UNIVERSITAT DE BARCELONA

Endothelial and myointimal cell functions related to vascular inflammation and remodeling in Giant-Cell Arteritis

Contribution of interleukin-23p19, interleukin-35 and endothelin-1

Ester Planas Rigol

Endothelial and myointimal cell functions related to vascular inflammation and remodeling in Giant-Cell Arteritis.

Contribution of interleukin-23p19, interleukin-35 and endothelin-1.

Thesis presented by

Ester Planas Rigol

For the degree of Doctor by the University of Barcelona

Thesis directed by

Maria Cinta Cid Xutglà

UNIVERSITAT DE BARCELONA

School of Medicine, University of Barcelona

Barcelona, November 2015

A la meva família, especialment als meus avis

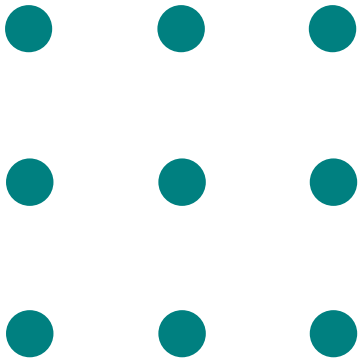

Moltes vegades la solució està en mirar-ho des d'un altre angle aparentment inexistent

Acknowledgments

Sense cadascuna de les persones que apareixen en les següents pàgines, aquesta tesi no hauria estat mai possible.

First of all, I would like to thank to Hynda Kleinman, Juan Cañete and Santiago Lamas as well as Manel Juan and Jordi Yagüe for their acceptance to evaluating my doctoral thesis. This is a great honor for me. Thank you so much. M'agradaria agraïr especialment el gran suport que he rebut per part del dr. Josep Maria Grau, sobretot els darrers mesos que és quan un més ho necessita.

Tot seguit m'agradaria continuar pel Vasculteam :
Mariona, sempre recordaré el primer cafè/entrevista en el que ja em vas fer sentir com a casa, a més de tots els congressos (sobretot els Keystone) i moments al bar de la facultat que hem viscut juntes. Gràcies perquè m'has fet veure art en la ciència i ciència en l'art. Gràcies Mariona, per donar-me l'oportunitat de créixer científicament i com a persona i per preocupar-te per nosaltres. Ets un geni que mai deixa de sorprendre amb l'enorme coneixement que té.

Marco por tu manera de ser tan servicial, tan agradecido y a la vez tan divertido, por hacerme sacar el duende loco que todos llevamos dentro y compartir la pasión por la ciencia. Gracias por los desayunos, tu ayuda en la parte más clínica y por las visitas sorpresa al despachillo. **Sergio** por tu buen carácter, el buen rollo que desprendes y tu profesionalidad, pero sobretodo por lo mucho que me has ayudado. **Itzi**, nuestra Audrey Hepburn**,** era genial cuando estabas en el lab siempre con tu enorme sonrisa que son de aquellas que se contagian. **Pepe** gràcies per ser un dels sèniors del grup que sempre té ganes d'explicar-te alguna cosa clínica que no entens. **Ana** per la teva capacitat resolutiva i per ser sempre un dels pilars dels l*abmeetings*, regalant-nos els comentaris o observacions adequats. **Georgina** pels projectes i vivències compartits que han acabat fent que ens coneguéssim i ens uníssim més. Qui m'havia de dir que la p19 aniria acompanyada d'una nova amiga! Però gràcies sobretot pel teu suport i per posar-me a ratlla quan toca.

Marc gràcies per obrir-me els braços de panda des del primer dia, sense tu el doctorat hauria estat totalment diferent. Trobo que som el *ying yang* perfecte. Gràcies per la calma que em transmets, per les mirades que ho diuen tot sense necessitat de parlar i pel teu suport, però sobretot per cuidar-me TANT. Ets d'aquells que és fàcil tenir ganes d'abraçar (més de 10 segons). T'has transformat en molt més que un company de feina : un grandiós amic. **Nekane, Neki, Neka,** què hauria fet jo sense les nostres converses dels vespres a més dels *labbirrings* improvisats, els viatges a EEUU i les nostres abraçades i moments punkis perquè si? Aprenc moltes coses amb tu i em fa feliç que confiïs en mi ja que t'has transofrmat en algú molt IMPORTANT. Ets d'aquelles que sempre hi és donant-ho tot sense esperar res a canvi. Moltes gràcies per ser tan sensible i evidentment GRÀCIES de veritat per demostrar ser una gran amigueta i tenir-te sempre aquí al meu costat (literal també!). Ets petiteta però a la vegada

exageradament GRAN! **Ester Lozi** pel curs intensiu que em vas fer quan vaig entrar al grup. Per les moltes vegades que m'has ajudat des d'EEUU o des d'aquí, per la teva capacitat de veure les coses de forma pràctica i per donar-me sempre bons consells. **Àlex** per omplir-me d'energia i ganes de fer experiments i fer-me qüestionar les coses amb les teves preguntes. Pel teu punt crític i les teves ganes de menjar-te la vida que tan m'agrada! Per transformar-te en un molt bon amic que sempre em fa il·lusió veure**. Stefania**, fu breve ma intensa!!

És molt important la gent del teu propi grup però també ho són les persones amb qui comparteixes el dia a dia, primer al lab 413, després al 302 i ara al 4B…
Glòria per ser la **jefa** màxima mito i del lab! Pels milions de converses sobre absolutament tot al tren, a cultius, esmorzant...Per fer-nos riure fins i tot quan estem plorant! Per preocupar-te de tot i tothom i fer que tots siguem una miqueta més feliços. Ets espectacular i per això em tens i el cor robat des de fa molt temps! Glo, ho saps oi que ets molt més que un 10? **Cons** pels viatgets "reparadors" compartits, per saber que sempre em tens present i per la teva enorme empatia, generositat i el teu sentit de l'humor. No he conegut mai cap persona igual a tu Cons, ets massa única. Fas treure el millor de nosaltres i això et fa molt gran. **Mariona** per fer que anar al labortari cada dia sigui encara millor. Per fer les coses difícils extremadament fàcils, pels teus detallets constants, pels teus somriures revitalitzants, la teva energia, el teu bon humor, i sobretot per fer que em senti com si et conegués de tota la vida des del primer mes. Per ser una gran amiga a qui tinc ganes d'explicar-li tot, sempre discreta però molt present. M'has demostrat moltíssim, moltes gràcies. **Marc Suri** gràcies per...TOT! Pels teus detalls, pels nostres moments de complicitat i pillades mentre faig coses absurdes, per saber que tinc uns braços on anar si tinc algun problema o una alegria, per contagiar-me la teva passió per la música i per no parar de sorprendre'm amb petites i grans coses. Ets màgic. **Diana,** eres muy padre, gracias por hacernos reír muchísimo, por tus ganas de aprender, por tus muestras de cariño y comprensión y por tu sentido del humor. **Adriana**, quina sort hem tingut de tenir-te uns mesets amb nosaltres. Mil gràcies per les teves històries, per la teva pau i per la teva atenció. Ets meravellosa, espero no allunyar-me de tu. **Íngrid** per fer-me sentir una amiga des del principi, per portar aire fresc al lab carregat de bon rotllo. Per mostrar-me que ets d'aquelles que es preocupa per les coses, i posa els seus granets de sorra per fer un món millor. Saps què? quan se que hi ets estic més contenta i no et cal fer res! Encara no se quin és el teu secret però el que si que se és que no es pot ser més encantadora! **Maria,** per les teves mostres de carinyo i l'alegria que desprens quan et tenim per aquí. Per ser tan mona i per fer-me sentir estimada. **Jenn** pel teu sentit de l'humor d'ogro i els teus vestidets! **Ester Tobías** pels teus detallets recoberts amb pipes i els teus "bon dia" ara acompanyats de l'Abraçada! Perquè se que puc comptar amb tu tan en lo personal com amb les cosetes del lab, i com no, pels nostres moments tallant biòpsies. Lo bueno abunda! **Palmi** per ser autèntica, modesta i ensenyar-nos coses útils cada dia sense adonar-te'n. Pels cafès de bon matí acompanyats d'històries i la teva energia a l'hora de muntar plans i sobretot per la teva constància. Pels palmimentos i per il·lusionar-te per les petites coses. M'encantes. **Merxe** per comprendre la part

més íntima de mi,pel teu punt hippie tan autèntic. Per cuidar-me i preocupar-te sempre per mi i per tots, per fer-me sentir important i per ser el Desembre 19…i sobretot per ser tu, la Merxe, algú senzill i que sap ser i fer feliç a qualsevol amb lo mínim. No podria escriure totes les coses bones perquè no tinc espai i crec que ets de les que prefereixes una abraçada. Gràcies per tenir la **Kine**, per portar-la amb nosaltres, i fer que també sigui la meva amigueta a la que tinc ganes de veure créixer i no parar mai de seguir-li la pista de ben a prop. **Gemma** quantes coses a agrair! Per començar per ser co-fundadora dels *labbirrings*, per les xerrades al lab quan ja no hi quedava ningú, per ser una bonica **enxaneta** però també saber fer pinya, pels moments d'emoció "xungo" al veure els limfos i els monos pel citòmetre i per fer-me aprendre paraules noves cada dia. **Francesc** per la teva capacitat de dir les coses tal qual i caure bé igual. Per uns grandiosos moments quan et teníem per aquí que per sort ens continues regalant. Ets una caixa de sorpreses!oi? **Siscu** per impregnar-nos de bromes constantment, per ajudar-me amb tècniques que havia de posar a punt, per fer-nos de guia i per fer-nos saber una miqueta més de coses sobre l'art i la ciència. Pels teus missatges preguntant com estic i les teves abraçades..bueno, depèn de quines. Per ser una personeta que tan m'agrada. Va, ves a trepitjar flors! **Sarai** per crear aquestes arrels tan profundes en el meu cor. Per ser tan carinyosa i tan especial. Per confiar plenament amb nosaltres i fer-nos sentir que el 302 és una gran família. Perquè vull seguir pujada a la teva furgoneta. I què dir de la **Gemma Sasot,** gràcies per les innumerables vegades que entres al despatx vascul i m'arrenques un somriure, o dos, o tres! Pels missatges dient que ens trobem a faltar quan fa un únic dia que no hem passat pel lab i sobretot pels teus : " estàs bé?". Per ser tan autèntica i bitxo!!
I també agraïr-te **Núria** la teva màgia, bona energia i la tranquil·litat que em desprens. Encara que no ens veiem gaire, sempre et tinc molt en compte. Gràcies per ser de les persones que em va regalar les primeres paraules al 413.

Gràcies també l'**Àlex predi,** per ser tan divertido y auténtico, con ganas de cantar y bailar y hacernos reir tanto! Y sobre todo por tu sinceridad!! A la **Rosa** pel teu somriure de bon dia**,** i per preguntar-me sempre com estic i per ajudar-me amb el format de la tesi! A la **Sara** por la tranquilidad que desprendes y tu buen rollo**,** a la **Laia** pel carinyo que sempre m'has donat i per la cançó de l'esquirol plim plim! A la **Irene** per la teva efusivitat a l'hora de fer les coses, a la **Margarita** pel teu somriure tendre i les teves ganes d'ajudar, a l'**Anna Creus**, per haver pogut compartir almenys uns mesets amb tu al lab, al **Jordi Casanova** per ser un crack i demostrar que amb poquetes eines es pot construir moltíssim i a la **Sílvia** per ajudar-me infinit quan ho necessito i sempre interessar-te per mi. A la **Didi**, per portar bon rotllo al lab des del primer dia i al **Sergio y Vicente**, vaya súper mitos! (I tots els nous que van passant!) Ha sido muy bonito teneros en el laboratorio.També al **senyor Bové**, qui sempre et saluda amb un enorme "bon dia" i es preocupa sempre perquè estem tots bé a més d'haver-me donat una cosa que ara per mi tindrà molt valor. I a les noves incorporacions de la planta com l'**Anna Boronat** qui amb molt poc temps ja m'ha demostrat que puc comptar amb ella i que és una persona meravellosa.

També és importantíssima la gent amb qui no tens la sort de compartir els espais però també estan rondant pel CELLEX o el CEK.
Al grup del Dr. Postigo, sobretot a l' **Ester Sánchez** per ser tan espectacular com a persona i com a científica. Per donar-me consells, per ajudar-me a dissenyar experiments, per deixar-me reactius, per no rendir-se mai. És d'aquelles persones que et fa venir ganes de menjar-te el món i continuar en ciència. Gràcies també a l'**Oriol**, per donar aquest bon rotllo sempre, fins i tot quan estàs atabalat. Pels teus comentaris graciosos i també les teves ganes d'ajudar. Per ser una persona a qui sempre tens ganes de veure. I a la **Laura, el Pablo, la Natàlia i l'Àngela** pels *labbirrings* compartits.

I també del grup del Dr. Elies Campo destacant la **Jara** per les nostres converses compartint penes i alegries. Per poder compartir amb algú la meva passió per la ciència. Ja ens havíem conegut a la uni però crec que ha sigut ara que realment ens hem re-descobert i m'encanta. Gràcies gràcies i gràcies preciosa! També a la **Marta** per empatitzar amb mi des del minut zero, per la teva mirada de comprensió i les teves abraçades i per la teva eficiència i capacitat de resolució. I el **Robert** i la **Carla**, pel "contrabando" de reactius! I a la **Laia Rosic** per ser d'aquelles persones que quan veus somrius molt perquè t'encanta trobar-te-les, va ser un súper descobriment del màster de biomedicina i totes les altres coses en les que hem anat coincidint.

En general, gràcies als veïns de bio cel·lular, però sobretot a la **Iona**, per compartir batalletes de les EEBB, i pels nostres cafès. I al **Carles** per ajudar-me amb les immunos i per preguntar-me sobre la tesi i donar-me ànims i consell cada cop que ens trobem pels passadissos!
Gràcies també a la **Maria Calvo**, a l'**Elisenda** i a l'**Anna** del servei de microscopia confocal per ajudar-me a posar les tècniques a punt i interessar-se sempre per com porto la tesi. S'agraeix infinit.

Durant els anys de doctorat he tingut la gran sort d'haver fet una estada al NIH, a Bethesda, on vaig descobrir gent a qui també podria agrair un munt de coses. A la **Giovanna Tosato** for offering me the opportunity to work in your lab. I will always remember those days in DC. I think I grow up as a person but also as a scientist. Thank you so much for making me feel like one more in the group since the first day I arrived and for the effort you've done to publish our appreciate p19! I would also like to thank all the people from the lab. **Hide**, for being my teacher in each experiment and being a super scientist, **Ombre** for your good mood and for making me feel happy every time I saw you and you called me "*figlia de la fiore*"! **Michael,** thanks for your questions during the lab meetings, the beers after work and your energy in the lab and outside the lab. **Henry** for making me laugh and dance a lot and making me feel comfortable in the lab. **Inn Inn** for all the plans you organized and for taking care of everybody in the lab. **Richard,** my friend Richard! Thanks for coming to my bench every afternoon with your big smile and some

cookies! Thanks as well for taking care of me like a daughter and for being my partner at Zoo Bar!

Sense deixar de mencionar els amics que vaig fer fora del lab : **Abelito y Mónica** por hacerme sentir querida e importante en todo momento, hacerme reír y tener a alguien con quien emocionarme con los pequeños detalles. Mil gracias también por preguntarme cada viernes si "mañana tengo que ir a dar vueltas a las células" pero sobretodo porque podemos mantener nuestra relación escribiéndonos estas cartas que tanta ilusión me siguen haciendo. **David** por ser mi ángel de la guarda de Washington, por los cafés de mañana y tarde, por las miradas de comprensión en miles de circunstancias surrealistas y por la ayuda inagotable en el laboratorio. En definitiva gracias por ser un gran AMIGO y la primera persona que me abrió la puerta en DC. **Aida** por ser mi compi de margaritas y de visitas a Nueva York fugaces. Por sacarme a pasear por Adams Morgan y contar conmigo siempre. **Sandra** per ser una persona única, vital, generosa, curiosa i amb una empatía exagerada i per pensar en mi en molts moments. Em vas robar el cor des del primer dia! Quin és el teu secret? **Gerard** per transformar-te en el GERARD des del dia del tornado allà al Rumba Café. Per les nostres "Blue Moon" a la pizzeria d'Adams envoltades de converses sobre una mica tot, per tenir un compi amb qui riure i plorar, per la teva ment crítica que et fa ser tan especial i per fer-me sentir valorada i recolzada. T'has transformat en un gran amic que tinc la sort que el tinc voltant per aquí de tant en tant.

També han sigut molt importants les persones que vaig conèixer durant la meva estada a Austràlia. **Nick Hayward**, to give me the opportunity to work in your lab. I still think it was a dream. I will never forget the help you gave me while I was in Oz and the work you did to change my visa. Thanks for becoming a friend, for being interested on everything in my life and being an awesome person. I really hope to see you soon. Thanks for helping me choosing the research way. Thanks to **Mitch** and **Maggie** and **Vanessa** and all the people from the G floor!

A més de persones que van estar amb mi mentre aprenia a viure la vida al mateix moment en que començava a agafar passió per la ciència com la **Keilie** , for the *somewhere to stay* bus trips, for meeting you around the world and make me understand that the best important thing in life is being happy and make me keep smiling. **Bruno and Misa** to become great friends with who could do a lot of trips around Oz, **Jin** for being the cutest girl ever!! And **Heeeeee** to become one of the best persons I've never met!

Ferran, et podria agrair moltíssimes coses però la que destaco és el fet d'impulsar-me a marxar a Austràlia, compartir aquella experiència amb tu va ser MERAVELLÓS. Moltíssimes gràcies, perquè gràcies a allò i a la teva bona energia ara estic aquí escrivint els agraïments de la meva tesi.

També han estat molt important el grup de Biologia Molecular de l'Hospital de Terrassa que és el primer laboratori on vaig treballar. Per això vull agraïr al **Miguel Carballo**, que suerte tuve de hacer las prácticas de Biotecnología con vosotros, y gracias por ofrecerme quedarme durante aquel año. Aprendí muchísimo! Ah! Y por llamarme hormiga atómica, aún lo pienso a veces

cuando voy como loca por el laboratorio. **Imma** gràcies per ser tan complerta, ho tens tot! Moltíssimes gràcies per regalar-me grans moments (com el del pastís del microscopi) i per apropar-te tant a mi, per la teva energia que es contagia, i per estar encara tant present. En definitiva, per ser tan guai! **Maria José** gràcies per fer que em sentís tan còmode amb vosaltres, per ser tan ordenada i pràctica i per confirar en mi i per cuidar-me tant. Gràcies per encara regalar-me aquestes abraçades que tan m'agraden quan ens trobem per Terrassa. Vosaltres dues em vau ensenyar a cuidar i transfectar les cèl·lules, a fer PCRs, a fer gels…tot! Les meves primeres teachers. Quin gran honor!

Als amiguet que he anat trobant als congressos sobretot al **Puneet** i la **Hanane**: I've been so lucky to share more than only a meeting with you! I a la **Jess** for being an awesome girl who is plenty of contagious energy!!

Crec que durant aquests anys, ha estat clau també el caliu que m'han donat els meus amics de la uni i per això mereixen una bona part d'aquests agraïments . Al **Jordi** per ser senzillament un crack, tenir capacitat de resoldre i tenir respostes sobre qualsevol dubte que se m'hagi plantejat en qualsevol moment. I pels momentazos mentre "estudiàvem" a l'hemeroteca. Per estar sempre al meu costat ja des del principi de biotecnologia, per l'estima que ens tenim i el vincle que hem creat que espero que no es trenqui mai. A la **Mercè** perquè des de que et vaig veure a la uni que ja vaig pensar : "amb aquesta noia segur que ens portem bé"… sembla que no em vaig equivocar…m'encanta compartir-ho tot amb tu, poder-te escoltar i que m'escoltis i has estat un pilar molt important tan en l'etapa uni com en l'etapa doctorat. Per ser una gran amiga. A la **Irma** perquè cada cop que em dius "petita" sento que hi ha algú allà a l'altra banda que m'estima. Per compartir aquest punt freak per la ciència i sobretot per la immuno. Per ser una persona GENIAL i dolça d'aquestes que sempre tens ganes d'abraçar. Per ser una gran amiga. A la **Gina** per ser tan autèntica, ensenyar-me que en la vida no hi ha "NO" que valgui, que si tens un objectiu has de lluitar per aquest i demostrar-m'ho constantment. Pel teu sentit de l'humor i la teva capacitat de caure bé a la gent sense fer cap esforç, com vas fer amb mi que se'm vas posar a la butxaca rapidíssimament i encara hi sóc! U,e! A la **Bàrbara** per tractar-me com una germana des del minut zero. Per les hores de practiques a biotecnologia. **Berna**t no hi ha paraules que valguin per dir-te tot el que t'hauria d'agrair. Suposo que notes lo molt que t'arribo a admirar. Des del primer moment que em vas ensenyar la teva part més optimista. Gràcies per compartir els teus pensaments i sentiments, per demostrar-me que confies en mi i em valores i per fer-te estimar tant, no conec ningú com tu i ets un gegantíssim amic que no penso perdre mai. Al **Ponsi** per ser tan únic. És impossible veure't i no tenir ganes de riure, sempre explicant batalletes que no pots deixar d'escoltar ni un segon. Per preguntar sempre com estic i per dir les coses tal qual són. Per tenir aquest toc irònic-cínic que amaguen la teva extrema sensibilitat que a mi tan m'agrada que surti.

Durant aquests anys de doctorat he tingut la sort de tenir-vos per aquí rondant, ja ens vam conèixer a la uni però amb la majoria de vosaltres ens han unit més els dinars al CEK : **Borja,** gràcies per les teves visites al lab i per riure-te'n sempre de la meva part de "floreta". Per demostrar-me que no s'ha de tenir por per fer les coses que a un li vénen de gust fer i per ser un gran amic. **Helena** per ser tan dolça i compartir aquests moments en els que estàvem pujades a una muntanya russa durant el doctorat. Pel dia en que em vas agafar a les pràctiques i em vas dir que anava amb tu amb aquell gran somriure i,evidentment per ser una gran amiga. **Laura**, per ser una persona preciosa, vital, empàtica i bona. Ets d'aquelles persones que desprenen una energía molt positiva i que tinc ganes de continuar tenint ben a prop. **Marta** per ser així tal qual. Per compartir el punt de massoca i amant de la ciència i per tot!!!

Laureta, Laura, Rodri (Juan), Meri, Carles, Pou, Alba,Marc,Francesc i molts d'altres de la uni, pels meravellosos anys de BIotecnologia i per les trobades que anem organitzant, encara que no haguem coincidit tant com amb d'altres de la uni, continueu sent gent molt important per mi.

Al **nen de la sele** per preguntar-me una cosa que sempre m'ha fet molta gràcia: "em pots tornar a recordar què fas en un dia normal al laboratori?" i per trobar-te en el moment/lloc més inesperat.

També m'agradaria agrair a **na Mari ,en Rafel i en Raul** per obrir-me les portes de casa vostra com si fos una filla o germana més. Pels moments de relax que he passat amb vosaltres a Menorca i per preocupar-vos sempre per com em van les coses i sobretot la meva tesi. Però sobretot al **Dani,** perquè m'has fet ser més forta, m'has cuidat i donat recolzament i incontables detalls i mostres de carinyo (fins i tot en moments una mica més crístics) que m'han fet ser més feliç aquests 4 anys. Tot i la distància se que podem continuar comptant l'un amb l'altre.

I com no, al **Marc Santín**, per la teva dosi d'energia i estima que em proporciones des de fa ja tants anys ja sigui des de la distància o amb les magnífiques abraçades quan ens trobem. Amb tu he tingut la sort de créixer i començar-me a definir com a persona. Hi ets sempre Marc. Petó-nas.

No poden faltar els meus **com-pis**….**Xavi** , has demostrat ser un fantàstic company de pis i encara més amic amb qui ens hem pogut explicar com ens sentíem i al mateix temps intercanviar informació dels nostres doctorats quan assentats al sofà descobríem que l'altre també estava fent gràfics de feina! Gràcies també per portar la **Mireia**, per favor, ja ric només d'escriure aquest paràgraf i pensar en tu bonica! Ets la millor medicina després d'un dia d'aquells cansats de lab en que el sofà t'està absorbint, i la millor companya d'històries

d'aquelles que et passen i creus que és millor que ningú mai les sàpiga! Ole tu! **Mireia**...quan et tenia al pis sabia que erets exageradament important per mi, però ara que no hi ets encara ho noto més. Trobo a faltar els nostres sofà-manta on qualsevol tema valia, la nostra comprensió amb i sense paraules i la teva manera de veure la vida (i tot, perquè ho veus tot!). Ets un tresoret que no vull perdre i amb qui he après molt. T'has convertit en una germaneta. **Laia ,** has sigut un gran descobriment, i una dosi de bon rotllo. Cada dia que passa penso que has aparegut al pis per algun motiu molt bo i de fet ja ho saps. T'has transformat en una gegantíssima amiga en un temps rècord. Gràcies per entendre-ho tot de mi sense que t'hagi d'explicar gaire...ets meravellosa! **Anna**, gràcies per donar-me consells, per preguntar-me com estic, per fer-me riure sense haver de fer cap esforç i per ensenyar-me tantes coses d'un món diferent al meu (you are killing it!).

A les meves ragazzes…**Glòria**, no sabria pas on posar-te ,perquè a part de ser la meva cosina ets també una gran amiga, una de les millors. Sempre fent-me sentir que el que faig val la pena i el que dic té sentit i sobretot ensenyant-me a fer passos ferms. La teva gran intel·ligència ,el teu sentit de l'humor i la teva empatia em tenen enamorada. Quina sort que tinc d'haver compartit tantes coses amb tu : els Nadals a casa els avis, els dinars de diumenge a Les Pedritxes, el tennis, la piscina, la música, i ara els viatgets i sopars juntament amb la Gemma. Ets una tia espectacular. Fem un baile de las primas per favor. I **Gemma,** gràcies per ser una de les amigues més constants...per estar sempre ja des de que fèiem jazz , tennis, els estius a Calafell, al Velcro i ara amb les ragazze…quina sort la meva i quan de suport he tingut sempre per part teva! Per mi ets molt especial, sempre comprensiva i pacient i mil qualitats que aquí no hi caben! Mil gràcies per ser així i compartir-ho amb mi. I **Roger**, gràcies per fer-me veure que la música heavy també té color, fer-me riure sempre que et tinc a prop, i demanar-me posar un toque científic als teus tatuatges!

Cristi , per ser preciosa per dins i per fora, per ser la meva millor amiga, algú a qui puc explicar-li TOT. M'has ajudat a veure millor les coses en els moments difícils i durs de la tesi i de la vida, i hem rigut (i molt) juntes en els moments més bonics. Has estat present en tots i cadascun dels moments importants, fent-me agafar força i confiança en mi mateixa. Ens robes el cor simplement per la teva manera de ser, tan sincera, empàtica i espontània. T'admiro molt i realment et necessito molt al meu costat. Gràcies a tu he conegut el teu **Xavi,** a qui també li agraïria el suport que m'ha donat sense adonar-se'n i les abraçades sorpresa quan les necessitava. **Puça**, pels cafès de divendres a l'Anticco, per interessar-te pel que faig al lab i explicar-me d'economia! Per ser un noiet tranquil , senzill i sensible i per estimar-me tant. Caminem junts des de fa molts anys i espero que en siguin més. En definitiva, gràcies per ser TU.

Als de jazz, sobretot a la **Laura Olivella**, perquè cada dimarts i dijous pugui desconnectar desfogant-me com millor m'agrada, ballant. A l'**Albert**, per preguntar-me sempre com estic i fer-

me tornar a treure l'àurea perduda i per portar sempre un segon casc. Juntament amb la **Cris** i les **Lídies,** la **Gemma** i la **Marina** per fer que anar a la xina sigui meravellós : una dosi de riures magnífica. I, evidentment gràcies també al recolzament que tinc sempre per part de les **mamis.**

A les nenes i nens de Matadepera : **Anna, la meva Anni...** perquè fa tants anys que ens coneixem que no hi ha res que no et pugui/vulgui/necessiti explicar. Ets una "chica 10" per mi i ho saps , una amigueta bonica per dins i per fora. Una de les meves millors amigues. **Mireia**, per poder compartir batalletes de l'hospital i de l'institut amb tu! Per fer-me enamorar de la teva manera de ser des del principi, de tu! Per transmetre'm aquesta energia *zen* que tan m'agrada. Sobren les paraules. **Alícia,** per ser la rata més guai del món mundial i pels magnífics moments que he passat, passo i passaré al teu costat mirant-nos! **Miona,** per ser tan autèntica i valorar-me tant, per ser constant, respectuosa, aplicada i sobretot bona amiga. **Judit** per ser tan divertida, per les nostres fotos intentant quedar bé i per riure-te'n del meu punt freak amb les cèl·lules! **Helena** (i Judit) per fer que el meu cumple sigui el 14 i a més el 15 i pels vermuts amb el teus peques que tan em carreguen les piles. Per ser-hi des de fa tants anys ja a la Plaça Vella. **Gigi,** per estar sempre tan a prop i per fer-me riure tant. Per fer-me veure les coses des d'un altre punt de vista (el killer) sempre tan necessari. **Alexandra**, ja fa temps que ens vem unir i quina sort la meva, gràcies per les múltiples converses sobre tot i per la teva vitalitat! I pels nostres bailes, la nostra medicina. **Berta** per ser tan mona i adaptable i portar sempre bon rotllo i fer riure tant!! Per fer-me preguntes i esperar un : "Millor". **Lara,** per ser un gran descobriment ja des de l'IES com si fossis una adtv. **Montse** per ser una persona tan adorable que sempre està allà disposada a regalar-te un somriure i ajudar-te. **Maria** per compartir amb mi el teu esperit aventurer i ganes de reinventar-te. **Norma** per contagiar aquesta pau i per entendre la meva part més de biòloga. **Núria** per regalar-me sempre aquest bonic gran somriure ja des de fa tants anys. **Lito,** per ser així de divertit, espavilat i interessar-te tan per mi, i sobretot per ser una persona tan espectacular. **Miki,** per tractar-me sempre com una princesa i per tots els anys que hem viscut fent plans, i per fer un component del *pack* que espero que no es trenqui mai. **Pol**, pels biquinis i birres que fèiem per trencar la setmana i per recordar-me sempre que és lluna plena. Tampoc em voldria deixar l'**Autonell,** el **Pep**, el **Marc Serrat**, el **Uris** (Villatoro i Pérez), el **Pepe** i el **Xavi Serra** pels súper plans que fèiem!

I també m'agradaria mencionar els meus **amics de Calafell (sobretot al Lalo, l'Edu ,el Gerardo, el Borràs, el Sergio, la Elena i el Queque)** que els conec des de que tinc 14 anys i encara ara ens continuem veient, sembla que no passin els anys. Mil gràcies per fer que els estius o els caps de setmana d'estiu es transformin en dosis de medicina energètica per combatre millor la setmana. Sou únics!I evidentment **l'Edu Varas** i el **Litus** que també m'han hagut d'escoltar mil vegades les meves batalletes amb el doctorat tot fent braves o guitarreando!

Voldria agrair especialment al **Ramón**, per haver entrat en la meva vida quan menys m'esperava. Per ser tan sorprenentment oportú i ser una font màgica d'energia inesgotable. Perquè cada cop que em mires entenc que em tens en compte i que estàs al meu costat donant-me tot allò que necessito i més. Perquè ajudes a que la meva vida sigui més fàcil i fas treure el millor de mi fent-me riure i ajudant-me a ser més feliç! Gràcies de veritat pel teu optimisme i suport absolut. No puc imaginar ningú millor al meu costat. Suposo que això deu ser al que es refereix la Bona Sort. Som afortunats d'haver-nos "trobat" just quan ens havíem de "trobar".

I finalment a la **meva família**. A la **súper Iaia Pilar** per la teva energia, bon humor, la teva manera de veure la vida, tan moderna... i per tenir sempre el teu suport! Tothom està orgullós de tu i t'estima perquè tu tens un cor gegant i ets tan autèntica que fas arrencar somriures a tothom amb qui et creues . Ets el pilar fort de la família. Jo de gran vull ser com tu. **A tu , Avi t'agraeixo ser el motor** dels dinars dels diumenges, com arriben a unir la família! Per agafar-me la mà quan menys m'ho espero i dir-me que tu tens clar que "jo ja se el que em faig" i que confies amb mi. Això a mi m'ajuda a fer passos més ferms. Per explicar-me batalletes de quan erets jove i ensenyar-me a ser treballadora. En definitiva, per ser-hi sempre, discret però constant observant-nos a tots amb la teva copa de cava a la mà i aquell mig somriure que tan trobaré a faltar. **Salvador , Rosa i les peques,** per omplir de vida la família, per fer que els diumenges siguin més divertits i per fer-me madrina de l'Helena, i cosina de la princeseta Júlia. **Sílvia** per demostrar a mi, i al món sencer, que un no aprèn si no vol i que els límits se'ls posa un mateix. Contagies força ,energia i uns valors humans admirables. M'encanta que siguis la meva tieta, a veure si se m'enganxa alguna cosa! Ara estem lluny però et sento més a prop que mai. Gràcies per compartir amb mi la clau de la vida : Saber esperar. T'admiro! **Xavi** per ser tan únic, m'encanta escoltar-te perquè sempre aprenc alguna cosa. Has demostrat capacitat de sacrifici i adaptació i ser un pare genial i a més sense perdre mai el teu sentit de l'humor. I òbviament els meus cosinets, el **Marc i el Gerard**, per fer-me entendre la vida des d'un altre punt de vista, dir-me Ister i ser magnífics. I a l'avi **Josep Maria** i la iaia **Mari**, i el **Toni** no sabeu com us trobem a faltar, espero que allà on sigueu ho pugueu notar.

A la **Laura** per l'ajuda incondicional. Per ser el meu referent des de fa 30 anys, sense ni tan sols adonar-te'n. Per ser la germana gran ideal i perfecte per dins i per fora que tothom voldria tenir. Si t'hagués fet a mida m'hauria quedat molt curta!! Gràcies per aplanar-me el camí de la vida però sobretot per ser com ets. SEMPRE hi has sigut i sempre hi seràs. I el **Jordi**, el meu cunyadet, a qui he tingut la sort de conèixer més i més els diumenges. M'encanta la teva manera de veure les coses, la teva ment crítica i la teva capacitat de resolució!
A la meva mare. **Mama**, no hi persona en la galàxia sencera que tingui més qualitats que tu. Sempre presumeixo de mare! Estimes i cuides a tothom, i com a filla, encara me'n beneficio més! Sense tu avui no seria qui sóc. No existeix la paraula que defineixi el meu sentiment cap a tu per això intento demostrar-t'ho al dia a dia com puc, espero que ho notis. La nostra connexió

arriba a esferes paranormals, que de vegades fan por! Ets, fas i em dones tot allò que una filla podria demanar a una mare. T'estimo mama.

Papa, el meu súper pare, és l'artista de la portada de la tesi. No puc imaginar ningú millor per fer-ho. Tu em vas fer treure també la petita artista que tenia dins, cosa que m'ha ajudat molt a conèixer-me a mi mateixa. Amb la teva serenitat, m'has escoltat i t'has interessat sempre sobre mi i, aquests anys, sobre la meva feina. M'has proporcionat estima, comprensió (i un munt de moments gravats amb la teva càmera que ara tinc la sort de poder mirar). En definitiva, m'has donat i em dones tot allò que una filla podria demanar a un pare. Ets magnífic. T'estimo papa.

Tinc una família petita, però creieu-me que per mi és **MOLT GRAN**!

Index

1. Abbreviations……27

2. Introduction……35

2.1 Vasculitis……37

2.2 Giant Cell Arteritis……38

History and description……38

Diagnosis……38

Histopathology……39

Clinical manifestations……41

Mechanisms of GCA……41

Genetic Background……41

Triggers…… 42

Pathogenesis of GCA……42

Additional mechanisms: Autoantibodies……46

GCA treatment……47

Glucocorticoids……47

Other approximations to GCA treatment……47

Functional models……48

In vivo model……48

Ex vivo model……48

2.3 Mechanisms and molecules involved in vascular inflammation……50

Leukocyte recruitment steps……50

Molecules involved in leukocyte recruitment……51

Selectins……51

Integrins……52

Adhesion molecules: ICAM-1 and VCAM-1……53

Chemokines……53

VSMC and pericytes in leukocyte recruitment……55

Cytokines……56

Cytokines involved in CD4+T differentiation……56

Cytokines involved in macrophage differentiation……57

JAK/STAT signaling……..59

The IL-12 superfamily of cytokines……62

Introduction……62

Receptors and signaling……63

IL-12 (p40+p35)……65

IL-23 (p19+p40)……65

IL-35 (p35+Ebi3)……68

IL-27 (Ebi3+p28)……71

2.4 Mechanisms contributing to vascular remodeling……73

VSMC in vascular remodeling……73

Cell migration……74

Molecules involved in cell migration……75

Integrins in cell migration……75

Rho family proteins……76

PI3K……76

FAK……78

Src……81

MAPK……83

Endothelin System……84

Description……84

ET-1 regulation……84

ET-1 biosynthesis……86

ET-1 receptors (ET_AR and ET_BR)……87

Endothelin in vascular remodeling and fibrosis……89

Endothelin involvement in disease……91

Endothelin therapies and new approaches……91

MMPs/TIMPs……93

2.5 Challenges in GCA……94

Persistence of inflammation in GCA. Related molecules……94

Vascular remodeling in GCA. Related molecules……98

3. Hypothesis……101

4. Aims of the study……105

5. Material and methods……109

5.1 Cell culture……111

Temporal artery biopsy culture on Matrigel……111

Primary cultures of VSMC……111

Other cell types obtaining and culture ……111

Peripheral blood mononuclear cells (PBMC)……111

Negative isolation of CD4+T cells and CD14+ from PBMC……112

Co-culture of CD4+T cells, monocytes (CD14+) or PBMC with VSMC……112

HUVEC (Human umbilical vein endothelial cells) culture……113

5.2 Flow cytometry……113

5.3 Quantitative real-time reverse transcription (RT)-PCR……114

5.4 Protein detection in cell lysates……114

Immunobloting……114

Immunoprecipitation……116

Nuclear and cytoplasm protein extraction ……116

5.5 Assessment of protein secretion……117

Immunoassay……117

TCA/DOC cell supernatant precipitation……117

Gelatin zymography……118

5.6 Cell proliferation assay……118

5.7 Adhesion assay……118

Leukocyte /VSMC adhesion assay……118

Leukocyte /HUVEC adhesion assay……119

5.8 Migration assays……119

Transendothelial migration assay……119

Cell migration assay (Boyden Chamber)……120

Scratch wound-healing assay……120

VSMC outgrowth from temporal artery biopsies cultured on Matrigel……120

5.9 Transient transfection of adherent cells (VSMC)……...121

5.10 Lentiviral vector production, purification and HUVEC infection……..121

5.11 Immunofluorescence……122

Cell staining……122

Tissue staining……123

Proximity ligation assay (PLA)……...124

5.12 Bioinformatic approximations……125

Gene promoter region analysis……..125

Molecular modeling……...125

5.13 Statistical analysis……126

5.14 Reagents ……126

6. Results……127

6.1 Identification of IL-23p19 as an endothelial proinflammatory peptide that promotes gp130-STAT3 signaling……....129

Results summary (part 1)…….....173

6.2 IL-35: A new cytokine involved in vascular inflammation……175

Results summary (part 2)……...211

6.3 Endothelin 1 induces a myofibroblastic phenotype in vascular smooth muscle cells. A mechanim potentially contributing to vascular remodeling and intimal hyperplasia in Giant-Cell arteritis……...213

Results summary (part 3)……...249

7. Discussion……...251

8. Conclusions……...271

9. Bibliography……275

10. Additional Data……...299

11. Annex……311

Abbreviations

Aa - Aminoacid

AECA - Anti-endothelial cells antibodies

ANG I or II - Angiopoietin 1 or 2

AoSMC - Aortic smooth muscle cells

ASA - Acetylslicylic acid

BCL- B-cell lymphoma

BM - Basal membrane

BSA - Bovine serum albumin

CD - Cluster of differentiation

CIA - Collagen Induced Arthritis

CCL - Chemokine CC ligand

CCR - Chemokine CC receptor

cDNA - Complementary deoxyribonucleic acid

CFL1 - Cytokine-like factor 1

CHB - Chronic hepatitis B

CIA - Collagen-induced-arthritis

CXCL - Chemokine CXC ligand

CXCR - Chemokine CXC receptor

Da - Dalton

DAG - Diacylglycerol

DC - Dendritic cell

DMEM - Dulbecco modified Eagle medium

DNA - Deoxyribonucleic acid

DAMPs - Damage- associated molecules patterns

EAE - Experimental autoimmune endephalomyelitis

EC - Endothelial cell

ECGS - Endothelial cell growth supplement

ECE - Endothelin converting enzyme

ECM - Extracellular matrix component

eNOS - Endothelial nitric oxyde synthase

ET - Endothelin

EDN - Endothelin (gene)

EDTA - Ethilenediaminetetraacetic acid

EGF - Endothelial growth factor

ELISA - Enzyme-linked immunoSorbent Assay

ERK - Extracellular signal-regulated kinase

ESAM - Endothelial adhesion molecule

ESGL-1 - E-selectin ligand 1

ETM - Endothelial/epithelial to mesenchymal

ET_AR - Endothelin A receptor

ET_BR - Endothelin B receptor

FAK - Focal adhesion kinase

FAT - Focal adhesion targeting

FBS - Fetal Bovine serum

Fc - Fragment crystallizable region

FERM - Four-point-one, ezrin, radixin, moesin

FGF - Fibroblast growth factor

FGFR - Fibroblast growth factor receptor

FNIII - Fibronectin III domain

FOXP3 - Forkhead box 3

FRNK - FAK-related-non-kinase

GAP - GTPase-activating protein

GC - Glucocorticoids

GCA - Giant-cell arteritis

GCSF - Granulocyte colony-stimulating factor

GEF - Guanosine nucleotide exchange factor

GiACTA - Giant cell arteritis clinical trial

Gp130 - Glicoprotein 130

GPCR – G-protein-coupled receptor

GRB - Growth factor receptor bound protein

GTPase - Guanosine triphosphate binding proteinase

HLA - Human leukocyte antigen

HMG-COA - 3-hidroxy-3-methylglutaryl-coenzyme A

HUVEC - Human umbilical vein endothelial cell

ICAM - Intercellular adhesion molecule

EL - Elastic layer

IFN - Interferon

Ig - Immunoglobulin

IL - Interleukin

ILRA - IL-1 receptor antagonist

IP_3 - Inositol 1,4, 5-triphosphate

JAM - Junctional adhesion molecule

JAK - Janus kinase

JNK - c-Jun N-terminal kinase

Leu - Leucine

LDL - Low density lipoprotein

LFA-1 - Lymphocyte function associated antigen 1

LVV - Large vessel vasculitis

MAC-1 - Macrophage-1 antigen

MAPK - Mitogen-activated protein kinase

MHC - Major histocompatibility complex

MICA - MHC class I related gene A

miR - MicroRNA

MLC - Myosine light chain

MLCK - Myosine light chain kinase

MMP - Matrix metalloproteinase

mRNA - Messenger ribonucleic acid

MTX - Methotrexate

M1 or M2 - Macrophage type 1 or 2

NFAT - Nuclera factor of activated T cells

NFκB - Nuclear factor kappa-light-chain-enhancer of activated B cells

NK - Natural killer

NO - Nitric oxide

NOD - Non obese diabetic

NOS - Nitric oxide synthase

PAMPs - Pathogen- associated molecules patterns

PBMC - Peripheral blood mononuclear cells

PBS - Phosphate buffer saline

PDGF - Platelet derived growth factor

PECAM - Platelet endothelial cell adhesion

PET - Positron emission tomography

PI3K - Phosphoinositide 3-kinase

PIP - Phoshphatidylinositol phosphate

PLA - Proximity ligation assay

PLC - Phospholipase C

PSGL-1 - P-selectin glycoprotein 1

PTEN - Phosphatidylinositol-3,4,5-triphosphatase

PTK - Protein tyrosine kinase

PtdIns (4, 5) P2 / PIP2 - Phosphatidylinositol-4,5-biphosphate

PtdIns (3, 4, 5) P3 /PIP3 - Phosphatidylinositol-3,4,5-triphosphate

PTPα - Protein tyrosine phosphatase alpha

PTPN22 - Protein tyrosin phophatase non-receptor type 2

RA - Rheumatoid arthritis

RIPA - Radioimmunoprecipitation assay

RNA - Ribonucleic acid

SCID - Sever combine immunodeficiency

Ser - Serine

SFK - Src family kinase

SH - Src homology domain

SLE - Systemic lupus erythematosus

SNP - Single nucleotide polymorphism

SOCS - Suppressor of cytokine signaling

STAT - Signal transducer and activation transcription

TA - Temporal artery biopsy

TAB - Temporal artery

TAK - Takayasu

TCR T - T cell receptor

TCZ - Tocilizumab

Teff - T effector cell

TF - Transcription factor

Tfh - T helper follicular cell

TGFβ - Transforming growth factor β

Th - T helper

Thr - Threonine

Tie - Tyrosine kinase with immunoglobulin-like and EGF-like domains

TLR - Toll like receptor

TIMP - Tissue inhibitor of metalloproteinase

TNFα - Tumor necrosis factor α

Treg - T regulatory cell

Tyr/Y - Tyrosine

VEGF - Vascular endothelial growth factor

VCAM - Vascular cell adhesion molecule

VLA-4 - Very late antigen 4

VSMC - Vascular smooth muscle cell

Introduction

2.1 Vasculitis

Vasculitis is a group of heterogeneous diseases characterized by inflammation of blood vessels. Vasculitis can be classified as large, medium or small vessel vasculitis (**Figure 1**). Large vessels include the aorta and its major branches. Medium vessels are mainly the visceral arteries and veins and their intimal branches, however small vessels include intraparenchymal arteries, arterioles, capillaries, venules and veins. Any of the vasculitis included into each of these three categories may occasionally affect any size artery (*5*).

In this thesis, we are focuse on large vessels vasculitis (LVV) which includes Takayasu disease (TAK) and Giant Cell Arteritis (GCA). Although GCA and TAK differ in their demographic and ethnic distribution, their histopathological features are nearly identical and both diseases may share immunopathogenic mechanisms. Moreover, TAK affects younger (less than 50) people than GCA (more than 50 years old).

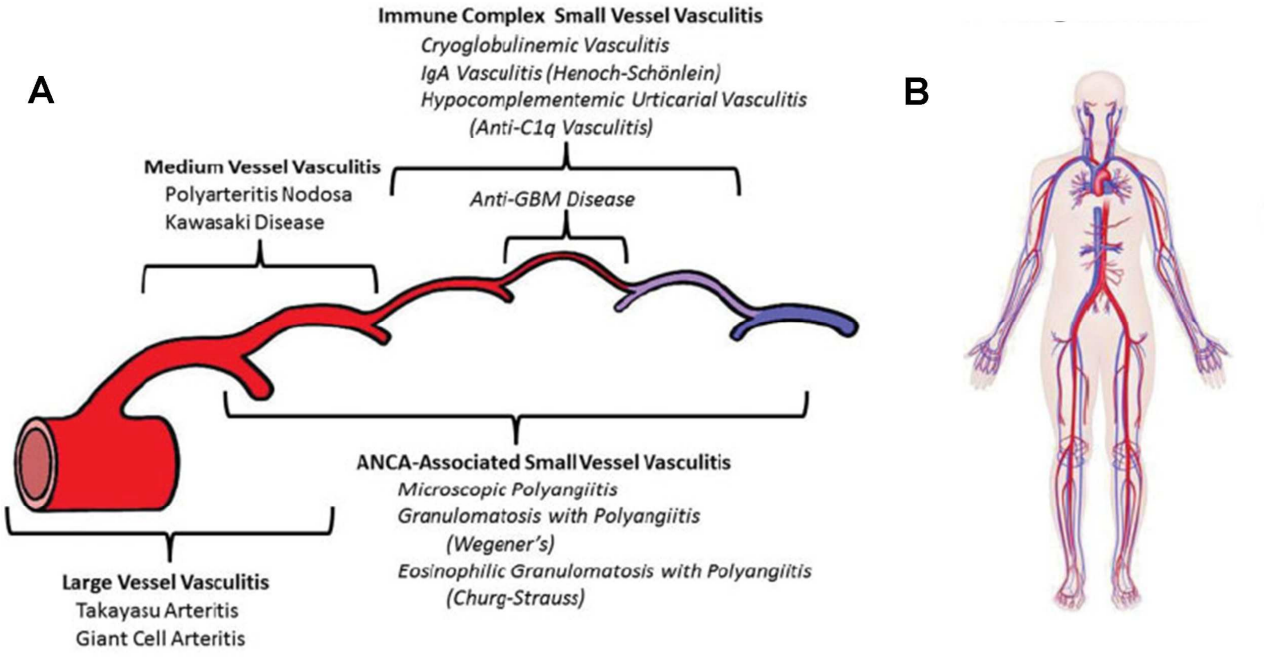

Figure1. (A) Vasculitis classified depending on the size of vessels predeominantly involved (large, medium and small). (B) Large vessels representation defined in the Chapel Hill Consensus Conference nomenclature system (2012) (*5*).

2.2 Giant Cell Arteritis

History and description

Giant Cell Arteritis (GCA) was clinically described by Jonathan Hutchinson in 1980. Although in 1932 was Bayard Horton who firstly obtained a temporal artery biopsy (TAB) which was an important contribution in order to characterize the histopathological substrate of the disease (*6*).

GCA is a systemic, granulomatous and chronic vasculitis affecting medium and large arteries. It predominantly affects of the carotid branches such as temporal artery (TA), ophthalmic artery or anterior ciliary arteries, but also the aorta and its major branches (*5, 7*). GCA is a disease of an unknown etiology and it is probably triggered by an immune response against still unknown antigen.

GCA patients are usually older than 50 years. Although is relatively rare, GCA is the most common primary form of vasculitis in the western countries. The incidence of the disease depends on the geographic region, being the major incidence in Scandinavia. In Scandinavia the incidence is more than 17 per 100.000 people per year in patients older than 50 years. In Mediterranean population, the incidence is lower, being less than 12 per 100.000 people per year in patients older than 50 years. The incidence, also changes depending on the age and the sex. The global incidence of GCA would be 1-2 to 10.000 person per year in patients older than 50 years although the peak appears at the age of 70-79 years being slightly more common in women than in men and the calculated prevalence of this disease is 1 for each 500 people (*8*).

Since vascular stenosis/occlusions can lead to irreversible tissue ischemia, such as blindness or stroke (*9*), prompt diagnosis and management is an absolute requirement for patients with GCA.

Diagnosis

Although there are emerging and promising imaging techniques such as positron emission tomography (PET) (*10*), computerized tomography (CT)-scan angiography, magnetic resonance imaging (MRI) angiography and color duplex ultrasonography which permit to detect abnormalities indicating large-vessel inflammation in GCA (*11*), the gold standard method for the diagnosis of GCA is still the temporal artery biopsy (TAB). Working with TABs permits to clearly observe the characteristic GCA histopathology which includes the presence of the

inflammatory infiltrate, granuloma formation with giant cells and the disruption of the normal artery layers (*12*).

Histopathology

In normal arteries the following well defined layers can be distinguished (**Figure 2**):

- **Adventitia layer**: Composed by connective tissue, collagen fibers and nervous fibers, tissue resident dendritic cells (DC), fibroblasts and endothelial cells (EC) forming the *vasa vasorum*. (*13*)
- **Media layer:** Composed by vascular smooth muscle cells (VSMC) surrounded by two elastic membranes (internal and external). VSMC serve under various circumstances both as agents of contraction and as the manufacturers of extracellular matrix proteins (ECM).
- **Intima layer**: It is located between the endothelial lumen (composed by a monolayer of EC) and the media layer. The intimal layer is mostly composed by myointimal cells and ECM.

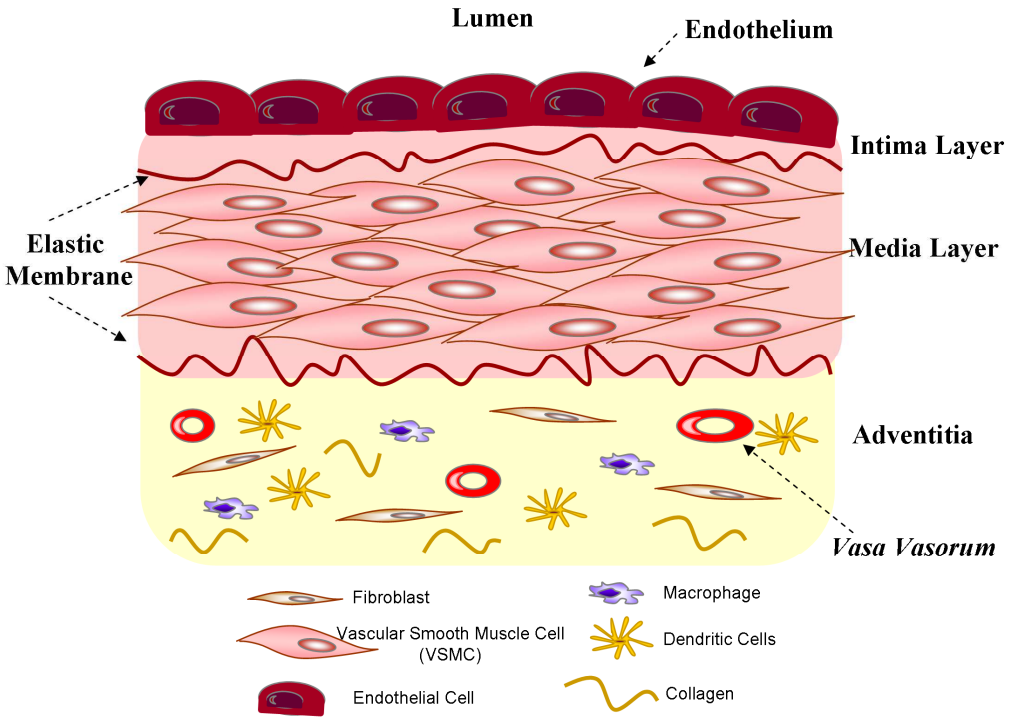

Figure2. Structure of a muscular artery is represented. A muscular artery is composed by different layers: Adventitia, media, intima and endothelium. The intima and media are mostly composed by endothelial cells (EC) or vascular smooth muscle cells (VSMC) respectively. The adventitia comprises a wide variety of cell types including resident dendritic cells (DC) and macrophages, fibroblasts, endothelial

cells forming the *vasa vasorum* and extracellular matrix proteins (ECM) such as collagens. Adapted from Stenmark *et al.*, (2013) (*13*).

As explained above, GCA histopathology observed in TAB is important for its diagnosis.

GCA is characterized by presenting an inflammatory infiltrate mostly composed by mononuclear cells (lymphocytes and macrophages are the main source) (*1, 14*)**.** Nevertheless it has been also demonstrated the presence of other cell types such neutrophils and B lymphocytes (*15*)**.** In the first stages of the disease, these infiltrating leukocytes are limited to the adventitia whereas in the advanced disease, they are found in the media. Importantly, GCA TAs are also characterized by presenting an intimal hyperplasia which promotes the vascular occlusion. As seen in **Figure 3A**, in which a TAB corresponding to a control is represented, all the artery layers explained are preserved. In contrast, in a TAB from GCA patient, GCA lesions are characterized by the presence of giant cells (arrows in **Figure 3B**), the presence of leukocytes, the presence of the neovessels in the entire artery, the neointima formation and the narrowed lumen and a clear disruption of all the artery layers, being difficult in most of the cases to determine the media layer. (The GCA pathology process is extensively explained in **Mechanism of GCA** section).

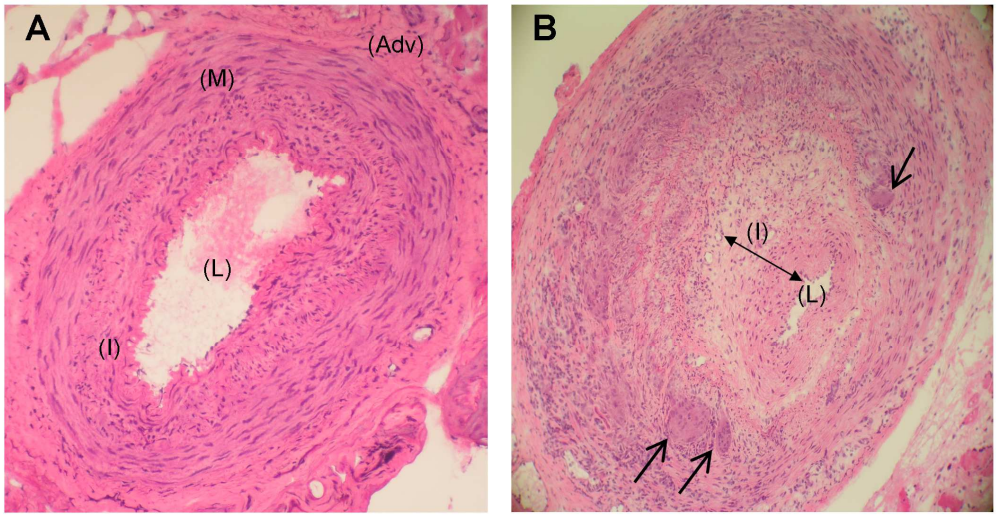

Figure3. Hematoxilin/eosin staining of temporal artery biopsies (TAB). (A) TAB staining from a control. (B) TAB obtained from a patient with GCA. Arrows in (B) pointed the presence of giant cells. (Adv) Adventitia, (M) Media, (I) Intima, (L) Lumen.

Clinical manifestations

The clinical manifestations of GCA can be classified in:

- **Arteritic symptoms.** These symptoms arise as a consequence of the local inflammation of the carotid branches such as TA, ophthalmic artery, anterior ciliary artery, and the aorta and its major branches. These symptoms tipicall occur in the cranial area and of visual loss, jaw claudication or cephalea.
- **Systemic symptoms.** Anorexia, malaise, weight loss and occasionally fevers.
- **Polymyalgia rheumatica symptoms**. Muscle pain and stiffness affecting the neck, the shoulder girdle, the pelvic girdle and only occasionally, the trunk.

Mechanisms of GCA

Genetic background

Genetic background in GCA is still poorly understood. However, GCA seems to be a polygenic disease. Several studies trying to associate single nucleotide polymorphism (SNP) to genes that contribute to immune response such as cytokines, chemokines (and their receptors) and class II major histocompatibility complex (MHCII) related molecules have been performed.

Regarding to MHC genetic variations, HLA class II alleles have been consistenty found to be associated to GCA (*16-18*).

Some genetic variations on genes related to autoimmune/inflammatory processes such as PTPN22 or NRL1 have also been found associated to GCA (*17, 19, 20*).

Some polymorphisms in GCA related cytokines such as IL-17 (*21*), IL-6. (*22*) , IL-10 (*23*), TNFα (*24*), VEGF (*25*),IL-33 (*26*) and other related molecules such as NOS2 or CCL2 (*22*) have been demonstrated.

Interestingly, in other studies have been characterized polymorphisms that seem to be associated not to GCA but to the different phenotypic expression of the disease. It is the case of polymorphisms in CD40 (a co-stimulatory protein found on antigen presenting cells required for their activation) which has also been associated to visual ischemic manifestations in individuals with biopsy-proven GCA (*27*).

Triggers

GCA etiology is still unknown based on the histopathologic findings and genetic association with HLA class II antigens, some studies trying to identify pathogens involved in GCA have been performed.

The infectious hypothesis has gained importance by the demonstration that DC (DCs)—typically activated by pathogens via Toll-like receptors (TLRs)—in inflamed arteries from patients with GCA have an 'activated' phenotype. For this reason, the existence of one or more pathogens driving this immune response or autoimmunity against an unknown antigen from the own vasculature has been an important point of interest for different research groups.

Some of the pathogens considered to be responsible for this inflammatory process are Varicella *Zoster Virus*, *Herpesvirus 6*, *Parvovirus B19* or *Chlamydia Pneumoniae*. There are some articles suggesting the presence of *parvovirus B19* (*28, 29*) *Varicella Zoster* (*30*) (*31*) or *Chlamydia Pneumoniae* (*32*) in GCA artery lesions. This matter has caused a lot of controversy since other groups failed on demonstrating association between these pathogens and GCA and their presence ar mostly related to the age of the patients (*28, 33-35*).

However, emerging data suggest that different microbe sequences may be present in noninflammatory and inflammatory LVV diseases. Whether variations in vascular microbial sequences are the cause or a secondary result of vessel injury remains to be determined (*36*).

Moreover, further investigation should be done in order to clearly distinguish between detection of remaining bacteria and virus as a consequence of the age of the patients or the presence of these pathogens causing GCA disease and other vasculities.

Pathogenesis of GCA

GCA pathogenesis is not completely characterized, although there is a well accepted model based on observation of the histopathology of the disease and immunopathology studies. Nevertheless, further investigation about the molecules and mechanisms contributing to the disease is needed.

Under inflammatory conditions, leukocytes that are circulating along the vessels of the body are challenged with attached to the blood vessel wall and transmigrate to the site of inflammation in order to eliminate the primary inflammation and contributing to tissue repair.

GCA related lesions start as a crosstalk between **innate and adaptive immune response** (*37*). The innate response is initiated in the adventitia layer due to the activation of resident DC (*1, 38*) which would react against a still unknown antigens through tool like receptors (TLR) (*39-41*) in which the main leukocyte recruitment will be neutrophils or other dendritic cells (*42*). Adaptive immune response would be triggered by the activation of DC or other sentinel cell such as tissue resident macrophages that, once activated, are able to process and present antigens to CD4+T lymphocytes promoting their activation and differentiation into T helper (Th) populations Th1 or Th17 (*43-45*) that will orchestrate the adaptive response (See **Cytokines section**). The participation of antigen-specific adaptive immune responses is supported by the demonstration of oligoclonal T cell expansion in lesions (*46*). Importantly, Th1 subsets are characterized by secreting IFNγ which promote chemokine secretion and additional leukocyte recruitment contributing to the chronic inflammation ((*47*), **Additional data**). In fact, one of the most relevant functions of IFNγ is macrophage activation, granuloma formation and differentiation into giant-cells, typical findings in GCA. In contrast, Th17 populations are associated to acute response (*43*). IL-17A is a proinflammatory cytokine with pleiotropic effects on a variety of cell types including macrophages, neutrophils, endothelial cells and fibroblasts and actively contributes to inflammatory cascades. Both Th1 and Th17 lymphocytes are increased in peripheral blood from patients with GCA where a Th1-Th17 double positive cell population can be also detected (*44*) (**Figure 4**).

The persistent leukocyte recruitment by the activated EC to the pathologic artery permits to **amplify vascular pro-inflammatory cascades** leading to chronic inflammation. This is a complex mechanism in which endothelial wall may initiate the process by promoting adherence of the leukocytes plus subsequent transmigration to the tissue in which the leukocyte will follow the chemoatractant signal in order to arrive to their final destination.

The port of entry for activated leukocytes may be the adventitial capillaries (*vasa vasorum*) which in proinflammatory conditions may overexpress adhesion molecules (i.e. ICAM-1 and VCAM-1) and chemokines promoting leukocyte adhesion and transmigration (*48*) (see **Leukocyte recruitment section**) (**Figure 4**). Moreover, the important angiogenic process promoting the formation of new microvessels in the media/intima junction may contribute to the aberrant leukocyte recruitment and promote persistence of the inflammation (*49*). The infiltrating

leukocytes would constantly secrete proinflammatory cytokines (i.e. IL-1β, IL-6 and TNFαbetween others) (*2, 50*) that contribute as well to amplify the inflammatory response activating downstream pathways. Moreover, these leukocytes would subsequently migrate to the inner artery layers interacting with the different cell types of the artery wall such as VSMC which can also acquire a proinflammatory phenotype contributing to cytokine production and leukocyte recruitment by expressing adhesion molecules (**Figure 4**).

Pathological vascular remodeling developes as a response to inflammatory injury. (See **vascular remodeling mechanisms section**). Macrophages recruitment and activation also contribute to GCA tissue lesions since they are able to either amplify proinflammatory cascades in the tissue by secreting chemokine and cytokine or by damaging the tissue through different mechanism. To invade the vessel walls, leukocyte may break the basement membrane of the *vasa vasorum* and disrupt the elastic layers (EL) during progression across the artery wall. Mechanisms of injury include production of free radicals and matrix metalloproteinases (MMPs) that would promote disruption of the elastic layers and cleavage of other matrix proteins (*39*). Growth factors and profibrotic molecules (i.e. PDGF, TGFβ1) generate the development of intimal hyperplasia (*51, 52*) released either by infiltrating leukocytes or VSMC. VSMC are essential to this process since, under proinflammatory conditions, are able to change its quiescent non-proliferative phenotype into a myofibroblastic-like phenotype. As a result of this process, VSMC would be able to migrate and proliferate towards the intima layer while secreting ECM contributing to the neointima formation and vasocclusion (*39*) (**Figure 4**).
An important unresolved issue is why vascular remodeling leads dilatation in some vessels like the aorta and stenosis in some others like TA (*11*).

All the molecules involved in each of the explained processes of the pathogenesis of GCA are explained in more detail in the section **Challenges in GCA**

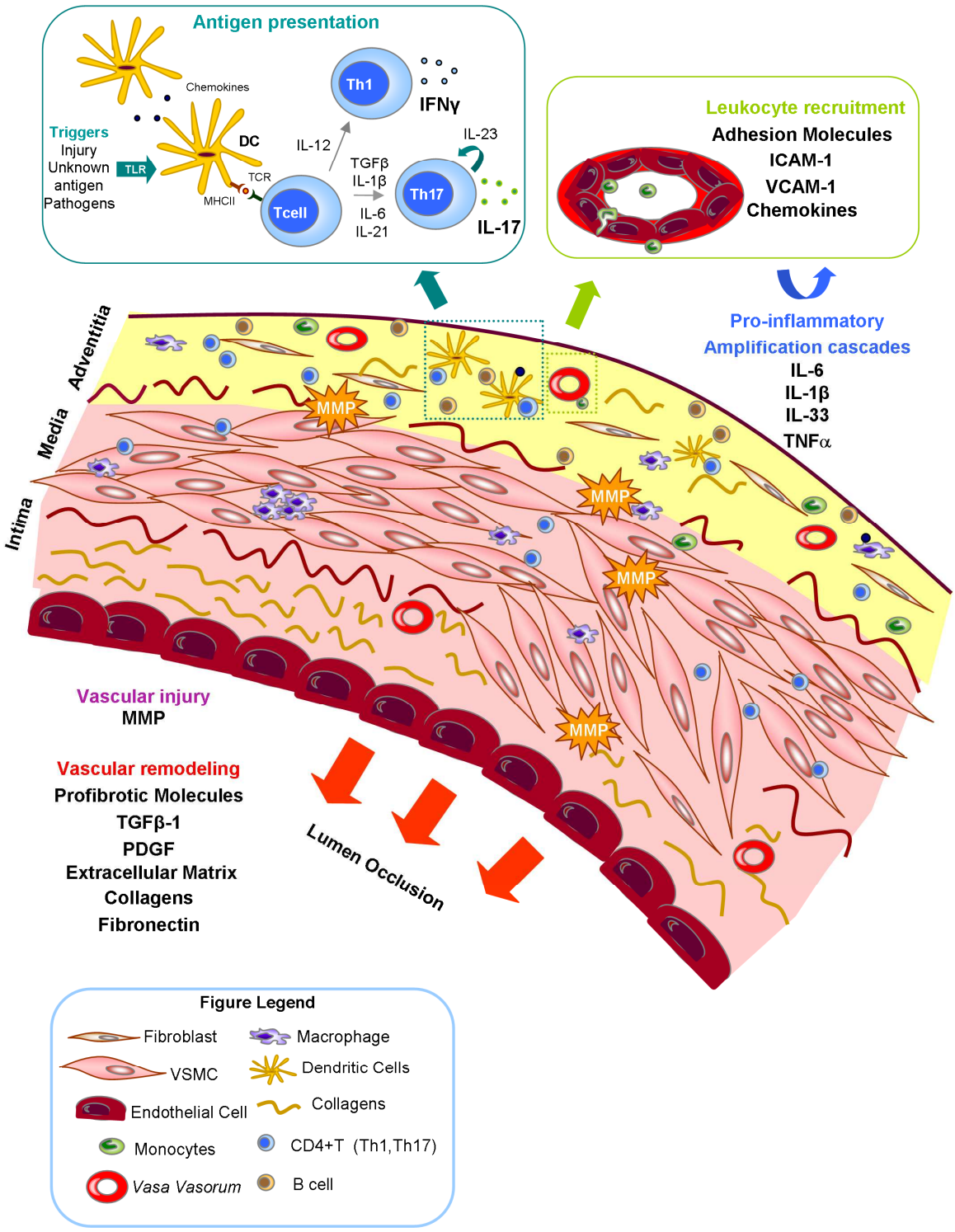

Figure4. Representation of GCA pathology. GCA requires the activation of DC from de adventitia, presentation of still unknown antigens and recognition by CD4+T lymphocytes and subsequent active cation of these and other cells such as EC. The permanent recruitment of leukocytes is facilitated by the neoformed microvessels which overexpres adhesion molecules (ICAM-1 and VCAM-1) and chemokines. T cells recruited mostly differentiate into Th1 and Th17 subsets, expressing cytokines IFNγ and IL-17 respectively. These cytokines activate and guide macrophages which would promote granuloma formation and secretion of several proinflammatory cytokines (i.e. but also IL-1β and TNFα). Infiltrating leukocytes migrate from the adventitia towards de media and intimal layer and together with the other vessel wall

components (i.e. VSMC) will respond to this immune injury by a pathological vascular remodeling. This would include production of growth factors (i.e. TGFβ and PDGF) and proteases that would degrade elastic layers and that would promote myofibroblast differentiation, proliferation, migration and production of ECM contributing to the intimal hyperplasia and vascular occlusion.

Additional mechanisms: Autoantibodies

Although B cells are not the predominant cells subsets in inflamed temporal arteries in GCA these cells are essential for T cell activation. Consistent with B cell importance in GCA, a few case report using Rituximab (a monoclonal antibody against CD20) which promotes B cell depletion) suggest that this treatment may ameliorate GCA disease activity (*53*).

Importantly, B cells may contribute to the presence of some auto-antibodies in GCA patients sera (*15*). Autoantibodies against the ferritin heavy polypeptidase (FTH1) have been detected in sera from 92% (*54*) or about 70% (*55*) patients with active GCA. Furthermore, early studies have indicated that deposits of immunoglobulins are present in inflamed temporal arteries of GCA patients (*56*). Moreover, antibodies against lamin C, human cytokeratin 15, mitochondrial cytochrome oxidase subunit II have been also found in GCA sera (*57*).

There are also some studies focusing on the search for autoantibodies against artery components like endothelial cells (AECAs) or VSMC. Although no function has been associated to these antibodies, the presence of autoantibodies against EC in systemic inflammation, autoimmune diseases and primary and secondary vasculitis (*58*) including GCA (*59*) has been reported.

A study using mice model demonstrated that serum autoantibodies directed to vascular vessel wall (primarily VSMC) were pathogenic and that the mechanisms that mediate the pathogenicity of the anti-VSMC antibodies in the animal model was mostly triggered by Tcells (*60*).

In other studies, IgGs obtained from the serum of GCA patients have been shown to react against some VSMC or EC proteins such as vinculin, lamin A/C and mitochondrial fumarate hidratase (*61*).

Nevertheless, none of these studies are conclusive enough to demonstrate a primary effect of these antibodies in GCA pathogenesis and it is likely that they are generated as a consequence of inflammation and tissue injury. In the study of Chakravarti *et a*l. (2015) (*62*) sera from 78% of patients with large-vessel vasculitis (including GCA, TAK or isolated aortitits) presented antibody reactivity against 14-3-3 proteins in aortic tissue. These proteins are ubicuously expressed in many tissues and are regulatory molecules which have the ability to bind several

signal proteins (i.e. kinases, phosphatases and transmembrane receptors). However, the role of these antibodies in LLVV is still unknown.

GCA treatment

Glucocorticoids

Glucocorticoids (GC) are the current treatment for GCA. Patients with GCA experience a rapid relief of their symptoms with high-dose glucocorticosteroids. However, disease activity may not be completely abrogated, and 40–60% of patients relapse when corticosteroids are tapered (*63, 64*).

During follow-up, GCA patients may develop vascular complications that GC are not able to prevent visual loss (15% of the patients with initial visual loss) (*65, 66*) , aortic dilatations (in 22.2%) (*9*) and extremity artery stenosis (in 5-15% of the patients) (*11*).

Although the majority of patients respond efficiently to the treatment, GC therapy does not prevent relapse in 40-60% of patients. Relapsing patients cumulate higher GC and develop more side effects. About 80% of the patients develop at least one adverse event attributable to GC after long-term follow-up. Side effects include: hypertension, miopathy, osteoporosi, glaucoma, gastrointestinal ulcer, cataracts, and increased susceptibility to infection.

For these reasons, active research is ongoing in order to identify new therapies that could replace or at least reduce GC treatment.

Other approximations to GCA treatment

Until present, the only therapy that has been partially successful as a steroid-sparing agent is **Methotrexate (MTX).** MTX is an inhibitor of folic acid with antiproliferative, antitumoral and immunosupressive properties. Besides being used for the treatment of cancers, it has also been successfully used for the treatment of other vasculities, including Wegener's granulomatosis and TAK arteritis (*67-69*).

According to the GCA pathogenesis model other approximations have been considered.

On one hand, targeting cell types participating in GCA immunopathogenesis has been considered. A clinical trial with Abatacept (recombinant Ig-CTLA-4) aimed to reduce Tcell activation is ongoing and preliminary results have shown some efficacy (*70*). B-cell depletion with **Rituximab** has provided benefit in a few case reports (*53*).

On the other hand, blocking proinflammatory cytokines expressed in GCA lesios has been tried. Although TNFα is abundantly detected in GCA lesions, studies developed in order to neutralize TNFα with **Infliximab** (chimeric monoclonal anti-TNFα) provide no evidence of benefit (*52, 71*) (*72*). Other studies trying to block TNF with **etanercept** (recombinant soluble TNF receptor) (*73*) or **adalimumab** (humanized monoclonal antibody anti-TNFα) (*74*) have also failed to demonstrate clear efficacy in GCA. Ongoing trials include blocking IL-1β using **anakinra** (recombinant IL-1RA) or **gevokizumab** (humanized monoclonal antibody anti IL-1β). Finally, IL-6 function blockade using **Tocilizumab** (humanized monoclonal antibody anti-IL-6 receptor) is being evaluated in a clinical trial called GiACTA (*75*).

Functional models

In vivo model

Research in order to amplify the knowledge about the mechanisms involved in GCA immunopathology is essential to find new therapeutic targets for the improvement of the treatment of GCA. Nevertheless several genetically modified mice develop large vessel vasculitis supporting the relevance of certain molecules (IRF, IL-1RA and IFNγ) in large-vessel inflammation (*76-78*). There are also models of small vessel vasculitis (*79, 80*) .

Ex vivo model

Some investigators of our group have developed an *ex vivo* model consisting of culturing TABs on a 3D basement membrane called Matrigel ^{TM} (*81*) (see **Material and Methods** section). This basal membrane proportionate the appropriate conditions to permit the preservation of the vascular structure and its inflammatory infiltrate up to 15 days of cultured (*82*).

Matrigel ^{TM} is a matrix derived from a tumor extract which contains several biological active components from the cellular basement membranes such as laminin, Type IV collagen, MMPs, profibrotic factors and growth factors. Basement membranes are thin sheets that separate the epithelium or endothelium from the stroma, and surrounding nerves, muscle fibers, smooth muscle cells and fat cells (*83*). Matrigel, is developed after a meticulous process from the EHS mouse tumor basement membrane in order to obtain an sterile matrix which becomes gel at 37ºC and is able to support the culture of several tissues and cell types (*81, 83, 84*). While 2-Dimentional (2D) cell culture on plastic substrate usually promote cellular proliferation but

inhibits their differentiation, 3-Dimentional (3D) cultures are more physiological models. Matrigel™ is used for various studies including cell differentiation, angiogenesis, tumor growth, tissue engineering and tissue conservation (*84*).

This TAB *ex vivo* model improves the NOD-SCID mice (a mice model which is extremely immunosuppressed). This consists on a xenotransplant model in which GCA-proven TABs or control specimens are engrafted subcutaneously into NOD-SCID mice allowing the structure preservation (*85*).

Either TAB cultured on Matrigel™ or NOD-SCID mice have been used in order to generate more information about the effects of GC on proinflammatory molecules involved in GCA.

In the following sections of this doctoral thesis various aspects related to the immunopathogenesis of GCA are extensively detailed in order to better understand the context of the generated results and their relevance: **leukocyte recruitment** into the inflamed arteries, proinflammatory molecules involved in the amplification of the inflammatory cascades promoting **persistence of the inflammation** and molecules involved in **vascular remodeling** as a response to persistent inflammation.

2.3 Mechanisms and molecules involved in vascular inflammation

Leukocyte recruitment steps

Leukocyte recruitment is developed by interactions between leukocyte and EC in the focus of inflammation. This process, which is driven by the combination of adhesion molecules, chemokines and integrins occurs through different steps including: tethering, rolling, adhesion strengthening and spreading and transmigration to the injury site (**Figure 5**). **Tethering** is the first step in which leukocyte weakly attached to the EC. **Rolling** is the process through which leukocytes transiently adhere to the selectins expressed by endothelium through carbohydrate ligands. While rolling, leukocytes respond to chemokines that active the leukocyte integrins. Integrins bind to endothelial adhesion molecules from the immunoglobulin superfamily which are up-regulated by inflammatory cytokines and this interacton promotes **adhesion and spreading.** Chemokines are also important for promoting the migration and polarization of the leukocyte to the injury site (*86*). At this point, leukocytes can either **transmigrate** through the endothelium junctions (paracellular migration) or through the body of the endothelium (transcellular migration) (*87*). This is just the first barrier because they also have to penetrate through endothelial-cell basement membrane and perycites. Interestingly, transmigration is a complex step which includes signaling through ICAM-1 on EC which promotes cytoskeleton changes through activation of p38 MAPK, increasing intracellular Ca^{2+} and activation of Ras homologue RHO (GTPase) leading to enhanced endothelial cell contraction and loosing cell-cell junctions such as VE-cadherin interactions (*87*). In this final step of leuckocyte recruitment, the molecules involved are immunoglobulin superfamily members such as platelet/EC adhesion molecule (PECAM-1), intercellular adhesion molecule 1 or 2 (ICAM-1 or ICAM-2), junctional adhesion molecules (JAMs), endothelial cell-selective adhesion molecules (ESAM), CD99 and their leukocyte ligands (*88, 89*).

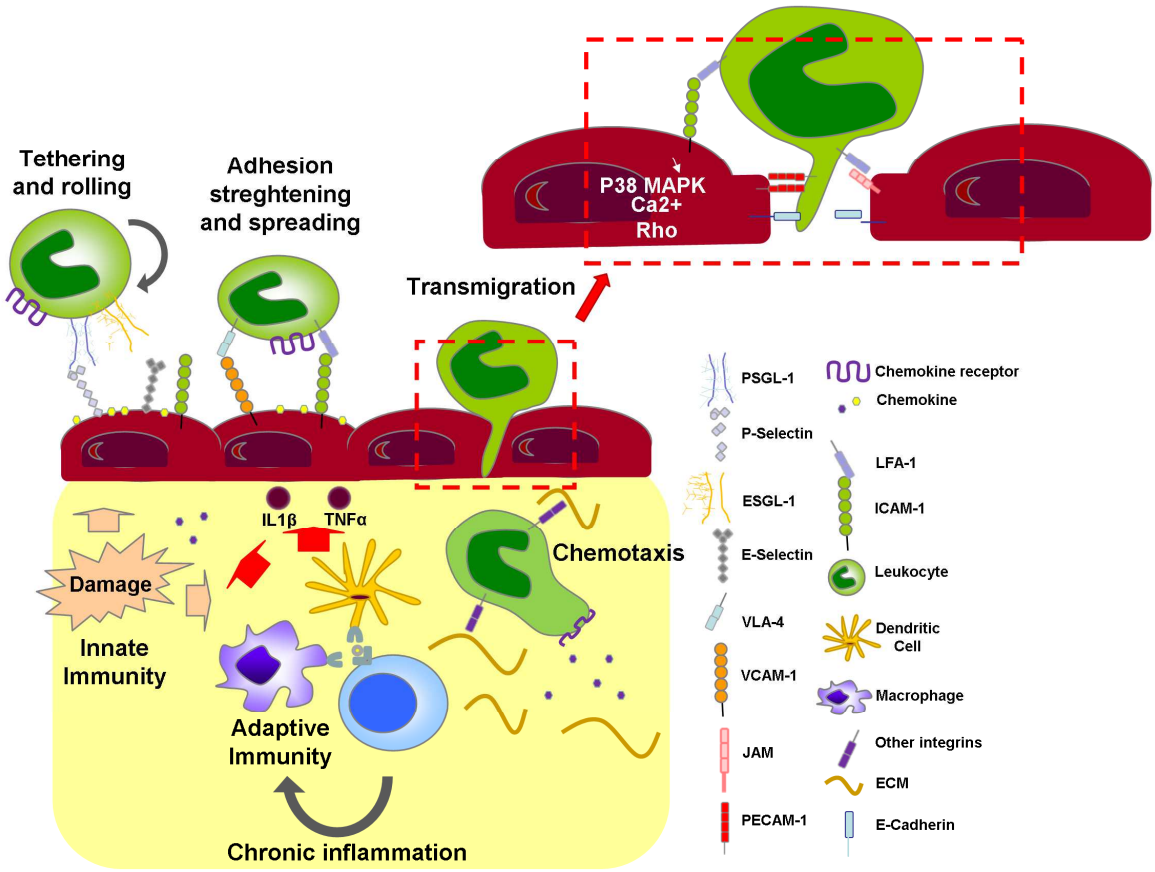

Figure5. Leukocyte recruitment by activated endothelium of *vasa vasorum* or neovessels in inflamed arteries. After antigen recognition by resident DC or macrophages, activated EC leads the overexpression of adhesion molecules allowing leukocyte recruitment and transmigration. Leukocyte recruitment is achieved by different steps (tethering and rolling, adhesion strengthening and spreading and transmigration to the injury site). In each step different molecules are involved. Chemokines are also secreted by the activated endothelium guiding the leukocytes to migrate towards the injury site. When activation signals do not decrease, inflammation becomes chronic. Adapted from Nourshargh *et al.* (2014) (*90*).

Molecules involved in leukocyte recruitment

Selectins

The first stages of leukocyte recruitment are promoted by overexpression of adhesion molecules called **selectins** by the EC. These proteins bind to their ligands with low affinity (attachment and detachment of individual bonds) and allo leukocyte rolling along the vessel wall (*91*).

EC activation can be driven in a rapid and protein-synthesis-independent manner (with minutes) usually induced by proinflammatory signal (i.e. histamine and its GPCRs receptor in EC) or

more slowly (within hours) involving transcriptional induction of molecules involved in leukocyte trafficking. This slow activation is usually driven by cytokines such as IL-1β, TNFα (*92*).

Selectins can be classified according to the cell type expressing them. **P-selectin** is expressed by EC and platelets while **E- selectin** is only expressed by EC. **L-selectins** are expressed by different leukocytes. P-selectins are important because they are already synthesized and stored into *Weibel-Palade* bodies and under some stimuli; they are translocated to the cell membrane. In contrast, E-selectin overexpression is *de novo* in response to inflammatory stimuli. Although both selectin types are important for leukocyte recruitment, they have different functions. While P-selectins are the first adhesion molecules promoting leukocyte attachment to the endothelial wall, E-selectins (expressed several hours later) permit persistence of the cell recruitment (*90, 93*).

Selectin ligands are expressed by leukocytes and include P-selectin glycoprotein 1 (PSGL-1) as a ligand for P-selectin and E-selectin ligand 1 (ESGL-1) and glycosilated CD44 as a ligand for E-selectin.

Integrins

Integrins are a family of transmembrane receptors that act in a bidirectional (inside-out and inside-in) signaling to integrate the extracellular and intracellular environment using cell-cell and ECM interaction (*94*). Integrins are also important for the rolling and firm leukocyte adhesion step. The most important integrins related to leukocyte attachment to endothelium are from the β1 and β2-integrin subfamilies. These integrins attach to the immunoglobulin superfamily members ICAM-1 or VCAM-1 (vascular cell adhesion molecule 1). Leukocyte, mostly activated monocyte and T cells express very late antigen 4 (VLA-4 or α4β1 integrin) which is the ligand for VCAM-1 (*95, 96*) whereas lymphocyte function-associated antigen 1 (LFA1 or αLβ2) which is expressed by T cells, macrophages, B cells and neutrophils is the ligand for ICAM-1 (*94*).

In the leukocyte arrest to endothelial cells, integrins (which are usually in a non- activated conformation) react to an inside-out stimulatory signal which induces a medium or high-affinity conformation which opening the ligand-binding pocket. This signal is usually triggered by **chemokines** which will activate G-protein-coupled receptors (GPCR) during the rolling process, at the same time, intracellular cell signaling that induces changes in the cytoskeleton (*97, 98*).

In the migration process, integrins are also important (see **Molecules involved in cell migration** section) because after transmigration through the EC, leukocytes are required to migrate through the perycite layer and basement membrane and interact with ECM in order to arrive to the inflamed tissue.

Transmigration not only allows leukocyte arrival to inflamed tissues but also functional changes in transmigrated leukocytes which exhibit enhanced survival and increased effector functions (i.e. greater ability to invade and to kill) (*99-101*) .

Adhesion molecules: ICAM-1 and VCAM-1

As mentioned, ICAM-1 and VCAM-1 belong to the immunoglobulin gene superfamily. Intracellular adhesion molecule 1 (**ICAM-1** also named CD54) is a protein of 90KDa which consist of 5 immunoglobulin-like domains, a transmembrane region and a cytoplasmic tail. It binds to β2 integrins (LFA-1 and MAC-1) expressed by leukocytes by promoting their recruitment (*102, 103*).

ICAM-1 is constituveley expressed by EC although it can be induced by cytokines such as IL-1β, TNFα or IFNγ (*104, 105*) in these cells. Nevertheless, ICAM-1 can also be expressed by other cell types such as macrophages and VSMC (*106*).

Vascular cell adhesion molecule-1 (**VCAM-1 or CD106)** is a cell surface glycoprotein expressed by cytokine-activated-endohtelium which mediates the adhesion and signal transduction of monocytes and lymphocytes through its activated ligand VLA-4 (β1 integrin).

Either ICAM-1 or VCAM-1 are important in both immune recognition and in leukocyte migration to sites of inflammation.

Chemokines

Chemokines are low molecular weight (7-15KDa) members of the cytokine family of regulatory proteins which stimulate polarization and chemotaxis of leukocytes (*107*). Chemokines induce directional movement of the cell expressing the corresponding chemokine receptor creating a chemical ligand gradient. This allows cells to move towards high local concentration of chemokines (*107*) (*108*). Importantly one chemokine can interact with more than one receptor and, at the same time, one specific receptor can interact with more than one chemokine (*109*) .

Chemokine molecular signature includes four conserved cystein residues that form 2 disulfide bonds pairing first and third cystein and second and fourth cystein. Depending on the first and

second cystein distribution from the N-terminal, they are classified in four families as following described (*110*):

CXC. There is another aminoacid betweed the first and second cystein

CC. The first and second cysteins are adjacent

CX3C. There are three different aminoacid between the first and second cysteins

(X)C. The first and the third cysteins are missing

In addition to their primary structure, chemokines can also be classified according to their function as inflammatory, angiogenic or homeostatic.

Inflammatory chemokines are those involved in the recruitment of leukocytes to inflamed tissues while the homeostatic chemokines are constitutively expressed and are involved in the physiological homing of lymphocytes to the lymphoid tissue (*111*) (**Table 1**).

In this thesis, we will focus on the inflammatory and angiogenic ones which are classified in the following table according to their receptors and the main producing cell types.

Human Chemokines			
Chemokine	**Other name**	**Receptor**	**Function**
CXC subfamily			
CXCL8	IL-8	CXCR1,CXCR2	(I,ANG) Neutrophils, basophils, Tcell recruitment
CXCL9	MIG	CXCR3	(I)Lymphocyte chemoattractant. Induced by IFNγ
CXCL10	IP-10	CXCR3	(I)Monocyte, NK and Tcell chemoattractant. Adhesion molecules modulation. Induced by IFNγ. Cleaved by MMP9
CXCL11	I-TAC	CXCR3,CXCR7	(I)Activated Tcell, neutrophils and monocytes recruitment.Induced by IFNγ. Cleaved by MMP8
CXCL12	SDF-1	CXCR4,CXCR7	(I,H,ANG)Activated Tcell, monocyte migration but inhibition of monocyte adhesion to ICAM
CC subfamily			
CCL2	MCP-1	CCR2	(I) Monocyte, basophil, memory Tcell, DC chemoattractant. Essential for granuloma formation.Induced by PDGF and activated by MMP12

Table1. Relevant chemokines involved in inflammation (I) and angiogenesis (ANG) or homeostatis (H).

VSMC and pericyte in leukocyte recruitment

Capillary mural cells consist of pericytes whereas artery mural cells are VSMC. Pericytes are irregularly located in the basement membrane (intima layer) interacting with EC. In contrast, VSMC are oriented circumferentially around the artery and separated from the basement membrane through the elastic membrane and are located in the media layer. VSMC are important on regulating vascular tone. Nevertheless, both mural cells may play a role in the recruitment of leukocytes. Although VSMC in normal conditions are not in contact to leukocytes, in vasculitis such as GCA the disruption of the elastic layers may generate cell-cell contact between the infiltrating leukocytes and VSMC which lose their orientation.

Leukocyte that have already transmigrated through EC, must cross the pericyte sheath and the venular basement membrane (BM) in order to arrive to the focus of inflammation (*112*). Pericytes are crucial for vascular development and function but also for immune response as they can express adhesion molecules (i.e. ICAM-1 and VCAM-1), chemokines, cytokines and proinflammatory cytokine receptors (*100*) (*113*).

Interaction of pericytes (ICAM-1) and leukocytes (LFA-1 or MAC-1) seems to be important on instructing infiltrating leukocytes for optimized navigation and effector response to the sites of inflammation. Nevertheless, more investigation is needed to better understand the consequences of pericyte-leukocyte interactions (*90*)**.**

ICAM-1 and VCAM-1 are also expressed by VSMC from atherosclerotic lesions. This induction may contribute to the inflammatory reaction and with the progression and stability of atherosclerotic plaques (*106*). In GCA where leukocytes interact with VSMC, ICAM-1 and VCAM-1 are also expressed by this cell type. The cytokines that induce the adhesion molecules in VSMC are IL-1β and TNFα. Recently studies have also demonstrated that IFNγ stimulates VSMC expression of ICAM-1 and some chemokines such as CXCL9, CXCL10, CXCL11 and CCL2 suggesting that VSMC may play a role in amplifying inflammation in GCA by recruiting and binding to infiltrating leukocytes ((*47*), **Additional data**).

In this thesis, a co-culture model of VSMC with leukocytes (or distinct subsets) has been used in order to better characterized bi-directional interactions since it seems to be a key point in the persistence of inflammation in GCA.

Cytokines

Cytokines encompases an heterogeneous group of pleiotropic molecules (proteins or peptides) which act as key intercellular communicators by interacting with specific receptors. They can be involved in biologic activities and differentiation of leukocytes and other cell types (lymphokines or monokines) and chemotaxis (chemokines). At the same time, cytokines can be divided into functional classes: **lymphocyte growth factors**, **proinflammatory** and **anti-inflammatory** molecules. Some cytokines need to be cleaved by converting enzymes, caspases or MMPs family to be activated (*114*). Cytokine response is regulated and maintained by a balance which in chronic inflammation, is disrupted. Cytokines that participate in acute inflammation in response to aggression (i.e. virus, bacteria) can also participate in chronic disease (i.e. autoimmune disease or transplant rejection).

Cytokines involved in CD4+T differentiation

Efficient host defense against invading pathogenic microorganisms is achieved through coordination of complex signaling networks that link the innate and adaptive immune systems. Antigen presenting cells (APC) including DC interact with CD4+T cells which differentiate into effector T cells: Th1, Th2, Th17, T follicular helper (Tfh) and induced regulatory T cells (iTregs) (**Figure 6**). This differentiation may be triggered by cytokines but also by the T cell-antigen presenting cell interaction (*115*). Th1 differentiation is triggered by IL-12 and these cells are IFN_{γ} producers through TXB21 transcription factor (TF). In contrast, Th2 cells are differentiate in response to IL-2 and produce IL-4, IL-5 and IL-13 through the activation of the TF GATA-3 (*116, 117*).

Th1 cells are mostly involved in the defense against intracellular pathogens and in granuloma formation whereas Th2 are involved in the production of immunoglobulin E (IgE) which is important in allergic processes and in eosinophils activation (*116*).

Besides Th1 and Th2 subsets, Th17 differentiation occurs in response to the master regulator RORc and is characterized by the production of IL-17, IL-21 and IL-22. For Th17 differentiation, TGFβ, IL-6, IL-1β and IL-21 are required. IL-23 it is also an important cytokine because it promotes Th17 expansion (*118, 119*). This subset is involved in inflammation and autoimmunity.Th1 and Th17 cells have essential roles in organ-specific autoimmunity (*120*).

Follicular B helper T cells (Tfh) are also important Th subsets. These cells regulate the maturation of B cells and are differentiating as a response to IL-21 through the TF BCL-6 (*121, 122*).

Moreover, recent investigation has characterized new CD4+T cell population such as Th21 and Th9. It is important to consider that there is plasticity among these cells and a differentiated subtype can differentiate into another one.

T regulatory cells (Treg) are important in limiting tissue damage (*120*). Treg have the role of maintenaining immune homeostasis by limiting Teff responses and preventing autoimmunity mostly by inhibiting Th1 and Th2 cytokine production (*123*).

These cells are regulated by forkhead transcription factor 3 (FOXP3) and can be classified into: natural Treg (nTreg/ CD4+CD25+) which are generated in the thymus or iTreg (induced T reg) which mostly differentiate as a response to TGFβ (*124, 125*). iTReg 35 have also been characterized as Treg that are differentiated through the IL-35, a cytokine from the IL-12 heterodimeric family of cytokines (*126*).

Cytokines involved in macrophage differentiation

Macrophages are mononuclear cells that play a critical role even in both innate and adapative immunity. Macrophages derive from monocyte activation by their recruitment through endothelium into inflamed tissue.

Macrophages form granulomas which are commonly found in some chronic diseases (*127*). Moreover, macrophages trigger recruitment of other cell types such as lymphocytes by secreting cytokines and chemokines.

Macrophages can also be polarized into different classes (M1 or M2) similar to T lymphochytes (**Figure 6**). M1 macrophage polarization is triggered by Th1 cytokines such as IFNγ or by LPS. This macrophage subtype is characterized by its ability to produce amount of proinflammatory cytokines such as IL-12, IL-1β, IL-23, TNFα (among others), high expression of MHCII, reactive

oxygen and nitrogen species and chemokines such as CXCL9 and CXCL10. M1, then are involved in Th1 recruitment and response and tissue-disruptive reaction (*128-130*).

In contrast, M2 macrophages are differentiated in response to Th2 cytokines such as IL-4 and IL-13 (*131*). M2 highly express IL1RA (IL-1 receptor antagonist) and the anti-inflammatory cytokine IL-10. M2 also secret chemokines (i.e. CCL17, CCL22 and CCL24) which receptors are mostly expressed by Treg and Th2 cells. In general, then, M2 are predominantly involved in immunoregulation, tissue remodeling , angiogenesis and Th2 response (*130*).

In GCA, the inflammatory infiltrate is mostly composed by CD4+T helper cells (Th1 and Th17) and macrophages (*1*). Since granuloma formation is a characteristic of the disease, and the proinflammatory cytokines expressed are Th1 related, it is likely that M1 macrophages may play an important role in the pathogenesis of GCA (*2, 3*). Nevertheless, there is an important angiogenic and tissue remodeling process in the disease in which M2 macrophages may also be involved.

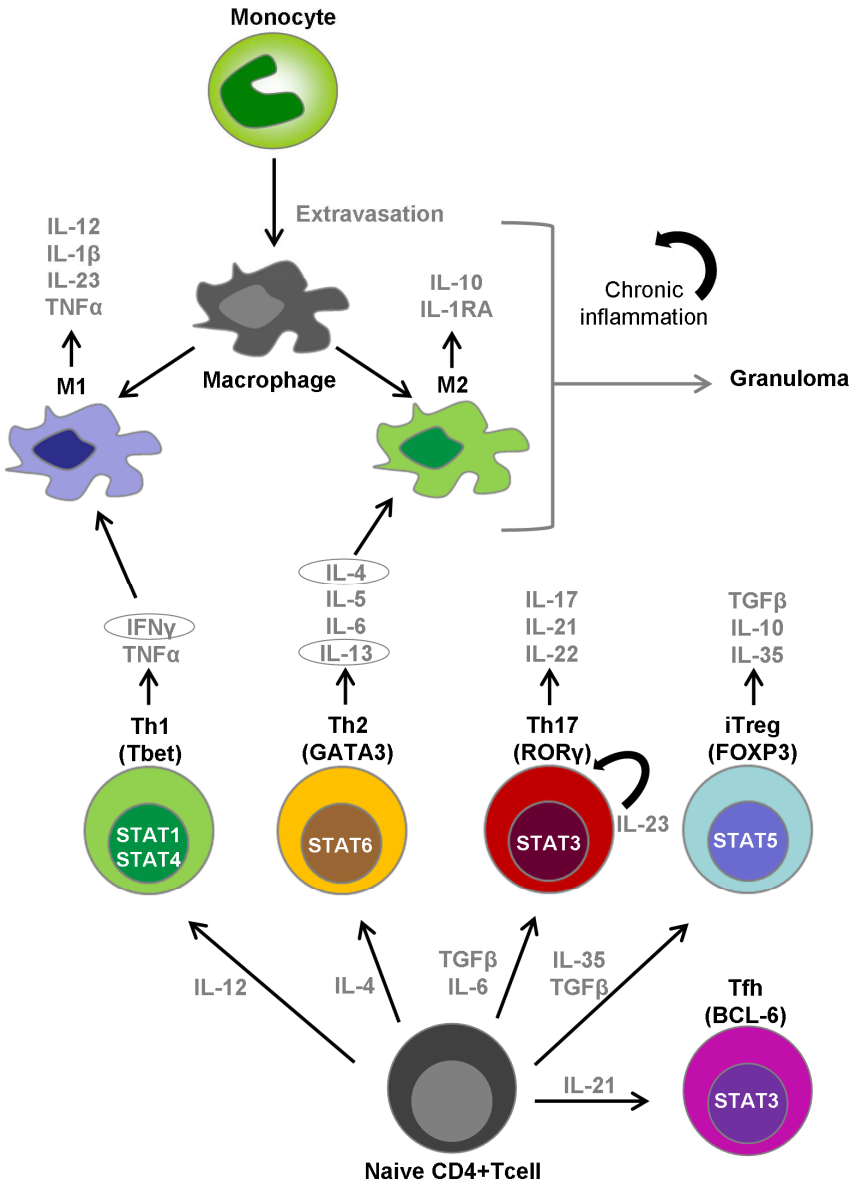

Figure6. Cytokines and transcription factors involved in CD4+T and macrophage differentiation. After interaction with APC naïve CD4+T cell can be differentiatied into different T helper (Th) subsets as represented. Each subset is triggered through a combination of different proinflammatory cytokines which would promote activation of different genes through specific transcriptor factors. Th cells are also involved in macrophage differentiation in M1 or M2 subsets. Accumulation of macrophages would form granuloma as a reponse to chronic inflammation. Adapted from Cid MC *et al.*, (2012) (*114*).

JAK/STAT signaling

As explained, cytokines trigger a variety of cell responses. Many cytokines signal through Janus kinases (JAK) and the STAT (signal transducer and activation of transcription) family of transcription factors is the remarkable pathway for membrane to nucleus signaling (*132*). Intracellular signaling occurs when a cytokine binds to its receptor (which probably will promote

its subunit multimerization). For JAK/STAT signaling the cytoplasmic domain of the receptor must associate to JAK tyrosine kinases (*133*) (**Figure 7**).

The JAK family is composed by JAK1, JAK2, JAK3 and Tyk2. For JAK activation, two JAK molecules need to be in close proximity, allowing trans-phosphorylation. Once it is activated, JAK also activates the receptors and other targets such as STATs, promoting their phosphorylation (*133*). STAT family is composed by 7 members of proteins of 750-850 amino acids (aa): STAT1, STAT2, STAT3, STAT4, STAT5a, STAT5b and STAT6. STATs are latent transcription factors that reside in the cytoplasm until activated. All the STATs contain aminoterminal, coiled-coil, SH2, DNA binding and transcriptional domains. SH2 is essential for STAT activation and function since STATs are phosphorylated by JAKs on a conserved tyrosine residue located in the SH2 domains. This allows dimerization with other STATs which can be homodimers or heterodimers depending on the stimuli and receptor activation.

Both STAT homodimers and heterodimers are translocated to the nucleus in a mechanism depending on importin α-5 (nucleoprotein interactor 1) and the Ran nuclear export pathway (*134*) . Once in the nucleus, dimerized STAT bind to specific regulatory DNA sequences to active or repress transcription of target genes (*133*) (**Figure 7**).

In addition to JAK/STAT there are also negative regulators of cytokine pathways. The most explored ones are the SOCS (suppressor of cytokine signaling proteins). SOCS family is composed by 8 members (SOCS1-SOCS7 and CIS). These molecules conform a negative feedback response where translocated STATs may activate SOCS gene transcription and its resulting protein may interact with phosphorylated JAK or receptors turning off the pathway (*135*).

Transcripts encoding SOCS1, SOCS2, SOCS3 and CIS are often present in cells at low or undetectable levels but are induced by several cytokines such as IFNγ, IL-6, IL-4, IL-2 or GM-CSF. Bioinformatics has revealed that CIS presents putative DNA binding sites for STAT5 in its promoter, while SOCS1 seems to have STAT1, STAT3 and STAT6 binding sites. Interestingly, SOCS3 is mainly transcribed as a response to STAT1 and STAT3 activation (*135*).

Among other important biological processes, JAK/STAT pathway plays an essential role in naïve CD4+T cell differentiation into T helper (*136*) (**Figure 6**).

STAT1 seems to be necessary for the Th1 differentiation and maintenance since IFNγ induce the expression of the TF TXB21 in a forward feedback mechanism enhancing Tcell procuction of more IFNγ. Th1 differentiation is also triggered by **STAT4** activation as a response to IL-12. STAT4 is essential for expressing IL12R and IL-18R in Th1 cells. STAT4 deficient mice are resistant to autoimmune disease characterized by Th1 response (i.e. mice model for rheumatoid arthritis or diabetes).

STAT3 is activated by IL-6, IL-21 and IL-23 which are cytokines involved in Th17 differentiation and manteinance. Accordingly, STAT3 specific deletion on T cells abrogates Th17 differentiation (*136*).

STAT5 is also related to T plasticity. The induced Treg cells may be differentiate as a response of cytokines such as TGFβ (*126*) and the main important master regulator seems to be FOXP3. Moreover, STAT5 activation seems to be important in this iTreg differentiation.

STAT6 is mainly activated by IL-4 and IL-13 which is also critical for Th2 differentiation. STAT6 regulates the expression of the TF GATA-3 (*132*).

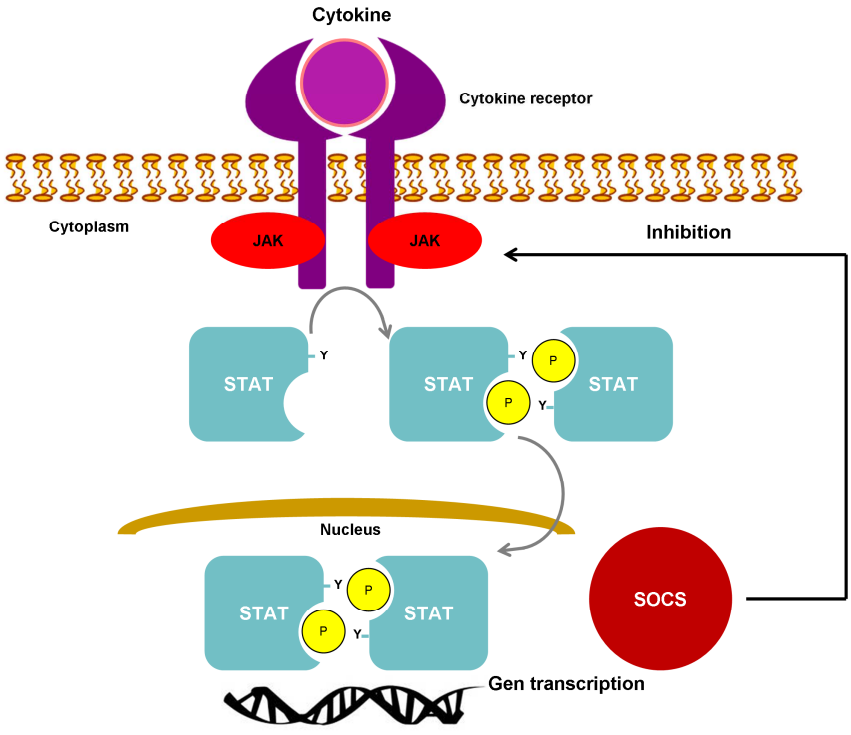

Figure7. JAK/STAT activation and STAT nuclear is representated. After cytokine stimulation JAK is phosphorylated and activated with subsequent STAT activation, dimerization and nuclear transloclation. Once in the nucleus, STAT homodimers promote transcription of various proinflammatory related gens including SOCS which inhibits JAK activation preventing STAT activation. Adapted from Shuai *et al*. (2013) (*137*) and Krebs D. *et al*. (2001) (*135*).

The IL-12 superfamily of cytokines

Introduction

Type I cytokines are composed by the IL-6 and IL-12 superfamilies. These groups of cytokines are characterized by presenting a four helix structure. Whereas IL-6 cytokines are secreted as homodimers, IL-12 cytokines are secreted as heterodimers (*138*). IL-12 superfamily of cytokines is associated with the regulation of innate and adaptive immune responses, operating in bacterial and parasitic infections as well as in autoimmune diseases (*139, 140*) .

IL-12 superfamily is composed by IL-12 (p35+p40), IL-23 (p40+p19), IL-35 (Ebi3+p35) and IL-27 (p28+Ebi3) (*140*) **(Figure 8)**.

The subunits that compose the IL-12 superfamily of cytokines are classified as α subunits (p19, p28 and p35) and β subunits (Ebi3 and p40) depending on their structural homology. The IL-12 family α subunits are characterized by a unique up-up-down-down four helix bundle conformation which is structurally homologous to IL-6 cytokine family that signals through gp130. In contrast, IL-12 family β subunits maintain homology with the extracellular domain of receptors of the IL-6 family (i.e. IL-6R) which contain a conserved amino-terminal immunoglobulin (Ig) domain and two tandem fibronectin type III (FNIII) domains responsible for cytokine binding. Interestingly, Ebi3 lacks of the Ig domain (*140, 141*). In fact, since the α subunits can pair with the β subunits it could be possible to find new molecules composed by Ebi3 and p19 or p40 and p28.

Both p35 and p19 have sequence homology to IL-6 and granulocyte colony-stimulating factor (G-CSF) which allows their inclusion into the gp130 class of long-chain cytokines (*142*).

The structure of these heterodimeric cytokines is complex, while IL-12 and IL-23 contain disulfide-linked bounds between p40 and the helical p35 or p19 respectively and are efficiently secreted, IL-27 and IL-35 subunits are linked trough non-covalent unions and, consequently, are secreted in much lower amounts (*140, 142, 143*). This raises the possibility that in cells that express multiple chains of the IL-12 cytokine family, such as activated DC, macrophages or B cells, the chains may compete for pairing and secretion.

In addition to their canonical function as heterodimers, some components of the IL-12 family can **function autonomously as monomers or homodimers**. Importantly, p40 subunits have independent function of p19 or p35 and can be secreted as a homodimers (p40+p40) or monomers (p40) (*94, 142*). In fact, p40 homodimers are shown to promote a negative IL-12

feedback loop by competitively binding to IL-12 receptor chain IL-12Rβ1. However p40 acts as a chemoattractant for macrophages (*94*) and promotes the migration of activated DC and the production of IFNγ by CD8+T cells (*144*). Interestingly, no independent secretion of p35 and p19 has been described yet. Moreover, some studies have shown that p40 seems to be necessary for the secretion of either p35 or p19 in order to form mature IL-12 and IL-23 respectively (*145, 146*).

Similar to p40, IL-27 subunit p28, can also be secreted independently of Ebi3. The IL-27 subunit p28 has been found in supernatant of cultured macrophages and DC from $Ebi3^{-/-}$ mice after the stimulation with LPS and IFNγ (*147*). Previous studies reported that overexpression of IL-27p28 by established cell lines leads to its secretion independently of Ebi3 (*148*) .

The p28 subunit can act as an antagonist of gp130 receptor. This subunit abrogates either IL-6 or IL-27 function. Regarding to IL-6, p28 inhibits IL-6-STAT3 activation, Th17 differentiation and IL-10 production but also IL-6 promoting germinal center formation (*147*). For this reason, it has been considered as a potential therapeutic tool.

There is still no evidence that p19 or p35 have functions or are secreted independently of p40. Recent studies by our group (see **Results section, part 1**) have demonstrated for the first time that p19 is independently induced in EC under proinflammatory conditions althought it is not secreted. This subunit can promote leukocyte recruitment by inducing endothelial adhesion molecules through intracellular gp130 receptor and STAT3 activation.

Receptors and signaling

The IL-12 superfamily cytokines trigger different response in spite of being constituted by a combination of the same subunits. Interchange of cytokine subunits is extended to their receptors which are also composed by combinations of shared chains.

The combination of signaling pathways might determine different cytokine functions. The receptor of IL-12 was first described by Chua *et al.* in 1994 (*149, 150*). It is an heterodimer composed by IL-12Rβ1 and IL-12Rβ2 whereas the receptor of IL-23 is composed by IL-23R and the shared IL-12Rβ1 (*151, 152*). IL-27 triggers its signal through the receptor composed by IL-27R (WSX1) which associates to gp130 (*153*). Importantly, the receptor of IL-35 is unconventional since it seems to be a combination of homodimers or heterodimers of IL-12Rβ2 and gp130 in T cells and heterodimer of IL-27R and IL-12Rβ2 in B cells (*154, 155*) **(Figure 8).**

As these receptor chains are expressed as monomers in the cell surface and form dimers after specific cytokine binding, it remains unclear which determines dimer formation in a context exposed to multiple cytokines from IL-12 superfamily. This is a field that still remains unknown and need to be further explored to better understand the mechanisms through which similar cytokines trigger quite different responses.

Signaling of these cytokines is also mediated by members of the JAK/STAT family. Although IL-12Rβ2 and IL-23R have long cytoplasm tails and mediate intracellular signaling, the IL-12Rβ1 cytoplasm tail is short and does not contain tyrosine residues (*150*). In addition, IL-12Rβ1 activates Tyk2 whereas both IL-23R and IL-12Rβ2 activate JAK2 (*92*).

IL-12 mediates signaling through dimers of STAT4 which are previously activated by JAK2/TyK2 (*156*), in contrast, IL-23 drives its signaling through heterodimers of STAT3 and STAT4 through the activation of JAK2/Tyk2 (*151, 152*). IL-27 drives it signaling through STAT3 and STAT1 (*157*) after activation of JAK1 and JAK2 and IL-35 uses a unique heterodimer of STAT4 and STAT1 after activation of JAK1/JAK2 to trigger its signal in T lymphocytes (*154*) or STAT1/STAT3 in B cells (*155*) (**Figure 8**).

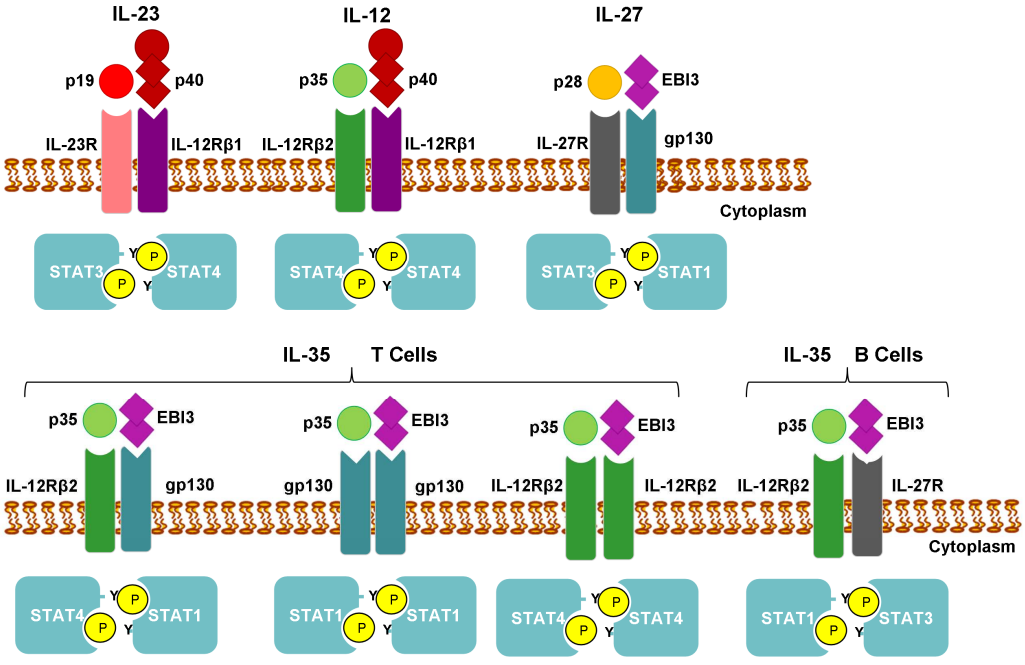

Figure8. Representation of IL-12 superfamily of heterodimeric cytokines and their receptors. JAK/STAT signaling pathways activated by each cytokine are also displayed. Adapted from Vignali D. *et al.*, (2012) (*140*) and Egwuagu C. *et al*., 2015 (*158*)

IL-12 (p40+p35)

IL-12 was firstly identified and purified from supernatants of Epstein-Barr virus (EBV) transformed lymphoblastoids cells (*159, 160*).

IL-12 is a proinflammatory cytokine produced by monocytes, macrophages and other antigen presenting cells (APC) including B cells and DC as a response to microbial pathogens and has a key role in the development of cell-mediated immunity *(139).* The major functions of IL-12 are the induction of IFNγ production from natural killer (NK) and T cells which, at the same time, promotes IL-12 production in a positive feedback manner (*139*). Importantly, IL-12 is also essential for the differentiation of naive T cells into Th1 cells and for enhancing cytotoxicity of NK cells (*139*) (**Figure 6**). Importantly, activated T cells induce IL-12 production by monocytes and DCs via CD40–CD40L ligand interaction.

Although IL-12 is important to host defense, overexpression of IL-12 can cause persistent inflammation leading to autoimmune diseases. For this reason IL-12 regulatory mechanisms are important to be explored. While IL-12 is upregulated by several TLR such as TLR-4, -5 and -9 it is downregulated by cytokines produced by Th2 differentiated cells such as IL-10 as a consequence of the decreased of NFκB and AP-1 activation (*161*) or TGFβ (*162*).

Mice deficient of either p35 or p40 exhibit reduced IFNγ secretion, impaired Th1 development, enhanced Th2 development, and increased NK cell lytic activity (*163*).

IL-23 (p19+p40)

IL-23 was firstly described by Oppman B. *et al.* (2000) (*152*). It is secreted by either activated mouse or human DCs. Oppman reported a new subunit, named p19, which shared about 40% of homology with p35 subunit of IL-12. p19 seemed to lack functional activity by itself, but in combination with p40 conformed the cytokine IL-23 (this part will be extensiveley commented in the **part one of the Results section**).

The subunit p19 was firstly identified by searching sequence databases with a computationally generated profile of IL-6 subfamily structures. This subunit presents a molecular weight of 18,7 KDa in humans. Although the presence of signal peptide in p19 structure suggested its secretion, Oppman *et al.* were only able to find little but biologically unfunctional p19 secretion by mouse p19 but not by human p19 transfected 293Tcells. The subunit p19 subunit was only secreted when cells were co-transfected with the p40 subunit. Co-transfection with other IL-6

related molecules such as Ebi3, soluble IL-6R and cytokine-like factor 1 (CFL1) was also assessed (*152*) (**Figure 9**). Moreover p19 but not p40 is induced by TNFα in mouse endothelial cells (*152*) suggesting and independent function in this cell type different than only form IL-23.

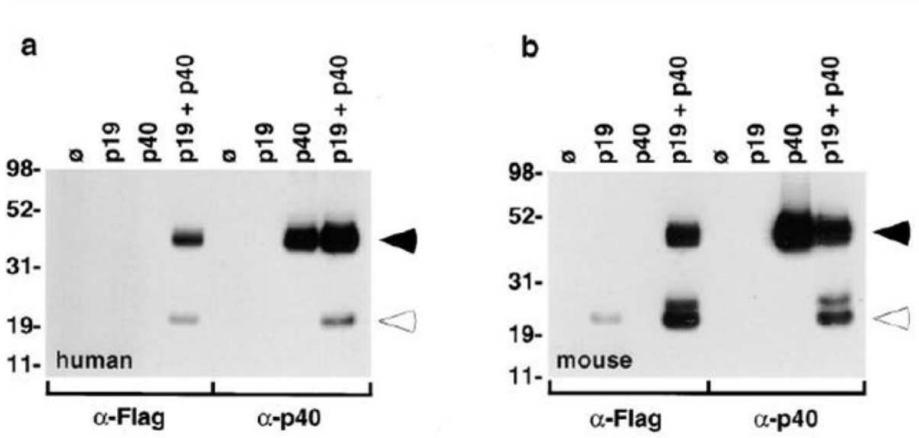

Figure9. Human and mouse IL-12p40 and p19 expression and secretion by transfected 293T cells. Each lane represents transfected 293T with empty vector (lanes 1 and 5) or expression vectors for p19-Flag (lanes 2 and 6), IL-12 p40 (lanes 3 and 7) or both (lanes 4 and 8). Either anti-Flag or anti-p40 antibodies were used to precipitate transfected cell supernates. Anti-p19 (white arrow) and p40 (black arrow) antibodies were used to detect both subunits. (A) Immunoprecipitation of human cell supernates. (B) Immunoprecipitation of mouse cell supernates (*152*).

IL-23 is a proinflammatory cytokine mainly produced by activated DC and macrophages as a response to microbial pathogens and it is enhanced by the co stimulatory molecule CD40 and its ligands (*140, 152*).

Moreover, IL-23 participates in a positive feedback loop promoting IL-12 production by DCs to enhance p19 transcription and further IL-23 production although in the absence of IL-23 the Th1 differentiation and IFNγ production is unaltered (*164*) (*165, 166*).

Although it was firstly thought that IL-23 was essential to Th17 population differentiation of naïve CD4+T cell through STAT3 activation (*164, 167, 168*) it was later demonstrated that it has a different function on this cell types. IL-23 has a key role in Th17 maintenance by stabilizing IL-17 expression and the Th17 phenotype but is not a differentiation factor for Th17 cells (*169*). In fact, Th17 differentiation is triggered mostly by IL-6 and TGFβ (*169*) although IL-1β and IL-21 are also important for its differentiation (**Figure 6**). The IL-23/IL-17 pathway plays an important role in terms of the induction of inflammatory cytokines contributing to autoimmunity as well as protective responses against infection. Consistently, IL-23R is undetected in naïve T even after TCR stimulation (*170*). Even though, IL-12Rβ1 is constitutively expressed by memory and naïve

T cells whereas IL-12Rβ2 is easily induced by naïve T cells after TCR stimulation (*140*). For this reason naïve T cells can respond to IL-12 promoting Th1 differentiation. This observation agrees with the fact that additional cytokines are required for IL-23R stimulation and subsequent Th17 development and IL-23 recognition in order to produce IL-17 (*167*). IL-23 receptor chains are predominantly co-expressed by activated/memory T cells, Th17 cell clones, and NK cell lines, but also at low levels by monocytes, macrophages, and DC populations (*167*) (*151*).

In vivo approximations have been used to better understand IL-12 and IL-23 functions (*170*). The first dichotomy observed between the IL-12 subunits was by the different response of IL-12p40 or IL-12p35 deficient mice response to experimental autoimmune encephalomyelitis (EAE). While p40 deficient mice were not able to develop disease, IL-12p35 deficient mice (similar as IFNγ deficient mice) showed more severe pathology than wildtype suggesting different functions for p40 and p35. The generation of p19 deficient mice by Cua *et al.* (2003) (*166*) firstly revealed a unique role for IL-23 but not IL-12 in autoimmune disease (EAE) and demonstrated different roles for IL-12 and IL-23 *in vivo*. In this study, it was demonstrated that mice lacking p40 or p19 did not develop disease whereas in p35 deficient mice EAE was developed. The authors concluded that IL-23, unlike IL-12 acts more broadly as an end-stage effector cytokine through direct activation of macrophages.

Using an animal model of collagen-induced-arthritis (CIA) it was demonstrated that while IL-12p35 deficient mice presented exacerbated arthritis, IL-23-deficient mice were resistant and this correlated with the absence of CD4+T cells that produce IL-17 (*165*).

To further investigate biological functions of IL-23 *in vivo* a transgenic mice that overexpressed p19 was developed by Wiekoswski *et al.* (2001) (*171*). In the study it was observed that p19 transgenic mice presented a prominent systemic inflammation phenotype, infertility and premature death. Interestingly, these animals presented lymphocytes and macrophages infiltrates in different tissues. Moreover, TNFα and IL-1β was highly detected in the serum of the transgenic mice as well as a high number of circulating neutrohpils. These findings were important since indicated that p19 shares biological properties with IL-6, IL-12 and G-CSF and specific expression is required for its biological activity.

In the study of Wiekowski *et al*., (2001) it was opened a new question about the possibility of p19 working independently of p40. Importantly for this hypothesis, no differences of p40 expression between control and p19 transgenic mice were observed suggesting p19 independent role (See **first part of the Results** section).

IL-35 (p35+Ebi3)

IL-35 is the newest cytokine described of the IL-12 superfamily although the hypothesis about p35 and p40 having other partners and other functions different than IL-12 formation has been suggested since the 90'. Some of the hypothesis originates from the observation that $p35^{-/-}$ and $p40^{-/-}$ animal models for different diseases does not present equal phenotypes. This issue firstly suggested a different partner for p40 in order to form another cytokine (IL-23, discussed above) but also suggested the possibility of another partner for p35. Morevoer, whereas p35 subunit of IL-12 is constitutively expressed in different cell types, p40 is inducible by different stimuli *(172).*

Ebi3 was firstly identified by Devergne *et al.* on 1996 (*173*). Ebi3 was clearly found expressed and secreted by *in vitro* B lymphocyte cell lines transformed with Epstein-Barr-virus (EBV). For this reason, it was called EBV-induced gene 3. EBI3 gene is localized in chromosome 19, band p13.3 which is translated into 33 KDa protein which preserves a 27% of homology with p40 subunit of IL-12. Moreover, both subunits have 3' untranslated 39 Alu repetitions, without transmembrane motifs and they are synthesized to be secreted.

This subunit is expressed *in vivo* by different human tissue such as placenta (in syncytiotrophoblast cells) localized mainly in the cytoplasm and endoplasmic reticulum, in the tonsils (by mononuclear cells such as macrophages) and in the spleen (mainly localized in the perifolicular area and vascular area). Interestingly, in most of the cells Ebi3 is localized in the cell cytoplasm or associated to the endoplasmic reticulum. Immature Ebi3 has also been found associated to calnexin in the endoplasmic reticulum suggesting that although its structure it may need a partner in order to be secreted.

In 1997, the same author demonstrated that Ebi3 is associated to p35 and the results were described as a novel, naturally occurring heterodimeric hemoprotein (*174*). Is in this work where it was determined using co-immunoprecipitations that both subunits interact with non-covalent junctions and that this interaction was necessary in order to be secreted similar as p40 which is

apparently needed by p35 and p19 in order to conform and secrete mature IL-12 and IL-23 respectively (*174*).

IL-35 was firstly named by Collison *et al.* (2007) (*175*). They firstly exposed a function for IL-35 as a potent inhibitory cytokine produced by resting and activated mouse and human Treg cell populations but not by T effector cells. The main studies about IL-35 functions have been done with Treg cells in which has been described that IL-35 suppresses T conv proliferation by inducing cell-cycle arrest in G1 phase (*140*).

Importantly, similar as TGFβ and IL-10, recombinant IL-35 *in vitro* treatment of either mouse or human T conv (CD4+Foxp3- T cells) induces a type of Treg called iTr35 (*126*). These cells do not express the common Treg TF FOXP3 and trigger their suppressive effects independently of IL-10 or TGFβ (*126*).

Importantly, IL-35 expression is different in mouse and human, while in mouse IL-35 is constitutiveley expressed by Foxp3 resting and activated T cells (*126*), human CD4+CD25+Foxp3+ Tregs do not constitutively express IL-35 (*176*). This fact is important to be considered since emerge controversial results in the literature.

Another important issue of this cytokine is the fact that whereas p35 gene is constitutively expressed at low levels in many cell types and therefore displays an almost ubiquitous expression, EBI3 gene expression is restricted to specific cell types and highly inducible so Ebi3 expression may be decisive for IL-35 formation. As explained, Ebi3 has found expressed at high levels in placental trophoblast cells and activated dendritic cells and at lower levels in macrophages and endothelial cells (*174*) but regarding to lymphocytes, Ebi3 expression is detected in activated normal B cells as well as tumoral B and T cells, but (in contrast to constitutive expression of p35) is undetectable in normal resting CD3T cells subsets (including effector T cells, naive and memory CD4+ T cells, CD8+ and γδ T cells) (*176*). Neither $CD25^+$ nor $FoxP3^+$ Tcells in human thymuses, lymph nodes, tonsils, spleens, and intestines co-expressed p35 with Ebi3. Importantly, and opposite of what happens in mice, T cell stimulation consistently induced Ebi3 in various CD4+ T cell subsets but no Ebi3 could be detected in stimulated Tregs (*176*) (**Figure 10**).

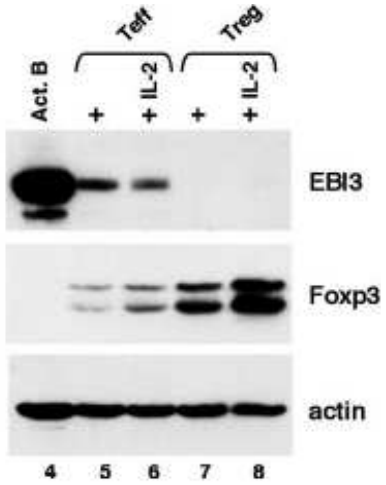

Figure10. Western blot analysis of Ebi3 expression in activated CD4+T cells (Teff or Treg). Teff and Treg cells were purified from the same donor and either stimulated for 2 days with beads coated with anti-CD3 and anti-CD28 Abs (+) plus IL-2 (+ IL-2). Cells lysates were analyzed by western blot with anti-Ebi3 or Foxp3. Positive control is activated B cells stimulated for 2 days with anti-CD40 Abs (*176*).

In contrast, in another study it was demonstrated that IL-35 production and released is induced in human peripheral blood CD4+ and CD8+ T cells by co-stimulation provided by human rhinoviruses activated DC promoting differentiation of IL-35 producing cells which are potent Treg (*177*). Moreover, T reg were assumed to have therapeutic effects on RA in which IL-35 may play a role (*178*).

In chronic hepatitis C patients present high levels of T reg are important for maintain immunoregulatory balance and it is dependent on IL-10 and IL-35 production (*179*). According to this data, Liu *et al*. (2011) (*180*) performed a study of IL-35 on patients with chronic hepatitis B (CHB). They showed that IL-35 could be detected in the peripheral blood of patients with CHB whereas it was undetectable in healthy individuals. The current study provided the first evidence that the novel cytokine IL-35 could be detected in the CD4+ T cells from the peripheral blood during human disease suggesting IL-35 as a new target for immunotherapy against chronic Hepatitis B virus infection.

Similar as happens with Treg cells, some studies have started to explored IL-35 functions in other lymphoid and myeloid cell types, as B cells. Recombinant mouse or human IL-35 inhibits proliferation of $CD19^{+}$ $B220^{hi}CD5^{-}$ B cells and also induces IL-10 B cell producers (i10-Breg) expansion *in vitro*. Interestingly then, recombinant mouse IL-35 can induced either B reg cells or

i10-Breg into a Breg cells that produces IL-35 cytokine which are named i35-Bcells and have suppressive effects either by IL-35 or IL-10 secretion (*155, 181*).

Importantly, the IL-35 receptor is unconventional since it can be homodimer or heterodimer of IL-12Rβ2 and gp130 chain (*154*). In Tconv, the gp130 chain is constitutively expressed and not inducible in the influence of proinflammatory agents. Meanwhile, IL-12Rβ2 is induced by IL-2 or IL-27 (*157, 182*). IL-35 promotes Tconv cells suppression either through gp130 or IL-12Rβ2. But in contrast, both chains are essential for Tconv cells to differentiate into iTr35. Downstream pathway is triggered by heterodimer of STAT1 (activated through gp130) and STAT4 (activated through IL-12Rβ2). In contrast, in B cells it seems that the receptor is composed by IL-27R and IL-12Rβ2 which activates STAT1 and STAT3 (*155*) (**Figure 8**).

Even though, these approximations have only been done in mice and should be also confirmed with human cells.

IL-35 will be extensively investigated and discussed in the **second part of the Results** section in which it has been found to be expressed by non-lymphoid cells such as VSMC as well as to promote proinflammatory phenotype in this cell type through different receptor and pathways previously described.

IL-27 (Ebi3+p28)

IL-27 is a cytokine of IL-12 superfamily which is highly expressed either by activated DC or macrophages (*183*).

While activated T cells and NK cells express the highest levels of the IL-27R there are a range of cells that coexpress IL-27ra and gp130, including naıve T cells, mast cells, endothelial cells, activated B cells, monocytes, Langerhan's cells and acti- vated dendritic cells. The expression of the full IL-27 receptor complex by these cell types indicates that they should be fully responsive to the effects of IL-27 (*184*).

IL-27 is mainly an inhibitory cytokine often genereated during autoimmune response by local APC. However, other stimuli different than TLR (n Treg cell, IFNβ, TLR ligand and statins) can also induce IL-27 by APC limiting the induction of the inflammation (*140*) (*184*).

Although IL-27 shares gp130 receptor with IL-6, IL-27 present different function than IL-6 such as upregulation of the Th1 transcription factor T-bet and the IL-12Rβ2 chain (*157*) while suppressing IL-6-driven T cell proliferation and Th17 differentiation (*185*).

IL-27 in combination of IL-12 can also promote IFNγ production by naïve CD4+Tcells and NK (*153, 157, 183*). Moreover, IL-27 inhibits development of Th17 cells (*186*) and the production of an IL-10-producing Tr1 cell–like regulatory population (*187, 188*) .

Nevertheless, proinflammatory function has also been associated to IL-27. For example, IL-27 facilitates the development of follicular helper T cells (Tfh) by the induction of IL-21 becoming a modulator of B cell function and development important in disorders by excessive germinal centers formation and high-affinity autoantibody production (*189*) .

	IL-12	IL-23	IL-27	IL-35
Cells that produce	DC, monocytes, macrophages, B cells, CD4+T	DC, monocytes, macrophages, Bcells	DC, monocytes, macrophages, Bcells, SMC (?)	FOXP3 T reg cells (?), activated CD4T and DC Bcells
Cells that respond	Naïve T cells, Th1 cells, NK	Memory T cells, Th1/Th17 cells and NK	T cells, Th1 cells, NK	Tconv cells, aorta SMC (?)
Function	Th1 activation, Th1 maintenance Th2 suppression	Th1 activation Th17 maintenance and proliferation	Th1 modulation Th17 suppression IL-10 induction B cell modulation Tfh development	Tconv suppression IL-10 production i35Treg and i35-Bcell differentition

Table2. IL-12 cytokine family biological characteristics and functions in human. Adapted from Collison *et al.* (2007) (*141*) and Bardel *et al.*, 2008 (*176*).

2.4 Mechanisms contributing to vascular remodeling

Vascular remodeling is a dynamic process which include at least 4 cellular processes: growth, death, migration, and synthesis/degradation of ECM (*190*). Vascular remodeling is depending on dynamic interactions between growth factors, vasoactive molecules and hemodynamic stimuli, being a dynamic process as a response to prolonged changes in hemodynamic conditions. Nevertheless, it also can be involved in vascular diseases and cardiovascular disorders (*191*).

VSMC in vascular remodeling

During vasculature maturation, formation and development, VSMC are an essential proliferative, contractile and synthetic component. In addition, during vasculature development, VSMC secrete extracellular matrix proteins, in order to create the essential matrix for the organization of the different layers. In these first steps, VSMC can be described as a fibroblast-like cells (*192*).

In a mature animal, VSMC are highly specialized cells whose principal functions are contraction and regulation of blood vessels tone-diameter, blood pressure and blood flow distribution. VSMC in adult animals still maintain remarkable plasticity and can undergo reversible changes in their phenotype as a response of the environment such as vascular injury. In this context, VSMC dramatically increase their proliferation rate and migration ability. These changes in their phenotype sometimes contribute in disease development such as atherosclerosis, cancer, hypertension or some vasculitis such as GCA (*193*).

VSMC switch between contractile and synthetic phenotypes throughout the lifespan, especially in the context of repair and remodeling.

According to VSMC changes in their phenotype, they can be divided in three groups (*194*): (note that this process is dynamic) (**Figure 11**)

- **Contractile or differentiated.** Quiescent cells, contraction phenotype in a maintenance of vascular tone in mature vessels
- **Synthetic or dedifferentiated.** Increased proliferation and migration rate and ECM synthesis as a response of vascular injury in order to repair damage in normal conditions.

- **Inflammatory.** Under various stimuli such as PBMC interaction or as a cytokine/chemokine response VSMC can secrete cytokines and express proinflammatory related molecules such as VCAM-1 and ICAM-1.

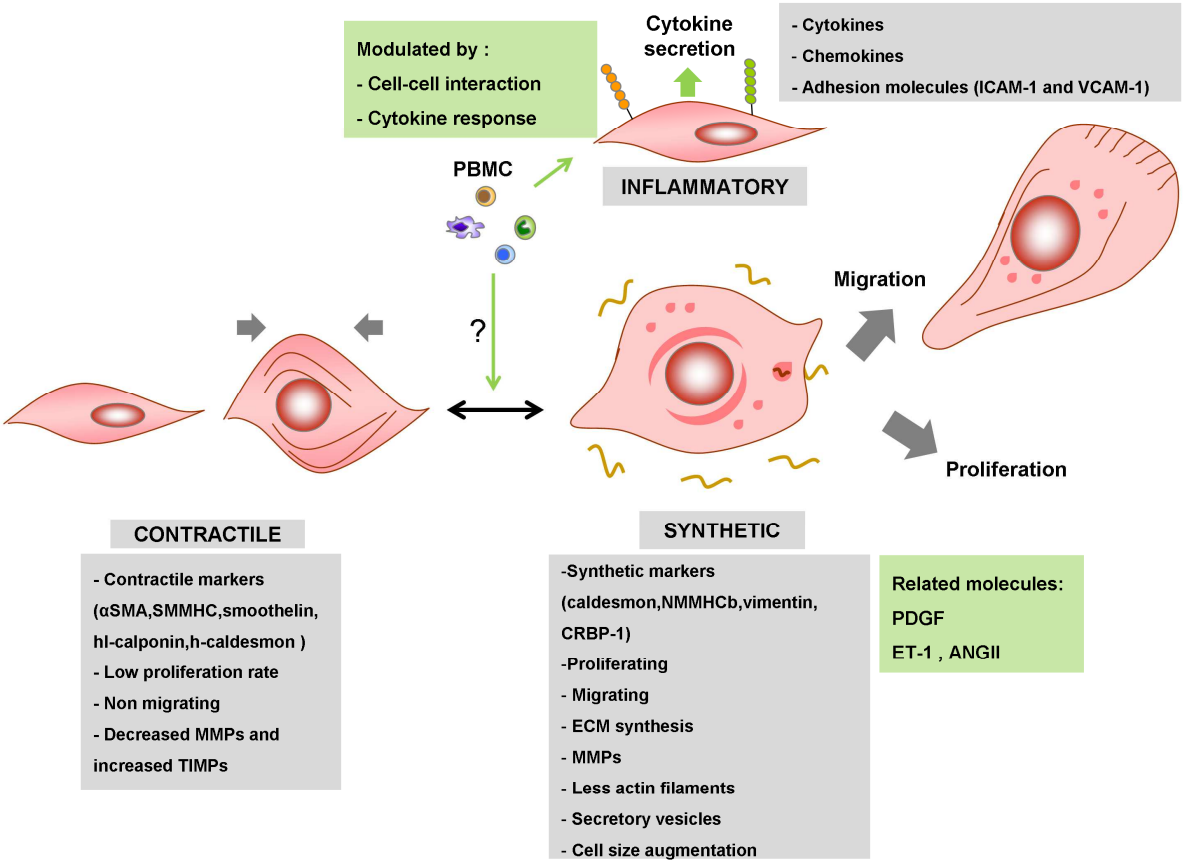

Figure11. Changes in vascular smooth muscle cells (VSMC) under different stimuli. VSMC present a high plasticity. Different conditions can promote VSMC changes in their phenotype. Contractile VSMC present different markers as labeled than synthetic phenotype a process that is involved in vascular remodeling and cell migration. Moreover, VSMC can also adopt a proinflammatory phenotype which consists on the modulation of adhesion molecules chemokines and cytokines secretion and it is usually prone by leukocyte interaction. Adapted from Reid Amy J, *et al.* (2012) (*195*) and Lula L. Hilensky K.(*194*).

Cell migration

Cell migration is a multistep process that orchestrates different essential functions in cells such as tissue repair or leukocyte infiltrating tissues. Moreover, cell migration contributes to several important pathological processes (i.e. cancer, chronic inflammatory diseases or vascular diseases) (*196*).

Cell migration must be understood as a dynamic and cyclic process in which the cell response to the stimuli is translated into its polarization and creation of protrusions (**Figure 12**) in the

direction of the migration (**leading edge**). This phenomenon is accompanied of the polymerization of actin filament in the site of protrusion. These filaments interact through integrins with ECM in order to establish the step as a point of traction for the cell movement (**focal adhesions**). In addition, in the **rear edge** of the migrating cell, old focal adhesions must be detached in order to allow cell contraction and movement.

Protrusions can be distinguished into **lamellipodia** or **filopodia** depending on the characteristics of actin distribution. While lamellipodia is a broad extension of organized actin filaments which is essential for cell migration because such organization push the cell along the plasma membrane, filopodia is a formation of long parallel bundles of actin filaments which serve as a sensors to explore the local cell environment (*197, 198*) (**Figure 12**).

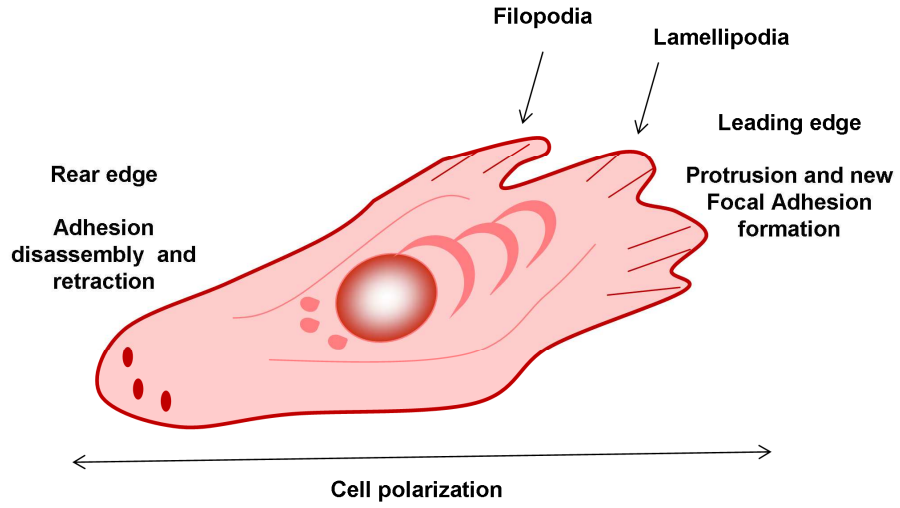

Figure12. Cell migration is characterized by cell polarization and cytoskeleton reorganization. Either formation of new focal adhesion in the leading edge or the disassembly of old focal adhesion from the rear edge is essential for cell migration. Lamellipodia and filopodia are created in the leading edge in order to migrate.

Molecules involved in cell migration

Integrins in cell migration

In cell adhesion, migration and spreading, integrins act as mediators of ECM and actin fibers of cell cytoskeleton. Integrins are important for the signaling from outside the cells (responding to ECM) triggering signaling to the cytoplasm of the cell. Integrin signal is mostly driven by G proteins. In addition to the integrins, other focal adhesion related molecules are needed such as Src, tallin, vinculin , paxillin and FAK (*199*).

Rho family proteins

Rho family small guanosine triphosphate (GTP) - binding proteins (GTPases) are central regulators of actin organization and protrusion formation. Between them, the most important ones in lamellipodia and filopodia formation are RhoG, Rac and CDc42. While CDc42 is mostly associated to filopodia formation, Rac promotes lamellipodia formation (*200*).

PI3K (Phosphatidylinositol-4, 5-bisphosphate 3-kinase)

According to structural features and lipid substrate preference, PI3K can be divided in three classes (class I, class II and class III). In cell migration process, the most important ones are class I PI3K which consists in heterodimers composed by a catalytic subunit and a regulatory domain. Class I PI3K can be distinguished in class I A which mostly trigger response through tyrosin kinases receptors and are conformed by 110KDa catalytic domain with three different isoforms described (p110α, β and δ) plus a 85 KDa adaptor regulatory domain with also three isoforms described (p85α, β and p55γ). Isoforms p110 α and β are widely distributed in mammal tissues while p110δ is mainly find in leukocytes (**Figure 13A**).

Importantly, the class IA PI3K activity can be driven not only by tyrosine kinase receptor but also by non-receptor tyrosine kinases such as FAK, src-family and JAK kinases. Interestingly, this class IA PI3K activation through this non receptor tyrosine kinases has been found involved in T and B cell antigen receptors , cytokine receptors, coestimulatory molecules and cell-cell interaction (*201, 202*). In contrast, class I B trigger their response through heterotrimeric G proteins-coupled receptors (GPCRs) and are composed by catalytic domain p110γ and regulatory domain p101 or p87 (*202, 203*). Class I B PI3Ks are directly activated by Gβγ subunits of GPCRs. This class of PI3Ks appears to be present only in mammals with restricted tissue distribution being abundant in white blood cells.

Interestingly, recent data suggest that most class I PI3K subunits might be activated by GPCRs either directly through Gβγ protein subunit or indirectly for example by RAS protein which can be activated both by Tyr kinase or GPCRs (*203*) since the catalytic domain of class I PI3K can be activated through RAS (*204*) (**Figure 13B**).

Class I PI3Ks have been associated to cell growth, DNA synthesis, regulation of apoptosis, and cytoskeleton changes. There are no findings of how PI3K affect to actin cytoskeleton although there are evidences suggesting that it could be through its lipid production pointing to the actin

cytoskeleton in the plasma membrane as a primary target for PI3K. This process seems to be triggered through guanosine nucleotide exchange factors (GEFs) and GTPase-activating proteins (GAPSs) and small GTPases (*202*).

Phosphatidylinositol 4, 5-bisphosphate (PtdIns (4, 5) P_2) or PIP_2 is a phospholipid of cell membrane which in *vivo,* PIP_2 is the substrate for class I PI3K which phosphorilates its 3-hydroxyl group of the inositol ring obtaining PIP_3 (PtdIns (3, 4, 5) P_3) (**Figure 13B**).

PIP_3 is a key signaling molecule that become rapidly and highly polarized in cells that are exposed to a gradient of chemoattractant. This amplification process involves both localized accumulation and activation of PI3Ks, which generate PIP_3.

PIP_3 and PI3K are accumulated and activated in the leading edge of a migratory cell while, in contrast, in the rear edge of the migrating cells phosphorylation and location of phosphatidylinositol-3,4,5-trisphosphate 3-phosphatase (PTEN) is abundant since it's the enzyme that reverts the PI3K reaction by removing the third phosphorylation to PIP3 obtaining again PIP2 (*196*) (**Figure 13C**).

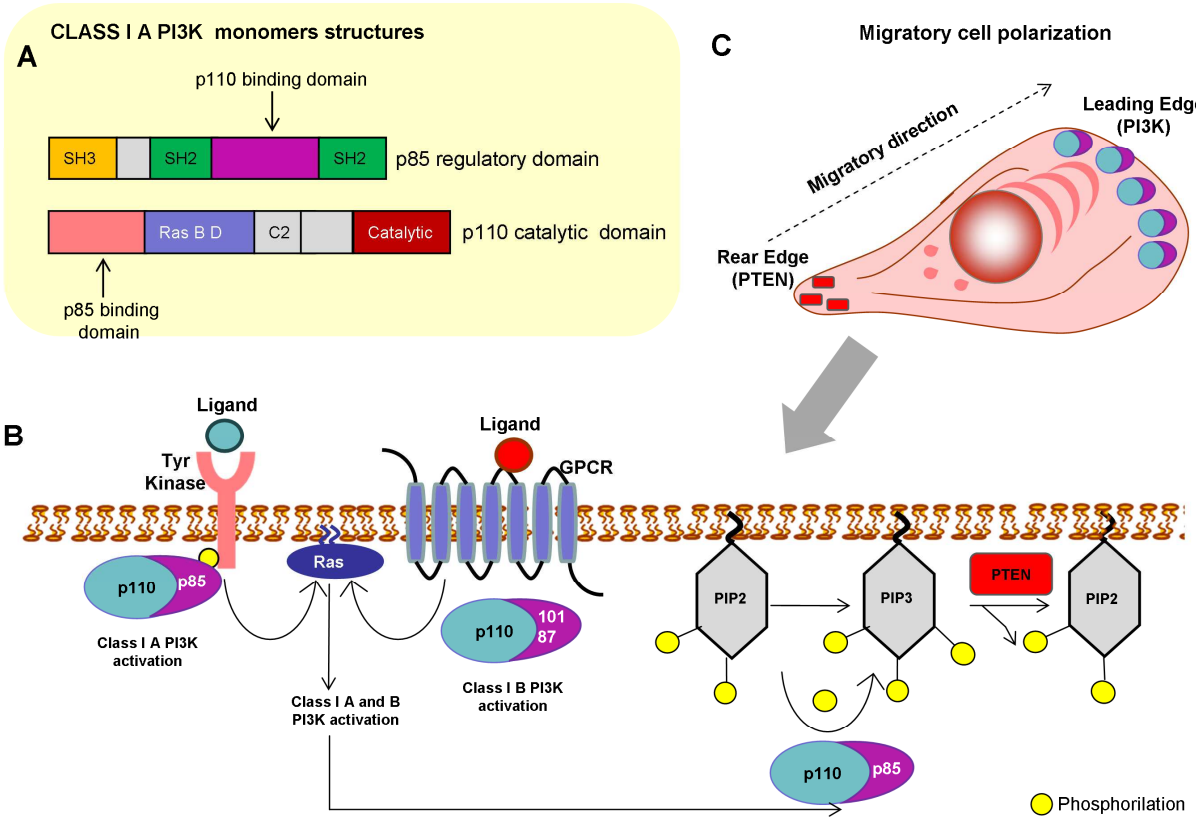

Figure13. Class I PI3K monomers structures and the involvement in cell migration. A) Class I A PI3Ks are composed by p85 regulatory domain plus P110 catalytic domain. B) PI3K can be activated either as a response of ligand binding to either tyrosin kinase receptor after or to GPCR activation after

Ras activation. Active PI3K proportionate the enzymatic reaction of phosphorylation PIP2 in order to form PIP3. C) PIP3 and active PI3K are localized in the leading edge of migratory cells whereas; PIP2 and the enzyme which promotes PIP3 to PIP2 conversion are localized in the rear edge of migratory cells. Adapted from Vanhaesebroeck *et al*., *(2010)* (*203*) and Ridley *et al*. *(* 2003) (*196*).Note that Class I A PI3K can also be induced by non-receptor Tyr kinase proteins although is not represented in this scheme . C2 domain in PI3K is a C^{2+} depending phospholipid binding protein, which is a common domain in proteins involved in signal transduction or membrane traffic (*202*).

The most important PI3K inhibitors are **wortmannin** and **LY294002.** Wortmannin is a fungal metabolite which potently inhibits all three classes of PI3K and so PI3K-related members (i.e. mTor). One important inconvenient of Wortmannin to be considered is its short half-life. Another inhibitor used to inhibit PI3K is LY294002 which is a flavonoid-based synthetic compound. This inhibitor works as an inhibitor of ATP site.

FAK (Focal adhesion kinase)

FAK is a tyrosine kinase protein of 125 KDa which was firstly described by Shaller *et al*. (1992) (*205*). FAK was highly found expressed in the focal adhesion of v-src transformed fibroblasts of chicken embryos. FAK is autophosphorylated and activated as a response of integrin interaction with ECM. These focal contacts are formed at ECM-integrin junctions that bring together cytoskeletal and signaling proteins during the processes of cell adhesion, spreading and migration (*206*). Many stimuli can induce tyrosine phosphorylation and activation of the catalytic activity of FAK, including growth factors, neuropeptides, molecules that stimulate G-protein coupled receptors and mechanical stimuli (*207*).

The main important FAK functions described are controlling cell motility, cell adhesion and transmitting cell survival signal from the extracellular matrix.

Inhibition of endogenous FAK signaling in fibroblasts is translated into reduction of cell motility, diminish of spread rate, exhibit and increased number of prominent focal adhesion and migrate poorly in response to chemotactic and haptotactic signals, even in some cases increase cell death (*208, 209*). In contrast, enhancing FAK signaling by exogenous expression increases cell motility and promote cell survival in the absence of a signal from the extracellular matrix (*210, 211*).

FAK structure consists in a catalytic domain which is flanked by two non-catalytic domains (**Figure 14**). The N-terminal domain (FERM) consists on a conserved domain with high

homology to ezrin, radixin and moesin. This domain is important for the interaction with the β subunit of cytoskeletal proteins (*212*). Moreover, it is able to interact with cytosolic domain of tyrosin kinase receptors (i.e. EGFR and PDGFR).

In contrast, C- terminal domain FAT (focal adhesion target) consists on a 4-helix bundle structure that contains sites for integrin-associated protein since it is rich in protein interaction sites (*206*). It is mostly associated to paxillin, tallin, and vinculin, which are proteins from the cytoskeleton important for driving focal adhesion formation. Interestingly, paxillin binds directly to the cytoplasmic domains of integrin receptors as well as to the focal adhesion protein tallin and paxillin may function as the 'docking partner' for FAK in adhesion complexes (*213*). C-terminmal not only harbors protein-protein interaction but also contains SH3-domain containing proteins. Site II allows the interaction with other docking proteins such as p130Cas, whereas site II interacts with regulators of small G proteins GRAF and GAP (*213*) which are associated to protein Rho GTPases which participate in cytoskeleton reorganization. Punctual mutation of FAT disrupts paxillin association and β1 interaction which promote the inhibition of FAK localization to focal contacts (*206*).

FAK can also be phosphorylated in different amino acids. The most important characterized one is the phosphosrilation on tyrosine 397 (Y397) which is located at FERM domain. This phosphorylation creates a docking site for proteins containing SH2 domain such as src-family kinases (SFKs), phospholipase Cγ (PLCγ), suppressor of cytokine signaling (SOCS), growth factor receptor bound protein 7 (GRB7), Shc adaptor protein, p120 RsGAP and p85 subunit of PI3K (*206*). Between them, the most important ones to be considered for this thesis would be the non-receptor cytoplasmic tyrosine kinase Src (*214*) and, p85 subunit of PI3K (*215*) which would trigger cell adhesion and migration (*216*). FAK is importantly involved in cell migration since FAK-deficient cells loose the ability of migrate (*208, 213*).

Binding of Src to phosphorylated Y397FAK results into a dual activated FAK-Src complex which leads to the phosphorylation of both tyrosine 861 and 925 (Y925). Activation of FAK Y861 promotes p130Cas binding to SH3 domain while Y925 FAK activation promotes the actin fibers formation with subsequent generation of the force need for the cell migration (*217*). Importantly, Y925 binds to SH2 protein domains such as Grb2 which is related to RAS and ERK2 (extracellular signal-regulated kinase 2) pathway. This is important since for cell migration, it is new focal adhesion formation are necessary to be recruited to the cell leading edge of the cell

but also the disruption of the old ones in the rear edge. Hunger-Glaser *et al*., (2004) (*218*) described that ERK2 activation as a response of FAK/Src complex would prone activation of myosin light chain kinase (MLCK) promoting focal contact dynamics in migrating cells and phosphorylation of Ser910 which would inhibit paxillin association to FAK and inhibiting FAK translocation to focal adhesion (*206*) .

There is some controversial about the involvement of G proteins in FAK activation, although in some studies has demonstrated Gβγ heterodimer role in regulating FAK activation in EC (*219*). Moreover, integrin may also play an important role in FAK activation so integrin β1 has also been discussed to be essential in the induction of fibrosis by fibroblast (*220*).

FRNK domain (FAK-related-non-kinase) functions as a negative regulator of kinase activity of certain expressing cells. Interestingly, FRNK is elevated in VSMC which is upregulated as a response to vascular injury (*221*). Moreover, cells overexpressing FRNK inhibits the rate of cell spreading, chemotactic and haptotactic migration. Overexpression of FRNK also inhibits the rate of cell spreading, chemotactic and haptotactic migration (*209, 221, 222*) (**Figure 14**).

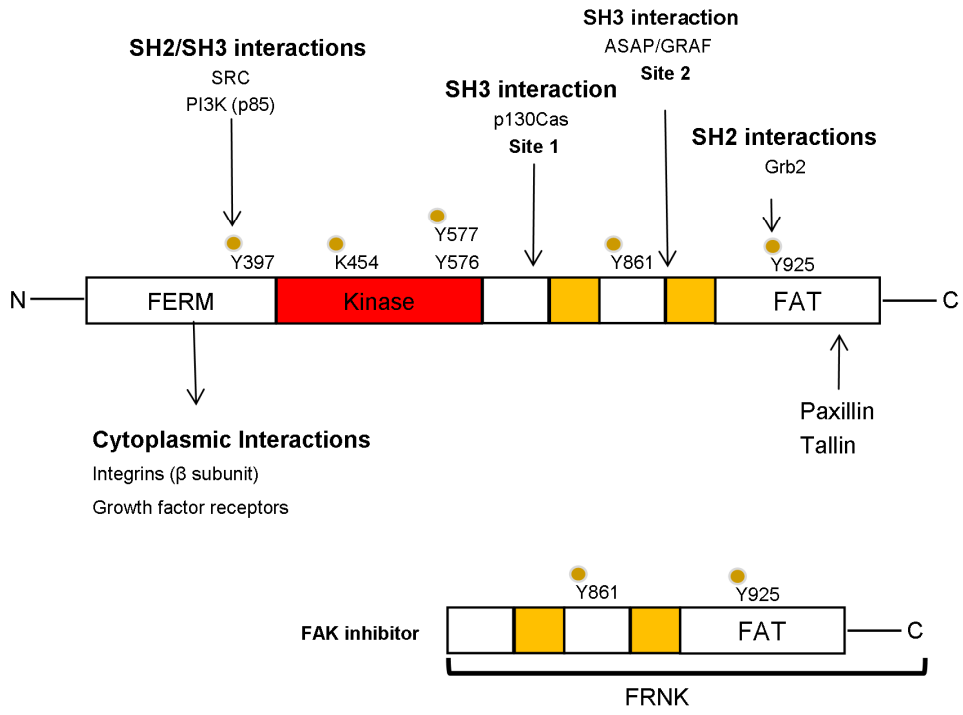

Figure14. FAK structure and organization. N-terminal (FERM) domain directs interactions with integrins and growth factor receptor as well as p85 of PI3K. FERM domain contains a tyrosine autophosphorylated site (Y397) which creats a docking site for SH2/SH3 domains of Src and PI3K. Catalytic domain contains

two tyrosine phosphosrilation sites (Y577 and Y576) to obtain complet FAK activation. C-terminal domain contains sites for multiple protein-protein interaction. Site 1 (S1) prone intarction with p130 Cas through its SH3 domain whereas site 2 (SH2) contribute to SH3 domain interactio of Graf related proteins. FAT domain, localized in the C-terminal interacts with proteins such as paxillin or tallin and contain a tyrosine domain (Y925) which also creats a docking site for SH3 domain of Grb2 proteins which promote ERK2 activation. FRNK is also represented an act as a FAK inhibitor. Adapted from Parsons *et al.* (1994) (*199*).

FAK signaling is modulated by expression of an endogenous FAK inhibitor termed FRNK (FAK-related nonkinase), which is expressed as an independent protein and consists of the carboxyl-terminal noncatalytic domain of FAK (**Figure 14**). FRNK is identical in sequence to the C-terminal domain of FAK at both nucleotide and amino acid levels. FRNK specific cDNAs are characterized by long 59 non-coding leader sequences indicating that expression of FRNK is mediated by alternative splicing or transcription of FRNK-specific sequences (*223, 224*). While FAK is ubiquitously expressed, FRNK is selectively expressed in a number of cell types such as VSMC (*221*). Importantly, FRNK is highly expressed by these cells during embryogenesis and downregulated in adult tissues although after artery injury it becomes upregulated. This increased of FRNK after injury may change VSMC phenotype into less proliferative and migratory cells regulating then the activity of FAK (*221*).

Src

Src is a tyrosin kinase protein of approximately 60 KDa which was derived from the oncogen v-src which is responsible of the tumor formation in chicken infected with the Rous sarcoma virus (*225*) and was determined as a member of the large family of structurally related tyrosin kinases expressed in many different cell types (*226*).

Src has peliotropic functions such as fundamental cellular processes including cell growth, differentiation, cell shape, migration, adhesion and survival (*227, 228*).

Similar as FAK deficient cells, Src $^{-/-}$ present less capability of migration and descontrolled formation of focal adhesion all around the cell which would loose the focal adhesion turnover necessary for migrate (*208*). Interestingly, Src is also important for cell adhesion and migration since (together with FAK activation) it is involved on the disruption of adherent junctions while promoting degradation of E-cadherin (a molecule ivolved in the cell-cell adhesion). This degradation of E-cadherin is also important for cell migration (*228*).

Src activity is regulated by intramolecular interactions controlled by tyrosine phosphorylation and it can interact with other proteins through its SH2 and SH3 domains which contain prolin-rich motifs.

The structure of Src family proteins consist in a c-Terminal tail containing a negative regulatory tyrosin (Y527 in chicken or Y530 in humans) and four Src homology domains (SH) plus an amino-terminal domain (*227, 228*) (**figure 15A**).

The SH domains consist on SH1 (kinase) which contains the autophosphorytation tyrosine site (Y416 in chicken or Y419 in human), SH2, SH3 which prone intramolecular and intermolecular interaction of Src and SH4 domain which promotes the interaction of Src with the membrane throughout the myristoylation site (*228*).

Src is negatively regulated by phosphorylation of a tyrosine residue (Y527) localized in the C-terminal. It is phosphorylated by Csk tyrosine kinase, promoting an inactive conformation of Src which consist on an intramolecular association of C-terminal with SH2 domain (*207, 226*) and a second intramolecular association involving SH3 domain. Defosforilation of this negative phosphorylation site can be performed by phosphatase (i.e. PTPα) which would activate Src (*229*). Although it also can be activated by disruption of the low intramolecular interaction between SH2 and SH3 Src domains by creating new SH2 SH3 interactions by their ligands (*207*) (*230*). SH2 Src domain highly binds to FAK in Y397 although upstream this tyrosine 397 of FAK is the sequence RALPSIPKL, which resembles the consensus Src SH3-domain binding motif, RXLPPLPRf. The close proximity of this putative SH3-binding site (residues 368–376) to the Src SH2-binding site in FAK (residues 397–400) suggests that both SH3 and SH2 domain interactions might mediate the association of Src with FAK. Interestingly Src can also be activated by interacting with pCas either in SH2 or SH3 domain resulting on the activated conformation of Src. Association of Src with other proteins such as p130Cas and paxillin (*230*) (*231, 232*) (**Figure 15B**). Moreover, Src present a autophosphorylated tyrosine (Y416) in the kinase domain which it only can be phosphorylated when Src it is on its active conformation (*233*).

Elevated expression of Src has been associated to some cancer such as breast and colon cancer (*228*) mostly in the later stages which seems to contribute to metastatic potential throughout effects on adhesion, invasion and cell motility.

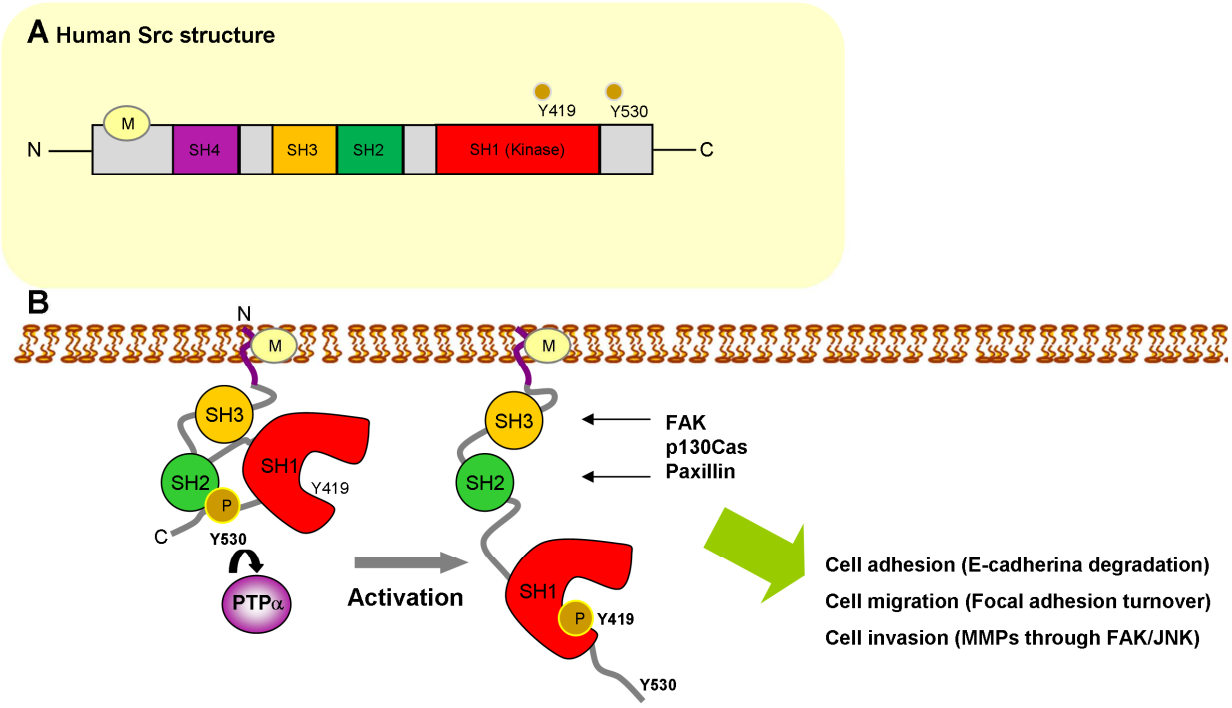

Figure15. Src structure, activation and functions. A) Structure of Src consists of four Src homology domains (SH) and an N-terminal domain containing a merystoylation syte (M). SH1 domain contain the kinase which can be activated (phosphorylation at Tyr 419) or inactive when is phosphorylated at Y530. (B) When Y530 is phophosrilated, it binds to SH2 and SH3 domains promoting an inactive Src conformation. Src activation occurs when C-terminal Y530 phosphorylated is removed (i.e. PTPα - Protein tyrosine phosphatase alpha) and Src conformation changes permitting Y419 phosphorylation and SH2 and SH3 interaction with other proteins such as FAK, p130 Cas and paxillin promoting Src associated functions. Adapted from Yeatman *et al.* (2004) (*228*).

MAPK (ERK)

Mitogen-activated protein kinases (MAPKs) are protein serine and threonine (Ser/Thr) kinases that convert extracellular stimuli into a wide range of cellular responses. In mammals, 14 MAPKs have been characterized. The most extensively studied groups of MAPKs are ERK1/2, JNK and p38 isoforms. MAPK are Ser/Thr kinases which are often activated either through phosphrylation or as a result of their interaction with a small GTP-binding protein Ras/Rho family as a response to extracellular stimuli (*234*).

ERK1 was the first mammalian MAPK to be characterized. It was originally found to be phosphorylated on Tyr and Thr residues as a response to growth factors such as PDGF, EGF or insulin. Moreover, they can also be activated by ligand for heterodimeric GPCRs, cytokines, osmotic stress and microtubule disorganization (*235*).

Interestingly, ERK1 and ERK2 present about 80% of homology. Both proteins, after activation can be translocated from cell cytoplasm to the nucleus. After stimulation are able to phosphorilate a wide number of substrates localized in different cell compartments (*236*).

Both ERK1 and ERK2 play a centrol role in the control of the cell proliferation but also cell motility. The important process in which ERK1/ERK2 are related to cell motility is through the activation of MLCK activity promoting MLC phosphorylation/activation (*237*).

As explained in the previous sections, the FAK/Src axis triggers ERK activation with subsequent MLC phosphorylation and cell migration (*206*).

Endothelin system

Description

Endothelin is a vasoconstrictor peptide which was isolated by Yanagisawa *et al*. (1998) (*238, 239*) from cultured porcine EC conditioned medium. The endothelin gene (END) encodes three different isoforms named ET-1, ET-2 and ET-3 (*240, 241*). Each of the three peptides consist of 21 aa residues and are expressed in different patterns depending on cell an tissue being ET-1 the main isoform produced by EC. These isoforms only present two or six aa different than ET-1 (**Figure 16A**).

ET-1, ET-2 and ET-3 are important in vasomotor tone, cell proliferation and hormone production (*242*).

The main functions of endothelins are vasoconstriction and mitogenic effects although it also can stimulates cytokine, growth factors (i.e. VEGF , EGF,PDGF), TGFβ ,ECM and fibronectin production (*241*).

Endothelins are produced by a wide variety of cell types such as macrophages, mastocytes, neurons, hepatocytes, leukocytes, fibroblast and epithelial cells. Nevertheless ET-1 is mostly produced by EC and VSMC (*242*). ET-1 can act in an autocrin or paractin way.

ET-1 regulation

Interestingly, ET-1 is the predominant isoform in the cardiovascular system and possesses multiple functions such as vasopressor action and cardiovascular remodeling. In endothelial cells, ET-1 can be either localized into secretory vesicles or stored in Weibel-Palade bodies (*238*). Since ET-1 present physiological role in the maintenance of vascular tone and at the

same time it also can be involved in cardiovascular diseases (i.e. atherosclerosis), the storage and secretion of ET-1 by EC can differ depending on its function. In normal conditions, ET-1 secretion is continuous and regulated at mRNA level (*240*). In these conditions, ET-1 is not stored and may be secreted through cell secretory vesicles. Both ECE and big ET-1 have also been found in these cell vesicles reinforcing this hypothesis. In addition, release of ET-1 in high concentrations may be via the regulated pathway which may involved the degranulation of Weibel-Palade bodies as a response of vascular injury or other stimuli (*238*).

Interestingly, ET-1 can be transcribed, synthesized and secreted within minutes as a stimuli respond. The half life of ET-1 mRNA is about 15-20 minutes. In addition, the half life of ET-1 in plasma is about 4-7 minutes (*240*).

ET-1 gene (EDN1) is located on the chromosome 6 (6p24.1). Molecular analyses of the sequences upstream of exon 1 have revealed the existence of a number of potential regulatory elements. The binding of specific transcription factors to these DNA sites modulate mRNA expression, although a detailed scheme on how the promoter works at the molecular level is not yet fully understood. Thrombin, phorpbol-ester, angiotensin II between others activate c-fos and c-jun complexes interacting with AP-1 binding site, cytokines such as IL1β, TNFα and IFNγ can also induce ET-1 mRNA expression by binding sites for nuclear factor-1 (NFκB) (*243*). Binding sites for GATA-2 protein, TGFβ-activated SMAD transcription factors, hypoxia-inducible factor 1 (HIF1) (*244*) and two consensus nuclear factor of activated T cells (NFAT) binding sites (*245*) have also been determined in EDN1 promoter region (*4, 242, 246*).

Interestingly, recent investigations have determined regulation of ET-1 mRNA by epigenetics such as DNA methylation, hystone modifications or microRNAs (i.e. mir-1) (*247*). In addition, EDN1 contains the motif AUUUA in the mRNA which is linked to proteins that stabilized mRNA and inhibits its degradation (*244, 248*).

ET-2 and 3 are not as well described as ET-1. ET-2 is mainly produced by intestine and kidney but also is detected in placenta and uterus although no clear functions are described. In contrast ET-3 is mainly expressed in the brain by neurons and astrocytes but also found in gastrointestinal tract, lung and kidney. Interestingly, ET-3, like ET-1 also circulates in the plasma and can inhibit ET-1 function (*242*) (*241*) .

Endothelin Biosynthesis

Endothelin biosynthesis has been extensiveley reported for ET-1 isoform although the other isoforms may present similar steps in order to become the mature and active corresponding endothelin form (ET-2 or ET-3). ET-1 mature form is produced by a precursor (**preproendothelin**) which consists in a 203 aa protein. A **furin-like peptidase** cleaves the signal peptide of this preproendothelin resulting a 39 aa form which is called **big-endothelin** (big-ET-1). Importantly, big-ET-1 can be secreted and it is found in plasma and maintain about 1/100 biological function of ET-1 (*242, 249*). ET-1 mature form is obtained by the cleavage between Tryp-21-Val-22 of this big-ET by endothelin by the **endothelin converting enzyme (ECE-1)** (*250*). Alternatively to ECEs, other mechanism has been described to obtain ET-1 (21aa) mature form such as non-ECE metallopreteinase and interestingly, a chymase (found involved in VSMC) which would cleave Big-ET-1 into Tyr31-Gly32 resulting in the formation of a 31aa mature ET-1 (*241*) (*251, 252*) (**Figure 16B**).

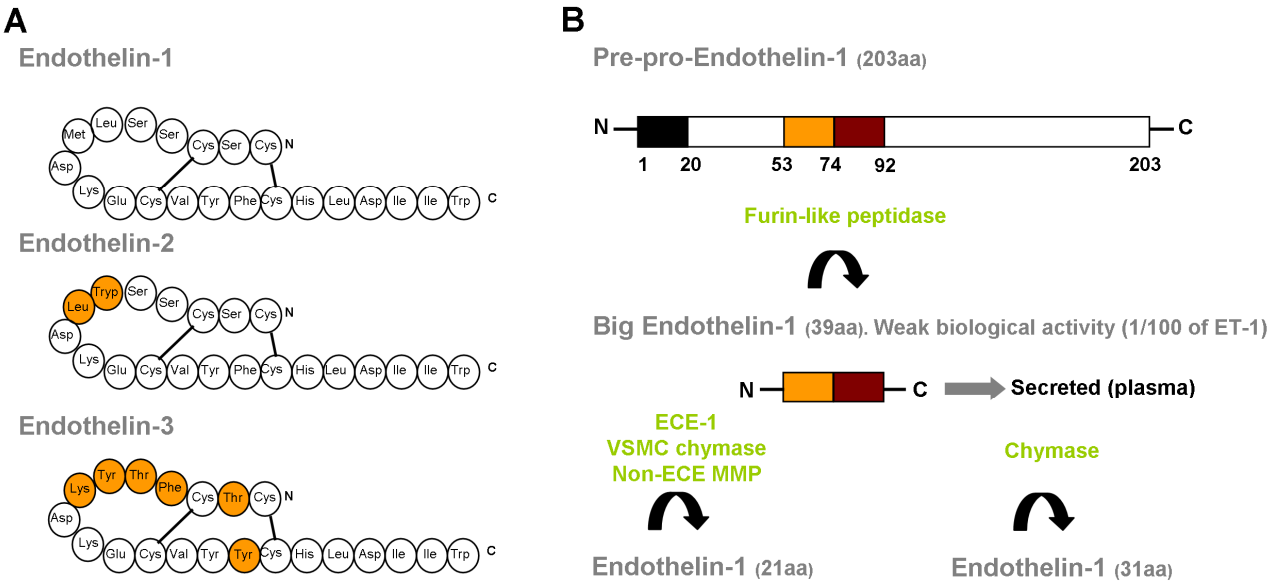

Figure16. Endothelin-1 structure and biosynthesis. A) Three isoforms of endothelin exist (ET-1, ET-2 and ET-3) and the aa sequences and bounding sites are also represented. In orange are highlighted the aa that differs from ET-2 and ET-3 to ET-1. B) Prepro-ET-1 mRNA is translated into prepro-ET-1 protein in a 203 aa peptide which is cleaved by furin-like peptidase to the 39 aa Big ET-1. Big ET-1 is processed into ET-1 (21aa) by endothelin converting enzyme (ECE-1), chymases or non-ECE matrix metalloporeinases (MMPs). Big ET-1 can aslso be processed into ET-1 (31aa) by being cleaved with a chymase. Adapted from Luscher *et al*., (2000) (*241*) and Masaki *et al.* (2004) (*249*).

ECEs are membrane bound $Zinc^{2+}$ dependent metalloproteinases which present structural homology to neutral endopeptidase 24.11 (*242*) . ECEs are expressed in different cell types such as EC, VSMC, cardiomyocytes and macrophages (*241*).

Three different ECEs have been described ECE-1, ECE-2 and ECE-3 (which is specific for big ET-3) (*253*) although ECE-1 appears to be the predominant ECE in huma. ECE-1 expressions is regulated through protein kinase C-dependent mechanism, ET_BR and the transcription factor ets-1 and some cytokines (*241*).

ECE-1 present four different isoforms derived by splicing of a unique gene: ECE-1 a, ECE-1 b, ECE-1 and ECE-1 d. Each of these isoforms can be expressed in different cell types and tissues .ECE-1 is abundant in EC and it is stored in cell vesicles in constitutively transported to membrane. In contrast, ECE-1 b is localized in the cytoplasm (Golgy complex) and ECE-1 c and d in the cell surface. Because of ECE-1 cell localization, it seems that may cleave big-ET-1 intracellular or in the cell surface (*249*).

In contrast to the high level of ECE that is expressed in EC, only low to moderate levels of expression has been detected in adjacent intimal and medial VSMC (*254*). Human umbilical vein SMC synthesize and secrete immunoreactive ET-1 and ET-3, indicating a possible physiological relevance of the smooth muscle converting enzyme (*255*).

ET-1 receptors (ET_AR and ET_BR)

In mammal cells, endothelins bind to endothelin receptor A or B (ET_AR or ET_BR). Both endothelin receptors are members of the seven transmembrane segments G_i-protein-coupled-receptor which are expressed in various tissues. The aa structure of the two types of receptor is approximately 60 % identical and each type is highly conserved across mammalian species (85 to 90 percent) with a size which range from 45,000 to 50,000 Da (*256*).

The structure of both receptors consists on a long extracellular amino terminal tail, seven hydrophobic transmembrane domains and an intracellular carboxy-tail. Interestingly, the third intracellular domain and the c-terminal tail present several putative phosphorylation sites (*256, 257*). Moreover, both receptors maintain a putative conserved binding site (Asp-Arg-Tyr) in the second intracellular loop involved in coupling G proteins.

Both receptors drive cell contraction by stimulation of phospholipase C (PLC) which at the same time forms insoitol 1, 4, 5-triphosphate (IP_3) and diacylglycol (DG) causing an increased of

intracellular Ca^{2+} concentration (*242, 256*). In contrast, nitric oxid (NO) stops the vasoconstriction by returning intracellular Ca^{2+} to its basal concentration (*242*) (*258*). Multiple G proteins may be involved in this process (**Figure 17**).

ET_AR is mostly associated to vasoconstriction and is highly expressed in VSMC and cardiac myocytes. In contrast, ET_BR is mostly associated to vasodilatation and is highly expressed by EC and in less extend on VSMC and macrophages (*242*). Importantly, endothelin A receptors are abundantly expressed in arteries whereas B receptors are mostly expressed in veins although in some diseases like arterial hypertension, can be overexpressed in VSMC (*259*).

While ET_AR binds ET-1 and ET-2 by 10 times more affinity than ET-3, ET_BR binds endothelins by similar affinity. Under **physiological conditions** in VSMC ET-1 binding to ET_AR trigger the induction of PCL, IP_3 and DG producing Ca^{2+} increment in the cell. In contrast in EC, ET-1 binding to ET_BR is linked to inhibitor G proteins that inhibit cyclic AMP formation and NA^+-H^+ activation. Moreover, ET_BR induce the production of NO and prostacyclin that would be secreted toward VSMC promoting vasodilatation (*241, 242*). Moreover this receptor in EC prevents apoptosis and inhibits ECE-1 expression and ET-1 clearance and degradation in order to dimish its signal (*260*) (**Figure 17**).

In contrast, as a consequence of ET-1 **overexpression under stimuli** both ET_AR and ET_BR can promote VSMC contraction, migration or quimiotaxis. A complex mechanism in which several tyrosin kinases proteins (PTK) promoting activation of RAK and MAPK but also through Rho kinases (**Figure 17**). Several therapies focused on blocking either receptor A or B have been studied and are further explained bellow.

ET-1 function and ET_BR induction by migratory VSMC from inflammatory vascular disease (GCA) has been evaluated and discussed in the **part 3 of the Results section** of this doctoral thesis.

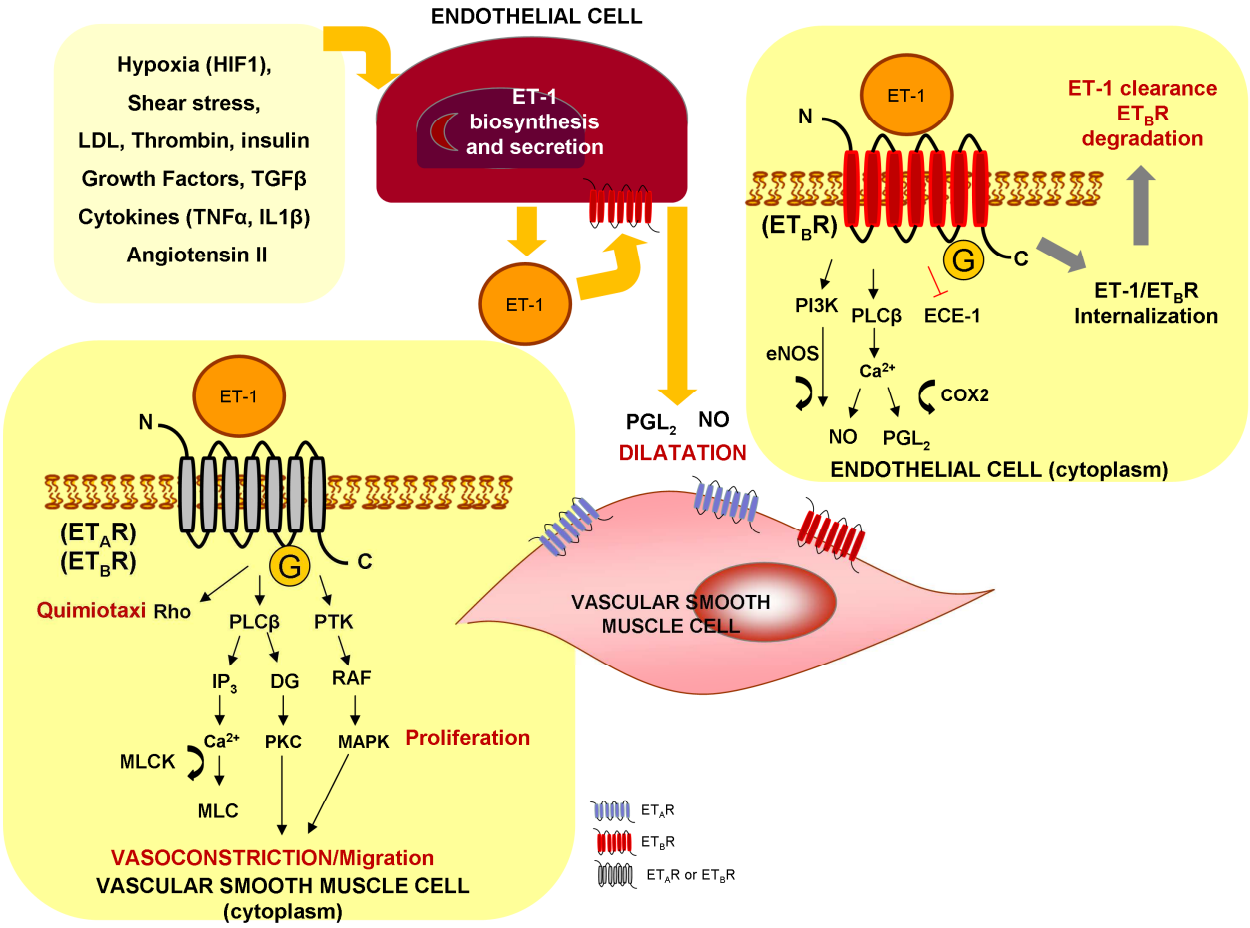

Figure17. Role of both ET-1 receptors (ET_AR and ET_BR) mediating signaling in the regulation of vascular tone. ET-1 biosynthesis and secretion by EC binds to VSMC ET_AR/ET_BR and increase vascular tone via G protein mediated Ca^{2+} dependent activation of MLCK (myosin light chain kinase) or by Rho kinase pathway activation of MLCP (Myosine light chain phosphatase). (PLCβ: phospholipase beta, IP3: inositol 1, 3, 4-trisphosphate, DAG: diacylglycerol, PKC: protein kinase C, PTK: (Protein tyrosin kinase), RAF/MAPK: Mitogen-activated protein kinase. ET-1 secreted by EC can also be recognized by ET_BR from EC which mediated signaling in the regulation of EC promoting NO and PGI2 (prostaglandin I2) release that will work as vasodilators on VSMC. The formation of NO can be driven either by PLCβ or through PI3K which both activated eNOs (endothelial nitric oxide synthase). The formation of PGL_2 is triggered by COX-2 (cyclooxygenase-2). Moreover, ET_BR promotes EC ET-1 clearance by membrane internalization and degradation. In addition ET_BR also inhibit ET-1 by inhibiting ECE. Different stimuli can induce ET-1 production in different cell types as labeled. Adapted from Levin *et al*. (1995),Horinouchi *et a*l. (2013) (*242, 261*) and Remuzzi *et al.* (2002) (*262*).

Endothelin in vascular remodeling and fibrosis

Although ET-1 is the most important vasoconstriction molecule it is also described that it is involved in the transformation of fibroblast to myofibroblast and in ETM (endothelial/epithelial to mesenchymal) processes which contributes in vascular remodeling and fibrosis. Fibrosis is characterized by the excess deposition of ECM plus remodeling. The fibrotic event is developed as a result of aberrant response to injury and persistent repair tissue that would induce

migration, proliferation and activation of myofibroblast differentiation (*263*). Importantly, ET-1 has been associated to fibrotic processes as a downstream mediator of TGFβ and PDGF promoting myofibroblast differentiation (*264*) and, as a consequence aberrant fibronectin and ECM deposition (*265, 266*).

Fibroblasts are usually localized in the connective tissue and are the main contributors of ECM deposition. In normal conditions, fibroblasts are in a quiescent phenotype although it can change after stimuli (i.e. vascular injury) as a contractile phenotype which is called myofibroblast. These cells are involved in normal wound repair although aberrant and persistent wound healing also contributes to extra deposition of ECM causing fibrosis in several tissues or vascular remodeling (*4*). The nature of the damage can be physical or chemical stimuli, or even as a consequence of proinflammatory cytokines or chemokines secreted by infiltrated leukocytes or even by the imbalance between vasoactive factors , NO and ET-1 production.

The mechanisms in which ET-1 triggers fibroblast to myofibroblast changes have been fully studied. Myofibroblast induced phenotype by ET-1 can be triggered by activation FAK (Y397) (*265*) (*220*). Moreover PI3K pathway (*267*) and MAPK (ERK) or G proteins (*268*) seems to be also involved. According to vascular remodeling, migration and invasion, protease secretion is also necessary for migratory cells. ET-1 also is involved in this process by inducing both production and secretion of proteases such as MMP2, MMP9 and increase the ratio between MMP and their inhibitor (TIMPS) turning fibroblasts into invasive phenotype (*244*). This is important process in solid tumor progression and metastasis, vascular remodeling and fibrotic diseases.

Maladaptive vascular remodeling in inflammation diseases of blood vessels leads to intimal proliferation and fibrosis, leading the lumen occlusion. ET-1 as a key mediator of this process is not completely elucidated (*4*). In the third project of the **results and discussion** section of this doctoral thesis, ET-1 effects on VSMC functions related to vascular remodeling and occlusion have been investigated.

Moreover ET-1 may also be involved in angiogenesis since it leads EC migration in autocrine manner (*269, 270*). This induction has been considered to be through ET_BR in cultured HUVEC (*271*). The same cells, cultured with ET-1 and seeded into Matrigel ^{TM} basement membrane increase their capacity of forming vascular cord-like structures indicating that ET-1 may be involved in angiogenesis process (*272*).

Endothelin involvement in disease

Although ET-1 is essential for controlling vascular tone in physiological conditions, its biosynthesis is stimulated by cardiovascular risk factors such as elevated levels of oxidized LDL cholesterol and glucose estrogen deficiency, obesity, cocaine use, hypoxia (ischemia), aging and procoagulant mediators such as thrombin, vasoconstrictors, growth factors cytokines, and adhesion molecules (*241*).

Aberrant ET-1 axis activation is associated to diseases such as pulmonary hypertension (*273*), cardiovascular disease, cancer (*244, 274*), atherosclerosis (*275*) vasospastic disorders, vascular inflammation (*276*) and fibrosis related diseases (*264, 265*) such as idiopathic pulmonary fibrosis and scleroderma (*277*) (*278*). Interestingly, the stimulated released of ET-1 by vasoactive agents such as thrombin is strongly increased in aged arteries, compared to endothelium from young arteries, a mechanism that may contribute to cardiovascular pathology in aging (*4, 279*). ET-1 axis is also common involved in solid tumor progression (ovarian, prostate, colon, breast, bladder and lung) in which ET-1 may induce proliferation, invasion and cell migration, resistance to apoptosis and stimulation of vessel formation (*244*).

ET-1 therapies and new approaches

The interest on the suppression of ET-1 axis has been gain intereste while gaining knowledge about ET-1 functions in non physiological conditions. For this reason, different ET-1 therapies have been tested in order to suppress ET-1-pathological functions.

Inhibitors of ET-1 synthesis include nitric oxide (NO), prostacyclin, atrial natriuretic peptides, and estrogens (*241*) have been proposed. Other approximations are the usage of ET-1 converting enzyme ECE-1 inhibitors although the identification of new mechanism contributing to mature ET-1 formation such as chymases or non-ECE MMPs limits the effectiveness of these drugs (*241*).

ET-1 partially mediates angiotensin (Ang) II–induced vascular changes *in vivo*. For this reason investigation of the effects of the angiotensin type 1 receptor antagonist losartan and the calcium channel blocker verapamil was used to diminish vascular reactivity and tissue ET-1 levels in aortas experimental rats (*280*). Although both antihypertensive agents lowered blood pressure and normalized endothelial function, only losartan prevented the increase in tissue ET-1 content, suggesting that angiotensin type 1 receptor antagonists but not calcium antagonists modulate tissue ET-1 *in vivo.* The inhibition of ET-1 with the usage of rennin-angiotenisin inhibitors or statins has also been tested in experimental animals (*280*).

Many pharmaceutical industries have been interested in the ET-1 system and research for ET-1 receptor antagonists in order to block ET-1 effects. The main important ET-1 recepetor inhibitor is **Bosentan**, which is a competitive antagonist of ET-1 at blocking both ET-1 receptors (ET_AR and ET_BR) althought it has slightly higher affinity to ET-1 receptor A than B. Another inhibitor of both ET-1 receptors is **Tezosentan**.

Moreover, selective antagonists for either ET_AR or ET_BR are also available. **BQ123** is a cyclopeptide which present a potent and selective antagonist activity against ET_AR and was firstly discobered by Ihara *et al.* in 1992 (*281*). In contrast, BQ788 is a potent and selective **ET_BR** antagonist (*282*). Other ET-1 receptor A selective inhibitors are **Ambrisentan, Atrasentan** and **Sitaxentan** among others.

Bosentan is the first orally active ET-1 receptor antagonist mainly used for the treatment of pulmonary arterial hypertension (PAH). In this disease, ET-1 receptors antagonists have been proven as effective anti-hypertensive drugs. These positive results may be caused by the special hypersensitivity that pulmonary circulation is sensitive to ET-1 regulation. Nevertheless Bosentan, has also been in trial for congestive heart failure, coronary-artery disease and scleroderma between others (*262*).

Moreover, both BQ123 and BQ788 are also in clinical trial for different disease related to vascular occlusion (www.clinicaltrials.gov) or in some cancers (*244*).

Nevertheless, new therapies involving biological molecular techniques such as anti-sense gene therapy may also be useful for the ET-1 blockade.

MMPs/TIMPs

Matrix metalloproteinases proteins (MMPs) family was identified in 1962 by Gross and Lapiere. MMPs are members of the metzincin group of proteases, which are named after the zinc ion and the conserved Met residue at the active site (*283*), It has been characterized 24 different human MMPs. Mammalian MMPs share a conserved domain structure that consists of a signal peptide, an amino-terminal pro-domain, a catalytic domain and a hemopexin carboxy-terminal domain that is important in determining substrate specificity and interactions with tissue inhibitors of metalloproteinases (TIMPs).

The pro-domain contains a conserved Cys residue that coordinates the active-site zinc to inhibit catalysis (*284*). When the pro-domain is destabilized or removed, the active site becomes available to cleave substrates (**Figure 18**). MMP2 and MMP9 also have fibronectin type II repeats, which mediate binding to collagens, inserted into the catalytic domain. Most of the MMPs are secreted proteins although also exist membrane type-MMPs (MT-MMPs) such as MMP14. MMPs were thought to function mainly as enzymes that degrade structural components of the ECM. However, MMP proteolysis can create space for cells to migrate, can produce specific substrate-cleavage fragments with independent biological activity, can regulate tissue architecture through effects on the ECM and intercellular junctions, and can activate, deactivate or modify the activity of signaling molecules, both directly and indirectly (*284-286*).

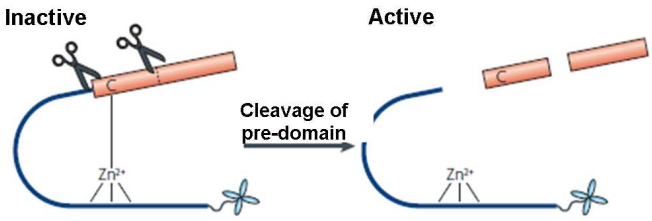

Figure18. Matrix metalloproteinases activation. Most of the MMPs are cell released inactive and different proteins must cleaved the pro–peptide into mature form which the active site becomes available for matrix degradation (*284*).

Most of the MMPs are secreted in a latent form and will be activated once they are released by other active MMPs. Even though, alternative mechanisms of action have also been observed, including functional intermolecular MMP complexes: MMP14 binds to tissue inhibitor of metalloproteinase-2 (TIMP2), which binds to pro-MMP2, thereby positioning it for activation by a second molecule of MMP14 (*285, 287*).

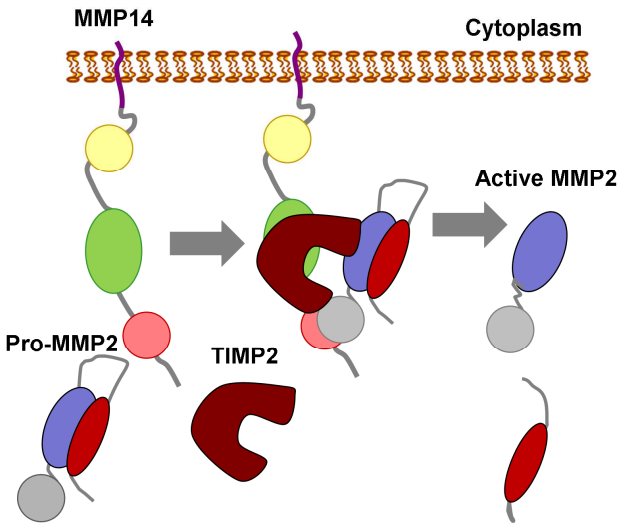

Figure19. MMP2 activation by MMP14 and TIMP2. Secreted pro-MMP2 need to interact with 1:1 TIMP and MMP14 in order to cleave pro-MMP2 into unfold and active MMP2. Adapted from Sternlicht and Werb (2001) (*285*).

MMP activity is blocked specific inhibitors, such as TIMPs. Four human TIMPs have been identified, which are anchored in the ECM or secreted extracellularly and bind MMPs 1:1 stoichiometrically (*284*).

Because their wide variety of biological functions, loss or uncontrolled function of MMPs and their inhibitors have been associated to several diseases including the following processes: blood vessel remodeling, inflammation and wounding, and bone modeling and remodeling (*284*).

2.5 Challenges in GCA

As previously explained either persistence of the inflammation or pathologic vascular remodeling are the main problems in GCA. For this reason there are several studies attempting to understand the pathological mechanism involved as well as the molecules related to this process but also to the disease.

Persistence of inflammation in GCA. Related molecules.

Molecules related to **leukocyte recruitment** and **amplification of cytokine cascades** have been investigated in order to amplify the knowledge of the mechanism involved in persistence of the inflammation in GCA.

Regarding to leukocyte recruitment, in GCA lesions has been observed that **P-selectin**, **ICAM-1, ICAM-2** and **PECAM-1** expression is induced by the *vasa vasorum* from the adventitia and highly expressed by the pathological microvessels from the intima-media junctions together with **VCAM-1** and **E-selectin**. Moreover, integrins type β2 (including **LFA1, MAC-1** and **gp150**) which are the receptors for ICAM-1 are highly expressed by leukocytes surrounding EC from the adventitial *vasa vasorum* and from the intima-media junction microvessels. In contrast, β1 integrin (**VLA-4**) which is a receptor for VCAM-1 is mostly limited to the EC from the adventitial *vasa vasorum*. Importantly, the treatment with GC does not affect to the the constitutively expressed molecules but diminished the expression of VCAM-1 and E-selectin (*48*). Moreover, soluble adhesion molecules have also been found overexpressed in GCA patients (*288*) even after one year of GC treatment (*52*). Interestingly, ICAM-1 has been found highly expressed in serum of GCA patient who relapses even after one year of GC treatment (*50, 52*).

Importantly **CCL2**, **MRP-8**, **S-100** are also overexpressed by GCA patients who relapse after GC treatment. To emphasize, CCL2, is clearly expressed by infiltrating leukocytes, VSMC and EC being stronger in granulomatous areas. Similar result is found with CCL2 receptor (CCR2) which is clearly expressed by leukocytes from the adventitia but also strongly by granulomatous areas from GCA lesions. CCL2 is also a chemoatactive molecule for EC, which may stimulate angiogenesis, and important mechanism for chronic inflammatory diseases. Importantly, CCL2 is associated to lower risk of ischemic complications (*289*). MRP8 and S-100 are molecules involved in the early recruitment of phagocytes (neutrophils and monocytes). MRP8 is also expressed by leukocytes located in the adventitia of GCA lesions in TA and also surrounding *vasa vasorum (289)*, which is thought to be the port of entry of leukocytes (*290*).

IL-33, a member of the IL-1 cytokine family, has recently been described as a novel activator of EC which promotes adhesion molecules and proinflammatory cytokine expression as well as angiogenesis in the endothelium (*291, 292*). IL-33 is expressed in GCA TA lesions but not by controls. Moreover, as well as its receptor **ST2**, IL33 is expressed by inflammatory mononuclear cells and EC from neovessels. Interestingly, IL-33 expression after GC treatment is similar to control arteries suggesting GC therapy modulation. This is an important finding, since IL-33 and its receptor may be involved in the earlier stages of the disease promoting angiogenesis,

vascular leakage and tissue infiltrating by inflammatory cells to the pathological artery which is essential for persistence of the inflammation in patients with GCA (*293*).

The subunit p19 of IL-23 is explored in this doctoral thesis as a new endothelial proinflammatory peptide. P19 contribute to ICAM-1 and VCAM-1 expression by EC through gp130 –STAT3 activation. This process seems to be crucial for leukocyte recruitment by EC as a port of entry of inflammation in GCA (see part one of the **Results section**)

As explained, immune response involved in GCA is either innate response or adaptive one. Moreover the interaction of different vasculature cell types and the infiltrating leukocyte may also amplify cytokine and chemokine release and consequently promote chronic inflammation. Several proinflammatory cytokines have been described to be associated to GCA.

In relation to Th subsets differentiation, both IFNγ and IL-17 have been explored in GCA lesions. Between Th1 related cytokines **IFNγ** is present in GCA lesions (*52, 85*) and induced by patients who relapse (*52*) together with **IL12p40** (*52*). IFNγ promotes the recruitment of macrophages to the injured artery during the first steps of the inflammation by promoting secretion of chemokines by EC or VSMC. Blocking IFNγ in *ex-vivo* model using TAB cultured in a three dimentional matrix suggested that blocking IFNγ diminishes macrophage recruitment by downregulating chemokine secretion ((*47*), **Additional data).**

According to Th17 differentiation, although **IL-17** cytokine is barely detected in serum, it is highly expressed at mRNA and protein levels by GCA lesions in all the entire TA. Interestingly, IL-17 is extremely reduced by GC treatment whereas patients who have strongest expression of IL17A in the origin of the disease, tend to experience less relapses and are able to reduce prednisone earlier than patients with weaker IL7A expression (*43*). The important finding is the observation that a subset of T reg cells which express FOXP3 are also able to express IL17A in tissue with active GCA (*43*).

Interestingly, IL-17A and IFNγ producing CD4+ Th1 cells were induced in PBMC from patients with active GCA even compared to controls or patients with remission. Remarkably**, IL-21** CD4+T producing cells were memory cells (CD45Ro+/CD27+) and were also associated to active GCA. Moreover, these cells correlated with the expansion of Th1 and Th17 cells. This was an important finding since Th1 and Th17 have already been associated to GCA pathology

by other authors and treatment with GC diminish more dramatically Th17 related genes than Th1 (*44*). For this reason, upstream mediator of Th1 or Th17 differentiation could be good targets for GCA treatment.

IL-32 has also been reported to be involved in the persistent inflammation of GCA (*294*). IL-32 is a Th1-related proinflammatory cytokine which is induced by IFNγ. It has functions in both innate and immune response and it is also expressed by EC. IL-32 is also associated to chronic inflammatory diseases such as rheumatoid arthritis (*295, 296*) or Crhon disease (*297*). Both mRNA and protein are highly expressed in GCA lesions of TA being expressed by leukocytes, VSMC and EC from the neovessels which provides strong evidence of pivotal role of IL-32 in the organization of the vascular inflammatory response. IL-32 is also accompanied by a strong overexpression of **IL-27** (p28 subunit) which is an inducer of Th1 differentiation inducing Th1 related cytokines such as IL-1β, and TNFα in monocytes or IL-6 in fibroblasts. Moreover, both IL-27 and IL-32 can be induced by innate response (TLR or NOD) and promote adaptive response, mostly Th1. For all these data, it is hypothesized that both IL-32 and IL-27 may participate by leading the induction and perpetuation of arterial inflammatory immune response. Nevertheless no association with GC treatment has been reported yet. Moreover IL-27 has been found involved in Th1 differentiation subsets in granulomatous diseases (*298*).

IL-35, a cytokine composed by Ebi3 (a subunit of IL-27) and p35 (a subunit of IL-12) has been explored in this doctoral as a cytokine expressed in GCA lesions. Moreover, the function of this molecule on VSMC is also explored in this section (see part 2 of the **Results section**)

Studies focused on the tissue expression of GCA related molecules have determined that the proinflammatory cytokines **TNFα, IL-1β and IL-6** (*2, 52*) are overexpressed in GCA TAB comparing to controls, being the granulomatous areas the higher areas where cytokine expression is found. Interestingly, TNFα, IL-1β, IL-6 expression is higher in patients with a strong systemic inflammatory reaction who require higher GC dose and longer duration of the treatment suggesting that these cytokines may be involved in vascular inflammation and persistence of the disease (*2, 52, 299*). Moreover, **IL-12p40** and **IFNγ** are highly expressed in the tissue of patients but also higher in patients who relapse in contrast to IL12p35. For this

reason, this response is thought to be associated to IL-23 cytokine instead of IL-12 being more interesting for the relapses the Th17 response (*52*). In fact, **IL-17** and also **p19** (the partner for p40 in order to form IL-23) are also overexpressed in patient who relapsed.

Interestingly, **TNFα**, **IL-6** and **IL-12p40** have been found highly expressed in serum of patient who relapses even after a long-term follow-up (*50, 52*).

Vascular remodeling in GCA. Related molecules.

Another important unresolved issue in GCA pathology is the vascular remodeling as a response to inflammatory injury which would promote the major complication in GCA. In this process, inflammatory infiltrate migration from the adventitia to the intima layer may promote loss of VSMC and also secretion of elastinolitic activity MMPs such us **MMP2**, **MMP9** and **MMP12** which degrade elastic layers and ECM (*300*). MMPs and their inhibitors have been also evaluated by different investigators in GCA disease (*300, 301*) (*302, 303*). Importantly, MMP9 (*304, 305*), MMP2 and **MMP14** proteolitic activity is higher in GCA lesions tan controls, by leukocyte surrounding the internal elastic membrane and also VSMC. Interestingly, pre-MMP2 but no other MMP tested is also expressed by VSMC (*300*). MMPs may be involved in leukocyte progression but also in vascular remodeling in GCA and related complications as aorta aneurism (*300*).

The mechanisms in which VSMC turn more migratory, proliferative and matrix deposition phenotype is still unknown but there's some molecules found in GCA lesion that are involved in this process such as **PDGF** (expressed by CD68 and VSMC) (*51, 306*) or **TGF-β** (*52, 85, 307*). PDGF induces VSMC ECM production, angiogenic (angiogenin) and chemoattractant (CCL2) factors and VSMC proliferation and migration (*289, 306*). Importantly, Imatinib mesylate (tyrosine kinase inhibitor used in the treatment of multiple cancers) strongly inhibits the PDGF-mediated response (*306*).

In GCA, the most frequent and devasting ischemic events occurs in territories supplied by carotid and vertebral artery branches, and include ischemic optic neuritis and stroke. About 15-20% of patients also develop an occlusive vasculopathy involving large-size and medium size vessels, particularly the aorta and limbs. Branches of the ophthalmic artery, particularly posterior ciliary and cilioretinal arteries supplying the optic nerve and retina may be directly

involved by typical GCA lesions. The most common ischemic complication in GCA is partial or totally visual loss appearing in 15-20% of patients. Transient visual loss (*amarurosis fugax*) may be due to the critical blood flow in the small arteries supplying the optic nerve (*308*) (*66*) suggests participation of vasospastic phenomena. For this reason the endothelin system (including **ET-1,** both receptors **ET_AR** and **ET_BR** and **ECE-1**) was explored in GCA and was found induced in GCA tissue. Moreover, serum ET was increased in patients with ischemic complications (*276*).

Using TA cultured on Matrigel ^{TM} it has been observed that some of the vascular remodeling and fibrosis related molecules are not dimished by the usage of glucocorticoids (Dexametasone) (*82*).

Therapies addressed to inactivate pathways involved in pathological vascular remodeling are key points of interestes in GCA treatment. Consequently, in this thesis we investigated the role of ET-1 in vascular remodeling associated to GCA as well as the effects of ET-1 receptor antagonist (BQ123 and BQ788) on responses related to vascular occlusionin order to explore potential therapeutic interventions aimed to reduce ischemic complications in GCA (see part 3 of the **Results section**)

Hypothesis

Persistent chronic inflammation and uncontrolled vascular remodeling are important challenges in GCA.

Regarding to persistence of the inflammation we hypothesized:

1) The port of entry of inflammatory cells to GCA-involved arteries is the EC from the adventitia *vasa vasorum* or from the neovessels which are formed in the entire pathological artery. Proinflammatory molecules (i.e. cytokines, chemokines) secreted by the inflammatory infiltrate may trigger EC phenotype changes to promote persistent leukocyte recruitment

> **Hypothesis 1**
>
> The subunits p19 and p40 (components of IL-23 cytokine) are differentially expressed in EC. While p19 can be induced by proinflammatory stimuli, p40 is not detected in EC. P19 peptide may have proinflammatory functions independent from p40 in inflamed EC. P19 may contribute to the persistence of inflammation by promoting EC phenotypical changes (i.e. overexpression of adhesion molecules or chemokines). This process may be contribute to leukocyte recruitment through *vasa vasorum* in *GCA*

2) Inflammatory infiltrates may interact with vascular wall components and induce a myofibroblastic or proinflammatory phenotype in VSMC
3) Either cell-cell interaction mediated by integrins (PBMC) and adhesion molecules (VSMC) or soluble molecules (cytokines) might be involved in VSMC proinflammatory phenotype changes.
4) Since dissociation in the expression of of p35 and p40 (conforming IL-12) has been observed in GCA lesions, the other known p35 partner (Ebi3) may be expressed by vascular components to conform the IL-35 cytokine under inflammatory conditions.
5) IL-35 may be produced by infiltrating leukocytes in GCA and may contribute to develop a proinflammatory phenotype in VSMC.

Hypothesis 2

The IL-12 subunit p35 (highly expressed by VSMC) may also contribute to vascular inflammation in GCA while interacting with Ebi3 in order to form IL-35 cytokine. Moreover, IL-35 may contribute to the persistence of the inflammation in GCA by inducing a proinflammatory phenotype in VSMC.

Regarding to pathological vascular remodeling present in GCA we hypothesized:

6) Since ischemic complications affects about 15% of patients with GCA and ET-1 has found expressed in tissue and increased in serum from patients with ischemic complications, ET-1 and related molecules may have an important role in vascular remodeling and fibrosis leading to vascular occlusion
    - ET-1 may promote VSMC migration and MMPs secretion.
7) Cell migration is a complex process in which turnover of focal adhesions is essential. In migratory cells these molecules trigger cell migration as a response of the interaction to ECM through integrins. ET-1 may prone cell migration by a downstream mechanism involving FAK, Src and PI3K pathways.

Hypothesis 3

Vascular remodeling leads vascular occlusion and subsequent ischemic complications in GCA. The ET-1 system, highly expressed in tissue and sera from ischemic GCA patients, may contribute to GCA vascular occlusion not only by promoting vasoconstriction but also by promoting VSMC migration and ECM deposition. ET-1 may trigger this response by activating migration- related kinases such as FAK, Src and PI3K.

Aims of the study

The main aim of this doctoral thesis is to generate new knowledge about the underlined challenges in GCA (persistence of the inflammation and pathological vascular remodeling) on the basis of the previously formulated hypothesis

1. Regarding to the first hypothesis that **p19 could be involved in the phenotypical differentiation of EC from the *vasa vasorum* promoting leukocyte recruitment**, we designed the following objectives:

- To determine which proinflammatory related molecules induce p19 in primary cultures of EC such as HUVEC or dermal EC.
- To evaluate p19 secretion in non-producing p40 primary EC.
- To analyze p19 functions (independent form p40) in EC studying leukocyte recruitment related molecules such as adhesion molecules (ICAM-1, VCAM-1 and PECAM-1) or chemokines in p19-expressing-HUVEC.
- To explore p19 endothelial receptor and downstream intracellular signaling pathways activated by p19 in p19-induced-HUVEC considering that these cells don not produce neither p40 nor IL-23R.
- To confirm intracellular p19 association with gp130-p19 and subsequent activation of STAT3 as a mechanism triggering p19 proinflammatory functions.
- To confirm this association in temporal artery biopsies from patients with GCA

2. To test the second hypothesis proposing that **IL-35 could be a new cytokine contributing to persistent vascular inflammation in GCA by inducing pronflammatory phenotype in VSMC** we established the following objectives :

- To determine which cell types produce p35 and its IL-35 conforming partner subunit Ebi3 in temporal arteries from patients with GCA and control arteries.
- To explore the soluble molecules and cell-cell interactions involved in Ebi3-p35 mRNA induction or mature IL-35 secretion by VSMC. To assess this point we have used co-cultures of isolated CD4T cells or macrophages together with VSMC.
- To investigate proinflammatory functions of recombinant IL-35 on VSMC (i.e. expression of adhesion molecules, IL-6, IL-1β among other cytokines).

3. To confirm the third hypothesis, that **ET-1 promotes migration of VSMC by activating kinases involved in focal adhesion turnover**, we have proposed the following objectives

- To determine expression of ET-1 and its both receptors (ET_AR and ET_BR) in GCA-involved and control arteries
- To explore bidirectional modulation of ET-1/ ET-1 receptor expression by VSMC and PBMC in co-culture.
- To explore the effects of ET-1 on VSMC cytoskeleton reorganization and migration.
- To explore ET-1 receptor downstream signaling pathways involved in ET-1 induction of VSMC migration as well as the effects of ET-1 receptor blockade in this process.
- To test ET-1 and ET-1 receptor inhibitors (BQ123 and BQ788) on myointimal cell outgrowth from temporal arteries form GCA patients cultured ex-vivo on Matrigel ^{TM}.

Material and methods

5.1 Cell Culture

Temporal artery biopsy culture on Matrigel™

Serial, 1mm thick sections from temporal artery biopsies, obtained for diagnostic purposes, are placed onto ice-cold reconstituted basement membrane Matrigel™ (BD Biosciences) and cultured in RPMI-1640 medium (Lonza, Verviers, Belgium) 10% fetal bovine serum (FBS) (Gibco, Life Technologies, Waltham, Massachusets, USA), supplemented with 2mM of L-Glutamine 200mM (Gibco), 50 µg/ml of Gentamicin (Braun, Melsungen, Germany) and 2,5 µg/mL of Amphotericin B (Life Technologies) and cultured at 37ºC in 5% CO2.

Primary cultures of VSMC

VSMC develop from the TA explanted sections in Matrigel™ cultured in Dulbecco modified Eagle medium (DMEM) (Lonza) within 1 week and reach confluence in 3 weeks. Cells are then released with 0.05% trypsin/ethilenediaminetetraacetic acid (EDTA) (Invitrogen, Life Technologies), transferred to uncoated flasks, and split 1:2 upon confluence to get the primary cultured of VSMC .The study is approved by the institutional review board of the Hospital Clínic of Barcelona and all patients signed an informed consent. Cells have been characterized by flow cytometry (*306*) , western blot and immunofluorescence using αSMA and type I and III collagens by quantitative real time reverse transcriptation (qRT-PCR).

Other cell types obtaining and culture

Peripheral blood mononuclear cells (PBMC)

Peripheral Blood Mononuclear Cells (PBMC) are obtained by density gradient centrifugation using Lymphoprep ™ (Axis-Shield, Oslo, Norway) in sterile conditions. Fresh blood is collected from volunteers or patients using EDTA tubes (Vacutainer EDTA tubes) and diluted 1:1 with PBS (1X). Ficoll-Lymphoprep is added at the same volume as blood into a 50ml conical centrifuge tube. Diluted blood is added carefully onto Ficoll (avoiding mixing). It is centrifuged at 660xG, 4ºC for 20 minutes (brake =0). With a Pasteur pipette the mononuclear layer is transferred into another centrifuge tube containing 20mL of PBS (1X) and it is then washed by centrifuging for three times at 350xG for 10 minutes (brake =9).

Negative isolation of CD4+T cells and CD14+ from PBMC

Dynabeads Untouched Human CD4+T Cell kit (Invitrogen) is used for isolate pure and viable CD4+T from PBMC by negative isolation. The Kit consists in a mixture of monoclonal mouse IgG antibodies against the non-CD4+T cells in order to deplete CD8+ T cells, B cells, NK cells, monocytes, platelets, dendritic cells, granulocytes and erythrocytes but collect CD4+T. **Dynabeads Untouched Human monocyte kit** (Invitrogen) is used for isolate pure and viable CD14+ (monocytes) from PBMC by negative isolation. The kit contains biotinylated monoclonal antibodies against T cells, B cells, NK cells, dendritic cells, granulocytes and erythrocytes.

$5x10^7$ PBMC (obtained as explained in section 3.2.1) are diluted in 500 µl of isolation buffer (containing 1X phosphate buffer salin (PBS) supplemented with 0.1% bovine serum albumin (BSA) and 2mM EDTA) and 100 µl blocking reagent (gamma globulin in 0.9% NaCL) for monocytes or FBS for CD4+T isolation is added together with the corresponding antibody mix. After incubation for 20 minutes at 2-8 ºC, either monocytes isolation or CD4+T isolation samples are washed by adding 4mL of isolation buffer and centrifuge at 350xG for 8 minutes at 2-8ºC. After discarding the supernatant, each sample is incubated with high rotation at 2-8ºC (monocytes) or 18-25ºC (CD4+T) for 15 minutes with the corresponding pre-washed dynabeads (500µl of dynabeads plus 500µl of isolation buffer). Samples are then resuspended with 4ml of isolation buffer and tubes are placed in a magnet for 2 minutes and supernatants contained either the untouched monocytes or the untouched CD4+T are placed into a new and sterile tube. Both kits allow getting isolated cell types in perfect shape for any functional assay and application. The protocol for both kits is followed as described in the manual provided by the manufacturers. Cell purity is analyzed by flow cytometry.

Co-culture of CD4+T cells, monocytes (CD14+) or PBMCs with VSMC (Figure 20)

VSMC are seeded at 90% confluence onto 6well plate and cultured with DMEM (10X FBS) overnight. PBMCs or untouched CD4+T cells or monocytes are counted using *Neubauer Chamber*. Media from the VSMC is replaced by 1 million isolated CD4+TCells or CD14+ in 10XFBS RPMI (Lonza). The co-cultured situations are compared by situations containing only VSMC, PBMC, CD4+TCells or CD14+. After 24, 48 and 72 hours supernatants are collected and RNA and Protein are extracted as explained bellow. Different cell populations of the co-culture are obtained and processed separately: Leukocytes that have not attached to the VSMC

are obtained by centrifuging the supernatants at 1000xG. Leukocytes that have been attached to VSMC are isolated by rinsing the wells with cold Versene (Invitrogen). VSMC are released using 0.05%Trypsin-EDTA (Invitrogen).

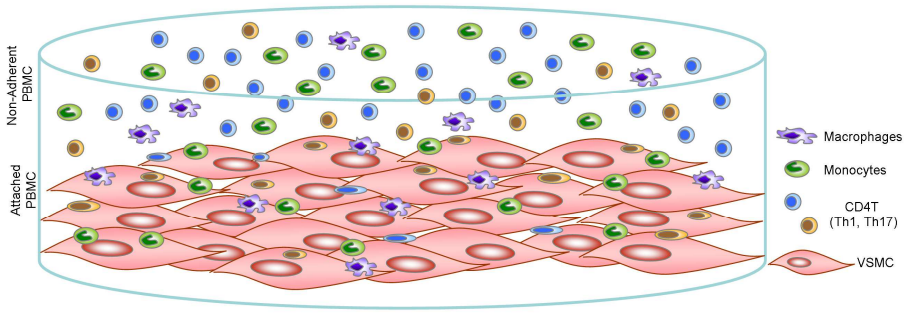

Figure20. PBMC-VSMC co-culture is represented.

HUVEC (Human umbilical vein endothelial cells) culture

HUVEC are cultured in RPMI (Lonza) supplemented with 20% of FBS (Gibco), 100mg of Endothelial Cell Growth Supplement (ECGS) (Collaborative Biomedical Products), 2500 units of Sodium Heparin (Rovi), 2mM of L-Glutamine (Life Technologies), 100 units/mL of Penicilin/Streptomicin (Gibco) , 2.5 µg/mL of Amphotericin B (Life Technologies) and 50 µg/ml of Gentamicin (B-Braun). HUVEC are cultured at 37ºC in 5% CO2 in 0.1% gelatin pre-coated 75cm^2 flasks with 0.1% gelatin (Bio-Rad Laboratories, Hercules, CA, USA) and split 1:4 before reach confluence .

5.2 Flow cytometry

After CD14+ and CD4+T negative isolation from PBMC, cells were counted and stained to test the efficiency of the isolation. Isolated cells were centrifuge at 400xG for 10 minutes and resuspended with 2% FBS in PBS (1X) for 2x10^6 cells/ml. 2µg of antibody for each 0.5x10^6 is calculated as suggested by the manufacturers. In this case, 0.1x10^6 cells are counted and diluted in 100µL of 2%FBS in PBS (1X) plus the corresponding volume of the conjugated antibody and incubated 30 minutes at 4ºC. All the antibodies are purchased from Invitrogen. After 30 minutes of incubation, tubes are filled with 1ml of 2%FBS and PBS (1X) and centrifuge

5 minutes at 1500xG. Supernatant is discarded and cells are resuspended with 200µl of 5% PBS.

Primary Antibodies (human)

Invitrogen : CD3+-FITC and CD14+-PE (mouse monoclonal)

BD Pharmigen : IgG1-FITC or IgG1-PE

5.3 Quantitative real-time reverse transcription (RT)-PCR

RNA is extracted from cultured VSMC, PBMC, CD4+T, CD14+ or HUVEC using TRIzol Reagent-Chloroform-Isopropanol (Invitrogen). RNA is resuspended with H_2O DEPC (Ambion, Life Technologies) and concentration is quantified using Quawell Q3000 UV spectrophotometer (Quawell Technology Inc.). Total RNA (1µg) is then reverse transcribed using High Capacity cDNA Reverse Transcription kit (Applied Biosystems, Life Technologies). Genes are measured by quantitative real-time RT-PCR with specific TaqMan gene expression assays (Applied Biosystems). Fluorescence is detected with an ABI PRISM 7900 Sequence Detection system and results re analyzed with the Sequence Detection Software version 2.3 (Applied Biosystems). All samples are normalized to the expression of the endogenous control GUSb. Comparative threshold cicles (C_t) method is used to assess the relative gene expression.

Human Taqman Gene expression probes

IL23p19, IL12p40, ICAM-1, VCAM-1, PECAM-1, CXCL9, CXCL10, CXCL11, GAPDH, ET-1, ET_AR, ET_BR, MMP2, MMP9, MMP12, MMP14, TIMP1 and TIMP2, IL12A (p35), Ebi3, IL27p28, IL17, IL10, IL6, IL1β, TNFα, IFNγ, gp130, IL12Rβ2 and Gusb

5.4 Protein detection in cell lysates

Immunoblotting

Cell lysates are obtained using modified radioimmunoprecipitation assay (RIPA) buffer supplemented with protease inhibitors (Boehringer, Mannheim, Germany), NaF (50mM), PMSF (1mM), protinine, leupeptine, pepstatine (1ng/ml) and orthovanadate (2mM) (Sigma-Aldrich, St. Louis, MO, USA). Protein is quantified using *BCA™ Protein Assay Reagent* A and B in a 50:1 proportion (Pierce, Thermo Fisher Scientific, Waltham, Massachusets, USA). A known concentration BSA standard curve is used to extrapolate the sample protein concentration.

Plate is incubated 30 minutes at 37ºC and the lecture is done using absorbance at 560nm (read at 620nm, if not possible). Twenty µg of protein per condition are resolved on 8% or 10% reducing sodium dodecyl sulfate (SDS)–polyacrylamide electrophoresis gels (125V 35mA) with the buffer 1X:25mM Tris Base, 192 mM Glycine, 0,1% SDS (w/v), ph 8.3. After electrophoresis, the gel is blotted at room temperature onto nitrocellulose membranes (Invitrogen) using the 10X buffer containing (0,25M Tris base, 2M glycine (30,25g + 144,25g Gly en 1L). Blocking is performed by incubating the membrane one hour at room temperature with Tris Buffer Saline with 0.1% Tween (50mM Tris (ph 6.8), 150mM NaCL) (TBST1X) with a 5% of Milk. Immunodetection is performed by incubating primary antibodies (diluted 1:100 or 1:500 following the manufacturers recommendations in TBST1X 5%BSA) at 4ºC overnight. After primary antibody incubation, three washes should be done with TBST1X followed by 1hour incubation with secondary antibody (1:2000 in TBST1X 5%BSA).

Chemiluminescence signal is measured with the LAS-4000 imaging system (Fujifilm Corporation, Tokyo, Japan) after incubating for 2 minutes the membrane with enhanced chemiluminescence (ECL) (Pierce, Thermo Fisher Scientific).

Image analysis and quantification is done by using even Image Gauge or Image J software.

Primary antibodies (human)

Chemicon (MD Millipore Billerica, MA, USA): MMP14 (rabbit polyclonal)

Cell Signaling (Danvers, MA, USA): p44/42 MAPK (Erk1/2), p-Src (Y416), Src, p-FAK (Tyr397 and Tyr925), total AKT, ICAM-1 (rabbit polyclonal), p-AKT (Ser473), p-p44/42 MAPK (ERK1/2), (Tr202/Tyr204), NF-κB p65, NF-κB p-p65 (Ser536), p-STAT1 (Y701), p-STAT3 (Y705), p-STAT4 (Y693), (rabbit polyclonal), STAT1, STAT3, STAT4 (mouse monoclonal),

Santa Cruz (Dallas, TX, USA): FAK (Rabbit polyclonal), laminB (mouse monoclonal)

Abcam: β-actin (rabbit monoclonal), alpha smooth muscle actin (mouse monoclonal) human

Sigma-Aldrich: IL23p19 (rabbit polyclonal), αTubulin (mouse monoclonal)

R&D Systems: IL-23 p19 (goat polyclonal), VCAM-1 (sheep polyclonal and mouse monoclonal), gp130 (mouse monoclonal)

BD-Pharmingen: CD31/PECAM-1 (mouse monoclonal)

Merck Millipore (Billerica, Massachussets, USA): gp130 (rabbit polyclonal)

Secondary Antibodies

Anti-rabbit IgG HRP-linked (Cell Signaling), goat anti-mouse IgG (HRP conjugate) (Biorad) and donkey anti goat IgG-HRP, donkey anti sheep IgG-HRP (Santa Cruz).

Immunoprecipitation

Protein extracts of cells (HUVEC or VSMC) are prepared in lysis buffer containing 10mM Tris-HCL (pH=7.5), 150mM NaCl, 0.2% NP-40 (Abcam), 1mM NaF, 1mM EDTA, 10% glycerol, Complete protease inhibitor cocktail (Roche Diagnostics, Basel, Switzerland), 2mM of sodium orthovanadate (Sigma-Aldrich) and 1µg/mL pepstatin A (Sigma-Aldrich), leupeptin hemisulfate salt (Sigma-Aldrich) and aprotinin (Thermo Scientific). Primary antibodies are individually incubated (4 µg) with washed Protein G Dynabeads (50 µl; Life Technologies) and incubate 10 min at room temperature. After magnet separation the antibody/beads complex is added to the cell lysates (500 µg) followed by incubation (18 hr at 4°C) with rotation. Beads/antibody/protein complexes are recovered by magnetic separation. Target antigen is eluted by heat treatment (10 min at 70 °C).

Primary antibodies (human)

Merck Millipore: gp130 (rabbit polyclonal)

R&D Systems: IL-23 p19 (goat polyclonal)

Nuclear and cytoplasm protein extraction

Nuclear and cytoplasm fractions are obtained from VSMC cultured on 6 well plates previously washed with cold PBS 1X to discard *debris* and albumin from the medium. Attached cells are obtained with scrapper and collected by centrifuging at 4ºC during 5 minutes at 1000rpm. P*ellet* obtained is ressuspended with Buffer I (1 mL de 1 M Hepes, pH 8.0 , 150 µl de 1 M MgCl2 ,1 mL de 1 M KCl,100 µl de 1 M dTT raised with dH2O up to 100 mL) supplemented with proteases and phosphatases inhibitors as previously described. Samples are ice incubated for 15 minutes and NP40 1% is added before vortex briefly. Samples are then centrifuged at 12.000 rpm for 5 minutes at 4ºC and supernatant are collected as a cytoplasm fraction. Pellets are resuspended with *Buffer* II (2 mL 1 M Hepes pH 8.0 ,150 µl 1 M $MgCl_2$,25 mL glycerol ,42 mL 1 M NaCl,40 µl 0.5 M EDTA, 100 µl 1 M DTT raised with dH2O up to 100 mL) supplemented with protease and phosphatase inhibitors.

5.5 Assessment of protein secretion

Immunoassay

ELISAs (Enzyme-Linked ImmunoSorbent Assay) is an assay used to quantify the protein concentration in different samples of cell supernatant, serum or plasma. In this study, cell supernatants are incubated into a microplate which has been pre-coated with monoclonal antibody against the target molecule. Standard (recombinant molecules in a specific concentration) is used to obtain the standard curve. The present molecules would be attached to the immobilized antibody in each well. Unbounded molecules are washed and enzyme-linked polyclonal antibody against the target molecule is added in each well. More washes are done in order to avoid inespecificity. Substrate solution is added to get colorimetric signal proportional of the amount of the target molecule present in each sample. Stop solution is added before get the absorbance at 450 nm using an absorbance microplate reader (Multiskan Ascent, Thermo Scientific).

Immunoassay kit (human)

ET-1, CXCL9, CXCL10, CXCL11, IL-6 Quantikine ELISA Kit (R&D Systems, Minneapolis, MN, USA), p-gp130 sandwich ELISA (R&D Systems), IL1β and IL-35 (USCN life science Inc., Wuha, China), IL-23p19 (Abcam, Cambridge, UK)

TCA/DOC cell supernatant precipitation

For supernatants precipitation, TCA (trichloroacetic) and DOC (sodium deoxycholate) have been used. Cell supernatants must be centrifuged and filtered before freezing in order to replace unattached cells. The supernatants (about 1 o 2ml) are placed into chilled centrifuge tubes and 1/10 of the total volume of DOC (0, 15 %) is added into each tube. After addition of DOC, each tube is vigorously centrifuged and incubated for 15 minutes at 4ºC. After incubation 1/10 of the initial total volume of pre-chilled TCA (72%) is added to each corresponding tube, vortex vigorously and incubate again during 15 minutes at 4ºC. Centrifuge at high speed (>12.000G) is then performed for 5 minutes at 4ºC. Supernatant is removed and pellet is then washed twice with cold acetone (previously stored at -20ºC) by centrifuging the samples at >12.000G for 5 minutes at 4ºC. After centrifugation, the supernatant is again discarded. If the pellet obtained is large, sonication can be performed after ressuspend the pellet with RIPA or the corresponding component for subsequent protein assay.

Gelatin zymography

Gelatin zymography is an eletrophoretic technique used to detect metaloproteinases (MMP) on serum free cell supernatants or cell lysates. Cells are cultured with serum-free DMEM in the presence or absence of different dose and times of the molecules analyzed. After incubation, cell supernatants are collected, centrifuged and stored at -80ºC. 100µL of each supernatant is then subjected to SDS-PAGE through 10% polyacrylamide gels copolymerized with 0.2 g/mL gelatin (Bio-Rad Laboratories). Gels are washed with 2.5% Triton-X-100 (Bio-Rad), rinsed with 10 mmol/L and ph=8 Tris (*Trizma base* from Sigma-Aldrich) and incubated overnight at 37°C in 50 mmol/L Tris, 5 mmol/L $CaCl_2$, and 1 µmol/L $ZnCl_2$. Gels are then fixed and stained with 0.2% Coomassie blue (Sigma-Aldrich). After distaining several times with 7% solution of acetic acid, MMP signal is quantified exposing the gel into light using LAS-4000 imaging system (Fujifilm Corporation, Tokyo, Japan)

5.6 Cell proliferation Assay

In order to evaluate cell proliferation, cells must be subconfluently seeded (for VSMC, usually 4000 cells per well) on 96-well plate (Nunc, Roskilde, Denmark) and serum starved for 24 hours and afterwards medium is replace by 1XFBS DMEM fresh medium or supplemented with the molecules that are wanted to evaluated. At several time-points, usually every 24 hours during 7 days, cells are fixed and stained with 0.2% crystal violet (Sigma-Aldrich) in 20% methanol for 20 min. Wells are washed, air-dried, and solubilized in 1% sodium dodecyl sulfate (SDS). Optical density is measured with a plate reader (Multiskan Ascent, Thermo Scientific) at 620 nm wavelength. Quadruplicates of each conditioned are performed.

5.7 Adhesion assay

Leukocyte /VSMC adhesion assay

Confluent monolayer of cells was generated in 96-well plates (5.000 cells per well) and half were treated with the tested molecule (rIL-35) for O/N. Human PBMC were isolated from the peripheral blood of volunteer donors and resuspended in serum-free RPMI medium to get 100.000 cells per well and co-cultured onto the pre-washed VSMC monolayer from 30 to 90 minutes at 5% CO_2 at 37ºC. After removal of non-adherent cells and washing (3 times in

1XPBS), 100 µl of crystal violet solution is added to each well (dried O/N) and lysate with 100µl of SDS (10X) per well. Absorbance is measured at 620 nm. The results are expressed as mean relative absorvance (±SEM of quadruplicate cultures).

Leukocyte /HUVEC adhesion assay

Leukocyte adhesion to endothelium is evaluated using CytoSelect Leukocyte-Endothelium Adhesion assay kit (Cell Biolabs Inc.), following the manufacturer's instructions. Confluent monolayers of vector only or p19-transduced HUVEC are generated in 96-well plates pre-coated with gelatin by 3-day HUVEC (25.000 cells/well) culture. Human PBMC isolated from the peripheral blood of volunteer donors ($1x10^6$ cells/ml), are labeled with LeukoTracker™ solution (1 hr incubation at 37ºC). After washing and suspension in serum-free medium, the labeled PBMC ($2x10^5$ cells/well in 200 µl) are incubated onto the pre-washed HUVEC monolayer (1.5 hr at 37ºC). After removal of non-adherent cells and washing 3 times in wash buffer, 150 µl lysis buffer (from kit) is added to each well (10 min incubation with shaking). Fluorescence in the supernatant (100 µl) is measured at 480/520 nm. The results are expressed as mean relative Fluorescence Units (±SD of triplicate cultures).

5.8 Migration assays

Transendothelial migration assay

Transendothelial migration assay is performed by using either control HUVEC or p19-infected HUVEC which are seeded (40.000 cells/well) onto the membrane (pre-coated with 0.1% gelatin) separating the top from the bottom chamber of transwells (5µm pore size; 96-well plates; Costar, Fisher Scientific) to generate a monolayer. Once formed, the monolayer is incubated overnight in complete HUVEC medium alone or with LPS (1 µg/ml) or TNFα+ IFNγ (20ng/ml each). Transendothelial migration of PBMC ($1x10^6$ cells/well of PBMC is added per well) is then carried out in RPMI 1640 medium with 0.5% BSA over 6 hour incubation at 5% CO_2 at 37ºC. Viable cells (using *Trypan Blue,* Life Technology) in the lower chamber are collected and counted using *Neubauer* chamber. The results of triplicate cultures are expressed as means (±SD).

Cell Migration Assay (Boyden Chamber)

Cell migration is measured in 48-well microchemotaxis *Boyden Chamber* using the specific pore polyester filters (Poretics, Osmonics Inc., Minnesota, USA) depending on the cells that are being evaluated. For VSMC pore size used is 10µm but for leukocyte is 5µm.

The number of cells also depends on the cells used. In this case, 5000 VSMC and 125.000 leukocytes are used per well. Stimuli supplemented or fresh DMEM (1x FBS) is added either in the bottom wells of the chamber or in the upper ones together with the cells depending on the assay. After 6 hours of incubation in 5% CO_2 at 37ºC, cells are removed from the upper surface and filters are fixed for 10 minutes at room temperature with methanol (Panreac) and stained with hematoxylin for 30 minutes at room temperature.

Slides are then mounted with mounting medium (Merck, Kenilworth, New Jersey, USA) and dry overnight and each stained pore represent one migrating cell. Four randomly selected fields per well are counted under a microscope at 20x magnification. Bars represent number of migrating cells (mean and SEM).

Scratch wound-healing assay

Cells (VSMC) are seeded at 80% confluent onto a 0.1% gelatin (Bio-Rad Laboratories) precoated 12 well plate and cultured overnight 5% CO_2 at 37ºC. One scratch per well is done using a sterile 200µL tip. Cells are then rinsed with PBS 1X to release debris and replaced with fresh DMEM 10XFBS supplemented with 50mM Hepes (Sigma-Aldrich) with or without the corresponding stimuli. Three pictures per well are automatically taken using phase contrast microscope (Leica Microsystems, Heildelberg, Germany) every 15 minutes during 24 hours. After 10 hours of culture, medium can be replaced by fresh one with the corresponding additives. Image J software (Wayne Rasband, Bethesda, Maryland, USA) is used to measure the lengths of each wound. 10 lengths are measure in each image to get multiple values. Bars represent percentatge of wound or scratch closure for each condition (mean and SEM).

VSMC outgrowth from temporal artery biopsies cultured on Matrigel ™

Temporal artery sections obtained from 3 untreated patients with biopsy-proven GCA or with negative artery are cultured on Matrigel™ in the presence or in the absence different molecules suggested to be tested. Daily photographs are taken from day 3 to day 17. Outgrowth of VSMC is scored by two investigators blinded to the conditions tested, as follows: 1=visible outgrowth of

scattered cells; 2=cells growing from the entire ring; 3=cells expanding at least two times the length of 2; and 4=cells covering the entire surface of the well. Agreement is achieved in 96% of measurements and each score is then represented in a graph.

5.9 Transient transfection of adherent cells (VSMC)

Before transfection, VSMC are seeded onto 12 well plates overnight. Complete DMEM medium is replaced by complete DMEM without antibiotics at least 6 hours before transfection is performed. Lipofectamin 2000 Reagent (Invitrogen) is used for transient transfection of VSMC (4µL of Lipofectamin 2000 + 100µl of serum-free Optimem medium for situation), using 2 µg of cDNA diluted on 100µl of medium Optimem (Gibco) for each well. Diluted DNA and Lipofetamin 2000 (Invitrogen) are mixed and incubated for 30 minutes at room temperature before adding to each well. After 6 hours of incubation at 5% CO_2 and 37ºC, the medium is replaced by 10X FBS DMEM with antibiotics. Transfected cells are used for experimental procedures 48 or 72hours post-transfection, all of them compared with VSMC transfected with the empty vector pcDNA3 (MOCK). Efficiency of transfection is verified both detecting total transfected protein by western blot or by immunofluorescence using pEGFP-C3 which contains a green fluorescent protein (GFP).

5.10 Lentiviral vector production, purification and HUVEC infection

Third generation lentiviral vectors are used for overexpression of the target protein (IL-23p19) in HUVEC. In order to obtain the lentiviral vectors, 293T cells are cultured with 10X DMEM onto 10 cm plates until achieving confluence. Complete 10X DMEM medium is replaced by complete DMEM without antibiotics 24 hours before being transfected. These cells are cotransfected with the 3 packaging plasmids and either the lentiviral vector containing the cassette that is desired to be overexpressed or the control. The packaging plasmids consist on: a CMV packaging construct expressing the *gag* and *pol* genes (pMDL), a Rous sarcoma virus construct expressing *rev (pRev)*, and a CMV construct expressing the *VSV-g* envelope (pEnv). The lentiviral vector for expression of human IL-23 p19 is purchased from GeneCopoeia (cat. No. EX-U1167-Lv105); and the pLVX-Puro vector is used as control. Both plasmids contain puromycin resistance for further selection of the infected cells. The final DNA amount that is

needed to transfect for each plasmid is: 3,5 µg for the pEnv, 2.5µg for the pRev, 5 µg for the pMDL and 12µg for the lentiviral vectors. After that, 1.5 ml of Optimem medium (serum free and without antibiotics) per each 10cm plate with the calculated volum for each packaging plasmid plus de lentiviral plasmid (either containing the IL23p19 cassette or the empty one) is prepared. In another tube, Lipofectamin 2000 dilution (60µL of Lipofectamin and 1.5ml of Optimem for each 10cm plate) is incubated. After 5 minutes incubation at room temperature, Lipofectamin 2000 and the diluted vectors are mixed and incubated together for 20 minutes at room temperature. The lentiviral vector and Lipofectamin 2000 mix is added to 293T cells and supplemented with 7ml of Optimem with 10X FBS for each 10cm plate. 12 hours later, medium should be replaced by 10XFBS DMEM with antibiotics. After 30 hours, 293T cells should form clusters of cells, which are the producers of the lentivirus that we need for the infection. Virus containing supernatant is collected (10mL per each 10cm plate) and filtered with 0.22 µm pore and supplemented with polybrene (EMB Bioscience) at a final concentration of 8µg/ml before being added to HUVEC which have been prepared at 90% confluence into 10cm plate. After centrifuging the plates at 2500rpm for 1 hour, HUVEC are incubated at 5% CO_2 and 37ºC overnight. Medium is then replaced by fresh complete HUVEC medium supplemented with 0.5µg/ml of puromycin.

5.11 Immunofluorescence

Cell staining

Immunofluorescence staining of the cells (VSMC or HUVEC) is performed in cultured cells onto 16 well chamber slides (Nunc). After washing the cells with PBS (1%), they were fixed ten minutes at RT with 4% paraformaldehyde (PFA) and incubated for 1hour at 4ºC with blocking buffer containing 1%BSA, 5% Donkey Serum (Sigma-Aldrich) in PBS (1%) supplemented or not with triton 0.1% if permeabilization is needed. Incubation of the primary antibodies is performed at 4ºC overnight at 1:100 or 1:50 dilution following manufacturer recommendations. Secondary antibodies are incubated at room temperature for one houre and used at 1:300 Molecular probes, Life Technologies). Actin is stained with Rhodamin Phalloidin (Molecular Probes) at 1:3000 dilution or anti-human αSMA (Abcam). Nuclei are stained using Hoechst (1:1000 in PBS

1X) and the slides are mounted with Prolong Gold Antifade Reagent (Molecular Probes, LifeTechnologies).

Tissue staining

Temporal artery biopsy are fixed with 4% paraforlmaldehyde (PFA) and incubated with increasing concentrations of sucrose (15% and 30%) before being frozen with OCT and stored at -80ºC. For staining, slides are re-fixed with 4% PFA for 10 min at room temperature, washed in PBS1X, and incubated for 1h at 4ºC with the blocking and permeabilization buffer containing 0.1% of Triton, 1% of BSA and 5% donkey serum (Sigma-Aldrich) in 1X PBS. Slides are incubated overnight with the primary antibodies which are diluted at 1:100 or 1:50 with the blocking and permeabilization buffer. After washing three times with 1X PBS with 0.1% Tween (PBST), slides are incubated for 2 hours at room temperature with secondary antibodies (Life Technologies) diluted 1:300. Hoechst (Molecular Probes, Life Technologies) (1:1000 in 1XPBS) is used for nuclei staining (incubation 5 minutes at room temperature). Slides are mounted with Prolong Gold Antifade Reagent (Molecular Probes, LifeTechnologies). Control of the technique is always realized by incubating the cells or the tissue with secondary but not with primary antibodies.

Either immunofluorescence staining of the cells or temporal artery biopsies are examined using a laser scanning confocal Leica TCS *SP5* microscope (Leica Microsystems). Images are processed with Leica Confocal software (LAS-AF Lite) and Image J software.

Primary antibodies:

Santa Cruz: IL12p40 and ET-1 (goat polyclonal), IL12p35 (rabbit polyclonal), EBI3 (mouse monoclonal), FAK (rabbit polyclonal), FAK (mouse monoclonal)

Cell Signaling: PI3K p85 and p-STAT3 (Tyr705) (rabbit monoclonal), p-FAK (Tyr397) (rabbit polyclonal)

Atlas Antibodies: IL12p35 (rabbit polyclonal)

Merck Millipore: gp130 (rabbit polyclonal)

R&D Systems: IL23p19 (goat polyclonal)

Abcam: αSMA, ET_BR and IL23p19 (rabbit polyclonal)

DAKO: CD31 (mouse monoclonal)

BD tranduction laboratories : ET_AR (mouse monoclonal)

Acris antibodies (San Diego, CA, USA): IL12p35 (mouse monoclonal)

Proximity Ligation Assay (PLA)

PLA is used to visualize proximity co-localization (<40 nm) in cells or tissue biopsies of temporal arteries using Duolink Detection kit (Olink Bioscience, Uppsala, Sweden). For cells staining using PLA, they are fixed (4% PFA for 20 min at room temperature) and stored in 50% glycerol. Tissue biopsies of temporal arteries are pre-treated as explained in the previous section. After blocking (1 hour in blocking buffer at room temperature), cells or tissues are incubated overnight at 4ºC with primary antibodies in blocking buffer (containing 0.1% of Triton, 1% of BSA and 5% donkey serum (Sigma-Aldrich) in 1X PBS) . After washing (5 min, twice in wash buffer: 0.1 M Tris-HCl pH 7.5, 0.5M NaCl, 5% Tween-20 in ultrapure water), slides are incubated (30 min at 37ºC) with PLA probe solution containing anti-rabbit MINUS and anti-mouse PLUS Duolink PLA probes. After washing, circularization and ligation of the oligonucleotides in the probes, an amplification tep is performed using polymerase solution (100 min at 37ºC). If a cell marker is needed cells or tissues are re-fixed in 4% PFA after staining with fluorescent onjugated mAb. After washing and re-fixation, the slides are mounted with Duolink II Mounting medium containing DAPI or with Prolong Gold Antifade Reagent (Life Technologies) after staining with Hoechst as explained in in the previous section. Images are obtained through a Carl Zeiss LSM 780 confocal microscope, using ZEN software (Carl Zeiss) or Leica TCS *SP5* microscope (Leica Microsystems). Quantification of PLA signal is calculated as mean (±SD) dots/cells. Total number of dots/area and total DAPI signal/area, were measured by Image J over multiple fields including at least 200 cells.

Primary antibodies (human):

Santa Cruz: IL12p35 (rabbit polyclonal), EBI3 (mouse monoclonal)

Millipore: gp130 (rabbit polyclonal)

Acris antibodies: IL12p35 (mouse monoclonal)

R&D Systems: gp130 (mouse monoclonal)

Sigma-Aldrich : IL23p19 (rabbit polyclonal)

5.12 Bioinformatic approximations

Gene promoter region analysis

Promoter sequence (5000bp) of the target gens (IL12p35 and EBI3) are obtained with *USNC Genome Browser*. Using *Chip Bioinformatics Mapper program,* the predicted transcription factor sequences in the promoter sequence of each gene are obtained. Only the predicted transcription factors with SCORE >3 and eValue <7 are considered as recommended by the authors of the program (*309*).

Molecular modeling

Molecular modeling is used to predict the hypothetical binding between two molecules. The experimental structural complex of vIL6-gp130 (*310*) (protein data bank PDB ID: 1I1R; http://www.rcsb.org/pdb/explore/explore.do?structureId=1I1R) is used as the template to model potential binding interactions between human (h) p19 and gp130. Multiple sequence alignments of vIL6, hp19 and hIL6 is used as a guidance to overlay the experimental structures of hp19 (PDB ID: 3D87) onto the vIL6-gp130 (PDB ID: 1ILR) to create a tetrameric p19-gp130 model complex. Sequence alignments are created by using T-COFFEE software (online Version_10.00.r1613; http://www.tcoffee.org/) in the Expresso mode (aligns protein sequences using structural information). The following TCOFFEE methods are chosen to compute the Expresso library: sap_pair, muscle_msa and t_coffee_msa. Option to automatically fetch PDB templates is turned on and all the remaining options are kept at the default mode. The validity of hp19-gp130 model and its binding interface compatibility are evaluated by comparing the key contact surface residues of vIL6-gp130. The non-similar residues in the binding interface and their compatibility to the newly created model are evaluated at the sequence and structural

levels using the NCBI tool (Amino Acid Explorer) (*311*) and molecular modeling software (Accelrys Discovery Studio Visualizer 3.5).

5.13 Statistical Analysis

Mann-Whitney was applied for non-parametric and independent samples using SPSS software, version PASW 18.0.

5.14 Reagents

The recombinant molecules, and inhibitors (as well as neutralizing antibodies) used in all the functional experiments performed in this thesis are listed below.

R&D: TNFα (10 or 20ng/ml), IFNγ (1-10ng/ml), hIL6 (200g/ml), IL6R (200ng/ml), PMA (10ng/ml), IL1β (10 ng/ml)

Sigma-Aldrich: LPS (1µg/ml), BQ123 (20µmol/L), BQ788 (20µmol/L), PF573228/FAK Inhibitor (1-10µg/ml), ICAM-1 (mouse monoclonal), VCAM-1 (mouse monoclonal)

Sino Biological (North Wales, USA)**:** rIL35 (20ng/ml)

MP Biomedical: ET-1(10^{-6}, 10^{-9} and 10^{-11}µmol/L)

Calbiochem (EMD Chemicals Inc., Gibbstown, NJ, USA)**:** Fibronectin (5µg/cm^2), LY294002 (PI3K inhibitor) (50µmol/l), PP2 (Src inhibitor) (10µmol/l),

PD98059 (MAPK 42/44 ERK1/2 inhibitor) (20µmol/l)

Immunotech (Westbrook, ME)**:** Anti-integrin β1

Abcam: anti-integrin α-4 antibody (HP2/1), anti-LFA1 (mouse), anti-integrin β2

Santa Cruz : control mouse IgG

Results

Identification of IL-23p19 as an endothelial pro-inflammatory peptide that promotes gp130-STAT3 signaling

Running Title: IL-23p19 is an endothelial pro-inflammatory peptide

Georgina Espigol-Frigole[1,2,¶]**, **Ester Planas-Rigol**[1,2,¶], Hidetaka Ohnuki[1], Ombretta Salvucci[1], Henry Kwak[1], Sarangan Ravichandran[3], Brian Luke[3], Maria C. Cid[2] and Giovanna Tosato[1]*

Acceptance subjected to major revision. Revision submitted.

Running Title: IL-23p19 is an endothelial pro-inflammatory peptide

Georgina Espigol-Frigole[1,2,¶]**, Ester Planas-Rigol[1,2,¶], Hidetaka Ohnuki[1], Ombretta Salvucci[1], Henry Kwak[1], Sarangan Ravichandran[3], Brian Luke[3], Maria C. Cid[2] and Giovanna Tosato[1]*

1 Laboratory of Cellular Oncology, Center for Cancer Research, National Cancer Institute, National Institutes of Health, Bethesda MD 20892, USA.

2 Department of Systemic Autoimmune Diseases, Clinical Institute of Medicine and Dermatology, Hospital Clinic, University of Barcelona, IDIBAPS-CRB CELLEX, Barcelona, Spain.

3 Advanced Biomedical Computing Center, Leidos Biomedical Research, Inc.; Frederick National Laboratory for Cancer Research, Frederick, Maryland 21702, USA

[¶]These authors contributed equally to this work

*Corresponding author. Tel: 301-5949596; Fax: 301-5943996; E-mail: Tosatog@mail.nih.gov

Acceptance subjected to major revision. Revision submitted.

(30/09/2015)

Dear Dr. Tosato,

Manuscript Number: aad2357

Thank you for sending us your manuscript entitled "Identification of IL-23p19 as an endothelial pro-inflammatory peptide that promotes gp130-STAT3 signaling." I'm very sorry for how long the process has taken. I've been waiting for a third referee to return their comments, but it's been over a month, so I've decided to go ahead with the two sets of comments that we already have. We are potentially interested in publishing your manuscript as a Research Article, but we are not prepared to accept it in its present form. Please revise your manuscript in accord with the referees' comments and the editorial comments, which are pasted at the end of this message. Because of the nature of the reviewers' comments and revisions required, we may send the revised manuscript back for further review

ABSTRACT

IL-23, a heterodimeric cytokine composed of the unique p19/IL-23A peptide and the shared IL-12p40/IL-12β chain is implicated in Crohn's disease, rheumatoid arthritis, psoriasis and other immune-mediated inflammatory diseases. No function has previously been attributed to the IL-23p19 peptide, despite its expression in endothelial cells and other cells without IL-12/IL-23p40 to enable IL-23 production. Here we show that intracellular IL-23p19 promotes ICAM-1 and VCAM-1 adhesion molecules expression in endothelial cells enhancing leukocyte attachment to endothelium and trans-endothelial migration. We find that intracellular p19 associates with gp130 signal transducer and induces gp130-STAT3 signaling. Pro-inflammatory signals promote IL-23p19 expression in endothelial cells, and adventitial capillaries of inflamed temporal arteries in patients with giant-cell arteritis (GCA) display endothelial p19-protein associated with gp130, but no IL-12/IL-23p40. Since adventitial capillaries are essential to inflammatory cells entry into arterial walls, p19 is likely a contributor to GCA disease and a novel therapeutic target. Our results provide evidence that IL-23p19 is a previously unrecognized endothelial pro-inflammatory peptide that promotes leukocyte transendothelial migration, advancing current understanding of the complexities of inflammatory responses.

INTRODUCTION

Inflammatory cells and inflammatory mediators play critical roles in the pathogenic cascade leading to vascular lesions that characterize different types of vasculitis. Giant-cell arteritis (GCA) is an inflammatory vasculitis that typically involves medium and large arteries, predominantly branches of the aortic arch (*1*). The condition is associated with systemic inflammatory symptoms (*1*) and is generally long-lasting (*2*). Luminal occlusion from intimal hyperplasia can lead to ischemic complications including loss of vision (*3*), and vascular wall injury may lead to aortic aneurysm or dissection (*4*).

The cause of GCA is unknown. Mechanistic studies have outlined activation of vessel wall-resident dendritic cells and recruitment of lymphocytes/monocytes to the vessel wall as key pathogenic events (*2, 5*). The adventitial capillaries (*vasa vasorum*) of GCA arteries are believed to be the port of entry for inflammatory cells, as they abnormally express a variety of adhesion molecules that promote leukocyte adhesion to endothelium and trans-endothelial migration (*6*). A key feature of GCA lesions is the abundance of various inflammatory cytokines, chemokines and other mediators, which produce systemic symptoms, amplify local inflammation and produce vascular pathology by targeting the endothelium and vascular smooth muscle cells and fibroblasts (*2*).

IL-23, a heterodimeric cytokine composed of the unique p19/IL-23A peptide and the shared IL-12p40/IL-12β chain (*7*), promotes development of a population of T cells, designated Th17 as they express IL-17, implicated in Crohn's disease, rheumatoid arthritis, psoriasis and other immune-mediated inflammatory diseases (*8*). Macrophages and dendritic cells, which express p19 and p40, secrete IL-23, whereas endothelial cells and certain T cell subsets express p19 mRNA, but not p40, and thus do not secrete IL-23 (*7*).

There is evidence for involvement of IL-23 in GCA, since Th17 cells are abnormally elevated in blood of untreated GCA patients, and circulating monocytes express abnormally elevated mRNA levels of IL-23p19 and IL-12p40 (*9*). GCA vascular lesions express abnormally elevated IL-17 mRNA (*10*), and pre-treatment GCA tissue specimens express IL-23p19 mRNA, which decreases after treatment (*11*). However, the role of IL-23 in GCA has not been fully investigated. Here we discovered a previously unrecognized role of IL-23p19 as pro-inflammatory peptide that is produced by the endothelium.

RESULTS

IL-23 p19 is detected in Temporal Arteritis tissue

Normal superficial temporal arteries display the characteristic central lumen limited by the endothelium of the *tunica intima*, the internal elastic membrane, the *tunica media* and the *adventitia* (Fig. 1A, left H&E staining; right DAPI staining). In GCA, diseased superficial temporal arteries are variously disrupted (Fig. 1B, left H&E; right DAPI): the lumen is narrowed, the intima is thickened, the internal elastic membrane is fragmented, and the *tunica media* contains inflammatory cells and occasional multinucleated giant cells (*2*). The blood capillaries (*vasa vasorum*), normally restricted to the adventitia, are also found in the *tunica media* of GCA temporal artery (*2*).

The endothelial cell marker CD31 identifies (red) the endothelium limiting the lumen of the normal temporal artery and the narrowed lumen of the GCA temporal artery (Fig. 1, C and D). CD31 additionally identifies an expansive network of adventitial neoangiogenic capillaries in the GCA vessel wall and scattered other cells (Fig. 1D) that are missing from the normal artery (Fig. 1C). We found that IL-23p19 (green, henceforth p19) is present in the $CD31^+$ pathological capillary network of GCA (Fig. 2E). By contrast, IL-12/IL-23p40 (white, henceforth p40) is generally absent from $CD31^+$ cells but is detected in occasional $CD31^-$ cells (Fig. 1E). The presence of CD31 and p19 without p40 was confirmed in two additional GCA temporal arteries. Consistent with previous results in cultured endothelial cells showing that this cell population does not express p40 (*7*), the current results demonstrate that p19, but not p40, is generally present in the capillary endothelium lining the pathological *vasa vasorum* of inflamed temporal arteries from GCA patients. Since previous studies have shown that p19 is only secreted extracellularly as a complex with p40 to form the IL-23 cytokine (*7*), the current results are consistent with p19 being an intracellular peptide in GCA endothelium.

Inflammatory signals induce p19 expression in endothelial cells

Since serum and tissue concentrations of TNFα, IL-6 and IL-1β are often abnormally elevated in active GCA patients (*5*), we tested whether pro-inflammatory signals promote p19 expression in primary endothelial cells. TNFα and LPS induced p19 mRNA expression in primary human umbilical vein endothelial cells (HUVEC) and in dermal microvascular

endothelial cells (HDMEC) (Fig. 2A), but not expression of p40 mRNA (Fig. 2B). In contrast, LPS expectedly induced p19 and p40 mRNA expression in normal peripheral blood mononuclear cells (PBMC) (Fig. 2, A and B). By immunoblotting, LPS and TNFα increased p19 protein levels in HUVEC and HDMEC lysates (Fig. 2C).

Immunoblotting (Fig. 2C) and a sensitive ELISA (Fig. 2D) failed to detect p19 protein in culture supernatants of endothelial cells even after LPS or TNFα activation, suggesting that endothelial cells secrete little/no p19 in the extracellular compartment. Instead, p19 was clearly detected in the culture supernatants of LPS-activated PBMC (Fig. 2D). Thus, consistent with earlier studies (*7*) activated endothelial cells fail to produce IL-23 as they do not express p40, and they do not secrete p19.

To investigate potential functions of p19 in endothelial cells, we took advantage of a lentiviral vector (LV) for stable expression of p19 in these cells. After puromycin selection, HUVEC consistently expressed p19 mRNA (Fig. 2E top) and protein (Fig. 2E, bottom). The transduced p19 was detected in the cytoplasm of HUVEC (Fig. 2E). We considered the possibility that p19 might promote p40 and IL-23R expression; however, we found no increase in p40 and IL-23R mRNAs in p19-transduced HUVEC (Fig. 2F). Multiple attempts at recovering p19 protein from culture supernatants of p19-transduced HUVEC were unsuccessful, despite supernatant concentration (Fig. 2G).

p19 induces adhesion molecules expression in endothelial cells

As the vascular endothelium critically regulates crawling, adhesion and transendothelial migration of circulating leukocytes, we investigated whether p19 can modulate endothelial cell expression of adhesion molecules that mediate these processes (*12*). We find that p19-transduced endothelial cells express higher levels of ICAM-1 and VCAM-1 mRNA and protein compared to control cells (Fig. 3, A and B). Levels of PECAM-1, a member of the Ig superfamily prominently expressed in endothelial intercellular junction, minimally differed between p19-expressing and control cells (Fig. 3, A and B). However, unlike LPS or IFN□ plus TNF□, p19 induced minimal expression of the cytokines CXCL9, CXCL10, CXC11 and IL-6 in endothelial cells (fig. S1).

The endothelial adhesion molecules VCAM-1 and ICAM-1 promote leukocyte adhesiveness to the endothelium by engagement of the LFA-1 and VLA-4 integrins (*13*), and induce critical signals to enhance transendothelial migration together with endothelial-derived inflammatory chemokines (*13*). We examined whether endothelial expression of p19 alters leukocyte attachment to endothelium and trans-endothelial migration. In cell attachment assays, we find that normal peripheral blood mononuclear cells attach significantly better to p19-expressing endothelium compared to control endothelium over a wide range of mononuclear cell concentrations (Fig. 3C). In cell transmigration assays, we observe that p19-expressing endothelium sustains greater leukocyte transmigration compared to control endothelium after activation with LPS or with TNFα and IFNγ (Fig. 3D).

p19 induces autocrine signaling in endothelial cells

We examined potential mechanisms underlying p19 transcriptional activation of adhesion molecules. A screening for Erk1/2, Akt, STAT1 and NF□B-p65 revealed that p19 does not induce the phosphorylation of these signaling mediators in HUVEC (fig. S2A). By contrast, we found that p19-expressing HUVEC display significantly increased ($p<0.05$) levels of STAT3 phosphorylation (p-STAT3; Tyr 705) compared to control cells (Fig. 3E). Selective activation of STAT3 but not STAT1 has previously been attributed to differences among activating signals, engagement of SOCS inhibitors and other factors (*14*). Consistent with p19 inducing STAT3 activation, p19-HUVEC displayed nuclear STAT3, whereas p19-negative cells did not (Fig. 3F and fig. S2B). Since IL-6 plus IL-6R induce gp130/STAT3 activation from the cell surface (*15*) whereas p19 is an intracellular peptide in endothelial cells, we measured p-STAT3 in p19-HUVEC activated by IL-6 plus IL-6R. We found that IL-6 plus soluble IL-6R time-dependently induced substantially more STAT3 activation in p19 HUVEC compared to control HUVEC at all time-points (Fig. 3G). These results provide evidence that p19 promotes STAT3 activation in endothelial cells. In addition, since ICAM-1 and VCAM-1 are transcriptional targets of IL-6-IL-6R/gp130/p-STAT3 signaling (*16*) (Champion Chip transcription factor Search portal, DECODE database, SABiosciences), these results suggested the possibility that p19 promotes transcriptional activation of ICAM-1 and VCAM-1 by inducing gp130/pSTAT3 signaling.

There is structural similarity (~16% sequence identity and 34.3% sequence similarity) between p19 and vIL-6 (*7)*, a viral cytokine product of KSHV/HHV-8 (*7, 17*). Intracellular vIL-6 binds to intracellular gp130 and promotes gp130 signaling from an intracellular location (*18, 19*). We hypothesized that intracellular p19 also binds to intracellular gp130 and activates gp130-STAT3 signaling. The experimental structure of the tetrameric complex of vIL-6-gp130 extracellular domain (*20*) (Fig. 4A, left) was used as a basis to evaluate possible p19-gp130 interaction. Based on the conservation of key binding residues (fig. S3, A to C and Molecular Modeling in Materials and Methods), we concluded that p19 has a high probability of forming a complex with gp130. A model for a predicted tetrameric structure of p19-gp130 is shown (Fig. 4A, right) next to the experimental structure of vIL-6-gp130 (Fig. 4A, left).

We tested for the possibility that p19 physically associates with gp130. First, we looked for recombinant p19 binding to immobilized recombinant gp130-Fc in a cell-free system. As shown, p19 dose-dependently bound to gp130-Fc as did control vIL-6, although at higher protein concentrations (Fig. 4B). Second, we utilized the murine BAF-130 cells, which are stably transduced with human gp130 to confirm p19 binding to gp130 in a cell-based system. We found that recombinant p19 time-dependently activates gp130 (Fig. 4C) and STAT3 (Fig. 4D) in BAF-130 cells similar to human IL-6 plus IL-6R. Third, we tested if endogenous gp130 associates with p19 in HUVEC transduced with p19. As shown (Fig. 4E, left), gp130-specific antibodies specifically immunoprecipitated p19 from cell lysates of p19-HUVEC with or without pre-activation with IL-6 plus IL-6R, which promotes gp130 expression (*21*). Re-blotting confirmed the specific immunoprecipitation of gp130 (Fig. 4E, right). Fourth, we used proximity ligation assay (PLA) to visualize proximity co-localization of p19 and gp130 in HUVEC. This assay generates dots that mark the co-localization of two molecules when their distance is <40 nm. We tested p19-transduced and control HUVEC prior to or after 15 min activation with IL-6 plus IL-6R, which induces gp130 is internalization and re-expression on the cell surface from translation of pre-existing mRNA (*15*). Since previous results have shown that vIL-6 associates with gp130 in the endoplasmic reticulum (*19*) and the current results suggested that vIL-6 and p19 similarly engage gp130, we reasoned that activation with IL-6 plus IL-6R could result in increased p19-gp130 proximity co-localization. Consistent with this, PLA detected specific association of p19-gp130 in p19-HUVEC, prior to and to a greater

degree after 15 min activation with IL-6 plus IL-6R (Fig. 5, A and B). Control HUVEC also displayed a low level specific (not detected in control PLA) association between p19 and gp130, likely reflecting the low-level p19 expression in endothelial cells (Fig. 2C) and the high sensitivity of PLA-based detection of p19-gp130 association. Together, these results demonstrate that intracellular p19 associates with gp130, and suggest that gp130 serves as a mediator of p19-induced signaling in endothelial cells.

Since the phosphorylation of specific gp130 tyrosine residues initiates STAT3 signaling, we tested whether p19 modulates gp130 phosphorylation. Using a quantitative ELISA, we found significantly greater gp130 tyrosine phosphorylation in lysates of p19-expressing HUVEC than in control lysates (Fig. 5C). Similarly, IL-6 plus IL-6R induced greater gp130 tyrosine phosphorylation in p19-HUVEC compared to control (Fig. 5C). These results demonstrate that p19 associates with gp130 and promotes gp130 tyrosine phosphorylation.

p19 specifically associates with gp130 in GCA temporal artery

The experiments *in vitro* predicted that p19 associates with gp130 in endothelial cells within GCA lesions. We used PLA to visualize the proximity co-localization of p19 and gp130, and CD31 immunostaining to mark endothelial cells (Fig. 6). Specificity controls, including PLA in a control GCA-negative temporal artery (fig. S4A, temporal artery from an elderly patient suffering from headaches of unknown etiology) and PLA with no primary antibody in GCA-positive temporal artery biopsy (fig. S4B) showed specificity of PLA for p19-gp130. As reflected by the specific PLA staining (red), p19 and gp130 co-localized in a proportion of $CD31^+$ cells (green) scattered in the GCA vessel wall (Fig. 6; fig. S5 and fig. S6). Little PLA signal was detected in the endothelium limiting the central lumen (fig. S6). PLA signal was also detected in a proportion of $CD31^-$ cells, possibly T lymphocyte subsets (Fig. 6 and fig. S6), which express p19 (*7*) and gp130 (*22*). Thus, p19 and gp130 co-localize in $CD31^+$ endothelial cells lining the *vasa vasorum* of GCA-affected arteries, providing an opportunity for p19/gp130 signaling at these sites.

DISCUSSION

These results show that IL-23p19, considered a biologically inactive intracellular peptide (*7*), plays a previously unrecognized role as an endogenous activator of endothelial inflammation, promoting leukocyte adhesion to endothelium and transendothelial migration. This pro-inflammatory function of p19 is independent of IL-23 and likely contributes to pathogenesis of GCA arteritis, as p19 is broadly expressed in the GCA adventitial capillaries, which are the principal port of entry for inflammatory cells into the vessel wall (*2, 6*). Mechanistically, by inducing endothelial VCAM-1 and ICAM-1 expression, p19 is expected to promote adventitial accumulation of leukocytes, which preferentially express VLA-4 and LFA-1, the cognate VCAM-1 and ICAM-1 leukocyte ligands (*6*). Since inflamed endothelium is common to a number of inflammatory disorders, the current results predict a broader proinflammatory role of p19 in other forms of vasculitis. In addition, besides endothelial cells, “polarized” T lymphocytes express p19, but not p40 (*7*); a potential function of p19 in this cell type has not been fully investigated. Furthermore, p19 mRNA is expressed at relatively higher levels than p40 in inflammatory macrophages (*7*), raising the possibility that p19 may play independent functional roles even in cells that secrete IL-23.

One of the limitations of this study is that the relative contribution of p19 to tissue inflammation could not be fully assessed as we have focused on endothelial cells to avoid confounding phenotypes associated with IL-23 secretion. Nonetheless, the identification of p19 as a previously unrecognized intracellular pro-inflammatory peptide presents an advance and offers a new therapeutic target.

p19-transgenic mice developed severe inflammation in many tissues associated with swollen abdomen, runting and early death despite having normal levels of circulating IL-12p40, supporting the possibility that p19 may be biologically active independent of p40 when expressed in certain cells (*23*). Consistent with this, IL-23 did not reproduce the phenotype of p19-transgenic mice when expressed systemically in mice at high levels over a prolonged period, promoting instead specific inflammation at the tendon-bone insertion (*24*). Although these phenotypic differences may reflect a spectrum of IL-23-related functions, they raise the possibility that the most severe phenotype of p19-transgenic mice is attributable in part to p19 activity on its own.

The viral cytokine vIL-6 and the p19 peptide share about 16% sequence identity and are mostly intracellular proteins. Similar to vIL-6, which forms a tetrameric intracellular complex with the gp130 signal transducer composed of two gp130 chains and two vIL-6 ($gp130_2$-$vIL\text{-}6_2$) molecules (*25, 26*), we found that intracellular p19 binds to gp130 and activates gp130-STAT3 signaling. Human IL-6 and vIL-6 share about 25% sequence identity, but human IL-6 forms hexameric signaling complexes at the cell surface, which include two gp80/IL-6R subunits in addition to two gp130 signal transducer chains and two IL-6 chains ($gp802\text{-}gp130_2\text{-}hIL\text{-}6_2$). Nonetheless, human IL-6 and vIL-6 initiate similar signaling from phosphorylated gp130 (*19, 27*). Thus p19, initially discovered through computational analysis as a member of the IL-6 family of cytokines, is now found to share gp130 signaling with a member of this family.

Most patients with GCA are treated effectively with steroid therapy, which improves systemic inflammatory symptoms, but steroids do not control all inflammatory pathways active in GCA (*2*). Disease flares are frequent after glucocorticoids are tapered, and prolonged use of glucocorticoids is associated with various complications; thus new drugs are needed. The current disclosure of a previously unrecognized pro-inflammatory role of intracellular p19 unveils a new potential therapeutic target in GCA and other inflammatory diseases in which p19 is expressed in the absence of p40. Neutralizing antibodies to p19, which hold promise as a treatment for psoriasis (*28*) are not likely effective against intracellular p19. Rather, JAK inhibitors (*29*) and SHP inhibitors (*30*) should be explored for pharmacologic targeting of p19 signaling in inflammatory diseases such as GCA.

MATERIALS AND METHODS

Experimental Design

This study was originally designed to evaluate functional roles of IL-23 in patients with GCA. After initiation of the study, a screen of GCA temporal arteries revealed that endothelial cells lining affected capillaries ("vasa vasorum") express the p19 chain of IL-23, but not the p40 chain, and are thus unable to secrete IL-23. Since no function has previously been attributed to p19, we examined potential functions of p19 in the endothelium. Through a series of controlled functional experiments *in vitro* using primary endothelial cells, we have demonstrated that p19 promotes leukocyte attachment to the endothelium and trans-endothelial migration. Based on structural modeling data suggesting that p19 could complex with gp130, we conducted a series of biochemical experiments, which demonstrated the binding of p19 to gp130. Further, we identified gp130/STAT3 signaling as a pathway mediating p19 function. An observational study of GCA tissue biopsies identified specific proximity colocalization of p19 and gp130, supporting a signaling role of p19/gp130 *in vivo*.

Cells, Reagents and Cell Culture

HUVEC were derived and propagated as described (*31*). HDMEC (Lonza) were maintained in EBM-2 endothelial growth medium supplemented with EGM-2 MV Bullet Kit (Clonetics). BAF-130 cells, murine BAF-B03 cells stably transduced with human gp130, were previously reported (*27*). Peripheral blood mononuclear cells (PBMC) were obtained from volunteer donors per approved protocol. Cells were stimulated with PMA (phorbol myristate acetate; R&D Systems, 10 ng/ml), LPS (Sigma 1µg/ml), human TNFα (R&D Systems, 20 ng/ml), human IFN□ (R&D Systems 1 or 10 ng/ml) over 24 hours in complete culture medium. To activate gp130/pSTAT3 signaling, HUVEC were stimulated (0-45 min) with p19 (1 µg/ml, Abnova) or with hIL-6 (200-1000 ng/ml, R&D Systems) plus IL-6R (200-2500 ng/ml, R&D Systems). In selected experiments IL-6 plus IL-6R were used to pre-activate HUVEC (18-24 hours). For production of serum-free supernatants, endothelial cells were cultured in M199 serum-free complete medium for 24-72 hours. Trichloroacetic acid (TCA) was used to precipitate protein from these supernatants. To reduce background activation, HUVEC were cultured for 18 hours in M199 medium with 0.5% BSA.

IL-23 p19 Transduction

The lentiviral vector for expression of human IL-23 p19 was from GeneCopoeia (cat. No. EX-U1167-Lv105); the pLVX-Puro vector (*31*) was used as control. Infection and puromycin selection of transduced cells were achieved as described (*31*).

Real-time RT-PCR

RNA was extracted using TRI Reagent (Molecular Research Center); cDNA was synthesized from 1 µg total RNA (High Capacity cDNA Reverse Transcription Kit; Applied Biosystems). mRNA was measured by real-time PCR with 1 µL cDNA and Taqman PCR Universal Master Mix (Applied Biosystems). Human Taqman Gene expression probes included: IL23p19, IL12p40, ICAM-1, VCAM-1, PECAM-1, CXCL9, CXCL10, CXCL11, IL-6 and GAPDH (Applied Biosystems). PCR reaction conditions were those recommended by the manufacturer.

ELISAs

Human IL-23 p19 ELISA kit was from Abcam; CXCL9, CXCL10 and CXCL11 Quantikine ELISA kits were from R&D Systems. Human phospho-gp130 was measured in cell lysates (25 and 12.5 □g/well) using a sandwich ELISA, following manufacturer's instructions (R&D Systems). The binding of p19 and vIL-6 to gp130 was measured using modification of a reported method (*27*). Recombinant human soluble gp130 (sgp 130; R&D Systems) was immobilized on ELISA plate wells (4HBX, Immulon) at 5□g/ml in PBS. After blocking (SuperBlock, Life Technologies), MBPvIL-6 (*27*) or p19 (IL23A, Abnova) was applied at various concentrations in 1% BSA/PBS, and incubated for 4 hours at room temperature. Bound protein was detected with polyclonal IgG rabbit antibodies anti-vIL-6 (*27*)or goat IgG anti-p19 (AF1716 R&D Systems), both used at (1 µg/ml), followed by HRP-conjugated donkey anti-rabbit IgG (NA934V, GE Healthcare Life Sciences) or rabbit anti-goat IgG (401504 Calbiochem) at 1:3000 dilution in PBS/0.05% Tween 20. Reactions were visualized with tetramethoxybenzene peroxidase substrate, followed by 2N H_2SO_4. Plates were read at 450 nm using a microplate reader.

Immunoprecipitation

Protein extracts of p19-transduced HUVEC untreated, treated with 200-1000 ng/mL human IL-6 (R&D Systems) plus 200-2500 ng/mL of soluble IL-6 receptor (R&D Systems) or treated with p19 protein (1µg/ml, Abnova) were prepared in lysis buffer containing 10mM Tris-HCL (pH=7.5), 150mM NaCl, 0.2% NP-40 (Abcam), 1mM NaF, 1mM EDTA, 10% glycerol, Complete protease inhibitor cocktail (Roche), 2mM of sodium orthovanadate (Sigma-Aldrich) and 1µg/mL pepstatin A (Sigma-Aldrich), leupeptin hemisulfate salt (Sigma-Aldrich) and aprotinin (Thermo Scientific). Rabbit polyclonal IgG antibody to human gp130 (Millipore) and control rabbit polyclonal IgG (Jackson Immunoresearch laboratories) were individually incubated (4 µg) with washed Protein G Dynabeads (50 µl; Life Technologies) and incubated 10 min at room temperature. After magnet separation the antibody/beads complex was added to the cell lysates (500 µg) followed by incubation (18 hours at 4℃) with rotation. Beads/antibody/protein complexes were recovered by magnetic separation. Target antigen was eluted by heat treatment (10 min at 70 ℃).

Immunoblotting

Immunoprecipitates and protein extracts prepared in SDS lysis buffer with protease inhibitor cocktail set III (Calbiochem, Darmstadt, Germany), 50 mM NaF, and 1mM sodium orthovanadate were resolved through NuPAGE 4-12%, Bis-Tris or 6% tris-glycine gels (Invitrogen) and transferred to nitrocellulose paper. After blocking, the membranes were incubated with antibodies: human IL23 p19 polyclonal rabbit antibody (Sigma-Aldrich), human IL-23 p19 polyclonal goat IgG (R&D Systems); human gp130 mouse monoclonal antibody (R&D), human gp130 rabbit polyclonal (Millipore) human VCAM-1 sheep polyclonal (R&D Systems), human ICAM-1 rabbit polyclonal (Cell Signaling Technology), CD31/PECAM-1 mouse mAb (BD-Pharmingen) and sheep polyclonal (R&D Systems); STAT1 rabbit polyclonal, p-STAT1 (Tyr701) rabbit mAb, STAT3 rabbit mAb, p-STAT3 (Tyr705) rabbit mAb, p44/42 MAPK (Erk1/2) rabbit polyclonal, phospho-p44/42 MAPK (ERK1/2) (Tr202/Tyr204) rabbit mAb, NF-□B p65 rabbit mAb, NFκB phospho-p65 (Ser536) rabbit mAb, AKT rabbit polyclonal, p-AKT (Ser473) rabbit mAb (all from Cell Signaling Technology); phosphotyrosine 4G10 mouse monoclonal antibody (Millipore) and β-actin goat antibody (Santa Cruz Biotechnology).

Horseradish peroxidase (HRP)-conjugated donkey anti-mouse IgG, anti-rabbit IgG or anti-sheep were from Amersham Pharmacia Biotech. Bound secondary antibodies were visualized by enhanced chemiluminescence (Amersham). Membranes were stripped and re-stained.

Tissues

Biopsies of temporal arteries were obtained for diagnostic purposes from eight patients with suspected GCA participating on institutionally approved study protocols of the Vasculitis Research Unit, Department of Autoimmune Diseases, "Hospital Clinic of Barcelona" (Spain). All participants in the study provided written informed consent after the nature and possible consequences of participation in the study were explained. Five of the patients had histological features of GCA in the biopsy (Table S1) and three of the patients did not have histological features of tissue inflammation and served as controls (Table S2).

Immunofluorescence Imaging

HUVEC cells were grown on Lab-tek chamber slides (Nunc, ThermoScientific), fixed (cold 4% paraformaldehyde in PBS) and stained with antibodies to IL23p19 (rabbit polyclonal, Abcam), IL-23p19 goat IgG polyclonal (R&D Systems), STAT3 (rabbit mAb; Cell Signaling Technology) and phospho-STAT3 (Tyr705) (rabbit mAb; Cell Signaling Technology). Secondary antibodies were Alexa fluor-conjugated anti-goat or anti-rabbit antibodies (Molecular Probes, Life Technologies). Nuclei were stained with DAPI. Fluorescence intensity of p-STAT3 from confocal imaging (Carl Zeiss LSM 780 confocal microscope) in HUVEC was measured by Image J, and was subsequently normalized by DAPI fluorescence intensity in each region to adjust for different cell density.

Temporal arteries tissues were fixed (cold 4% paraformaldehyde in PBS), cryo-protected in 15% and 30% sucrose, embedded in OCT, and processed for histology. For staining, slides were further fixed with 4% paraformaldehyde for 10 min at room temperature, washed in PBS, and soaked in PBS with 0.1% of Triton, 1% of BSA and 5% donkey serum (Sigma-Aldrich) for 1h at 4ºC. Primary antibodies were incubated overnight at 4℃: human CD31 (mouse monoclonal Ab, DAKO), human IL23p19 (rabbit polyclonal, Abcam) and human IL12p40 (goat polyclonal Ab, Santa Cruz Biotechnology). Slides were washed in PBS (5 min,

three times), followed by incubation with secondary antibodies (spectrally-distinct Alexa Fluor-conjugated antibodies to goat, mouse and rabbit IgG; Molecular Probes, Life Technologies). Nuclei were visualized with DAPI. Images were obtained by laser scanning confocal Leica TCS *SP5* microscope (Leica Microsystems, Heidelberg, Germany). Images were processed with Leica Confocal software (LAS-AF Lite) and Image J software (Wayne Rasband, Bethesda, Maryland, USA).

Proximity Ligation Assay (PLA)

PLA was used to visualize proximity co-localization (<40 nm) of p19 and gp130 in HUVEC and tissue biopsies of temporal arteries using Duolink Detection kit (Olink Bioscience). HUVEC were fixed (4% PFA for 20 min at room temperature) and stored in 50% glycerol. After blocking for (1 hour in blocking buffer at room temperature), cells were incubated overnight at 4ºC with anti-human p19 rabbit polyclonal Ab (2µg/ml, Sigma) and anti-human gp130 mouse IgG1 mAb (10µg/ml R&D Systems) in blocking buffer. After washing (5 min, twice in wash buffer: 0.1 M Tris-HCl pH 7.5, 0.5M NaCl, 5% Tween-20 in ultrapure water), cells were incubated (30 min at 37ºC) with PLA probe solution containing anti-rabbit MINUS and anti-mouse PLUS Duolink PLA probes. After washing, circularization and ligation of the oligonucleotides in the probes, an amplification step was performed using polymerase solution (100 min at 37ºC). After washing, re-fixation in 4% PFA and additional washing, the cells were stained with AlexaFluor 488-Zenon-labeled mouse anti-human CD31 mAb antibody (Covance/EMD Millipore) or with FITC-conjugated mouse mAb to human CD31 (ImmunoTools). After washing and re-fixation in 4% PFA, the slides were mounted with Duolink II Mounting medium containing DAPI. Images were obtained through a Carl Zeiss LSM 780 confocal microscope, using ZEN software (Carl Zeiss). Quantification of PLA signal was calculated as mean (±SD) dots/cells. Total number of dots/area and total DAPI signal/area, were measured by Image J over multiple fields including at least 200 cells.

Leukocyte-endothelium Adhesion Assay

Leukocyte adhesion to endothelium was evaluated using CytoSelect Leukocyte-Endothelium Adhesion assay kit, following the manufacturer's instructions. Briefly, confluent monolayers of vector only or p19-transduced HUVEC were generated in 96-well plates pre-coated with gelatin by 3-day HUVEC (25,000 cells/well) culture. Human PBMC isolated from the peripheral blood of volunteer donors ($1x10^6$ cells/ml), were labeled with LeukoTracker™ solution (1 hour incubation at 37ºC). After washing and suspension in serum-free medium, the labeled PBMC ($2x10^5$ cells/well in 200 µl) were incubated onto the pre-washed HUVEC monolayer and incubated (1.5 hour at 37ºC). After removal of non-adherent cells and washing (3 times in wash buffer), 150 µl lysis buffer (from kit) was added to each well (10 min incubation, shaking). Fluorescence in the supernatant (100 µl) was measured at 480/520 nm. The results are expressed as mean relative Fluorescence Units (±SD of triplicate cultures).

Transendothelial Migration Assay

The assay was performed essentially as described (*32*). Vector only or p19-infected HUVEC were seeded (40,000 cells/well) onto the membrane (pre-coated with 0.1% gelatin) separating the top from the bottom chamber of transwells (5□m pore size; 96-well plates; Costar, Fisher Scientific) to generate a monolayer. Once formed, the monolayer was incubated overnight in complete medium alone, with LPS (1 µg/ml) or with TNFα plus IFNγ. Transendothelial migration of PBMC ($1x10^6$ cells/well) was carried out in RPMI 1640 medium with 0.5% BSA over 6 hours incubation at 37ºC. Viable cells in the lower chamber were collected and counted. The results of triplicate cultures are expressed as means (±SD).

Molecular Modeling

The experimental structural complex of vIL6-gp130 (*20*) (protein data bank PDB ID: 1I1R; http://www.rcsb.org/pdb/explore/explore.do?structureId=1I1R) was used as the template to model potential binding interactions between human (h) p19 and gp130. Multiple sequence alignments of vIL6, hp19 and hIL6 was used as a guidance to overlay the experimental structures of hp19 (PDB ID: 3D87) onto the vIL6-gp130 (PDB ID: 1ILR) to create a tetrameric p19-gp130 model complex. Sequence alignments were created by using T-COFFEE software

(online Version_10.00.r1613; http://www.tcoffee.org/) in the Expresso (aligns protein sequences using structural information) mode. The following TCOFFEE methods were chosen to compute the Expresso library: sap_pair, muscle_msa and t_coffee_msa. Option to automatically fetch PDB templates was turned on and all the remaining options were kept at the default mode. The validity of hp19-gp130 model and its binding interface compatibility were evaluated by comparing the key contact surface residues of vIL6-gp130. The non-similar residues in the binding interface and their compatibility to the newly created model were evaluated at the sequence and structural levels using the NCBI tool (Amino Acid Explorer) (*33*) and molecular modeling software (Accelrys Discovery Studio Visualizer 3.5).

Statistical Analysis

The results are presented as mean ±SD. The statistical significance of differences between two groups was calculated using two-tailed Student *t*-test. The results are provided as *P* values, where <0.05 is considered significant.

SUPPLEMENTARY MATERIALS

Fig. S1. CXCL9, CXCL10 or CXCL11 are not detected in HUVEC transduced with p19.

Fig. S2. Analysis of signaling mediators in HUVEC transduced with p19.

Fig. S3. Molecular modeling of p19-gp130 interactions.

Fig. S4. PLA controls.

Fig. S5. PLA (p19+gp130) and CD31 immunostaining of GCA temporal artery.

Fig. S6. CD31 immunostaining and PLA (p19+gp130) of GCA temporal artery.

Table S1. GCA patients: clinical and laboratory findings.

Table S2. Control patients: clinical and laboratory findings.

REFERENCES AND NOTES

1. C. Salvarani, F. Cantini, G. G. Hunder, Polymyalgia rheumatica and giant-cell arteritis. *Lancet* **372**, 234-245 (2008); published online EpubJul 19 (10.1016/S0140-6736(08)61077-6).

2. C. M. Weyand, J. J. Goronzy, Immune mechanisms in medium and large-vessel vasculitis. *Nature reviews. Rheumatology* **9**, 731-740 (2013); published online EpubDec (10.1038/nrrheum.2013.161).

3. S. S. Hayreh, B. Zimmerman, Visual deterioration in giant cell arteritis patients while on high doses of corticosteroid therapy. *Ophthalmology* **110**, 1204-1215 (2003); published online EpubJun (10.1016/S0161-6420(03)00228-8).

4. M. C. Cid, A. Garcia-Martinez, E. Lozano, G. Espigol-Frigole, J. Hernandez-Rodriguez, Five clinical conundrums in the management of giant cell arteritis. *Rheumatic diseases clinics of North America* **33**, 819-834, vii (2007); published online EpubNov (10.1016/j.rdc.2007.08.001).

5. J. Hernandez-Rodriguez, M. Segarra, C. Vilardell, M. Sanchez, A. Garcia-Martinez, M. J. Esteban, C. Queralt, J. M. Grau, A. Urbano-Marquez, A. Palacin, D. Colomer, M. C. Cid, Tissue production of pro-inflammatory cytokines (IL-1beta, TNFalpha and IL-6) correlates with the intensity of the systemic inflammatory response and with corticosteroid requirements in giant-cell arteritis. *Rheumatology* **43**, 294-301 (2004); published online EpubMar (10.1093/rheumatology/keh058).

6. M. C. Cid, M. Cebrian, C. Font, B. Coll-Vinent, J. Hernandez-Rodriguez, J. Esparza, A. Urbano-Marquez, J. M. Grau, Cell adhesion molecules in the development of inflammatory infiltrates in giant cell arteritis: inflammation-induced angiogenesis as the preferential site of leukocyte-endothelial cell interactions. *Arthritis and rheumatism* **43**, 184-194 (2000); published online EpubJan (10.1002/1529-0131(200001)43:1<184::AID-ANR23>3.0.CO;2-N).

7. B. Oppmann, R. Lesley, B. Blom, J. C. Timans, Y. Xu, B. Hunte, F. Vega, N. Yu, J. Wang, K. Singh, F. Zonin, E. Vaisberg, T. Churakova, M. Liu, D. Gorman, J. Wagner, S. Zurawski, Y. Liu, J. S. Abrams, K. W. Moore, D. Rennick, R. de Waal-Malefyt, C. Hannum, J. F. Bazan, R. A. Kastelein, Novel p19 protein engages IL-12p40 to form a

cytokine, IL-23, with biological activities similar as well as distinct from IL-12. *Immunity* **13**, 715-725 (2000); published online EpubNov

8. S. L. Gaffen, R. Jain, A. V. Garg, D. J. Cua, The IL-23-IL-17 immune axis: from mechanisms to therapeutic testing. *Nature reviews. Immunology* **14**, 585-600 (2014); published online EpubAug 22 (10.1038/nri3707).
9. J. Deng, B. R. Younge, R. A. Olshen, J. J. Goronzy, C. M. Weyand, Th17 and Th1 T-cell responses in giant cell arteritis. *Circulation* **121**, 906-915 (2010); published online EpubFeb 23 (10.1161/CIRCULATIONAHA.109.872903).
10. G. Espigol-Frigole, M. Corbera-Bellalta, E. Planas-Rigol, E. Lozano, M. Segarra, A. Garcia-Martinez, S. Prieto-Gonzalez, J. Hernandez-Rodriguez, J. M. Grau, M. U. Rahman, M. C. Cid, Increased IL-17A expression in temporal artery lesions is a predictor of sustained response to glucocorticoid treatment in patients with giant-cell arteritis. *Annals of the rheumatic diseases* **72**, 1481-1487 (2013); published online EpubSep 1 (10.1136/annrheumdis-2012-201836).
11. S. Visvanathan, M. U. Rahman, G. S. Hoffman, S. Xu, A. Garcia-Martinez, M. Segarra, E. Lozano, G. Espigol-Frigole, J. Hernandez-Rodriguez, M. C. Cid, Tissue and serum markers of inflammation during the follow-up of patients with giant-cell arteritis--a prospective longitudinal study. *Rheumatology* **50**, 2061-2070 (2011); published online EpubNov (10.1093/rheumatology/ker163).
12. J. J. Campbell, E. C. Butcher, Chemokines in tissue-specific and microenvironment-specific lymphocyte homing. *Current opinion in immunology* **12**, 336-341 (2000); published online EpubJun
13. Z. Shulman, V. Shinder, E. Klein, V. Grabovsky, O. Yeger, E. Geron, A. Montresor, M. Bolomini-Vittori, S. W. Feigelson, T. Kirchhausen, C. Laudanna, G. Shakhar, R. Alon, Lymphocyte crawling and transendothelial migration require chemokine triggering of high-affinity LFA-1 integrin. *Immunity* **30**, 384-396 (2009); published online EpubMar 20 (10.1016/j.immuni.2008.12.020).
14. S. A. Jones, J. Scheller, S. Rose-John, Therapeutic strategies for the clinical blockade of IL-6/gp130 signaling. *The Journal of clinical investigation* **121**, 3375-3383 (2011); published online EpubSep (10.1172/JCI57158).

15. Y. Wang, G. M. Fuller, Phosphorylation and internalization of gp130 occur after IL-6 activation of Jak2 kinase in hepatocytes. *Molecular biology of the cell* **5**, 819-828 (1994); published online EpubJul

16. M. Romano, M. Sironi, C. Toniatti, N. Polentarutti, P. Fruscella, P. Ghezzi, R. Faggioni, W. Luini, V. van Hinsbergh, S. Sozzani, F. Bussolino, V. Poli, G. Ciliberto, A. Mantovani, Role of IL-6 and its soluble receptor in induction of chemokines and leukocyte recruitment. *Immunity* **6**, 315-325 (1997); published online EpubMar

17. P. S. Moore, C. Boshoff, R. A. Weiss, Y. Chang, Molecular mimicry of human cytokine and cytokine response pathway genes by KSHV. *Science* **274**, 1739-1744 (1996); published online EpubDec 6

18. M. B. Meads, P. G. Medveczky, Kaposi's sarcoma-associated herpesvirus-encoded viral interleukin-6 is secreted and modified differently than human interleukin-6: evidence for a unique autocrine signaling mechanism. *The Journal of biological chemistry* **279**, 51793-51803 (2004); published online EpubDec 10 (10.1074/jbc.M407382200).

19. D. Chen, G. Sandford, J. Nicholas, Intracellular signaling mechanisms and activities of human herpesvirus 8 interleukin-6. *Journal of virology* **83**, 722-733 (2009); published online EpubJan (10.1128/JVI.01517-08).

20. D. Chow, X. He, A. L. Snow, S. Rose-John, K. C. Garcia, Structure of an extracellular gp130 cytokine receptor signaling complex. *Science* **291**, 2150-2155 (2001); published online EpubMar 16 (10.1126/science.1058308).

21. M. Saito, K. Yoshida, M. Hibi, T. Taga, T. Kishimoto, Molecular cloning of a murine IL-6 receptor-associated signal transducer, gp130, and its regulated expression in vivo. *Journal of immunology* **148**, 4066-4071 (1992); published online EpubJun 15

22. M. Lotz, F. Jirik, P. Kabouridis, C. Tsoukas, T. Hirano, T. Kishimoto, D. A. Carson, B cell stimulating factor 2/interleukin 6 is a costimulant for human thymocytes and T lymphocytes. *J Exp Med* **167**, 1253-1258 (1988); published online EpubMar 1

23. M. T. Wiekowski, M. W. Leach, E. W. Evans, L. Sullivan, S. C. Chen, G. Vassileva, J. F. Bazan, D. M. Gorman, R. A. Kastelein, S. Narula, S. A. Lira, Ubiquitous transgenic expression of the IL-23 subunit p19 induces multiorgan inflammation, runting,

infertility, and premature death. *Journal of immunology* **166**, 7563-7570 (2001); published online EpubJun 15

24. J. P. Sherlock, B. Joyce-Shaikh, S. P. Turner, C. C. Chao, M. Sathe, J. Grein, D. M. Gorman, E. P. Bowman, T. K. McClanahan, J. H. Yearley, G. Eberl, C. D. Buckley, R. A. Kastelein, R. H. Pierce, D. M. Laface, D. J. Cua, IL-23 induces spondyloarthropathy by acting on ROR-gammat+ CD3+CD4-CD8- entheseal resident T cells. *Nature medicine* **18**, 1069-1076 (2012); published online EpubJul (10.1038/nm.2817).
25. J. Molden, Y. Chang, Y. You, P. S. Moore, M. A. Goldsmith, A Kaposi's sarcoma-associated herpesvirus-encoded cytokine homolog (vIL-6) activates signaling through the shared gp130 receptor subunit. *The Journal of biological chemistry* **272**, 19625-19631 (1997); published online EpubAug 1
26. D. Chen, J. Nicholas, Structural requirements for gp80 independence of human herpesvirus 8 interleukin-6 (vIL-6) and evidence for gp80 stabilization of gp130 signaling complexes induced by vIL-6. *Journal of virology* **80**, 9811-9821 (2006); published online EpubOct (10.1128/JVI.00872-06).
27. Y. Aoki, M. Narazaki, T. Kishimoto, G. Tosato, Receptor engagement by viral interleukin-6 encoded by Kaposi sarcoma-associated herpesvirus. *Blood* **98**, 3042-3049 (2001); published online EpubNov 15
28. T. Kopp, E. Riedl, C. Bangert, E. P. Bowman, E. Greisenegger, A. Horowitz, H. Kittler, W. M. Blumenschein, T. K. McClanahan, T. Marbury, C. Zachariae, D. Xu, X. S. Hou, A. Mehta, A. S. Zandvliet, D. Montgomery, F. van Aarle, S. Khalilieh, Clinical improvement in psoriasis with specific targeting of interleukin-23. *Nature* **521**, 222-226 (2015); published online EpubMay 14 (10.1038/nature14175).
29. J. J. O'Shea, Y. Kanno, A. C. Chan, In search of magic bullets: the golden age of immunotherapeutics. *Cell* **157**, 227-240 (2014); published online EpubMar 27 (10.1016/j.cell.2014.03.010).
30. G. M. Fuhler, S. H. Diks, M. P. Peppelenbosch, W. G. Kerr, Widespread deregulation of phosphorylation-based signaling pathways in multiple myeloma cells: opportunities

for therapeutic intervention. *Molecular medicine* **17**, 790-798 (2011)10.2119/molmed.2011.00013).

31. M. Segarra, H. Ohnuki, D. Maric, O. Salvucci, X. Hou, A. Kumar, X. Li, G. Tosato, Semaphorin 6A regulates angiogenesis by modulating VEGF signaling. *Blood* **120**, 4104-4115 (2012); published online EpubNov 8 (10.1182/blood-2012-02-410076).
32. L. Yao, O. Salvucci, A. R. Cardones, S. T. Hwang, Y. Aoki, M. De La Luz Sierra, A. Sajewicz, S. Pittaluga, R. Yarchoan, G. Tosato, Selective expression of stromal-derived factor-1 in the capillary vascular endothelium plays a role in Kaposi sarcoma pathogenesis. *Blood* **102**, 3900-3905 (2003); published online EpubDec 1 (10.1182/blood-2003-02-0641).
33. P. S. Cooper, D. Lipshultz, W. T. Matten, S. D. McGinnis, S. Pechous, M. L. Romiti, T. Tao, M. Valjavec-Gratian, E. W. Sayers, Education resources of the National Center for Biotechnology Information. *Briefings in bioinformatics* **11**, 563-569 (2010); published online EpubNov (10.1093/bib/bbq022).

Acknowledgements: We thank Drs. S. Sakakibara, D. Maric, S. Garfield, B. Adler, D. Lowy and members of the Laboratory of Cellular Oncology for helping in aspects of this work. **Funding:** This work is supported by the intramural research program of CCR/NCI/NIH. The computational analysis in this project was funded with Federal funds from the National Cancer Institute, National Institutes of Health, under Contract No. HHSN261200800001E, and does not necessarily reflect the views or policies of the Department of Health and Human Services, nor does mention of trade names, commercial products, or organizations imply endorsement by the U.S. Government. E. Planas-Rigol and M. C. Cid were funded by the Ministerio de Economía y Competitividad (SAF 11/30073). G. Espígol-Frigolé was partially funded by the Instituto de Salud Carlos III. **Author contributions:** G E.-F., E. P.-R., H. O., H.K., O. S. performed the experiments. G E.-F., E. P.-R. and G. T. planned the experiments. S. R. and B. L. performed computational analyses. G. E-F and M. C. C. provided care of the patients. G. E.-F., E. P.-R. and G. T. interpreted the data and wrote the manuscript.

Competing interests: The authors declare that they have no competing interests.

FIGURE LEGENDS

Figure 1. IL-23p19 expression in GCA temporal arteritis. (A,B) Histology of normal (A) and GCA (B) temporal arteries; narrowing lumen, inflammatory infiltrates in the vessel wall and disrupted internal elastic membrane in B; H&E (left) DAPI (right). L: lumen; I: *tunica intima*; M: *tunica media*; Adv: *adventitia*; E: internal elastic membrane. **(C,D)** CD31 (red) in sections of normal temporal artery (C) showing selective presence of CD31 in the endothelium lining the temporal artery, and in sections of GCA temporal artery (D) showing CD31 (red) in the endothelium lining the narrow lumen and in cells scattered throughout the vessel wall. Nuclei are stained with DAPI (blue). **(E)** CD31 (red), p19 (green), p40 (white) immunostaining in the *adventitia* of the GCA temporal artery (magnification of the boxed areas 1-3 in D), showing CD31/p19 co-localization (yellow, pointed by the arrows) in capillary structures and other isolated cells. Boxed areas in the bottom panels limit $p40^+$ (white) cells. Results are representative of 3 arteries from 3 GCA patients; at least 3 sections/sample were evaluated.

Figure2. Inflammatory signals induce p19 in endothelial cells. Effects of PMA, LPS and TNFα on endothelial cell (HUVEC and HDMEC) expression of p19 **(A)** and p40 mRNA **(B)**. Results are from qPCR (fold increase after 24 hour culture; means±SD; n=3/group; triplicate measurements). **(C)** LPS and TNFα induce p19 in HUVEC and HDMEC; no p19 is detected in TCA-precipitates of serum-free HDMEC supernatants (SN, 20 ml). Cell lysates of LPS-activated PBMC are used as control. Representative immunoblotting results from 3 experiments. **(D)** p19 is detected in culture supernatants from LPS-activated PBMC ($2x10^6$/ml), but not in culture supernatants of HUVEC and HDMEC ($1x10^6$/ml); all cell types were cultured in complete culture medium for 24 hours. ELISA results (means±SD; n=4 experiments; triplicate measurements). **(E)** p19 mRNA (left upper bar graphs) and protein (left lower blots) is detected in HUVEC transduced by p19 lentivirus (p19LV) but not control lentivirus (control); qPCR (fold increase $x10^3$; means±SD triplicate measurements) and immunoblotting results (representative of 5 and 6 experiments, respectively). p19 is visualized in the cytoplasm of HUVEC transduced with p19 (right lower panel) but not control (right lower panel) lentivirus; % cells with cytoplasmic p19/DAPI: 92±6.3% (n=6 experiments). **(F)** Expression of p40 and IL-23R in non-transduced HUVEC, HUVEC transduced with p19 and

control lentivirus and in LPS-activated PBMC. Results are from qPCR (fold increase; means±SD; triplicate measurements). **(G)** p19 protein is detected in supernatants from LPS-activated PBMC but not from p19-transduced HUVEC. Cells were cultured ($1x10^6$/ml) in serum-free medium for 24 (1) and 72 (2) hours; protein was TCA-precipitated from the conditioned media (100 ml from p19 HUVEC and 20 ml from LPS-activated PBMC). Cells lysates (cells) of p19-HUVEC and LPS-activated PBMC (after 72 hours culture) were used as controls. Representative results from 3 experiments.

Figure3. p19 induces adhesion molecules and STAT3 phosphorylation in endothelial cells. Lentiviral p19 (p19) but not vector (control) promotes ICAM-1 and VCAM-1 mRNA **(A)** and protein **(B)** expression in HUVEC; qPCR results (fold increase; means ±SD; n=3 experiments, triplicate measurements); representative immunoblotting results (left); bar graph (right): band intensity ratios relative to β-actin (means±SD, 3 experiments). **(C)** PBMC attach better onto monolayers of p19-transduced HUVEC compared to control (vector-transduced) HUVEC. The results (means±SD of triplicates) reflect a representative experiment (5 performed). **(D)** Transendothelial migration of normal peripheral blood PBMC through monolayers of p19-transduced or control (vector-transduced) HUVEC cultured in medium only or activated with LPS or TNFα plus IFNγ. The results reflect the (means±SD, 3 experiments; each experiment includes PBMC from 3-4 blood donors). **(E)** p-STAT3) in p19 and control HUVEC is detected by Western blotting. STAT3 and β-actin are from membrane re-probing; representative immunoblotting results (left); the bar graph (right): band intensity ratios relative to STAT3 and β-actin (means±SD, 3 experiments). **(F)** STAT3 nuclear localization (green, pointed by arrow) in p19-expressing HUVEC (red); nuclei are stained with DAPI (blue). **(G)** IL-6 plus IL-6R induce more p-STAT3 in p19-HUVEC compared to control HUVEC; time course: 0-45 min. After immunostaining for p-STAT3 and visualization of nuclei with DAPI, immunofluorescence was quantified in at least 500 cells from 10 fields at each time-point. Bar graph: time 0 results with expanded scale; the line graph reflects the results at 0-45 min. P values (two-tailed Student t-test): **: $p< 0.01$; *$p < 0.05$.

Figure4. p19 binds to gp130. (A) Structure similarity of the vIL-6-gp130 and p19-gp130 tetrameric complexes. The vIL-6-gp130 complex representation (left) is based on the published experimental structure; the p19-gp130 complex representation (right) is based on modeling predictions. **(B)** p19 and vIL-6 bind to immobilized gp130 as detected by ELISA. Purified soluble gp130 immobilized to plastic wells was incubated with serial dilutions of recombinant human p19 (78-250 ng/ml) or vIL-6 (1.5-50 ng/ml); bound protein was detected with specific antibodies. The results represent the means of triplicate measurements. **(C)** Recombinant human p19 (1□g/ml) time-dependently induces gp130 activation in mouse BAF-130 cells stably transduced with human gp130; human IL-6 (1 µg/ml) plus IL6R (2.5 µg/ml) were added to culture 15 min. Cell lysates were immunoprecipitated with rabbit anti-gp130 antibody or rabbit IgG. The immunoprecipitates were immunoblotted with anti-phosphotyrosine antibody; after stripping, the membrane was re-probed with anti-gp130 antibody. **(D)** Recombinant human p19 (1µg/ml) time-dependently induces p-STAT3 in mouse BAF-130 cells stably transduced with human gp130. IL-6 plus IL-6R were used as a positive control (conditions are the same as in C). Membranes were re-probed with β-actin antibody. **(E)** gp130 binds to endogenous p19 in HUVEC as detected by immunoprecipitation (IP) and immunoblotting (IB). IP: rabbit IgG to human gp130 or rabbit IgG. IB: rabbit anti-human p19 and mouse anti-human gp130 antibodies. Lysates of p19-HUVEC (sample 1 and 3) and p19-HUVEC pre-activated (18 hours) with IL-6 plus IL6R (sample 2) were immunoprecipitated with human gp130 rabbit IgG antibody (samples 1 and 2) or rabbit IgG (sample 3); gp130 and p19-related bands are marked by the arrows.

Figure5. p19 co-localizes with gp130 in endothelial cells and activates gp130. (A) PLA imaging shows that intracellular p19 associates with gp130 in HUVEC. The red dots mark the proximity (<40 nm) co-localization of p19 and gp130 in p19-HUVEC and control HUVEC prior to activation (time 0) or after 15 min activation with IL-6 plus IL6R. CD31 immunostaining (green) marks the endothelial cell surface membrane; representative images (of 5 larger fields/condition). The panels on the left reflect representative images from control PLA documenting PLA specificity. Nuclei are identified by DAPI (blue) staining. **(B)** Quantitation of p19+gp130 proximity co-localization in p19-HUVEC and control HUVEC prior to and 15 min

after activation with IL-6 plus IL6R. The results (mean±SD dots/cell) are from analysis of at least 200 cells from 5 fields/condition. **(C)** Relative tyrosine-phosphorylated (p-Tyr) gp130 detected in cell lysates of control and p19-infected HUVEC prior to (0 min) and 5 min after activation with IL-6 plus IL-6R. Results are from ELISA (±SD triplicate measurements).

Figure6. Endothelial co-localization of p19 and gp130 in GCA temporal artery. PLA imaging shows that p19 associates with gp130 in $CD31^+$ vascular structures from the *adventitia* (Adv) of a temporal artery affected with GCA. The red staining marks the proximity (<40 nm) co-localization of p19 and gp130 in the tissue. The green staining marks CD31 immunostaining and blue (DAPI) marks the cell nuclei. White arrows point to PLA (p19+gp130) red signal and the corresponding $CD31^+$ green signal. Upper left: low magnification image; the two boxed areas (labeled 1 and 2) are magnified on the right (3 panels, corresponding to box 1) and below (3 panels, corresponding to box 2). The results are representative of 3 patients with GCA; at least 3 sections/patient were evaluated.

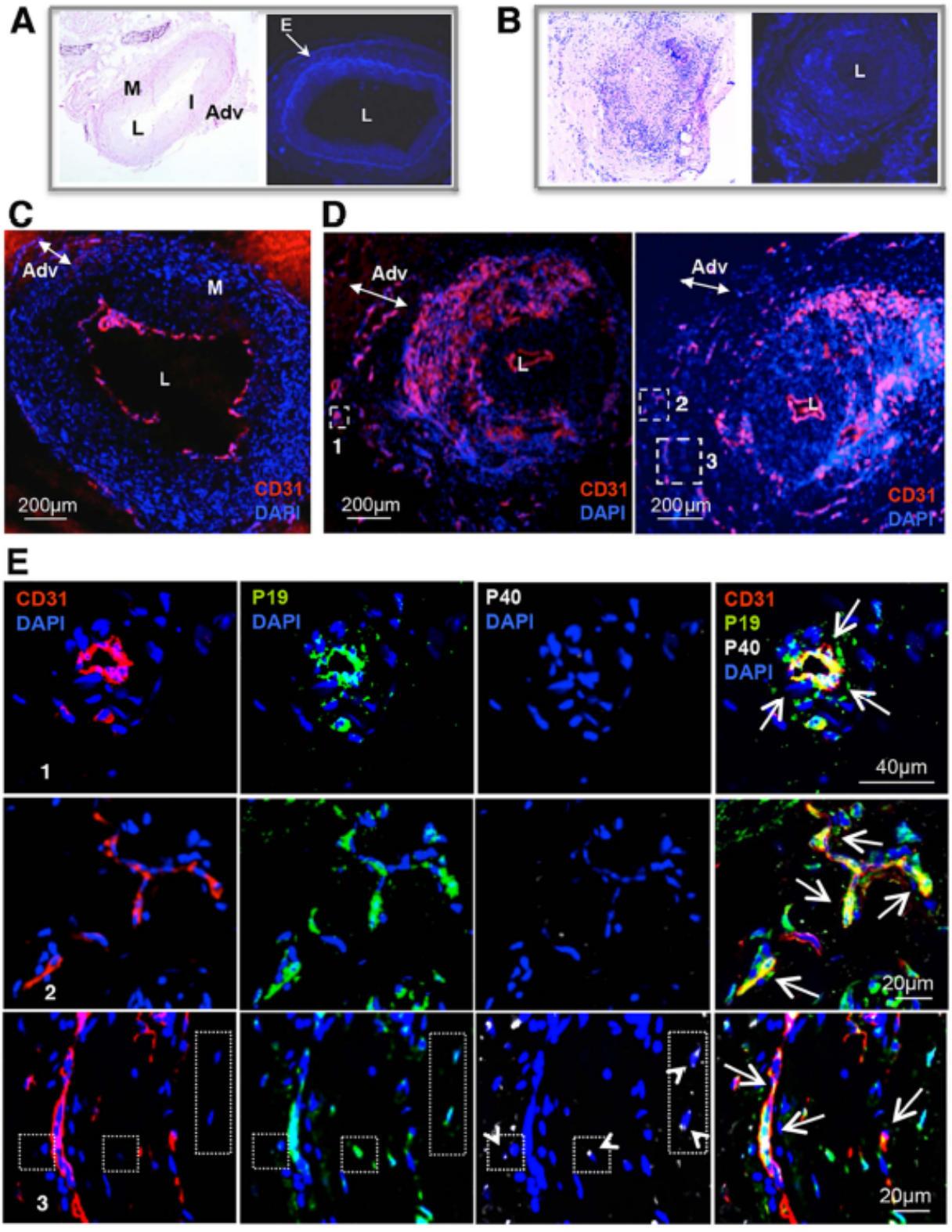
A
M
I
Adv
L
E
L
B
L
C
Adv
M
L
200μm
CD31
DAPI
D
Adv
L
1
200μm
CD31
DAPI
Adv
2
L
3
200μm
CD31
DAPI
E
CD31
DAPI
1
P19
DAPI
P40
DAPI
CD31
P19
P40
DAPI
40μm
2
20μm
3
20μm

Figure 1

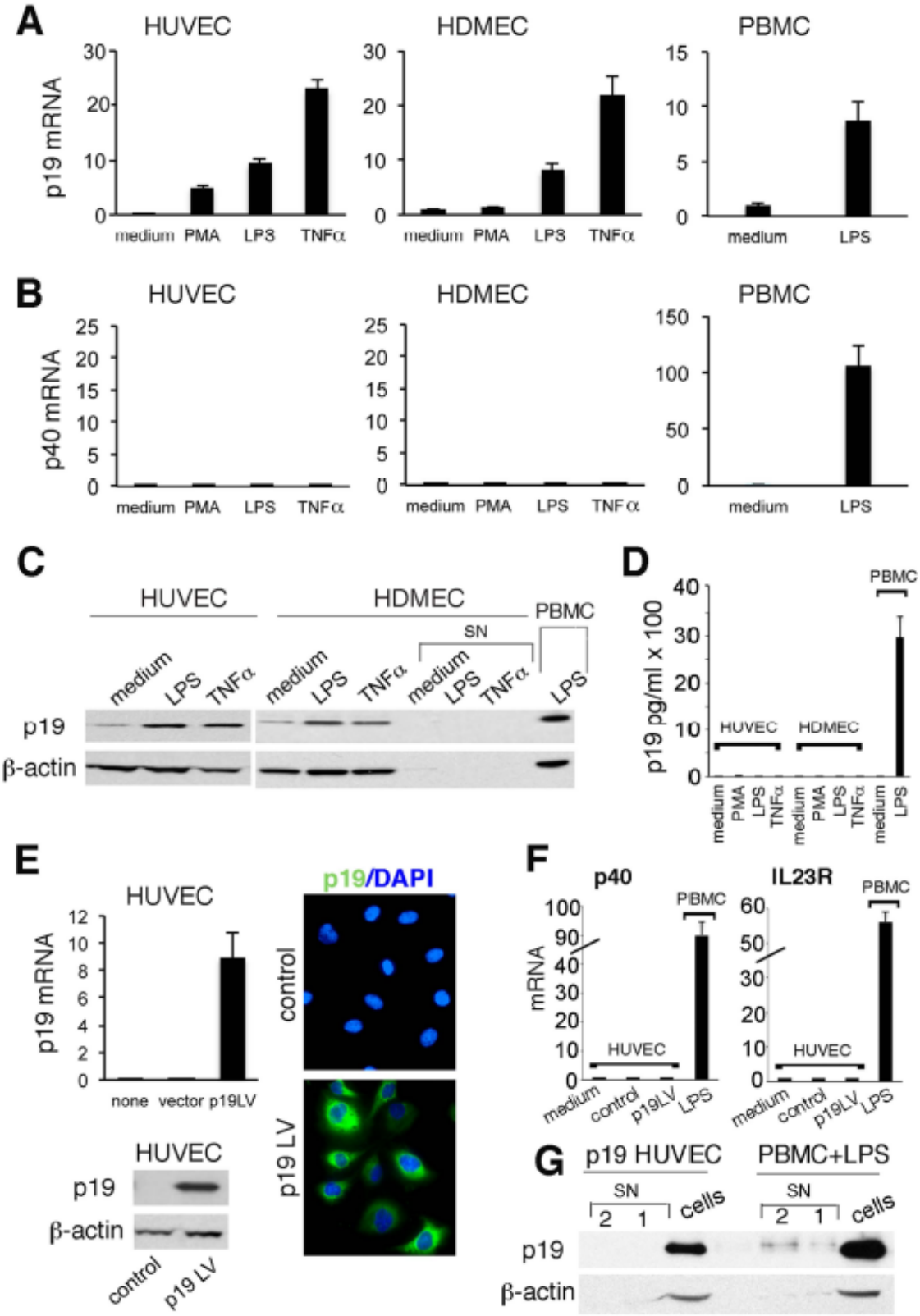
A
HUVEC
HDMEC
PBMC
p19 mRNA
medium PMA LPS TNFα
medium LPS
B
p40 mRNA
C
p19
β-actin
SN
D
p19 pg/ml x 100
E
p19/DAPI
control
p19 LV
none vector p19LV
F
p40
IL23R
mRNA
G
p19 HUVEC
PBMC+LPS
cells

Figure 2

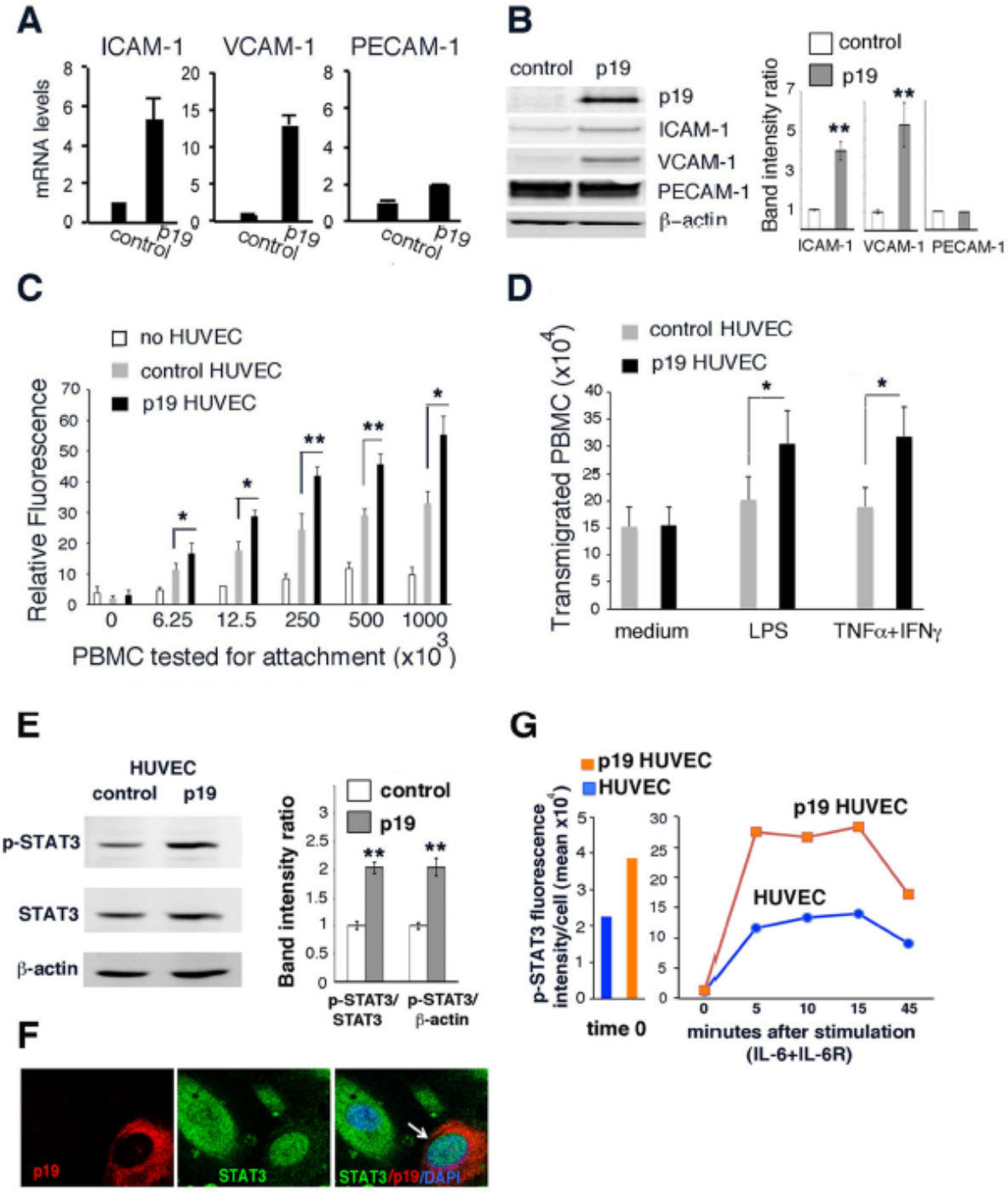
A
ICAM-1
VCAM-1
PECAM-1
mRNA levels
control
p19
B
control
p19
p19
ICAM-1
VCAM-1
PECAM-1
β-actin
Band intensity ratio
C
no HUVEC
control HUVEC
p19 HUVEC
Relative Fluorescence
PBMC tested for attachment (x10³)
D
control HUVEC
p19 HUVEC
Transmigrated PBMC (x10⁴)
medium
LPS
TNFα+IFNγ
E
HUVEC
p-STAT3
STAT3
β-actin
Band intensity ratio
p-STAT3/ STAT3
p-STAT3/ β-actin
F
p19
STAT3
STAT3/p19/DAPI
G
p19 HUVEC
HUVEC
p-STAT3 fluorescence intensity/cell (mean x10⁴)
time 0
minutes after stimulation (IL-6+IL-6R)

Figure 3

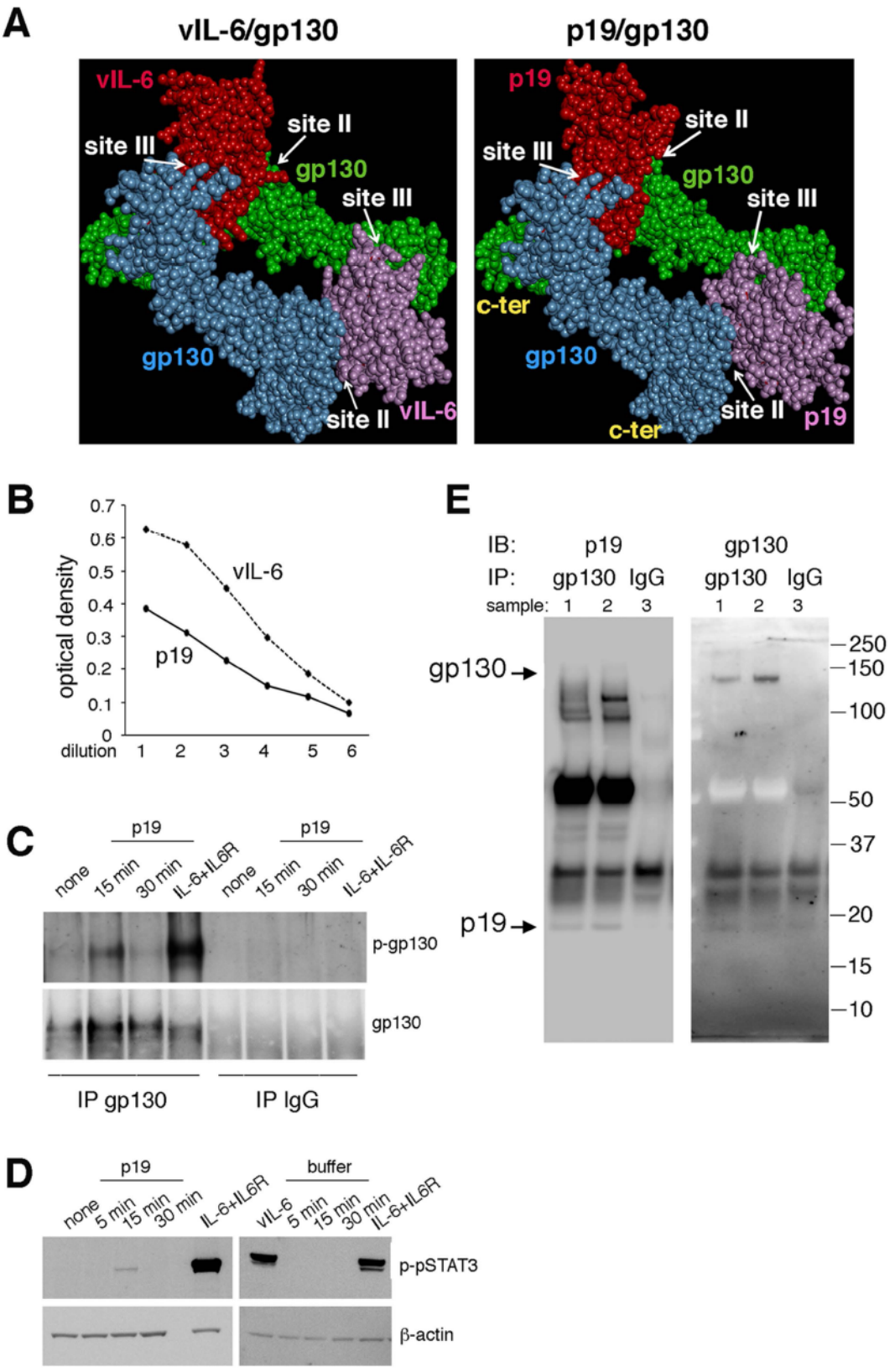
A
vIL-6/gp130
vIL-6
site II
site III
gp130
site III
gp130
site II
vIL-6
p19/gp130
p19
site II
site III
gp130
site III
c-ter
gp130
site II
p19
c-ter
B
optical density
0.7
0.6
0.5
0.4
0.3
0.2
0.1
0
dilution 1 2 3 4 5 6
vIL-6
p19
C
p19
p19
none
15 min
30 min
IL-6+IL6R
none
15 min
30 min
IL-6+IL6R
p-gp130
gp130
IP gp130
IP IgG
D
p19
buffer
none
5 min
15 min
30 min
IL-6+IL6R
vIL-6
5 min
15 min
30 min
IL-6+IL6R
p-pSTAT3
β-actin
E
IB:
p19
gp130
IP:
gp130
IgG
gp130
IgG
sample:
1
2
3
1
2
3
gp130
p19
250
150
100
50
37
20
15
10

Figure 4

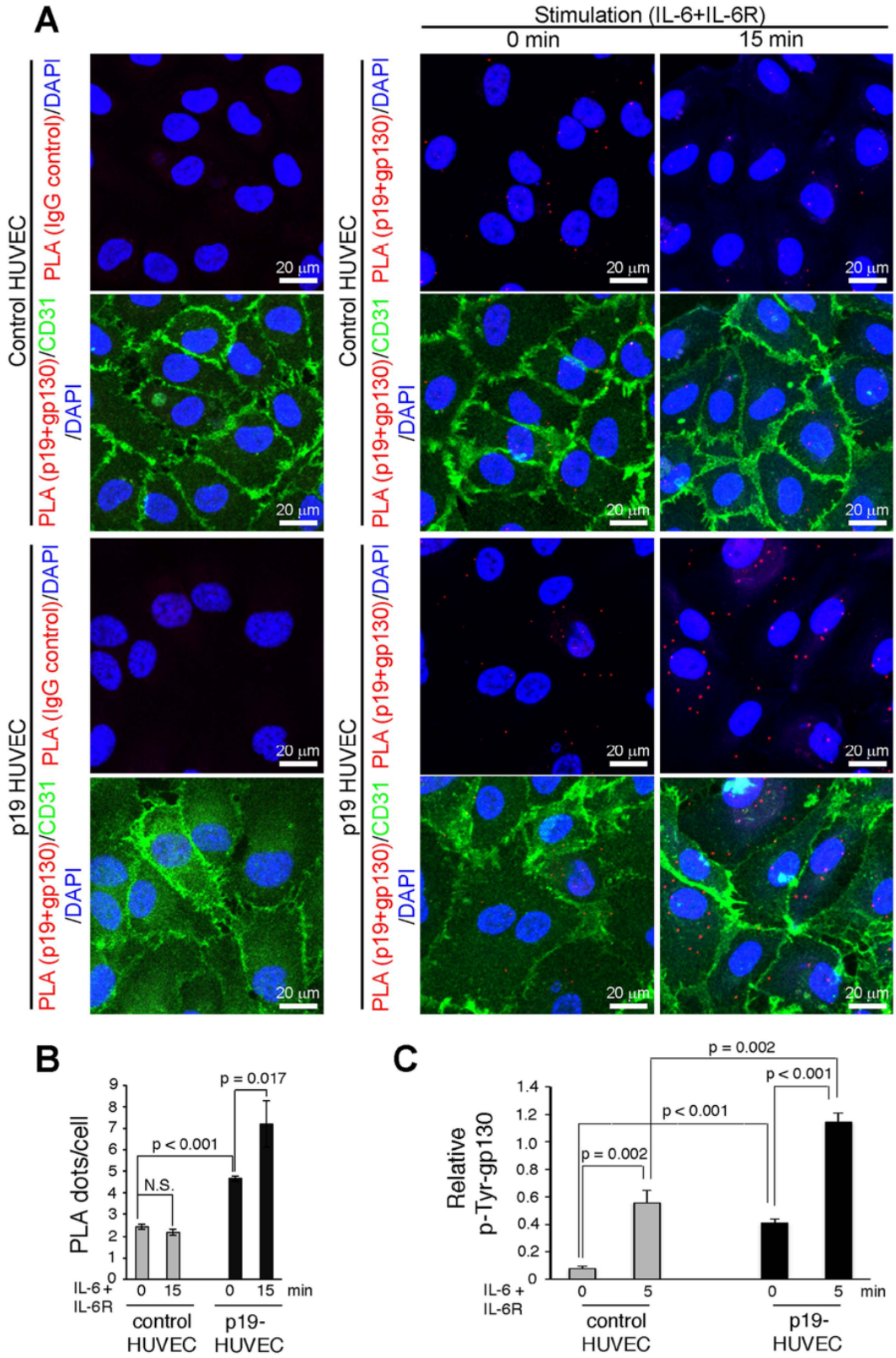
A
Stimulation (IL-6+IL-6R)
0 min
15 min
Control HUVEC
PLA (IgG control)/DAPI
PLA (p19+gp130)/CD31 /DAPI
p19 HUVEC
20 μm
B
PLA dots/cell
p = 0.017
p < 0.001
N.S.
IL-6 + IL-6R
0 15 0 15 min
control HUVEC
p19-HUVEC
C
Relative p-Tyr-gp130
p = 0.002
p < 0.001
p < 0.001
p = 0.002
0 5 0 5 min
control HUVEC
p19-HUVEC

Figure 5

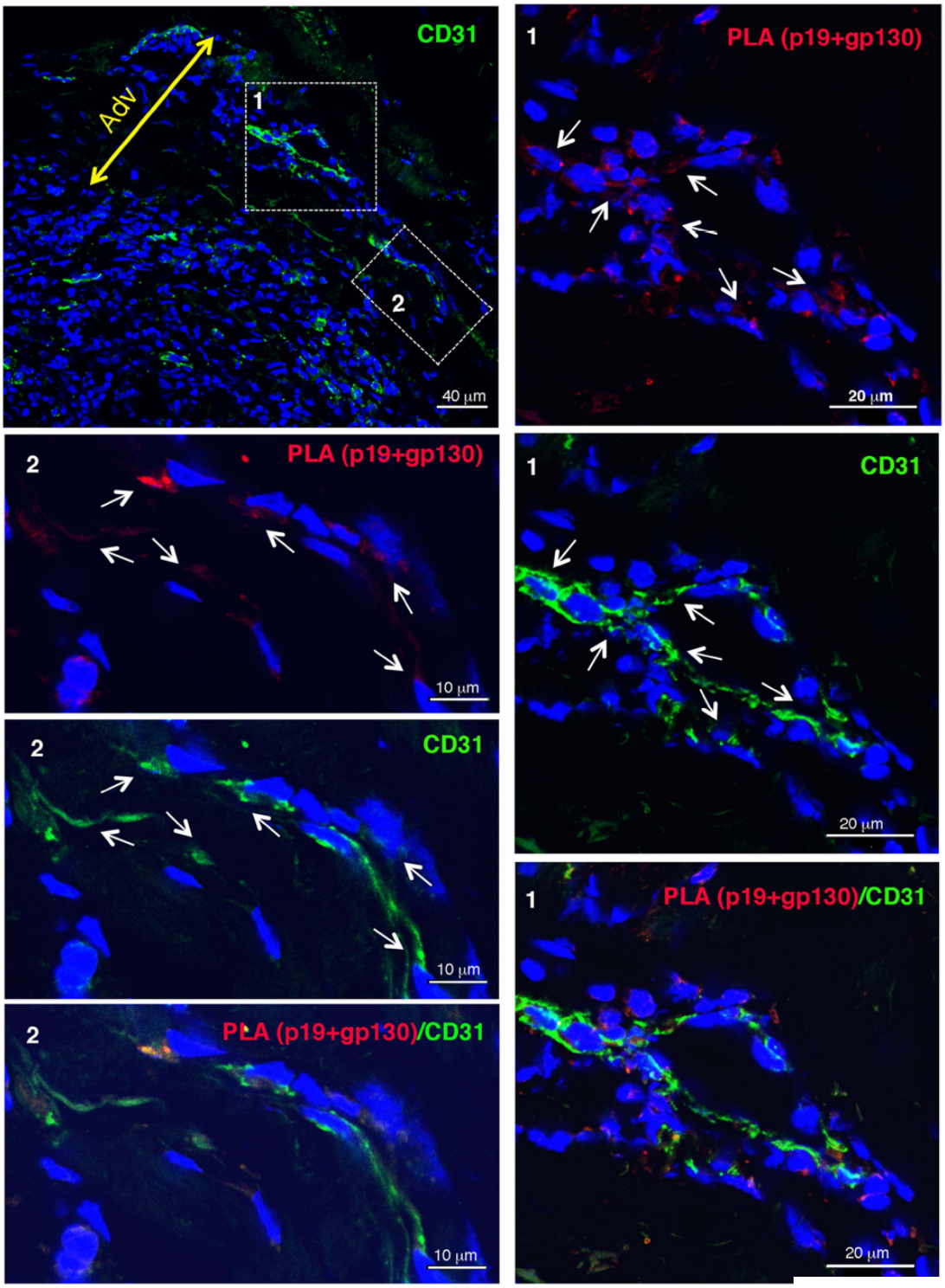
CD31
Adv
1
2
40 μm
1
PLA (p19+gp130)
20 μm
2
PLA (p19+gp130)
10 μm
1
CD31
20 μm
2
CD31
10 μm
1
PLA (p19+gp130)/CD31
20 μm
2
PLA (p19+gp130)/CD31
10 μm

Figure 6

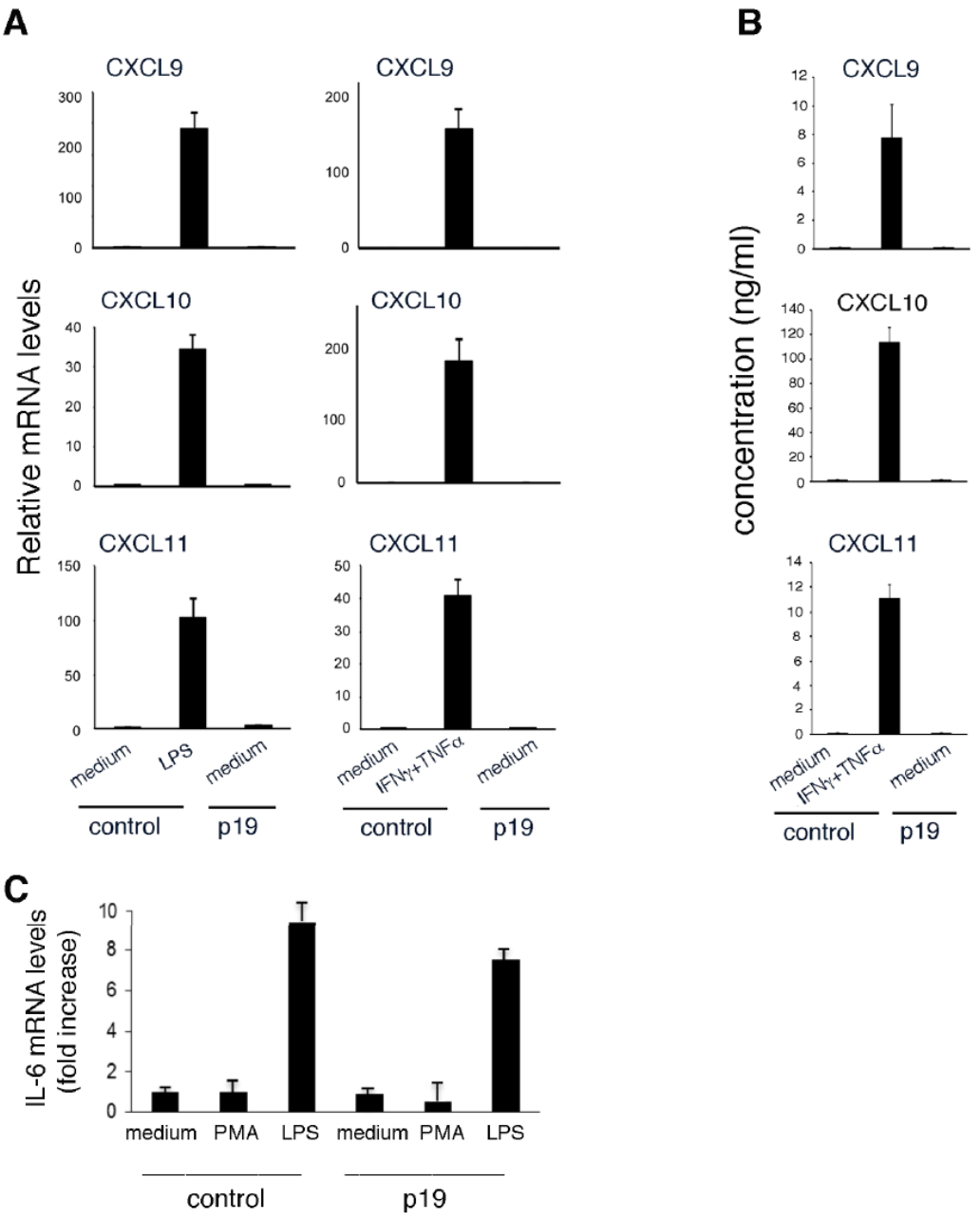

Fig. S1. Effects of p19 on HUVEC expression of CXCL9, CXCL10, CXCL11 and IL-6. qPCR **(A)** and ELISA **(B)** results for the chemokines CXCL9, CXCL10 and CXCL11. **(C)** IL-6 mRNA levels from qPCR. The results (means ±SD of triplicate measurements) are representative of 3 experiments. Control (vector-transduced) and p19 (p19-transduced) HUVEC.

Supplementary figure 1

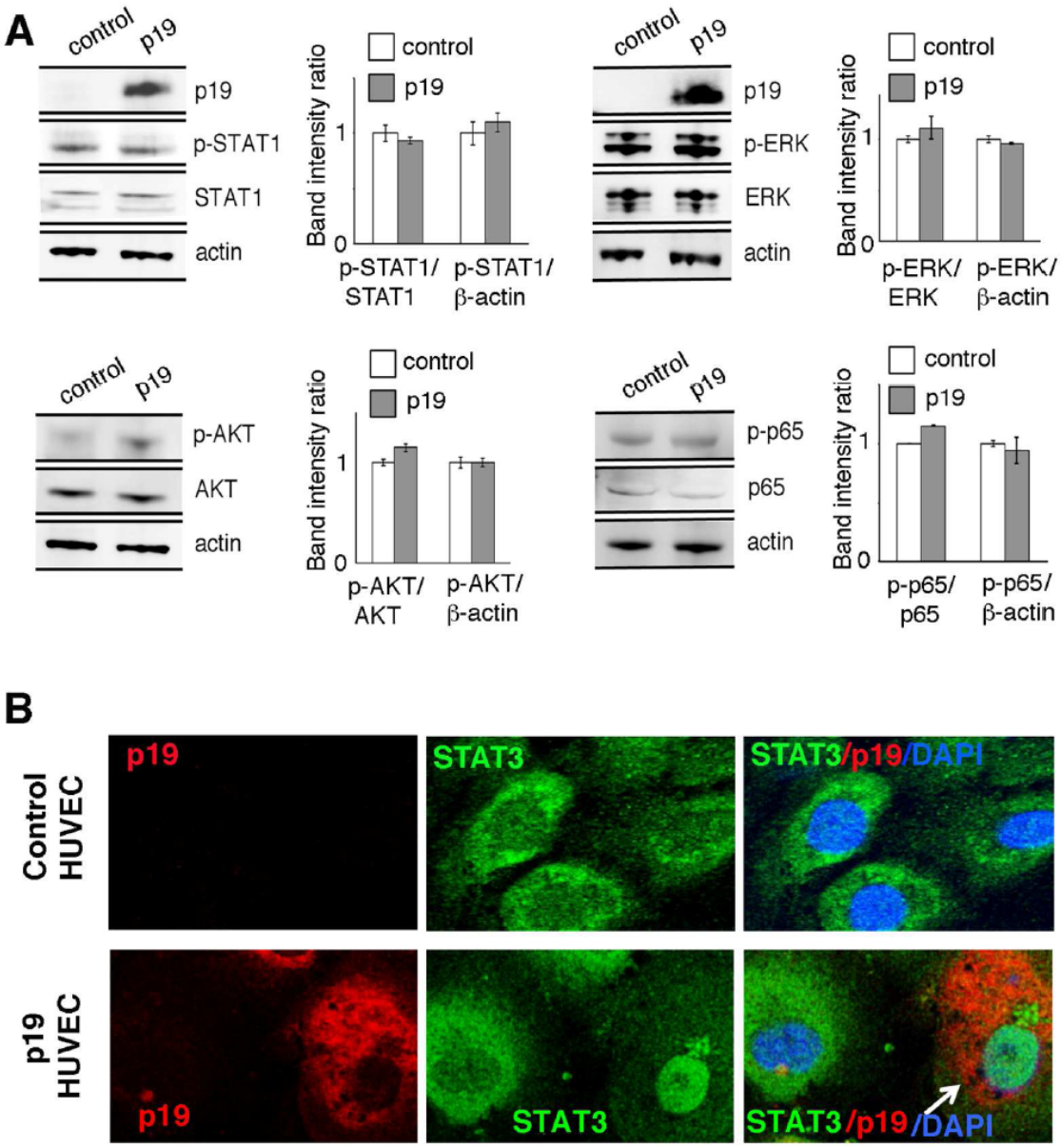

Fig. S2. Analysis of signaling mediators in HUVEC transduced with p19. Signaling mediators detected by immunoblotting in control (vector-transduced) and p19-transduced HUVEC. Representative immunoblotting; results of relative band intensity measurements are shown in the bar graphs (means ± of 3 experiments). **(A)**. Selective STAT3 nuclear localization in p19 expressing HUVEC **(B)**.

Supplementary figure 2

A

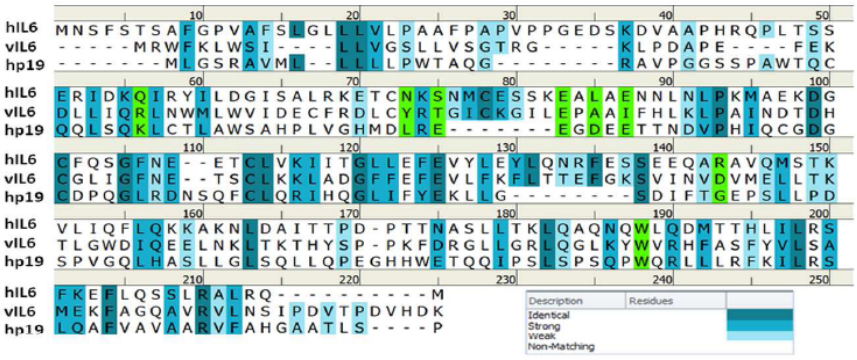

H-bonded vIL-6 residues and corresponding residues in hIL-6 and p19 are highlighted in green

B

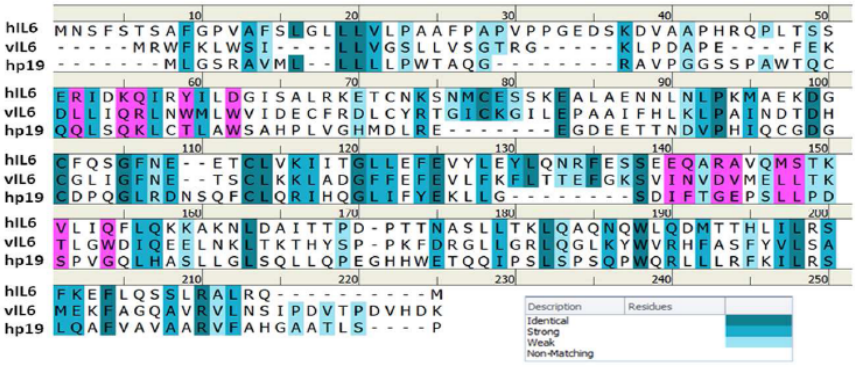

Surface residues from vIL6-gp130 complex site II and corresponding residues in hIL6 and p19 are highlighted in pink

C

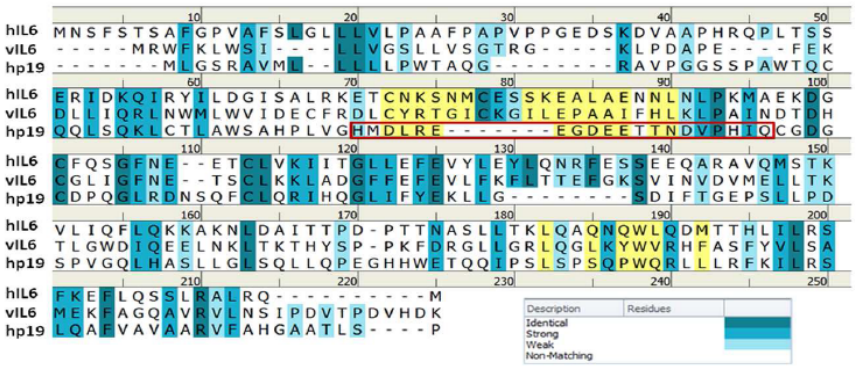

Surface residues from vIL6-gp130 complex site III and corresponding residues in hIL6 and p19 are highlighted in yellow. The red box identifies the loop region linking the A and B helices.

Fig. S3. Molecular modeling of p19-gp130 interactions. H-bond interactions **(A)**, Site II interaction **(B)** and Site III interaction **(C)**.

Supplementary figure 3

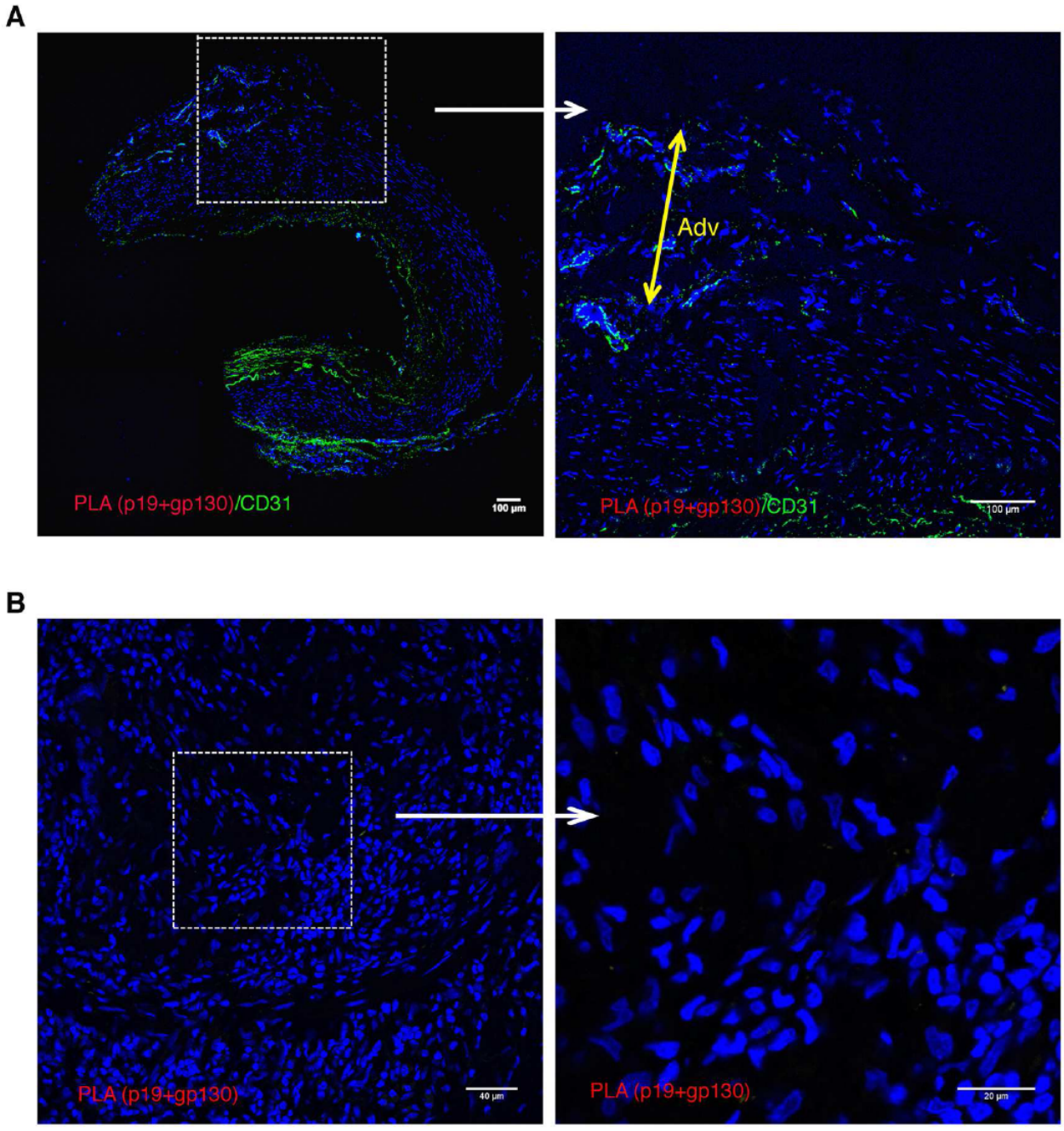

Fig. S4. PLA controls. PLA (p19+gp130, red) and CD31 immunostaining (green) of temporal artery from a patient suffering from persistent headaches of unknown cause. **(A)**. Control PLA (p19+gp130) of GCA artery without primary antibodies **(B)**. DAPI (blue) depicts cell nuclei. The results are representative of 3 control patients and 3 patients with GCA; at least 3 sections/patient were evaluated.

Supplementary figure 4

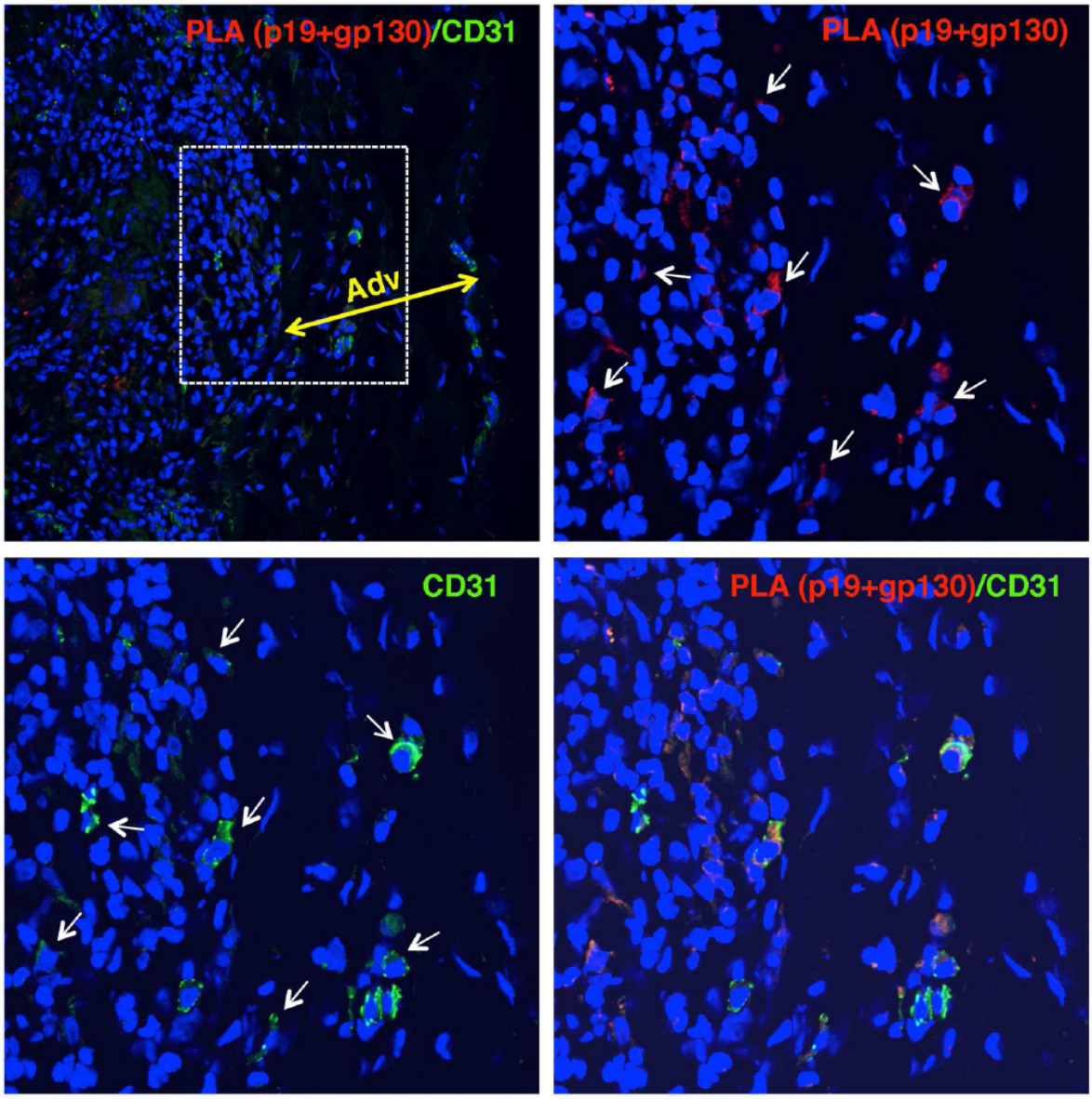

Fig. S5. PLA (p19+gp130) and CD31 immunostaining of GCA temporal artery. PLA imaging shows the proximity co-localization (<40 nm) of p19 and gp130 in $CD31^+$ cells within the *adventitia* (Adv) of a GCA temporal artery. PLA (red); CD31 immunostaining (green); DAPI (blue.) White arrows point to PLA signal and corresponding $CD31^+$ signal. Upper left: low magnification image (PLA signal is not detected at this magnification); the boxed area is magnified in the other 3 panels (PLA signal is detected). The results are representative of 3 patients with GCA; at least 3 sections/patient were evaluated.

Supplementary figure 5

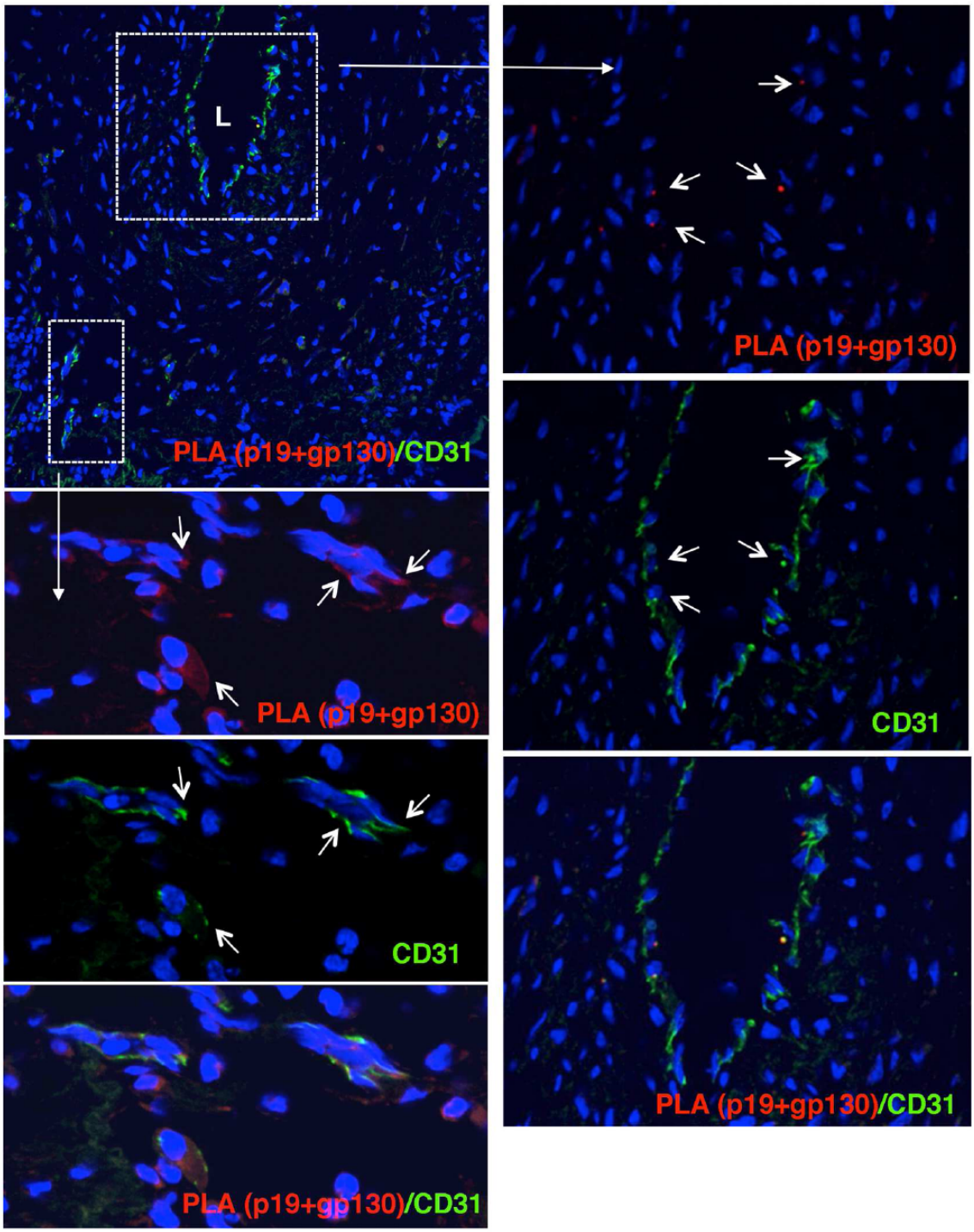

Fig. S6. PLA (p19+gp130) and CD31 immunostaining of GCA temporal artery. Boxed areas (upper left; PLA signal not visible) are magnified. PLA: red; CD31: green; DAPI: blue. Lumen (L). Representative of 3 GCA patients.

Supplementary figure 6

Table S1. GCA patients: clinical and laboratory findings at diagnosis

Age (median years ±SD)	73.10 ± 7.69
Gender (male/female) ratio	0/5
Clinical manifestations at diagnosis	
Cranial Symptoms	
Headache	4 (80%)
Scalp tenderness	2 (40%)
Jaw claudication	2 (40%)
Diplopia	0
Visual loss	0
Systemic Symptoms	
Fever	3 (60%)
Weight loss	2 (40%)
Polymyalgia rheumatica	3 (60%)
Laboratory results at diagnosis	
Erythrocyte Sedimentation Rate (ESR, mm/hr)	104.19 ± 21.61
C-Reactive Protein (CRP, mg/dL)	11.32 ± 9.04
Hemoglobin (Hgb, g/dL	9.55 ± 1.1

Table S2. Control patients: demographic data and diagnosis

Age (median years ±SD)	77.126 ± 8.14
Gender (male/female) ratio	0/3
Diagnosis	
Non-arteritic anterior ischemic neuritis	1
Chronic multifactorial anemia	1
Non-specific headache in patient with multiple pathologies	1

Supplementary table 1

Identification of IL-23p19 as an endothelial proinflammatory peptide that promotes gp130-STAT3 signaling

Running Title: IL-23p19 is an endothelial proinflammatory peptide

Georgina Espigol-Frigole, Ester Planas-Rigol, Hidetaka Ohnuki, Ombretta Salvucci, Henry Kwak, Sarangan Ravichandran, Brian Luke, Maria C. Cid and Giovanna Tosato

Results summary (part 1)

1) We have demonstrate that p19, but not p40, is expressed in the capillary endothelium lining the pathological *vasa vasorum* of inflamed temporal arteries from GCA patients by immunofluorescence staining comparing inflamed TAB (from GCA patients) vs controls.
2) TNFα and LPS induce p19 mRNA and protein expression in primary cultures of EC whereas p40 is not detectable.
3) No evidences on the secretion of p19 by these stimulated cells are present suggesting intracellular function.
4) Over-expression of p19 induces adhesion molecules (ICAM-1 and VCAM-1) mRNA and protein expression in HUVEC.
5) Endothelial expression of p19 promotes leukocyte attachment to endothelium and trans-endothelial migration.
6) p19-expressing HUVEC display increased levels of STAT3 phosphorylation (p-STAT3; Tyr 705) as well as STAT3 nuclear translocation. Moreover, IL-6 plus soluble IL-6R induce greater STAT3 activation in p19 expressing HUVEC.
7) Molecular modeling approximations predict that p19 has a high probability of forming a complex with gp130 similar to viral IL-6 (vIL-6).
8) Various functional experiments using either HUVEC or tissues have demonstrated p19 interaction with the gp130 receptor.
    a. p19 dose-dependently binds to immobilized recombinant gp130-Fc in a cell-free system.

b. Recombinant p19 time-dependently activates STAT3 in BAF-130 cells (which are stably transfected with human gp130 and don't express IL-6R) similar to vIL-6 and to human IL-6 plus IL-6 receptor (IL-6R).

c. In p19-HUVEC lysates, p19 co-immunoprocipitates with gp130 with or without prior activation with IL-6 plus IL-6R.

d. Proximity ligation assay detected specific association of p19 and gp130 in p19-HUVEC. Moreover this interaction was enhanced by previous activation of p19-HUVEC cells with IL-6 plus soluble IL-6R.

e. p19 and gp130 co-localize in $CD31^+$ endothelial cells lining the *vasa vasorum* of GCA-affected arteries, allowing p19/gp130 signaling at these sites.

IL-35: A new cytokine involved in vascular inflammation.

E.Planas-Rigol, M.Corbera- Bellalta, N.Terrades-Garcia, Georgina Espígol-Frigolé, Marco A. Alba, S. Prieto, MC.Cid.

Department of Systemic Autoimmune Diseases. Hospital Clínic. IDIBAPS. University of Barcelona (Spain).

(In preparation)

Vasculitis Research Unit, Department of Autoimmune Diseases. Hospital Clínic. University of Barcelona. Institut d'Investigacions Biomèdiques August Pi i Sunyer (IDIBAPS). Fundació CELLEX. Barcelona, Spain

Correspondence

Maria Cinta Cid Xutglà.
Department of Autoimmune Diseases. Hospital Clínic
Villarroel, 170
08036-Barcelona, Spain
Email: mccid@clinic.ub.es
Phone number: 93 227 54 00 ext 3111

ABSTRACT:

Giant cell arteritis (GCA) is a chronic inflammatory disease of blood vessels in which Th1 and Th17 pathways are involved. Our previous results have demonstrated a dissociation of the IL-12 subunits (p40 and p35) expression in arterial biopsies from patients with GCA. While p40 is hardly detected in normal arteries and induced in GCA lesions, p35 is constitutively expressed by vascular smooth muscle (VSMC) cells from the media layer. Another partner for p35 (EBI3) has been described to conform IL-35 which is also a component of the IL-12 super family of heterodimeric cytokines together with IL-23, IL-27 and IL-12.

In this study it has been observed that p35 mRNA was equally expressed in control or GCA arteries whereas Ebi3 was increased in GCA specimens. Interestingly, p35 and Ebi3 co-expressed in VSMC and leukocytes within the inflammatory infiltrates. Moreover, co-culture of CD4T or CD14+ with VSMC induced p35 and Ebi3 mRNA expression and IL-35 secretion by VSMC either through soluble molecules such as IL-1β, TNFα or IFNγ or cell-contact such as β2-ICAM-1. Importantly, recombinant IL-35 promotes proinflammatory phenotype of VSMC by inducing expression of ICAM-1, IL1β and IL-6 through gp130 receptor and STAT1/STAT3 activation.

It's the first time that it has been demonstrated that IL-35 is expressed in vascular lesions from patients with GCA driven by interactions between inflammatory cells and VSMC in which IL-35 induces a proinflammatory phenotype in VSMC.

INTRODUCTION

Giant cell arteritis (GCA) is a chronic inflammatory disease of blood vessels mostly affecting medium and large vessels from the upper extremities, neck, and head with frequently affectation to temporal artery (TA) (*1*) (*2*). The pathogenesis of the disease is characterized by presenting and inflammatory infiltrate composed by mononuclear cells being lymphocytes and macrophages the main source (*3*)**.** These cells may infiltrate the artery through the endothelial cells (EC) from the adventitial *vasa vasorum* and from the neovessels which are present in the entire pathological artery. The infiltrating leukocytes migrate from the outer artery layers (adventitia) to the inner ones (intima) with the occasionally formation of giant cells. Moreover, these cells interact with cell types from the artery wall such as vascular smooth muscle cells (VSMC). The inflammatory infiltrate is mostly composed by macrophages and T lymphocytes (CD4+T) (*3, 4*) in which Th1 (IL-12 triggering IFNγ) and Th17 (IL-23 triggering IL-17) inflammatory pathways are mainly involved (*5*) (*6, 7*).

IL-12 superfamily of heterodimeric cytokines (IL-12, IL-23, IL-27 and IL-35) play an essential role on Th1/Th17 differentiation and maintenance (*8*). Between them both IL-12 (composed by IL-12p40 (p40) and IL-12p35 (p35)) and IL-23 (composed by IL-23p40 and IL-23p19 (p19)) have been explored in GCA lesions. A clear dissociation between IL-12 subunits (p40 and p35) was found in GCA specimens (*9*). While p35 was constitutively expressed by VSMC from the media layer, p40 was induced in GCA specimens. Interestingly, the L-12 subunit p35 can also be associated to Epstein-Barr virus induced 3 (Ebi3) in order to conform cytokine IL-35 (*10*) (*11*) which is also a component of the IL-12 family of heterodimeric cytokines. Although these cytokines are composed by same subunits, they trigger different response (*8*). The complexity of these cytokines is also due to the combination of their receptor chains. The IL-12 receptor is the combination of IL-12Rβ1 and IL-12Rβ2 (*12, 13*), while the IL-23 is the combination of IL-23R and IL-12Rβ1 (*14*). IL-27 receptor is composed by IL-27R (WSX-1) and gp130 (*15*) and, interestingly, IL-35 may triggers its response through either heterodimers or homodimers of IL-12Rβ2/gp130 in CD4+T lymphocytes (*16*) or IL-12Rβ2 and IL-27R in B cells (*17*).

Anti-inflammatory effects of IL-35 have been described as proliferation suppressor for T conventional cells (Tconv) and promoting differentiation of these cells into high suppressive induced T regulatory cells (iTreg) which are named iTr35 and are able to produce IL-35 (*11, 18*).

The same observations have been assumed by B cells which in response to IL-35 may promote the differentiation into specific Breg that produce IL-35 (*17*).

Since the expression of IL-12 subunit p35, in contrast to p40, is also expressed by non-immune cells in GCA lesions, the aim of our study is to explore the expression of p35 IL-35 related partner Ebi3 in GCA specimens as well as to explore the IL-35 function in vascular inflammatory diseases such as GCA. Interestingly, both Ebi3 and p35 co-expressed in VSMC from GCA tissues and were induced under proinflammatory context promoted by leukocyte infiltration. Moreover, IL-35 developed proinflammatory phenotype in VSMC suggesting that IL-35 could play an important role in GCA immunopathogenesis.

MATERIAL AND METHODS

Isolation and culture of VSMC from human TA biopsies cultured on Matrigel ™

VSMC were developed and characterized from explanted Temporal artery (TA) sections obtained for diagnostic purposes placed onto Matrigel™ as previously explained (*19, 20*).

CD4+T cells, monocytes (CD14+) and VSMC co-culture

VSMC were seeded at 90% confluence onto 6well plate and cultured overnight with complete DMEM medium (Lonza, Hopkinton, MA USA) with 10% of FBS. Peripheral Blood Mononuclear Cells (PBMCs) were obtained by density gradient centrifugation using Lymphoprep ™ (Axis-Shield, Oslo, Norway). PBMCs were counted using Neubauer chamber and Untouched human CD4+T or CD14+ (monocytes) Dynabead kits (Invitrogen, Grand Island, NY, USA) were used to obtain the isolated cells. Efficiency of isolation was tested using flow cytometry staining with CD3+-FITC and CD14+-PE (mouse monoclonal) purchased from Invitrogen. Media from the VSMC was replaced by 1 million isolated CD4+T or CD14+ in 10% FBS complete medium RPMI (Lonza). The co-cultured situations were compared with situations containing only VSMC, CD4+T or CD14+. After 24, 48 and 72 hours supernatants were collected and mRNA and protein were extracted. Different cell populations of the co-culture were obtained and processed separately: CD4+T or CD14+ that did not attach to the VSMC (Non-Adherent) were obtained by centrifuging the supernatants. CD4+T or CD14+ that were attached to VSMC were isolated rising the well with cold Versene (Invitrogen Grand Island, NY, USA) (Adherent). VSMC were released using Trypsin-EDTA (Invitrogen). In some occasions, *transwell* of 0.4µm pore (Thermo Scientific, Waltham, Massachusetts, USA) were used to inhibit the cellular contact of the co-cultures.

Reagents

Human recombinant IL-35 (rIL-35) was purchased from Sino Biological Inc (North Wales, USA). Recombinant human IL-1β, IFNγ and TNFα were from R&D Systems (Minneapolis, Minnesota, USA). For the blockade experiment mouse monoclonal anti-human ICAM-1 and VCAM-1 (R&D Systems), anti-integrin α-4 antibody (HP2/1) from Abcam (Cambridge, UK), anti- integrin β1 (Immunotech, Westbrook, ME), anti-LFA1 (mouse), anti-integrin β2 and mouse IgG (Santa Cruz) were used.

Quantitative real-time reverse transcription (RT)-PCR

RNA was extracted from cultured VSMC using TRIzol Reagent (Invitrogen). Total RNA (1µg) was reverse transcribed using Archive *High Capacity cDNA Reverse Transcription kit* (Applied Biosystems, Foster City, California, USA). IL-12A (p35), IL-12B (p40), Ebi3, IL-27p28, IL-23A(p19), IL-17, IL-10, IL-6, IL1β , TNFα, IFNγ, gp130, IL-12Rβ2, ICAM-1, VCAM-1 mRNA were measured by quantitative real-time RT-PCR with specific TaqMan gene expression assays from Applied Biosystems (Foster City, CA, USA). All samples were normalized to the expression of the endogenous control GUSb and analyzed with Sequence Detection Software 2.3 (Applied Biosystems).

Western blot analysis

Cell lysates were obtained in modified radioimmunoprecipitation assay (RIPA) buffer and supplemented with protease and phosphatases inhibitors (Complete, Boehringer Mannheim, Mannheim, Germany), NaF (50mM), PMSF (1mM), protinine, leupeptine, pepstatine (1ng/ml) and orthovanadate (2mM) (Sigma-Aldrich, St. Louis, Missouri, USA). Twenty micrograms of protein per condition was resolved on 10% reducing sodium dodecyl sulphate (SDS)–polyacrylamide gel electrophoresis gels and blotted overnight at 4ºC onto nitrocellulose membranes (Invitrogen). Immunodetection was performed with the following antibodies: rabbit polyclonal anti-human ICAM-1, phospho-STAT1, phospho-STAT3, phospho-STAT4, mouse monoclonal anti-human STAT1, STAT3 and STAT4 (Cell Signaling, Danvers, MA, USA), mouse monoclonal or sheep polyclonal anti-human VCAM-1 (R&D Systems), rabbit polyclonal anti-human βactin (Abcam), mouse monoclonal anti-human LaminB (Santa Cruz) and rabbit polyclonal anti-human alpha tubulin (Sigma-Aldrich). Chemiluminescence signals were measured with the LAS-4000 imaging system (Fujifilm Corporation, Tokyo, Japan).

Assessment of protein secretion by immunoassay

USNC life science Inc. (Wuhan, China) immunoassay was used to measure secreted IL-35 and IL-1β in cell supernatants. IL-6 Quantikine ELISA kit was purchased from R&D Systems.

Leukocyte-VSMC Adhesion Assay

Confluent monolayer of VSMC was generated in 96-well plates (5.000 cells/well) treated with or without rIL-35 for overnight. Human PBMC were isolated from the peripheral blood of volunteer and resuspended in serum-free RPMI medium to get 100.000 cells per well and incubated onto

the pre-washed VSMC monolayer from 30 to 90 minutes at 37ºC. After removal of non-adherent cells and washing (3 times in 1% PBS), 100 µl of crystal violet solution was added to each well (dried O/N) and lysate with 100µl of SDS (10X) per well. Absorbance was measured at 620 nm. The results are expressed as mean relative Absorbance (± SEM of quadruplicate cultures).

Bioinformatics gene promoter region analysis

Promoter sequences (5.000bp) of IL-12A (p35) and EBI3 (Ebi3) genes were obtained with *USNC Genome Browser*. Using *Chip Bioinformatics Mapper program,* the predicted transcription factor sequences in the promoter sequence of each gene were obtained. Only the predicted transcription factors with SCORE >3 and eValue <7 were considered as recommended by the authors of the program (*21*).

Nuclear and cytoplasm protein extraction

Nuclear and cytoplasmic fractions were obtained from VSMC cultured on 6 well plates previously washed with cold 1% PBS to discard *debris* and albumin from the medium. The attached cells were collected by centrifuging at 4ºC during 5 minutes at 1.000 rpm. *Pellet* obtained was ressuspended with Buffer I (1 mL de 1 M Hepes, pH 8.0 , 150 µl de 1 M MgCl2 ,1 mL de 1 M KCl,100 µl de 1 M dTT raised with dH2O up to 100 mL) supplemented with protease and phosphatase inhibitors as previously described. Samples were ice incubated for 15 minutes and NP40 (1%) was added before vortex briefly. Samples were then centrifuged at 12.000 rpm for 5 minutes at 4ºC and supernatants were collected as a cytoplasm fraction. Pellets were resuspended with Buffer II (2 mL 1 M Hepes pH 8.0 ,150 µl 1 M MgCl2,25 mL glycerol ,42 mL 1 M NaCl,40 µl 0.5 M EDTA, 100 µl 1 M DTT raised with dH_2O up to 100 mL) supplemented with protease and phosphatase inhibitors as previously described .

Immunofluorescence staining and confocal microscopy of VSMC and TA biopsies

Immunofluorescence staining on VSMC was performed culturing the cells on sixteen well chamber slides (Nunc, Waltham, MA, USA). After washing the cells with PBS (1%), they were fixed ten minutes at RT with 4% paraformaldehyde (PFA) and incubated for 1hour at 4ºC with blocking buffer containing (1%BSA, 5% Donkey Serum in PBS (1%)) supplemented or not with triton 0.1% if permeabilization is needed. Primary antibodies incubation was performed at 1:100 or 1:50 dilution at 4ºC overnight. Secondary antibodies were used at 1:300 and were purchased from Molecular probes. Primary antibodies used were: mouse monoclonal anti-human Ebi3

(Santa Cruz, Dallas, Texas, USA), rabbit anti-human gp130 (Millipore, Billerica, Massachusetts, USA), mouse monoclonal anti-human IL12p35 (Acris Antibodies, San Diego, CA, USA). Temporal artery tissues were fixed with PFA 4% and incubated with increasing concentrations of sucrose before being frozen with OCT and stored at -80ºC. The immunofluorescence staining was performed as described for VSMC. Primary antibodies used were: goat polyclonal anti-human IL12p40 and mouse monoclonal anti-human Ebi3 (Santa Cruz), and rabbit polyclonal anti-human IL12A (Atlas). Secondary antibodies were used at 1:300 and were purchased from Molecular Probes (Life Technologies Ltd, Paisley, UK).

Proximity Ligation Assay (PLA)

PLA was used to visualize proximity co-localization (<40 nm) of p35 and Ebi3 (on TA sections) as well as Ebi3 or p35 with gp130 in VSMC using Duolink Detection kit (Olink Bioscience, Uppsala, Sweden). Either frozen TA biopsies or cultured cells were fixed (4% PFA for 10 min at room temperature) before blocking for one hour in blocking buffer 4ºC. as previously described in immunofluorescence section. Primary antibodies were incubated overnight 4ºC and were used at 1:100 or 1:50 dilution. The primary antibodies used were: mouse monoclonal anti-human Ebi3 (Santa Cruz), mouse monoclonal anti-human IL12A (Acris antibodies) and rabbit polyclonal anti-human gp130 (Millipore). After washing (5 min, twice in wash buffer: 0.1 M Tris-HCl pH 7.5, 0.5M NaCl, 5% Tween-20 in ultrapure water), incubation (30 min at 37ºC) with PLA probe solution containing anti-rabbit MINUS and anti-mouse PLUS Dulolink PLA probes was done. After washing, circularization and ligation of the oligonucleotides in the probes, an amplification step was performed using polymerase solution (100 min at 37ºC) and finally re-fixed with 4% PFA.

Hoechst (Molecular Probes) (1:1000) was used for nuclear staining. Slides were mounted with Prolong Gold Antifade Reagent (Molecular Probes, Life Technologies). Samples were examined using a laser scanning confocal Leica TCS *SP5* microscope (Leica Microsystems, Heidelberg, Germany). Images were processed with Leica Confocal software (LAS-AF Lite) and Image J software (Wayne Rasband, Bethesda, Maryland, USA).Control of the technique was realized incubating with secondary but not with primary antibodies.

Statistical analysis Mann-Whitney was applied for non-parametric and independent samples using SPSS software, version PASW 22.0.

RESULTS

Ebi3 and p35 are co-expressed by leukocyte and VSMC from GCA lesions.

Either Th1 (i.e. IFNγ and IL-12) or Th17 (i.e. IL-6, IL-23 and IL-17) related molecules have been explored in several diseases involving chronic inflammation such as GCA (*5, 6, 9, 22*). Other proinflammaoty cytokines such as TNFα or IL-1β have also been associated to GCA persistent immunopathology (*23*). Interestingly, together with IL-23 and IL-12, another IL-12 superfamily of heterodimeric cytokines related molecule IL-27 has also been associated to GCA promoting Th1 differentiation (*24*). Nevertheless, IL-35 association to GCA and other related diseases remains unknown.

Previous immunohistochemistry results already demonstrated dissociation between IL-12 subunits (p40 and p35) in GCA specimens (*9*). In here, expression of p35 partner to form IL-35 (Ebi3) is also investigated in GCA lesions. Ebi3 and p35 presented a similar expression pattern but different than p40 subunit. While both IL-35 subunits were detected in the media layer of control specimens (Figure 1A), both subunits were also found in GCA lesions expressed by either leukocytes or VSMC from the media junction (Figure 1B). In contrast, p40 was hardly detected in controls and overexpressed in GCA specimens limited to the leukocytes (Figure 1A, B). To assure p35 binding to Ebi3 in this tissue, proximity ligation assay (PLA) was also performed (figure 1C-E). Some p35/Ebi3 signal was detected in the media layer from the controls (Figure 1C). This signal was significantly stronger in the media layer of the GCA lesions (figure 1E) either produced by VSMC (Figure 1 e1) or leukocytes mostly from the media-intima junction (Figure 1 e2). Interestingly VSMC that expressed more IL-35 were the ones that were localized together with the infiltrating leukocytes (Figure 1E). Specificity of the antibodies and PLA signal was demonstrated by negative control of the technique (Figure 1D).

IL-35 subunits (p35 and Ebi3) are induced in VSMC co-cultured together with leukocyte

We observed that both IL-35 subunits (p35 and Ebi3) are highly expressed by the VSMC surrounded by infiltrated leukocytes that are localized in the adventitial-media junctions of GCA lesions (Figure 1). For this reason, in order to mimic this phenomenon, co-cultures of primary VSMC derived from TA biopsies cultured on Matrigel ^{TM} (*20*) together with PBMC obtained from volunteers were used to evaluate IL-35 subunits modulation in VSMC. Both Ebi3 and p35

mRNA expression was induced by leukocytes in VSMC (Figure 2A, B). Moreover this *in vitro* model was validated by co-culturing PBMC obtained from a biopsy-proven GCA patient together with the corresponding VSMC derived from TA biopsy from the same patient demonstrating no differences at the studied times (Supplementary Figure 1A).

Since macrophages and CD4+T lymphocytes are the main source of infiltrating leukocytes involved in GCA inflammatory (*3, 4*), CD4+T cells and CD14+ (monocytes) were negatively isolated from PBMC and their purity and viability was validated using flow cytometry (Supplementary Figure 1B).

According to immunofluorescence staining results, isolated VSMC expressed either p35 or Ebi3 and, in addition, both subunits were dramatically induced by co-culturing these cells with CD4+T or monocytes (Figure 2 C, D). Secretion of IL-35 by isolated CD4+T, CD14+, VSMC and both co-cultures was also evaluated using immunoassay. Interestingly, VSMC secreted the mature cytokine and this secretion was higher when VSMC were co-cultured together with CD4+T or CD14+ (Figure 3G).

To further investigate leukocyte-VSMC mechanisms involved in p35 and Ebi3 modulation, co-cultures of whole PBMC, isolated CD4+T or monocytes were performed using *transwell* in order to avoid cell-cell interaction (Figure 2A, B, E, F).The results demonstrated that nor p35 or Ebi3 were induced by co-culturing VSMC with CD4+T lymphocytes when cell-contact was abolished. In contrast, both p35 and Ebi3 expression remained upregulated in VSMC when co-cultured with PBMC or CD14+ even when cell-cell interaction was suppressed with *transwell*. IL-35 secretion by VSMC was again evaluated by immunoassay and the results obtained agreed with the mRNA ones (Figure 2H).

Interestingly, isolated CD4+T cells did not produced the mature IL-35, but, in contrast isolated CD14+ secreted this cytokine only when they were in contact with VSMC or attached to the plastic of the plate (mainly differentiated macrophages) (Figure 2G,H).

IL-12p40 (p35 partner to form IL-12) and IL-27p28 (Ebi3 partner to form IL-27) were also evaluated in this co-culture system. Both subunits were hardly detected by isolated VSMC although their expression was induced by co-culturing VSMC together with leukocytes, such induction was limited to cell-cell interaction (Supplementary Figure 2).

IL-35 is induced either by NFκB or IRF pathway

Some predictive studies have already been explored in the promoter of EBI3 (Ebi3 gene) and IL12A (p35 gene) (*25*). In our study EBI3 and IL12A promoter regions were also explored in order to investigate which soluble molecules secreted by co-cultured monocytes could be involved in the IL-35 modulation in VSMC. For this reason, we used the bioinformatic program *USCN genome Browser* and *Chip Bioinformatic Mapper* and followed the manufacturer instructions (*21*). Interestingly, EBI3 and IL12A shared NFκB and IRF putative transcription factor (TF) binding sites in their promoter regions suggesting that proinflammatory context is needed for IL-35 induction.

To confirm these bioinformatic predicted results, functional studies testing the main important NFκB inductors (IL1β and TNFα) and IRF related molecules (IFNγ) were tested as possible IL-35 inductors in cultured human VSMC. Both p35 and Ebi3 were significantly induced by all these molecules by VSMC (Figure 3A, B). IL-35 immunoassay showed that IL-35 secretion was dramatically induced when VSMC were cultured with IL1β or TNFα and, in less extension when cultured with IFNγ (Figure 3C).

IL-35 subunits (p35 and Ebi3) are induced by β2-ICAM1 interaction in VSMC co-cultured with either CD4+T or CD14+ cells.

As seen in Figure 3, IL-35 subunits (p35 and Ebi3) are modulated by the presence of leukocytes and, in some cases, cell contact is essential. Although leukocyte attachment to endothelium has been fully investigated, the mechanisms through which leukocyte interact to VSMC remains unknown. In this study, co-cultures of CD14+ and CD4+T with VSMC have shown that leukocyte/VSMC interaction induce IL-35 expression by VSMC. In order to explore which interactions are essential for IL-35 modulation by VSMC we blocked different adhesion molecules expressed by VSMC such as ICAM-1 and VCAM-1 and their corresponding ligands expressed by leukocytes such as integrins β2 (i.e. LFA1), integrins β1 and integrins α4. VSMC co-cultures of CD4+T or CD14+ were used as basal conditions or as positive controls respectively of IL-35 subunits modulation (Figure 4). Interestingly, overexpression of p35 and Ebi3 in VSMC co-cultured with either CD4+T or CD14+ was abrogated by blocking cell-cell interaction with the neutralizing antibodies against β2 integrins and the adhesion molecule

ICAM-1 (Figure 4A). Similar results were obtained by blocking β2 integrins (including LFA-1 neutralizing antibody) and ICAM-1 in CD4+T or CD14+/VSMC co-cultures.

According to this observations, ICAM-1 and VCAM-1 mRNA expression was explored in VSMC co-cultured together with CD4+T or CD14+ in the presence or in the absence of cell-cell interaction. Interestingly, both adhesion molecules were induced in VSMC when co-cultured together with CD4+T cells or monocytes (Supplementary Figure 3).

Glucocorticoid treatment does not modulate IL-35 subunits

Glucocorticoid therapy (GC) is the current treatment for GCA. Nevertheless, about 40-60% of the patients relapse (*26, 27*). For this reason, research attempting to improve the ineffective current treatment of GCA is needed. According to the previous data in which we have shown that IL-35 is induced by proinflammatory stimuli in VSMC (mostly promoted by infiltrating leukocytes) we considered that IL-35 could be involved in GCA immunopathology. We next explored the effect of GC on the modulation of both IL-35 subunits. First, we evaluated mRNA expression of IL-35 subunits (p35 and Ebi3) comparing 10 fresh control specimens and 20 biopsy-proven GCA TA biopsies including 10 patients who had received GC treatment and 10 patient who did not received this treatment (Figure 5A). Both Ebi3 and p35 subunits were found expressed by controls and GCA specimens. Whereas Ebi3 was significantly overexpressed in GCA patients ($p=0.002$), equal p35 mRNA expression was detected between both populations. Interestingly, both IL-35 subunits (p35 and Ebi3) remained upregulated even in the patients who had received GC treatment (Figure 5A).

Immunofluorescence staining of Ebi3, p35 and p40 was again performed in different TA from patients with GCA who had received or not GC treatment. Interestingly, and according to the previous observations, both Ebi3 and p35 subunits remained detectable by GCA TA biopsies from GC treated patients whereas p40 (p35 partner to form IL-12) was undetectable in this patients (Figure 5B).

These results were also confirmed by co-culturing VSMC with fresh PBMC in the presence of dexamethasone (Figure 5C). Interestingly, p35 expression by isolated VSMC was not modulated by the presence of GC neither was Ebi3. Moreover, according to the previous

results, both subunits were induced in VSMC by the presence of leukocyte, but while p35 reached basal expression under dexamethasone treatment, Ebi3 expression was upregulated by GC.

IL-35 induce proinflammatory phenotype in VSMC

We observed that IL-35 is secreted by either activated CD14+ cells or VSMC under proinflammatory context. Even so, IL-35 function in non-leukocyte cells has not previously been explored. In order to understand IL-35 function in VSMC, *in vitro* studies using recombinant IL-35 (rIL-35) were performed. Proinflammatory cytokines (IL1β, IL-6, IL-12p40, IL-17, IL-23, IFNγ and TNFα) and adhesion molecules (ICAM-1 and VCAM-1) previously described to be involved in GCA immunopathology were explored as well as the anti-inflammatory cytokine IL-10. Among the molecules explored, IL-6 (Figure 6A) and IL1β (Figure 6B) mRNA expression was induced by rIL-35 in VSMC. In contrast, only IL-6 was detected in the cell supernatant of VSMC which was also induced by rIL-35 in this cell type. Interestingly, ICAM-1 was highly induced by rIL-35 although VCAM-1 was slightly modulated by the presence of the cytokine (Figure 6 C, D). In addition, same results were obtained when protein modulation of ICAM-1 and VCAM-1 was evaluated in VSMC which were previously treated with rIL-35 (Figure 6E). Following with these observations, leukocytes attachment to VSMC was also evaluated. Importantly, PBMC attachment to rIL-35 pre-treated VSMC was about two fold higher compared to PBMC attachment to untreated VSMC (Figure 6F).

IL-35 binds to gp130 in VSMC

A few reports have explored IL-35 receptor. The main important findings suggest that IL-35 binds to either homodimers or heterodimers of gp130 and IL-12Rβ2 chains in mice Tconv and that both chains are necessary for IL-35 subunit induction (*16*). In contrast, in mice Bcells IL-35 signals through heterodimers of IL-27R and IL-12Rβ2 chains (*17*). In here, we have demonstrated that VSMC lack of IL-12rβ2 chain (Figure 7A) even after stimulation with rIL-35 (data not shown). In contrast, gp130 was constitutively expressed by VSMC (Figure 7A) although rIL-35 stimulation did not modulate this chain (Figure 7B). According to this data, neither p35 nor Ebi3 subunits were induced by rIL-35 in VSMC (Supplementary Figure 4).

Although further studies should be done in order to explore and characterize IL-35 receptor in VSMC, our results suggested that IL-35 function in VSMC should be triggered through gp130. Bioinformatic remodelling analysis had already demonstrated that Ebi3 and p35 might interact with gp130 (*16*). Since it is well known that Ebi3 when it is linked to p28 to form IL-27 binds to gp130, and p35 subunit of IL-12 binds to IL-12Rβ2 but not gp130, we focused on the unexplored interaction between p35 and gp130 in VSMC. To demonstrate this happening, immunofluorescence staining of p35 and gp130 was performed on rIL-35 pre-treated VSMC. Interestingly co-expression of gp130 and p35 was strongly found in most of the evaluated cells (Figure 7C). In addition, proximity ligation assay (PLA) between p35 and gp130 or Ebi3 and gp130 (as a positive control of the technique) was performed on VSMC. Again, PLA signal of both p35 and EbiI3 –gp130 interaction was detected in VSMC (Figure 7D).

IL-35 induces STAT3 and STAT1 but not STAT4 phosphorylation and nuclear translocation in VSMC

As a consequence of IL-35 binding to IL-12Rβ2/gp130 on Tconv cells, a unique heterodimer STAT1/STAT4 is activated (in which STAT1 would be trigger trough gp130 receptor and STAT4 through IL-12Rβ2 receptor) (*16*). In contrast, in B cells, IL-35 promotes activation of STAT1/STAT3 heterodimer (*17*). Our results demonstrated that IL-35 may interact with gp130 but not IL-12Rβ2 in order to induce ICAM-1 and IL-6 expression by VSMC. To further investigate IL-35/gp130 downstream pathway in VSMC, we analyzed STAT1, STAT3 and STAT4 activation. Interestingly, rIL-35 induced STAT1 and STAT3 phosphorylation (Tyr 705) but not STAT4 (Figure 7E).

DISCUSSION

Mechanisms contributing to chronic inflammation are essential to be understood in order to improve the current treatment for vascular inflammation diseases such as GCA. For this reason, either proinflammatory cytokines or cell types involved in this process are essential to be studied. In GCA, the crosstalk between the innate and adaptive immune responses orchestrates the secretion of proinflammatory cytokine cascades that would contribute to the differentiation of Th1 or Th17 subsets as well as macrophage differentiation.

Several proinflammatory cytokines have been investigated in GCA. In here we report for the first time that IL-35 (a member of the IL-12 superfamily of heterodimeric cytokines) is involved in the immunopathogenesis of GCA.

Although in most of the reports using mouse models for different disease has shown that IL-35 is a suppressive and anti-inflammatory cytokine (*17, 25, 28*) there is still some controversy about IL-35 function. Some of this studies using mouse models have revealed that IL-35 induced suppressive Treg (iTr35) (*18*) and Bcells (iB35) (*17*).

In here, we have demonstrated that *in vitro* activated human CD14+ cells produce either mRNA of IL-35 subunits (p35 and Ebi3) or mature cytokine. In contrast, CD4+T cells obtained from peripheral blood of volunteers did not express IL-35 subunits neither secret the mature cytokine according to the observations published by others (*29, 30*).

As observed in GCA lesions, VSMC surrounded by infiltrating leukocytes produced IL-35. Moreover, *in vitro* co-cultures of VSMC together with PBMC, CD4+T or CD14+ cells demonstrated that even cell-cell interaction (through integrin β2 binding to ICAM-1) or production of soluble molecules related to NFκB (TNFα or IL-1β) or IRF (IFNγ) significantly induced IL-35 expression and secretion by VSMC suggesting that production of IL-35 by VSMC is a phenomenon depending on proinflammatory context.

Most of the reports found in the literature explore IL-35 function in mice lymphoid and myeloid cells and before our observations little was known about IL-35 function different than the observed as a suppressive cytokine. According to our observations recent studies have started to evaluate IL-35 expression in non-lymphoid cell types such as endothelial cells (EC), VSMC and macrophages (*25*).

Interestingly, human VSMC not only produced IL-35 but also respond to this cytokine. Recombinant IL-35 (rIL-35) induced proinflammatory phenotype in VSMC (by promoting the upregulation of proinflammatory molecules ICAM-1, VCAM-1, IL-6 and IL1β). Furthermore, adhesion molecules upregulation by IL-35 in VSMC contributed to leukocyte attachment to VSMC, a mechanism that is involved in persistence of inflammation in GCA as seen by other proinflammatory cytokines such as IFNγ (*22*). Moreover, this phenomenon could also be a positive feedback for IL-35 expression by VSMC since we have observed that leukocyte interaction with VSMC through β2 and ICAM-1 induces both IL-35 subunits (p35 and Ebi3). Nevertheless, we have not evaluated here if this interaction also promotes induction of other proinflammatory cytokines by VSMC but it should be further investigated.

According to our data, a recent study have shown that aorta VSMC respond to recombinant IL-35 (rIL-35) by promoting apoptosis and ICAM-1 expression although the mechanisms involved in this process are not characterized (*31*).

The mechanism in which IL-35 triggers its signal is not understood yet. Although it seems that in mice Tconv cells, it is triggered either by binding to homodimers or heterodimers of gp130 and IL-12Rβ2 chains promoting STAT1 and STAT4 dimerization and activation (*16*), in B cells the receptor is thought to be composed by heterodimers of IL-12Rβ2 and IL-27R chains (*17*). Although VSMC respond to rIL-35, these cells lack of IL-12Rβ2 expression but constitutively express gp130. In contrast to the previous observations by others, our studies demonstrated that rIL-35 binding to gp130 promotes STAT1/STAT3 phosphorylation and nucleus translocation but not STAT4 activation in human VSMC.

Either IL-6, IL1β, VCAM-1 and ICAM-1 have a predictive binding site for STAT3 or STAT1 in their promoter region (Champion Chip transcription factor Search portal, DECODE database, SABiosciences) suggesting that rIL-35 binding gp130 and subsequent STAT1/STAT3 activation and nuclear translocation might be the responsible mechanisms that would promote ICAM-1, VCAM-1, IL1β and IL-6 overexpression observed in VSMC.

Although most of the studies in human diseases have demonstrated that IL-35 function as an anti-inflammatory cytokine (*32-34*) a recent study using samples from patients with rheumatoid

arthritis (RA) has suggested that IL-35 might also have a proinflammatory role in this disease (*35*).

Surprisingly, neither p35 nor Ebi3 mRNA and protein expression is modulated by glucocorticoids (GC), the current treatment for GCA. This finding was important since GC dramatically downregulates other proinflammatory cytokines (*19*).

Taking all this data together, we report here that IL-35, a member of the IL-12 superfamily of cytokines is associated to GCA. Moreover, IL-35 is expressed by either leukocytes from the inflammatory infiltrate but also by cells from the vascular wall such as VSMC. In addition, IL-35 may contribute to sustaining inflammatory cascades in GCA by inducing a proinflammatory phenotype in VSMC.

BIBLIOGRAPHY

1. J. C. Jennette *et al.*, 2012 revised International Chapel Hill Consensus Conference Nomenclature of Vasculitides. *Arthritis and rheumatism* **65**, 1 (Jan, 2013).
2. T. A. Kermani *et al.*, Large-vessel involvement in giant cell arteritis: a population-based cohort study of the incidence-trends and prognosis. *Annals of the rheumatic diseases* **72**, 1989 (Dec, 2013).
3. M. C. Cid *et al.*, Immunohistochemical analysis of lymphoid and macrophage cell subsets and their immunologic activation markers in temporal arteritis. Influence of corticosteroid treatment. *Arthritis and rheumatism* **32**, 884 (Jul, 1989).
4. D. O. Adams, Molecular interactions in macrophage activation. *Immunology today* **10**, 33 (Feb, 1989).
5. G. Espigol-Frigole *et al.*, Increased IL-17A expression in temporal artery lesions is a predictor of sustained response to glucocorticoid treatment in patients with giant-cell arteritis. *Annals of the rheumatic diseases* **72**, 1481 (Sep 1, 2013).
6. J. Deng, B. R. Younge, R. A. Olshen, J. J. Goronzy, C. M. Weyand, Th17 and Th1 T-cell responses in giant cell arteritis. *Circulation* **121**, 906 (Feb 23, 2010).
7. B. Terrier *et al.*, Interleukin-21 modulates Th1 and Th17 responses in giant cell arteritis. *Arthritis and rheumatism* **64**, 2001 (Jun, 2012).
8. D. A. Vignali, V. K. Kuchroo, IL-12 family cytokines: immunological playmakers. *Nature immunology* **13**, 722 (Aug, 2012).
9. S. Visvanathan *et al.*, Tissue and serum markers of inflammation during the follow-up of patients with giant-cell arteritis--a prospective longitudinal study. *Rheumatology* **50**, 2061 (Nov, 2011).
10. O. Devergne, M. Birkenbach, E. Kieff, Epstein-Barr virus-induced gene 3 and the p35 subunit of interleukin 12 form a novel heterodimeric hematopoietin. *Proceedings of the National Academy of Sciences of the United States of America* **94**, 12041 (Oct 28, 1997).
11. L. W. Collison *et al.*, The inhibitory cytokine IL-35 contributes to regulatory T-cell function. *Nature* **450**, 566 (Nov 22, 2007).
12. A. O. Chua *et al.*, Expression cloning of a human IL-12 receptor component. A new member of the cytokine receptor superfamily with strong homology to gp130. *Journal of immunology* **153**, 128 (Jul 1, 1994).
13. A. O. Chua, V. L. Wilkinson, D. H. Presky, U. Gubler, Cloning and characterization of a mouse IL-12 receptor-beta component. *Journal of immunology* **155**, 4286 (Nov 1, 1995).
14. C. Parham *et al.*, A receptor for the heterodimeric cytokine IL-23 is composed of IL-12Rbeta1 and a novel cytokine receptor subunit, IL-23R. *Journal of immunology* **168**, 5699 (Jun 1, 2002).
15. S. Pflanz *et al.*, WSX-1 and glycoprotein 130 constitute a signal-transducing receptor for IL-27. *Journal of immunology* **172**, 2225 (Feb 15, 2004).

16. L. W. Collison *et al.*, The composition and signaling of the IL-35 receptor are unconventional. *Nature immunology* **13**, 290 (Mar, 2012).
17. R. X. Wang *et al.*, Interleukin-35 induces regulatory B cells that suppress autoimmune disease. *Nature medicine* **20**, 633 (Jun, 2014).
18. L. W. Collison *et al.*, IL-35-mediated induction of a potent regulatory T cell population. *Nature immunology* **11**, 1093 (Dec, 2010).
19. M. Corbera-Bellalta *et al.*, Changes in biomarkers after therapeutic intervention in temporal arteries cultured in Matrigel: a new model for preclinical studies in giant-cell arteritis. *Annals of the rheumatic diseases* **73**, 616 (Mar, 2014).
20. E. Lozano, M. Segarra, A. Garcia-Martinez, J. Hernandez-Rodriguez, M. C. Cid, Imatinib mesylate inhibits in vitro and ex vivo biological responses related to vascular occlusion in giant cell arteritis. *Annals of the rheumatic diseases* **67**, 1581 (Nov, 2008).
21. V. D. Marinescu, I. S. Kohane, A. Riva, MAPPER: a search engine for the computational identification of putative transcription factor binding sites in multiple genomes. *BMC bioinformatics* **6**, 79 (2005).
22. P.-R. E. Corbera-Bellalta M., Lozano E., Terrades N., Alba M., Prieto-González S., García-Martínez A., Albero R., Enjuanes A., Espígol-Frigolé G.,Hernández-Rodríguez J.,Roux-Lombard P., Ferlin W., Dayer JM., Kosko-Vilbois M.,Cid MC., Blocking interferon gamma reduces expression of chemokines cxcl9, cxcl10 and cxcl11 and decreases macrophage infiltration in ex-vivo cultured arteries from patients with Giant-cell arteritis *Annals of Rheumatic Diseases* (2015).
23. J. Hernandez-Rodriguez *et al.*, Tissue production of pro-inflammatory cytokines (IL-1beta, TNFalpha and IL-6) correlates with the intensity of the systemic inflammatory response and with corticosteroid requirements in giant-cell arteritis. *Rheumatology* **43**, 294 (Mar, 2004).
24. F. Ciccia *et al.*, Expression of interleukin-32 in the inflamed arteries of patients with giant cell arteritis. *Arthritis and rheumatism* **63**, 2097 (Jul, 2011).
25. X. Li *et al.*, IL-35 is a novel responsive anti-inflammatory cytokine--a new system of categorizing anti-inflammatory cytokines. *PloS one* **7**, e33628 (2012).
26. M. C. Cid, A. Garcia-Martinez, E. Lozano, G. Espigol-Frigole, J. Hernandez-Rodriguez, Five clinical conundrums in the management of giant cell arteritis. *Rheumatic diseases clinics of North America* **33**, 819 (Nov, 2007).
27. A. Proven, S. E. Gabriel, C. Orces, W. M. O'Fallon, G. G. Hunder, Glucocorticoid therapy in giant cell arteritis: duration and adverse outcomes. *Arthritis and rheumatism* **49**, 703 (Oct 15, 2003).
28. W. Niedbala *et al.*, IL-35 is a novel cytokine with therapeutic effects against collagen-induced arthritis through the expansion of regulatory T cells and suppression of Th17 cells. *European journal of immunology* **37**, 3021 (Nov, 2007).

29. E. Bardel, F. Larousserie, P. Charlot-Rabiega, A. Coulomb-L'Hermine, O. Devergne, Human CD4+ CD25+ Foxp3+ regulatory T cells do not constitutively express IL-35. *Journal of immunology* **181**, 6898 (Nov 15, 2008).
30. F. Liu, F. Tong, Y. He, H. Liu, Detectable expression of IL-35 in CD4+ T cells from peripheral blood of chronic hepatitis B patients. *Clinical immunology* **139**, 1 (Apr, 2011).
31. W. Skowron *et al.*, The effect of interleukin-35 on the integrity, ICAM-1 expression and apoptosis of human aortic smooth muscle cells. *Pharmacological reports : PR* **67**, 376 (Apr, 2015).
32. S. Kempe *et al.*, Epstein-barr virus-induced gene-3 is expressed in human atheroma plaques. *The American journal of pathology* **175**, 440 (Jul, 2009).
33. B. Langhans *et al.*, Core-specific adaptive regulatory T-cells in different outcomes of hepatitis C. *Clinical science* **119**, 97 (Jul, 2010).
34. M. C. Boissier *et al.*, Regulatory T cells (Treg) in rheumatoid arthritis. *Joint, bone, spine : revue du rhumatisme* **76**, 10 (Jan, 2009).
35. M. Filkova *et al.*, Pro-inflammatory effects of interleukin-35 in rheumatoid arthritis. *Cytokine* **73**, 36 (May, 2015).

Figure legends

Figure1. IL-35 subunits distribution in GCA lesions. p35 (green), Ebi3 (blue) and IL-12p40 (red). Three untreated samples were analyzed. (A) Control sample. VSMC are mostly observed. B) Immunostaining of GCA TA biopsy-proven. b1) Magnification of VSMC from the disrupted media layer surrounded by leukocytes. Note that both p35 and Ebi3 are expressed by either VSMC or leukocytes whereas p40 staining is limited to leukocytes. C-E) Proximity ligation assay (PLA) of the same TA biopsies analyzed in A and B. Red signal represent p35 and Ebi3 interaction (<40nm). C) Control TA biopsy. D) Negative control of the technique in which no primary antibodies are used. E) PLA staining of GCA biopsy-proven TA showing the media-adventitial junction. e1) Magnification of VSMC surrounded by leukocytes. e2) Magnification of leukocytes surrounding VSMC. **(A or Adv) adventitia, (M) media, (I) intima, (L) lumen.**

Figure2. IL-35 subunits expression by co-cultured VSMC together with PBMC or isolated CD4+T or CD14+. A and B) VSMC mRNA expression of p35 and Ebi3 when co-cultured with PBMCs even with cell-cell contact or using transwell chamber. C and D) VSMC mRNA expression of p35 and Ebi3 when co-cultured with isolated CD4+T cells or CD14+ as labelled. E and F) VSMC mRNA expression of p35 and Ebi3 when co-cultured with isolated CD4+T cells and CD14+ avoiding cell-cell interaction using transwell chambers. G) Immunoassay detecting mature IL-35 secretion in cell supernatant of CD4+T cells, CD14+ or VSMC even in basal conditions or when co-cultured. H) Same as G but using transwell chamber to avoid cell-cell interaction. Each co-cultured is the representation of triplicates using different cells and different PBMC donors.

Figure3. IL-35 mRNA and protein expression by *in vitro* VSMC submitted to different stimuli as labelled (TNFα, IL-1β and IFNγ, used at 20ng/mL). A and B) IL-35 subunits p35 (A) and Ebi3 (B) mRNA expression after treatment of VSMC with the corresponding recombinant molecules for 6, 24 and 48 hours. C) Immunoassay detecting mature IL-35 in supernatants of VSMC pre-treated with the corresponding recombinant molecules and labelled doses for 48 hours. Triplicates are represented in bars (mean and SEM).

Figure4. IL-35 subunits mRNA expression by VSMC co-cultured with either CD4+T lymphocytes or CD14+ cells with previously blockade of intregins and adhesion molecules as labelled. A) p35 and Ebi3 representation of VSMC co-cultured with CD4+T. B)

p35 and Ebi3 respresentation of VSMC co-cultured with CD14+ in the presence of the labelled blocking antibodies.

Legend: IgG mouse (negative control), LFA1 (Limphocyte function associated antigen -1), HP2/1 (neutralizing antibody against α4 integrin subunit), β2 (neutralizing antibody against integrin β2), β1 (neutralizing antibody against integrin subunit β1), ICAM-1 and VCAM-1 (neutralizing antibodies against adhesion molecules ICAM-1 and VCAM-1). VSMC (VSMC cultured alone), Untreated (VSMC co-cultured with either CD4+T cells or CD14+ without the addition of the previous neutralizing antibodies). Triplicates are represented in bars corresponding to mean and SEM.

Figure5. IL-35 subunits analyzed under glucocorticoid (GC) treatment. A) Ebi3 and p35 mRNA expression from fresh control TAs (n=10), GCA patients who had not received GC treatment (n=10) and GCA patients who had received GC treatment. Statistical analysis is also represented using Mann Whitney test for independent samples. B) Immunofluorescence of p35 (green), Ebi3 (blue) and IL-12p40 (red) from untreated GCA biopsy-proven patient *vs*. GCA patient who receive GC treatment. Two patients for each condition were explored. C) IL-35 subunits (p35 and Ebi3) mRNA expression of VSMC co-cultured with CD4+T or CD14+ in the absence or presence of dexamethasone. Triplicates are respresented in bars corresponding to mean and SEM.

Figure6. Recombinant IL-35 (rIL-35) proinflammatory functions in primary cultures of VSMC. A) IL-6 mRNA expression and protein secretion (immunoassay) by untreated *vs.* rIL-35 treated VSMC at 6, 24 and 48 hours. B) IL-1β mRNA expression by untreated *vs.* rIL-35 treated VSMC at 6, 24 and 48 hours. C and D) Molecule adhesion mRNA expression comparing untreated VSMC or rIL-35 treated VSMC as labelled. (C) mRNA expression of ICAM-1 (D) mRNA expression of VCAM-1. Either A, B, C and D panels correspond to triplicates and results are represented in bars corresponding to mean and SEM. E) Western blot of 24 hours cultured VSMC in the absence or presence of different stimuli (IL-35, IL-1β or TNFα; 20ng/mL) as labelled. ICAM-1, VCAM-1 and βactin are represented. Immunoblot correspond to a representation of three independent experiments. F) Adhesion assay showing leukocyte attachment (45 minutes) to untreated or pre-treated VSMC with increasing dose of rIL-35 (24 hours of treatment). Bars represent mean and SEM of quadruplicates of the same experiment.

Figure7. IL-12Rβ2 and gp130 expression in VSMC. A) IL-12Rβ2 and gp130 chain mRNA expression by VSMC, PBMC, CD4+T or CD14+. 24hours of culture is represented. B) gp130 expression by VSMC under treatment with rIL-35 (20ng/mL). (A and B) Triplicates are represented as means and SEM. C) Immunofluorescence staining of p35 (red) and gp130 (green) in VSMC. Co-expression of both molecules is represented in merge. D) Proximity ligation assay (PLA) of gp130 together with Ebi3 (positive control) or p35. Red signal indicates that both molecules are separated less than 40nm suggesting direct interaction. Picture correspond to a representation of several other stained cells with same results. VSMC were previously stimulated with 20ng/ml of rIL-35 for 6 hours either for immunofluorescence or for PLA staining. E) Immunoblot of p-STAT1, p-STAT3 and p-STAT4 comparing with total corresponding STAT and βactin at 5, 15, 30 and 60 minutes after VSMC stimulation with 20ng/mL of rIL-35.

Supplementary Figure legends

Supplementary Figure1. A) p35 and Ebi3 mRNA expression of VSMC derived from TA biopsy taken from GCA patients co-cultured with PBMC either from the same patient or obtained by a volunteer. Time = 24 hours. B) Flow cytometry representation comparing total lymphocytes (CD3+) or monocytes (CD14+) either from PBMC or from isolated CD4+T or CD14+ cells using Untouched Dynabeads kits. Enrichment of the populations is determined.

Supplementary Figure2. IL-27p28 (partner of Ebi3 to form IL-27) and IL-12p40 (partner of p35 to form IL-35) mRNA expression by VSMC co-cultured with PBMC either allowing cell –cell interaction or using transwell at 24 and 48 hours.

Supplementary Figure3. ICAM-1 and VCAM-1 expression by VSMC co-cultured together with isolated CD4+T or CD14+ cells allowing cell –cell interaction or using transwell. Different times were explored: 24, 48 and 72 hours of co-culture.

Supplementary Figure4. IL-35 subunits (p35 and Ebi3) expression by VSMC previously stimulated for 6, 24 and 48 hours with rIL-35 (20ng/ml). Error bars correspond to mean and SEM for triplicates samples of each condition.

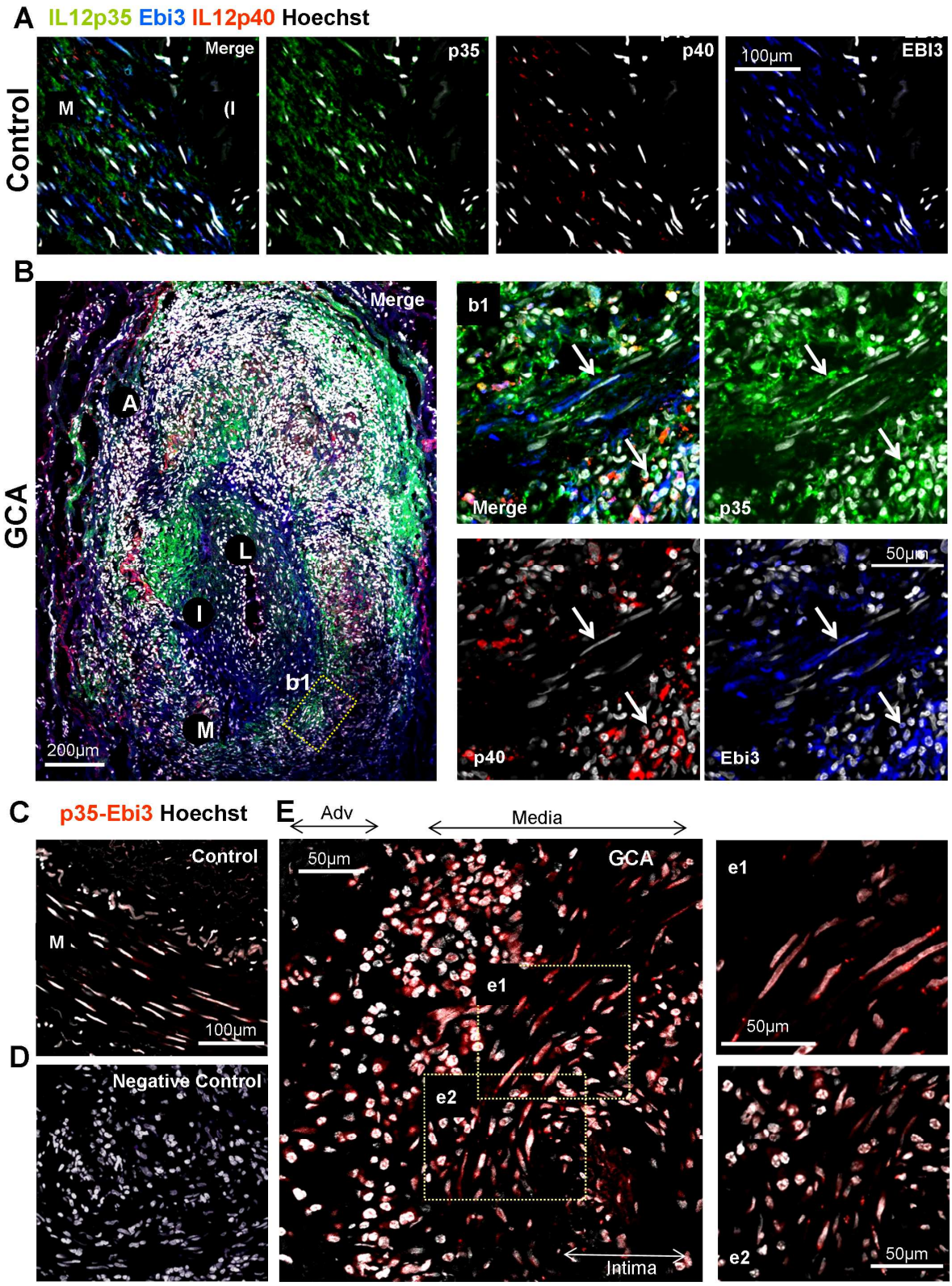
A
IL12p35 Ebi3 IL12p40 Hoechst
Control
Merge
p35
p40
EBI3
100µm
M
(I
B
GCA
Merge
A
L
I
b1
M
200µm
b1
Merge
p35
p40
Ebi3
50µm
C
p35-Ebi3 Hoechst
Control
M
100µm
D
Negative Control
E
Adv
Media
50µm
GCA
e1
e2
Intima
e1
50µm
e2
50µm

Figure 1

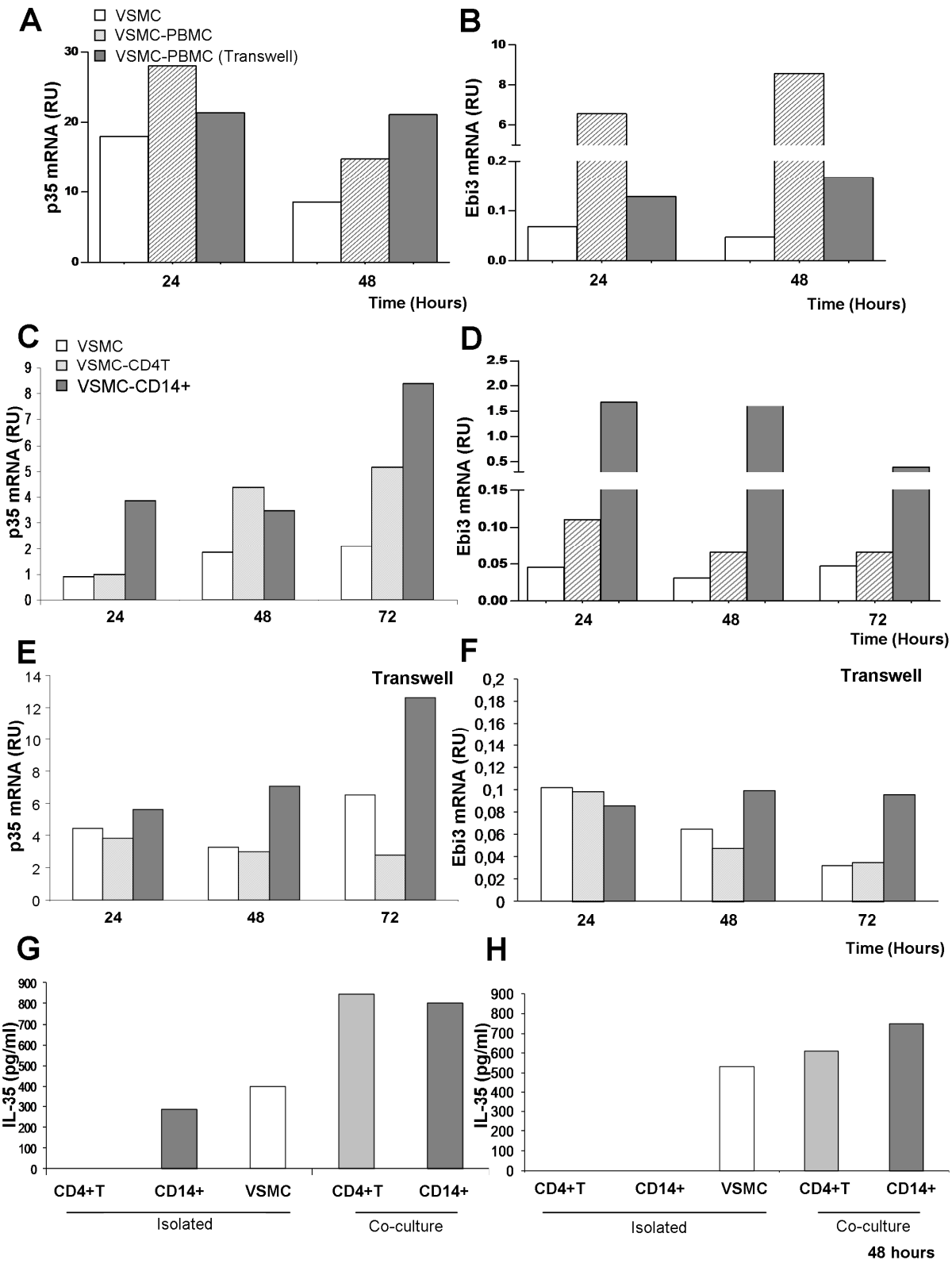
A
VSMC
VSMC-PBMC
VSMC-PBMC (Transwell)
p35 mRNA (RU)
Time (Hours)
B
Ebi3 mRNA (RU)
Time (Hours)
C
VSMC
VSMC-CD4T
VSMC-CD14+
p35 mRNA (RU)
D
Ebi3 mRNA (RU)
Time (Hours)
E
Transwell
p35 mRNA (RU)
F
Transwell
Ebi3 mRNA (RU)
Time (Hours)
G
IL-35 (pg/ml)
CD4+T
CD14+
VSMC
CD4+T
CD14+
Isolated
Co-culture
H
IL-35 (pg/ml)
CD4+T
CD14+
VSMC
CD4+T
CD14+
Isolated
Co-culture
48 hours

Figure 2

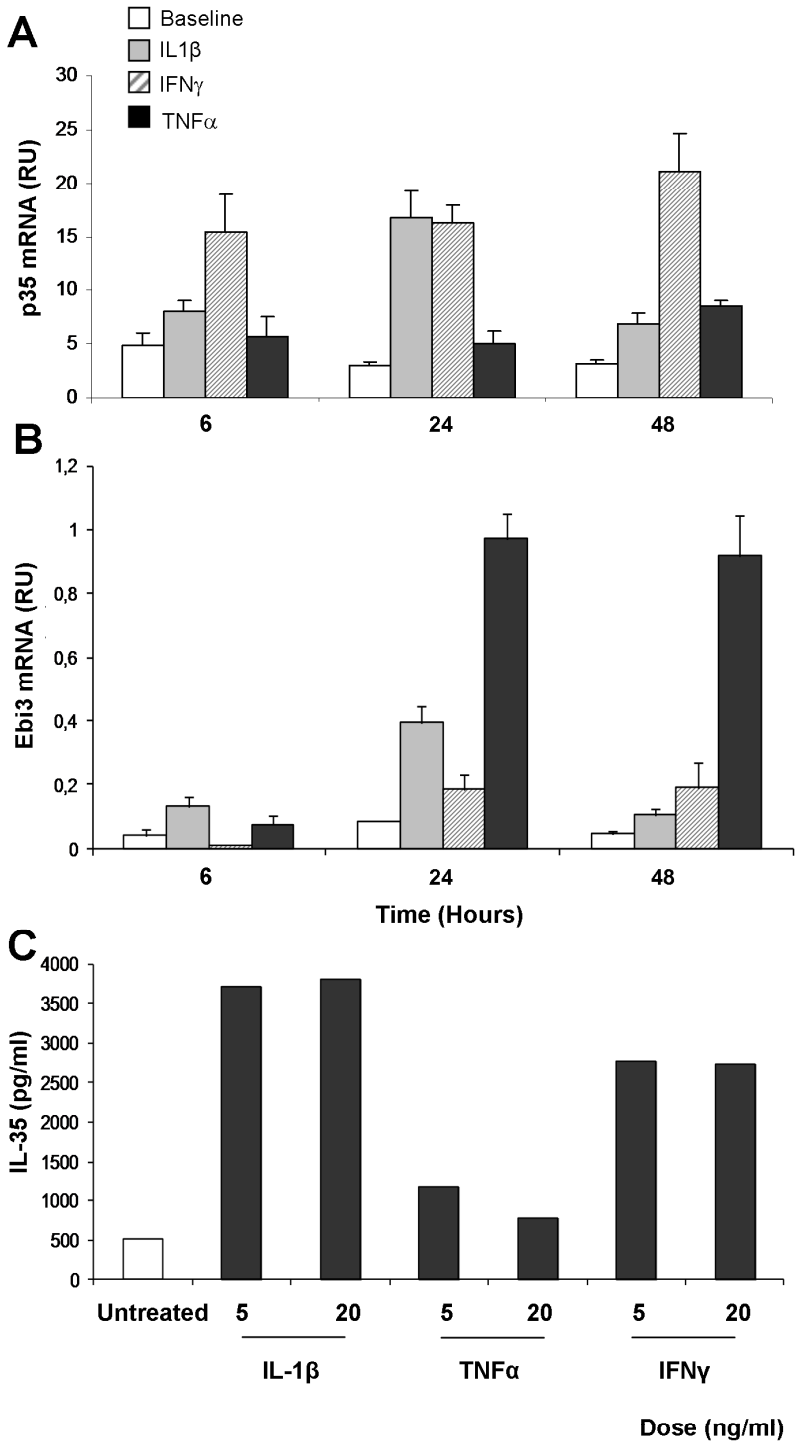
A
Baseline
IL1β
IFNγ
TNFα
p35 mRNA (RU)
30
25
20
15
10
5
0
6
24
48
B
Ebi3 mRNA (RU)
1,2
1
0,8
0,6
0,4
0,2
0
6
24
48
Time (Hours)
C
IL-35 (pg/ml)
4000
3500
3000
2500
2000
1500
1000
500
0
Untreated
5
20
5
20
5
20
IL-1β
TNFα
IFNγ
Dose (ng/ml)

Figure 3

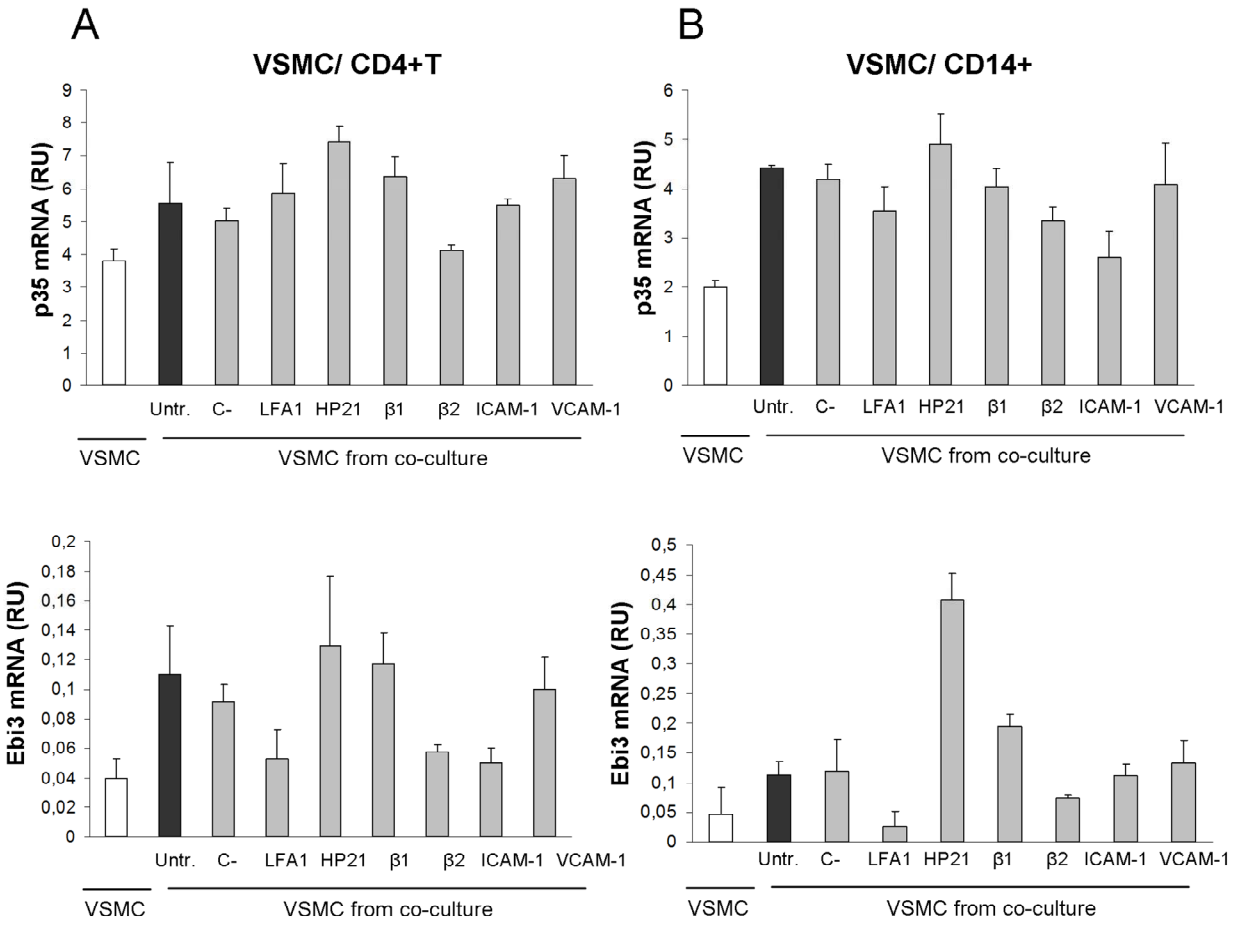
A
VSMC/ CD4+T
p35 mRNA (RU)
Untr.
C-
LFA1
HP21
β1
β2
ICAM-1
VCAM-1
VSMC
VSMC from co-culture
B
VSMC/ CD14+
p35 mRNA (RU)
Ebi3 mRNA (RU)

Figure 4

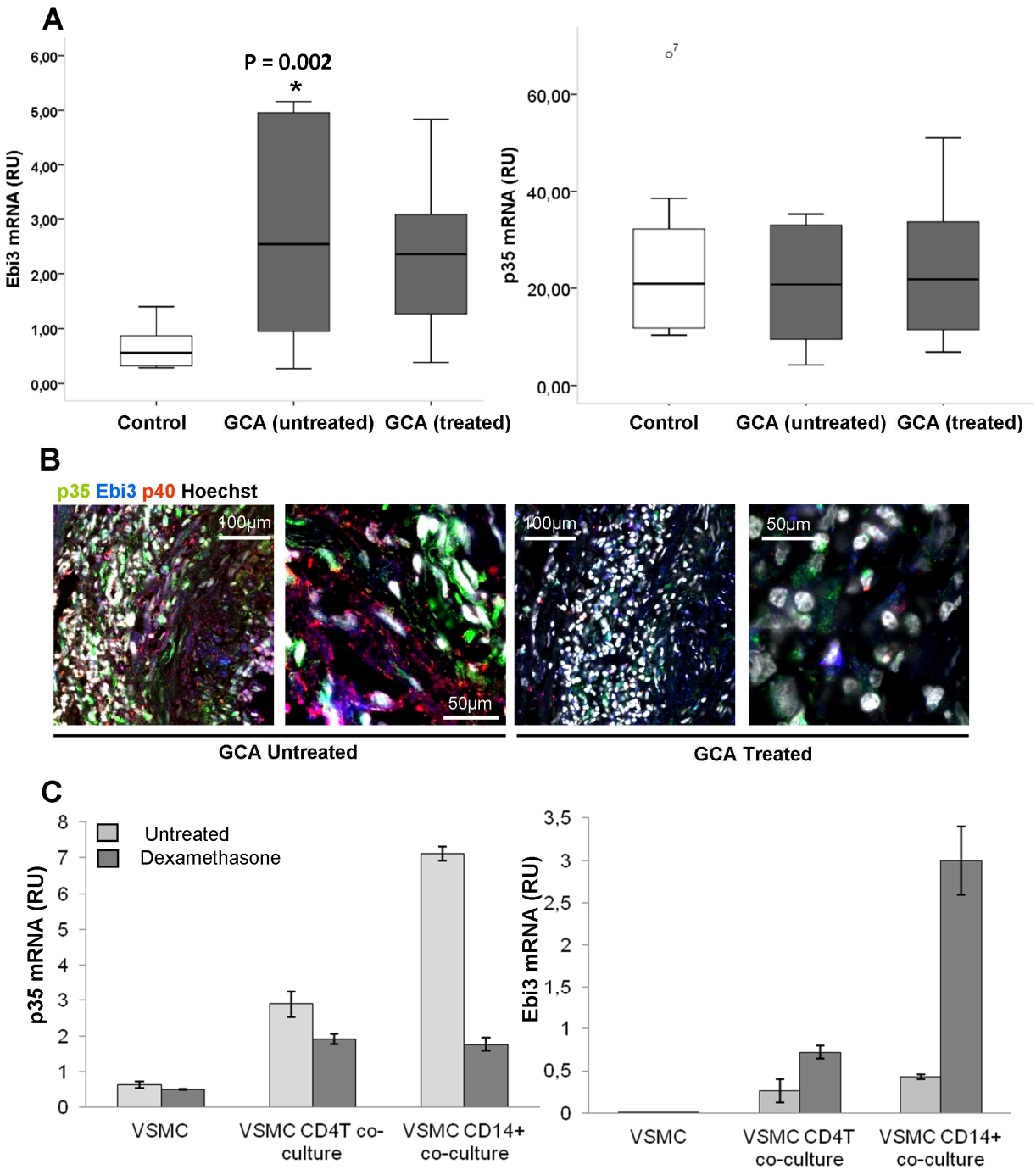
A
P = 0.002
*
Ebi3 mRNA (RU)
6,00
5,00
4,00
3,00
2,00
1,00
0,00
Control
GCA (untreated)
GCA (treated)
p35 mRNA (RU)
60,00
40,00
20,00
0,00
Control
GCA (untreated)
GCA (treated)
B
p35 Ebi3 p40 Hoechst
100µm
50µm
100µm
50µm
GCA Untreated
GCA Treated
C
Untreated
Dexamethasone
p35 mRNA (RU)
8
7
6
5
4
3
2
1
0
VSMC
VSMC CD4T co-culture
VSMC CD14+ co-culture
Ebi3 mRNA (RU)
3,5
3
2,5
2
1,5
1
0,5
0
VSMC
VSMC CD4T co-culture
VSMC CD14+ co-culture

Figure 5

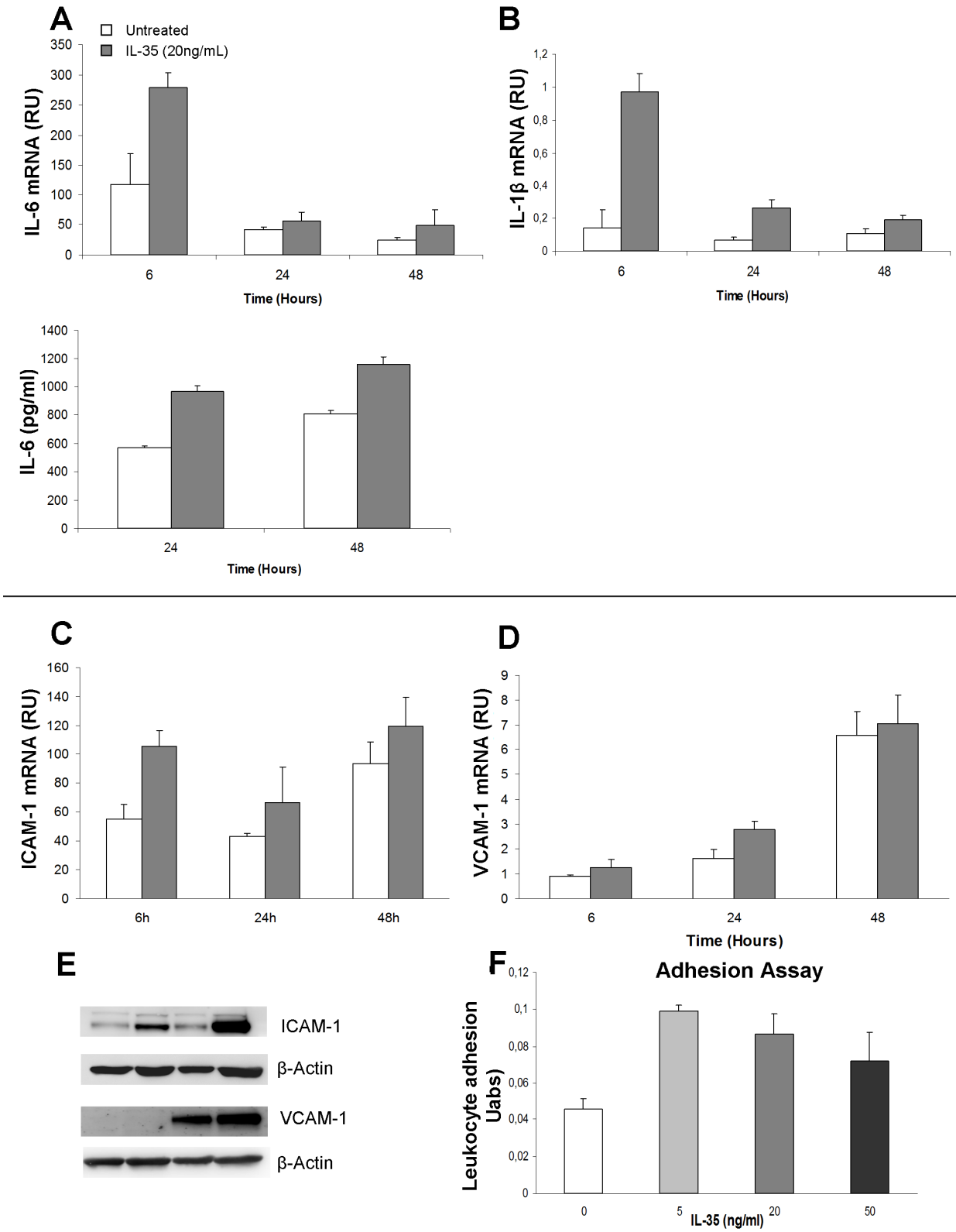
A
Untreated
IL-35 (20ng/mL)
IL-6 mRNA (RU)
Time (Hours)
B
IL-1β mRNA (RU)
Time (Hours)
IL-6 (pg/ml)
Time (Hours)
C
ICAM-1 mRNA (RU)
6h
24h
48h
D
VCAM-1 mRNA (RU)
Time (Hours)
E
ICAM-1
β-Actin
VCAM-1
β-Actin
F
Adhesion Assay
Leukocyte adhesion Uabs)
IL-35 (ng/ml)

Figure 6

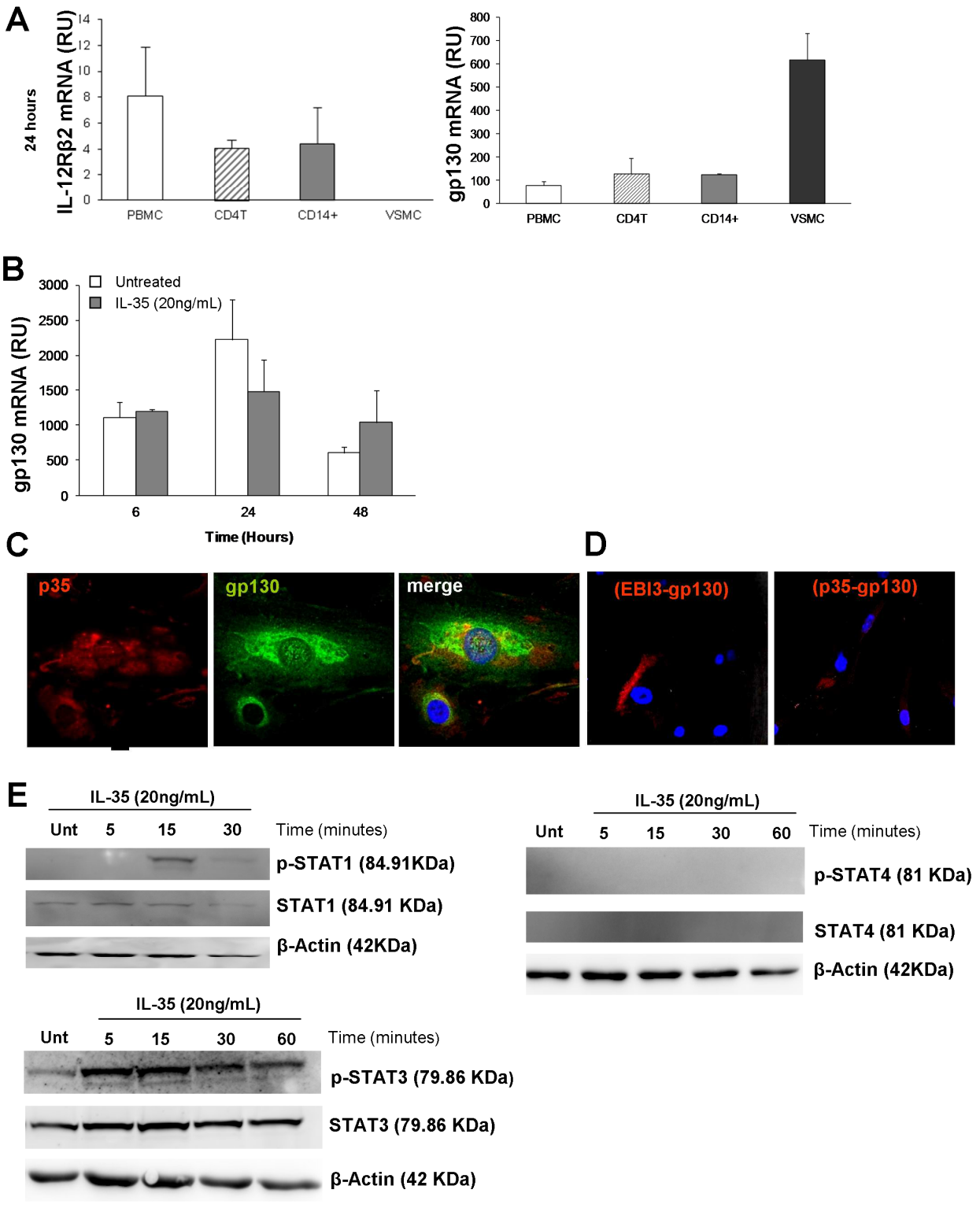
A
24 hours
IL-12Rβ2 mRNA (RU)
PBMC
CD4T
CD14+
VSMC
gp130 mRNA (RU)
B
Untreated
IL-35 (20ng/mL)
gp130 mRNA (RU)
Time (Hours)
C
p35
gp130
merge
D
(EBI3-gp130)
(p35-gp130)
E
IL-35 (20ng/mL)
Unt
Time (minutes)
p-STAT1 (84.91KDa)
STAT1 (84.91 KDa)
β-Actin (42KDa)
p-STAT4 (81 KDa)
STAT4 (81 KDa)
p-STAT3 (79.86 KDa)
STAT3 (79.86 KDa)
β-Actin (42 KDa)

Figure 7

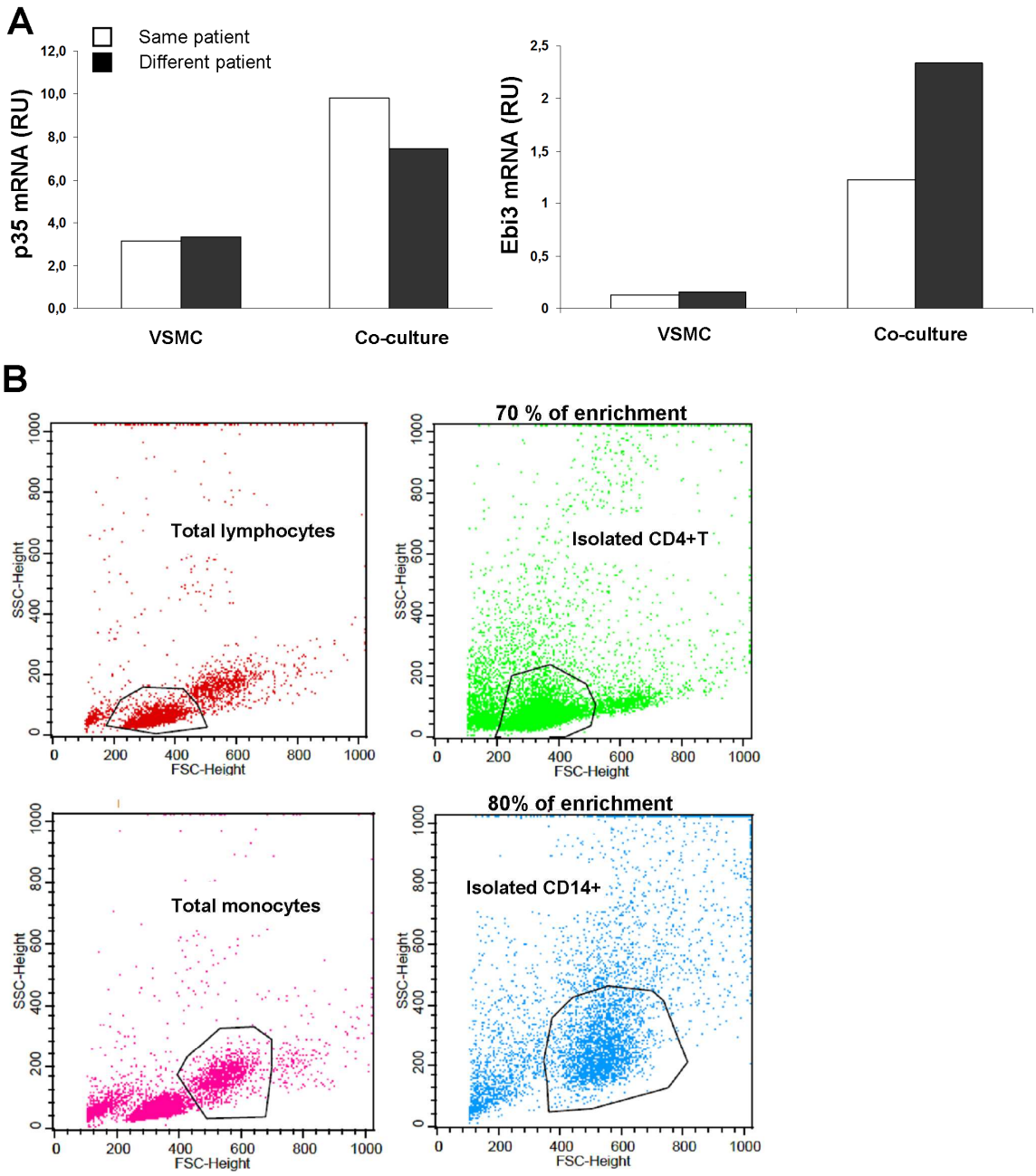

Supplementary Figure 1

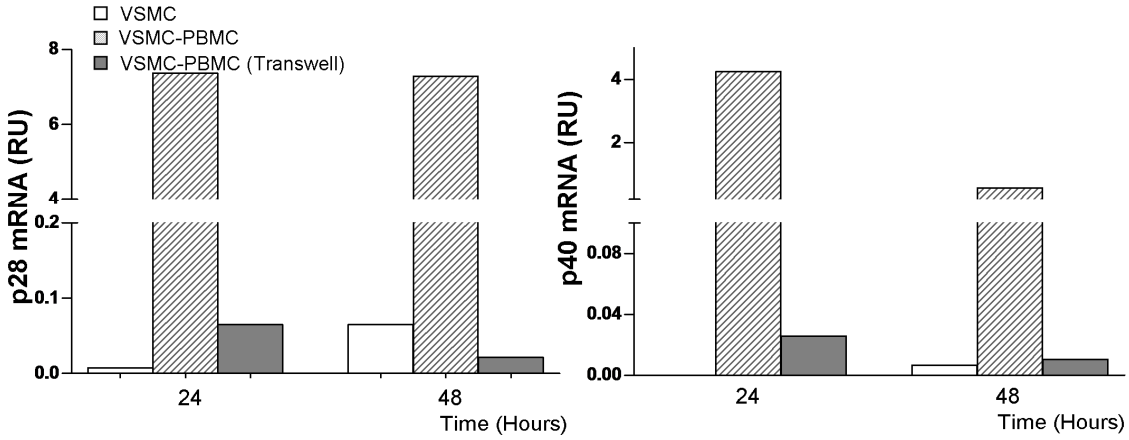

Supplementary Figure 2

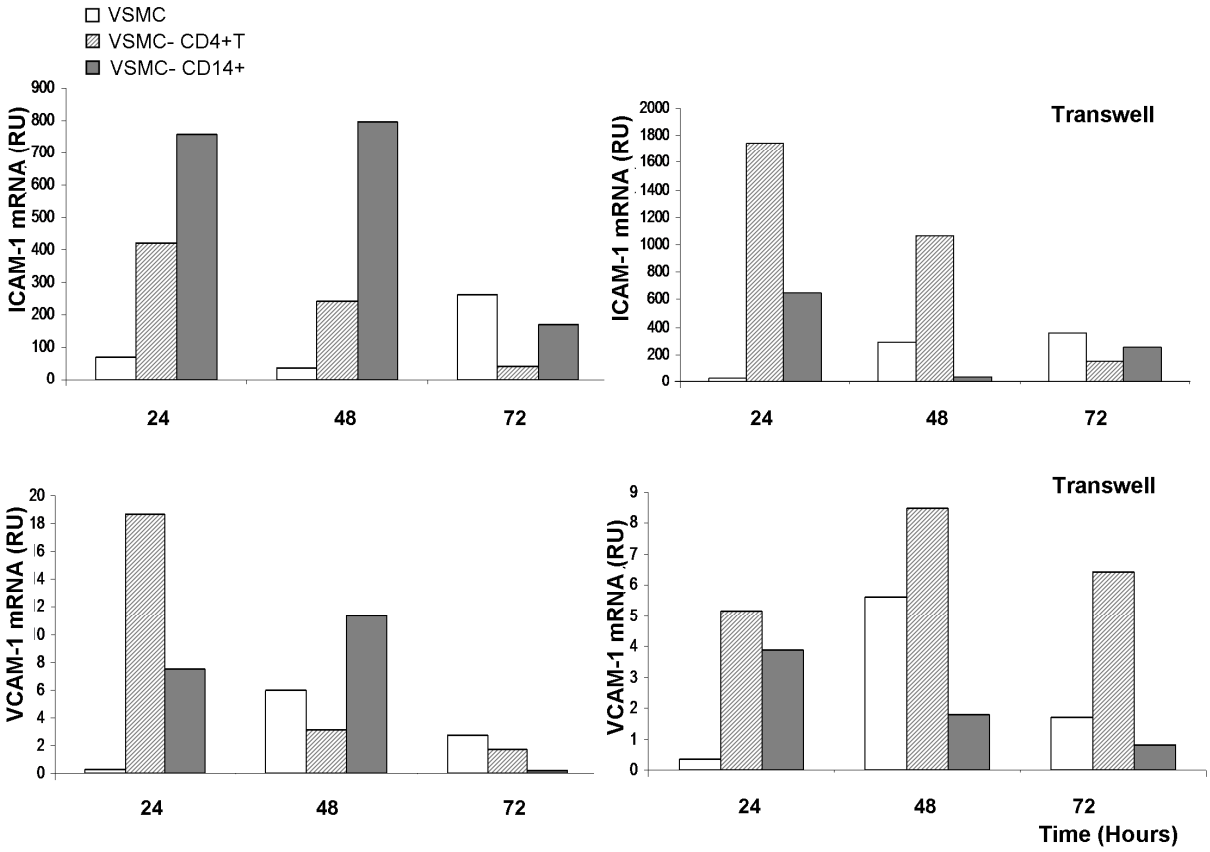

Supplementary Figure 3

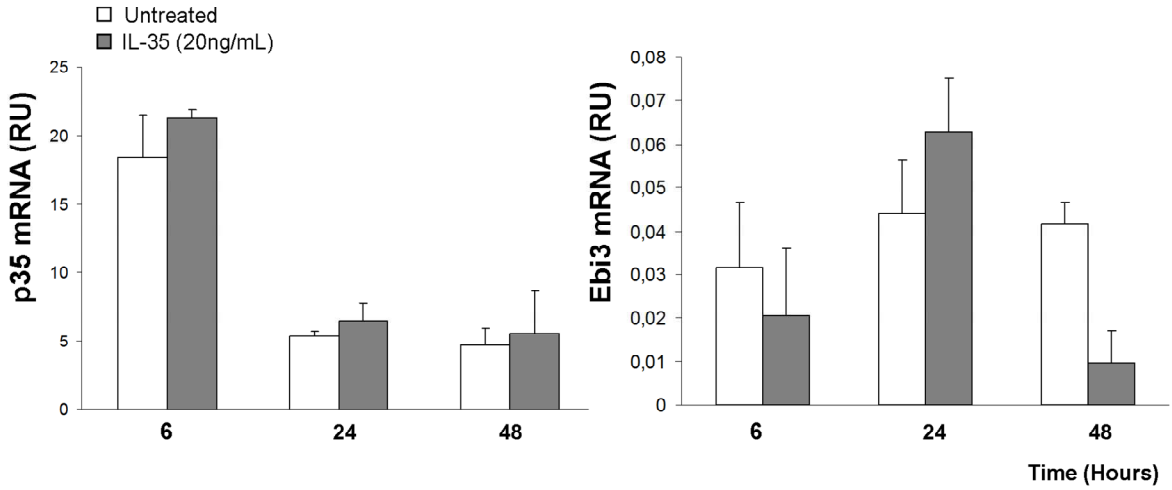

Supplementary Figure 4

IL-35: A new cytokine involved in vascular inflammation.

E.Planas-Rigol, M.Corbera- Bellalta, N.Terrades-Garcia, Georgina Espígol-Frigolé, Marco A. Alba, S. Prieto, MC.Cid.

Results summary (part 2)

1) Ebi3 and p35 are expressed in GCA lesions either by VSMC or infiltrating leukocytes.
2) IL-35 subunits (p35 and Ebi3) are induced in VSMC co-cultured with PBMC.
    a. The soluble molecules involved in IL-35 induced-production by VSMC are NFkB related molecules (IL-1β, TNFα) and IFNγ.
    b. Cell-cell contact (through integring β2 and ICAM-1) is also important for IL-35 expression by VSMC.
3) Recombinant IL-35 induces proinflammatory phenotype in VSMC by inducing IL-6 production and increasing adhesion molecule ICAM-1expression.
    a. Recombinant IL-35 promotes VSMC adhesion to PBMC.
4) Recombinant IL-35 induce STAT1 and STAT3 phosphorylation but not STAT4 phosphorylation in VSMC.
5) In contrast to what has been described in CD4+Tconv cells or Bcells, recombinant IL-35 interacts with gp130 but not with IL-12rβ2 in VSMC.

Endothelin 1 induces a myofibroblastic phenotype in vascular smooth muscle cells. A mechanism potentially contributing to vascular remodeling and intimal hyperplasia in Giant Cell Arteritis

Ester Planas-Rigol, PhD[1], Nekane Terrades-Garcia, PhD[1], Marc Corbera-Bellalta, PhD[1], Ester Lozano, PhD[1], Marco A. Alba, MD[1], Georgina Espígol-Frigolé, Sergio Prieto, MD [1], Jose Hernández, Marta Segarra, PhD[1], Sara Preciado, PhD[2], Rodolfo Lavilla, PhD[2], Maria C. Cid, MD[1]

[1]Vasculitis Research Unit, Department of Autoimmune Diseases. Hospital Clínic. University of Barcelona. Institut d'Investigacions Biomèdiques August Pi i Sunyer (IDIBAPS). Fundació CELLEX. Barcelona, Spain

[2] Laboratory of Organic Chemistry. Faculty of Pharmacy, Barcelona. Science Park, Baldiri Reixac, 10-12, 08028 Barcelona, Spain

Short Title. ET-1 involvement in vascular remodeling in GCA.

Correspondence
Maria Cinta Cid Xutglà
Department of Autoimmune Diseases. Hospital Clínic
Villarroel, 170
08036-Barcelona, Spain
Email: mccid@clinic.ub.es
Phone number: 93 227 54 00 ext 3111

Short title: ET-1 potential role in vascular remodeling of GCA.

Subject codes: [115] Remodeling, [82] Cell signaling/signal transduction, [151] Ischemic biology - basic Studies, [162] Smooth muscle proliferation and differentiation, [97] Other Vascular biology

ABSTRACT

Background: Giant-cell arteritis (GCA) is an inflammatory disease of large/medium-sized arteries, frequently involving the temporal artery (TA). Inflammation-induced vascular remodeling leads to vaso-occlusive events. Circulating ET-1 is increased in GCA patients with ischemic complications suggesting a role for ET-1 in vascular occlusion beyond its vasoactive function.

Objective: To investigate whether ET-1 induces a migratory myofibroblastic phenotype in human TA-derived vascular smooth muscle cells (VSMC) leading to intimal hyperplasia and vascular occlusion in GCA.

Methods and results: Inmunofluorescence/confocal microscopy showed increased ET-1 expression in GCA-lesions compared to control arteries. In inflamed arteries, ET-1 was expressed by infiltrating mononuclear cells whereas ET-receptors, particularly ET_BR, were expressed by VSMC. Accordingly, when co-cultured *in vitro*, TA-derived VSMC increased ET-1 expression by mononuclear cells. ET-1 increased α-smooth muscle actin (αSMA) expression by cultured TA-derived VSMC, promoted VSMC migration *in vitro,* and migration from the media to the intima in cultured TA explants. ET-1 promoted VSMC motility by increasing activation of focal adhesion kinase (FAK), a crucial molecule in the turnover of focal adhesions during cell migration. FAK activation resulted in Y397 autophosphorylation, permitting association with Src kinases and interaction with p85 subunit of PI3Kinase which, upon ET-1 exposure, co-localized with FAK at the focal adhesions of migrating VSMC. Accordingly, FAK or PI3K inhibition abrogated ET-1-induced migration *in vitro*. Consistently, ET_AR and ET_BR antagonists inhibited VSMC outgrowth from cultured GCA-involved artery explants.

Conclusions: ET-1 is up-regulated in GCA lesions and promotes VSMC migration towards the intimal layer contributing to intimal hyperplasia and vascular occlusion in GCA.

NON-STANDARD ABBREVIATIONS AND ACRONYMS

αSMA Alpha smooth muscle actin

BDNF Brain-derived neurotrophic factor

EC Endothelial cells

ECE Endothelin converting enzyme 1

ECM Extracellular matrix

EGF Epidermal growth factor

ERK Extracellular signal -regulated kinase

ET-1 Endothelin 1

ET_AR Endothelin type A receptor

ET_BR Endothelin type B receptor

FAK Focal Adhesion Kinase

FN Fibronectin

GCA Giant Cell Arteritis

GPCR G-Protein coupled receptor

MMP Matrix metalloproteinase

NFG Nerve-growth factor

PDGF Platelet derived growth factor

PBMC Peripheral blood mononuclear cells

PI3K Phosphatidylinositol-4, 5-bisphosphate 3-kinase

Src Proto-oncogene tyrosine-protein kinase Src

TA Temporal artery

TGFβ Transforming growth factor beta

TIMP Tissue inhibitor of metalloproteinase

VSMC Vascular smooth muscle cells

INTRODUCTION

Giant Cell Arteritis (GCA) is a granulomatous vasculitis preferentially targeting large and medium-sized arteries in aged individuals and frequently involving the cranial arteries [1, 2]. Inflammation induced vascular remodeling leads to vascular lumen reduction and, consequently, patients develop symptoms of vascular insufficiency [3, 4]. Irreversible ischemic complications, particularly partial or complete visual loss resulting from optic nerve ischemia, and less frequently stroke, occur in 20% of patients [5]. Pathogenic mechanisms leading to vascular remodeling and eventual occlusion in GCA are incompletely understood and remain largely unexplored. It is generally assumed that vascular smooth muscle cells (VSMC) acquire a myofibroblastic phenotype, proliferate and migrate through disrupted elastic fibers towards the intima where they produce abundant matrix proteins. Preliminary studies suggest that several growth factors, including PDGF, TGFβ, EGF, NGF or BDNF, may participate in this process. Their role is supported by their expression in GCA lesions and their ability to stimulate proliferation and/or migration of temporal artery-derived VSMC *in vitro* [6, 7]. However, underlying mechanisms remain virtually unexplored.

Visual loss in GCA is frequently preceded by characteristic transient episodes of blindness (*amaurosis fugax*) suggesting that vasospastic phenomena may also contribute to flow reduction in small arteries supplying the optic nerve [5].

Endothelins (ET) encompass a family of potent vasoactive peptides involved in the regulation of vascular tone, ET-1 is the main endothelin peptide expressed in the vascular system. The product of the ET-1 transcript is subjected to sequential cleavages yielding a 39 amino-acid peptide, big endothelin with weak biological effects. Its subsequent processing by endothelin converting enzyme -1 (ECE-1) results in a 21 amino acid mature and active endothelin-1 (ET-1) [8].

ET-1 is mainly expressed by endothelial cells although VSMC and macrophages may also produce it [9, 10]. ET-1 signals through two G-protein coupled receptors (GPCR): endothelin-1 receptor A and B (ET_AR and ET_BR). ET_AR and ET_BR mediate VSMC contraction. However, signalling through ET_BR on endothelial cells stimulates production of nitric oxide and prostacyclin which drives paracrine vasodilatation [11].

Although the majority of previous studies on ET-1 functions have focused on VSMC contraction and regulation of vascular tone, in recent years, skin, liver and lung fibroblasts have been identified as important targets of ET-1[12, 13]. ET-1 promotes myofibroblast differentiation of fibroblasts, a crucial step in the development of fibrogenic diseases such as systemic sclerosis or cardiac, pulmonary or hepatic fibrosis [14].

We and others have recently shown that ET-1, ET_AR, ET_BR and ECE-1 are up-regulated in GCA-involved arteries [9, 15] although the specific cells expressing the ET-1 system components have not been determined. Moreover, plasma ET-1 concentrations are elevated in patients with cranial ischemic complications [9].

We hypothesized that in addition to its well known vaso-active function ET-1 might contribute to vascular occlusion in GCA by stimulating a migratory myofibroblast phenotype in VSMC and favoring the development of intimal hyperplasia. Consequently we investigated the effect of ET-1 in stimulating human temporal artery-derived VSMC migration *in vitro* and *ex-vivo* as well as the signaling pathways involved in this process.

METHODS

Patient's samples

Temporal artery (TA) biopsies were performed to eight patients with suspected GCA. Four TA biopsies showing histopathological features of GCA were used in the indicated procedures whereas four others with no inflammatory infiltrate served as controls. The study was approved by the local Ethics Committee (Hospital Clinic of Barcelona) and patients signed informed consent.

Isolation and culture of VSMC derived from human temporal arteries

Human temporal artery-derived VSMC were obtained from explanted sections of temporal arteries (TA) cultured on Matrigel™ as described [16] and characterized by flow cytometry [6].

Reagents

Human ET-1 was purchased from MP Biomedical (Aurora, Ohio, USA). Fibronectin (FN) was obtained by Calbiochem (EMD Chemicals Inc., Gibbstown, NJ, USA) and used at 5µg/cm^2. Polylysine was acquired by Sigma-Aldrich (St. Louis, MO, USA) and used at 10µg/mL.

ET_AR antagonist BQ123 was chemically synthesized through solid phase peptide synthesis and chromatographically identical to a commercial sample. ET_BR antagonist BQ788 and PF-573228 (FAK inhibitor) were purchased from Sigma-Adrich. LY294002 (PI3K inhibitor), PP2 (Src inhibitor) and PD98059 (ERK inhibitor) were acquired from Calbiochem.

Transient transfection

FAK wild-type cDNA and FAK point mutants Y397F and Y925F were generated as previously described and expressed using the pCDNA3 vector containing the hemagglutinin (HA) epitope [17, 18]. Lipofectamin 2000 Reagent (Invitrogen, Waltham, Massachusetts, USA) was used for transient transfection of VSMC following the protocol advised by the manufacturer.

Quantitative real-time reverse transcription (RT)-PCR

RNA was extracted from cultured VSMC using TRIzol Reagent (Life Technologies, Ltd, Paisley, UK). ET-1, ET_AR, ET_BR, MMP2, MMP9, MMP12, MMP14, TIMP1 and TIMP2 mRNA (1µg) was measured by quantitative RT-PCR with specific TaqMan gene expression assays from Applied Biosystems (Foster City, CA, USA) as previously described [16 9, 19] .

Assessment of ET-1 secretion by immunoassay

R&D Quantikine ELISA Kit (Minneapolis, MN, USA) was used to measure ET-1 in cell supernatants.

Western blot

Cell lysates were obtained as described in the online supplement. Twenty µg of protein/lane were resolved on 8% or 10% reducing sodium dodecyl sulfate (SDS)–polyacrylamide electrophoresis gels and blotted at room temperature onto nitrocellulose membranes (Invitrogen). Immunodetection was performed with the following antibodies: rabbit polyclonal anti-human MMP14 (Chemicon, MD Millipore Billerica, MA, USA), rabbit polyclonal anti-human phospo-ERK, total ERK, phospo Y416-Src, total Src, phospho-Y397FAK and Y925 FAK (Cell Signaling, Danvers, MA, USA), rabbit polyclonal anti-human FAK (Santa Cruz, Dallas, TX, USA), rabbit polyclonal anti-human βactin (Abcam, Cambridge, UK), and mouse monoclonal anti-human alpha smooth muscle actin (αSMA) (Abcam). Chemiluminescence signals were measured with Image Quant LAS-4000 (GE Health Care Life Science, Pittsburgh, USA).

Gelatin zymography

VSMC were seeded at 80 confluence in a twelve well plate and cultured in serum-free DMEM (Lonza, Verviers, Belgium) with increasing doses of ET-1 (0, 10^{-11}, 10^{-9} and 10^{-6} mol/L). One hundred µL of each supernatant was subjected to SDS-PAGE through 10% polyacrylamide gels copolymerized with 0.2 g/mL gelatin (Bio-Rad Laboratories, Hercules, CA, USA) as previously described [18].

CD4+T cells, monocytes (CD14+) and VSMC co-culture

VSMC were seeded at 90% confluence. Peripheral Blood Mononuclear Cells (PBMC) were obtained by density gradient centrifugation using Lymphoprep™ (Axis-Shield, Oslo, Norway). Untouched CD4+T or CD14+ cells were isolated with Dynabead kits (Invitrogen).

VSMC outgrowth from *ex vivo* cultured TA sections from patients with GCA

TA sections obtained from 3 treatment-naive patients with GCA were cultured on Matrigel™ in the presence or in the absence of ET-1 (10^{-9} mol/L), BQ123 or BQ788 (20 µmol/L). Outgrowth of VSMC was scored by two investigators blinded to the conditions tested as previously described[6].

Migration assay

VSMC migration was performed by using Boyden Chamber and 10 µm pore polyester filters (Poretics Osmonics Inc., Minnesota, MN, USA). VSMC in DMEM (1% FBS) were placed at 5000 cells/well in the upper chambers. Cells were pre-incubated with or without BQ123, BQ788, or combination of both (20 µmol/L) for 1 hour and then ET-1 (10-9 mol/L) or were added at different concentrations either in the bottom or the upper chambers in quadruplicate wells. After 6-hour incubation, cells were removed from the upper surface and filters were fixed with methanol and stained with hematoxylin as depicted in the online supplementary methods. Four pictures of stained membranes were taken for each quadruplicate. After fixation and staining, purple pores were counted and represented.

Scratch wound-healing assay

VSMC were seeded at 80% confluent onto a 0.1% gelatin pre-coated 12-well plate and cultured overnight. One scratch per well was done before adding fresh DMEM supplemented with 50 mmol/L of Hepes (Sigma-Aldrich) and BQ123, BQ788 (20 µmol/L) or combination of both inhibitors. Subsequent addition of ET-1 (10^{-9} mol/L) or fresh medium was added to each corresponding well. Results were analyzed as explained in online supplement.

Proliferation assay

VSMC were plated at 4000 cells/well in flat-bottom 96-well plates (Nunc, Waltham, MA, USA) in medium 1% FBS as previously described [6]. Cells were exposed ET-1 (10^{-9}mol/L). Cells were fixed and stained with 0,2% crystal violet (Sigma-Adrich) in 20% methanol at various time-points and cell quantity was measured as detailed in online supplementary methods

Immunofluorescence Imaging

Immunofluorescence staining was performed in VSMC cultured on 16-well chamber slides (Nunc), fixed (4% paraformaldehyde) and stained overnight with 1:100 or 1:50 dilution of the corresponding antibodies to FAK (rabbit polyclonal, Santa Cruz), p85 and Y397-FAK (rabbit polyclonal, Cell Signaling). Secondary antibodies were used at 1:300 and were purchased from Molecular Probes (Oregon, USA). Actin was stained with Rhodamin Phalloidin (Molecular Probes) at 1:1000 dilution or mouse anti-human αSMA (Abcam).

TA tissues were fixed with 4% paraformaldehyde (PFA) and incubated with increasing concentrations of saccharose before being frozen with OCT (Sakura, Flemingweg, The

Netherlands) and stored at -80ºC. Before incubating with primary antibodies, tissues were refixed with 4%PFA and permeabilized. Antibodies to ET-1 (goat polyclonal, Santa Cruz), ET_AR (mouse monoclonal, BD Transduction Laboratories), ET_BR (rabbit polyclonal, Abcam), Y397 FAK (rabbit polyclonal, Cell Signaling), FAK (mouse monoclonal, Santa Cruz) and αSMA (mouse monoclonal, Abcam) were used at 1:50 or 1:100 dilution. Secondary antibodies were used at 1:300 and were purchased from Molecular Probes.

Hoechst (Molecular Probes) (1:1000) was used nuclear staining. Slides were mounted with Prolong Gold Antifade Reagent (Molecular Probes). Preparations were examined using a laser scanning confocal Leica TCS *SP5* microscope (Leica Microsystems, Heildelberg, Germany). Images were processed with Leica Confocal software (LAS-AF Lite) and Image J software.

Statistical analysis

Mann-Whitney was applied for non-parametric and independent samples using SPSS software, version PASW 22.0.

RESULTS

Distribution of the ET-1 system in GCA lesions compared to controls

Components of ET-1 system (ET-1, ET_AR, and ET_BR) are known to be overexpressed in GCA lesions compared to normal arteries [9] but their cellular distribution has not been characterized. In control arteries ET-1 expression was observed in concentrically organized, αSMA expressing VSMC in the media layer (Figure 1A). In contrast, in GCA-involved arteries, the muscular layer was disrupted and αSMA expressing VSMC were mostly localized in the neointima and did not substantially express ET-1 (Figure 1B). Scattered αSMA and ET-1 co-expressing cells were observed at the intima/media junction (Figure 1 b.2, b.3). ET-1 was mostly and intensively expressed by clusters of infiltrating inflammatory cells surrounding VSMC (Figure 1 b.1). In addition, ET-1 expression by the luminal endothelium was increased in GCA (Figure 1B) compared to control arteries where endothelial expression of ET-1 was weaker (Figure 1A).

Expression of ET_AR and ET_BR (Figure 1C-F) was explored in the same specimens. In control arteries, ET_AR was expressed by VSMC in the media whereas ET_BR was slightly expressed even by the endothelium (Figure 1C). In GCA, both ET_AR and ET_BR receptors were strongly expressed, particularly in cells located in the intima-media junction which included inflammatory

cells and presumably migrating VSMC (Figure 1 E, F). Endothelial cells and scattered cells in the intimal layer also expressed ET receptors (Figure 1C, E and F).

In order to further characterize the cell types responsible for ET-1 production in GCA lesions, primary cultures of TA-derived VSMC [6] were co-cultured with purified CD4+T cells or monocytes (CD14+) from healthy donors to mimic vascular inflammatory infiltrates. Primary VSMC expressed and secreted high levels of ET-1 (Figure 1G) similar as cultured human umbilical vein endothelial cells (HUVEC) as a source of EC. Interestingly, an induction of mRNA expression and secretion of ET-1 by CD4+ T cells and also CD14+ monocytes was observed when co-cultured with VSMC (Figure 1H) suggesting that VSMC promotes ET-1 production by infiltrating lymphocytes and macrophages in GCA lesions.

ET-1 promotes VSMC cytoskeleton reorganization and migration through ET_AR and ET_BR receptors

Based on the remarkable change in αSMA-expressing VSMC location from the media to the intima observed in GCA-involved arteries, we further investigated whether ET-1 was involved in VSMC migration. ET-1 elicited spreading of VSMC with a striking formation of cytoplasm protrusions (Figure 2A). This phenotype was not induced in VSMC cultured on poylysine and was more remarkable when VSMC were cultured on fibronectin, suggesting participation of integrin-mediated signaling pathways in this process (Figure 2A). Spreading was reverted by blocking ET-1 signaling with ET_AR and ET_BR antagonists BQ123 and BQ788, respectively (Figure 2A).

ET-1 phenotype changes in VSMC were associated with an increased migratory activity. Scratch wound healing assays with cultured VSMC showed that treatment with ET-1 resulted in significantly faster scratch-wound closure (Figure 2B, C). ET_AR and ET_BR antagonists (BQ123 and BQ788, respectively) and combination of both inhibitors significantly abrogated ET-1-induced migration of VSMC indicating implication of both receptors in this process (Figure 2B, C).

ET-1 also induced VSMC migration in Boyden chambers when added to the upper compartment (Figure 2D). In contrast, when ET-1 was added to the lower compartment, no differences in migration were observed indicating that ET-1 has no chemoattractant activity (Figure 2D). ET-1

induced migration in Boyden chambers was again reduced with BQ788 and completely abrogated with BQ123 or the combination of both (Figure 2E).

ET-1 recruits FAK to the VSMC leading edge. ET-1/Y397FAK axis is essential for the ET-1 induction of VSMC migration

We next explored the involvement of focal adhesion kinase (FAK) in ET-induced VSMC migration. FAK is a docking and signaling tyrosine kinase with a seminal role in focal adhesion turnover required for cell migration in response to integrin engagement or growth factor signaling [20]. FAK activation results in auto-phosphorylation of several crucial tyrosines [21] . ET-1 induced phosphorylation of Y397 and Y925 FAK residues, which was abrogated by ET_AR or ET_BR antagonists BQ123 and BQ788 (Figure 3A).

In addition to FAK phosphorylation, ET-1 induced FAK recruitment at the cell protrusions and co-localization with αSMA (Figure 3B). To further confirm the role of FAK in ET-1 induced VSMC migration, we investigated the effect of PF-573228, an inhibitor of FAK kinase activity. At concentrations able to inhibit FAK phosphorylation (Supplementary Figure 1A, B), PF-573228 significantly reduced ET-1-induced migration in a dose response manner (Figure 3C). Furthermore, transient transfection of expression vectors containing wild-type FAK or FAK point mutations Y397F or Y925F, were used to evaluate the relative contribution of both phosphorylation sites in ET-1-induced VSMC migration (Figure 3D). Transient transfection of VSMC with wild type FAK significantly increased VSMC migration through Boyden chambers showed a significantly cell migration induction by FAK transfected cells *vs.* MOCK (PCDNA3) ($p<0.01$). Similar results were observed in the FAK925-HA transfected ($p<0.01$). In contrast FAK397-HA transfected VSMC did not show increased migration (Figure 3D) indicating that phosphorylation of Y397 but not Y925 is required for ET-1- mediated migration in primary VSMC.

ERK, Src, and PI3K are essential for ET-1/ Y397FAK axis induced VSMC migration

Considering that FAK activated form (Y397) and total FAK were clearly found localized on the protrusions of the ET-1 treated cells, we next explored FAK downstream pathways involved on migration including ERK, Src and PI3K [21-23] .Consistent with our previous results, phosphorylation of ERK and Src (Y416) were induced by ET-1 and abrogated by both ET-1 receptor antagonists BQ123 and BQ788 (Figure 4A).

In order to further explore the contribution of ERK ,Src and PI3K to ET-1/FAK downstream migration pathway, we next performed Boyden Chamber assays with VSMC pre incubated with the Src, ERK and PI3K inhibitors (PP2, PD98059, and LY294002 respectively) with or without ET-1. No differences in cell viability was observed using Trypan Blue staining (data not shown). ERK inhibitor (PD98059) and Src inhibitor (PP2) completely abrogated both basal and ET-1-induced migration ($p<0.05$). Interestingly, PI3K inhibitor (LY294002) only abrogated ET-1-induced migration (Figure 4B). PI3K p85 subunit can be involved in cell cytoskeleton reorganization as a response of integrin and G proteins; hence it can be associated to Y397 FAK [24]. Since Y397 FAK is activated through ET-1 we wanted to evaluate whether PI3K p85 is associated to FAK in the cell protrusions in response to ET-1. To this end, we performed immunofluorescence staining of p85 (green) total FAK (red) and cytoskeleton (blue). Indeed, ET-1 induced p85/FAK recruitment to the leading edge of VSMC comparing with untreated cells (Figure 4D). Cells pre-incubated with either BQ123 or BQ788 showed co-expression of p85/FAK but none of them was localized in the cell protrusions. In addition, cells pre-incubated with PI3K inhibitor showed FAK/p85 co-localization but this complex was not recruited to the cell protrusion. Moreover, formation of immature focal adhesion was observed only when ET-1 was added together with PI3K inhibitor LY294002 (Figure 4D and Supplementary Figure 2). Intriguingly, VSMC pre-treated with PI3K inhibitor did not show the spread phenotype observed in ET-1-treated cells (Figure 4C). In line with our results, FAK inhibitor also abrogates the ET-1 induced elongated VSMC phenotype (Figure 4C) and FAK/p85 recruitment to the cell protrusions (Figure 4D). Overall, our data demonstrate that signaling pathways though FAK, ERK, Src and PI3K are required for VSMC migration induced by ET-1.

ET-1 promotes secretion of MMP2 by VSMC

In GCA lesions, migration of infiltrating leukocytes and VSMC from the media layer to the neointima requires disruption of elastic membranes. Gelatinases MMP9 and MMP2 have elastinolytic activity and their expression, activation, and proteolytic activity have been demonstrated in GCA lesions [19, 25]. It has been previously reported that integrin engagement and FAK signaling trigger rapid secretion of gelatinases by lymphoid [18, 26]. Based on the important role of ET-1 in inducing FAK activation and VSMC migration we explored whether ET-1 modulated secretion of gelatinases and their inhibitors TIMPs. To this end, VSMC were

treated with ET-1 for 6 and 24 hours and expression of MMP2, MMP9, MMP14, TIMP1, and TIMP2 were analyzed. No significant differences in MMPS or TIMPs mRNA expression were observed after ET-1 stimulation (Supplementary Figure 3A) although a slightly induction on mRNA expression of these molecules was observed and inhibited by BQ123 and BQ788 (Supplementary Figure 3B). Nevertheless, ET-1 clearly induced secretion of pre-MMP2 and mature MMP2 (figure 5A) and this effect was partially abrogated by BQ123 (ET_AR antagonist) and importantly abrogated by BQ788 (ET_BR antagonist) (Figure 5B). In contrast, MMP14 expression was not modulated by ET-1 (Figure 5C). Furthermore, increased secretion of TIMP2 on the supernatants of ET-1 treated VSMC was observed which could lead to an increment of the mature MMP2 (Figure 5D).

ET-1 blockade through ET_AR and ET_BR antagonists efficiently abrogates VSMC outgrowth and Y397FAK phosphorylation from *ex vivo* temporal arteries

As previously demonstrated, ET-1 is highly expressed by GCA lesions [9, 15]. In here we report that ET-1 may be involved in the VSMC migration from the media layer to the intima. We investigated whether ET-1 was also involved in VSMC outgrowth from *ex vivo* TAs from patients with GCA cultured on Matrigel™ [16]. The outgrowth of the cells was scored as previously described [6]. Blocking ET_BR with BQ788 remarkably inhibited VSMC outgrowth from GCA-involved arteries. The effect of blocking ET_AR with BQ123 was less intense but also delayed VSMC outgrowth (Figure 6A). To confirm that it was not an inhibition of the proliferation but of the migration we performed a proliferation assay with VSMC in presence of absence of ET-1. Results clearly showed that ET-1 may not play a role in the proliferation of these cells (Supplementary Figure 4). Our functional data in this *ex vivo* model of GCA suggest that ET-1 plays an important role in promoting migration and outgrowth of VSMC.

Moreover, cultured TA sections from patients with GCA were assessed for FAK phosphorylation. As shown in figure 6C, Y397-phosphorylated FAK was detected in GCA lesions, particularly at the intima and intima/media junction and FAK phosphorylation decreased upon exposure to ET_AR and ET_BR antagonists.

ET-1 induces neointima formation in *ex vivo* cultured normal temporal arteries

Control TAs were cultured on Matrigel™ [16] with or without ET-1 supplemented medium for 5 days. The specimens were then collected, fixed and immunofluorescence stained for αSMA in

order to study changes in the artery morphology (Figure 7). Interestingly, a dramatic induction of αSMA expression was observed in the ET-1 treated sections (Figure 7). Moreover, concentric organization of quiescent VSMC was disrupted and VSMC migrated towards the intima.

DISCUSSION

ET-1 is known to be expressed in TA from patients with GCA but its cellular distribution and function has not been investigated[6, 15]. The observation that GCA patients with disease-related ischemic complications have significantly elevated circulating ET-1, suggest a role for ET-1 in permanent vascular occlusion beyond its vasoconstrictor function[6]. Moreover, arteries involved by GCA are larger than resistance arteries controlling vascular tone.

While in normal TA ET-1 peptide was slightly detectable, in GCA lesions, an intense expression of ET-1 by inflammatory cells and endothelial cells was observed. Slight expression of ET-1 by VSMC was also detected. Interestingly, interactions between lymphocytes or monocytes with cultured VSMC, intensively increased ET-1 production. This observation indicates that cross-talk between inflammatory cells and vascular components strongly increases ET-1 production in the context of vascular inflammation.

In GCA lesions VSMC distribution underwent a dramatic change compared with normal arteries. While in control arteries VSMC appeared organized in concentric layers, in GCA the muscular layer was disorganized and intensively expressing αSMA cells predominated in the intima. Interestingly, ET-1 stimulated expression of both ET_AR and and ET_BR receptors, rendering VSMC more receptive to the effects of ET-1. However, while constitutive expression of ET_AR predominated in normal arteries, ET_BR expression was clearly increased in GCA lesions. ET-1 stimulated a myofibroblast phenotype in VSMC by up-regulating αSMA expression, cytoskeletal organization and migratory activity through both ET_AR and ET_BR, *in vitro* and in *ex vivo* cultured TA explants. Overall, the inhibitory effect of ET_BR blockade on VSMC migration and related responses was more remarkable than the effect of inhibiting ET_AR.

ET-1 stimulated VSMC migration through FAK activation, revealed by ET-1 enhanced FAK auto-phopsphorylation at Y397, which mediates binding of Src kinase and the p85 regulatory subunit of PI3kinase, a crucial process in cell motility [21, 22]. ET-1 promoted co-localization of activated FAK and p85 PI3 kinase at the focal adhesions. Subsequent signaling cascades

participating in cell motility in other cell types, such as ERK were also activated. Interestingly, while FAK, Src and ERK inhibitors strongly reduced both baseline and ET-1 induced migration, PI3kinase inhibitor selectively inhibited the increase in migration induced by ET-1.

PI3kinase operates downstream of G-protein –coupled receptors [28, 30]. Class I PI3kinases are activated by tyrosine kinases whereas class II PI3kinases are activated through G-protein coupled receptors. It is likely that ET-1 promotes activation of both classes of PI3kinases through FAK activation and through G-protein coupled receptors ET_AR and ET_BR.

It has been previously shown that FAK coordinates migration with matrix metalloproteinase release, which is necessary for cell progression through the extra-cellular matrix[18]. ET-1 stimulated release of MMP2 by VSMC, a process mostly mediated by ET_BR in our experimental conditions. Since MMP2 has elastinolytic activity, induction and release of MMP-2 mediated by ET-1 may be relevant to the disruption of the internal elastic lamina, characteristically observed in GCA lesions, allowing VSMC migration from the muscular to the intimal layer[19, 31, 32].

FAK has received substantial attention in pathological processes where cell migration is seminal including cancer and fibrosis[12, 33]. In the field of vascular biology interest has focused on the role of endothelial FAK in angiogenesis. Our data suggests a seminal role for FAK in vascular remodeling. Supporting our findings a recent study has evidenced Y397 phosphorylated FAK in the resistance arteries undergoing vascular remodeling in hypertension[34].

Consequently, our results indicate that ET-1-mediated activation of FAK in VSMC may have a seminal role in vascular remodeling in the context of vascular inflammation where ET-1 is mainly produced by inflammatory cells and their production is amplified through interactions with VSMC. These newly recognized functions of ET-1 on VSMC may have a broader impact and may operate in vascular diseases with prominent vascular remodeling beyond GCA. To date, in the field of vascular biology attention has mainly focused on the vasoconstriction role of ET-1 and only responses related to vascular reactivity or hypertension have been explored after conditional deletion of ET_AR in VSMC[35,36]. Based on its presumed major function, ET-1 has been considered a therapeutic target for vascular diseases where vasoconstriction is thought to play a major role such as systemic or pulmonary hypertension or, more recently, fibrotic diseases, such scleroderma or lung fibrosis, according to the newly recognized functions of ET-1 on fibroblasts [12, 13, 35, 36]. However, to date, clinical trials with ET-1 receptor antagonists have

shown the best efficacy for diseases with prominent vascular remodeling such as ischemic ulcers in systemic sclerosis or pulmonary hypertension rather than vasoconstriction or fibrotic diseases [35, 36].

There is an unmet need of treatments reducing inflammation-induced vascular remodeling in GCA since patients with systemic vasculitis may develop complications derived from vascular occlusion in spite of glucocorticoid or immunosuppressive therapy. Our data underline an unprecedented and seminal role for ET-1 in inducing vascular remodeling and vascular occlusion in the context of vascular inflammation and point towards endothelial receptor antagonists as potential therapeutic targets to avoid maladaptive vascular remodeling in inflammatory diseases of blood vessels.

Acknowledgments

The authors would thank to Dr. Ester Sánchez-Tillo for helping with the vector production and Ester Tobias for the technical support on processing TA biopsies and be processed by immunofluorescence. We also thank Anna Bosch, Elisenda and Maria Calvo from the Advanced Optical Microscopy department of the University of Barcelona for the technical support on the images of the confocal microscopy. We also thank Dr. Jara Palomero, Marta Rodriguez and Robert Albero from the group of Dr. Elias Campo.

Sources of funding

Supported by the Ministerio de Economía y Competitividad (SAF 11/30073), BQU-CTQ2012-30930) and Instituto de Salud Carlos III (PIE13/00033)

Disclosures

None

REFERENCES

1. Salvarani C, Pipitone N, Versari A, Hunder GG. Clinical features of polymyalgia rheumatica and giant cell arteritis. *Nature reviews. Rheumatology*. 2012;8:509-521
2. Jennette JC, Falk RJ, Bacon PA, Basu N, Cid MC, Ferrario F, Flores-Suarez LF, Gross WL, Guillevin L, Hagen EC, Hoffman GS, Jayne DR, Kallenberg CG, Lamprecht P, Langford CA, Luqmani RA, Mahr AD, Matteson EL, Merkel PA, Ozen S, Pusey CD, Rasmussen N, Rees AJ, Scott DG, Specks U, Stone JH, Takahashi K, Watts RA. 2012 revised international chapel hill consensus conference nomenclature of vasculitides. *Arthritis and rheumatism*. 2013;65:1-11
3. Cid MC, Font C, Oristrell J, de la Sierra A, Coll-Vinent B, Lopez-Soto A, Vilaseca J, Urbano-Marquez A, Grau JM. Association between strong inflammatory response and low risk of developing visual loss and other cranial ischemic complications in giant cell (temporal) arteritis. *Arthritis and rheumatism*. 1998;41:26-32
4. Salvarani C, Cimino L, Macchioni P, Consonni D, Cantini F, Bajocchi G, Pipitone N, Catanoso MG, Boiardi L. Risk factors for visual loss in an italian population-based cohort of patients with giant cell arteritis. *Arthritis and rheumatism*. 2005;53:293-297
5. Font C, Cid MC, Coll-Vinent B, Lopez-Soto A, Grau JM. Clinical features in patients with permanent visual loss due to biopsy-proven giant cell arteritis. *British journal of rheumatology*. 1997;36:251-254
6. Lozano E, Segarra M, Garcia-Martinez A, Hernandez-Rodriguez J, Cid MC. Imatinib mesylate inhibits in vitro and ex vivo biological responses related to vascular occlusion in giant cell arteritis. *Annals of the rheumatic diseases*. 2008;67:1581-1588
7. Ly KH, Regent A, Molina E, Saada S, Sindou P, Le-Jeunne C, Brezin A, Witko-Sarsat V, Labrousse F, Robert PY, Bertin P, Bourges JL, Fauchais AL, Vidal E, Mouthon L, Jauberteau MO. Neurotrophins are expressed in giant cell arteritis lesions and may contribute to vascular remodeling. *Arthritis research & therapy*. 2014;16:487
8. Russell FD, Skepper JN, Davenport AP. Endothelin peptide and converting enzymes in human endothelium. *Journal of cardiovascular pharmacology*. 1998;31 Suppl 1:S19-21
9. Lozano E, Segarra M, Corbera-Bellalta M, Garcia-Martinez A, Espigol-Frigole G, Pla-Campo A, Hernandez-Rodriguez J, Cid MC. Increased expression of the endothelin system in arterial lesions from patients with giant-cell arteritis: Association between elevated plasma endothelin levels and the development of ischaemic events. *Annals of the rheumatic diseases*. 2010;69:434-442
10. Ehrenreich H, Anderson RW, Fox CH, Rieckmann P, Hoffman GS, Travis WD, Coligan JE, Kehrl JH, Fauci AS. Endothelins, peptides with potent vasoactive properties, are produced by human macrophages. *The Journal of experimental medicine*. 1990;172:1741-1748

11. Luscher TF, Barton M. Endothelins and endothelin receptor antagonists: Therapeutic considerations for a novel class of cardiovascular drugs. *Circulation*. 2000;102:2434-2440
12. Lagares D, Busnadiego O, Garcia-Fernandez RA, Lamas S, Rodriguez-Pascual F. Adenoviral gene transfer of endothelin-1 in the lung induces pulmonary fibrosis through the activation of focal adhesion kinase. *American journal of respiratory cell and molecular biology*. 2012;47:834-842
13. Lagares D, Garcia-Fernandez RA, Jimenez CL, Magan-Marchal N, Busnadiego O, Lamas S, Rodriguez-Pascual F. Endothelin 1 contributes to the effect of transforming growth factor beta1 on wound repair and skin fibrosis. *Arthritis and rheumatism*. 2010;62:878-889
14. Leask A. Potential therapeutic targets for cardiac fibrosis: Tgfbeta, angiotensin, endothelin, ccn2, and pdgf, partners in fibroblast activation. *Circulation research*. 2010;106:1675-1680
15. Dimitrijevic I, Andersson C, Rissler P, Edvinsson L. Increased tissue endothelin-1 and endothelin-b receptor expression in temporal arteries from patients with giant cell arteritis. *Ophthalmology*. 2010;117:628-636
16. Corbera-Bellalta M, Garcia-Martinez A, Lozano E, Planas-Rigol E, Tavera-Bahillo I, Alba MA, Prieto-Gonzalez S, Butjosa M, Espigol-Frigole G, Hernandez-Rodriguez J, Fernandez PL, Roux-Lombard P, Dayer JM, Rahman MU, Cid MC. Changes in biomarkers after therapeutic intervention in temporal arteries cultured in matrigel: A new model for preclinical studies in giant-cell arteritis. *Annals of the rheumatic diseases*. 2014;73:616-623
17. Tamura M, Gu J, Danen EH, Takino T, Miyamoto S, Yamada KM. Pten interactions with focal adhesion kinase and suppression of the extracellular matrix-dependent phosphatidylinositol 3-kinase/akt cell survival pathway. *The Journal of biological chemistry*. 1999;274:20693-20703
18. Segarra M, Vilardell C, Matsumoto K, Esparza J, Lozano E, Serra-Pages C, Urbano-Marquez A, Yamada KM, Cid MC. Dual function of focal adhesion kinase in regulating integrin-induced mmp-2 and mmp-9 release by human t lymphoid cells. *FASEB journal : official publication of the Federation of American Societies for Experimental Biology*. 2005;19:1875-1877
19. Segarra M, Garcia-Martinez A, Sanchez M, Hernandez-Rodriguez J, Lozano E, Grau JM, Cid MC. Gelatinase expression and proteolytic activity in giant-cell arteritis. *Annals of the rheumatic diseases*. 2007;66:1429-1435
20. Vicente-Manzanares M, Choi CK, Horwitz AR. Integrins in cell migration--the actin connection. *Journal of cell science*. 2009;122:199-206
21. Schaller MD, Parsons JT. Focal adhesion kinase and associated proteins. *Current opinion in cell biology*. 1994;6:705-710

22. Chen HC, Appeddu PA, Isoda H, Guan JL. Phosphorylation of tyrosine 397 in focal adhesion kinase is required for binding phosphatidylinositol 3-kinase. *The Journal of biological chemistry*. 1996;271:26329-26334
23. Mitra SK, Hanson DA, Schlaepfer DD. Focal adhesion kinase: In command and control of cell motility. *Nature reviews. Molecular cell biology*. 2005;6:56-68
24. Parsons JT. Focal adhesion kinase: The first ten years. *Journal of cell science*. 2003;116:1409-1416
25. Rodriguez-Pla A, Bosch-Gil JA, Rossello-Urgell J, Huguet-Redecilla P, Stone JH, Vilardell-Tarres M. Metalloproteinase-2 and -9 in giant cell arteritis: Involvement in vascular remodeling. *Circulation*. 2005;112:264-269
27. Kedzierski RM, Yanagisawa M. Endothelin system: The double-edged sword in health and disease. *Annual review of pharmacology and toxicology*. 2001;41:851-876
28. Reiske HR, Kao SC, Cary LA, Guan JL, Lai JF, Chen HC. Requirement of phosphatidylinositol 3-kinase in focal adhesion kinase-promoted cell migration. *The Journal of biological chemistry*. 1999;274:12361-12366
29. Vanhaesebroeck B, Leevers SJ, Ahmadi K, Timms J, Katso R, Driscoll PC, Woscholski R, Parker PJ, Waterfield MD. Synthesis and function of 3-phosphorylated inositol lipids. *Annual review of biochemistry*. 2001;70:535-602
30. Shi-Wen X, Chen Y, Denton CP, Eastwood M, Renzoni EA, Bou-Gharios G, Pearson JD, Dashwood M, du Bois RM, Black CM, Leask A, Abraham DJ. Endothelin-1 promotes myofibroblast induction through the ETA receptor via a rac/phosphoinositide 3-kinase/Akt-dependent pathway and is essential for the enhanced contractile phenotype of fibrotic fibroblasts. *Mol Biol Cell* 2004;15:2707-19
31. Hernández-Rodríguez J, Murgia G, Villar I, Campo E, Mackie SL, Chakrabarty A, Hensor EM, Morgan AW, Font C, Prieto-González S, Espígol-Frigolé G, Grau JM, Cid MC. Description and validation of histological patterns and proposal of a dynamic model of inflammatory infiltration in giant-cell arteritis. *Medicine (Baltimore)* 2016 Feb;95(8):e2368.
32. Planas-Rigol E, Corbera-Bellalta M, Espígol-Frigolé G, Terrades-García N, Alba MA, Prieto-González S, Hernández-Rodríguez J, Lozano E and Cid MC. Giant-cell arteritis: immunopathogenic mechanisms involved in vascular inflammation and remodeling. *J Vasc* 2016; 2: 1-7.
33. Sulzmaier FJ, Jean C, Schlaepfer DD. FAK in cancer: mechanistic findings and clinical applications. *Nat Rev Cancer* 2014;14:598-610
34. Heerkens EH, Quinn L, Withers SB, Heagerty AM. β Integrins mediate FAK Y397 autophosphorylation of resistance arteries during eutrophic inward remodeling in hypertension. *J Vasc Res* 2014;51:305-14
35. Rodríguez-Pascual F, Busnadiego O, Lagares D, Lamas S. Role of endothelin in the cardiovascular system. *Pharmacol Res* 2011;63:463-72.

36. Davenport AP, Hyndman KA, Dhaun N, Southan C, Kohan DE, Pollock JS, Pollock DM, Webb DJ, Maguire JJ. Endothelin. *Pharmacol Rev* 2016;68:357-418.

FIGURE LEGENDS

Figure1. Changes in histological distribution of the ET-1 system in GCA lesions. L: Lumen, M: Media, I: Intima, Adv: Adventitia. One representative experiment out of two TA is represented. (A) Staining of αSMA (green), ET-1 (red) and nuclei (blue) in control TA. (a.1) Magnification of ET-1 and αSMA positive cells localized in the media layer are highlighted with arrows. (B) Immunofluorescence of GCA TA stained with ET-1 (red), αSMA (green) and nuclei (blue) at low magnification. Magnification of Figure 1B showing ET-1 staining in the endothelium (arrow) (b.1), co-expressing ET-1 and αSMA cells (b.2 and b.3) or ET-1 positive cells surrounding αSMA positive cells (b.3) are represented. (C) Control TA in which ET_AR (red) is detected by VSMC and endothelium (arrow) while ET_BR (green) is slightly detected. Nuclei are stained in blue. (D) Negative control of the staining. (E) ET_AR and ET_BR positive cells localized in the intima and endothelium (arrow) of GCA TA. (F, f.1) GCA lesions and corresponding magnification of cells localized in the media-intimal junctions highly expressing ET_AR and ET_BR. (G) ET-1 secretion by HUVEC, VSMC and isolated CD4+T or CD14+ cells detected by immunoassay. Sensitivity of the assay is 0,207pg/mL. (H) ET-1 mRNA expression and immunoassay of supernatants of isolated CD4+T, CD14+ or co-cultured with VSMC at 24 hours.

Bar represent the number of cells (mean and SEM)

Figure2. ET-1 induces cytoskeleton reorganization in VSMC promoting migration through ET_AR and ET_BR receptor. (A) Immunofluorescence of VSMC cytoskeleton stained with Phalloidin (red) and nuclei using Hoechst (blue). ET-1 (10^{-9} mol/L) was added at the same time of seeding. VSMC were pre-incubated 30 minutes with BQ123 and BQ788 (20µmol/L) before ET-1 was added. Three hours after cells were seeded several pictures of each situation were taken and a representative picture of each situation is shown in (A) as labeled. Pre-coating with fibronectin (5µg/cm^2) or polylysine (10µg/mL) were used as a positive and negative control. (B) Representative pictures of wound healing assay of VSMC. Untreated, ET-1 (10^{-9} mol/L), BQ123 (20 µmol/L), BQ788 (20 µmol/L) or combination of both peptides with the following addition of

ET-1 as labeled are represented. (C) One scratch per well was done and 3 pictures per well were analyzed. Percentage of wound closure *vs.* time of each condition is represented. Three independent experiments were performed. (D) Migration assay using Boyden Chamber. Untreated VSMC, ET-1 added in the lower compartment or ET-1 added in the upper compartment. (E) Untreated, ET-1 (10^{-9} mol/L) and BQ123, BQ788 or combination of both peptides (20µmol/L) before adding ET-1. (*) $p<0.05$ for untreated cells *vs.* ET-1 treated cells. Bars represent number of cells (mean and SEM). (#) $p<0.05$ comparing ET-1 treated cells vs. peptide pre-incubated cells.

Figure3. ET-1 recruits FAK to the VSMC leading edge. ET-1/Y397FAK axis is essential for the ET-1 induction VSMC migration. (A) Immunoblot and corresponding quantifications of VSMC treated with ET-1 (10^{-9}mol/L) for 90 minutes as labeled. Three independent experiments are represented and quantified. (B) Immunofluorescence of total FAK (green) or Y397 FAK (green), Hoechst (blue) and cytoskeleton stained with Phalloidin or αSMA (red) of VSMC cultured in the presence or absence of ET-1 (10^{-9} mol/L) as labeled. Total FAK distribution in the cell protrusion of ET-1-treated VSMC is represented with arrow. Co-localization of αSMA and phospho Y397FAK in the pseudopodia is also highlighted with arrows. (C) Boyden chamber assay quantification of VSMC pre-incubated for 45 minutes with increasing dose of FAK inhibitor (PF-573228) with or without the subsequent addition of ET-1 (10^{-9}mol/L) as labeled. (D) Boyden Chamber Assay using VSMC three days post-transfected with control pcDNA3 (MOCK), wild type FAK (FAK) and the phosphorylation mutated forms Y397F and Y925F. Either C or B are representations of quadruplicates. Bar represent the number of cells (mean and SEM) and (*) $p<0.05$ for untreated cells *vs.* ET-1 treated cells (C) or FAK transfected cells (D). (#) $p<0.05$ comparing ET-1 treated cells *vs.* inhibitor pre-incubated cells (C) or phosphorylation mutated FAK forms transfected VSMC (D).

Figure4. ERK, Src, and PI3K are essential for ET-1/ Y397FAK axis induced VSMC migration. (A) Immunoblot of VSMC treated with ET-1 (10^{-9}mol/L) for 90 minutes. Three independent experiments are represented and quantified as labeled. Phosphorylation of ERK and Src (Y416) is represented *vs*. total corresponding protein. (B) Boyden Chamber Assay with VSMC pre-incubated for 45 minutes with Src inhibitor PP2 (10µmol/L) and ERK inhibitor PD98059 (20µmol/L) or PI3K inhibitor LY294002 (50µmol/L), with or without the subsequent

addition of ET-1. Quadruplicates are represented. Bar represent the number of cells (mean and SEM). (*) $p<0.05$ between untreated cells *vs.* ET-1 incubated cells, (#) $p<0.05$ between ET-1 treated cells *vs.* pre-incubated VSMC with the inhibitors and subsequent addition of ET-1. (C) Immunofluorescence of VSMC cytoskeleton (red) and nuclei (blue). ET-1 (10^{-9} mol/L) was added at the same time of seeding. VSMC were pre-incubated 30 minutes with FAK inhibitor (PF-573228) and PI3K inhibitor (LY284002) before ET-1 was added. Three hours after cells were seeded several pictures of each situation were taken and a representative picture of each situation is shown as labeled. (D) Cytoskeleton (blue), p85 (green), total FAK (red) and nuclei (white) immunofluorescence staining of VSMC treated with ET-1, or ET-1 plus 30 minutes pre-incubation with ET_AR antagonist (BQ123), ET_BR antagonist (BQ788), PI3K inhibitor (LY294002) and FAK inhibitor (PF-573228) as labeled. Cells were seeded at the same time as ET-1 was added and fixed after 3 hours. Arrows highlight p85 and FAK co-localization in the cell protrusion of the ET-1 treated VSMC or p85/FAK clusters of immature focal adhesion formations in ET-1 plus LY284002 condition. Each picture is a representation of several cells.

Figure5. Binding of ET-1 to ET_AR or ET_BR promotes secretion of MMP2 and TIMP2 by VSMC. (A) Gelatin zymography of serum free supernatants of VSMC treated with or without ET-1 at indicated concentrations and times. (B) Gelatin zymography of MMP2 using ET-1 (10^{-9} mol/L) and its receptor antagonists BQ123 and BQ788 (20 µmol/L) at 24 hours. (C) MMP14 immunoblot and βActin of VSMC lysates treated with ET-1 at the indicated doses. (D) TIMP2 immunoassay of VSMC supernatants as used in (A).

Figure6. ET-1 blockade through ET_AR and ET_BR inhibitors efficiently abrogates VSMC outgrowth from *ex vivo* temporal arteries. (A) Representation of the outgrowth of VSMC from three GCA TA biopsies cultured on Matrigel™ at day 5 and 12 as labeled. (B) Outgrowth quantification score of each situation was tested at the indicated days and conditions: untreated, BQ123 (20µmol/L) or BQ788 (20µmol/L). (C) Immunofluoresce of Y397 FAK (green), total FAK (red) and nuclei (blue) of GCA TA previously cultured on Matrigel™ for 5 days even untreated or treated with ET_AR or ET_BR antagonists (BQ123 and BQ788 respectively) at 20µmol/L. Arrows show co-expression of phospho FAK (Y397) and total FAK in the media-intimal junction or adventitia-media junction of the untreated GCA tissue. (L): Lumen, (I) Intima layer, (M) Media layer, (Adv): Adventitia.

Figure7. ET-1 induces αSMA and migration of VSMC from the media layer of temporal Arteries. (L): Lumen, (I) Intimal layer, (M) Media layer. Representation of three different control TAs cultured on Matrigel^{TM} for 5 days with fresh medium (A) or medium supplemented with ET-1 (10^{-9} mol/L) (B) and processed for immunofluorescence staining with αSMA (green) and nuclei (blue). Whereas untreated sections maintained the normal arterial structure, the addition of ET-1 upregulated αSMA expression and artery layer disorganization. Of note, some VSMC were found migrating from the media to the intimal layer (arrows in B).

SUPLEMENTARY DATA (Figure legends)

Figure1. FAK inhibition using PF-573228 and transicient transfection of FAK phosphorylated mutated sites. PF-573228 was used at different concentrations in VSMC. Cell lysates were collected at 90 minutes. (A) Immunoblot of phosphorylated forms of FAK (Y397 and Y925) *vs.* total FAK. (B) Y397/total FAK or Y925/ total FAK quantification. (D) GFP detection (green) of non- transfected VSMC *vs.* GFP pcDNA3 transfected cells. 30% of transfection was obtained. (E) Immunoblot of total FAK of transfected VSMC with the corresponding vectors compared with control (MOCK) and its corresponding quantifications in (F).

Figure2. Immunofluorescence of p85 PI3K and total FAK by VSMC. VSMC were seeded and stained by p85 (green), total FAK (red), cytoskeleton (blue) and nuclei (white). LY294002 was used at 50µmol/L. Several pictures were done in order to evaluate PI3K p85 and FAK recruitment to the cell protrusions.

Figure3. mRNA expression of MMP2, MMP14, TIMP2, MMP9 and TIMP1. (A) mRNA expression of MMP2, MMP14, TIMP2, MMP9 and TIMP1 in VSMC treated with different dose of ET-1 at 6 and 24 hours. (B) MMP2, MMP14, TIMP2, MMP9 and TIMP1 mRNA expression of VSMC with the ET-1 receptor antagonists (BQ123 and BQ788). Bars represent triplicates (mean and SEM). Note that Y axis is different.

Figure4. Proliferation assay of VSMC. VSMC were cultured at 4000 c/well of a 96 well plate, serum starved for 24 hours and medium was replaced with fresh one (at 1% FBS) or the same with ET-1 at 10^{-9}M. Each plate was fixed and stained with violet crystal each day from day 1 to 7 days. Absorbance at 620nm was read and represented.

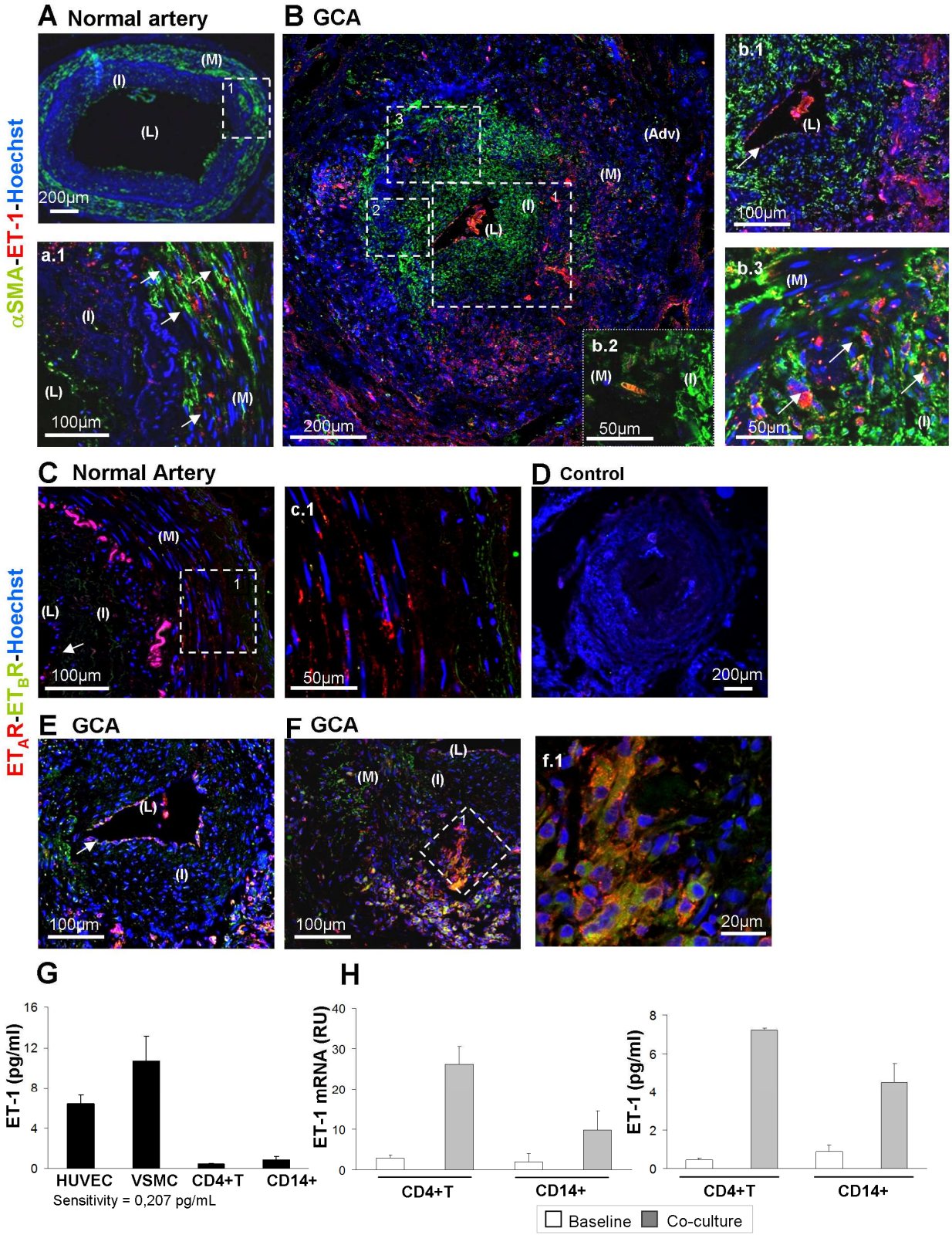
A Normal artery
B GCA
αSMA-ET-1-Hoechst
(M)
(I)
(L)
1
200µm
a.1
100µm
2
3
(Adv)
b.1
b.2
b.3
50µm
C Normal Artery
D Control
c.1
ETAR-ETBR-Hoechst
E GCA
F GCA
f.1
20µm
G
ET-1 (pg/ml)
HUVEC
VSMC
CD4+T
CD14+
Sensitivity = 0,207 pg/mL
H
ET-1 mRNA (RU)
Baseline
Co-culture

Figure 1

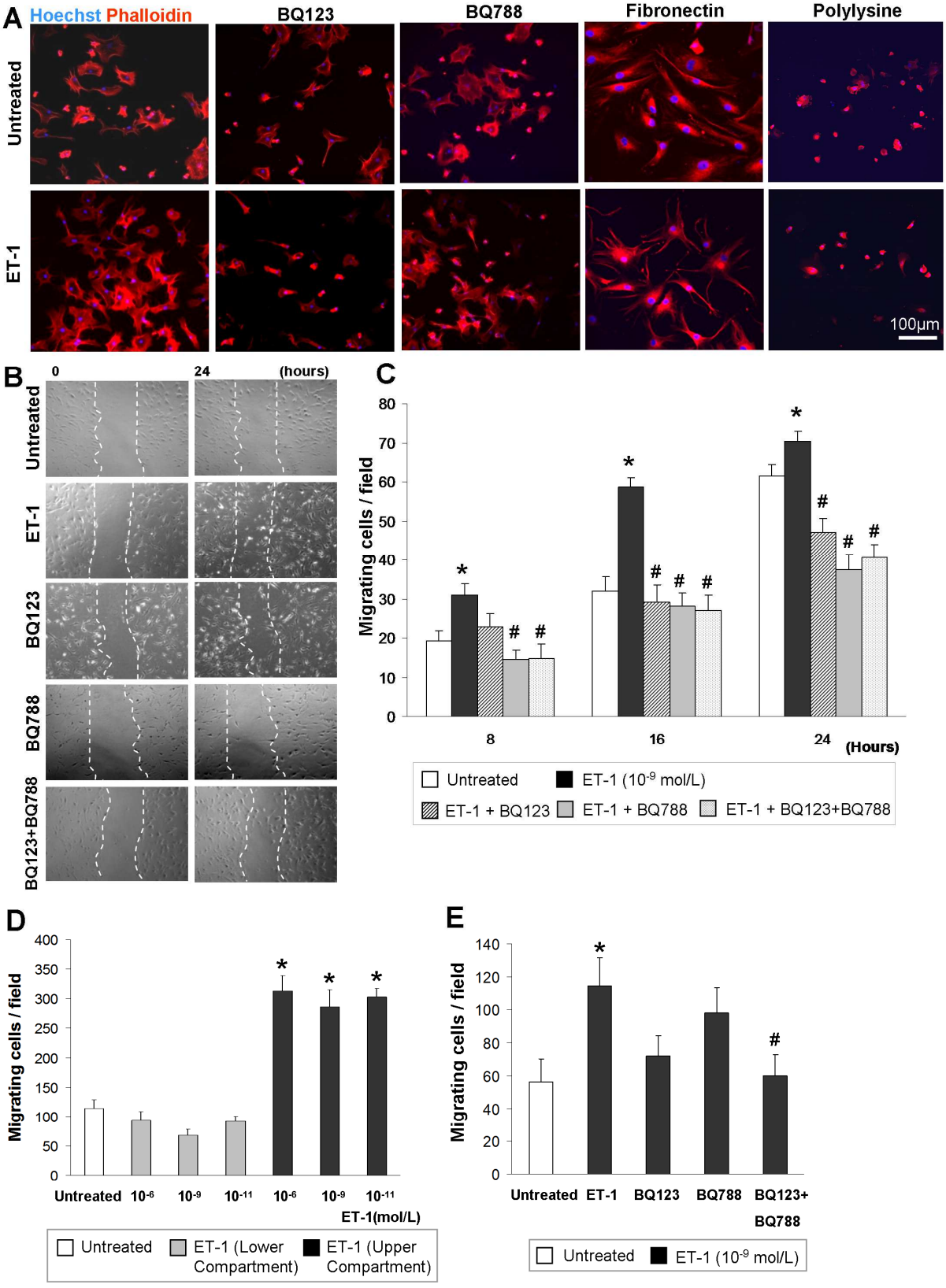
A
Hoechst Phalloidin
BQ123
BQ788
Fibronectin
Polylysine
Untreated
ET-1
100µm
B
0
24
(hours)
Untreated
ET-1
BQ123
BQ788
BQ123+BQ788
C
Migrating cells / field
8
16
24
(Hours)
Untreated
ET-1 (10-9 mol/L)
ET-1 + BQ123
ET-1 + BQ788
ET-1 + BQ123+BQ788
D
Migrating cells / field
Untreated
10-6
10-9
10-11
ET-1(mol/L)
Untreated
ET-1 (Lower Compartment)
ET-1 (Upper Compartment)
E
Migrating cells / field
Untreated
ET-1
BQ123
BQ788
BQ123+ BQ788
Untreated
ET-1 (10-9 mol/L)

Figure 2

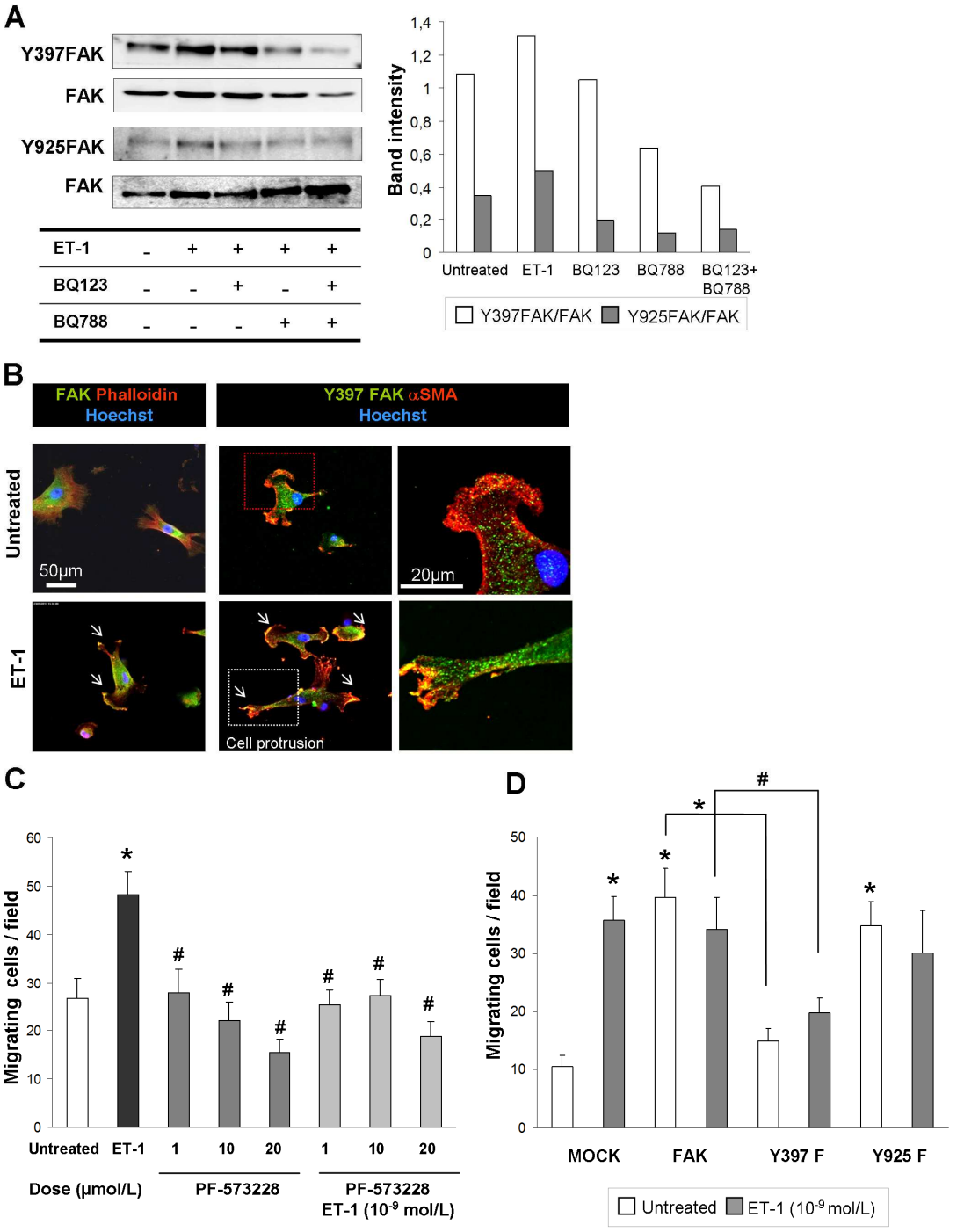
A
Y397FAK
FAK
Y925FAK
FAK
ET-1 - + + + +
BQ123 - - + - +
BQ788 - - - + +
Band intensity
1,4
1,2
1
0,8
0,6
0,4
0,2
0
Untreated
ET-1
BQ123
BQ788
BQ123+ BQ788
Y397FAK/FAK
Y925FAK/FAK
B
FAK Phalloidin Hoechst
Y397 FAK αSMA Hoechst
Untreated
ET-1
50µm
20µm
Cell protrusion
C
Migrating cells / field
Untreated
ET-1
1
10
20
1
10
20
Dose (µmol/L)
PF-573228
PF-573228 ET-1 (10-9 mol/L)
D
Migrating cells / field
MOCK
FAK
Y397 F
Y925 F
Untreated
ET-1 (10-9 mol/L)

Figure 3

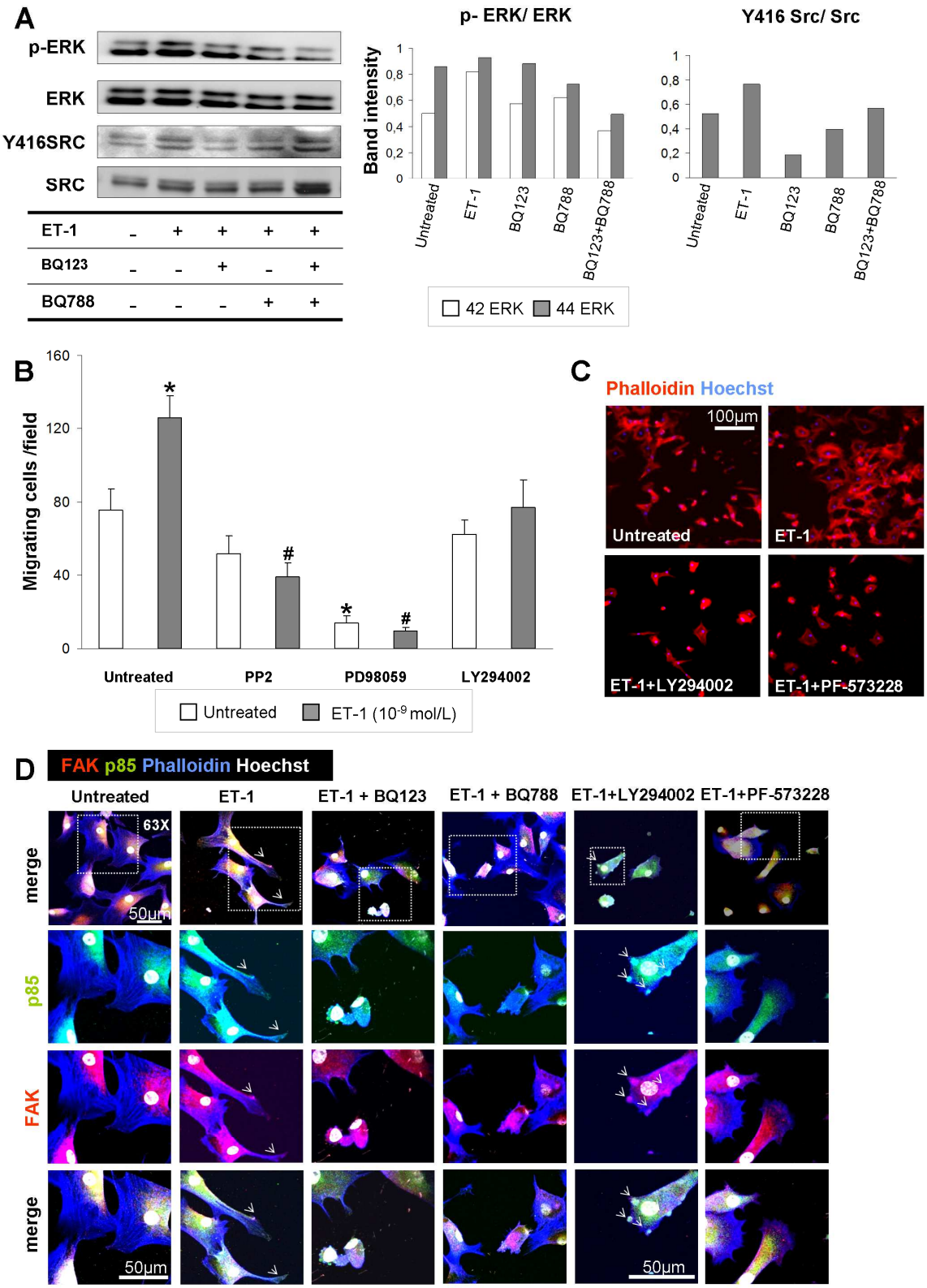
A
p-ERK
ERK
Y416SRC
SRC
ET-1 - + + + +
BQ123 - - + - +
BQ788 - - - + +
p- ERK/ ERK
Band intensity
Untreated
ET-1
BQ123
BQ788
BQ123+BQ788
42 ERK
44 ERK
Y416 Src/ Src
B
Migrating cells /field
Untreated
PP2
PD98059
LY294002
Untreated
ET-1 (10-9 mol/L)
C
Phalloidin Hoechst
100µm
Untreated
ET-1
ET-1+LY294002
ET-1+PF-573228
D
FAK p85 Phalloidin Hoechst
Untreated
ET-1
ET-1 + BQ123
ET-1 + BQ788
ET-1+LY294002
ET-1+PF-573228
merge
p85
FAK
merge
63X
50µm

Figure 4

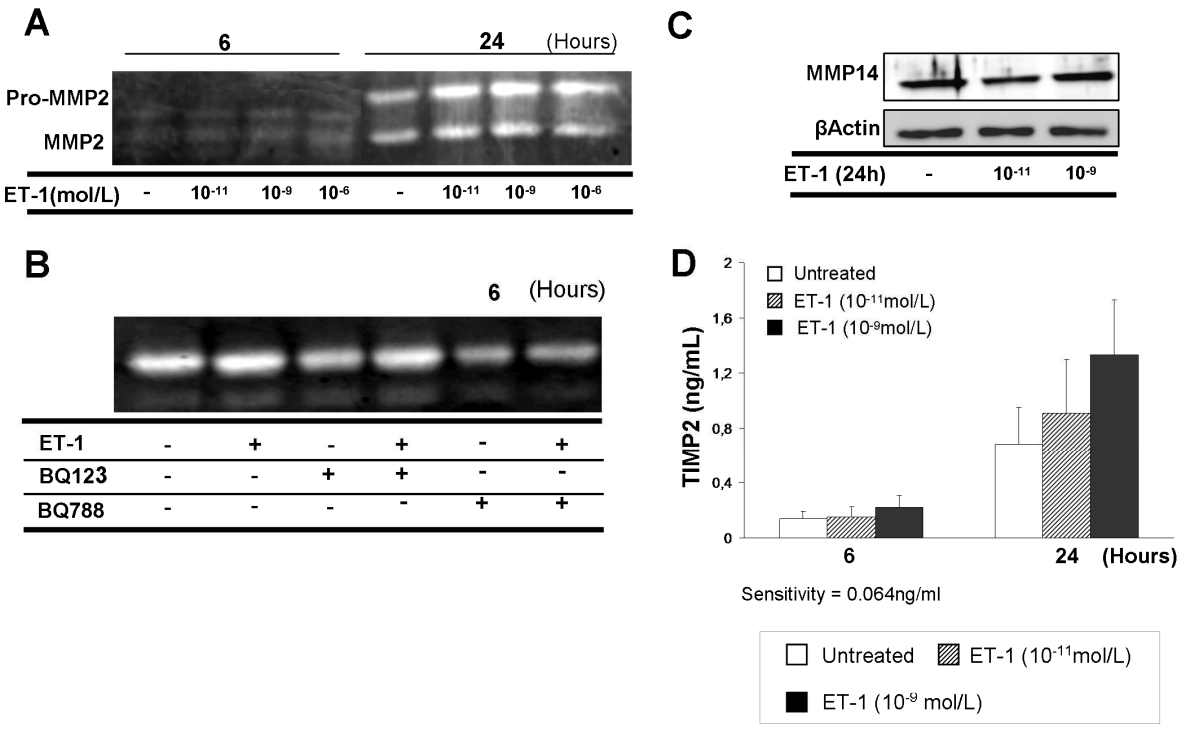
A
6
24
(Hours)
Pro-MMP2
MMP2
ET-1(mol/L) - 10-11 10-9 10-6 - 10-11 10-9 10-6
B
6
(Hours)
ET-1 - + - + - +
BQ123 - - + + - -
BQ788 - - - - + +
C
MMP14
βActin
ET-1 (24h) - 10-11 10-9
D
Untreated
ET-1 (10-11mol/L)
ET-1 (10-9mol/L)
TIMP2 (ng/mL)
2
1,6
1,2
0,8
0,4
0
6
24
(Hours)
Sensitivity = 0.064ng/ml
Untreated
ET-1 (10-11mol/L)
ET-1 (10-9 mol/L)

Figure 5

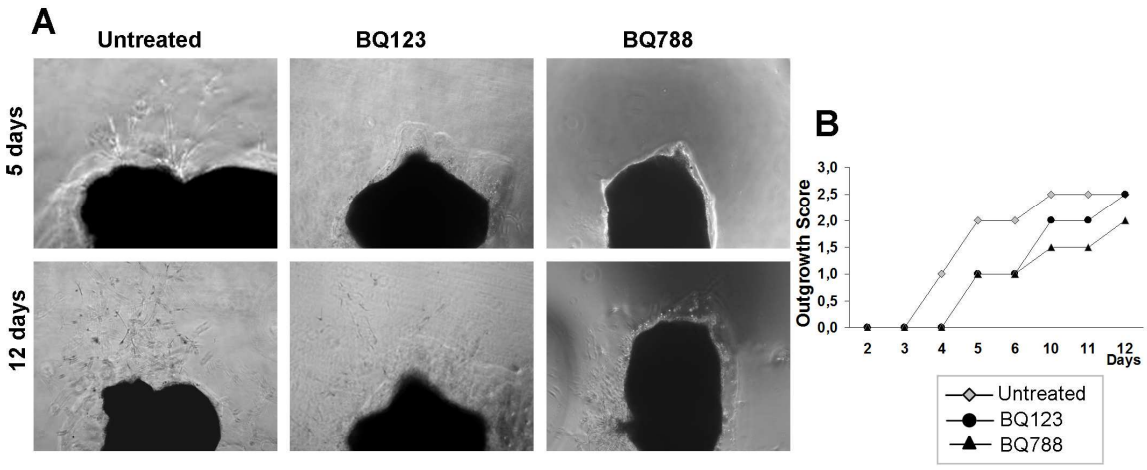
A
Untreated
BQ123
BQ788
5 days
12 days
B
Outgrowth Score
3,0
2,5
2,0
1,5
1,0
0,5
0,0
2
3
4
5
6
10
11
12
Days
Untreated
BQ123
BQ788

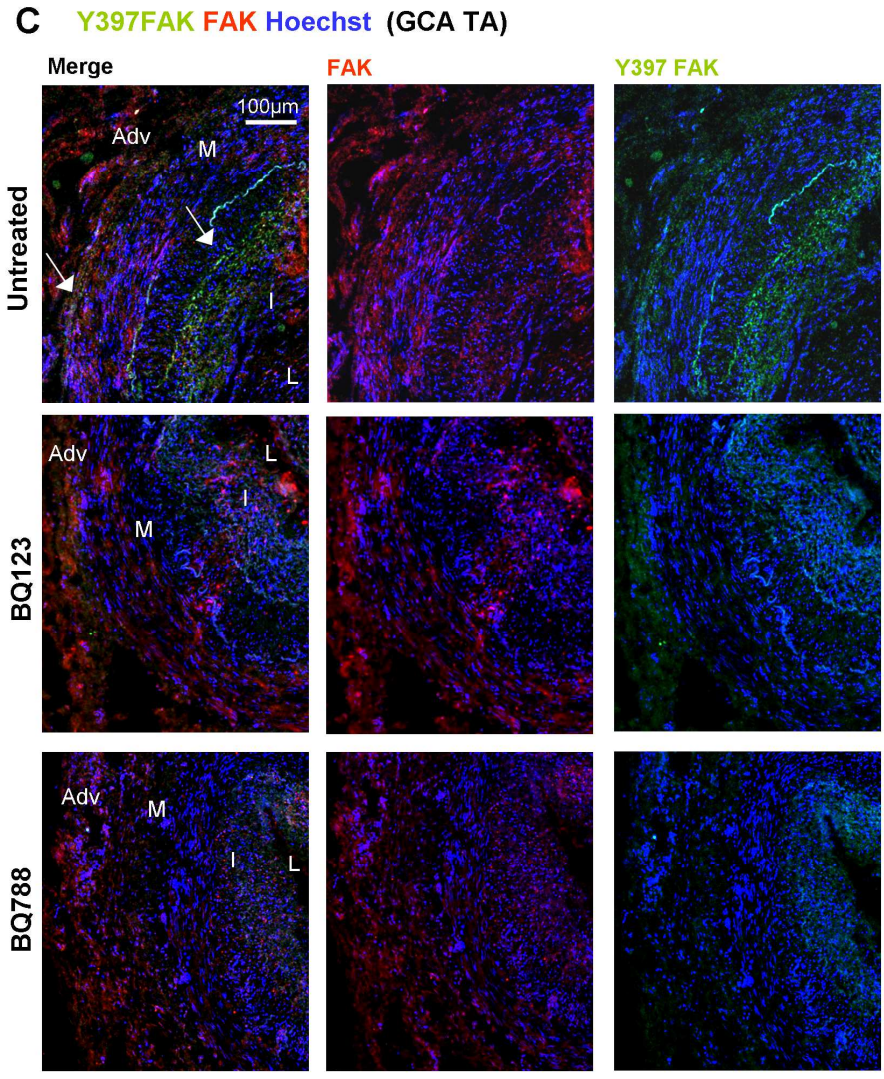
C Y397FAK FAK Hoechst (GCA TA)
Merge
FAK
Y397 FAK
100µm
Adv
M
I
L
Untreated
BQ123
BQ788

Figure 6

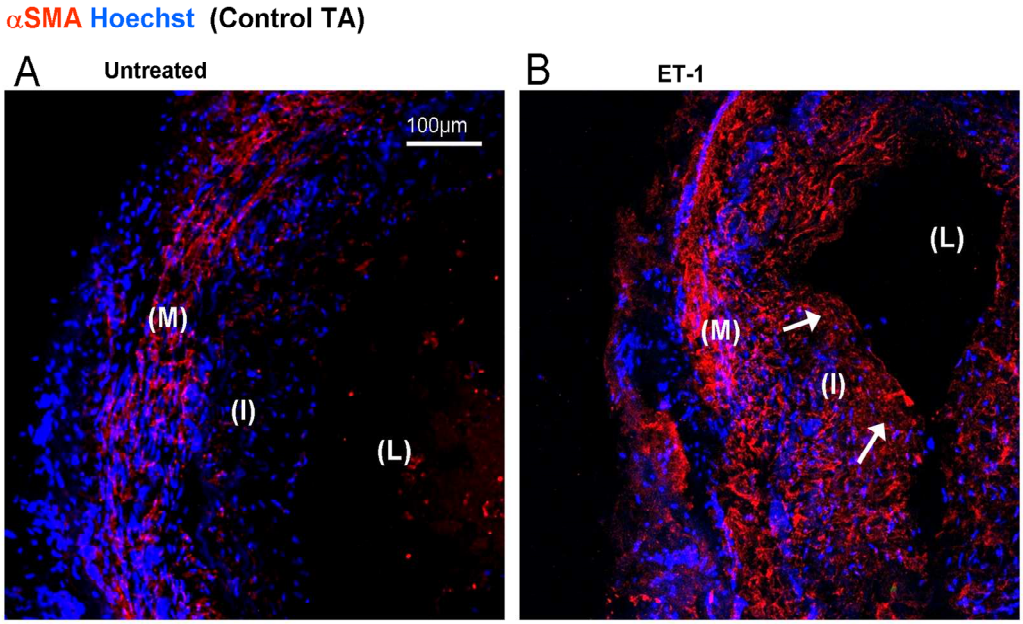

Figure 7

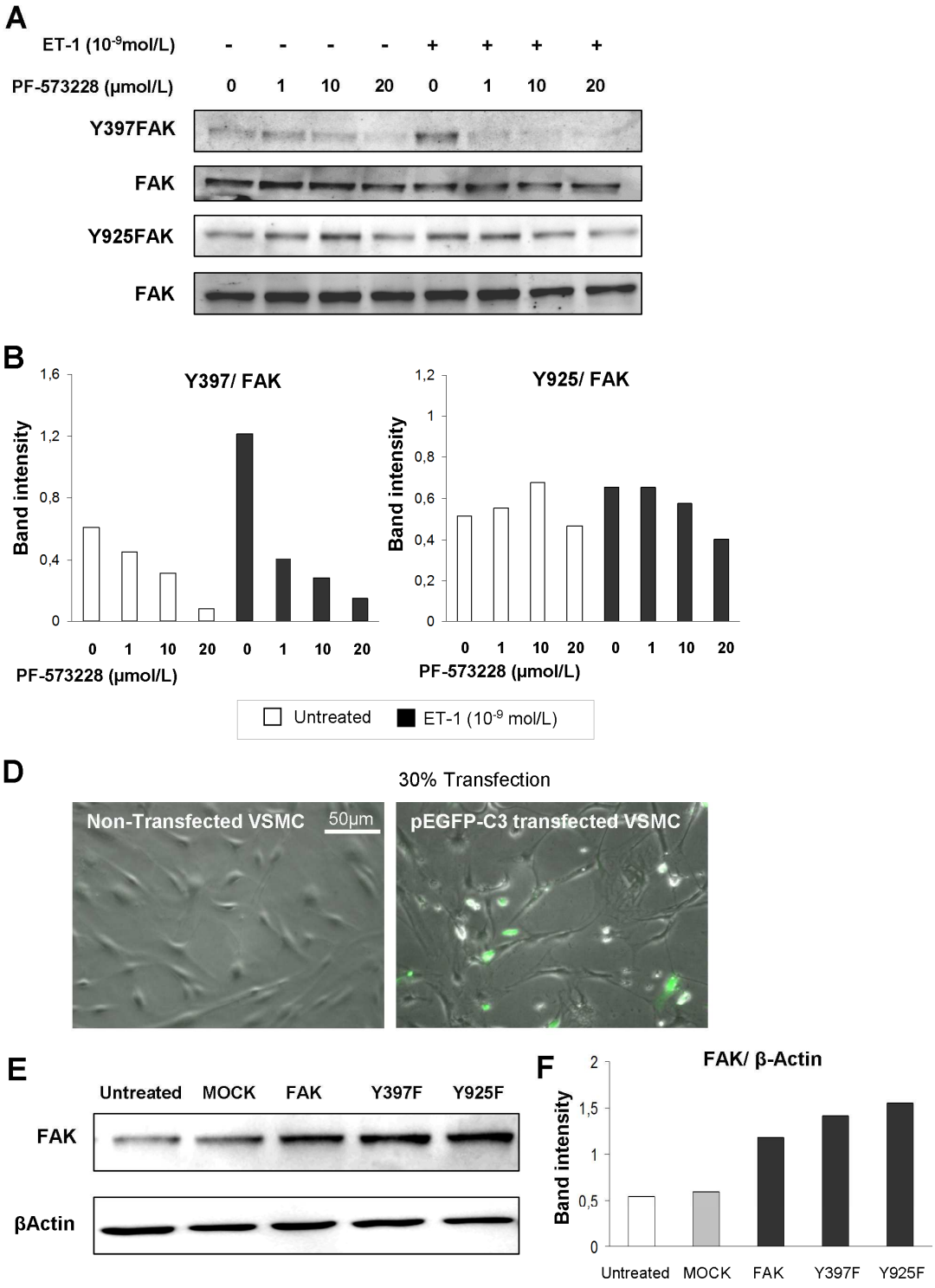

Supplementary Figure 1

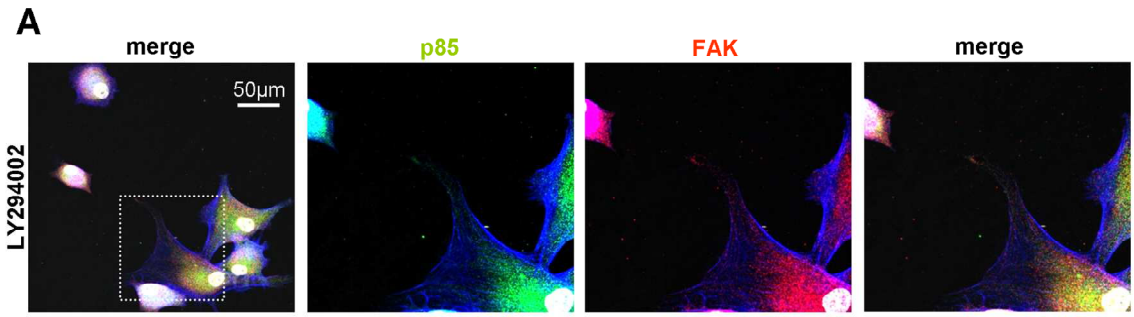

Supplementary Figure 2

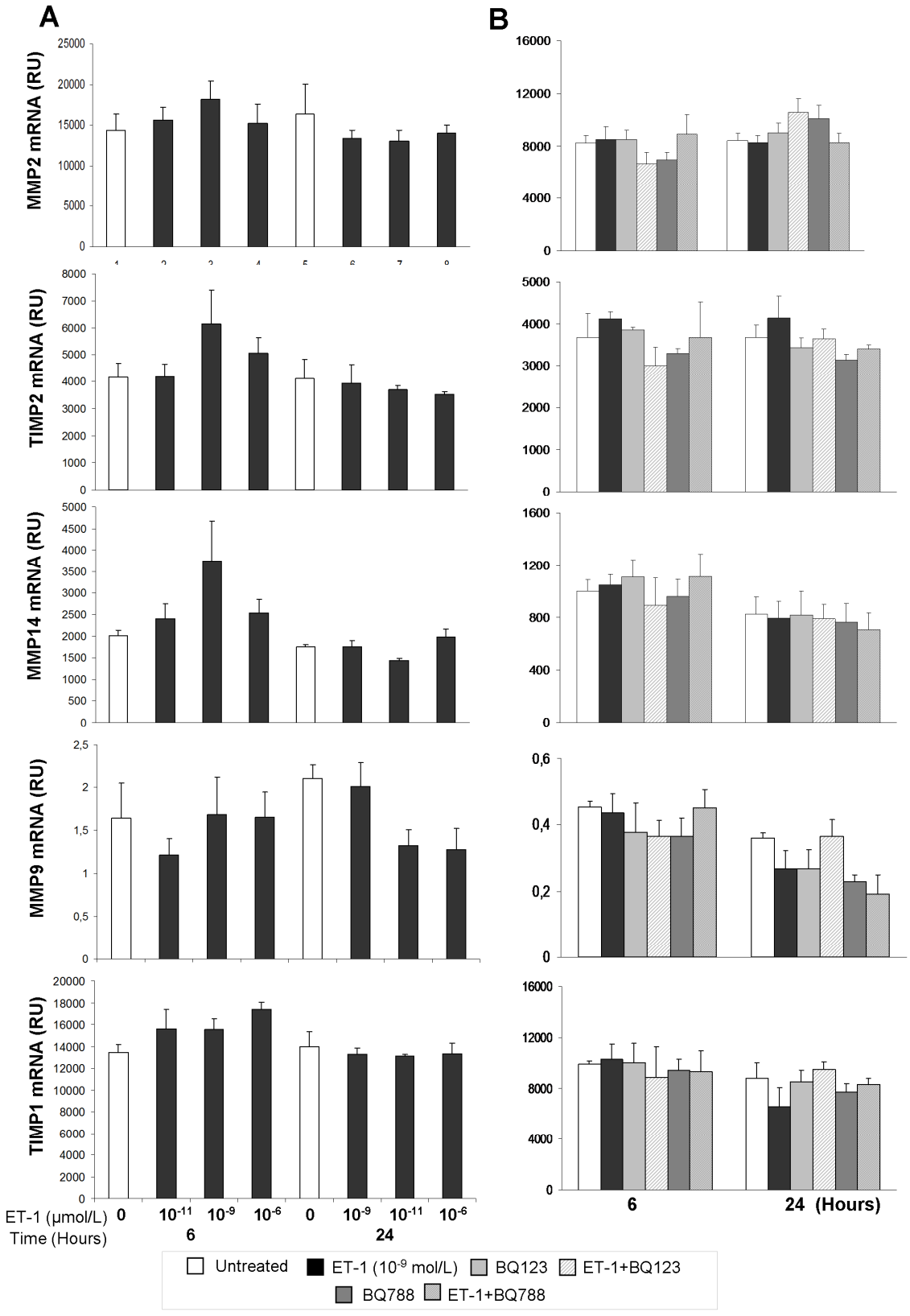

Supplementary Figure 3

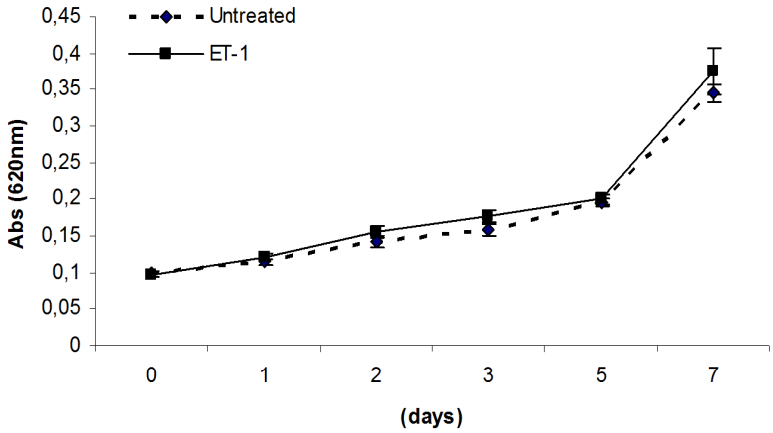

Supplementary Figure 4

Endothelin 1 induces a myofibroblastic phenotype in vascular smooth muscle cells. A mechanism potentially contributing to vascular remodeling and intimal hyperplasia in Giant Cell Arteritis

Ester Planas-Rigol, Nekane Terrades-Garcia, Marc Corbera-Bellalta, Ester Lozano, Marco A. Alba, Georgina Espígol, Sergio Prieto, Marta Segarra, Jose Hernández, Sara Preciado, Rodolfo Lavilla, Maria C. Cid.

Results summary (part 3)

1) ET-1 is expressed by the luminal endothelium and VSMC from the media layer in control temporal arteries.
2) ET-1 is mostly expressed by VSMC and inflammatory cells from the media and intima layer in GCA-involved temporal arteries.
3) ET_AR is expressed by VSMC in the media layer of control TABs whereas ET_BR is hardly detected. Interestingly, in GCA lesions, ET_BR is highly expressed by VSMC migrating from the media to the intimal layer.
4) ET-1 induces cytoskeleton reorganitzation in VSMC either cultured on plastic or on a matrix of fibronectin. Both endothelin receptor inhibitors (BQ123 and BQ788) abrogate this induced ET-1 phenoype by VSMC.
5) Activated (Y397) FAK is recruited to the VSMC leading edge after ET-1 stimulation. This ET-1 FAK recruitment is also abrogated by both ET-1 receptor antagonists.
6) ET-1 promotes FAK Y397 and Y925 phosphorylation and both phosphorylations are abrogated by BQ123 or BQ788. Moreover, FAK point mutations demonstrate that Y397 is essential for ET-1 induction of VSMC migration. FAK inhibitor (PF-573228) confirms that ET-1 induction of VSMC migration is triggered through FAK kinase activation.
7) FAK downstream pathways related to cell migration (Src, ERK and PI3K) are also activated by ET-1. Functional abrogation of these molecules using their corresponding inhibitors demonstrates that these pathways are essential for ET-1-induced migration of VSMC.

8) PI3K subunit p85 is also recruited to the VSMC leading edge after ET-1 stimulation. Moreover, when PI3K inhibitor is used in the presence of ET-1 immature focal adhesions are generated.
9) Secretion of MMP2 is induced by ET-1 treatment and abrogated by both ET-1 receptor inhibitors.
10) Both ET_AR and ET_BR inhibitors efficiently abrogate VSMC outgrowth from *ex vivo* cultured GCA –involved arteries.
11) ET-1 induces αSMA and VSMC migration from the media layer to the intimal layer in control TABs cultured on Matrigel ^{TM}

Discussion

Persistence of the inflammation and the ensuing vascular remodeling is an unresolved problem in chronic inflammation diseases of blood vessels such as GCA. For this reason, the study of these two issues has become a key point of interest for several researchers.

As already explained, the main aim of this doctoral thesis was to contribute knowledge to both issues especially in the setting of a chronic inflammation vasculopathy with frequent ischemic complications such as GCA. In this context the contributions of the studies included in this doctoral thesis are discussed below.

The IL-12 superfamily of cytokines is highly related to Th1 and Th17 CD4+T cell differentiation. IL-12 superfamily encompasses four different cytokines composed by shared subunits: IL-12 (p40 and p35), IL-23 (p19 and p40), IL-35 (p35 and Ebi3) and IL-27 (p28 and Ebi3) (*140*). Among them, IL-12 and IL-23 are the best characterized. IL-12 is mainly associated with Th1 differentiation and IFNγ production whereas IL-23 is involved in maintaining Th17 differentiation and production of IL-17 (*164*).

Both Th1 and Th17 cytokines are involved in autoimmune disease independently one of the other but it is also thought that both effector Tcell subsets may collaborate during the inflammatory response. For this reason both Th1 and Th17 related cytokines would be interesting therapeutic targets for patients suffering from autoimmune diseases and have been fully investigated.

Nevertheless, *in vivo* approximations have evidenced some dichotomy between IL-12 superfamily cytokine subunits. This is the case for IL-12 subunits (p40 and p35). Several studies comparing $p40^{-/-}$ and $p35^{-/-}$ in different animal models (i.e. experimental autoimmune endephalomyelitis (EAE) mice which is an animal model for multiple sclerosis (*166*) or in collagen induced arthritis (CIA) mice as a model for RA (*165*)) dislosed that p40 but not p35 was essential to develop the disease.

Another important approach which is consistent with this IL-12 subunit dichotomy is the study by Visvanathan *et al.* (2001) (*52*). In this study a gene approximation analysis in paired TA biopsies pre and post 1-year of glucocorticoid (GC) treatment revealed that, in relapsing GCA patients p40 but not p35 was overexpressed suggesting a different role for p40 with respect to p35 in

sustaining GCA disease activity. Another important point was the fact that immunohistochemistry demonstrated that p35 and p40 were differentially expressed in GCA specimens. While p35 was expressed by both VSMC and leukocytes in GCA lesions and only VSMC expression remained after GC treatment, p40 was mostly expressed by leukocytes but not by VSMC (*52*).

Dissociation between both IL-12 subunits indicate that p40 and p35 may have independent functions either working as independent units or combined with other partners in order to form cytokines.

Regarding to the possibility of p40 or p35 association with other partners in order to form cytokines different from IL-12, it was demonstrated that p40 can also bind to p19 peptide in order to form the cytokine IL-23 (*152*) but in contrast, p35 when is linked to Ebi3 subunit conform the cytokine IL-35 (*174*). Many questions remain unanswered regarding to IL-23 and IL-35 cytokine expression and function.

The possibility that IL-23, IL-12 and IL-35 subunits may also function independently is also an interesting point. Currently, it is only fully accepted that p40 is secreted as an homodimer and can act as an agonist of IL-12 by blocking IL-12Rβ1 and acting as a chemoattractant for macrophages (*144*). In contrast, no information about p35, p19 or Ebi3 potential independent functions is available.

According to these previous observations in **the Results section (part 1 and part 2)** of this doctoral thesis we report novel independent functions for the IL-23p19 subunit and unravel previously unknown roles for the cytokine IL-35 in vascular inflammation in GCA.

The first hypothesis generated in this doctoral thesis considers from the possibility that IL-23 subunit p19 may also have a role itself different than the attributable functions of the cytokine IL-23 in activated endothelium.

Hypothesis 1

The subunits p19 and p40 (components of IL-23 cytokine) are differentially expressed in endothelial cells (EC). While p19 can be induced by proinflammatory stimuli, p40 is not detected in EC. P19 peptide may have proinflammatory functions independent from p40 in inflamed EC. P19 may contribute to the persistence of inflammation by promoting EC phenotypical changes (i.e. overexpression of adhesion molecules or chemokines). This process may contribute to leukocyte recruitment through *vasa vasorum* in GCA

Two relevant previous studies have been essential to generate this hypothesis.

On one hand, the study published by Wiekowski *et al*. (2001) (*171*) described the phenotype of a p19 transgenic mouse who developed systemic inflammation with increased proinflammatory cytokines (TNFα and IL-1β) or the presence of leukocyte infiltrate in different tissues. Considering that p19 transgenic mice express same amounts of p40 comparing with control animals this observation suggested for the first time that p19 may have a function different than p40 association to form IL-23.

On the other hand, the study of Oppman *et al.*, (2000) (*152*) also demonstrated that p19 is induced under proinflammatory conditions in mice endothelial cells (EC) whereas neither p35 nor p40 are expressed by these cells either after stimulation. This was a critical point suggesting again, that p19 alone may have a role independent from its dimerization with p40.

Our study is consistent with the previous ones, demonstrating again that p19 is also induced by proinflammatory stimuli in human EC from various sources independently from p40. The most important finding in this issue is that, for the first time, we found that p19 had an unrecognized role as an endogenous activator of endothelial inflammation promoting leukocyte adhesion to endothelium and transendothelial migration.

All these functions have great interest in inflammation disease since activated EC are essential for leukocyte recruitment to the inflamed tissues. Endothelium activation and leukocyte recruitment requires complex and essential steps in which a wide range of molecules are involved (*90*). With regards to GCA, some studies have postulated that leukocyte recruitment

might be prone by EC from the pathological microvessels mostly compressed in the adventitial layer of the arteries (*48*). In this scenario, under proinflammatory vascular stimuli p19 but not p40 might be induced by EC from the microvessels assisting leukocyte recruitment.

According to our results (ELISA assay and immunobloting of cell supernatant precipitates) p19 is not secreted (or very little) by activated EC. These results are consistent with those obtained by Oppman *et al*. (2000) (*152*) who concluded that p19 required p40 subunit in order to be secreted. Other cytokines, such as IL-1α have been demonstrated to have intracellular functions: IL-1α binds to receptors localized either in the cell surface or in the cytoplasm with subsequent translocation to the nucleus acting as a transcription factor (*312*).

According to this point, the subunit p19 subunit is considered an α subunit, with homology with p35 and p28 of the IL-12 superfamily of cytokines, whereas p40 is considered a β subunit together with Ebi3. Both Ebi3 and p40 are essential for p35 or p19 secretion to form mature IL-35/IL-12 or IL-23 respectively suggesting that p19 could also interact with Ebi3 in order to form a new cytokine. This is something that should definitely be further investigated.

Furthermore, p19 mRNA is expressed at higher levels than p40 in inflammatory macrophages (*152*) suggesting that p19 may play, in these cells, a function idependent secreted mature IL-23 as it happens in EC.

In order to study intracellular p19 function, EC stably expressing p19 were developed. Although these cells express higher amounts of p19 than activated EC under physiologic conditions, this was a suitable tool to better understand p19 functions in cultured EC.

Using this system we could demonstrate that endogenous p19 subunit induces both adhesion molecules ICAM-1 and VCAM-1 as well as promotes leukocyte adhesion and transmigration *in vitro*. Consistent with these *in vitro* assays, in GCA tissue p19 was highly expressed and p40 undetected in the EC from the *vasa vasorum*, suggesting that p19 expressed by the *vasa vasorum* may promote recruitment of LFA-1 and VLA-4 expressing leukocytes through up-regulation of ICAM-1 and VCAM-1 respectively (*48*). This is an important finding that has been observed in GCA lesions but it may also exist in other chronic inflamed diseases.

The mechanism through which endogenous p19 signals to induce this described active phenotype in EC was also unknown. IL-23 signal is triggered by IL-23 receptor (IL-23R) which is a heterodimer composed by IL-12Rβ1 and IL-23R (*151*). While IL-23R directly binds to p19 and is expressed by activated memory Tcells, natural killer (NK), monocyte, macrophages and dendritic cells (DC); IL-12Rβ1 binds to p40 and is expressed by Tcells, NK and DC. Interestingly for this study, IL-12Rβ1 is expressed by EC and modulated under proinflammatory conditions (data not shown) whereas EC does not produce IL-23R chain neither under proinflammatory conditions nor by p19 overexpression. For this reason, we thought that endogenous p19 could trigger its signal via another receptor. As previously explained, p19 is considered an α subunit that is characterized by a unique up-up down-down four helix bundle conformation which is structurally homologous of IL-6 family cytokines that signal through gp130 (*140*). These observations, together with the fact that viral IL-6 (vIL-6) shares a 16% homology with p19 and that both act mainly as intracellular proteins, it was thought that p19 could act similarly to vIL6. While IL-6 receptor (IL-6R) is composed by a hexameric structure of two gp130 and two IL-6R (gp80) localized in the cell surface plus two IL-6 molecules (*313*), vIL6 forms a tetrameric structure together with intracellular gp130 composed by two molecules of gp130 and two molecules of vIL6 (*314, 315*). What is important for both IL-6 and vIL-6 signaling is gp130 phosphorylation (*316*) (*317*). According to these observations, different approximations including bioinformatic predictive modeling, *in silico* experiments and *in vitro* experiments including primary EC or tissue samples were used to demonstrate p19 binding and activation of gp130 similarly to vIL-6. Nevertheless, the possibility that p19 could also be associated to another unknown intermediate molecule promoting stabilization of gp130/p19 complex cannot be excluded.

Among the molecules investigated as downstream p19/gp130 mediators, STAT3 was the only one that was found activated and also translocated to the nucleus. Although ICAM-1 and VCAM-1 (induced by endogenous p19) are mostly related to STAT1 activation, they also present a predictive site of STAT3 in their promoter region (Champion Chip transcription factor Search portal, DECODE database, SABiosciences)**.** Moreover, consistent with our findings, other cytokines that drive STAT3 activation such as IL-6 are also inducers of adhesion molecules through gp130 /STAT3 activation (*318*). Various approximations were assessed in

order to demonstrate p19 functions independently of IL-6 induction. In p19 overexpressing EC (which lack IL-23R), IL-6 expression was not modulated. Consistent with these data, in BAF130 cells (which lack IL-6R but overexpress gp130) p19 promoted STAT3 activation independently than IL-6R suggesting again a mechanism independently of IL-6 expression.

The discovery of intracellular p19 functions generates the convenience of designing new therapeutic tools to block the intracellular subunit. Antibodies to block secreted p19 to treat inflammatory disorders have been generated but these do not neutralize intracellular p19. The IL-23/Th17 axis is important for several autoimmune diseases. Since increased expression of both p19 and p40 but not p35 has been detected in the lesions of patients with psoriasis, suggesting IL-23 related disease (*319*), several antibody-based therapies are being explored for the treatment of this condition either by blocking p40 (*320*) or by blocking p19. Neutralizing antibodies against p19, which hold promise as a treatment for this disease (*321*) are not likely effective against intracellular p19. The same happens with IL-23 blockade as a treatment for ankylosing spondylitis (*322*).

Since we have characterized a new intracellular function for p19 through binding to gp130, an alternative therapeutic option would be to block this receptor but gp130 is widely expressed by many cell types in many tissues (*154*). Since endogenous p19 signal through STAT3, inhibitors of STAT3 pathway would probably be more effective than blocking extracellular p19 simultaneously would reduce the effect of additional cytokines. The same would happen using JAK/STAT inhibitors (*323*).

A summary of the most important points discussed in this doctoral thesis is represented in the following graphical abstract (Figure 21).

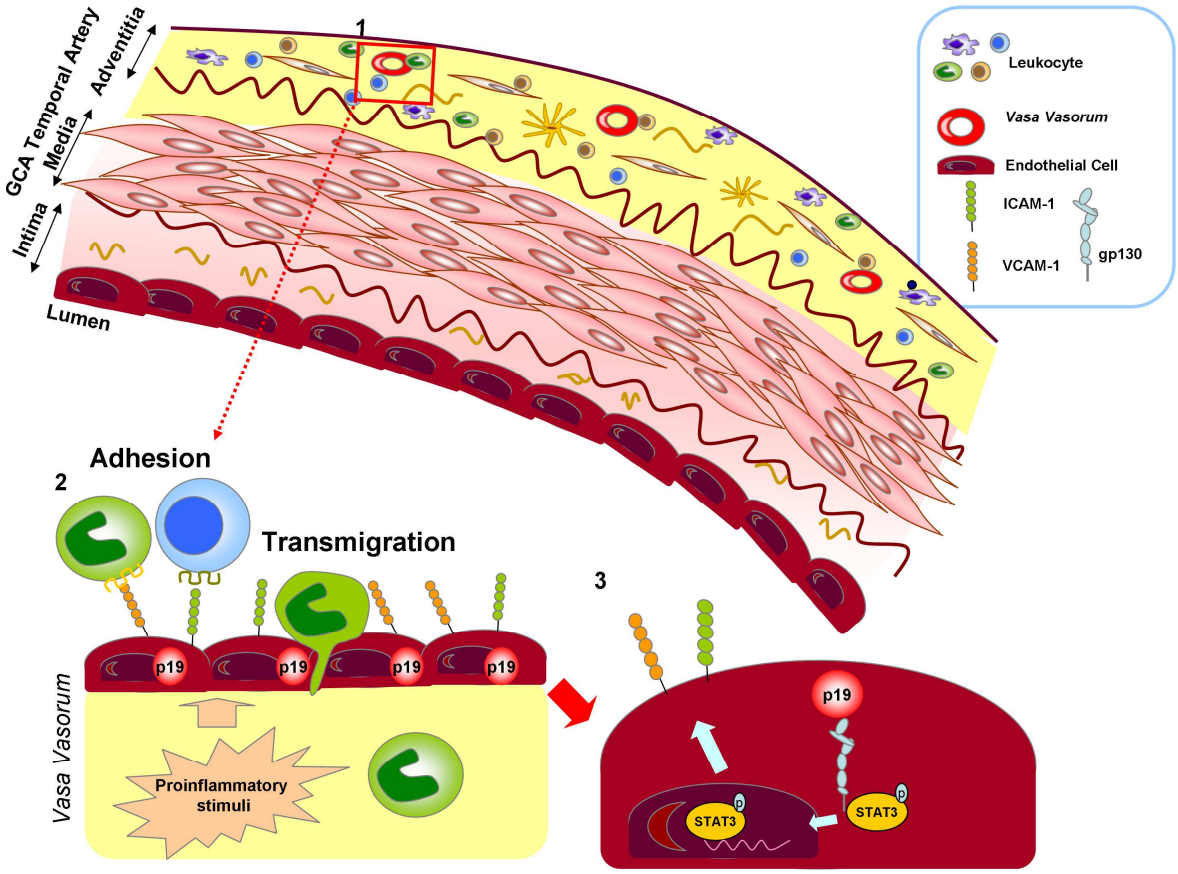

Figure21. Summary of the IL-23p19 involvement in GCA. 1) Adventitial *vasa vasorum* expressing p19 but not p40 in GCA lesions. 2) p19 induction under proinflammatory stimuli (TNFα or LPS) by EC. In p19 overexpressing EC it is induced adhesion molecule expression (ICAM-1 and VCAM-1) is induced, promoting leukocyte attachment and EC transmigration to the inflamed tissue. 3) This is a mechanism which is triggered by endogenous p19 binding to gp130 receptor plus phosphorylation and nucleus translocation of STAT3 that would work as a transcription factor of both ICAM-1 and VCAM-1.

Continuing with the IL-12 superfamily of cytokines, differences in p40 and p35 function and derived phenotypes in animals models for autoimmune diseases such as multiple sclerosis (*166*) and rheumatoid arthritis (RA) (*165*) introduced the hypothesis of alternative partners for both p40 and p35.

IL-35 is a new cytokine of the IL-12 superfamily of cytokines composed by Ebi3 and p35 (*174, 175*). IL-35 has been strongly related to immunoregulatory pathways and more specifically to the induction of specific and powerful Treg cells which are named iTr35 (*126*). The observation by Visvanathan *et al*. (*52*) indicating the presence of p35 but not p40 in VSMC from the media layer of TA from patients with GCA suggested that, p35 may have a role either as an

independent unit or by dimerizing with other partner different from p40. The second hypothesis of this doctoral thesis was originated from these observations.

Hypothesis 2

The IL-12 subunit p35 (highly expressed by VSMC) may also contribute to vascular inflammation in GCA while interacting with Ebi3 in order to form IL-35 cytokine. Moreover, IL-35 may contribute to the persistence of the inflammation in GCA by inducing a proinflammatory phenotype in VSMC.

In our study we demonstrated that p35 binds to Ebi3 in VSMC in order to form IL-35 subunits in GCA lesions. This finding is important because it is the first time that IL-35 has been explored in VSMC and also that this new cytokine has been found expressed in vascular inflammation lesions by non-leukocyte cells. This interesting information was translated into several questions:

- Is IL-35 associated to GCA immunopathology? How?
- How is IL-35 regulated in VSMC?
- Are VSMC able to respond to IL-35?
- Which is the receptor of IL-35 in VSMC?

Our results demonstrated that p40 (the p35 parter to form IL-12) had a different immuno staining pattern than p35 and Ebi3 subunits in a serial number of different biopsy proven-GCA TAs. Interestingly, p35 and Ebi3 were both expressed by VSMC from control arteries as well as by VSMC and leukocytes from GCA lesions. In contrast, p40 was hardly detected in control TAs and only expressed by infiltrating leukocytes but not VSMC in GCA specimens. Moreover PLA technique allowed us to confirm that p35 and Ebi3 were co-expressed conforming IL-35.

The fact that VSMC from control arteries express high amounts of p35 and some Ebi3 is an important issue and it is similar as happens with IL-6 cytokine which is also expressed by controls and induced in the inflammatory context (*2*). Both cytokines may be involved in vascular biology. Although this is an interesting issue, this aspect has not been explored yet.

VSMC co-cultured together with different populations of isolated PBMCs showed that both p35 and Ebi3 are induced in VSMC by the presence of inflammatory infiltrates. These results were

consistent with the observation that immuno staining of IL-35 subunits in inflamed tissue was stronger VSMC surrounded by the infiltrating leukocytes. Although some leukocytes also co-expressed both IL-35 subunits, we did not explore which leukocyte types express IL-35 in GCA lesions. According to the literature, they could be either CD4+T, Treg or B cells (*140, 155, 176*). In GCA, we hypothesize that IL-35-expressing-IL-35 could be macrophages since in our *in vitro* experiments demonstrated that monocytes that are co-cultured with VSMC or that are attached to the plate (which are mainly differentiated into macrophages) but not CD4+T cells isolated from the peripheral blood are able to produce and secrete mature IL-35. Moreover, in this study we mainly focused on the expression of IL-35 by VSMC as well as on exploring IL-35 functions on these cells. Nevertheless, the presence of Treg and IL-35 producing B cells or macrophages in GCA lesions and in other related inflammatory vascular diseases should be further explored in order to better understand the function of this complex cytokine.

The mechanisms involved in the modulation and secretion of mature IL-35 by VSMC was also an interesting point. The fact that this cytokine was induced by NFκB and IRF related molecules (such as IL-1β, TNFα and IFNγ) which are also overexpressed in GCA lesions was an important finding. Although we have just investigated IL-35 production by VSMC it is possible that the mechanisms identified may operate in other non-lymphoid cell types present in the artery wall such as fibroblast or EC.

Another interesting point in IL-35 subunit modulation was also the role of cell-cell interaction between leukocytes and VSMC in IL-35 production. We found that either adhesion molecule ICAM-1 expressed by VSMC or integrin β2 expressed by leukocytes but not VCAM-1 or their corresponding ligand β1 integrins may be essential for Ebi3 transcripitional regulation.

Although only IL-35 has been tested, it may be possible that cell-cell interactions mediated by leukocyte integrin β2 and ICAM-1 expressed by VSMC may contribute to the induction of other proinflammatory cytokines in GCA.

Consistent with this observation, IFNγ ((*47*), **Additional data**), IL-6, as well as co-culture with leukocytes promotes adhesion molecules expression by VSMC. There is an important gap in the literature regarding the processes regulated by leukocyte-VSMC interactions. Exploring VSMC phenotypic and functional changes induced by leukocytes may provide a better

understanding of mechanisms involved in the persistence of inflammation in GCA and other vascular inflammatory diseases.

Since the most of the pro-inflamamtory cytokines that are known to be involved in GCA lesions and other inflammatory vasculopathies are modulated with glucocorticoids (GC) (*82*), we also evaluated the effects of GC on IL-35 subunit expression since GC are the cornerstone of GCA treatment. Surprisingly, our experiments demonstrated that GC treatment does not seem to modulate the expression of IL-35 subunit Ebi3. Therefore, IL-35 could be also involved in persistence of the inflammation in GCA lesions and other related diseases.

Another unresolved question about IL-35 was wether this cytokine would have any effect on non-lymphoid cells such as VSMC. In our studies, we observed that recombinant IL-35 (rIL-35) clearly induced a proinflammatory phenotype in VSMC by promoting the induction of the proinflammatory cytokines (IL-1β, IL-6) and adhesion molecules (ICAM-1 and slightly VCAM-1) related to GCA immunopathology. This was an important finding leading to the identification of new functions for this cytokine since previous studies have mainly focused on lymphid and myeloid cells.

Recent studies propose IL-35 receptor as a complex heterodimer or homodimer combining gp130 and IL-12Rβ2 subunit in mice (*154*). This seems plausible since Ebi3 binds to gp130 when it is a subunit of IL-27 and p35 binds to IL-12Rβ2 when is a subunit of IL-12. Collison *et al.* (2010) (*126*) demonstrated that for the IL-35 differentiation of induced Treg (iTr35), STAT1 and STAT4 (as a consequence of IL-12Rβ2 and gp130 dimerization) was required. IL-12Rβ2 and gp130 would form an heterodimer transducing IL-35 downstream signal. In contrast, homodimers of gp130 or IL-12Rβ2 activate STAT1 or STAT4 respectively. Importantly, it is also concluded by the author that up-regulation of both Ebi3 and p35 expression requires the IL-35 heterodimeric receptor (*154*). On the other hand, in IL-35 producing B cells, the IL-35 response is triggered by STAT1/STAT3 and the receptor seems to be composed by IL-27α and IL-12Rβ2 (*155*). Interestingly, VSMC lack of expressing IL-12Rβ2 chain even after stimulation with rIL-35. Consistent with the fact that both IL-12Rβ2 and gp130 are essential for Ebi3 and p35 induction (*154*), rIL-35 did not promote the induction of either p35 or Ebi3 transcription in VSMC.

Moreover, rIL-35 only activated STAT1 and STAT3 but not STAT4 phosphorylation and nuclear translocation in VSMC. Similar to what happens with p19 and IL-6, IL-35-induced-STAT1/STAT3-nucleus-translocation might promote either IL-6, IL-1β, ICAM-1 or VCAM-1 expression in VSMC since all these molecules present predictive sites for STAT1 or STAT3 in their promoter region (Champion Chip transcription factor Search portal, DECODE database, SABiosciences).

It is intriguing that gp130 may functional as an independent receptor signaling. This pathway has only been observed in vIL-6 and after our studies, by endogenous p19. It is not strange that p35, which is also an α subunit and maintains homology with p19 and IL-6 related cytokines may also interact with gp130. It is extremely interesting the observation that both p19 and IL-35 can bind to gp130 and selectively activate STAT3. This is the first time that this unique signal has been reported for IL-12 family of cytokines. In this point, it would be interesting to test IL-35 function on EC as well as p19 function on VSMC. Moreover, we have not tested the possibility that IL-35 may interact with IL-27R or IL-23R in VSMC. This would be also a possibility because of the conserved homology between the α subunits p19, p35 and p28.

Although IL-35 has begun to be investigated in non-leukocyte cell types (*324-326*) there is still a highly controversial opinion about the function of IL-35 in humans. Most of the information that has been obtained is from the animal models in which IL-35 is produced by different cell types than in humans (*176*). Most of the studies on IL-35 using animal models suggest that IL-35 is an anti-inflammatory and suppressive cytokine (*175*). IL-17 suppresion is one of the relevant IL-35 functions indentified in mice (*165*),(*155, 327*).

According to our findings, scattered reports have recently demonstrated IL-35 expression and function by non-lymphoid cells. Li *et al*. (2012) (*325*) demonstrated Ebi3 and p35 expression by cells other than Treg or iTR35, as well as IL-35 subunit induction by various proinflammatory stimuli. Similar results were obtained by culturing human aortic SMC (AoSMCs) were both TNFα and IFNγ induced IL-35 subunits expression (*326*). In the same study, it was found that both Ebi3 and p35 subunits were expressed in SMC from atheroma lesions but no functions were explored. Other interesting study has suggested that IL-35 could induce ICAM-1 and

apoptosis in AoSMCs although no mechanism were neither explored (*324*). Importantly, in the study of Filková *et al.* (2015) (*328*) it was observed that both IL-35 subunits (Ebi3 and p35) are induced in rheumatoid arthritis lesions. Both subunits were expressed by macrophages, DC, B and T cells and also fibroblasts. This information agree with the one we have observed in GCA lesions in which inflammatory infiltrate expressed both subunits and, in addition, VSMC may also produce IL-35 in a proinflammatory context.

Controversial data between animals and humans suggest that IL-35 functions vary depending on the experimental model used as well as the cell type explored. Therefore, it is important to consider that generalization about mechanisms or extrapolation of results from a single genetically modified animal or experimental disease model may not be accurate. Considering these data together we may conclude that even animal models are important to better understand the function and signaling pathways of this new cytokine, it is important to characterize IL-35 function in humans. Since IL-35 responses seem to be cell dependent, it would be interesting to study its function in different human cell types.

As is summarized in the graphical abstract (**Figure 22**), our results demonstrate that IL-35 can be involved in GCA immunopathology by inducing a proinflammatory phenotype in VSMC through gp130 receptor and STAT1/STAT3 activation. These important findings suggest that IL-35 could be also invoved in GCA persistence of the inflammation. Even though, more studies of IL-35 function and cell association in other human vascular inflammation related diseases should be done to better understand this new and complex cytokine in humans.

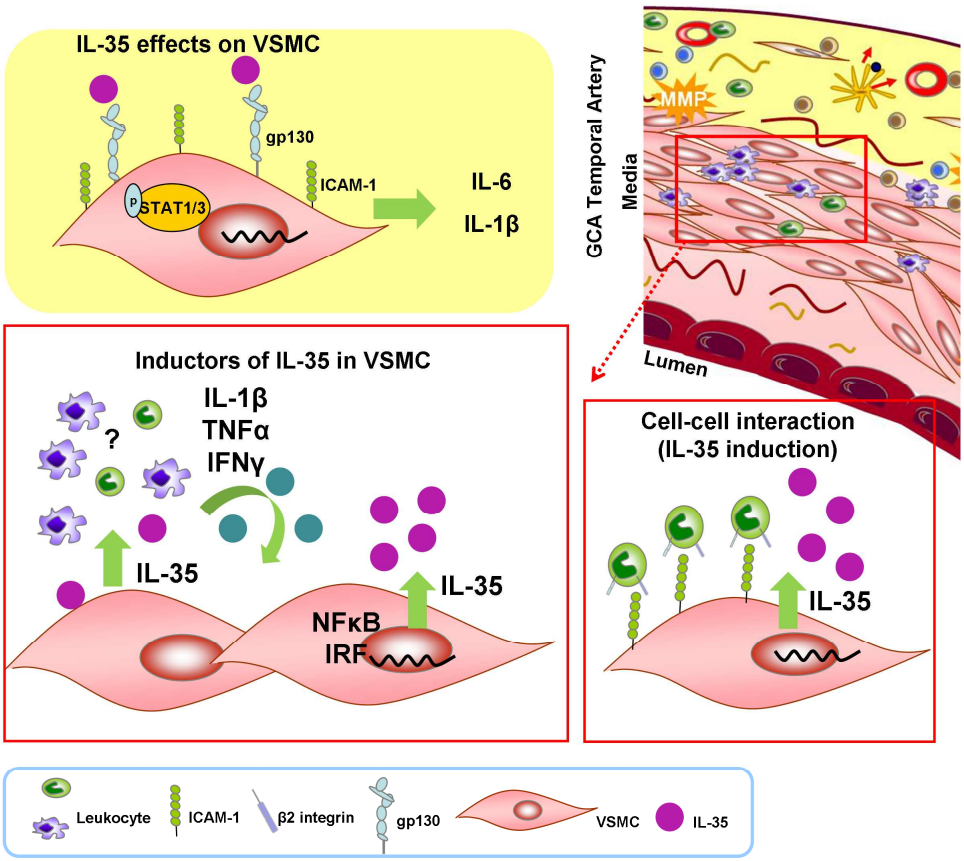

Figure22. Summary of IL-35 involvement in GCA. After leukocyte infiltration to the pathological artery these cells interact with cells from the vasculature wall such as VSMC. Leukocytes induce the expression of both IL-35 subunits (p35 and Ebi3) by VSMC. On one hand, this mechanism is triggered through NFκB activating molecules (IL-1β, TNFα) and IRF related molecules such as IFNγ. On the other hand IL-35 modulation is triggered by leukocyte-VSMC interaction mostly through integrin (β2) plus the adhesion molecule (ICAM-1). Moreover, rIL-35 induce proinflammatory phenotype on VSMC.

Another unresolved challenge in GCA is the **pathological vascular remodeling** as a consequence of chronic inflammation. As already discussed, this process is complex and requires acquisition of a proliferating and migratory myofibroblast phenotype by VSMC as well as aberrant ECM deposition. Nevertheless, the mechanisms which promote VSMC turning into more migratory, proliferative and matrix deposition phenotype are still unknown. Although other studies have demonstrated that some molecules expressed in GCA lesions are involved in this process such as PDGF (*51, 306*), TGFβ (*85*) or metalloproteinases (MMP) (*300*) further investigation is needed.

The most common ischemic complication in GCA is the partial or totally visual loss appearing in 15-20% of patients. Transient visual loss (*amarurosis fugax*) may be due to intermittent critically

reduced blood flow through the small arteries supplying the optic nerve, and suggest the participation of vasospastic mechanisms. Previous studies by our grup demonstrated expression of ET-1 system (including both receptors (ET_AR and ET_BR) and endothelin converting enzyme (ECE-1)) to the ischemic complications present in GCA (*276*). However, the functional role of ET-1 system and the molecular mechanisms underlying the development of the intimal hyperplasia and vascular occlusion in GCA are still unknown.

Although ET-1 is the most potent vasoconstriction molecule identified, it is also involved in the transformation of fibroblast to myofibroblast and in ETM (endothelial/epithelial to mesenchymal transition), a process which contributes to vascular remodeling and fibrotic disease models (*4, 264*). Among others, myofibroblast induced phenotype by ET-1 in fibroblasts can be triggered through FAK phosphorylation in Tyrosin 397 (Y397) (*265*) (*220*). Moreover PI3K pathway (*267*) and MAPK (ERK) or G proteins (*268*) seems to be also involved. Nevertheless, no association of ET-1 in pathological vascular remodeling in vascular inflammation has been reported yet.
The following hypothesis was originated from these previous observations.

Hypothesis 3

Vascular remodeling leads vascular occlusion and subsequent ischemic complications in GCA. The ET-1 system, highly expressed in tissue and sera from ischemic GCA patients, may contribute to GCA vascular occlusion not only by promoting vasoconstriction but also by promoting VSMC migration and ECM deposition. ET-1 may trigger this response by activating migration- related kinases such as FAK, Src and PI3K.

Our observations demonstrated that, in GCA lesions, quiescent VSMC from the media layer (expressing αSMA) were reorganized in the neointimal layer suggesting cytoskeleton changes, migration and myofibroblast differentiation. Interestingly, ET-1 expressing cells were mostly leukocytes which surrounded these migratory cells. Importantly, overexpresion of ET-1 receptors (mostly ET_BR) in GCA lesions by the cells localized in the media/intimal junction

suggested that these cells would be more capable to respond to ET-1 than the quiescents ones and this ET-1 receptor induction may be triggered by the presence of the inflammatory infiltrate.

Further more, ET-1 was expressed and secreted *in vitro* by cultured primary VSMC, isolated CD4+T cells, monocytes (CD14+) and EC. Interestingly, CD4+T cells and monocytes increased their ET-1 production when co-cultured with VSMC which agreed with the immunofluorescence observations in GCA tissue. These results, suggest that the high amount of ET-1 observed in GCA lesions might be mostly produced by the presence of active inflammatory infiltrate like macrophages and CD4+T cells.

From these results, we hypothesized that ET-1 secreted by the activated leukocytes would promote myofibroblast differentiation of VSMC and increased their migratory capacity.

Interestingly, ET-1 promoted cytoskeleton reorganization and induced VSMC migration by recruiting both Y397 activated FAK and PI3K in the cell protrusions of migratory cells. Moreover, this mechanism was triggered by ET-1 either receptor A or receptor B, since the usage of antagonist of both receptors (BQ123 or BQ788 respectively) abrogated ET-1 induction of FAK and PI3K recruitment by these migratory cells. Importantly, PI3K inhibitor abrogated its recruitment to the cell leading edge but even more interestingly it dramatically induced the formation of immature focal adhesion suggesting that PI3K would be essential for VSMC migration induced by ET-1. These results are consistent with the fact that phosphorylation of Y397 FAK leads the association to PI3K p85 subunit through its SH2 domain (*215*) triggering cell adhesion and migration (*216*).

Class I PI3K are activated through tyrosin kinases and heterotrimeric G protein-coupled receptors (GPCR) (*202*). There is no precise information about how PI3K affects organization of the cell actin cytoskeleton although this process seems to be triggered by guanosine nucleotide exchange factors (GEFs), GTPase-activating proteins (GAPS) and small GTPases (*202*). Although we have not fully studied the downstream ET_AR or ET_BR mechanism, both ET-1 receptors are GPCRs which may induce G proteins and as a consequence it is possible that would mediate PI3K and FAK activation.

FAK activation leads to autophosphorylation of several tyrosine including Y397 or Y925 (*199*). While activation of Y397 can be triggered through integrin interaction or by growth factor

receptors and promotes SH2 interaction with Src and PI3K; Y925 phosphorylation is the essential site for paxillin and tallin interaction as well as for the induction of MAPK (*199*).

It is essential to consider that cell migration is a dynamic process in which FAK activation turnover is needed. This process would include the assembly of new focal adhesions in the cell leading edge promoting the recruitment of p85 PI3K, Y397FAK and activated Src but also the disruption of old focal adhesions from the cell rear edge where PTEN and Y925FAK may also be involved but we have not assessed this question in our experiments. Interestingly, ET-1 induced migration depends mostly by Y397 FAK and Y925 FAK phosphorylations as well as Src and ERK activation.

FAK/Src complex also regulates extracellular and intracellular proetolitic events. FAK regulates both expression and activation of MMPs and tissue inhibitors of MMPs (TIMPs). Moreover it has also been repoted that ET-1 induces both production and secretion of proteases such as MMP2, MMP9 by fibroblast from tumor microenvironment, and increase the ratio between MMP and their inhibitor (TIMPS) turning fibroblasts into invasive phenotype (*244*). Similar to what happens with fibroblasts, ET-1 induced release of activated MMP2 by VSMC, a phenomenon which was also abrogated by both ET-1 receptor antagonists BQ123 and BQ788. Activated MMPs (MMP2, MMP9 and MMP14) are expressed in GCA lesions (*300*). While MMP9 and MMP2 are both expressed by leukocytes, pre-mature MMP2 is constitutiveley expressed by VSMC from the media layer of control TA. Previous studies using lymphocyte cell lines, also showed that FAK activation and phosphorylation of Y397 was essential to cell migration and MMP release and that PI3K, ERK and Src were also ivolved (*275*).

ET-1 inducing VSMC migration is also confirmed with the fact that control TA treated with ET-1 for 5 days induced myofibroblastic phenotype in VSMC (overexpression of αSMA and neointima formation) thus, GCA TA treated with ET-1 receptor antagonists (BQ123 amd BQ788) inhibited VSMC outgrowth from the artery sections as well as Y397 FAK phosphorylation in GCA specimens suggesting again that ET-1 may play an essential role in pathological vascular remodeling in GCA.

Interestingly, although ET-1 induces migration and proliferation of other cell types such as EC, in VSMC ET-1 did not function as a chemoattractant neither induced proliferation in VSMC.

An important point to keep in mind is the fact that in aged arteries compared to endothelium from young arteries; ET-1 may be stimulated by vasoactive agents such as thrombin. This mechanism may contribute to cardiovascular pathology in aging (*4, 279*) and, in this case it could be related to GCA which is a disease affecting patients older than 50 years. Because of we used primary cultures of VSMC derived from aged arteries (even controls) we cannot discard the possibility that ET-1 is overexpressed in these cells.

Although ET-1 is involved in controlling vascular tone in physiological conditions aberrant ET-1 axis activation is associated to diseases such as pulmonary hypertension (*273*), cardiovascular disease, cancer (*244, 274*), atherosclerosis (*275*) vasospastic disorders, vascular inflammation (*276*) and fibrotic diseases (*264, 265*) such as idiopathic pulmonary fibrosis and scleroderma (*277*) (*278*). For this reason, ET-1 suppression has gained interest when pathological new functions of ET-1 have been discovered. ET-1 receptor antagonists (i.e. bosentan) are approved for the treatment of pulmonary hypertension and vascular ulcers of patients with scleroderma. Clinial trials with ET-1 receptor antagonists BQ123 and BQ788 are also ongoing (www.clinicaltrials.gov). Interestingly, while pro-myofibroblastic functions of ET-1 have been mostly investigated and characterized in skin or lung fibroblasts, ET-1 receptor antagonists have been more efficient in diseases in which vascular remodeling is significant such as pulmonary hypertension or scleroderma vasculopathy. These observations underline the relevance of our studies in VSMC and re-inforce and important role for ET-1 in inflammation-induced vascular remodeling in GCA.

Taking this data together (as it is represented in **Figure 23**) we provide data supporting that ET-1 is involved in the generation of intimal hyperplasia and vascular occlusion in GCA not only as a vasoconstriction molecule but also by inducing a myofibroblastic phenotype in VSMC through both ET_AR or ET_BR. Both ET-1 receptor antagonists (BQ123 and BQ788) abrogate ET-1 induced myofibrobast phenotype in cultured VSMC. Even so, whereas ET_AR is constitutively expressed by quiescent VSMC from the non pathologic artery media layer, ET_BR is overexpressed in migratory VSMC from the media to intimal junctions in GCA lesions

suggesting that blocking ET_BR under proinflammatory context may be more specific than blocking ET_AR in GCA.

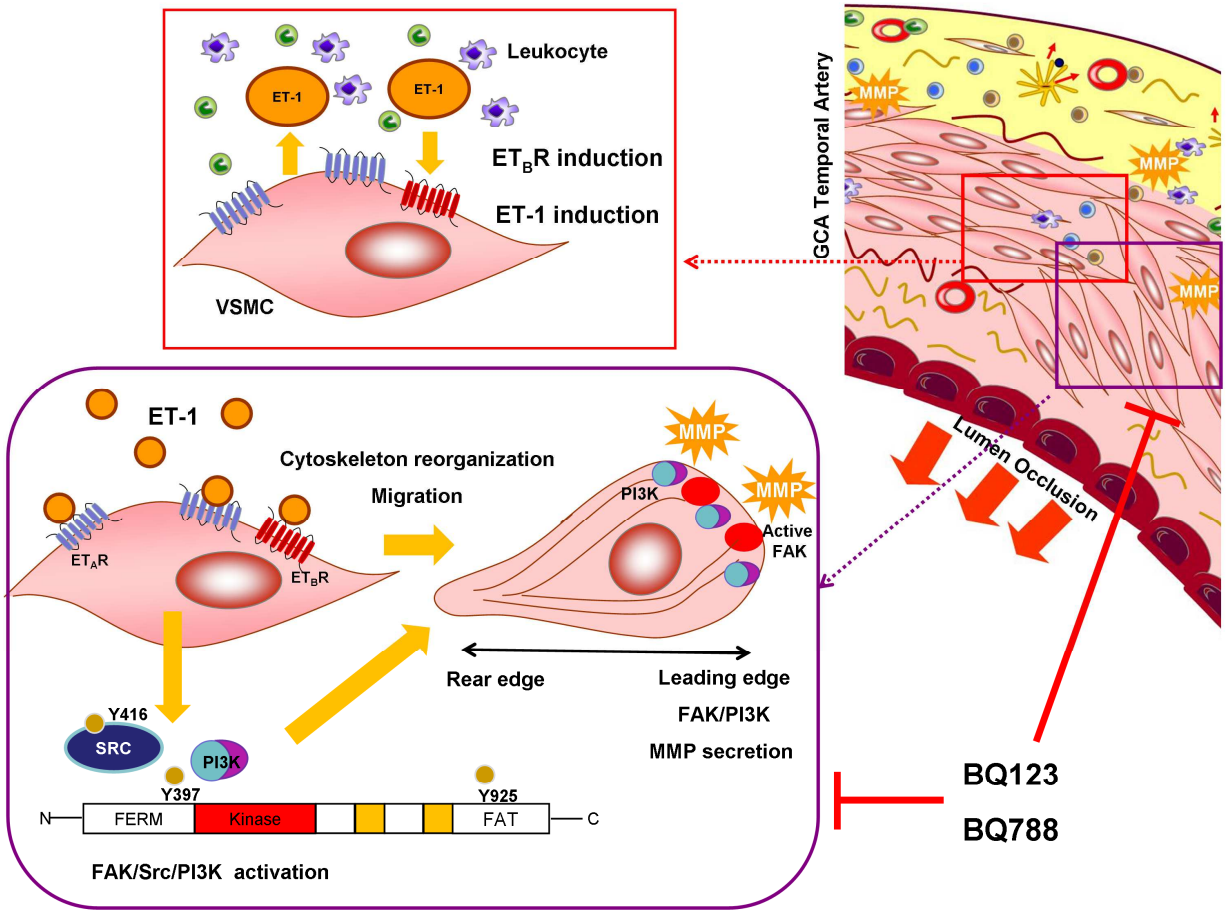

Figure23. Summary of ET-1 system in GCA. In vascular inflammation lesions, ET_BR is induced in migratory VSMC from the media/intimal junction. ET-1 is also up-regulated in leukocytes interacting with VSMC. ET-1 binding to either receptor A or B promotes myofibroblastic phenotye involving cytoskeleton reorganization and induction of cell migration by cultured VSMC. This mechanism involves FAK protein phosphorylation in Tyr 397 which promotes activation of both Tyrosin kinase proteins Src and PI3K. Both activated FAK and PI3K are recruited to the leading edge of the migratory VSMC induced by ET-1. The ET-1 receptor antagonist BQ123 and BQ788 abrogates *in vitro* ET-1 induced VSMC migration.

Although we have contributed knowledge to different unresolved aspects of chronic inflammation diseases of blood vessels such as GCA, further research is still needed to better understand the molecules and mechanisms explained in this doctoral thesis (IL-23p19, IL-35 and ET-1) as well as other molecules that may also contribute to persistence of the inflammation and vascular remodeling.

Conclusions

1. **IL-23p19 but not IL-12/IL-23p40 is induced under proinflammatory stimuli (i.e. TNFα, LPS) in endothelial cells (EC) suggesting a novel role for p19 independent from its dimerization with p40 in order to conform IL-23.**

2. **Endogenous p19 acts as a proinflammatory peptide in EC contributing to adhesion molecules overexpression which promotes EC leukocyte adhesion and transmigration. This mechanism is triggered through p19 association to gp130 receptor and subsequently phosphorylation and nuclear translocation of STAT3.**

3. **While p40 is undetectable in EC from the adventitial *vasa vasorum* of giant-cell arteritis (GCA) specimens, p19 co expression with gp130 is clearly found in this area suggesting p19 involvement in vascular inflammation mainly by promoting leukocyte recruitment.**

4. **IL-35 (p35 and Ebi3) is expressed in temporal arteries from GCA patients either by the infiltrating leukocytes or by vascular smooth muscle cells (VSMC)s. In addition, VSMC respond by producing more IL-35 when co-cultured with leukocytes, a mechanism triggered either by cell-cell interaction or by NFκB-activating molecules.**

5. **In contrast to previous studies describing anti-inflammatory effects of IL-35 on T regulatory cells (T_{reg}) and B cells, IL-35 promotes a proinflammatory phenotype in VSMC. The observed differences in IL-35 functions indicate that these may be cell-specific and dependent on receptor expression and downstream signaling pathways.**

6. **IL-35 may play a role in sustaining inflammatory cascades in GCA.**

7. **ET-1 is expressed in GCA lesions by either inflammatory infiltrate, migratory VSMC or endothelial cells.**

8. **ET-1 induces VSMC cytoskeleton reorganization by activating and recruiting FAK, Src and PI3K to the cell leading edge, a mechanism that promotes VSMC migration**

9. **ET-1 may be involved in GCA vascular occlusion by promoting VSMC migration to the intimal layer. A mechanism involving either ET_AR or ET_BR receptors.**

10. **Both ET-1 receptor antagonists (BQ123 and BQ788) abrogate ET-1 induced myofibrobast phenotype in cultured VSMC. Even so, whereas ET_AR is constitutively expressed by quiescent VSMC from the non pathologic artery media layer, ET_BR is overexpressed in migratory VSMC from the media to intimal junctions of GCA lesions suggesting that blocking ET_BR under proinflammatory context may be more specific than blocking ET_AR.**

Bibliography

1. M. C. Cid *et al.*, Immunohistochemical analysis of lymphoid and macrophage cell subsets and their immunologic activation markers in temporal arteritis. Influence of corticosteroid treatment. *Arthritis and rheumatism* **32**, 884 (Jul, 1989).
2. J. Hernandez-Rodriguez *et al.*, Tissue production of proinflammatory cytokines (IL-1beta, TNFalpha and IL-6) correlates with the intensity of the systemic inflammatory response and with corticosteroid requirements in giant-cell arteritis. *Rheumatology* **43**, 294 (Mar, 2004).
3. H. L. Rittner *et al.*, Tissue-destructive macrophages in giant cell arteritis. *Circulation research* **84**, 1050 (May 14, 1999).
4. F. Rodriguez-Pascual, O. Busnadiego, D. Lagares, S. Lamas, Role of endothelin in the cardiovascular system. *Pharmacological research : the official journal of the Italian Pharmacological Society* **63**, 463 (Jun, 2011).
5. J. C. Jennette *et al.*, 2012 revised International Chapel Hill Consensus Conference Nomenclature of Vasculitides. *Arthritis and rheumatism* **65**, 1 (Jan, 2013).
6. C. J. Boes, Bayard Horton's clinicopathological description of giant cell (temporal) arteritis. *Cephalalgia : an international journal of headache* **27**, 68 (Jan, 2007).
7. T. A. Kermani *et al.*, Large-vessel involvement in giant cell arteritis: a population-based cohort study of the incidence-trends and prognosis. *Annals of the rheumatic diseases* **72**, 1989 (Dec, 2013).
8. H. Petri, A. Nevitt, K. Sarsour, P. Napalkov, N. Collinson, Incidence of giant cell arteritis and characteristics of patients: data-driven analysis of comorbidities. *Arthritis care & research* **67**, 390 (Mar, 2015).
9. A. Garcia-Martinez *et al.*, Development of aortic aneurysm/dilatation during the followup of patients with giant cell arteritis: a cross-sectional screening of fifty-four prospectively followed patients. *Arthritis and rheumatism* **59**, 422 (Mar 15, 2008).
10. S. Prieto-Gonzalez *et al.*, Positron emission tomography assessment of large vessel inflammation in patients with newly diagnosed, biopsy-proven giant cell arteritis: a prospective, case-control study. *Annals of the rheumatic diseases* **73**, 1388 (Jul, 2014).
11. M. C. Cid *et al.*, The spectrum of vascular involvement in giant-cell arteritis: clinical consequences of detrimental vascular remodelling at different sites. *APMIS. Supplementum*, 10 (Jun, 2009).
12. J. Vilaseca, A. Gonzalez, M. C. Cid, J. Lopez-Vivancos, A. Ortega, Clinical usefulness of temporal artery biopsy. *Annals of the rheumatic diseases* **46**, 282 (Apr, 1987).
13. K. R. Stenmark *et al.*, The adventitia: essential regulator of vascular wall structure and function. *Annual review of physiology* **75**, 23 (2013).
14. D. O. Adams, Molecular interactions in macrophage activation. *Immunology today* **10**, 33 (Feb, 1989).
15. K. S. van der Geest *et al.*, Disturbed B cell homeostasis in newly diagnosed giant cell arteritis and polymyalgia rheumatica. *Arthritis & rheumatology* **66**, 1927 (Jul, 2014).

16. C. M. Weyand, K. C. Hicok, G. G. Hunder, J. J. Goronzy, The HLA-DRB1 locus as a genetic component in giant cell arteritis. Mapping of a disease-linked sequence motif to the antigen binding site of the HLA-DR molecule. *The Journal of clinical investigation* **90**, 2355 (Dec, 1992).
17. F. D. Carmona, M. A. Gonzalez-Gay, J. Martin, Genetic component of giant cell arteritis. *Rheumatology* **53**, 6 (Jan, 2014).
18. M. A. Gonzalez-Gay *et al.*, Contribution of MHC class I region to genetic susceptibility for giant cell arteritis. *Rheumatology* **46**, 431 (Mar, 2007).
19. A. Serrano *et al.*, Identification of the PTPN22 functional variant R620W as susceptibility genetic factor for giant cell arteritis. *Annals of the rheumatic diseases* **72**, 1882 (Nov, 2013).
20. A. Serrano *et al.*, Evidence of association of the NLRP1 gene with giant cell arteritis. *Annals of the rheumatic diseases* **72**, 628 (Apr, 2013).
21. A. Marquez *et al.*, Influence of the IL17A locus in giant cell arteritis susceptibility. *Annals of the rheumatic diseases* **73**, 1742 (Sep, 2014).
22. A. Enjuanes *et al.*, Association of NOS2 and potential effect of VEGF, IL6, CCL2 and IL1RN polymorphisms and haplotypes on susceptibility to GCA--a simultaneous study of 130 potentially functional SNPs in 14 candidate genes. *Rheumatology* **51**, 841 (May, 2012).
23. L. Boiardi *et al.*, Interleukin-10 promoter polymorphisms in giant cell arteritis. *Arthritis and rheumatism* **54**, 4011 (Dec, 2006).
24. D. L. Mattey *et al.*, Association of giant cell arteritis and polymyalgia rheumatica with different tumor necrosis factor microsatellite polymorphisms. *Arthritis and rheumatism* **43**, 1749 (Aug, 2000).
25. L. Boiardi *et al.*, Vascular endothelial growth factor gene polymorphisms in giant cell arteritis. *The Journal of rheumatology* **30**, 2160 (Oct, 2003).
26. A. Marquez *et al.*, A candidate gene approach identifies an IL33 genetic variant as a novel genetic risk factor for GCA. *PloS one* **9**, e113476 (2014).
27. L. Rodriguez-Rodriguez *et al.*, Influence of CD40 rs1883832 polymorphism in susceptibility to and clinical manifestations of biopsy-proven giant cell arteritis. *The Journal of rheumatology* **37**, 2076 (Oct, 2010).
28. A. S. Bhatt *et al.*, In search of a candidate pathogen for giant cell arteritis: sequencing-based characterization of the giant cell arteritis microbiome. *Arthritis & rheumatology* **66**, 1939 (Jul, 2014).
29. R. Alvarez-Lafuente *et al.*, Human parvovirus B19, varicella zoster virus, and human herpes virus 6 in temporal artery biopsy specimens of patients with giant cell arteritis: analysis with quantitative real time polymerase chain reaction. *Annals of the rheumatic diseases* **64**, 780 (May, 2005).
30. B. M. Mitchell, R. L. Font, Detection of varicella zoster virus DNA in some patients with giant cell arteritis. *Investigative ophthalmology & visual science* **42**, 2572 (Oct, 2001).

31. M. A. Nagel *et al.*, Varicella zoster virus in the temporal artery of a patient with giant cell arteritis. *Journal of the neurological sciences* **335**, 228 (Dec 15, 2013).
32. G. Haugeberg, R. Bie, S. A. Nordbo, Temporal arteritis associated with Chlamydia pneumoniae DNA detected in an artery specimen. *The Journal of rheumatology* **28**, 1738 (Jul, 2001).
33. S. E. Gabriel *et al.*, The role of parvovirus B19 in the pathogenesis of giant cell arteritis: a preliminary evaluation. *Arthritis and rheumatism* **42**, 1255 (Jun, 1999).
34. P. G. Kennedy, E. Grinfeld, M. M. Esiri, Absence of detection of varicella-zoster virus DNA in temporal artery biopsies obtained from patients with giant cell arteritis. *Journal of the neurological sciences* **215**, 27 (Nov 15, 2003).
35. A. Rodriguez-Pla *et al.*, No detection of parvovirus B19 or herpesvirus DNA in giant cell arteritis. *Journal of clinical virology : the official publication of the Pan American Society for Clinical Virology* **31**, 11 (Sep, 2004).
36. A. Clifford, G. S. Hoffman, Evidence for a vascular microbiome and its role in vessel health and disease. *Current opinion in rheumatology* **27**, 397 (Jul, 2015).
37. C. M. Weyand, J. J. Goronzy, Immune mechanisms in medium and large-vessel vasculitis. *Nature reviews. Rheumatology* **9**, 731 (Dec, 2013).
38. W. Ma-Krupa *et al.*, Activation of arterial wall dendritic cells and breakdown of self-tolerance in giant cell arteritis. *The Journal of experimental medicine* **199**, 173 (Jan 19, 2004).
39. M. C. Cid, 3. Pathogenesis of giant cell arteritis. *Rheumatology* **53 Suppl 2**, i2 (May, 2014).
40. C. M. Weyand, J. J. Goronzy, Giant cell arteritis as an antigen-driven disease. *Rheumatic diseases clinics of North America* **21**, 1027 (Nov, 1995).
41. J. Deng *et al.*, Toll-like receptors 4 and 5 induce distinct types of vasculitis. *Circulation research* **104**, 488 (Feb 27, 2009).
42. W. M. Krupa *et al.*, Trapping of misdirected dendritic cells in the granulomatous lesions of giant cell arteritis. *The American journal of pathology* **161**, 1815 (Nov, 2002).
43. G. Espigol-Frigole *et al.*, Increased IL-17A expression in temporal artery lesions is a predictor of sustained response to glucocorticoid treatment in patients with giant-cell arteritis. *Annals of the rheumatic diseases* **72**, 1481 (Sep 1, 2013).
44. J. Deng, B. R. Younge, R. A. Olshen, J. J. Goronzy, C. M. Weyand, Th17 and Th1 T-cell responses in giant cell arteritis. *Circulation* **121**, 906 (Feb 23, 2010).
45. B. Terrier *et al.*, Interleukin-21 modulates Th1 and Th17 responses in giant cell arteritis. *Arthritis and rheumatism* **64**, 2001 (Jun, 2012).
46. C. M. Weyand *et al.*, Distinct vascular lesions in giant cell arteritis share identical T cell clonotypes. *The Journal of experimental medicine* **179**, 951 (Mar 1, 1994).
47. P.-R. E. Corbera-Bellalta M., Lozano E., Terrades N., Alba M., Prieto-González S., García-Martínez A., Albero R., Enjuanes A., Espígol-Frigolé G.,Hernández-Rodríguez J.,Roux-Lombard P., Ferlin W., Dayer JM., Kosko-Vilbois M.,Cid MC., Blocking

interferon gamma reduces expression of chemokines cxcl9, cxcl10 and cxcl11 and decreases macrophage infiltration in ex-vivo cultured arteries from patients with Giant-cell arteritis *Annals of Rheumatic Diseases* (2015).

48. M. C. Cid *et al.*, Cell adhesion molecules in the development of inflammatory infiltrates in giant cell arteritis: inflammation-induced angiogenesis as the preferential site of leukocyte-endothelial cell interactions. *Arthritis and rheumatism* **43**, 184 (Jan, 2000).
49. M. Kaiser, B. Younge, J. Bjornsson, J. J. Goronzy, C. M. Weyand, Formation of new vasa vasorum in vasculitis. Production of angiogenic cytokines by multinucleated giant cells. *The American journal of pathology* **155**, 765 (Sep, 1999).
50. A. Garcia-Martinez *et al.*, Clinical relevance of persistently elevated circulating cytokines (tumor necrosis factor alpha and interleukin-6) in the long-term followup of patients with giant cell arteritis. *Arthritis care & research* **62**, 835 (Jun, 2010).
51. M. Kaiser, C. M. Weyand, J. Bjornsson, J. J. Goronzy, Platelet-derived growth factor, intimal hyperplasia, and ischemic complications in giant cell arteritis. *Arthritis and rheumatism* **41**, 623 (Apr, 1998).
52. S. Visvanathan *et al.*, Tissue and serum markers of inflammation during the follow-up of patients with giant-cell arteritis--a prospective longitudinal study. *Rheumatology* **50**, 2061 (Nov, 2011).
53. A. Bhatia, P. J. Ell, J. C. Edwards, Anti-CD20 monoclonal antibody (rituximab) as an adjunct in the treatment of giant cell arteritis. *Annals of the rheumatic diseases* **64**, 1099 (Jul, 2005).
54. N. T. Baerlecken *et al.*, Association of ferritin autoantibodies with giant cell arteritis/polymyalgia rheumatica. *Annals of the rheumatic diseases* **71**, 943 (Jun, 2012).
55. A. Regent *et al.*, Contribution of antiferritin antibodies to diagnosis of giant cell arteritis. *Annals of the rheumatic diseases* **72**, 1269 (Jul, 2013).
56. J. R. Park, B. L. Hazleman, Immunological and histological study of temporal arteries. *Annals of the rheumatic diseases* **37**, 238 (Jun, 1978).
57. R. Schmits, B. Kubuschok, S. Schuster, K. D. Preuss, M. Pfreundschuh, Analysis of the B cell repertoire against autoantigens in patients with giant cell arteritis and polymyalgia rheumatica. *Clinical and experimental immunology* **127**, 379 (Feb, 2002).
58. P. Guilpain, L. Mouthon, Antiendothelial cells autoantibodies in vasculitis-associated systemic diseases. *Clinical reviews in allergy & immunology* **35**, 59 (Oct, 2008).
59. M. Navarro *et al.*, Anti-endothelial cell antibodies in systemic autoimmune diseases: prevalence and clinical significance. *Lupus* **6**, 521 (1997).
60. D. C. Baiu, B. Barger, M. Sandor, Z. Fabry, M. N. Hart, Autoantibodies to vascular smooth muscle are pathogenic for vasculitis. *The American journal of pathology* **166**, 1851 (Jun, 2005).
61. A. Regent *et al.*, Identification of target antigens of anti-endothelial cell and anti-vascular smooth muscle cell antibodies in patients with giant cell arteritis: a proteomic approach. *Arthritis research & therapy* **13**, R107 (2011).

62. R. Chakravarti *et al.*, 14-3-3 in Thoracic Aortic Aneurysms: Identification of a Novel Autoantigen in Large Vessel Vasculitis. *Arthritis & rheumatology* **67**, 1913 (Jul, 2015).
63. M. C. Cid, A. Garcia-Martinez, E. Lozano, G. Espigol-Frigole, J. Hernandez-Rodriguez, Five clinical conundrums in the management of giant cell arteritis. *Rheumatic diseases clinics of North America* **33**, 819 (Nov, 2007).
64. A. Proven, S. E. Gabriel, C. Orces, W. M. O'Fallon, G. G. Hunder, Glucocorticoid therapy in giant cell arteritis: duration and adverse outcomes. *Arthritis and rheumatism* **49**, 703 (Oct 15, 2003).
65. C. Font, M. C. Cid, B. Coll-Vinent, A. Lopez-Soto, J. M. Grau, Clinical features in patients with permanent visual loss due to biopsy-proven giant cell arteritis. *British journal of rheumatology* **36**, 251 (Feb, 1997).
66. C. Salvarani *et al.*, Risk factors for visual loss in an Italian population-based cohort of patients with giant cell arteritis. *Arthritis and rheumatism* **53**, 293 (Apr 15, 2005).
67. G. S. Hoffman *et al.*, A multicenter, randomized, double-blind, placebo-controlled trial of adjuvant methotrexate treatment for giant cell arteritis. *Arthritis and rheumatism* **46**, 1309 (May, 2002).
68. J. A. Jover *et al.*, Combined treatment of giant-cell arteritis with methotrexate and prednisone. a randomized, double-blind, placebo-controlled trial. *Annals of internal medicine* **134**, 106 (Jan 16, 2001).
69. R. F. Spiera *et al.*, A prospective, double-blind, randomized, placebo controlled trial of methotrexate in the treatment of giant cell arteritis (GCA). *Clinical and experimental rheumatology* **19**, 495 (Sep-Oct, 2001).
70. D. C. Carol A. Langford, Steven R. Ytterberg, Nader A. Khalidi, Paul A. Monach, Simon Carette, Philip Seo, Larry W. Moreland, Michael Weisman, Curry L. Koening, Antoine G., Robert F. Spiera, Carol McAlear, Kenneth J. Warrington, Christian Pagnoux, Kathleen Maksimowicz-McKinnon, Lindsy J. Forbess, Gary S. Hoffman, Renee Borchin, Jeffrey Krischer, Peter A. Merkel, A Randomized Double-Blind Trial of Abatacept and Glucocorticoids for the Treatment of Giant Cell Arteritis. *American college or rheumatology (ACR) Abstract Supplemented, San Francisco*, 3949 (2015).
71. G. S. Hoffman *et al.*, Infliximab for maintenance of glucocorticosteroid-induced remission of giant cell arteritis: a randomized trial. *Annals of internal medicine* **146**, 621 (May 1, 2007).
72. P. Riha, D. Dumas, V. Latger, S. Muller, J. F. Stoltz, The cooperative effect of L-selectin clusters and velocity-dependent bond formation that stabilizes leukocyte rolling. *Biorheology* **40**, 161 (2003).
73. V. M. Martinez-Taboada *et al.*, A double-blind placebo controlled trial of etanercept in patients with giant cell arteritis and corticosteroid side effects. *Annals of the rheumatic diseases* **67**, 625 (May, 2008).

74. R. Seror *et al.*, Adalimumab for steroid sparing in patients with giant-cell arteritis: results of a multicentre randomised controlled trial. *Annals of the rheumatic diseases* **73**, 2074 (Dec, 2014).
75. S. Unizony *et al.*, Tocilizumab for the treatment of large-vessel vasculitis (giant cell arteritis, Takayasu arteritis) and polymyalgia rheumatica. *Arthritis care & research* **64**, 1720 (Nov, 2012).
76. Q. Chen *et al.*, IRF-4-binding protein inhibits interleukin-17 and interleukin-21 production by controlling the activity of IRF-4 transcription factor. *Immunity* **29**, 899 (Dec 19, 2008).
77. K. E. Weck *et al.*, Murine gamma-herpesvirus 68 causes severe large-vessel arteritis in mice lacking interferon-gamma responsiveness: a new model for virus-induced vascular disease. *Nature medicine* **3**, 1346 (Dec, 1997).
78. M. J. Nicklin, D. E. Hughes, J. L. Barton, J. M. Ure, G. W. Duff, Arterial inflammation in mice lacking the interleukin 1 receptor antagonist gene. *The Journal of experimental medicine* **191**, 303 (Jan 17, 2000).
79. H. Xiao *et al.*, Antineutrophil cytoplasmic autoantibodies specific for myeloperoxidase cause glomerulonephritis and vasculitis in mice. *The Journal of clinical investigation* **110**, 955 (Oct, 2002).
80. Y. Hamano *et al.*, Genetic dissection of vasculitis, myeloperoxidase-specific antineutrophil cytoplasmic autoantibody production, and related traits in spontaneous crescentic glomerulonephritis-forming/Kinjoh mice. *Journal of immunology* **176**, 3662 (Mar 15, 2006).
81. G. Benton, J. George, H. K. Kleinman, I. P. Arnaoutova, Advancing science and technology via 3D culture on basement membrane matrix. *Journal of cellular physiology* **221**, 18 (Oct, 2009).
82. M. Corbera-Bellalta *et al.*, Changes in biomarkers after therapeutic intervention in temporal arteries cultured in Matrigel: a new model for preclinical studies in giant-cell arteritis. *Annals of the rheumatic diseases* **73**, 616 (Mar, 2014).
83. H. K. Kleinman *et al.*, Basement membrane complexes with biological activity. *Biochemistry* **25**, 312 (Jan 28, 1986).
84. H. K. Kleinman, G. R. Martin, Matrigel: basement membrane matrix with biological activity. *Seminars in cancer biology* **15**, 378 (Oct, 2005).
85. A. Brack *et al.*, Glucocorticoid-mediated repression of cytokine gene transcription in human arteritis-SCID chimeras. *The Journal of clinical investigation* **99**, 2842 (Jun 15, 1997).
86. F. Sanchez-Madrid, M. A. del Pozo, Leukocyte polarization in cell migration and immune interactions. *The EMBO journal* **18**, 501 (Feb 1, 1999).
87. K. Ley, C. Laudanna, M. I. Cybulsky, S. Nourshargh, Getting to the site of inflammation: the leukocyte adhesion cascade updated. *Nature reviews. Immunology* **7**, 678 (Sep, 2007).

88. W. A. Muller, Leukocyte-endothelial-cell interactions in leukocyte transmigration and the inflammatory response. *Trends in immunology* **24**, 327 (Jun, 2003).
89. A. J. Huang *et al.*, Endothelial cell cytosolic free calcium regulates neutrophil migration across monolayers of endothelial cells. *The Journal of cell biology* **120**, 1371 (Mar, 1993).
90. S. Nourshargh, R. Alon, Leukocyte migration into inflamed tissues. *Immunity* **41**, 694 (Nov 20, 2014).
91. R. Alon, D. A. Hammer, T. A. Springer, Lifetime of the P-selectin-carbohydrate bond and its response to tensile force in hydrodynamic flow. *Nature* **374**, 539 (Apr 6, 1995).
92. J. S. Pober, W. C. Sessa, Evolving functions of endothelial cells in inflammation. *Nature reviews. Immunology* **7**, 803 (Oct, 2007).
93. K. Ley, G. S. Kansas, Selectins in T-cell recruitment to non-lymphoid tissues and sites of inflammation. *Nature reviews. Immunology* **4**, 325 (May, 2004).
94. A. Salas *et al.*, Rolling adhesion through an extended conformation of integrin alphaLbeta2 and relation to alpha I and beta I-like domain interaction. *Immunity* **20**, 393 (Apr, 2004).
95. J. R. Chan, S. J. Hyduk, M. I. Cybulsky, Chemoattractants induce a rapid and transient upregulation of monocyte alpha4 integrin affinity for vascular cell adhesion molecule 1 which mediates arrest: an early step in the process of emigration. *The Journal of experimental medicine* **193**, 1149 (May 21, 2001).
96. Y. Huo, A. Hafezi-Moghadam, K. Ley, Role of vascular cell adhesion molecule-1 and fibronectin connecting segment-1 in monocyte rolling and adhesion on early atherosclerotic lesions. *Circulation research* **87**, 153 (Jul 21, 2000).
97. R. Alon, S. W. Feigelson, Chemokine signaling to lymphocyte integrins under shear flow. *Microcirculation* **16**, 3 (Jan, 2009).
98. M. H. Ginsberg, A. Partridge, S. J. Shattil, Integrin regulation. *Current opinion in cell biology* **17**, 509 (Oct, 2005).
99. S. Nourshargh, P. L. Hordijk, M. Sixt, Breaching multiple barriers: leukocyte motility through venular walls and the interstitium. *Nature reviews. Molecular cell biology* **11**, 366 (May, 2010).
100. K. Stark *et al.*, Capillary and arteriolar pericytes attract innate leukocytes exiting through venules and 'instruct' them with pattern-recognition and motility programs. *Nature immunology* **14**, 41 (Jan, 2013).
101. J. Herter, A. Zarbock, Integrin Regulation during Leukocyte Recruitment. *Journal of immunology* **190**, 4451 (May 1, 2013).
102. S. D. Marlin, T. A. Springer, Purified intercellular adhesion molecule-1 (ICAM-1) is a ligand for lymphocyte function-associated antigen 1 (LFA-1). *Cell* **51**, 813 (Dec 4, 1987).
103. R. Rothlein, M. L. Dustin, S. D. Marlin, T. A. Springer, A human intercellular adhesion molecule (ICAM-1) distinct from LFA-1. *Journal of immunology* **137**, 1270 (Aug 15, 1986).

104. M. L. Dustin, R. Rothlein, A. K. Bhan, C. A. Dinarello, T. A. Springer, Induction by IL 1 and interferon-gamma: tissue distribution, biochemistry, and function of a natural adherence molecule (ICAM-1). *Journal of immunology* **137**, 245 (Jul 1, 1986).

105. J. S. Pober *et al.*, Overlapping patterns of activation of human endothelial cells by interleukin 1, tumor necrosis factor, and immune interferon. *Journal of immunology* **137**, 1893 (Sep 15, 1986).

106. M. Braun, P. Pietsch, K. Schror, G. Baumann, S. B. Felix, Cellular adhesion molecules on vascular smooth muscle cells. *Cardiovascular research* **41**, 395 (Feb, 1999).

107. J. J. Oppenheim, C. O. Zachariae, N. Mukaida, K. Matsushima, Properties of the novel proinflammatory supergene "intercrine" cytokine family. *Annual review of immunology* **9**, 617 (1991).

108. D. K. Vassilatis *et al.*, The G protein-coupled receptor repertoires of human and mouse. *Proceedings of the National Academy of Sciences of the United States of America* **100**, 4903 (Apr 15, 2003).

109. H. Nomiyama, N. Osada, O. Yoshie, A family tree of vertebrate chemokine receptors for a unified nomenclature. *Developmental and comparative immunology* **35**, 705 (Jul, 2011).

110. A. Zlotnik, O. Yoshie, The chemokine superfamily revisited. *Immunity* **36**, 705 (May 25, 2012).

111. B. Moser, M. Wolf, A. Walz, P. Loetscher, Chemokines: multiple levels of leukocyte migration control. *Trends in immunology* **25**, 75 (Feb, 2004).

112. J. S. Pober, G. Tellides, Participation of blood vessel cells in human adaptive immune responses. *Trends in immunology* **33**, 49 (Jan, 2012).

113. M. B. Voisin, S. Nourshargh, Neutrophil transmigration: emergence of an adhesive cascade within venular walls. *Journal of innate immunity* **5**, 336 (2013).

114. C.-B. M. Cid Xutgla M. C., Planas-Rigol E., Lozano E, Espígol-Frigolé G, García-Martínez A, Hernández-Rodríguez J, Segarra M., *Inflammatory Diseases of Blood Vessels*. (ed. Second, 2012).

115. R. J. Boyton, D. M. Altmann, Is selection for TCR affinity a factor in cytokine polarization? *Trends in immunology* **23**, 526 (Nov, 2002).

116. J. J. O'Shea, W. E. Paul, Mechanisms underlying lineage commitment and plasticity of helper CD4+ T cells. *Science* **327**, 1098 (Feb 26, 2010).

117. C. Dong, R. A. Flavell, Control of T helper cell differentiation--in search of master genes. *Science's STKE : signal transduction knowledge environment* **2000**, pe1 (Sep 12, 2000).

118. Z. Chen, A. Laurence, J. J. O'Shea, Signal transduction pathways and transcriptional regulation in the control of Th17 differentiation. *Seminars in immunology* **19**, 400 (Dec, 2007).

119. Y. K. Lee, R. Mukasa, R. D. Hatton, C. T. Weaver, Developmental plasticity of Th17 and Treg cells. *Current opinion in immunology* **21**, 274 (Jun, 2009).

120. L. Zhou, M. M. Chong, D. R. Littman, Plasticity of CD4+ T cell lineage differentiation. *Immunity* **30**, 646 (May, 2009).
121. A. Vogelzang *et al.*, A fundamental role for interleukin-21 in the generation of T follicular helper cells. *Immunity* **29**, 127 (Jul 18, 2008).
122. N. Fazilleau, L. Mark, L. J. McHeyzer-Williams, M. G. McHeyzer-Williams, Follicular helper T cells: lineage and location. *Immunity* **30**, 324 (Mar 20, 2009).
123. J. M. Kim, J. P. Rasmussen, A. Y. Rudensky, Regulatory T cells prevent catastrophic autoimmunity throughout the lifespan of mice. *Nature immunology* **8**, 191 (Feb, 2007).
124. W. Chen *et al.*, Conversion of peripheral CD4+CD25- naive T cells to CD4+CD25+ regulatory T cells by TGF-beta induction of transcription factor Foxp3. *The Journal of experimental medicine* **198**, 1875 (Dec 15, 2003).
125. M. A. Curotto de Lafaille, J. J. Lafaille, Natural and adaptive foxp3+ regulatory T cells: more of the same or a division of labor? *Immunity* **30**, 626 (May, 2009).
126. L. W. Collison *et al.*, IL-35-mediated induction of a potent regulatory T cell population. *Nature immunology* **11**, 1093 (Dec, 2010).
127. D. O. Adams, The granulomatous inflammatory response. A review. *The American journal of pathology* **84**, 164 (Jul, 1976).
128. S. Gordon, P. R. Taylor, Monocyte and macrophage heterogeneity. *Nature reviews. Immunology* **5**, 953 (Dec, 2005).
129. A. Mantovani *et al.*, The chemokine system in diverse forms of macrophage activation and polarization. *Trends in immunology* **25**, 677 (Dec, 2004).
130. S. K. Biswas, A. Mantovani, Macrophage plasticity and interaction with lymphocyte subsets: cancer as a paradigm. *Nature immunology* **11**, 889 (Oct, 2010).
131. P. Loke *et al.*, IL-4 dependent alternatively-activated macrophages have a distinctive in vivo gene expression phenotype. *BMC immunology* **3**, 7 (Jul 4, 2002).
132. J. J. O'Shea, M. Gadina, R. D. Schreiber, Cytokine signaling in 2002: new surprises in the Jak/Stat pathway. *Cell* **109 Suppl**, S121 (Apr, 2002).
133. J. S. Rawlings, K. M. Rosler, D. A. Harrison, The JAK/STAT signaling pathway. *Journal of cell science* **117**, 1281 (Mar 15, 2004).
134. K. M. McBride, G. Banninger, C. McDonald, N. C. Reich, Regulated nuclear import of the STAT1 transcription factor by direct binding of importin-alpha. *The EMBO journal* **21**, 1754 (Apr 2, 2002).
135. D. L. Krebs, D. J. Hilton, SOCS proteins: negative regulators of cytokine signaling. *Stem cells* **19**, 378 (2001).
136. Z. Chen, J. J. O'Shea, Th17 cells: a new fate for differentiating helper T cells. *Immunologic research* **41**, 87 (2008).
137. K. Shuai, B. Liu, Regulation of JAK-STAT signalling in the immune system. *Nature reviews. Immunology* **3**, 900 (Nov, 2003).
138. L. L. Jones, D. A. Vignali, Molecular interactions within the IL-6/IL-12 cytokine/receptor superfamily. *Immunologic research* **51**, 5 (Oct, 2011).

139. K. Gee, C. Guzzo, N. F. Che Mat, W. Ma, A. Kumar, The IL-12 family of cytokines in infection, inflammation and autoimmune disorders. *Inflammation & allergy drug targets* **8**, 40 (Mar, 2009).
140. D. A. Vignali, V. K. Kuchroo, IL-12 family cytokines: immunological playmakers. *Nature immunology* **13**, 722 (Aug, 2012).
141. L. W. Collison, D. A. Vignali, Interleukin-35: odd one out or part of the family? *Immunological reviews* **226**, 248 (Dec, 2008).
142. P. J. Lupardus, K. C. Garcia, The structure of interleukin-23 reveals the molecular basis of p40 subunit sharing with interleukin-12. *Journal of molecular biology* **382**, 931 (Oct 17, 2008).
143. L. L. Jones, V. Chaturvedi, C. Uyttenhove, J. Van Snick, D. A. Vignali, Distinct subunit pairing criteria within the heterodimeric IL-12 cytokine family. *Molecular immunology* **51**, 234 (Jun, 2012).
144. A. M. Cooper, S. A. Khader, IL-12p40: an inherently agonistic cytokine. *Trends in immunology* **28**, 33 (Jan, 2007).
145. S. Gillessen *et al.*, Mouse interleukin-12 (IL-12) p40 homodimer: a potent IL-12 antagonist. *European journal of immunology* **25**, 200 (Jan, 1995).
146. F. P. Heinzel, A. M. Hujer, F. N. Ahmed, R. M. Rerko, In vivo production and function of IL-12 p40 homodimers. *Journal of immunology* **158**, 4381 (May 1, 1997).
147. J. S. Stumhofer *et al.*, A role for IL-27p28 as an antagonist of gp130-mediated signaling. *Nature immunology* **11**, 1119 (Dec, 2010).
148. O. Shimozato *et al.*, The secreted form of p28 subunit of interleukin (IL)-27 inhibits biological functions of IL-27 and suppresses anti-allogeneic immune responses. *Immunology* **128**, e816 (Sep, 2009).
149. A. O. Chua *et al.*, Expression cloning of a human IL-12 receptor component. A new member of the cytokine receptor superfamily with strong homology to gp130. *Journal of immunology* **153**, 128 (Jul 1, 1994).
150. A. O. Chua, V. L. Wilkinson, D. H. Presky, U. Gubler, Cloning and characterization of a mouse IL-12 receptor-beta component. *Journal of immunology* **155**, 4286 (Nov 1, 1995).
151. C. Parham *et al.*, A receptor for the heterodimeric cytokine IL-23 is composed of IL-12Rbeta1 and a novel cytokine receptor subunit, IL-23R. *Journal of immunology* **168**, 5699 (Jun 1, 2002).
152. B. Oppmann *et al.*, Novel p19 protein engages IL-12p40 to form a cytokine, IL-23, with biological activities similar as well as distinct from IL-12. *Immunity* **13**, 715 (Nov, 2000).
153. S. Pflanz *et al.*, WSX-1 and glycoprotein 130 constitute a signal-transducing receptor for IL-27. *Journal of immunology* **172**, 2225 (Feb 15, 2004).
154. L. W. Collison *et al.*, The composition and signaling of the IL-35 receptor are unconventional. *Nature immunology* **13**, 290 (Mar, 2012).

155. R. X. Wang *et al.*, Interleukin-35 induces regulatory B cells that suppress autoimmune disease. *Nature medicine* **20**, 633 (Jun, 2014).
156. W. E. Thierfelder *et al.*, Requirement for Stat4 in interleukin-12-mediated responses of natural killer and T cells. *Nature* **382**, 171 (Jul 11, 1996).
157. L. Hibbert, S. Pflanz, R. De Waal Malefyt, R. A. Kastelein, IL-27 and IFN-alpha signal via Stat1 and Stat3 and induce T-Bet and IL-12Rbeta2 in naive T cells. *Journal of interferon & cytokine research : the official journal of the International Society for Interferon and Cytokine Research* **23**, 513 (Sep, 2003).
158. C. E. Egwuagu, C. R. Yu, L. Sun, R. Wang, Interleukin 35: Critical regulator of immunity and lymphocyte-mediated diseases. *Cytokine & growth factor reviews* **26**, 587 (Oct, 2015).
159. A. D'Andrea *et al.*, Production of natural killer cell stimulatory factor (interleukin 12) by peripheral blood mononuclear cells. *The Journal of experimental medicine* **176**, 1387 (Nov 1, 1992).
160. A. D'Andrea *et al.*, Interleukin 10 (IL-10) inhibits human lymphocyte interferon gamma-production by suppressing natural killer cell stimulatory factor/IL-12 synthesis in accessory cells. *The Journal of experimental medicine* **178**, 1041 (Sep 1, 1993).
161. M. Aste-Amezaga, X. Ma, A. Sartori, G. Trinchieri, Molecular mechanisms of the induction of IL-12 and its inhibition by IL-10. *Journal of immunology* **160**, 5936 (Jun 15, 1998).
162. M. H. Branton, J. B. Kopp, TGF-beta and fibrosis. *Microbes and infection / Institut Pasteur* **1**, 1349 (Dec, 1999).
163. J. Magram *et al.*, IL-12-deficient mice are defective in IFN gamma production and type 1 cytokine responses. *Immunity* **4**, 471 (May, 1996).
164. S. Aggarwal, N. Ghilardi, M. H. Xie, F. J. de Sauvage, A. L. Gurney, Interleukin-23 promotes a distinct CD4 T cell activation state characterized by the production of interleukin-17. *The Journal of biological chemistry* **278**, 1910 (Jan 17, 2003).
165. C. A. Murphy *et al.*, Divergent pro- and antiinflammatory roles for IL-23 and IL-12 in joint autoimmune inflammation. *The Journal of experimental medicine* **198**, 1951 (Dec 15, 2003).
166. D. J. Cua *et al.*, Interleukin-23 rather than interleukin-12 is the critical cytokine for autoimmune inflammation of the brain. *Nature* **421**, 744 (Feb 13, 2003).
167. R. A. Kastelein, C. A. Hunter, D. J. Cua, Discovery and biology of IL-23 and IL-27: related but functionally distinct regulators of inflammation. *Annual review of immunology* **25**, 221 (2007).
168. C. L. Langrish *et al.*, IL-23 drives a pathogenic T cell population that induces autoimmune inflammation. *The Journal of experimental medicine* **201**, 233 (Jan 17, 2005).
169. E. Bettelli *et al.*, Reciprocal developmental pathways for the generation of pathogenic effector TH17 and regulatory T cells. *Nature* **441**, 235 (May 11, 2006).

170. C. A. Hunter, New IL-12-family members: IL-23 and IL-27, cytokines with divergent functions. *Nature reviews. Immunology* **5**, 521 (Jul, 2005).
171. M. T. Wiekowski *et al.*, Ubiquitous transgenic expression of the IL-23 subunit p19 induces multiorgan inflammation, runting, infertility, and premature death. *Journal of immunology* **166**, 7563 (Jun 15, 2001).
172. D. S. Schoenhaut *et al.*, Cloning and expression of murine IL-12. *Journal of immunology* **148**, 3433 (Jun 1, 1992).
173. O. Devergne *et al.*, A novel interleukin-12 p40-related protein induced by latent Epstein-Barr virus infection in B lymphocytes. *Journal of virology* **70**, 1143 (Feb, 1996).
174. O. Devergne, M. Birkenbach, E. Kieff, Epstein-Barr virus-induced gene 3 and the p35 subunit of interleukin 12 form a novel heterodimeric hematopoietin. *Proceedings of the National Academy of Sciences of the United States of America* **94**, 12041 (Oct 28, 1997).
175. L. W. Collison *et al.*, The inhibitory cytokine IL-35 contributes to regulatory T-cell function. *Nature* **450**, 566 (Nov 22, 2007).
176. E. Bardel, F. Larousserie, P. Charlot-Rabiega, A. Coulomb-L'Hermine, O. Devergne, Human CD4+ CD25+ Foxp3+ regulatory T cells do not constitutively express IL-35. *Journal of immunology* **181**, 6898 (Nov 15, 2008).
177. M. Seyerl *et al.*, Human rhinoviruses induce IL-35-producing Treg via induction of B7-H1 (CD274) and sialoadhesin (CD169) on DC. *European journal of immunology* **40**, 321 (Feb, 2010).
178. M. C. Boissier *et al.*, Regulatory T cells (Treg) in rheumatoid arthritis. *Joint, bone, spine : revue du rhumatisme* **76**, 10 (Jan, 2009).
179. B. Langhans *et al.*, Core-specific adaptive regulatory T-cells in different outcomes of hepatitis C. *Clinical science* **119**, 97 (Jul, 2010).
180. F. Liu, F. Tong, Y. He, H. Liu, Detectable expression of IL-35 in CD4+ T cells from peripheral blood of chronic hepatitis B patients. *Clinical immunology* **139**, 1 (Apr, 2011).
181. P. Shen *et al.*, IL-35-producing B cells are critical regulators of immunity during autoimmune and infectious diseases. *Nature* **507**, 366 (Mar 20, 2014).
182. W. Liao, J. X. Lin, L. Wang, P. Li, W. J. Leonard, Modulation of cytokine receptors by IL-2 broadly regulates differentiation into helper T cell lineages. *Nature immunology* **12**, 551 (Jun, 2011).
183. S. Pflanz *et al.*, IL-27, a heterodimeric cytokine composed of EBI3 and p28 protein, induces proliferation of naive CD4+ T cells. *Immunity* **16**, 779 (Jun, 2002).
184. J. S. Stumhofer, C. A. Hunter, Advances in understanding the anti-inflammatory properties of IL-27. *Immunology letters* **117**, 123 (May 15, 2008).
185. M. Batten, N. Ghilardi, The biology and therapeutic potential of interleukin 27. *Journal of molecular medicine* **85**, 661 (Jul, 2007).

186. J. S. Stumhofer *et al.*, Interleukin 27 negatively regulates the development of interleukin 17-producing T helper cells during chronic inflammation of the central nervous system. *Nature immunology* **7**, 937 (Sep, 2006).
187. D. C. Fitzgerald *et al.*, Suppression of autoimmune inflammation of the central nervous system by interleukin 10 secreted by interleukin 27-stimulated T cells. *Nature immunology* **8**, 1372 (Dec, 2007).
188. A. Awasthi *et al.*, A dominant function for interleukin 27 in generating interleukin 10-producing anti-inflammatory T cells. *Nature immunology* **8**, 1380 (Dec, 2007).
189. M. Batten *et al.*, IL-27 supports germinal center function by enhancing IL-21 production and the function of T follicular helper cells. *The Journal of experimental medicine* **207**, 2895 (Dec 20, 2010).
190. N. F. Renna, N. de Las Heras, R. M. Miatello, Pathophysiology of vascular remodeling in hypertension. *International journal of hypertension* **2013**, 808353 (2013).
191. G. H. Gibbons, V. J. Dzau, The emerging concept of vascular remodeling. *The New England journal of medicine* **330**, 1431 (May 19, 1994).
192. J. E. Hungerford, C. D. Little, Developmental biology of the vascular smooth muscle cell: building a multilayered vessel wall. *Journal of vascular research* **36**, 2 (Jan-Feb, 1999).
193. G. K. Owens, M. S. Kumar, B. R. Wamhoff, Molecular regulation of vascular smooth muscle cell differentiation in development and disease. *Physiological reviews* **84**, 767 (Jul, 2004).
194. L. L. H. K., in *Vascular Medicine: A Companion to Braunwald's Heart Disease* B. J. Creager M., Loscalzo J, Ed. (2013), pp. 25-42.
195. M. D. M. Reid Amy J., *Inflammatory Disease of Blood Vessels*. (ed. Second, 2012).
196. A. J. Ridley *et al.*, Cell migration: integrating signals from front to back. *Science* **302**, 1704 (Dec 5, 2003).
197. M. D. Welch, R. D. Mullins, Cellular control of actin nucleation. *Annual review of cell and developmental biology* **18**, 247 (2002).
198. T. D. Pollard, G. G. Borisy, Cellular motility driven by assembly and disassembly of actin filaments. *Cell* **112**, 453 (Feb 21, 2003).
199. J. T. Parsons *et al.*, Focal adhesion kinase: structure and signalling. *Journal of cell science. Supplement* **18**, 109 (1994).
200. B. Shen, M. K. Delaney, X. Du, Inside-out, outside-in, and inside-outside-in: G protein signaling in integrin-mediated cell adhesion, spreading, and retraction. *Current opinion in cell biology* **24**, 600 (Oct, 2012).
201. A. Khwaja, P. Rodriguez-Viciana, S. Wennstrom, P. H. Warne, J. Downward, Matrix adhesion and Ras transformation both activate a phosphoinositide 3-OH kinase and protein kinase B/Akt cellular survival pathway. *The EMBO journal* **16**, 2783 (May 15, 1997).

202. B. Vanhaesebroeck *et al.*, Synthesis and function of 3-phosphorylated inositol lipids. *Annual review of biochemistry* **70**, 535 (2001).

203. B. Vanhaesebroeck, J. Guillermet-Guibert, M. Graupera, B. Bilanges, The emerging mechanisms of isoform-specific PI3K signalling. *Nature reviews. Molecular cell biology* **11**, 329 (May, 2010).

204. P. Rodriguez-Viciana *et al.*, Phosphatidylinositol-3-OH kinase as a direct target of Ras. *Nature* **370**, 527 (Aug 18, 1994).

205. M. D. Schaller *et al.*, pp125FAK a structurally distinctive protein-tyrosine kinase associated with focal adhesions. *Proceedings of the National Academy of Sciences of the United States of America* **89**, 5192 (Jun 1, 1992).

206. S. K. Mitra, D. A. Hanson, D. D. Schlaepfer, Focal adhesion kinase: in command and control of cell motility. *Nature reviews. Molecular cell biology* **6**, 56 (Jan, 2005).

207. M. D. Schaller, Biochemical signals and biological responses elicited by the focal adhesion kinase. *Biochimica et biophysica acta* **1540**, 1 (Jul 25, 2001).

208. D. Ilic *et al.*, Reduced cell motility and enhanced focal adhesion contact formation in cells from FAK-deficient mice. *Nature* **377**, 539 (Oct 12, 1995).

209. A. Richardson, R. K. Malik, J. D. Hildebrand, J. T. Parsons, Inhibition of cell spreading by expression of the C-terminal domain of focal adhesion kinase (FAK) is rescued by coexpression of Src or catalytically inactive FAK: a role for paxillin tyrosine phosphorylation. *Molecular and cellular biology* **17**, 6906 (Dec, 1997).

210. L. A. Cary, J. F. Chang, J. L. Guan, Stimulation of cell migration by overexpression of focal adhesion kinase and its association with Src and Fyn. *Journal of cell science* **109 (Pt 7)**, 1787 (Jul, 1996).

211. S. M. Frisch, K. Vuori, E. Ruoslahti, P. Y. Chan-Hui, Control of adhesion-dependent cell survival by focal adhesion kinase. *The Journal of cell biology* **134**, 793 (Aug, 1996).

212. M. D. Schaller, C. A. Otey, J. D. Hildebrand, J. T. Parsons, Focal adhesion kinase and paxillin bind to peptides mimicking beta integrin cytoplasmic domains. *The Journal of cell biology* **130**, 1181 (Sep, 1995).

213. J. T. Parsons, Focal adhesion kinase: the first ten years. *Journal of cell science* **116**, 1409 (Apr 15, 2003).

214. M. D. Schaller, J. T. Parsons, Focal adhesion kinase and associated proteins. *Current opinion in cell biology* **6**, 705 (Oct, 1994).

215. H. C. Chen, P. A. Appeddu, H. Isoda, J. L. Guan, Phosphorylation of tyrosine 397 in focal adhesion kinase is required for binding phosphatidylinositol 3-kinase. *The Journal of biological chemistry* **271**, 26329 (Oct 18, 1996).

216. H. R. Reiske *et al.*, Requirement of phosphatidylinositol 3-kinase in focal adhesion kinase-promoted cell migration. *The Journal of biological chemistry* **274**, 12361 (Apr 30, 1999).

217. N. Karavitaki *et al.*, What is the natural history of nonoperated nonfunctioning pituitary adenomas? *Clinical endocrinology* **67**, 938 (Dec, 2007).

218. I. Hunger-Glaser, R. S. Fan, E. Perez-Salazar, E. Rozengurt, PDGF and FGF induce focal adhesion kinase (FAK) phosphorylation at Ser-910: dissociation from Tyr-397 phosphorylation and requirement for ERK activation. *Journal of cellular physiology* **200**, 213 (Aug, 2004).
219. G. H. John, I. May, M. J. Sarsfield, D. Collison, M. Helliwell, Dimeric uranyl complexes with bridging perrhenates. *Dalton transactions*, 1603 (Apr 28, 2007).
220. D. Lagares *et al.*, Inhibition of focal adhesion kinase prevents experimental lung fibrosis and myofibroblast formation. *Arthritis and rheumatism* **64**, 1653 (May, 2012).
221. J. M. Taylor *et al.*, Selective expression of an endogenous inhibitor of FAK regulates proliferation and migration of vascular smooth muscle cells. *Molecular and cellular biology* **21**, 1565 (Mar, 2001).
222. A. Richardson, T. Parsons, A mechanism for regulation of the adhesion-associated proteintyrosine kinase pp125FAK. *Nature* **380**, 538 (Apr 11, 1996).
223. K. Nolan, J. Lacoste, J. T. Parsons, Regulated expression of focal adhesion kinase-related nonkinase, the autonomously expressed C-terminal domain of focal adhesion kinase. *Molecular and cellular biology* **19**, 6120 (Sep, 1999).
224. M. D. Schaller, C. A. Borgman, J. T. Parsons, Autonomous expression of a noncatalytic domain of the focal adhesion-associated protein tyrosine kinase pp125FAK. *Molecular and cellular biology* **13**, 785 (Feb, 1993).
225. B. M. Sefton, T. Hunter, K. Beemon, W. Eckhart, Evidence that the phosphorylation of tyrosine is essential for cellular transformation by Rous sarcoma virus. *Cell* **20**, 807 (Jul, 1980).
226. S. M. Thomas, J. S. Brugge, Cellular functions regulated by Src family kinases. *Annual review of cell and developmental biology* **13**, 513 (1997).
227. S. J. Parsons, J. T. Parsons, Src family kinases, key regulators of signal transduction. *Oncogene* **23**, 7906 (Oct 18, 2004).
228. T. J. Yeatman, A renaissance for SRC. *Nature reviews. Cancer* **4**, 470 (Jun, 2004).
229. X. M. Zheng, Y. Wang, C. J. Pallen, Cell transformation and activation of pp60c-src by overexpression of a protein tyrosine phosphatase. *Nature* **359**, 336 (Sep 24, 1992).
230. J. W. Thomas *et al.*, SH2- and SH3-mediated interactions between focal adhesion kinase and Src. *The Journal of biological chemistry* **273**, 577 (Jan 2, 1998).
231. T. Nakamoto, R. Sakai, K. Ozawa, Y. Yazaki, H. Hirai, Direct binding of C-terminal region of p130Cas to SH2 and SH3 domains of Src kinase. *The Journal of biological chemistry* **271**, 8959 (Apr 12, 1996).
232. M. R. Burnham *et al.*, Regulation of c-SRC activity and function by the adapter protein CAS. *Molecular and cellular biology* **20**, 5865 (Aug, 2000).
233. G. S. Martin, The hunting of the Src. *Nature reviews. Molecular cell biology* **2**, 467 (Jun, 2001).

234. M. Cargnello, P. P. Roux, Activation and function of the MAPKs and their substrates, the MAPK-activated protein kinases. *Microbiology and molecular biology reviews : MMBR* **75**, 50 (Mar, 2011).

235. M. Raman, W. Chen, M. H. Cobb, Differential regulation and properties of MAPKs. *Oncogene* **26**, 3100 (May 14, 2007).

236. S. Yoon, R. Seger, The extracellular signal-regulated kinase: multiple substrates regulate diverse cellular functions. *Growth factors* **24**, 21 (Mar, 2006).

237. R. L. Klemke *et al.*, Regulation of cell motility by mitogen-activated protein kinase. *The Journal of cell biology* **137**, 481 (Apr 21, 1997).

238. F. D. Russell, A. P. Davenport, Secretory pathways in endothelin synthesis. *British journal of pharmacology* **126**, 391 (Jan, 1999).

239. M. Yanagisawa *et al.*, A novel potent vasoconstrictor peptide produced by vascular endothelial cells. *Nature* **332**, 411 (Mar 31, 1988).

240. A. Inoue *et al.*, The human endothelin family: three structurally and pharmacologically distinct isopeptides predicted by three separate genes. *Proceedings of the National Academy of Sciences of the United States of America* **86**, 2863 (Apr, 1989).

241. T. F. Luscher, M. Barton, Endothelins and endothelin receptor antagonists: therapeutic considerations for a novel class of cardiovascular drugs. *Circulation* **102**, 2434 (Nov 7, 2000).

242. E. R. Levin, Endothelins. *The New England journal of medicine* **333**, 356 (Aug 10, 1995).

243. S. J. Wort *et al.*, Synergistic induction of endothelin-1 by tumor necrosis factor alpha and interferon gamma is due to enhanced NF-kappaB binding and histone acetylation at specific kappaB sites. *The Journal of biological chemistry* **284**, 24297 (Sep 4, 2009).

244. L. Rosano, F. Spinella, A. Bagnato, Endothelin 1 in cancer: biological implications and therapeutic opportunities. *Nature reviews. Cancer* **13**, 637 (Sep, 2013).

245. K. A. Strait, P. K. Stricklett, R. M. Kohan, D. E. Kohan, Identification of two nuclear factor of activated T-cells (NFAT)-response elements in the 5'-upstream regulatory region of the ET-1 promoter. *The Journal of biological chemistry* **285**, 28520 (Sep 10, 2010).

246. M. E. Lee, K. D. Bloch, J. A. Clifford, T. Quertermous, Functional analysis of the endothelin-1 gene promoter. Evidence for an endothelial cell-specific cis-acting sequence. *The Journal of biological chemistry* **265**, 10446 (Jun 25, 1990).

247. D. Li *et al.*, The inhibitory effect of miRNA-1 on ET-1 gene expression. *FEBS letters* **586**, 1014 (Apr 5, 2012).

248. L. R. Stow, M. E. Jacobs, C. S. Wingo, B. D. Cain, Endothelin-1 gene regulation. *FASEB journal : official publication of the Federation of American Societies for Experimental Biology* **25**, 16 (Jan, 2011).

249. T. Masaki, Historical review: Endothelin. *Trends in pharmacological sciences* **25**, 219 (Apr, 2004).

250. D. Xu *et al.*, ECE-1: a membrane-bound metalloprotease that catalyzes the proteolytic activation of big endothelin-1. *Cell* **78**, 473 (Aug 12, 1994).
251. H. Kido *et al.*, Human chymase, an enzyme forming novel bioactive 31-amino acid length endothelins. *Biological chemistry* **379**, 885 (Jul, 1998).
252. F. Kishi *et al.*, Novel 31-amino-acid-length endothelins cause constriction of vascular smooth muscle. *Biochemical and biophysical research communications* **248**, 387 (Jul 20, 1998).
253. F. D. Russell, A. P. Davenport, Evidence for intracellular endothelin-converting enzyme-2 expression in cultured human vascular endothelial cells. *Circulation research* **84**, 891 (Apr 30, 1999).
254. A. P. Davenport, R. E. Kuc, J. W. Mockridge, Endothelin-converting enzyme in the human vasculature: evidence for differential conversion of big endothelin-3 by endothelial and smooth-muscle cells. *Journal of cardiovascular pharmacology* **31 Suppl 1**, S1 (1998).
255. J. C. Yu, A. P. Davenport, Secretion of endothelin-1 and endothelin-3 by human cultured vascular smooth muscle cells. *British journal of pharmacology* **114**, 551 (Jan, 1995).
256. C. B. Neylon, Vascular biology of endothelin signal transduction. *Clinical and experimental pharmacology & physiology* **26**, 149 (Feb, 1999).
257. T. Sakurai, M. Yanagisawa, T. Masaki, Molecular characterization of endothelin receptors. *Trends in pharmacological sciences* **13**, 103 (Mar, 1992).
258. M. S. Goligorsky *et al.*, Termination of endothelin signaling: role of nitric oxide. *Journal of cellular physiology* **158**, 485 (Mar, 1994).
259. R. M. Kedzierski, M. Yanagisawa, Endothelin system: the double-edged sword in health and disease. *Annual review of pharmacology and toxicology* **41**, 851 (2001).
260. V. Raoch *et al.*, Nitric oxide decreases the expression of endothelin-converting enzyme-1 through mRNA destabilization. *Arteriosclerosis, thrombosis, and vascular biology* **31**, 2577 (Nov, 2011).
261. T. Horinouchi, K. Terada, T. Higashi, S. Miwa, Endothelin receptor signaling: new insight into its regulatory mechanisms. *Journal of pharmacological sciences* **123**, 85 (2013).
262. G. Remuzzi, N. Perico, A. Benigni, New therapeutics that antagonize endothelin: promises and frustrations. *Nature reviews. Drug discovery* **1**, 986 (Dec, 2002).
263. T. A. Wynn, Common and unique mechanisms regulate fibrosis in various fibroproliferative diseases. *The Journal of clinical investigation* **117**, 524 (Mar, 2007).
264. A. Leask, Potential therapeutic targets for cardiac fibrosis: TGFbeta, angiotensin, endothelin, CCN2, and PDGF, partners in fibroblast activation. *Circulation research* **106**, 1675 (Jun 11, 2010).
265. D. Lagares, O. Busnadiego, R. A. Garcia-Fernandez, S. Lamas, F. Rodriguez-Pascual, Adenoviral gene transfer of endothelin-1 in the lung induces pulmonary fibrosis through

the activation of focal adhesion kinase. *American journal of respiratory cell and molecular biology* **47**, 834 (Dec, 2012).

266. X. Shi-wen *et al.*, Endothelin is a downstream mediator of profibrotic responses to transforming growth factor beta in human lung fibroblasts. *Arthritis and rheumatism* **56**, 4189 (Dec, 2007).
267. X. Shi-Wen *et al.*, Endothelin-1 promotes myofibroblast induction through the ETA receptor via a rac/phosphoinositide 3-kinase/Akt-dependent pathway and is essential for the enhanced contractile phenotype of fibrotic fibroblasts. *Molecular biology of the cell* **15**, 2707 (Jun, 2004).
268. A. Segarra *et al.*, Dual transcriptomics of virus-host interactions: comparing two Pacific oyster families presenting contrasted susceptibility to ostreid herpesvirus 1. *BMC genomics* **15**, 580 (2014).
269. Z. Daher, J. Noel, A. Claing, Endothelin-1 promotes migration of endothelial cells through the activation of ARF6 and the regulation of FAK activity. *Cellular signalling* **20**, 2256 (Dec, 2008).
270. C. Castanares *et al.*, Signaling by ALK5 mediates TGF-beta-induced ET-1 expression in endothelial cells: a role for migration and proliferation. *Journal of cell science* **120**, 1256 (Apr 1, 2007).
271. L. Morbidelli, C. Orlando, C. A. Maggi, F. Ledda, M. Ziche, Proliferation and migration of endothelial cells is promoted by endothelins via activation of ETB receptors. *The American journal of physiology* **269**, H686 (Aug, 1995).
272. D. Salani *et al.*, Endothelin-1 induces an angiogenic phenotype in cultured endothelial cells and stimulates neovascularization in vivo. *The American journal of pathology* **157**, 1703 (Nov, 2000).
273. A. H. Chester, M. H. Yacoub, The role of endothelin-1 in pulmonary arterial hypertension. *Global cardiology science & practice* **2014**, 62 (2014).
274. J. P. Knowles *et al.*, Endothelin-1 stimulates colon cancer adjacent fibroblasts. *International journal of cancer. Journal international du cancer* **130**, 1264 (Mar 15, 2012).
275. M. Segarra *et al.*, Dual function of focal adhesion kinase in regulating integrin-induced MMP-2 and MMP-9 release by human T lymphoid cells. *FASEB journal : official publication of the Federation of American Societies for Experimental Biology* **19**, 1875 (Nov, 2005).
276. E. Lozano *et al.*, Increased expression of the endothelin system in arterial lesions from patients with giant-cell arteritis: association between elevated plasma endothelin levels and the development of ischaemic events. *Annals of the rheumatic diseases* **69**, 434 (Feb, 2010).
277. Y. Chen *et al.*, Contribution of activin receptor-like kinase 5 (transforming growth factor beta receptor type I) signaling to the fibrotic phenotype of scleroderma fibroblasts. *Arthritis and rheumatism* **54**, 1309 (Apr, 2006).

278. D. J. Abraham *et al.*, Increased levels of endothelin-1 and differential endothelin type A and B receptor expression in scleroderma-associated fibrotic lung disease. *The American journal of pathology* **151**, 831 (Sep, 1997).
279. A. Goel *et al.*, Increased endothelial exocytosis and generation of endothelin-1 contributes to constriction of aged arteries. *Circulation research* **107**, 242 (Jul 23, 2010).
280. L. V. d'Uscio, S. Shaw, M. Barton, T. F. Luscher, Losartan but not verapamil inhibits angiotensin II-induced tissue endothelin-1 increase: role of blood pressure and endothelial function. *Hypertension* **31**, 1305 (Jun, 1998).
281. M. Ihara *et al.*, In vitro biological profile of a highly potent novel endothelin (ET) antagonist BQ-123 selective for the ETA receptor. *Journal of cardiovascular pharmacology* **20 Suppl 12**, S11 (1992).
282. K. Ishikawa *et al.*, Biochemical and pharmacological profile of a potent and selective endothelin B-receptor antagonist, BQ-788. *Proceedings of the National Academy of Sciences of the United States of America* **91**, 4892 (May 24, 1994).
283. W. Stocker *et al.*, The metzincins--topological and sequential relations between the astacins, adamalysins, serralysins, and matrixins (collagenases) define a superfamily of zinc-peptidases. *Protein science : a publication of the Protein Society* **4**, 823 (May, 1995).
284. A. Page-McCaw, A. J. Ewald, Z. Werb, Matrix metalloproteinases and the regulation of tissue remodelling. *Nature reviews. Molecular cell biology* **8**, 221 (Mar, 2007).
285. M. D. Sternlicht, Z. Werb, How matrix metalloproteinases regulate cell behavior. *Annual review of cell and developmental biology* **17**, 463 (2001).
286. C. M. Overall, C. Lopez-Otin, Strategies for MMP inhibition in cancer: innovations for the post-trial era. *Nature reviews. Cancer* **2**, 657 (Sep, 2002).
287. Z. Wang, R. Juttermann, P. D. Soloway, TIMP-2 is required for efficient activation of proMMP-2 in vivo. *The Journal of biological chemistry* **275**, 26411 (Aug 25, 2000).
288. B. Coll-Vinent *et al.*, Circulating soluble adhesion molecules in patients with giant cell arteritis. Correlation between soluble intercellular adhesion molecule-1 (sICAM-1) concentrations and disease activity. *Annals of the rheumatic diseases* **58**, 189 (Mar, 1999).
289. M. C. Cid *et al.*, Association between increased CCL2 (MCP-1) expression in lesions and persistence of disease activity in giant-cell arteritis. *Rheumatology* **45**, 1356 (Nov, 2006).
290. D. Foell *et al.*, Early recruitment of phagocytes contributes to the vascular inflammation of giant cell arteritis. *The Journal of pathology* **204**, 311 (Nov, 2004).
291. Y. S. Choi *et al.*, Interleukin-33 induces angiogenesis and vascular permeability through ST2/TRAF6-mediated endothelial nitric oxide production. *Blood* **114**, 3117 (Oct 1, 2009).

292. S. Demyanets *et al.*, Interleukin-33 induces expression of adhesion molecules and inflammatory activation in human endothelial cells and in human atherosclerotic plaques. *Arteriosclerosis, thrombosis, and vascular biology* **31**, 2080 (Sep, 2011).
293. F. Ciccia *et al.*, IL-33 is overexpressed in the inflamed arteries of patients with giant cell arteritis. *Annals of the rheumatic diseases* **72**, 258 (Feb, 2013).
294. F. Ciccia *et al.*, Expression of interleukin-32 in the inflamed arteries of patients with giant cell arteritis. *Arthritis and rheumatism* **63**, 2097 (Jul, 2011).
295. B. Heinhuis *et al.*, Tumour necrosis factor alpha-driven IL-32 expression in rheumatoid arthritis synovial tissue amplifies an inflammatory cascade. *Annals of the rheumatic diseases* **70**, 660 (Apr, 2011).
296. G. Alsaleh *et al.*, Innate immunity triggers IL-32 expression by fibroblast-like synoviocytes in rheumatoid arthritis. *Arthritis research & therapy* **12**, R135 (2010).
297. M. Shioya *et al.*, Epithelial overexpression of interleukin-32alpha in inflammatory bowel disease. *Clinical and experimental immunology* **149**, 480 (Sep, 2007).
298. F. Larousserie *et al.*, Expression of IL-27 in human Th1-associated granulomatous diseases. *The Journal of pathology* **202**, 164 (Feb, 2004).
299. J. Hernandez-Rodriguez *et al.*, A strong initial systemic inflammatory response is associated with higher corticosteroid requirements and longer duration of therapy in patients with giant-cell arteritis. *Arthritis and rheumatism* **47**, 29 (Feb, 2002).
300. M. Segarra *et al.*, Gelatinase expression and proteolytic activity in giant-cell arteritis. *Annals of the rheumatic diseases* **66**, 1429 (Nov, 2007).
301. T. Tomita, K. Imakawa, Matrix metalloproteinases and tissue inhibitors of metalloproteinases in giant cell arteritis: an immunocytochemical study. *Pathology* **30**, 40 (Feb, 1998).
302. A. D. Wagner, J. J. Goronzy, C. M. Weyand, Functional profile of tissue-infiltrating and circulating CD68+ cells in giant cell arteritis. Evidence for two components of the disease. *The Journal of clinical investigation* **94**, 1134 (Sep, 1994).
303. A. Rodriguez-Pla *et al.*, Metalloproteinase-2 and -9 in giant cell arteritis: involvement in vascular remodeling. *Circulation* **112**, 264 (Jul 12, 2005).
304. S. T. Nikkari, M. Hoyhtya, J. Isola, T. Nikkari, Macrophages contain 92-kd gelatinase (MMP-9) at the site of degenerated internal elastic lamina in temporal arteritis. *The American journal of pathology* **149**, 1427 (Nov, 1996).
305. D. Sorbi *et al.*, Elevated levels of 92-kd type IV collagenase (matrix metalloproteinase 9) in giant cell arteritis. *Arthritis and rheumatism* **39**, 1747 (Oct, 1996).
306. E. Lozano, M. Segarra, A. Garcia-Martinez, J. Hernandez-Rodriguez, M. C. Cid, Imatinib mesylate inhibits in vitro and ex vivo biological responses related to vascular occlusion in giant cell arteritis. *Annals of the rheumatic diseases* **67**, 1581 (Nov, 2008).
307. F. Ciccia *et al.*, Difference in the expression of IL-9 and IL-17 correlates with different histological pattern of vascular wall injury in giant cell arteritis. *Rheumatology*, (Apr 9, 2015).

308. M. C. Cid *et al.*, Association between strong inflammatory response and low risk of developing visual loss and other cranial ischemic complications in giant cell (temporal) arteritis. *Arthritis and rheumatism* **41**, 26 (Jan, 1998).

309. V. D. Marinescu, I. S. Kohane, A. Riva, MAPPER: a search engine for the computational identification of putative transcription factor binding sites in multiple genomes. *BMC bioinformatics* **6**, 79 (2005).

310. D. Chow, X. He, A. L. Snow, S. Rose-John, K. C. Garcia, Structure of an extracellular gp130 cytokine receptor signaling complex. *Science* **291**, 2150 (Mar 16, 2001).

311. P. S. Cooper *et al.*, Education resources of the National Center for Biotechnology Information. *Briefings in bioinformatics* **11**, 563 (Nov, 2010).

312. M. Buryskova, M. Pospisek, A. Grothey, T. Simmet, L. Burysek, Intracellular interleukin-1alpha functionally interacts with histone acetyltransferase complexes. *The Journal of biological chemistry* **279**, 4017 (Feb 6, 2004).

313. M. Hibi *et al.*, Molecular cloning and expression of an IL-6 signal transducer, gp130. *Cell* **63**, 1149 (Dec 21, 1990).

314. D. Chen, J. Nicholas, Structural requirements for gp80 independence of human herpesvirus 8 interleukin-6 (vIL-6) and evidence for gp80 stabilization of gp130 signaling complexes induced by vIL-6. *Journal of virology* **80**, 9811 (Oct, 2006).

315. J. Molden, Y. Chang, Y. You, P. S. Moore, M. A. Goldsmith, A Kaposi's sarcoma-associated herpesvirus-encoded cytokine homolog (vIL-6) activates signaling through the shared gp130 receptor subunit. *The Journal of biological chemistry* **272**, 19625 (Aug 1, 1997).

316. Y. Aoki, M. Narazaki, T. Kishimoto, G. Tosato, Receptor engagement by viral interleukin-6 encoded by Kaposi sarcoma-associated herpesvirus. *Blood* **98**, 3042 (Nov 15, 2001).

317. D. Chen, G. Sandford, J. Nicholas, Intracellular signaling mechanisms and activities of human herpesvirus 8 interleukin-6. *Journal of virology* **83**, 722 (Jan, 2009).

318. M. Romano *et al.*, Role of IL-6 and its soluble receptor in induction of chemokines and leukocyte recruitment. *Immunity* **6**, 315 (Mar, 1997).

319. X. Chen *et al.*, The expression of interleukin-23 (p19/p40) and interleukin-12 (p35/p40) in psoriasis skin. *Journal of Huazhong University of Science and Technology. Medical sciences = Hua zhong ke ji da xue xue bao. Yi xue Ying De wen ban = Huazhong keji daxue xuebao. Yixue Yingdewen ban* **26**, 750 (2006).

320. G. G. Krueger *et al.*, A human interleukin-12/23 monoclonal antibody for the treatment of psoriasis. *The New England journal of medicine* **356**, 580 (Feb 8, 2007).

321. T. Kopp *et al.*, Clinical improvement in psoriasis with specific targeting of interleukin-23. *Nature* **521**, 222 (May 14, 2015).

322. H. Jethwa, P. Bowness, The interleukin (IL)-23/IL-17 axis in ankylosing spondylitis: new advances and potentials for treatment. *Clinical and experimental immunology*, (Jun 17, 2015).

323. J. J. O'Shea, Y. Kanno, A. C. Chan, In search of magic bullets: the golden age of immunotherapeutics. *Cell* **157**, 227 (Mar 27, 2014).
324. W. Skowron *et al.*, The effect of interleukin-35 on the integrity, ICAM-1 expression and apoptosis of human aortic smooth muscle cells. *Pharmacological reports : PR* **67**, 376 (Apr, 2015).
325. X. Li *et al.*, IL-35 is a novel responsive anti-inflammatory cytokine--a new system of categorizing anti-inflammatory cytokines. *PloS one* **7**, e33628 (2012).
326. S. Kempe *et al.*, Epstein-barr virus-induced gene-3 is expressed in human atheroma plaques. *The American journal of pathology* **175**, 440 (Jul, 2009).
327. W. Niedbala *et al.*, IL-35 is a novel cytokine with therapeutic effects against collagen-induced arthritis through the expansion of regulatory T cells and suppression of Th17 cells. *European journal of immunology* **37**, 3021 (Nov, 2007).
328. M. Filkova *et al.*, Proinflammatory effects of interleukin-35 in rheumatoid arthritis. *Cytokine* **73**, 36 (May, 2015).

Additional Data

ARD Online First, published on December 23, 2015 as 10.1136/annrheumdis-2015-208371

EXTENDED REPORT

Blocking interferon γ reduces expression of chemokines CXCL9, CXCL10 and CXCL11 and decreases macrophage infiltration in ex vivo cultured arteries from patients with giant cell arteritis

Marc Corbera-Bellalta,[1] Ester Planas-Rigol,[1] Ester Lozano,[1] Nekane Terrades-García,[1] Marco A Alba,[1] Sergio Prieto-González,[1] Ana García-Martínez,[2] Robert Albero,[3] Anna Enjuanes,[4] Georgina Espígol-Frigolé,[1] José Hernández-Rodríguez,[1] Pascale Roux-Lombard,[5] Walter G Ferlin,[6] Jean-Michel Dayer,[7] Marie H Kosco-Vilbois,[5] Maria C Cid[1]

Handling editor Tore K Kvien

▶ Additional material is published online only. To view please visit the journal online (http://dx.doi.org/10.1136/annrheumdis-2015-208371).

For numbered affiliations see end of article.

Correspondence to
Dr Maria C Cid, Department of Autoimmune Diseases, Hospital Clínic, Villarroel 170, Barcelona 08036, Spain; mccid@clinic.ub.es

Received 4 August 2015
Revised 26 October 2015
Accepted 6 November 2015

ABSTRACT

Background Interferon γ (IFNγ) is considered a seminal cytokine in the pathogenesis of giant cell arteritis (GCA), but its functional role has not been investigated. We explored changes in infiltrating cells and biomarkers elicited by blocking IFNγ with a neutralising monoclonal antibody, A6, in temporal arteries from patients with GCA.

Methods Temporal arteries from 34 patients with GCA (positive histology) and 21 controls were cultured on 3D matrix (Matrigel) and exposed to A6 or recombinant IFNγ. Changes in gene/protein expression were measured by qRT-PCR/western blot or immunoassay. Changes in infiltrating cells were assessed by immunohistochemistry/immunofluorescence. Chemotaxis/adhesion assays were performed with temporal artery-derived vascular smooth muscle cells (VSMCs) and peripheral blood mononuclear cells (PBMCs).

Results Blocking endogenous IFNγ with A6 abrogated STAT-1 phosphorylation in cultured GCA arteries. Furthermore, selective reduction in CXCL9, CXCL10 and CXCL11 chemokine expression was observed along with reduction in infiltrating CD68 macrophages. Adding IFNγ elicited consistent opposite effects. IFNγ induced CXCL9, CXCL10, CXCL11, CCL2 and intracellular adhesion molecule-1 expression by cultured VSMC, resulting in increased PBMC chemotaxis/adhesion. Spontaneous expression of chemokines was higher in VSMC isolated from GCA-involved arteries than in those obtained from controls. Incubation of IFNγ-treated control arteries with PBMC resulted in adhesion/infiltration by CD68 macrophages, which did not occur in untreated arteries.

Conclusions Our ex vivo system suggests that IFNγ may play an important role in the recruitment of macrophages in GCA by inducing production of specific chemokines and adhesion molecules. Vascular wall components (ie, VSMC) are mediators of these functions and may facilitate progression of inflammatory infiltrates through the vessel wall.

To cite: Corbera-Bellalta M, Planas-Rigol E, Lozano E, *et al*. *Ann Rheum Dis* Published Online First: [*please include* Day Month Year] doi:10.1136/annrheumdis-2015-208371

INTRODUCTION

Giant cell arteritis (GCA) is a chronic inflammatory disease targeting large and medium-sized arteries in aged individuals.[1] In spite of the initial response to high-dose glucocorticoids (GCs), 40–60% of patients relapse when GCs are tapered and prolonged GC treatment results in significant side effects.[2]

Search for new therapeutic options requires better understanding of pathogenesis. GCA has been classically considered a Th1-mediated disease based on the granulomatous nature of inflammatory lesions with the presence of giant cells.[1 3] Moreover, while transcripts of several cytokines (ie, interleukin (IL)-6, tumour necrosis factor-α (TNFα) can be detected in unaffected temporal artery biopsies (TABs),[4–7] IFNγ, the distinctive cytokine produced by Th1 lymphocytes, is selectively expressed in GCA lesions.[4 7–12] Recently, Th17-mediated mechanisms are also emerging as a relevant component of GCA pathogenesis.[9–13]

IFNγ has important roles in innate and adaptive immunity. It is primarily expressed by Th1 and natural killer (NK) cells and also by plasmacytoid dendritic cells, B cells and macrophages.[14 15] IFNγ signals by inducing dimerisation of its receptor chains, which, in turn, induces phosphorylation of JAK 1 and JAK 2, creating binding sites for STAT-1.[14 16 17] STAT-1 phosphorylation results in STAT-1 dimerisation or formation of multimolecular complexes (ie, ISFG3 composed by STAT-1, STAT-2 and IRF9 molecules) subsequently inducing transcription of genes bearing gamma-activated sequences or interferon-stimulated responsive elements (ISREs), respectively, in their promoter regions.[14 16 17] Some of the STAT-1-induced target genes are themselves transcription factors (ie, IRFs), creating subsequent waves of inflammatory molecule expression.[18] Adding complexity, IFNγ may also induce STAT-3, particularly in conditions of STAT-1 paucity.[19] IFNγ promotes NK cell activity, macrophage activation, Th1 differentiation and expression of class I and class II major histocompatibility complex molecules on antigen-presenting cells.[14–21] Based on these functions, IFNγ is thought to have a major role in GCA. Its expression by adventitial infiltrates in early GCA lesions suggests a relevant role from the initial steps of vascular inflammation.[11 22]

To date, no mechanistic studies assessing the role of IFNγ in the development of full-blown lesions in GCA have been performed. In this study, we explored functional roles of IFNγ on GCA lesions by exposing cultured temporal artery sections from patients with GCA to a neutralising anti-human IFNγ monoclonal antibody.

PATIENTS AND METHODS

Patient samples

TABs were performed to 55 patients with suspected GCA for diagnostic purposes. A 5–15 mm segment was saved for the present study. Thirty-four patients had histopathological features of GCA in their TAB. Thirteen of them had started GC treatment 3.6±3.2 days before TAB. Twenty-one patients had no inflammatory infiltrates and served as controls. Clinical data of GCA patients and final diagnosis in control patients are disclosed in online supplementary tables S1 and S2, respectively.

Neutralising, monoclonal antibody A6 against IFNγ

A6 is a fully human monoclonal antibody generated in the laboratories of Novimmune (Geneva, Switzerland) from human immunoglobulin libraries using in vitro display technologies. A6 binds to human IFNγ and neutralises its bioactivity.

Temporal artery culture

Temporal artery sections from patients with GCA and controls were embedded in Matrigel to ensure prolonged survival, cultured ex vivo as described[7] with or without A6 antibody (10 µg/mL), recombinant IFNγ at 100 ng/mL (R&D Systems, Minneapolis, Minnesota, USA), human non-immune immunoglobulin IgG1 at 10 µg/mL (Sigma, Ayrshire, UK) as a negative control or dexamethasone (0.5 µg/mL, Sigma). Each condition was tested in 3–4 replicate wells. Biopsies were frozen in TRIzol reagent (Life Technologies) for RNA extraction or in radioimmunoprecipitation assay buffer with protease and phosphatase inhibitors for western blot studies.

Cell culture

Vascular smooth muscle cells (VSMCs) were isolated from TABs as previously described[22] and used after 3–8 doubling passages. Peripheral blood mononuclear cells (PBMCs) were obtained from whole blood of healthy donors using Lymphoprep (Axis-Shield, Oslo, Norway) (see culture details in online supplementary methods).

In specific experiments, VSMCs were seeded in 12-well plates and cultured alone or with 0.5×10^6 PBMC/well. At the end of the co-culture period, PBMCs were isolated from supernatants by centrifugation. The underlying VSMCs were separately recovered after gentle treatment with EDTA (Versene, Life Technologies) to remove adherent PBMC.

Gene expression analysis

Total RNA was obtained from cultured arteries or cells and cDNA was obtained by reverse-transcription (see online supplementary methods). Specific pre-developed TaqMan probes from Applied Biosystems (TaqMan Gene Expression Assays) (see online supplementary table S3) were used for PCR amplification. Fluorescence was detected with ABI PRISM 7900 Hardware and results were analysed with the Sequence Detection Software V.2.3 (Applied Biosystems). Gene expression was normalised to the expression of the endogenous control GUSb using comparative ΔCt method.[5–7 11] mRNA concentration was expressed in relative units with respect to GUSb expression.

Chemokine secretion

CXCL9, CXCL10 and CXCL11 concentrations in supernatants were measured by immunoassay using Quantikine (R&D Systems).

STAT-1 and STAT-3 phosphorylation in cultured arteries

Lysates were obtained from cultured artery sections or VSMC and phospho-STAT-1/total STAT-1 and phosho-STAT-3/total STAT-3 were assessed by western blot (see online supplementary methods).

Immunohistochemistry and immunofluorescence staining

Detailed immunostaining of cultured temporal artery sections or VSMC, as well as primary and secondary antibodies used, are depicted in online supplementary methods.

Chemotaxis assay

PBMC chemotaxis was assessed using Boyden chambers with 5 µm pore polycarbonate filters (see specific details in online supplementary methods).

Cell adhesion assays

VSMCs were grown to confluence in 96-well plates and stimulated with recombinant IFNγ. After 24 h 7.5×10^4 PBMCs per well were added and incubated at 37°C for 30 min. Wells were gently rinsed with phosphate-buffered saline and cells were fixed and stained with 0.2% crystal violet in 20% methanol for 10 min. Plates were extensively washed and crystal violet was solubilised with 1% sodium dodecyl sulfate (50 µL/well). Optical density was assessed by spectrophotometry at 560 nm wavelength.

Statistical analysis

Student's t test, when applicable, or Mann–Whitney test was applied for independent or paired samples for statistical analysis using SPSS software, PASW V.18.0.

RESULTS

Clone A6, a neutralising human monoclonal antibody against IFNγ, recognises IFNγ in GCA lesions and interferes with IFNγ-mediated signalling

Since A6 was screened and selected by its potential to neutralise IFNγ in vitro, we assessed its ability to bind IFNγ expressed in GCA lesions. As shown in figure 1, biotinylated A6 antibody immunostained GCA-involved temporal artery sections, whereas immunostaining with biotinylated human IgG1 was negative. Moreover, immunostaining of non-inflamed temporal artery sections from a control individual was negative according to the absence of IFNγ expression in normal arteries.[4 7]

Temporal artery culture in 3-D matrix has been shown to be a suitable model to test the effects of easily diffusing molecules such as dexamethasone.[7] However, it is not known whether complex molecules such as monoclonal antibodies are able to elicit biological responses in this system. To test this point, we investigated whether A6 was able to interfere with IFNγ-mediated signalling in cultured arteries by exploring the phosphorylation status of the transcription factors STAT-1 and STAT-3. As shown in figure 1E, F, normal arteries in culture had a remarkable constitutive expression and phosphorylation of STAT-3 but not STAT-1. Involved GCA arteries in culture had increased expression and phosphorylation of STAT-1 and decreased expression and phosphorylation of STAT-3 compared with cultured normal arteries. A6 antibody decreased expression and phosphorylation of STAT-1, whereas STAT-3 expression/

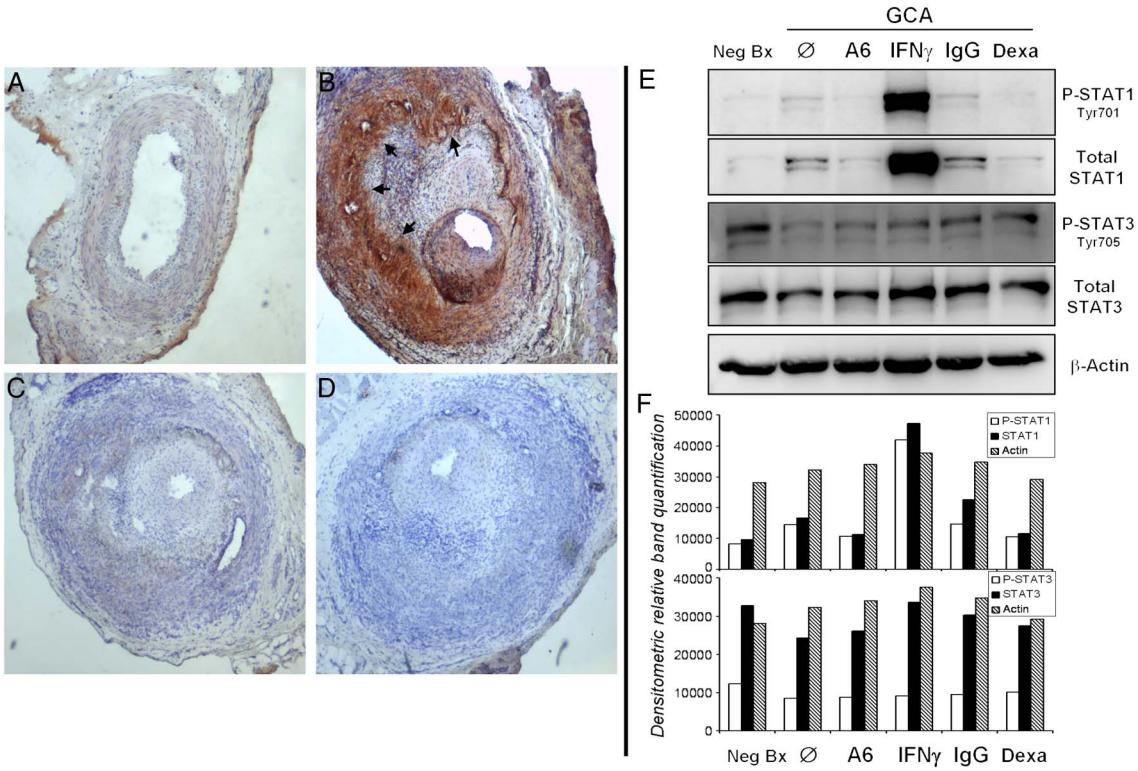

Figure 1 Interferon γ (IFNγ) expression in arteries with giant cell arteritis (GCA) and the effects of IFNγ on cultured temporal arteries from patients with GCA. (A–D) Immunostaining with A6 or control IgG1 on normal temporal arteries or GCA-involved arteries. (A) Histologically negative temporal artery from a control individual incubated with biotinylated A6 (negative control). (B) GCA-involved artery incubated with biotinylated A6 antibody (brown staining reflects IFNγ expression). (C) A GCA-involved artery incubated with biotinylated non-immune human IgG1 (isotype control). (D) A GCA-involved artery incubated with the detection system reagents but no A6 (negative control). (E) Western blot performed to assess phosphorylated or total STAT-1 and STAT-3 in protein extracts of a cultured histologically negative biopsy (Neg Bx) and a cultured GCA-involved biopsy (GCA) untreated (Ø), exposed to A6 (10 μg/mL), IFNγ (100 ng/mL), human IgG1 (IgG; 10 μg/mL) or dexamethasone (Dexa; 0.5 μg/mL) for 5 days. The experiment was repeated twice with consistent results and a representative blot is shown. β-Actin was used as a control for loading. (F) Densitometric analysis of bands obtained in western blot experiments is exemplified in (E).

phosphorylation was not substantially affected. Treatment with recombinant IFNγ strongly increased expression and phosphorylation of STAT-1.

Neutralising endogenous IFNγ production selectively downregulates CXCL9, CXCL10, CXCL11 chemokines and STAT-1 expression in cultured GCA arteries: adding exogenous IFNγ elicits opposite effects

We investigated the effects of neutralising IFNγ with A6 on the expression of a variety of candidate molecules relevant to the pathogenesis of vascular inflammation and remodelling in GCA.[3 5 11 22–30] Molecules investigated included transcription factors involved in T-cell functional differentiation, proinflammatory cytokines, chemokines/chemokine receptors, adhesion molecules, growth factors, metalloproteinases and their natural inhibitors, and extracellular matrix proteins (table 1 and figure 2). Since the temporal artery culture conveys by itself a downregulation of IFNγ expression with respect to the original fresh arteries, which may have minimised these results,[7] we sought to confirm the potential effects of IFNγ revealed by inhibition with A6 antibody by treating cultured GCA arteries with recombinant IFNγ.

Among the molecules tested, neutralising endogenous IFNγ with A6 mainly downregulated STAT-1 and chemokine CXCL9, CXCL10 and CXCL11 mRNAs (figure 2A). As shown in figure 2B, exposure of cultured GCA arteries to IFNγ elicited the expected opposite effects and induced strong expression of STAT-1 and chemokines CXCL9, CXCL10 and CXCL11 (figure 2B). CXCL9 and CXCL10 concentrations in the supernatant fluid were also reduced upon A6 antibody treatment and increased under exposure to recombinant IFNγ (figure 2C). Concentrations of CXCL11 were around the detection level and were not substantially modified by A6 antibody or recombinant IFNγ, suggesting that CXCL11 is not secreted or is retained in the extracellular matrix.

Table 1 shows the effect of blocking IFNγ with A6, as well as the effect of adding recombinant IFNγ on the additional molecules tested. Neutralising IFNγ with A6 tended to decrease HLA-DRA, TBX21, NOS-2, TNFα, IL-6, CCL2, CXCR3, intracellular adhesion molecule-1 (ICAM-1) and platelet-derived growth factor A mRNAs and, consistently, these tended to increase upon exposure to recombinant IFNγ. However, with the exception of TNFα, differences were not statistically significant, possibly due to the relatively low number of specimens analysed and the wide individual variability in expression of inflammatory products. Dexamethasone was able to markedly downregulate additional relevant molecules not influenced by A6 (table 1).

VSMCs contribute to chemokine production induced by IFNγ

Most of the effects of IFNγ have been investigated in T cells, monocytes and endothelial cells. To mimic vascular inflammatory infiltrates, we co-cultured PBMC from healthy donors with human temporal artery-derived VSMC, the main component of the arterial wall. Co-culture induced a variety of chemokines

Table 1 Mean fold change in mRNA of selected representative genes related to T helper functional differentiation, inflammation and vascular remodelling in cultured temporal arteries from 34 patients with GCA and 21 controls subjected to different treatments (control IgG1, A6, recombinant IFNγ or dexamethasone)

	GCA/control	GCA biopsies		
Fold increase		Clone A6/IgG1	IFNγ/untreated	Dexa/ untreated
Transcription factors				
TBX21	3.1154*	**0.7133**	**2.7776***	0.9522
GATA3	1.7611*	1.1780	1.3536	0.7716
RORC	3.6482*	0.8558	1.3571	0.8380*
STAT-3	0.5913	0.9232	1.6143	1.0565
Proinflammatory molecules				
Cytokines				
IL-1β	3.6162*	0.9041	1.1481	0.0342
TNFα	1.6621*	**0.7561***	**2.7333***	0.3047*
IL-6	1.4685	**0.7026**	**1.5621**	0.0757*
IFNγ	15.0840*	0.9119	0.6848	0.3869*
IL17A	103.5418*	1.4793	0.5557	0.0279*
Chemokines				
CCL2	1.6839	**0.8950**	**1.2292**	0.3424*
CCL3	6.3415*	0.9815	0.4381	0.2125*
CCL4	13.9455*	1.0598	0.1611	0.2058
CCL5	4.8446*	1.2153	1.3709	0.6600
CXCL8	1.3023	0.9805	0.9512	0.0748*
Chemokine receptors				
CCR2	6.9054*	1.3463	2.6116	0.5746
CXCR3	10.0717*	**0.6640**	**2.1125***	Not done
Adhesion molecules				
ICAM-1	1.7275	**0.8225**	**2.0204**	0.1137
VCAM-1	0.7031	0.9611	1.6861	0.0787
Other				
HLADRA	3.8304*	**0.7373**	**3.0312***	0.8810
NOS-2	1.7010	**0.2443**	**2.7067**	1.7251
Vascular remodelling-related molecules				
Growth factors				
PDGFA	0.4752*	**0.7690**	**1.6640**	0.4331
PDGFB	0.6820	0.8081	1.0921	0.6338
TGFβ	0.6106*	1.0119	1.2298	0.5117
Extracellular matrix proteins				
FN1	0.8757	1.0473	Not done	2.3182
COL1	1.9086	0.9953	Not done	0.9594
COL3	0.9037	0.8602	Not done	1.0790
Metalloproteases				
MMP-2	0.5738*	0.9101	0.5082	0.5827
MMP-9	2.3692*	0.8468	0.8204	0.0708*
MMP inhibitors				
TIMP1	1.8323*	0.9844	1.0956	0.3405*
TIMP2	0.5663*	0.9815	0.9614	0.7737

Number of specimens analysed: negative biopsies: 21; untreated GCA: 29; GCA treated with A6: 21; GCA treated with IgG1: 18; GCA treated with IFNγ: 9; GCA treated with dexamethasone: 11.
Bold values indicate consistent opposite results achieved by blocking IFNγ with A6 or by adding recombinant IFNγ.
*p<0.05.
Clone A6, anti-human IFNγ monoclonal antibody; GCA, giant cell arteritis; IgG1, isotype-matched control immunoglobulin; ICAM, intracellular adhesion molecule; IFNγ, recombinant interferon γ; MMP, matrix metalloproteinases; PDGF, platelet-derived growth factor.

not only in PBMC but also in VSMC, indicating that VSMCs are an active source of chemokines in an inflammatory microenvironment (figure 3A). IFNγ was produced and secreted by PBMC, basally and in co-culture (see online supplementary figure S1). In accordance with the previous results, neutralising IFNγ with A6 strongly and selectively inhibited CXCL9, CXCL10 and CXCL11 chemokine expression by all cell types (figure 3A). A slight, non-significant, reduction in STAT-1 and adhesion molecule ICAM-1 was observed. No effects of A6 were observed on the expression of STAT-3, VCAM-1 or other chemokines tested in this multicellular system (figure 3A and online supplementary figure S2).

To confirm that VSMC are an important source of chemokines upon IFNγ influence, we exposed human temporal artery-derived VSMC to IFNγ, which elicited a remarkable increase in STAT-1 (figure 3B). An induction of CXCL9, CXCL10 and CXCL11 and upregulation of constitutive CCL2 was obtained, whereas expression of other chemokines related to Th1 responses (ie, CCL3, CCL4 or CCL5) or CXCL8 was not significantly induced (figure 3B). Promoter analysis (4 kb upstream and 1 kb downstream of the transcription initiating sequence) of chemokine genes was performed using Chip Bioinformatics Mapper (http://snpper.chip.org/mapper/mapper-main).[31] The promoters of CXCL9, 10, and 11 as well as CCL2 shared ISRE sequences, whereas the remaining chemokines tested did not, supporting the exquisite sensitivity of these cytokines to IFNγ exposure. However, although IFNγ significantly upregulated constitutive CCL2 expression by cultured VSMC, A6 failed to downregulate CCL2 in multicellular systems such as PBMC/VSMC co-culture or whole GCA arteries where other inducers may be present (table 1 and figure 3A).

As previously demonstrated in other settings,[18 32 33] IFNγ also upregulated STAT-1 and adhesion molecule ICAM-1 expression by cultured VSMC and induced a slight expression of VCAM-1 and STAT-3 (figure 3B).

We next cultured temporal artery-derived VSMC from 8 patients and 11 controls and investigated chemokine production at passage zero to avoid phenotypic changes induced by prolonged culture. As shown in figure 3C, patient-derived VSMC conserved IFNγ signature and expressed significantly higher mRNA concentrations of IFNγ-induced chemokine CXCL9 and a tendency to increased expression of CXCL10 and CCL2 than VSMC derived from control individuals. Higher mRNA concentrations of other chemokines not clearly influenced by IFNγ in our experiments, particularly CCL4, were also observed. This may indicate VSMC exposure to stimuli other than IFNγ or to second-wave IFNγ-induced mediators in the complex multicellular and multimolecular microenvironment existing in GCA lesions.

Functional relevance of chemokine and adhesion molecule expression by VSMC

Treatment of cultured temporal artery-derived VSMC with IFNγ resulted in an increase in adhesion to PBMC (figure 4A).

The effect of IFNγ on ICAM-1 expression by VSMC was confirmed in GCA lesions. VSMC expressed ICAM-1 in cultured GCA arteries, particularly in the vicinity of inflammatory infiltrates. ICAM-1 expression was reduced in sections treated with A6 antibody and increased in sections treated with IFNγ (figure 4B). As already described,[25] ICAM-1 expression was also observed in *vasa vasorum* endothelial cells and inflammatory cells (figure 4B).

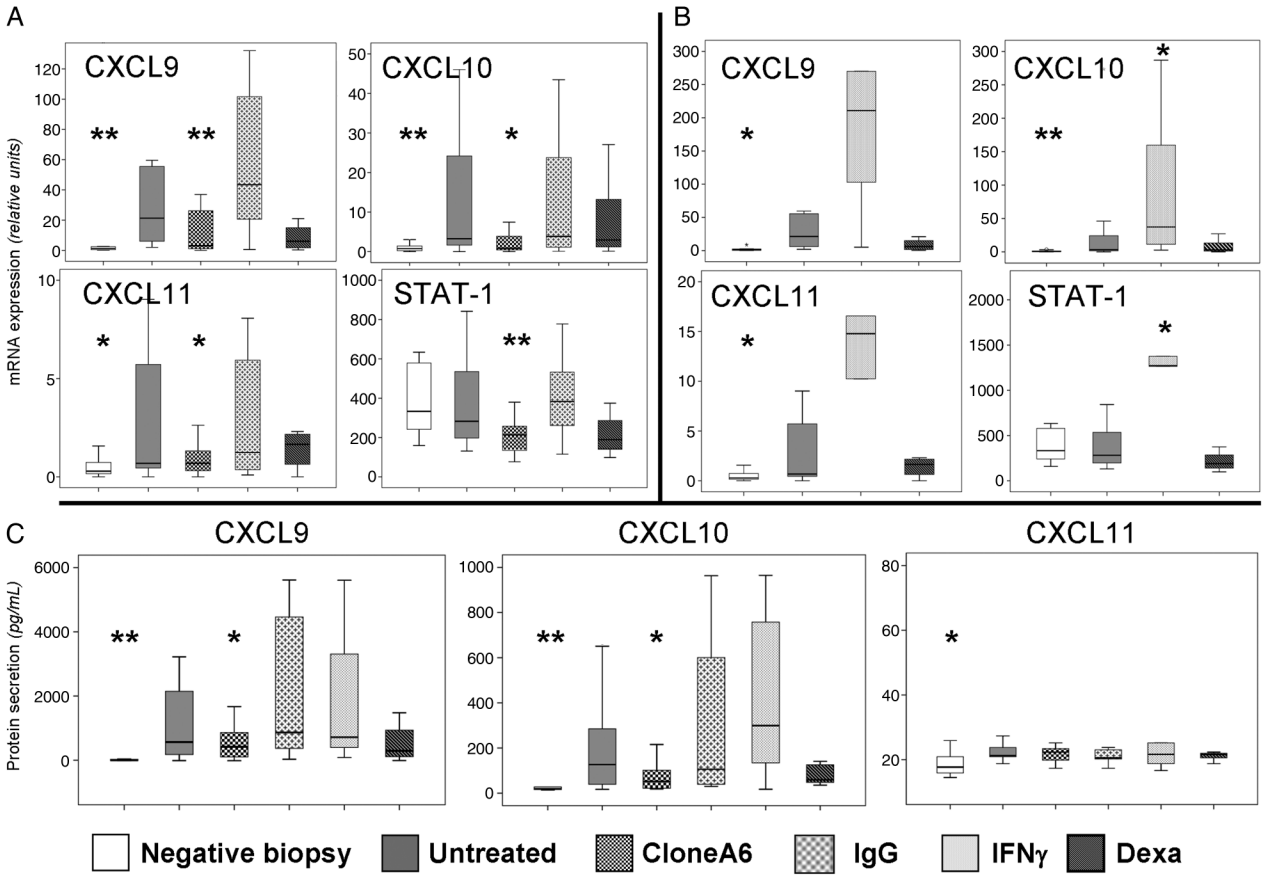

Figure 2 Changes in gene expression and protein secretion induced by blocking interferon γ (IFNγ) with A6 or adding additional IFNγ on cultured giant cell arteritis (GCA) biopsies. (A) mRNA concentrations (relative units) of CXCL9, CXCL10, CXCL11 and STAT-1 in cultured control arteries (negative biopsy) versus cultured GCA-involved arteries untreated or exposed to A6, human IgG1, or dexamethasone (Dexa) at the same concentrations as in figure 1. Statistical comparisons was performed between histologically negative and GCA-involved arteries and between IgG1-treated and A6-treated GCA involved arteries. *p<0.05; **p<0.005. Notice that the Y scale is different for each molecule. (B) mRNA concentrations (relative units) of CXCL9, CXCL10, CXCL11 and STAT-1 in cultured histologically negative arteries (negative biopsy) versus GCA-involved arteries untreated, or exposed to IFNγ or dexamethasone (Dexa) at the same concentrations as in figure 1 in a different set of experiments. Statistical comparison was performed between histologically negative and GCA-involved arteries and between GCA arteries untreated or treated with recombinant IFNγ. *p<0.05; **p<0.005. Notice that the Y scale is different for each molecule. (C) CXCL9, CXCL10 and CXCL11 concentrations (pg/mL) in the supernatants of cultured normal arteries and GCA-affected arteries untreated or exposed to A6, human IgG1, IFNγ or Dexa at the same concentrations as in figure 1. Statistical comparison was performed between histologically negative and GCA-involved arteries and between IgG1-treated and A6-treated GCA involved arteries. *p<0.05; **p<0.005.

Chemokine-rich supernatant of VSMC exposed to IFNγ stimulated PBMC chemotaxis in Boyden chambers (figure 4C), and this increase was abrogated by an antagonist of CXCR3, chemokine receptor common to CCL9, CXCL10 and CXCL11.

Effects of IFNγ neutralisation on infiltrating mononuclear cells in cultured temporal arteries from patients with GCA

The above findings suggest an important role for IFNγ in the initial recruitment of inflammatory cells in temporal arteries from patients with GCA and the participation of VSMC, the major component of normal arteries in this process. To confirm this hypothesis, normal temporal arteries were exposed to recombinant IFNγ and induction of CXCL9, CXCL10 and CXCL11 was confirmed (figure 5A). Incubation of IFNγ-treated normal arteries with PBMC from healthy donors resulted in infiltration of the artery wall by CD68 macrophages, which formed aggregates resembling giant cells (figure 5B). No CD3-positive cells penetrated the artery walls.

We next exposed cultured temporal arteries from patients with GCA to A6 and explored changes in the number of infiltrating T cells (CD3) and macrophages (CD68). Blocking IFNγ did not decrease the number of T cells (data not shown) but reduced the number of CD68-expressing cells and abrogated the presence of giant cells (figures 5C, D).

DISCUSSION

In this study, the first attempt to investigate the functional role of IFNγ in GCA, blocking endogenous IFNγ with a neutralising anti-IFNγ antibody, led to a significant reduction of STAT-1 and chemokine CXCL9, CXCL10 and CXCL11 expression in ex vivo cultured GCA arteries. Moreover, neutralising IFNγ resulted in decreased infiltration by CD68-expressing macrophages and reduced expression of TNFα along with a non-significant trend to decrease inflammatory molecules typical of a proinflammatory (M1-like) phenotype (HLA-DRA and inducible nitric oxide synthase).[20] These molecules, previously known to be expressed in GCA, are modulated by IFNγ in other

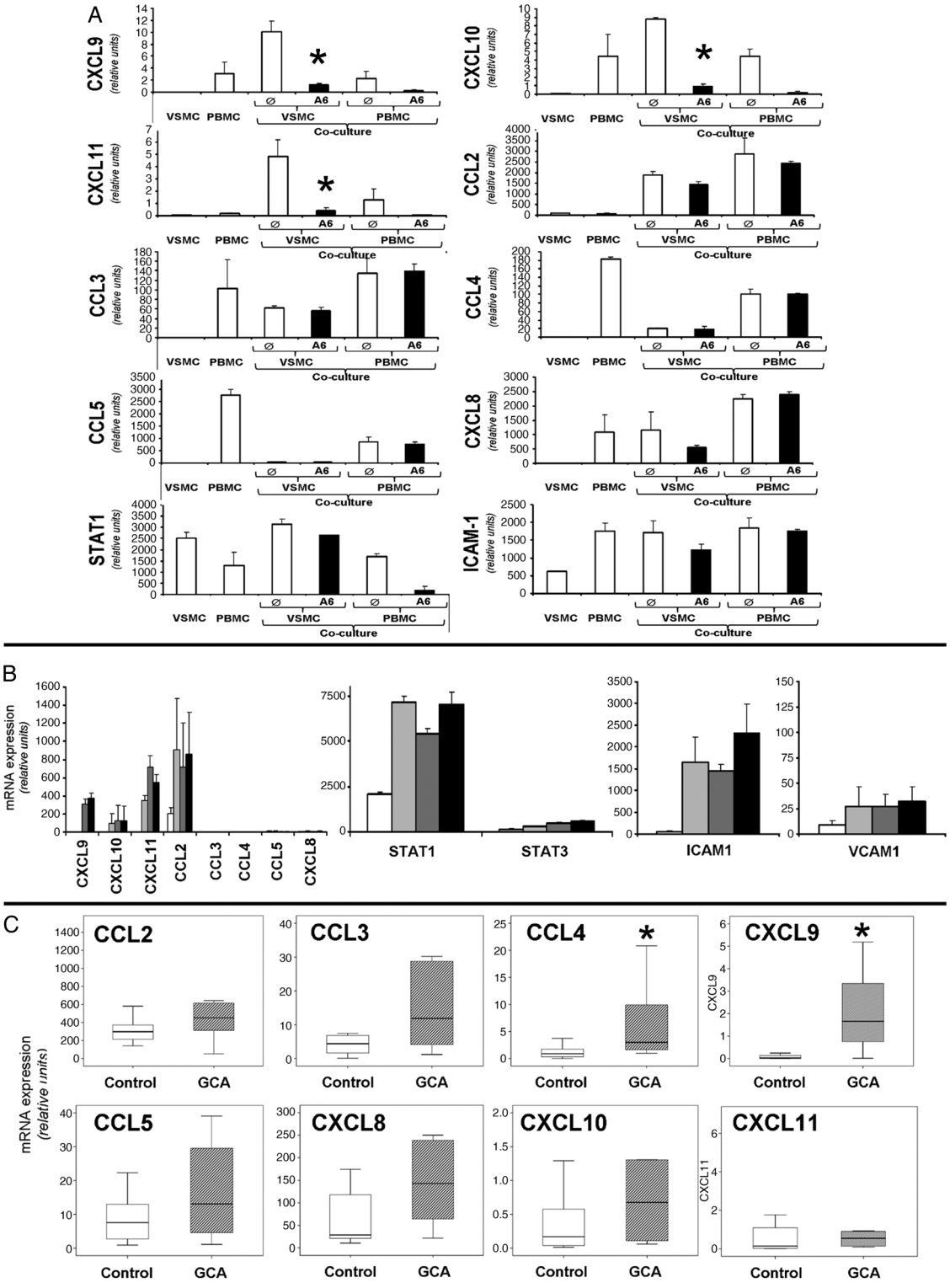

Figure 3 Effect of blocking the spontaneous interferon γ (IFNγ) production by co-cultured vascular smooth muscle cells (VSMCs) and peripheral blood mononuclear cells (PBMCs) on chemokine expression and effect of adding IFNγ on chemokine expression by temporal artery-derived VSMC. (A) VSMCs from normal temporal arteries were incubated alone or with PBMC (healthy donor) per well for 24 h. PBMCs were also cultured alone as a control. Cells were cultured with (A6) (filled bars) or without (Ø) (empty bars) the anti-IFNγ mAb A6 (10 μg/mL). After co-culture, PBMCs (adherent and non-adherent) were separated from VSMC. RNA was extracted from each individualized cell type: PBMC cultured alone, VSMC cultured alone, co-cultured PBMC (adherent and non-adherent) and co-cultured VSMC, and mRNA levels of various chemokines was determined. Notice that the Y scale is different for each molecule. The experiment was repeated three times with consistent results. *Significant reduction by A6 $p<0.05$ (B) Cultured VSMCs obtained from histologically normal temporal arteries were exposed to increasing concentrations of recombinant IFNγ(0-20-50-100 ng/mL) for 24 h and expression of transcription factors STAT-1 and STAT-3, chemokines and adhesion molecules intracellular adhesion molecule (ICAM)-1 and vascular adhesion molecule (VCAM)-1 was assessed by real-time quantitative RT-PCR. All increases in expression of chemokines, ICAM-1, STAT-1 and VCAM-1 were statistically significant ($p<0.05$) compared to baseline. Increase in STAT-3 was significant ($p<0.05$) at the highest IFNγ concentration. (C) Spontaneous chemokine mRNA expression (relative units) by primary cultures of VSMC obtained from 11 normal arteries (empty boxes) or giant cell arteritis (GCA)-involved arteries (filled boxes). *$p<0.05$.

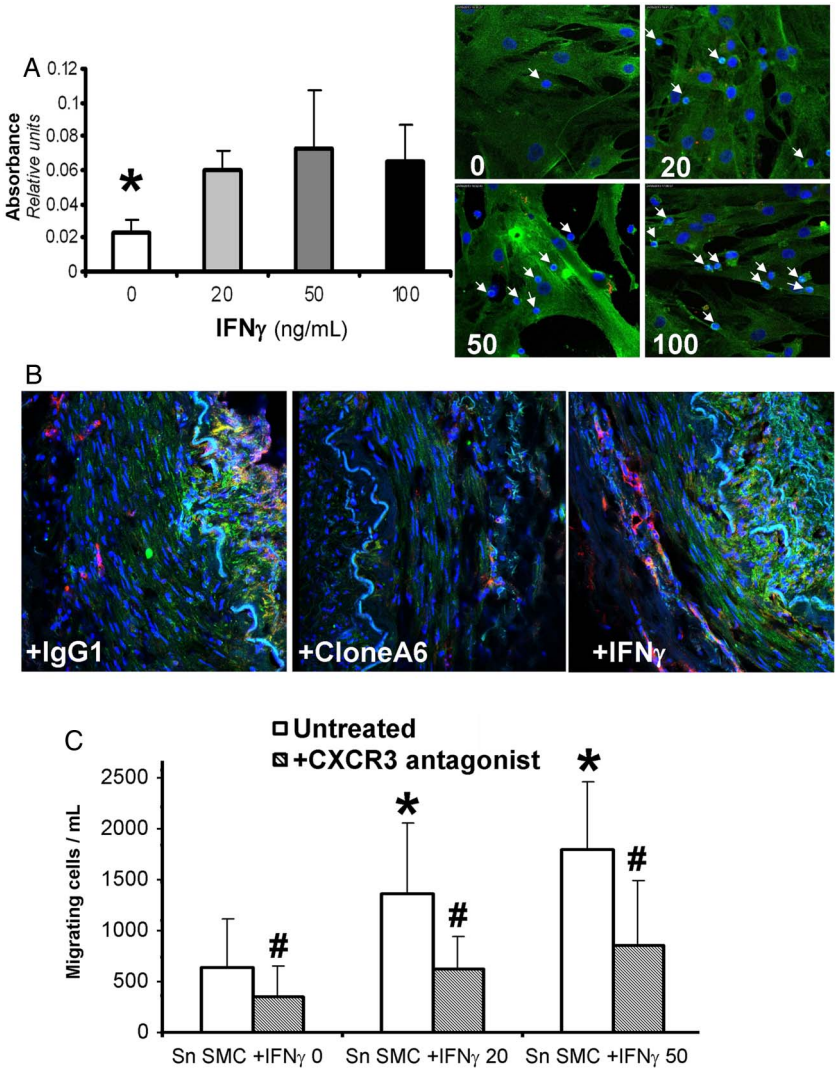

Figure 4 Changes in vascular smooth muscle cell (VSMCs) adhesiveness and chemoattraction to peripheral blood mononuclear cells (PBMCs) upon exposure to interferon γ (IFNγ). (A) PBMC adhesion to VSMC obtained from histologically normal temporal arteries and exposed to increasing concentrations of IFNγ. VSMC cultured in 96-well plates were exposed to increasing concentrations of IFNγ (0–20–50–100 ng/mL) for 24 h. PBMCs (75 000/well) were added and incubated for 1 h, washed and stained with crystal violet. Bars represent absorbance of solubilised dye in VSMC incubated with PBMC after subtraction of absorbance obtained from VSMC alone. *p<0.05. In parallel confirmatory experiments, VSMCs were seeded in chamber slides (Nunc, Waltham, Massachusetts, USA), and VSMCs were immunostained with a mouse monoclonal anti-human alpha smooth muscle actin antibody (ab54723, Abcam) (green). Nuclei were stained with DAPI (blue). The size of PBMC nuclei (indicated by arrows) are smaller than those from VSMC and can be easily distinguished. (B) Expression of intracellular adhesion molecule (ICAM)-1 (green) and CD31 (red) in temporal arteries from a patient with giant cell arteritis (GCA) exposed to IgG1 (10 μg/mL), A6 (10 μg/mL) or IFNγ (100 ng/mL)for 5 days. Nuclei were stained with DAPI (blue). VSMCs (elongated cells) express ICAM -1, particularly in the vicinity of infiltrating mononuclear cells. Co-expression of CD31 and ICAM-1 (merged, yellow) is observed on endothelial cells from adventitial vasa vasorum and neovessels. ICAM-1 expression is clearly reduced by A6 antibody. (C) Chemotactic activity of PBMC to the supernatant of VSMC exposed to IFNγ. Supernatants from VSMC obtained from histologically normal arteries incubated with increasing concentrations IFNγ (0–20–50 ng/mL) for 24 h were used to assess the induction of PBMC chemotaxis in the presence or in the absence of the CXCR3 inhibitor 500486. Bars represent the number of cells/mL that migrated to the lower chamber after 6 h incubation (mean±SD of three counts). *p<0.05 (increase in migration at any IFNγ concentration versus baseline). #p<0.05 (inhibition by CXCR3 antagonist).

settings.[5 19 20 23 26] Treatment of GCA arteries with exogenous IFNγ elicited opposite effects and tendencies, supporting the specificity of these findings.

Blocking IFNγ in our system led to a highly selective inhibition of ISRE-containing chemokine genes CXCL 9, 10 and 11. Although IFNγ also induced ISRE-dependent CCL2 in isolated VSMC, the effect of blocking IFNγ on CCL2 expression in GCA arteries was not apparent probably due to the remarkable constitutive expression of CCL2 in aged temporal arteries and the presence of potential additional inducers.[34] Since CXCL 9, 10 and 11 are powerful chemoattractants of mononuclear cells and these are able to interact with ICAM-1 expressing microvessels in inflamed arteries, our findings support a relevant role for IFNγ in the development and perpetuation of inflammatory infiltrates.

Based on the potent known effects of IFNγ on macrophages, and their predominance in GCA lesions, we expected that blocking IFNγ would have higher impact in the expression of downstream macrophage inflammatory products such as HLA-DR, NOS-2 and monokines.[20] In our model, IFNγ

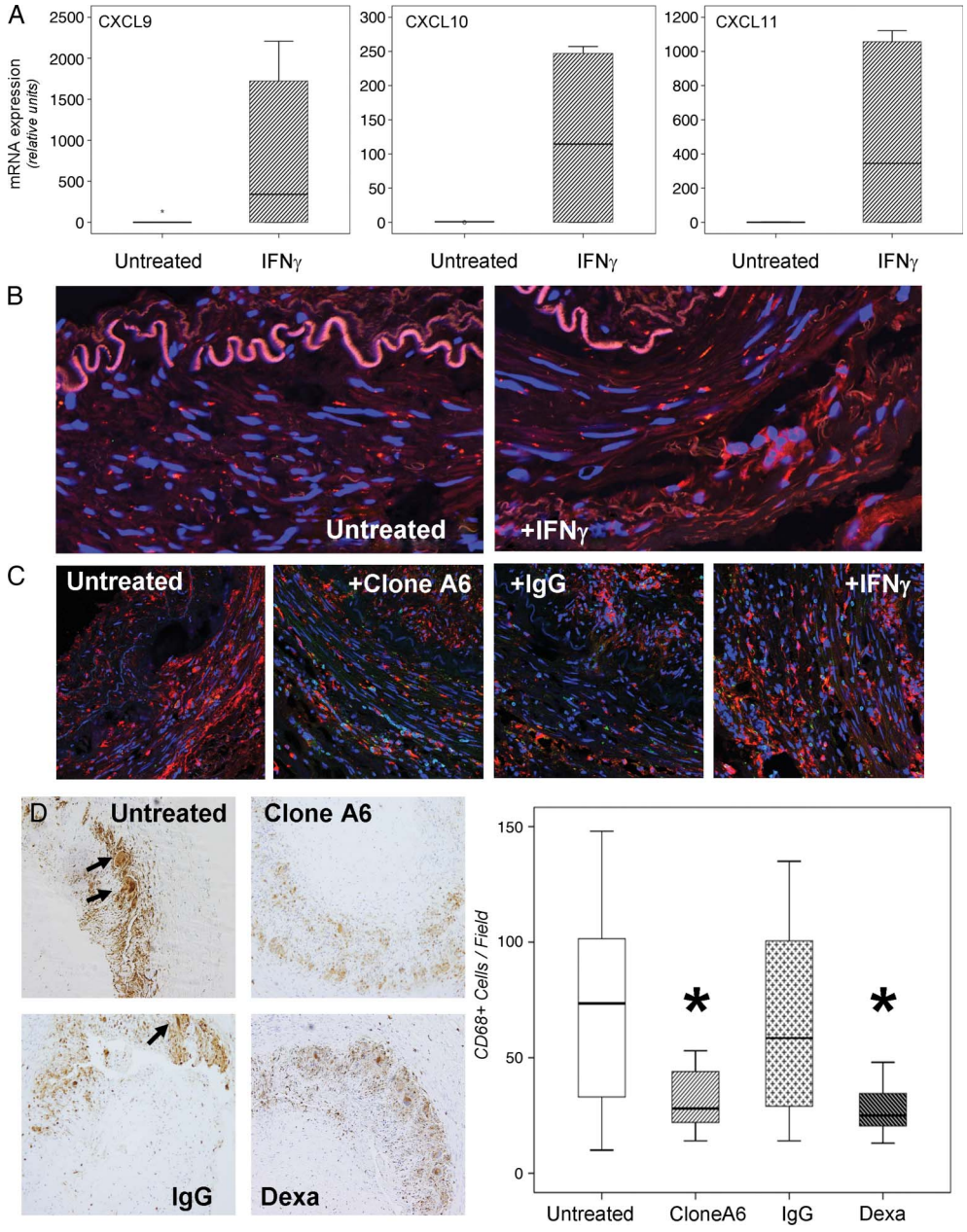

Figure 5 Effect of interferon γ (IFNγ) on chemokine expression and macrophage infiltration of histologically normal temporal arteries and reduction of macrophage infiltration in giant cell arteritis (GCA)-involved arteries following IFNγ blockade. (A) Histologically normal temporal arteries (N=6) were cultured on Matrigel with or without IFNγ (100 ng/mL) for 5 days and chemokine mRNA expression was assessed (relative units) by RT-PCR. (B) Histologically normal temporal arteries cultured in 24-well plates as above were incubated in medium alone or in medium containing IFNγ (100 ng/mL) for 4 days and were subsequently exposed to PBMC from a healthy donor (0.25×10^6/well) for 5 days. Cryosections of the retrieved arteries were processed for immunofluorescence, sectioned and immunostained with an anti-CD68 mAb (red). Nuclei were stained with DAPI (blue). (C) GCA affected temporal arteries were cultured in medium alone or in medium containing A6 antibody (10 μg/mL), control IgG1 (10 μg/mL) or recombinant IFNγ (100 ng/mL) for 5 days, washed and processed for immunofluorescence and immunostained with anti-CD68 mAb as in (B). Nuclei were stained with DAPI (blue). (D) Cryosections of GCA-affected temporal arteries, cultured as in (C), were immunostained with an anti-CD68 mAb. Notice reduction in immunostained CD68 cells and disappearance of giant cells (arrows) following anti-IFNγ or dexamethasone (Dexa) (0.5 μg/mL) treatment. Graph shows number of CD68+ cells/field (×100) in cultured GCA-involved temporal arteries untreated or exposed to A6, control IgG1 or dexamethasone (Dexa). Twelve fields/condition were assessed. *p<0.05.

neutralisation slightly modified or did not modify at all a number of relevant proinflammatory molecules that were, indeed, suppressed by GC. This may be determined by concomitant activation of IFNγ-independent pathways. In this regard, neutralisation of IFNγ did not substantially reduce expression and activation of STAT-3, which appears to be highly activated in normal arteries and in GCA lesions, in accordance with the remarkable production of IL-6 in normal and inflamed arteries.[4–6] Concomitant activation of STAT-3 and nuclear factor-κB may sustain expression of many inflammatory molecules in spite of IFNγ blockade.[35–37]

Most of the studies investigating IFNγ proinflammatory functions have explored its effects on macrophages and endothelial cells.[18 33] In vascular biology, the effects of IFNγ have been

essentially investigated in the setting of atherosclerosis and graft vasculopathy.[38 39] In these models, IFNγ is expressed in lesions and production of IFNγ induced chemokines have been attributed to endothelial cells and inflammatory cells and only occasionally related to myofibroblasts.[38] In VSMC, the effects of IFNγ have been mainly related to vascular remodelling and neointima formation.[39] In recent years, it has become apparent that VSMC may acquire a strong proinflammatory phenotype in the appropriate context.[40 41] Our findings indicate that, in GCA, VSMC are also important targets for IFNγ, which renders them active producers of chemokines and adhesion molecules, especially ICAM-1. Consequently, VSMCs likely contribute to the progression of inflammatory infiltrates through the medial layer of the artery wall and to the development of full-blown granulomatous lesions in GCA.

GC, the cornerstone of current GCA treatment, rapidly downregulate the expression of a variety of inflammatory cytokines (ie, IL-1β, TNFα, IL-6, IL-17), adhesion molecules (ie, ICAM-1) and matrix metalloproteinases (ie, MMP-9).[7 11 27 28] However, GC do not repress IFNγ transcription.[35] Although prolonged GC treatment eventually results in decreased IFNγ expression by other mechanisms,[11 42–44] acute GC effects on IFNγ expression in GCA lesions are less dramatic than that observed with other cytokines.[7 27 35] This has led to the hypothesis that incomplete suppression of IFNγ accounts for GCA relapses during GC tapering or withdrawal,[29] and IFNγ has been considered a potential therapeutic target.[29 35] However, our findings indicate that reducing STAT-1 expression and activation by blocking IFNγ may not be sufficient to abrogate inflammatory activity in full-blown GCA lesions, which may require blockade of multiple pathways. However, interfering with IFNγ might be useful in preventing relapses, given the relevant role of IFNγ in the recruitment of inflammatory cells since the very early inflammatory stages.[11 45]

In considering IFNγ as a potential therapeutic target, it is important to consider that IFNγ may have a protective role by limiting tissue injury.[16 46] Blocking IFNγ worsens, indeed, experimental arthritis by promoting Th17 differentiation and exacerbation of IL-17-mediated inflammatory responses.[47] In addition, an infectious trigger of GCA has been postulated, although no causative agents have been consistently identified.[48] In this regard, IFNγ-deficient mice infected with murine herpesvirus HV68 develop necrotising large-vessel vasculitis, supporting the well-known role of IFNγ in host defence against viruses but also suggesting a role in limiting vascular injury.[46 49] Moreover, in some experimental settings, but not in others, IFNγ deficiency exacerbates aortic aneurysm development, which is one of the important delayed complications of GCA.[50–56]

Our study has several limitations. On the one hand, it explores functional activities of IFNγ in a target organ isolated from a functional immune system and variations in chemokine and adhesion molecule expression could not result in effective changes in leucocyte recruitment. It is likely that, in vivo, inhibition of lymphocyte and monocyte recruitment and subsequent macrophage activation would result in greater impact on the generation of downstream inflammatory products. In addition, as mentioned, the culture itself downregulates IFNγ expression,[7] which may have minimised the effect of IFNγ neutralisation in our model. GC treatment of some patients prior to the TAB may also have influenced results.[7]

In spite of these limitations, our findings indicate an important role for IFNγ in the recruitment and activation of macrophages, which may sustain and amplify subsequent waves of proinflammatory cascades in GCA. Moreover, our findings support the suitability of the temporal artery culture model to test functional activities not only of pharmacological agents or chemicals but also of complex molecules such as biological agents.

Author affiliations
[1]Vasculitis Research Unit, Department of Autoimmune Diseases, Hospital Clínic, University of Barcelona, Institut d'Investigacions Biomèdiques August Pi i Sunyer (IDIBAPS), Barcelona, Spain
[2]Department of Emergency Medicine, Hospital Clínic, University of Barcelona, Institut d'Investigacions Biomèdiques August Pi i Sunyer (IDIBAPS), Barcelona, Spain
[3]Hematopathology Section, Department of Anatomic Pathology, Hospital Clínic, University of Barcelona, Institut d'Investigacions Biomèdiques August Pi i Sunyer (IDIBAPS), Barcelona, Spain
[4]Genomics and Haematopathology Unit, Hospital Clínic, University of Barcelona, Institut d'Investigacions Biomèdiques August Pi i Sunyer (IDIBAPS), Barcelona, Spain
[5]Division of Immunology and Allergy, University Hospital and Medical School, University of Geneva, Geneva, Switzerland
[6]Novimmune, Geneva, Switzerland
[7]Medical School, University of Geneva, Geneva, Switzerland

Contributors MCC and MC-B designed the study. MHK-V and J-MD contributed important input to its design. MC-B, EP-R, EL and NT performed the experimental work. MAA, SP-G, AG-M, GE-F and JH-R contributed to clinical selection and contributed to the experimental work. RA and AE supervised in silico promoter regions studies. All authors evaluated and criticised the data and PR-L and MHK-V provided important contributions to their interpretation. MC-B and MCC wrote the manuscript. All authors read, made improvements and approved the final version.

Funding Supported by Ministerio de Economía y Competitividad (SAF 11/30073 and SAF 14/57708-R) and by Instituto de Salud Carlos III (PIE13/00033) and Fondo europeo de Desarrollo Regional (FEDER)

Competing interests MHK-V and WGF are full employees by Novimmune. MCC, J-HR, GE-F and SP-G are currently participating in a clinical trial of tocilizumab (anti-IL-6R) in giant cell arteritis sponsored by Hoffmann-La Roche.

Patient consent Obtained.

Ethics approval Ethics committee of Hospital Clínic of Barcelona.

Provenance and peer review Not commissioned; externally peer reviewed.

REFERENCES

1 Salvarani C, Pipitone N, Versari A, *et al*. Clinical features of polymyalgia rheumatica and giant cell arteritis. *Nat Rev Rheumatol* 2012;8:509–21.
2 Alba MA, García-Martínez A, Prieto-González S, *et al*. Relapses in patients with giant cell arteritis: prevalence, characteristics, and associated clinical findings in a longitudinally followed cohort of 106 patients. *Medicine* 2014;93:194–201.
3 Cid MC, Font C, Coll-Vinent B, *et al*. Large vessel vasculitides. *Curr Opin Rheumatol* 1998;10:18–28.
4 Weyand CM, Hicok KC, Hunder GG, *et al*. Tissue cytokine patterns in patients with polymyalgia rheumatica and giant cell arteritis. *Ann Intern Med* 1994;121:484–91.
5 Hernández-Rodríguez J, Segarra M, Vilardell C, *et al*. Tissue production of pro-inflammatory cytokines (IL-1beta, TNF alpha and IL-6) correlates with the intensity of the systemic inflammatory response and with corticosteroid requirements in giant-cell arteritis. *Rheumatology (Oxford)* 2004;43:294–301.
6 Hernández-Rodríguez J, Segarra M, Vilardell C, *et al*. Elevated production of interleukin-6 is associated with a lower incidence of disease-related ischemic events in patients with giant-cell arteritis: angiogenic activity of interleukin-6 as a potential protective mechanism. *Circulation* 2003;107:2428–34.
7 Corbera-Bellalta M, García-Martínez A, Lozano E, *et al*. Changes in biomarkers after therapeutic intervention in temporal arteries cultured in Matrigel: a new model for preclinical studies in giant-cell arteritis. *Ann Rheum Dis* 2014;73:616–23.
8 Ciccia F, Alessandro R, Rizzo A, *et al*. Expression of interleukin-32 in the inflamed arteries of patients with giant cell arteritis. *Arthritis Rheum* 2011;63:2097–104.
9 Deng J, Younge BR, Olshen RA, *et al*. Th17 and Th1 T-cell responses in giant cell arteritis. *Circulation* 2010;121:906–15.
10 Terrier B, Geri G, Chaara W, *et al*. Interleukin-21 modulates Th1 and Th17 responses in giant cell arteritis. *Arthritis Rheum* 2012;64:2001–11.
11 Visvanathan S, Rahman MU, Hoffman GS, *et al*. Tissue and serum markers of inflammation during the follow-up of patients with giant-cell arteritis—a prospective longitudinal study. *Rheumatology (Oxford)* 2011;50:2061–70.
12 Samson M, Audia S, Fraszczak J, *et al*. Th1 and Th17 lymphocytes expressing CD161 are implicated in giant cell arteritis and polymyalgia rheumatica pathogenesis. *Arthritis Rheum* 2012;64:3788–98.
13 Espígol-Frigolé G, Corbera-Bellalta M, Planas-Rigol E, *et al*. Increased IL-17A expression in temporal artery lesions is a predictor of sustained response to glucocorticoid treatment in patients with giant-cell arteritis. *Ann Rheum Dis* 2013;72:1481–7.

14 Schroder K, Hertzog PJ, Ravasi T, *et al*. Interferon-gamma: an overview of signals, mechanisms and functions. *J Leukoc Biol* 2004;75:163–89.
15 Qiao Y, Giannopoulou EG, Chan CH, *et al*. Synergistic activation of inflammatory cytokine genes by interferon-γ-induced chromatin remodeling and toll-like receptor signaling. *Immunity* 2013;39:454–69.
16 Hu X, Ivashkiv LB. Cross-regulation of signaling pathways by interferon-gamma: implications for immune responses and autoimmune diseases. *Immunity* 2009;31:539–50.
17 Saha B, Jyothi Prasanna S, Chandrasekar B, *et al*. Gene modulation and immunoregulatory roles of interferon gamma. *Cytokine* 2010;50:1–14.
18 Hu X, Park-Min KH, Ho HH, *et al*. IFN-gamma-primed macrophages exhibit increased CCR2-dependent migration and altered IFN-gamma responses mediated by Stat1. *J Immunol* 2005;175:3637–47.
19 Qing Y, Stark GR. Alternative activation of STAT1 and STAT3 in response to interferon-gamma. *J Biol Chem* 2004;279:41679–85.
20 Murray PJ, Wynn TA. Protective and pathogenic functions of macrophage subsets. *Nat Rev Immunol* 2011;11:723–37.
21 Gough DJ, Levy DE, Johnstone RW, *et al*. IFNγ signalling- does it mean JAK-STAT? *Cytokine Growth Factor Rev* 2008;19:383–94.
22 Lozano E, Segarra M, García-Martínez A, *et al*. Imatinib mesylate inhibits in vitro and ex vivo biological responses related to vascular occlusion in giant cell arteritis. *Ann Rheum Dis* 2008;67:1581–8.
23 Cid MC, Campo E, Ercilla G, *et al*. Immunohistochemical analysis of lymphoid and macrophage cell subsets and their immunologic activation markers in temporal arteritis. Influence of corticosteroid treatment. *Arthritis Rheum* 1989;32:884–93.
24 Cid MC, Hoffman MP, Hernández-Rodríguez J, *et al*. Association between increased CCL2 (MCP-1) expression in lesions and persistence of disease activity in giant-cell arteritis. *Rheumatology (Oxford)* 2006;45:1356–63.
25 Cid MC, Cebrián M, Font C, *et al*. Cell adhesion molecules in the development of inflammatory infiltrates in giant cell arteritis: inflammation-induced angiogenesis as the preferential site of leukocyte-endothelial cell interactions. *Arthritis Rheum* 2000;43:184–94.
26 Weyand CM, Wagner AD, Björnsson J, *et al*. Correlation of the topographical arrangement and the functional pattern of tissue-infiltrating macrophages in giant cell arteritis. *J Clin Invest* 1996;98:1642–9.
27 Brack A, Rittner HL, Younge BR, *et al*. Glucocorticoid-mediated repression of cytokine gene transcription in human arteritis-SCID chimeras. *J Clin Invest* 1997;99:2842–50.
28 Segarra M, García-Martínez A, Sánchez M, *et al*. Gelatinase expression and proteolytic activity in giant-cell arteritis. *Ann Rheum Dis* 2007;66:1429–35.
29 Weyand CM, Goronzy JJ. Immune mechanisms in medium and large-vessel vasculitis. *Nat Rev Rheumatol* 2013;9:731–40.
30 Ly KH, Regent A, Tamby MC, *et al*. Pathogenesis of giant-cell arteritis: more than just an inflammatory condition?. *Autoimmunity Rev* 2010;9:635–45.
31 Marinescu VD, Kohane IS, Riva A. The MAPPER database: a multi-genome catalog of putative transcription factor binding sites. *Nucleic Acids Res* 2005;33:D91–7.
32 Braun M, Pietsch P, Felix SB, *et al*. Modulation of intercellular adhesion molecule-1 and vascular cell adhesion molecule-1 on human coronary smooth muscle cells by cytokines. *J Mol Cell Cardiol* 1995;27:2571–9.
33 Nourshargh S, Alon R. Leukocyte migration into inflamed tissues. *Immunity* 2014;41:694–707.
34 Wang M, Jiang L, Monticone RE, *et al*. Proinflammation: the key to arterial aging. *Trends Endocrinol Metab* 2014;25:72–9.
35 Weyand CM, Kaiser M, Yang H, *et al*. Therapeutic effects of acetylsalicylic acid in giant cell arteritis. *Arthritis Rheum* 2002;46:457–66.
36 Shin WS, Hong YH, Peng HB, *et al*. Nitric oxide attenuates vascular smooth muscle cell activation by interferon-gamma. The role of constitutive NF-kappa B activity. *J Biol Chem* 1996;271:11317–24.
37 Kovacic JC, Gupta R, Lee AC, *et al*. Stat3-dependent acute Rantes production in vascular smooth muscle cells modulates inflammation following arterial injury in mice. *J Clin Invest* 2010;120:303–14.
38 Zhao DX, Hu Y, Miller GG, *et al*. Differential expression of the IFN-gamma-inducible CXCR3-binding chemokines, IFN-inducible protein 10, monokine induced by IFN, and IFN-inducible T cell alpha chemoattractant in human cardiac allografts: association with cardiac allograft vasculopathy and acute rejection. *J Immunol* 2002;169:1556–60.
39 Tellides G, Tereb DA, Kirkiles-Smith NC, *et al*. Interferon-gamma elicits arteriosclerosis in the absence of leukocytes. *Nature* 2000;403:207–11.
40 Tellides G, Pober JS. Inflammatory and immune responses in the arterial media. *Circ Res* 2015;116:312–22.
41 Libby P, Hansson GK. Inflammation and immunity in diseases of the arterial tree: players and layers. *Circ Res* 2015;116:307–11.
42 Ogilvie RL, Sternjohn JR, Rattenbacher B, *et al*. Tristetraprolin mediates interferon-gamma mRNA decay. *J Biol Chem* 2009;284:11216–23.
43 Ishmael FT, Fang X, Galdiero MR, *et al*. Role of the RNA-binding protein tristetraprolin in glucocorticoid-mediated gene regulation. *J Immunol* 2008;180:8342–53.
44 Liberman AC, Refojo D, Druker J, *et al*. The activated glucocorticoid receptor inhibits the transcription factor T-bet by direct protein-protein interaction. *FASEB J* 2007;21:1177–88.
45 Wagner AD, Björnsson J, Bartley GB, *et al*. Interferon-gamma-producing T cells in giant cell vasculitis represent a minority of tissue-infiltrating cells and are located distant from the site of pathology. *Am J Pathol* 1996;148:1925–33.
46 Kelchtermans H, Billiau A, Matthys P. How interferon-gamma keeps autoimmune diseases in check. *Trends Immunol* 2008;29:479–86.
47 Kelchtermans H, Schurgers E, Geboes L, *et al*. Effector mechanisms of interleukin-17 in collagen-induced arthritis in the absence of interferon-gamma and counteraction by interferon-gamma. *Arthritis Res Ther* 2009;11:R122.
48 Bhatt AS, Manzo VE, Pedamallu CS, *et al*. In search of a candidate pathogen for giant cell arteritis: sequencing-based characterization of the giant cell arteritis microbiome. *Arthritis Rheumatol* 2014;66:1939–44.
49 Weck KE, Dal Canto AJ, Gould JD, *et al*. Murine gamma-herpesvirus 68 causes severe large-vessel arteritis in mice lacking interferon-gamma responsiveness: a new model for virus-induced vascular disease. *Nat Med* 1997;3:1346–53.
50 Shimizu K, Shichiri M, Libby P, *et al*. Th2-predominant inflammation and blockade of IFN-gamma signaling induce aneurysms in allografted aortas. *J Clin Invest* 2004;114:300–8.
51 King VL, Lin AY, Kristo F, *et al*. Interferon-gamma and the interferon-inducible chemokine CXCL10 protect against aneurysm formation and rupture. *Circulation* 2009;119:426–35.
52 Tang PC, Yakimov AO, Teesdale MA, *et al*. Transmural inflammation by interferon-gamma-producing T cells correlates with outward vascular remodeling and intimal expansion of ascending thoracic aortic aneurysms. *FASEB J* 2005;19:1528–30.
53 García-Martínez A, Hernández-Rodríguez J, Arguis P, *et al*. Development of aortic aneurysm/dilatation during the followup of patients with giant cell arteritis: a cross-sectional screening of fifty-four prospectively followed patients. *Arthritis Rheum* 2008;59:422–30.
54 Robson JC, Kiran A, Maskell J, *et al*. The relative risk of aortic aneurysm in patients with giant cell arteritis compared with the general population of the UK. *Ann Rheum Dis* 2015;74:129–35.
55 Kermani TA, Warrington KJ, Crowson CS, *et al*. Large-vessel involvement in giant cell arteritis: a population-based cohort study of the incidence-trends and prognosis. *Ann Rheum Dis* 2013;72:1989–94.
56 García-Martínez A, Arguis P, Prieto-González S, *et al*. Prospective long term follow-up of a cohort of patients with giant cell arteritis screened for aortic structural damage (aneurysm or dilatation). *Ann Rheum Dis* 2014;73:1826–32.

Annex

Other contributions

1. Marc Corbera-Bellalta, **Ester Planas-Rigol**, Ester Lozano , Nekane Terrades-Garcia,Marco A. Alba, Sergio Prieto-González, Ana García-Martínez,Robert Albero, Anna Enjuanes,Georgina Espigol-Frigole, Jose Hernández-Rodríguez,Pascale Roux-Lombard, Waslter G.Ferlin, Jean-Michel Dayer,Marie H Kosko-Vilbois,M.C. Cid.

Blocking interferon γreduces expression of chemokines CXCL9,CXCL10 and CXCL11 and decreases macrophage infiltration in ex-vivo cultured arteries from patients with giant-cell arteritis.

Ann Rheum Dis. 2015 Dec 23. doi: 10.1136/annrheumdis-2015-208371. [Epub ahead of print]

IF:10.377 (Included in theadditional data section)

2. Jara Palomero, Maria Carmela Vegliante, Marta Leonor Rodríguez, Álvaro Eguileor, Giancarlo Castellano**, Ester Planas-Rigol**, Pedro Jares, Inmaculada Ribera-Cortada, Maria C Cid, Elias Campo, Virginia Amador

SOX11 promotes tumor angiogensis through transcriptional regulation of PDGFA in mantle cell lymphoma

Blood. 2014 Oct 2;124(14):2235-47. doi: 10.1182/blood-2014-04-569566. Epub 2014 Aug 4.

IF:10.452

3. Alba MA, García-Martínez A, Prieto-González S, Tavera-Bahillo I, Corbera-Bellalta M, Planas-Rigol E, Espígol-Frigolé G, Butjosa M, Hernández-Rodríguez J, Cid MC.

Relapses in patients with giant cell arteritis:prevalence,characteristics,and associated clinical findings in a longitudinally followed cohort of 106 patients.

Medicine (Baltimore). 2014 Jul;93(5):194-201.Doi:10.1097/MD.0000000000000033. **IF:5.723**

4. Prieto-González S,Depetris M, García-Martínez A,Espígol-Frigolé G, Tavera-Bahillo I,Corbera-Bellalta M, **Planas-Rigol E**, Alba Ma,Hernández-Rodríguez J, Grau JM, Lomeña F, Cid MC.

Positron emission tomography assessment of large vessel inflammation in patients with newly diagnosed, biopsy-proven giant cell arteritis: a prospective, case-control study.

Ann Rheum Dis. 2014 Jul;73(7):1388-92. doi: 10.1136/annrheumdis-2013-204572. Epub 2014 Mar 24. **IF:10.377**

5. Corbera-Bellalta M, García-Martínez A, Lozano E, **Planas-Rigol E**, Tavera-Bahillo I, Alba MA, Prieto-González S, Butjosa M, Espígol-Frigolé G, Hernández-Rodríguez J, Fernández PL, Roux-Lombard P, Dayer JM, Rahman MU, Cid MC.

Changes in biomarkers after therapeutic intervention in temporal arteries cultured in Matrigel: a new model for preclinical studies in giant-cell arteritis.

Ann Rheum Dis. 2014 Mar;73(3):616-23. doi: 10.1136/annrheumdis-2012-202883. Epub 2013 Apr 27. **IF:10.377**

6. Espígol-Frigolé G, Corbera-Bellalta M, **Planas-Rigol E**, Lozano E, Segarra M, García-Martínez A, Prieto-González S, Hernández-Rodríguez J, Grau JM, Rahman MU, Cid MC.

***Increased IL-17A expression in temporal artery lesions is a predictor of sustained response to glucocorticoid treatment in patients with giant-cell arteritis*.**

Ann Rheum Dis. 2012 Sep 19Article**. IF:10.377**

Letters

1. Prieto-González S, Depetris M, García-Martínez A, Espígol-Frigolé G, Tavera-Bahillo I, Corbera-Bellalta M, Planas-Rigol E, Alba MA, Hernández-Rodríguez J, Grau JM, Lomeña F, Cid MC.

Authors' response to the eletter by Moiseev et al.

Ann Rheum Dis. 2014 Nov;73(11):e71. doi: 10.1136/annrheumdis-2014-206231. Epub 2014 Aug 8. IF:10.377

2. Corbera-Bellalta M, Planas-Rigol E, Espígol-Frigolé G, Lozano E, Cid MC

Functionally relevant treg cells are present in giant cell arteritis lesions: comment on the article by Samson et al.

Arthritis Rheum. 2013 Apr;65(4):1133-4. Letter. IF 7.477

LYMPHOID NEOPLASIA

SOX11 promotes tumor angiogenesis through transcriptional regulation of PDGFA in mantle cell lymphoma

Jara Palomero,[1] Maria Carmela Vegliante,[1] Marta Leonor Rodríguez,[1] Álvaro Eguileor,[1] Giancarlo Castellano,[1] Ester Planas-Rigol,[2] Pedro Jares,[1] Inmaculada Ribera-Cortada,[3] Maria C. Cid,[2] Elias Campo,[1,3] and Virginia Amador[1]

[1]Hematopathology Unit, Pathology Department, and [2]Vasculitis Research Unit, Department of Autoimmune Diseases, Institut d'Investigacions Biomèdiques August Pi i Sunyer, and [3]Department of Anatomic Pathology, Pharmacology and Microbiology, Hospital Clínic, University of Barcelona, Barcelona, Spain

Key Points

- SOX11 mediates regulation of angiogenesis via the PDGFA signaling pathway in MCL.
- SOX11-dependent increased angiogenesis contributes to a more aggressive MCL phenotype.

SOX11 is overexpressed in several solid tumors and in the vast majority of aggressive mantle cell lymphomas (MCLs). We have recently proven that SOX11 silencing reduces tumor growth in a MCL xenograft model, consistent with the indolent clinical course of the human SOX11-negative mantle cell lymphoma (MCL). However, the direct oncogenic mechanisms and downstream effector pathways implicated in SOX11-driven transformation remain poorly understood. Here, we observed that SOX11-positive xenograft and human primary MCL tumors overexpressed angiogenic gene signatures and had a higher microvascular density compared with their SOX11-negative counterparts. Conditioned media of SOX11-positive MCL cell lines induced in vitro endothelial cell proliferation, migration, tube formation, and activation of downstream angiogenic pathways. We identified *PDGFA* as a SOX11 direct target gene upregulated in MCL cells whose inhibition impaired SOX11-enhanced in vitro angiogenic effects on endothelial cells. In addition, platelet-derived growth factor A (PDGFA) was overexpressed in SOX11-positive but not in SOX11-negative MCL. In vivo, imatinib impaired tumor angiogenesis and lymphoma growth in SOX11-positive MCL xenograft tumors. Overall, our results demonstrate a prominent role for SOX11 as a driver of proangiogenic signals in MCL, and highlight the SOX11-PDGFA axis as a potential therapeutic target for the treatment of this aggressive disease. (*Blood*. 2014;124(14):2235-2247)

Introduction

Mantle cell lymphoma (MCL) is an aggressive lymphoid neoplasia derived from mature B cells genetically characterized by the presence of the t(11;14)(q13;q32) translocation causing cyclin D1 overexpression.[1] Furthermore, other secondary genetic alterations also contribute to the development and aggressiveness of MCL.[2] However, recent studies have identified a subset of MCL with indolent clinical behavior that tends to present with leukemic disease instead of extensive nodal infiltration and patients may not need chemotherapy for long periods.[3-5] Recently, molecular studies have identified *SOX11* (SRY [*sex determining region-Y*]-*box11*), as one of the best characterized discriminatory genes between these 2 clinical subtypes of MCL tumors.[6]

SOX11, together with *SOX4* and *SOX12*, belongs to the subgroup C of the *SOX* gene family encoding for transcription factors which play a critical role in embryonic development and cell differentiation.[7,8] SOX11 plays an important role in the regulation of neuronal cell survival and neurite growth, and is highly expressed in different central nervous system malignancies, solid tumors, aggressive MCL, and at lower levels in a subgroup of Burkitt and lymphoblastic lymphomas.[9-14] However, the oncogenic mechanisms of SOX11 contributing to the development and progression of these tumors are largely unknown.

We have recently demonstrated the in vivo tumorigenic potential of SOX11 in a MCL xenograft model. SOX11 blocks the terminal B-cell differentiation through direct positive regulation of PAX5[15] but the specific mechanisms regulated by SOX11 promoting the oncogenic and rapid tumor growth of aggressive MCL still remain to be elucidated.

To further characterize the potential oncogenic mechanisms regulated by SOX11 in MCL, we have investigated the gene and protein expression profiling of SOX11-positive and -knockdown MCL xenograft tumors, cell lines, and primary SOX11-positive and SOX11-negative MCL. We have identified that SOX11 modulates angiogenesis in MCL, and this mechanism is mediated by the upregulation of several proangiogencic factors, principally platelet-derived growth factor A (PDGFA). The inhibition of the PDGFA pathway not only impairs angiogenic development both in vitro and in vivo but also MCL tumor growth in vivo, offering a promising novel therapeutic strategy for the treatment of aggressive MCL.

Submitted April 16, 2014; accepted July 19, 2014. Prepublished online as *Blood* First Edition paper, August 4, 2014; DOI 10.1182/blood-2014-04-569566.

The microarray data reported in this article have been deposited in the Gene Expression Omnibus database (accession numbers GSE52892, for the xenograft tumor gene expression arrays).

The online version of this article contains a data supplement.

There is an Inside *Blood* Commentary on this article in this issue.

The publication costs of this article were defrayed in part by page charge payment. Therefore, and solely to indicate this fact, this article is hereby marked "advertisement" in accordance with 18 USC section 1734.

Methods

Cell lines and primary tumors

Three well-characterized SOX11-expressing MCL cell lines (Z138, GRANTA519, and JEKO1) were used for SOX11 silencing, xenograft experiments, western blot (WB), chromatin immunoprecipitation–quantitative polymerase chain reaction (ChIP-qPCR), in vitro experiments, and immunohistochemical studies. These 3 cell lines carry the t(11;14) and cyclin D1 overexpression.[16] Human umbilical vein endothelial cells (HUVECs) were used for in vitro angiogenesis experimental studies.

Microarray gene expression profiling (GEP) data from 38 primary MCL tumors, 16 SOX11-expressing, and 22 SOX11-negative were used for gene set enrichment analyses (GSEAs) (GSE36000).[17] In addition, 17 splenic MCL, 8 SOX11-expressing, and 9 SOX11-negative, were also investigated for the expression of PDGFA, CD31, CD34 by immunohistochemistry. Details on cell culture and human primary tumor information are provided in supplemental Methods (available on the *Blood* Web site).

Xenograft mouse model

With the use of a protocol approved by the animal testing ethical committee of the University of Barcelona, CB17-severe combined immunodeficient (CB17-SCID) mice (Charles River Laboratories) were subcutaneously inoculated into their lower dorsum with Z138, JEKO1, and GRANTA519 shControl, shSOX11.1, and shSOX11.3 cells as previously described,[15] generating SOX11-positive and -knockdown xenograft tumors (shControl, shSOX11.1, and shSOX11.3, respectively).

When tumor volumes reached 75 to 100 mm^3, mice were randomized to receive imatinib (LC Laboratories) dissolved in phosphate-buffered saline (PBS; Roche Applied Science) at 45 mg/kg or vehicle PBS twice daily by intraperitoneal (IP) injections for 2 weeks. Animals were euthanized according to institutional guidelines, and tumor xenografts were paraffin embedded on saline-coated slides in a fully automated immunostainer (Bond Max; Vision Biosystems) for immunohistochemical analysis and on Tissue-Tek OCT (Sakura) frozen in dry ice and stored at −80°C for RNA and protein extraction.

GEP and GSEA analyses

To identify oncogenic pathways related to SOX11 high expression in MCL, we performed GSEA[18] on expression data sets derived from MCL primary tumors (GSE36000),[17] in vitro SOX11 silencing experiments (GSE34763),[15] and MCL xenografts (GEP derived from Z138 shControl, n = 4; shSOX11.1, n = 5; and shSOX11.3, n = 5). Experimental details on RNA extraction and GEP from xenograft tumors and GSEA are provided in supplemental Methods.

Angiogenesis proteome profiler antibody array

Total protein extracts from in vitro and xenograft SOX11-positive and SOX11-negative cells were used to study the human angiogenesis proteome profiler antibody array (R&D Systems) following the manufacturer's protocol. Experimental details on protein extraction and proteome array are provided in supplemental Methods.

HUVECs in vitro angiogenesis studies

HUVECs were resuspended in RPMI + 10% fetal bovine serum (FBS) or SOX11-positive or SOX11-negative conditioned media (CM) and after the corresponding incubation time, their tube formation, proliferation, and migration were analyzed. Experimental details are provided in supplemental Methods.

HUVEC WB and PDGF pathway phosphospecific antibody array experiments

HUVECs were incubated in RPMI + 10% FBS or SOX11-positive or SOX11-negative CM for 3 hours, and WB experiments[19] and PDGF pathway phosphospecific antibody array were performed. Experimental details are provided in supplemental Methods.

Custom human quantibody array

SOX11-positive and SOX11-negative CM were incubated in the protein arrays for the quantification of the secreted levels of 8 proangiogenic factors (ANG, ANGPT1, ANGPT2, FGF1, FGF2, PDGFA, PDGFB, and VEGF) according to the manufacturer's protocol (RayBiotech). Experimental details are provided in supplemental Methods.

ChIP and ChIP-qPCR experiments

ChIP was carried out using the HighCell #ChIP kit (Diagenode). Briefly, Z138 and JEKO1 MCL cell lines were fixed and then sonicated with Biorupter sonicator (Diagenode). SOX11 antibody was used to immunoprecipitate protein-DNA complexes, and after immunoprecipitation, DNA was purified and quantified.

Primers for ChIP-qPCR were designed for SOX11 ChIP-enriched genomic DNA, and SOX11-ChIP DNA and 1:100 diluted input samples were analyzed in duplicate by qRT-PCR regions. Experimental details on ChIP, primers for ChIP-qPCR, and ChIP gene ontology (GO) categories analysis are provided in supplemental Methods.

Reporter plasmid constructs and luciferase assay

The SOX11-binding site to the regulatory region of *PDGFA* gene was amplified, cloned in front of a minimal promoter luciferase reporter vector pGL4.23[*luc2*/minP] (Promega), and used for transient cotransfection experiments and luciferase activity assays in HEK293 cells. Experimental details are provided in supplemental Methods.

In vitro PDGFA inhibition experiments

HUVECs were treated with 1μM imatinib or 10 μg/mL neutralizing antibody against human PDGFR-α (MAB322; R&D Systems) for 1 hour, and resuspended in RPMI + 10% FBS or SOX11-positive or SOX11-negative CM. HUVEC tube formation and migration were studied as previously described. Experimental details are provided in supplemental Methods.

Immunohistochemical staining and MVD quantification

Immunohistochemical staining studies were performed as previously described.[14,20] CD31 or CD34-positive microvessel density (MVD) areas were calculated as the sum of areas of MVD (μm^2) evaluated divided by the total area of the core analyzed (μm^2) as previously described.[21] Experimental details on immunohistochemical staining, antibodies used, and MVD quantification are provided in supplemental Methods.

Statistical analysis

Data are represented as mean ± standard deviation (SD) of 3 independent experiments. Statistical tests were performed using SPSS, v16.0 software (SPSS). Comparison between 2 groups of samples was evaluated by independent sample Student *t* test, and results were considered statistically significant when $P < .05$.

Results

SOX11 induces the expression of proangiogenic factors and promotes angiogenesis in MCL xenograft tumors

To investigate the mechanisms regulated by SOX11 promoting MCL tumor growth, we first compared the GEPs of SOX11-positive and SOX11-knockdown xenograft tumors.[15] GSEA showed that SOX11-positive xenografts were significantly enriched in gene signatures related to tumor angiogenesis among other tumor microenvironment prosurvival signals, including phosphatidylinositol 3-kinase cascade (Figure 1A, Table 1). At the protein level, SOX11-positive xenografts had a significantly increased expression of

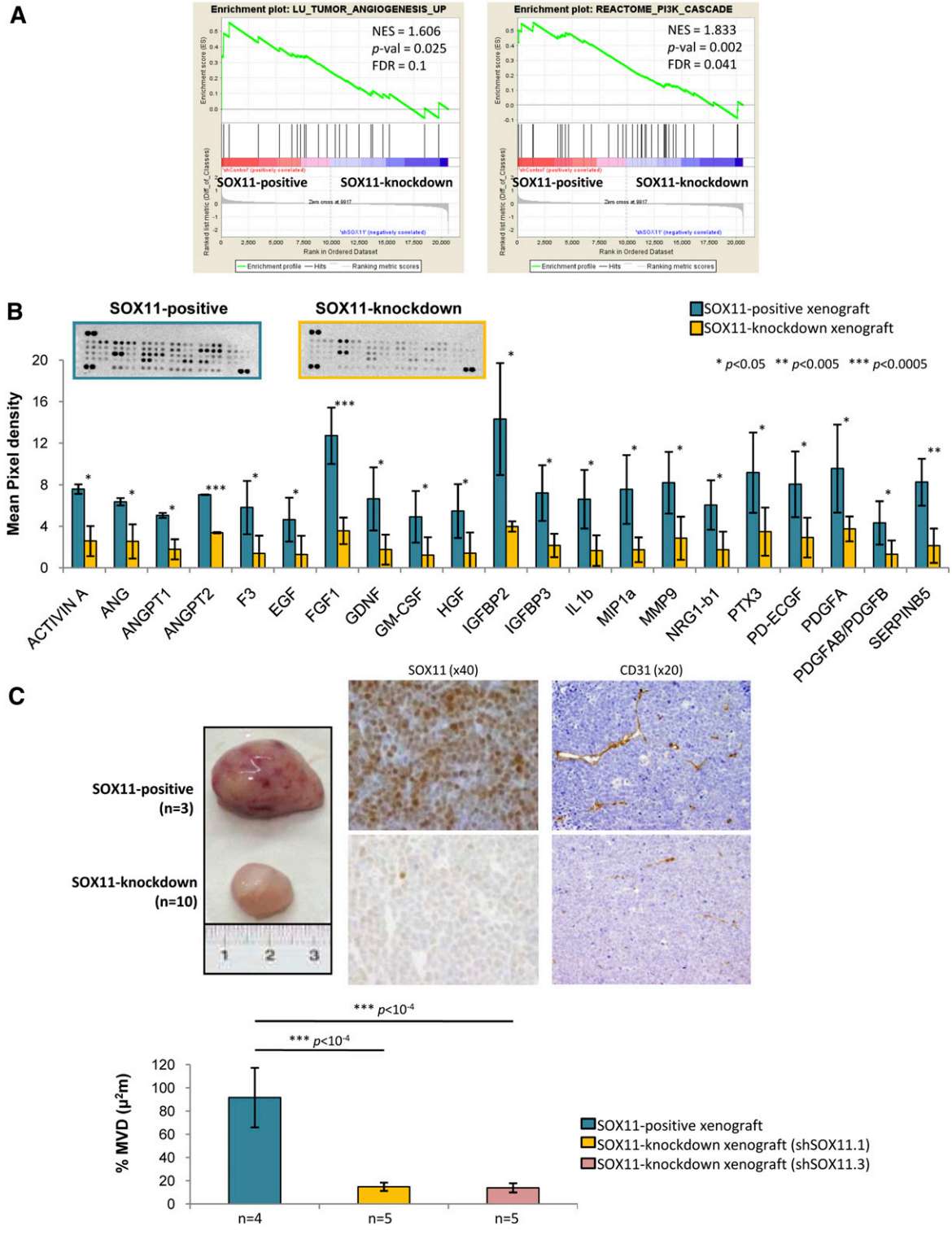

Figure 1. SOX11 induces the expression of proangiogenic factors and promotes angiogenesis in xenograft MCL-derived tumors. (A) GSEA analysis on expression data set from SOX11-positive and SOX11-knockdown xenograft tumors showing enriched gene sets related to angiogenesis pathways. NES, *P*-val, and FDR are represented. Statistical significance is considered when FDR <0.2. (B) Top panel, Representative images showing human-specific angiogenesis antibody array membranes incubated with protein extracts from SOX11-positive (n = 2) and SOX11-knockdown (n = 2) xenograft tissue lysates. Bottom panel, Quantification of the mean pixel densities showing 21 angiogenic proteins significantly upregulated in SOX11-positive compared with SOX11-knockdown xenografts. (C) Top panel, Macroscopic appearance and consecutive histological sections from representative SOX11-positive and SOX11-knockdown xenografts (Z138 shControl, n = 3; shSOX11.1, n = 5; and shSOX11.3, n = 5) stained with a specific antibody anti-human SOX11 (×40) and a specific antibody anti-mouse CD31 (×20). Bottom panel, Density (% of CD31-positive microvessel areas) of CD31-positive MVD areas in SOX11-positive and SOX11-knockdown tumors delineated by the presence of CD31-positive staining. Bar plot represents the mean percentage ± SD. *P*-val are shown. The significance of difference was determined by the independent samples Student *t* test. FDR, false discovery rate; NES, normalized enrichment score; *P*-val, *P* value.

Table 1. Angiogenic gene signatures

Gene set	*P* value		FDR *q* value	Upregulated in class
	NES	Nominal		
Enriched in SOX11-positive (n = 4) vs SOX11-knockdown (n = 10) xenograft tumors				
LU_TUMOR_ANGIOGENESIS_UP	1.606	.025	0.1	Z138 SOX11-positive xenograft tumors
REACTOME_PI_3K_CASCADE	1.833	.002	0.04	Z138 SOX11-positive xenograft tumors
Enriched in leukemic SOX11-expressing (n = 16) vs SOX11-negative (n = 22) MCL primary tumors				
LU_TUMOR_VASCULATURE_UP	1.51	.03	0.12	SOX11-expressing leukemic MCL primary tumors
ANGIOGENESIS	1.51	.02	0.1	SOX11-expressing leukemic MCL primary tumors
VASCULATURE_DEVELOPMENT	1.44	.04	0.18	SOX11-expressing leukemic MCL primary tumors
REGULATION_OF_ANGIOGENESIS	1.44	.04	0.14	SOX11-expressing leukemic MCL primary tumors
LU_TUMOR_ENDOTHELIAL_MARKERS_UP	1.60	.02	0.11	SOX11-expressing leukemic MCL primary tumors
Enriched in SOX11-positive (n = 2) vs SOX11-silenced (n = 4) MCL cell lines				
LU_TUMOR_ANGIOGENESIS_UP	1.646	.01	0.06	Z138 SOX11-positive MCL cell line

GSEA was used to test for significant enrichment of defined gene signatures related to angiogenesis. NES and FDR *P* values are shown and significance is considered when FDR <0.2. Gene signatures were downloaded from the MSigDB, Molecular Signature Database of Broad Institute.

FDR, false discovery rate; NES, normalized enrichment score.

21 proangiogenic factors compared with SOX11-knockdown xenografts including ANG, MMP9, PDGFA, and PDGFAB/PDGFB (Figure 1B). Moreover, SOX11-positive xenografts displayed higher CD31-positive MVD areas than SOX11-knockdown ones (90% ± μm^2 vs 15% ± μm^2, respectively, $P < 1 \times 10^{-4}$) (Figure 1C). Together, these results suggest that SOX11 may facilitate tumor growth by upregulating different proangiogenic factors and enhancing MCL tumor angiogenesis in vivo.

Conditioned media from SOX11-positive cell lines promote in vitro angiogenesis

We next analyzed the effects of the CM derived from SOX11-positive and -silenced MCL cell lines on several angiogenic responses of endothelial cells in vitro. We first performed tube formation assays using cultured HUVECs on Matrigel matrix.[22] As shown in Figure 2A, SOX11-positive CM significantly promoted a prominent increase in tube formation compared with CM from SOX11-negative cells and RPMI + 10% FBS. Conversely, SOX11-negative CM did not have an effect on tube formation compared with RPMI + 10% FBS. Concordantly, HUVECs displayed significantly increased proliferation (Figure 2B) and migration (Figure 2C) toward SOX11-positive CM of the 3 cell lines compared with SOX11-negative CM. We next confirmed that SOX11-positive CM media induced phosphorylation of Akt, FAK, and Erk1/2 compared with SOX11-negative CM or RPMI + 10% FBS whereas basal levels of these proteins did not change (Figure 2D). These results suggest that SOX11-positive CM may contain soluble factors that promote endothelial tube formation, proliferation, migration, and activation of signaling pathways required for angiogenesis.

SOX11 drives transcriptional activation of *PDGFA*

To identify the angiogenic factors expressed and secreted by SOX11-positive cells, we first performed a GSEA of the differential gene expression data sets of our MCL cell lines[15] and observed that, similarly to the xenograft tumors, SOX11-positive cell lines were also enriched in gene signatures related to tumor angiogenesis (Figure 3A, Table 1). We next investigated the expression levels of several angiogenic factors in the protein extracts of SOX11-positive and SOX11-silenced cells. Although the number of proangiogenic proteins differentially expressed between SOX11-positive and SOX11-silenced cell lines was much lower than in the tumor xenograft lysates, SOX11-positive cells still expressed significantly higher levels of the proangiogenic factors Activin A, ANGPT2, PDGFA, and VEGF compared with SOX11-silenced ones (Figure 3B).

To determine whether MCL cells secreted these factors in vitro, we analyzed SOX11-CM using a quantibody angiogenesis array and observed that SOX11-positive CM had significantly increased levels of PDGFA secretion compared with SOX11-negative CM (Figure 3C). No other proangiogenic factors analyzed (PDGFB, ANG, ANGPT1, ANGPT2, VEGF, FGF1, or FGF2) were detected in any MCL CM.

We performed a GO term analysis of our previous genome-wide promoter ChIP-chip study,[15] which showed that blood vessel development was one of the most significant biological processes overrepresented among the SOX11-bound genes (Figure 3D). However, among the proangiogenic factors overexpressed in the SOX11-positive cell lines (Figure 3B), *PDGFA* was the only one identified as a SOX11-bound gene by ChIP experiments, with no significant binding to *Activin A*, *ANGPT2*, or *VEGF* regulatory regions. Following on these results, we validated the specific binding of SOX11 to the regulatory region of *PDGFA* by ChIP-qPCR experiments. We observed a ±twofold and ±fourfold enrichment for *PDGFA* in Z138 and JEKO1, respectively, demonstrating that SOX11 directly binds to regulatory regions of *PDGFA* (Figure 3E).

Luciferase reporter assays with a *PDGFA* regulatory construct encompassing the SOX11 binding site showed a significant threefold induction ($P < 1 \times 10^{-4}$) in luciferase activity upon coexpression of SOX11 but not with an inactive truncated SOX11 protein lacking the High Mobility Group (HMG) domain (ΔHMGSOX11). Similar results were obtained with a *PAX5*-enhancer-luciferase reporter vector,[15] used as a positive control (Figure 3F).

Together, these findings verify the positive transcriptional effect of SOX11 on the *PDGFA* regulatory region and suggest that PDGFA may be the major mediator of angiogenic in SOX11-positive MCLs.

Inhibition of the PDGFA signaling pathway on endothelial cells impairs SOX11-enforced angiogenesis in MCL

To validate the involvement of PDGFA in promoting angiogenesis in MCL, we analyzed the phosphorylation level of endogenous PDGFR-α in HUVECs upon incubation with Z138 SOX11-positive

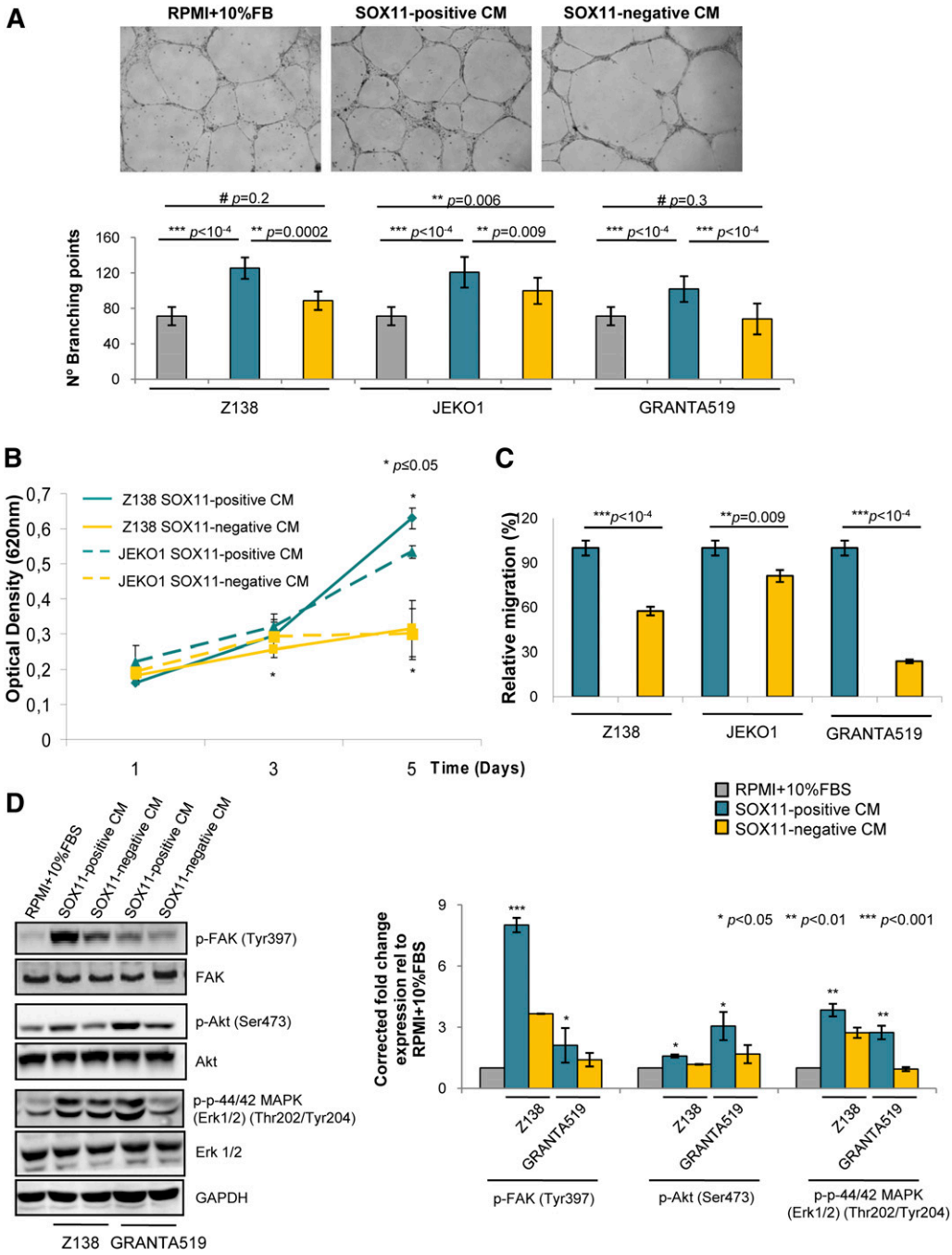

Figure 2. SOX11 promotes endothelial tube formation, cell proliferation and migration, and activation of angiogenic signaling cascades in vitro. (A) Top panel, Representative images showing the capillary tube formation by HUVECs growing on Matrigel matrix for 6 hours in the presence of control RPMI + 10% FBS, SOX11-positive or SOX11-negative CM on Matrigel matrix. Bottom panel, Quantification of the number of branching points representing tube formation by HUVECs cultured for 6 hours in RPMI + 10% FBS or SOX11-positive and SOX11-negative CM from Z138, JEKO1, and GRANTA519 MCL cell lines. SOX11-positive CM significantly promoted a prominent increase in tube formation compared with CM from SOX11-negative cells (126 vs 89 branching points, $P = .0002$, 121 vs 100 branching points, $P = .009$, and 102 vs 70 branching points, $P < 1 \times 10^{-4}$ in Z138, JEKO1, and GRANTA519) and RPMI + 10% FBS (126 vs 76 branching points, $P < 1 \times 10^{-4}$, 121 vs 76 branching points, $P < 1 \times 10^{-4}$, and 102 vs 76 branching points, $P < 1 \times 10^{-4}$ in Z138, JEKO1, and GRANTA519). Conversely, SOX11-negative CM did not have an effect on tube formation compared with RPMI + 10% FBS (89 vs 76 branching points, $P = .2$, 70 vs 76 branching points, $P = .3$ in Z138 and GRANTA519). (B) Kinetics of HUVEC growth in SOX11-positive CM (blue) or SOX11-negative CM (yellow) derived from SOX11-positive and SOX11-silenced Z138 (solid line) and JEKO1 (dashed line) MCL cell lines. Graph showing the optical density (620 nm) after staining the HUVECs with 0.2% crystal violet and measured at 620-nm wavelengths at the indicated time points (1, 3, and 5 days). (C) Graph displaying the percentage of migratory HUVEC cells toward SOX11-positive and SOX11-negative CM from Z138, JEKO1, and GRANTA519 MCL cell lines, relative to the percentage of migratory HUVEC cells toward RPMI + 10% FBS. HUVECs displayed significantly increased migration toward SOX11-positive CM cell lines (±90% migration) compared with SOX11-negative CM (±30%-70% migration, in Z138 and GRANTA519 [$P < 1 \times 10^{-4}$] and JEKO1 [$P = .009$]). (D) Left panel, WB experiments showing expression levels of basal and phosphorylated forms of FAK, Akt, and Erk1/2 proteins in HUVECs cultured in RPMI + 10% FBS or SOX11-positive and SOX11-negative CM from Z138 and GRANTA519 MCL cell lines for 3 hours. GAPDH was used as a loading control. Right panel, Fold change differences of phosphorylated forms of FAK, Akt, and Erk1/2 proteins in HUVECs cultured in RPMI + 10% FBS or SOX11-positive and SOX11-negative CM from Z138 and GRANTA519 MCL cell lines for 3 hours, correlated by quantification of GAPDH expression levels. Bar plot represents the mean percentage ± SD, n = 3. *P*-val is shown. The significance of difference was determined by independent samples Student *t* test. GAPDH, glyceraldehyde-3-phosphate dehydrogenase.

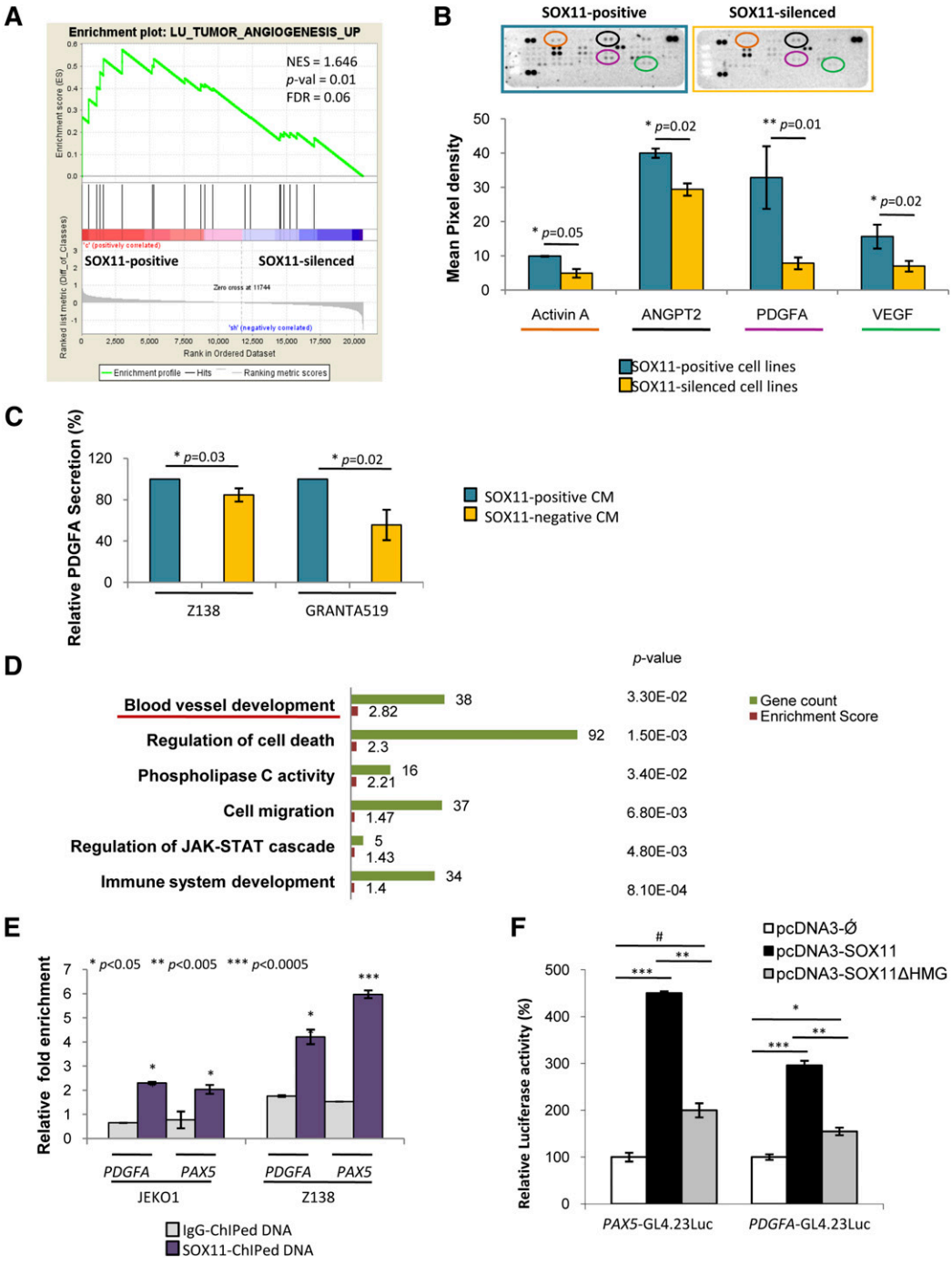

Figure 3. SOX11 binds to regulatory regions of *PDGFA* and positively regulates its transcription. (A) GSEA analysis on expression data set from SOX11-positive and SOX11-silenced MCL cell lines showing enriched gene sets related to angiogenesis pathways. NES, *P*-val, and FDR are represented. Statistical significance is considered when FDR < 0.2. (B) Top panel, Image showing human-specific angiogenesis antibody array membranes incubated with protein lysates from Z138 SOX11-positive (n = 2) and SOX11-silenced (n = 2) MCL cell lines. Bottom panel, Quantification of mean pixel density of the proangiogenic factors Activin A, ANGPT2, PDGFA, and VEGF comparing SOX11-positive and SOX11-silenced MCL cell lines. (C) Graph displaying the relative levels of PDGFA secreted by SOX11-positive and SOX11-silenced CM derived from Z138 and GRANTA519 MCL cell lines. Concentration was analyzed by a quantibody human angiogenesis array. Results are shown as relative percentage of PDGFA secretion compared with SOX11-positive CM. (D) Graph displaying the GO term results obtained from DAVID functional annotation tool of the high confidence SOX11-bound genes identified by ChIP-chip experiments (GSE3502).[15] The 6 most significant biological process GO terms and their gene count, enrichment score, and *P*-val are shown. Underlined is the blood vessel development GO biological term. (E) ChIP-qPCR analysis of specific binding of SOX11 to the regulatory regions of *PDGFA* in JEKO1 and Z138 MCL cell lines. Binding to *PAX5* was used as a positive internal control.[15] Relative DNA enrichment was measured by qPCR using specific primers for the respective regulatory regions (see "Methods"), and is displayed as fold enrichment relative to their respective input chromatin. Purple bars represent ChIP-qPCR enrichment of the SOX11 pull-down (SOX11-ChIPed DNA) while gray bars represent the negative control (IgG-ChIPed DNA). (F) Luciferase assays in transient cotransfections of *PAX5*-GL4.23 Luc and *PDGFA*-GL4.23 Luc with SOX11 full-length (pcDNA3-SOX11) and the truncated SOX11 proteins (pcDNA3-SOX11ΔHMG) expression vectors in HEK293 cells. Results are shown as the percentage of fold induction relative to luciferase activity in cotransfection with the empty vector (pcDNA3-Ø). Bar plot represents the mean percentage ± SD of 3 independent experiments. *P*-val are shown. The significance of difference was determined by independent samples Student *t* test.

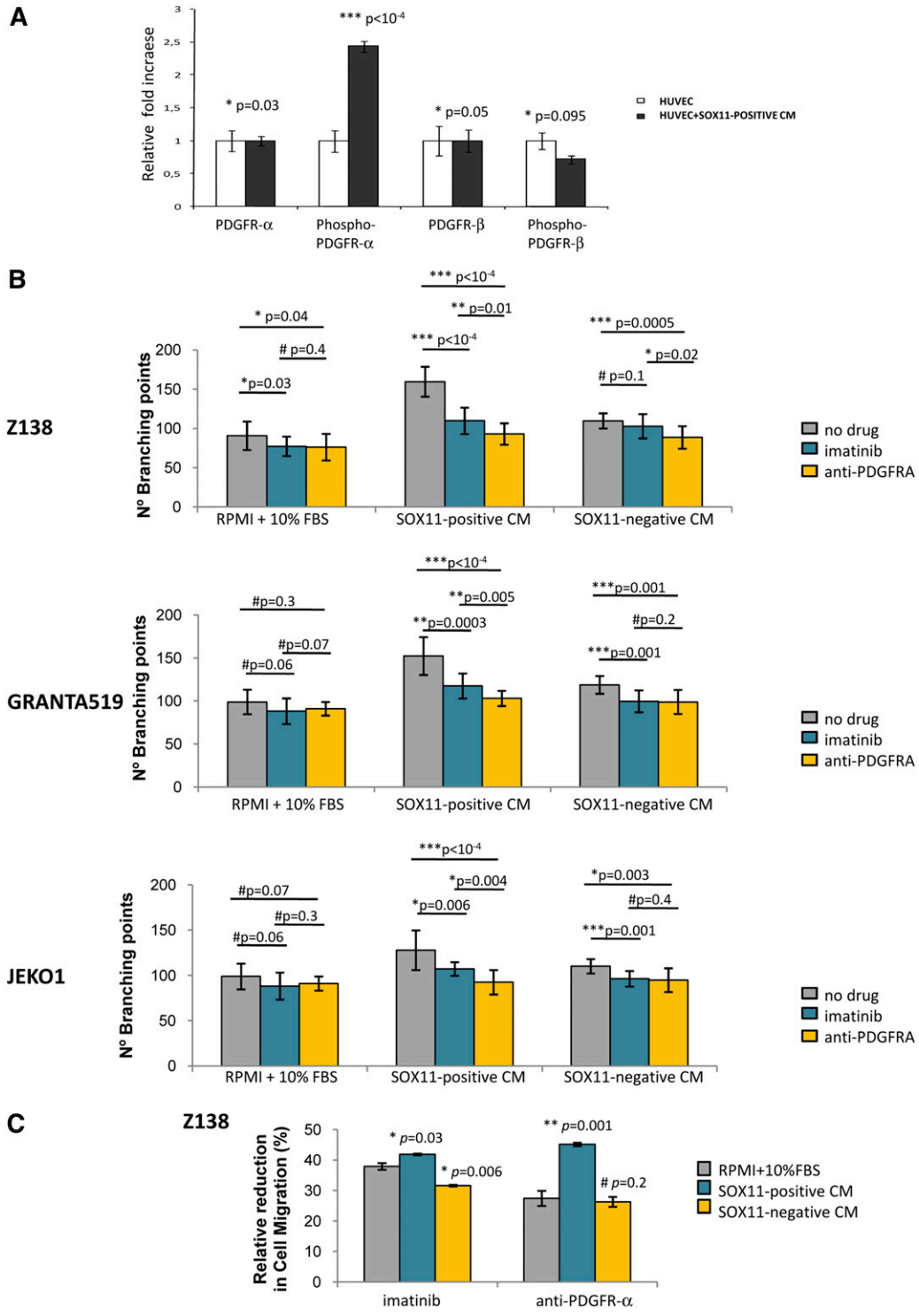

Figure 4. PDGFA inhibition on endothelial cells impairs SOX11-enforced angiogenesis in MCL. (A) Graph showing the relative fold change expression levels of the basal and phosphorylated forms of PDGFRα and PDGFRβ by HUVEC cells upon 3-hour incubation with RPMI + 10% FBS (HUVEC) or Z138 SOX11-positive CM (HUVEC+ SOX11-positive CM). Results are shown as fold increase relative to the corresponding expression levels by the HUVECs incubated with RPMI + 10% FBS. (B) Graphs showing number of branching points representing tube formation by HUVECs. HUVECs were pretreated with control PBS (gray), imatinib (blue), or a neutralizing antibody anti-PDGFRα (yellow) for 1 hour, and then incubated for 6 hours with RPMI + 10% FBS, SOX11-positive or SOX11-negative CM from Z138, GRANTA519, and JEKO1 MCL cell lines. (C) Graph displaying the relative perctage reduction in migration of HUVECs. HUVECs were pretreated with control PBS, imatinib, or a neutralizing antibody anti-PDGFRα for 1 hour, and then allowed to migrate toward RPMI + 10% FBS (gray), SOX11-positive CM (blue) or SOX11-negative CM (yellow) from Z138 MCL cell line. Upon overnight incubation, migratory cells were quantified and represented as the percentage of migration HUVECs compared with no drug (control PBS) treatment. Bar plot represents the mean percentage ± SD of 3 independent experiments. *P*-val are shown. The significance of difference was determined by independent samples Student *t* test.

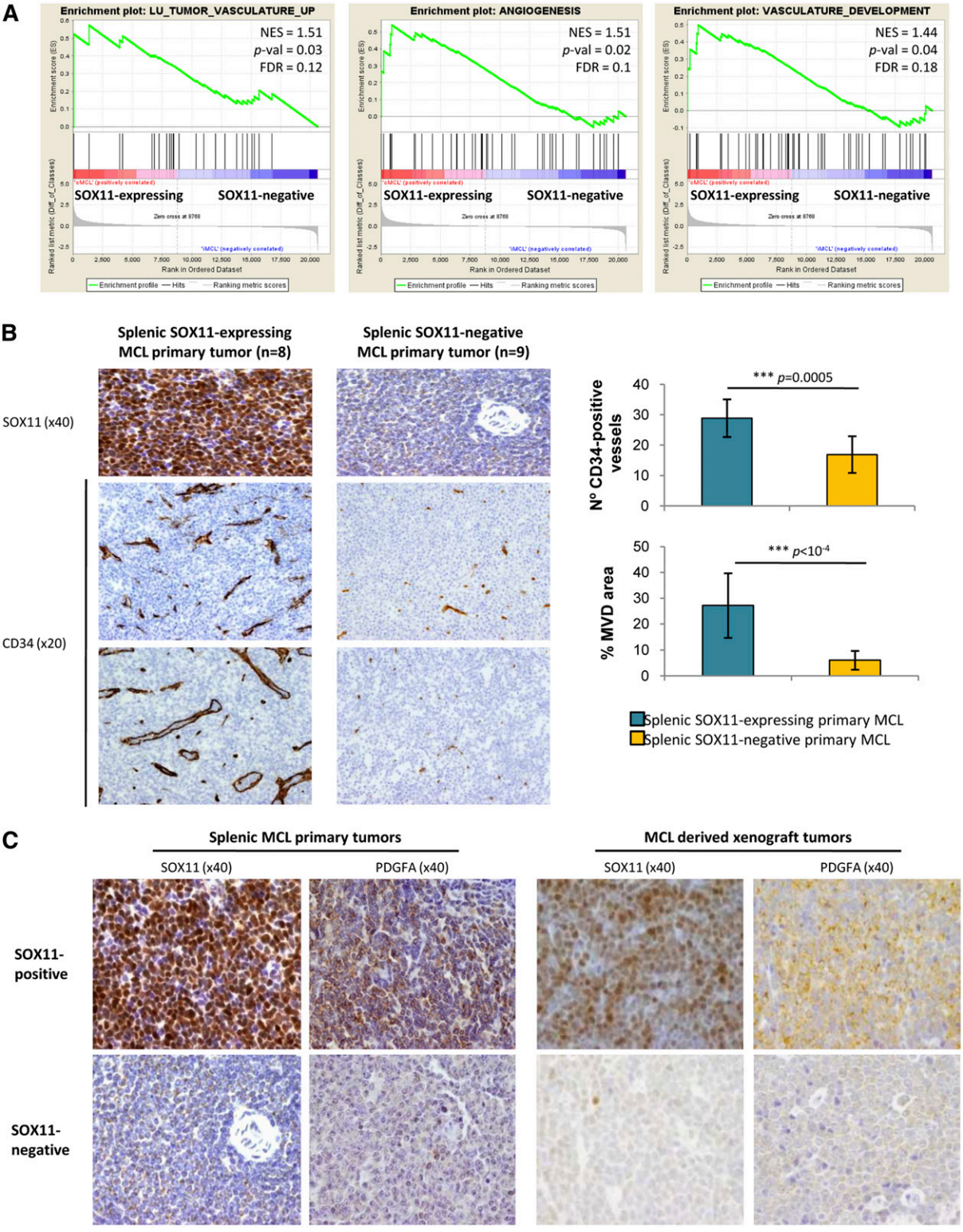

Figure 5. SOX11-positive MCL tumors have increased tumor angiogenesis network and PDGFA overexpression. (A) GSEA analysis on expression data sets from leukemic MCL primary tumors (16 SOX11-expressing and 22 SOX11-negative (GSE36000)[17] showing enriched gene sets related to angiogenesis pathways. NES, *P*-val, and FDR are shown. Statistical significance is considered when FDR < 0.2. (B) Left panel, Histological sections from representative SOX11-expresing (n = 8) and SOX11-negative (n = 9) splenic MCL primary tumors stained with specific antibodies against human SOX11 (×40) and CD34 (×20). Right panel, Graph showing quantification of number of CD34-positive vessels and percentage of CD34-positive MVD areas of the splenic MCL primary tumors. Bar plot represents the mean percentage ± SD. *P*-val are shown. The significance of difference was determined by independent samples *t* test. (C) Representative histological sections from SOX11-positive and SOX11-negative tumors from splenic MCL primary samples (n = 8 and n = 9, respectively) and MCL xenograft tumors (n = 3 and n = 10, respectively) stained with a specific antibody anti-human SOX11 (×40) and PDGFA (×40).

Table 2. Clinical and pathological characteristics of MCL with splenic involvement

	SOX11-negative MCL	SOX11-positive MCL
Patients		
No.	9	8
Median age, y (range)	70 (62-75)	65 (42-89)
Sex		
Male (%)	6 (67)	6 (75)
Female (%)	3 (33)	2 (25)
Histology		
Small cell (%)	4/9 (44)	1/8 (13)
Classic (%)	5/9 (56)	7/8 (87)
Ki67 index, mean ± SD	12.1 ± 9.83	28.63 ± 16.21
Ann Arbor stage		
I/II (%)	0/5 (0)	0/5 (0)
III/IV (%)	5/5 (100)	5/5 (100)
LDH level > normal (%)	2/5 (40)	0/2 (0)
Nodal involvement (%)	2/9 (22)	3/8 (38)
Leukemic involvement (%)	7/7 (100)	4/4 (100)
BM involvement (%)	5/5 (100)	5/5 (100)
Therapy		
Chemotherapy (%)	2/8 (25)	5/6 (83)
Only splenectomy (%)	6/8 (75)	1/6 (17)
Mean survival, mo (range)	96 (76-116)	49 (31-67)

BM, bone marrow; LDH, L-lactate dehydrogenase.

CM. We observed a significant 2.4-fold increase ($P < 1 \times 10^{-4}$) in PDGFR-α but not in PDGFR-β phosphorylation when HUVECs were cultured in Z138 SOX11-positive CM compared with RPMI + 10% FBS (Figure 4A), demonstrating the paracrine activation of the PDGFA/PDGFR-α angiogenic pathway on endothelial cells in MCL. Furthermore, we treated HUVECs with imatinib, a tyrosine kinase inhibitor of PDGFR, or a neutralizing antibody against human PDGFR-α, and then performed tube formation and migration assays in the presence of RPMI + 10% FBS or SOX11-positive CM. The tube formation induced by SOX11-positive CM of Z138, GRANTA519, and JEKO1 was significantly decreased when HUVECs were pretreated with imatinib or the neutralizing PDGFR-α antibody (Figure 4B). Both pretreatments also caused a significant reduction on HUVEC migration toward SOX11-positive CM when compared with no drug treatment (Figure 4C).

To determine whether PDGFR-α was expressed in MCL cells lines and primary tumors, we analyzed its messenger RNA (mRNA) levels in the GEP microarray data of our primary MCL tumors and MCL cell lines using as positive and negative references the previously published data of peripheral T-cell lymphoma (PTCL), a tumor known to express high levels of PDGFR-α, and the GEP of normal mature T cells, a subset of cells known to be negative for this receptor.[23] We confirmed the high levels of PDGFR-α in the PTCL whereas all our primary MCL and MCL cell lines had undetectable levels similarly to normal T lymphocytes (supplemental Figure 1). These findings indicate the lack of expression of PDGFR-α in MCL cells and support the idea that the secreted PDGFA must have a paracrine effect on the endothelial cells rather than an autocrine action on the MCL cells. Altogether, these results demonstrate that the enhanced angiogenic activity of the SOX11-positive CM is mediated by PDGFA expression, and its inhibition impairs SOX11-promoted angiogenic effects on endothelial cells.

Human SOX11-positive primary MCL overexpress PDGFA and have increased angiogenesis

To determine whether SOX11 could be regulating angiogenesis in vivo, we analyzed gene expression signatures of primary human MCL samples. GSEA revealed that SOX11-expressing human primary tumors were also significantly enriched in signatures related to angiogenesis such as tumor vasculature, angiogenesis, vasculature development, regulation of angiogenesis, and tumor endothelial markers (Figure 5A, Table 1). We then analyzed the MVD in an independent series of human MCL primary tumors (Table 2) by staining splenic tissue sections of 8 SOX11-expressing and 9 SOX11-negative tumors for CD31 and CD34. Both antibodies provided similar results with SOX11-positive tumors showing a significantly higher number of vessels than SOX11-negative MCL (±30 microvessels per μm^2 vs ±15 per μm^2, respectively, $P = .0005$) and larger vascular areas (30% ± μm^2 vs 5% ± μm^2, $P < 1 \times 10^{-4}$) (Figure 5B). These results confirm that SOX11 may also promote angiogenesis in primary human MCL.

We next investigated whether PDGFA mRNA was also overexpressed in human primary SOX11-positive MCL using the data of our microarray GEP of 38 primary MCL tumors, 16 SOX11-expressing, and 22 SOX11-negative and found a significant 1.6-fold increased level in SOX11-positive tumors ($P = .0303$) (supplemental Figure 2). Concordantly, high PDGFA expression was immunohistochemically demonstrated on the tumor cells of 8 SOX11-expressing MCL whereas it was not detected in the tumor cells of 9 SOX11-negative tumors. These results were also confirmed in the SOX11-positive and SOX11-negative xenograft tumors (Figure 5C). Therefore, these findings indicate that SOX11 upregulates PDGFA expression in MCL both in vitro and in vivo, mediating the SOX11-enforced angiogenesis that may contribute to the aggressiveness of these tumors.

Imatinib reduces tumor growth and angiogenesis of SOX11-positive MCL xenograft tumors

To demonstrate whether the in vitro inhibitory effect of imatinib on the SOX11-induced angiogenesis may also occur in vivo and, consequently, have an effect on tumor growth, we treated SOX11-positive and SOX11-negative MCL xenografts with imatinib or vehicle PBS and followed tumor growth up. In these experiments, imatinib treatment significantly suppressed tumor growth of the SOX11-positive xenografts compared with vehicle-treated controls (Figure 6A-B) bringing down the growth of SOX11-positive MCL xenograft to that of SOX11-knockdown tumors (Figure 6B).

To determine whether tumor growth reduction upon imatinib treatment was associated with impaired angiogenesis, tumor microvasculature was visualized by histologically staining imatinib- or PBS-treated xenografts with CD31. Compared with PBS treatment, administration of imatinib was strongly associated with a loss of microvasculature in the SOX11-positive xenografts, equaling the number of CD31-positive vessels and MVD areas to those observed in the SOX11-knockdown tumors (Figure 6C), suggesting that the abolishment in MVD was responsible for the tumor reduction observed in the imatinib-treated xenografts. Altogether, these results indicate that PDGFA inhibition could be effective to improve disease outcome of SOX11-positive MCL.

Discussion

Our study shows that increased tumor angiogenesis is a prominent feature of SOX11-positive MCL required for effective tumor growth, and provides evidences to support the inhibition of this mechanism as a new strategy for the management of aggressive MCL patients.

Angiogenesis deregulation is one of the hallmarks of cancer widely investigated in solid malignancies where it has been

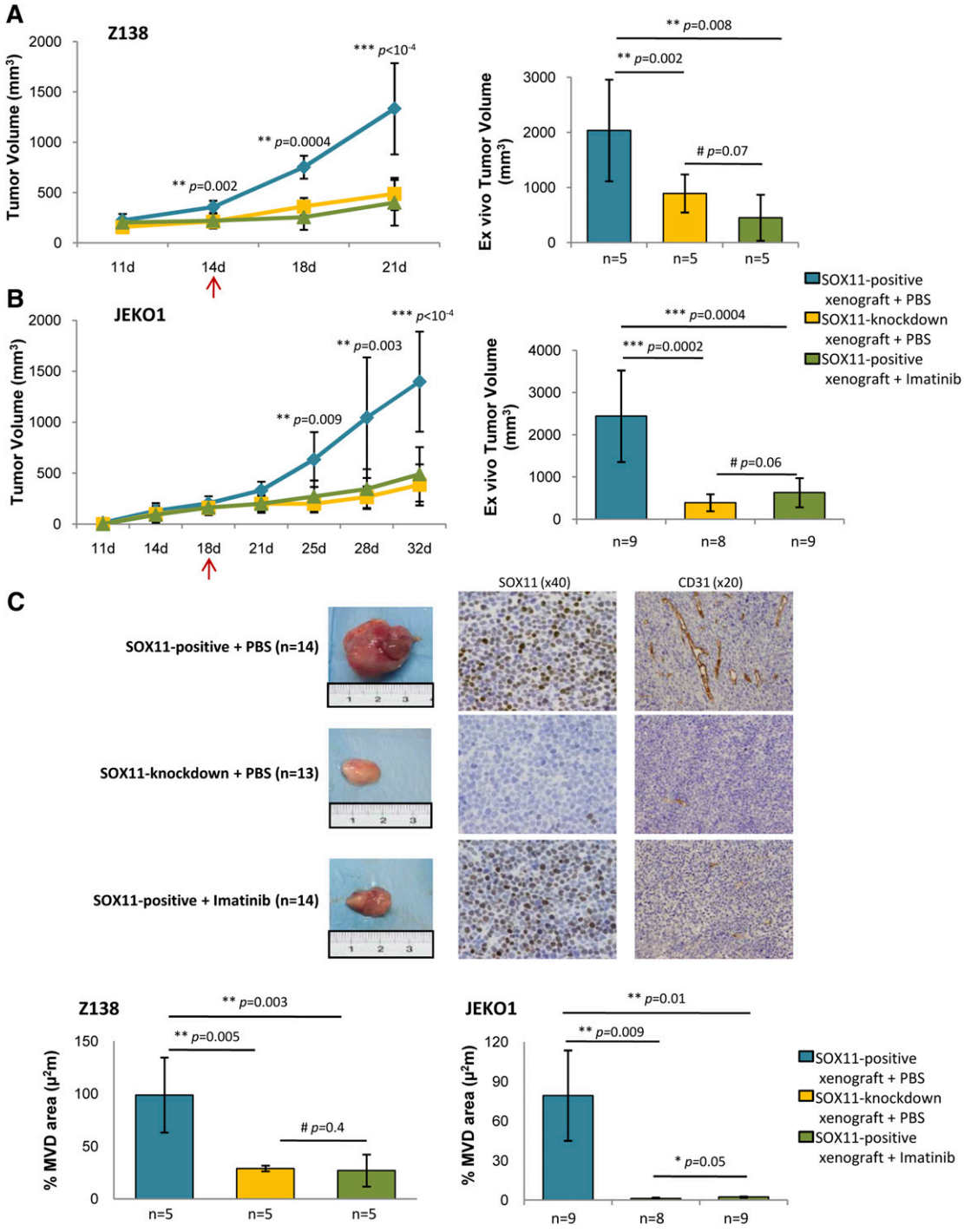

Figure 6. Imatinib reduces MCL tumor growth and angiogenesis of SOX11-positive MCL xenograft tumors. (A-B) Left panel, Tumor growth represented by tumor volumes (mm^3) at the indicated days PI of Z138 and JEKO1 SOX11-positive xenografts treated with IP injections of imatinib (n = 5, n = 9) (green) or vehicle PBS (n = 5, n = 9) (blue) and SOX11-knockdown xenografts treated with IP of vehicle PBS (n = 5, n = 8) (yellow). Right panel, Graph displaying tumor volumes (mm^3) at the time of tissue harvest, comparing imatinib (green) vs vehicle PBS (blue) treated SOX11-positive xenografts and (yellow) vehicle PBS-treated SOX11-knockdown xenografts. Compared with vehicle PBS, imatinib treatment significantly suppressed tumor growth of the SOX11-positive xenografts observed during follow-up (400 mm^3 vs 1330 mm^3, $P < 1 \times 10^{-4}$, and 490 mm^3 vs 1400 mm^3, $P < 1 \times 10^{-4}$ in Z138 and JEKO1, respectively) and ex vivo measurements (450 mm^3 vs 2000 mm^3, $P = .008$, and 630 mm^3 vs 2400 mm^3, $P = .0004$ in Z138 and JEKO1, respectively). (C) Top panel, Macroscopic appearance and consecutive histological sections from representative SOX11-positive (n = 14) and SOX11-knockdown xenograft tumors (n = 13) upon imatinib or vehicle PBS treatment. Immunohistochemical stainings were performed with a specific antibody anti-human SOX11 (×40) and an anti-mouse CD31 (×20). Bottom panel, Graph displaying the percentage of density of CD31-positive MVD areas in Z138 and JEKO1 xenograft tumors in (green) imatinib or (blue) vehicle PBS-treated SOX11-positive xenografts and (yellow) vehicle PBS-treated SOX11-knockdown xenografts, delineated by the presence of CD31-positive staining. Bar plot represents the mean percentage ± SD. *P*-val are shown. The significance of difference was determined by independent sample Student *t* test. PI, postinoculation.

associated with neoplastic growth and progression.[24-26] Recent studies have also revealed the pathogenic relevance and clinical impact of the "angiogenic switch" in lymphoid neoplasms but the mechanisms regulating this phenomenon are not well known.[26,27] In this study, we have shown that the more aggressive SOX11-positive MCL xenografts were enriched in angiogenic gene signatures and displayed much larger microvascular density areas than their SOX11-negative counterparts, concurring with other observations that an increased MVD correlates with disease progression in lymphoid neoplasms.[28,29] We therefore postulated that SOX11-positive MCL cells could promote a pronounced vasculature development and obtain an increased and deregulated blood supply that may contribute to their aggressive progression.

Interestingly, SOX11-positive CM promoted vascular tube formation, endothelial cell proliferation, and migration, and activation of relative angiogenic downstream pathways in HUVECs, indicating that SOX11-positive MCL cells secrete soluble factors that enhance signaling pathways related to cell migration and survival which are known to be activated by PDGFs in other cell types.[30] Concordant with our results, a recent study in zebrafish has reported the involvement of SOX11b, the human ortholog of SOX11, in promoting sprouting angiogenesis of caudal vein plexus.[31]

The gene transcriptional profile of SOX11-positive MCL cell lines was enriched in signatures related to angiogenesis and expressed higher levels of several proangiogenic factors than SOX11-negative ones. On the other hand, the number of proangiogenic factors upregulated in SOX11-positive tumor xenografts was much larger than in the respective cell lines, highlighting the cross-talk between tumor and accessory cells of the microenvironment in the regulation of angiogenesis. Among the proangiogenic factors overexpressed by SOX11-positive MCL cell lines in vitro, we could only detect secreted PDGFA at high levels in their corresponding CM, and *PDGFA* was the only gene directly bound by SOX11 in our ChIP-chip study, strongly supporting the idea that this gene could be one of the main SOX11-dependent factors regulating angiogenesis in MCL.

PDGFA is a member of the PDGF family of proangiogenic factors which may participate in the development of a vascular tumor microenvironment through a direct effect on the endothelium but also indirectly by recruiting mesenchymal stromal cells that release additional angiogenic elements.[32-35] The PDGF family consists of 5 isoforms that exert their cellular effects by binding to PDGFR-α or PDGFR-β with different affinities. PDGFA only binds to PDGFR-α, activating their downstream pathways involved in several oncogenic mechanisms including angiogenesis.[36,37] Several studies have demonstrated that PDGFR-α is expressed by HUVECs and solid tumor endothelial cells,[38,39] and here we demonstrated an increased phosphorylation of PDGFR-α but not PDGFR-β in HUVECs upon SOX11-positive CM incubation. Furthermore, we have demonstrated the activation of AKT, ERK, and FAK upon SOX11-positive CM incubation. The activation of these signaling pathways mediates proliferation, survival, and migration of endothelial responses required by the complex and multistep process of angiogenesis.

Pretreatment of HUVECs with imatinib or a specific neutralizing antibody against PDGFR-α inhibited their tube formation and migration promoted by the SOX11-positive CM. Although imatinib does not specifically target PDGFR kinases,[40-42] the lack of expression of PDGFR-α and the 2 other target kinases c-KIT and BCR-ABL in MCL cell lines and primary tumors indicates that its inhibitory effects on HUVEC angiogenic capacities are due to a blockade of the PDGFA/PDGFR-α angiogenic pathway cascade. The similar inhibitory effects obtained using the specific neutralizing antibody against PDGFR-α corroborate the blockade of the PDGFA/PDGFR-α axis by imatinib impairing HUVEC angiogenic abilities and support the idea that PDGFA promotes angiogenesis in MCL by a direct paracrine effect on endothelial cells.

SOX11-positive primary MCL showed a significant enrichment in angiogenic-related expression signatures and higher MVD than negative tumors. In addition, PDGFA was strongly expressed in SOX11-positive MCL but not detected in negative tumors, strongly supporting that the SOX11-PDGFA–related angiogenic development identified in the experimental models also plays a role in human tumors. SOX11-negative MCL usually present clinically with non-nodal leukemic disease whereas SOX11-positive tumors involve lymph nodes and have extensive extranodal infiltration.[4,5] The SOX11-dependent "angiogenic switch" discovered in this study may explain MCL clinical heterogeneity because the low angiogenic potential of SOX11-negative cells may impair their tissue infiltration and retain them in the bloodstream whereas SOX11-induced angiogenesis facilitates tissue infiltration and growth of the SOX11-expressing MCL cells.

The importance of tumor angiogenesis in the development and clinical progression of lymphoid neoplasias has suggested that these mechanisms may be potential targets for new therapies.[43] Imatinib has proven antiangiogenic effects in a DLBCL xenograft model targeting pericytes via PDGFR-β,[44] and lenalidomide impairs lymphangiogenesis in MCL preclinical models.[45] The striking growth impairment of the SOX11-positive xenografts due to a significant reduction in MVD and an impaired angiogenesis, together with the direct endothelial inhibitory effect of imatinib similar to the anti-PDGFR-α in the in vitro experiments, suggest that angiogenic pathway may represent a novel therapeutic strategy for the treatment of aggressive MCL. However, imatinib treatment may have some limitations in the clinical context since the development of MCL has been observed in 2 patients during treatment of chronic myelogenous leukemia (CML) with this tyrosine kinase inhibitor.[46,47] These 2 MCL cases were "blastoid" variants that had accumulated complex karyotypes including deletions of chromosome 9 (*INK4a*) and *ATM* and *TP53* mutations. These genetic alterations are associated with an angiogenic switch through different mechanisms such as induction of VEGF, HIF-1, and downregulation of thrombospondin-1, respectively.[48-50] Therefore, blastoid tumors may develop angiogenic stimuli alternative to the PDGFA–PDGFR-α axis.

In conclusion, we provide unique evidences on the SOX11-mediatied regulation of angiogenesis via the PDGFA pathway in MCL that in turn facilitates tumor growth. These findings in experimental models and primary human tumors support the oncogenic role of SOX11 in the aggressive behavior of MCL. Targeting the SOX11-PDGFA axis, which regulates the maintenance, migration, and proliferation of vascular endothelial cells, represents an attractive strategy to dismantle the lymphoma vasculature and therefore the growth and progression of this tumor. Modulation of this angiogenic pathway may therefore constitute a potential novel therapeutic strategy for the treatment of aggressive MCL.

Acknowledgments

This work was supported by the Ministerio de Economía y Competitividad (BFU2009-09235, BFU2012-30857, and RYC-2006-002110 [V.A.]), the Fundació La Marató de TV3 (TV3-Cancer-I3/20130110 [V.A.]), and the Instituto de Salud Carlos III (SAF2012-38432 and PIE13/00033 [E.C.] and SAF11/30073 [M.C.C.]). Fondo Europeo de Desarrollo Regional. Unión Europea. Una manera de hacer Europa.

Authorship

Contribution: J.P. performed all of the in vitro and in vivo experiments, and quantified MVD in both xenograft and MCL primary tumors; M.C.V. performed ChIP experiments; M.L.R. performed WB experiments; A.E. performed luciferase assays; G.C. performed statistical analysis; E.P.-R. performed angiogenic experiments in vitro; P.J. performed GEP analysis; I.R.-C. performed immunohistochemistry experiments and quantified MVD in MCL primary tumors; M.C.C. supervised the angiogenic experiments in vitro; E.C. identified morphologically MCL tumors, analyzed data, and supervised experiments; V.A. designed, performed, and supervised experiments, analyzed data, and wrote the manuscript; and all authors discussed the results and commented on the manuscript.

Conflict-of-interest disclosure: The authors declare no competing financial interests.

Correspondence: Virginia Amador, Centre Esther Koplowitz (CEK), C/Rosselló 153, Barcelona-08036, Spain; e-mail: vamador@clinic.ub.es.

References

1. Swerdlow SH, Campo E, Harris NL, et al. *WHO Classification of Tumours of Haematopoietic and Lymphoid Tissues*. Lyon, France: AIRC Press; 2008.
2. Jares P, Colomer D, Campo E. Molecular pathogenesis of mantle cell lymphoma. *J Clin Invest.* 2012;122(10):3416-3423.
3. Orchard J, Garand R, Davis Z, et al. A subset of t(11;14) lymphoma with mantle cell features displays mutated IgVH genes and includes patients with good prognosis, nonnodal disease. *Blood.* 2003;101(12):4975-4981.
4. Fernàndez V, Salamero O, Espinet B, et al. Genomic and gene expression profiling defines indolent forms of mantle cell lymphoma. *Cancer Res.* 2010;70(4):1408-1418.
5. Espinet B, Ferrer A, Bellosillo B, et al. Distinction between asymptomatic monoclonal B-cell lymphocytosis with cyclin D1 overexpression and mantle cell lymphoma: from molecular profiling to flow cytometry. *Clin Cancer Res.* 2014;20(4): 1007-1019.
6. Royo C, Navarro A, Clot G, et al. Non-nodal type of mantle cell lymphoma is a specific biological and clinical subgroup of the disease. *Leukemia.* 2012;26(8):1895-1898.
7. Sock E, Rettig SD, Enderich J, Bösl MR, Tamm ER, Wegner M. Gene targeting reveals a widespread role for the high-mobility-group transcription factor Sox11 in tissue remodeling. *Mol Cell Biol.* 2004;24(15):6635-6644.
8. Haslinger A, Schwarz TJ, Covic M, Lie DC. Expression of Sox11 in adult neurogenic niches suggests a stage-specific role in adult neurogenesis. *Eur J Neurosci.* 2009;29(11): 2103-2114.
9. Mu L, Berti L, Masserdotti G, et al. SoxC transcription factors are required for neuronal differentiation in adult hippocampal neurogenesis. *J Neurosci.* 2012;32(9):3067-3080.
10. Lin L, Lee VM, Wang Y, et al. Sox11 regulates survival and axonal growth of embryonic sensory neurons. *Dev Dyn.* 2011;240(1):52-64.
11. Weigle B, Ebner R, Temme A, et al. Highly specific overexpression of the transcription factor SOX11 in human malignant gliomas. *Oncol Rep.* 2005;13(1):139-144.
12. de Bont JM, Kros JM, Passier MM, et al. Differential expression and prognostic significance of SOX genes in pediatric medulloblastoma and ependymoma identified by microarray analysis. *Neuro-oncol.* 2008;10(5): 648-660.
13. Dictor M, Ek S, Sundberg M, et al. Strong lymphoid nuclear expression of SOX11 transcription factor defines lymphoblastic neoplasms, mantle cell lymphoma and Burkitt's lymphoma. *Haematologica.* 2009;94(11): 1563-1568.
14. Mozos A, Royo C, Hartmann E, et al. SOX11 expression is highly specific for mantle cell lymphoma and identifies the cyclin D1-negative subtype. *Haematologica.* 2009;94(11):1555-1562.
15. Vegliante MC, Palomero J, Pérez-Galán P, et al. SOX11 regulates PAX5 expression and blocks terminal B-cell differentiation in aggressive mantle cell lymphoma. *Blood.* 2013;121(12):2175-2185.
16. Salaverria I, Perez-Galan P, Colomer D, Campo E. Mantle cell lymphoma: from pathology and molecular pathogenesis to new therapeutic perspectives. *Haematologica.* 2006;91(1):11-16.
17. Navarro A, Clot G, Royo C, et al. Molecular subsets of mantle cell lymphoma defined by the IGHV mutational status and SOX11 expression have distinct biologic and clinical features. *Cancer Res.* 2012;72(20):5307-5316.
18. Subramanian A, Tamayo P, Mootha VK, et al. Gene set enrichment analysis: a knowledge-based approach for interpreting genome-wide expression profiles. *Proc Natl Acad Sci USA.* 2005;102(43):15545-15550.
19. Vegliante MC, Royo C, Palomero J, et al. Epigenetic activation of SOX11 in lymphoid neoplasms by histone modifications. *PLoS ONE.* 2011;6(6):e21382.
20. Roué G, Pérez-Galán P, Mozos A, et al. The Hsp90 inhibitor IPI-504 overcomes bortezomib resistance in mantle cell lymphoma in vitro and in vivo by down-regulation of the prosurvival ER chaperone BiP/Grp78. *Blood.* 2011;117(4): 1270-1279.
21. Cardesa-Salzmann TM, Colomo L, Gutierrez G, et al. High microvessel density determines a poor outcome in patients with diffuse large B-cell lymphoma treated with rituximab plus chemotherapy. *Haematologica.* 2011;96(7): 996-1001.
22. Kubota Y, Kleinman HK, Martin GR, Lawley TJ. Role of laminin and basement membrane in the morphological differentiation of human endothelial cells into capillary-like structures. *J Cell Biol.* 1988;107(4):1589-1598.
23. Piccaluga PP, Agostinelli C, Zinzani PL, Baccarani M, Dalla Favera R, Pileri SA. Expression of platelet-derived growth factor receptor alpha in peripheral T-cell lymphoma not otherwise specified. *Lancet Oncol.* 2005;6(6):440.
24. Yancopoulos GD, Davis S, Gale NW, Rudge JS, Wiegand SJ, Holash J. Vascular-specific growth factors and blood vessel formation. *Nature.* 2000; 407(6801):242-248.
25. Hanahan D, Weinberg RA. Hallmarks of cancer: the next generation. *Cell.* 2011;144(5):646-674.
26. Baeriswyl V, Christofori G. The angiogenic switch in carcinogenesis. *Semin Cancer Biol.* 2009; 19(5):329-337.
27. Lenz G, Wright G, Dave SS, et al; Lymphoma/Leukemia Molecular Profiling Project. Stromal gene signatures in large-B-cell lymphomas. *N Engl J Med.* 2008;359(22):2313-2323.
28. Perry AM, Cardesa-Salzmann TM, Meyer PN, et al. A new biologic prognostic model based on immunohistochemistry predicts survival in patients with diffuse large B-cell lymphoma. *Blood.* 2012;120(11):2290-2296.
29. Korkolopoulou P, Thymara I, Kavantzas N, et al. Angiogenesis in Hodgkin's lymphoma: a morphometric approach in 286 patients with prognostic implications. *Leukemia.* 2005;19(6): 894-900.
30. Lozano E, Segarra M, García-Martínez A, Hernández-Rodríguez J, Cid MC. Imatinib mesylate inhibits in vitro and ex vivo biological responses related to vascular occlusion in giant cell arteritis. *Ann Rheum Dis.* 2008;67(11): 1581-1588.
31. Schmitt CE, Woolls MJ, Jin SW. Mutant-specific gene expression profiling identifies SRY-related HMG box 11b (SOX11b) as a novel regulator of vascular development in zebrafish. *Mol Cells.* 2013;35(2):166-172.
32. Risau W, Drexler H, Mironov V, et al. Platelet-derived growth factor is angiogenic in vivo. *Growth Factors.* 1992;7(4):261-266.
33. Dong J, Grunstein J, Tejada M, et al. VEGF-null cells require PDGFR alpha signaling-mediated stromal fibroblast recruitment for tumorigenesis. *EMBO J.* 2004;23(14):2800-2810.
34. Ferrara N, Kerbel RS. Angiogenesis as a therapeutic target. *Nature.* 2005;438(7070): 967-974.
35. Ding W, Knox TR, Tschumper RC, et al. Platelet-derived growth factor (PDGF)-PDGF receptor interaction activates bone marrow-derived mesenchymal stromal cells derived from chronic lymphocytic leukemia: implications for an angiogenic switch. *Blood.* 2010;116(16): 2984-2993.
36. Heldin CH. Targeting the PDGF signaling pathway in tumor treatment. *Cell Commun Signal.* 2013;11:97.
37. Andrae J, Gallini R, Betsholtz C. Role of platelet-derived growth factors in physiology and medicine. *Genes Dev.* 2008;22(10):1276-1312.
38. Gerber DE, Gupta P, Dellinger MT, et al. Stromal platelet-derived growth factor receptor α (PDGFRα) provides a therapeutic target independent of tumor cell PDGFRα expression in lung cancer xenografts. *Mol Cancer Ther.* 2012; 11(11):2473-2482.
39. Zhu K, Pan Q, Zhang X, et al. MiR-146a enhances angiogenic activity of endothelial cells in hepatocellular carcinoma by promoting PDGFRA expression. *Carcinogenesis.* 2013;34(9): 2071-2079.
40. Goldman JM, Melo JV. Chronic myeloid leukemia—advances in biology and new approaches to treatment. *N Engl J Med.* 2003; 349(15):1451-1464.
41. Milojkovic D, Apperley J. Mechanisms of resistance to imatinib and second-generation tyrosine inhibitors in chronic myeloid leukemia. *Clin Cancer Res.* 2009;15(24):7519-7527.

42. Tauchi T, Ohyashiki K. Molecular mechanisms of resistance of leukemia to imatinib mesylate. *Leuk Res.* 2004;28(suppl 1):S39-S45.

43. Ruan J, Hajjar K, Rafii S, Leonard JP. Angiogenesis and antiangiogenic therapy in non-Hodgkin's lymphoma. *Ann Oncol.* 2009;20(3): 413-424.

44. Ruan J, Luo M, Wang C, et al. Imatinib disrupts lymphoma angiogenesis by targeting vascular pericytes. *Blood.* 2013;121(26):5192-5202.

45. Song K, Herzog BH, Sheng M, et al. Lenalidomide inhibits lymphangiogenesis in preclinical models of mantle cell lymphoma [published correction appears in *Cancer Res*. 2014;74(4):1284]. *Cancer Res.* 2013;73(24):7254-7264.

46. Garzia M, Sora F, Teofili L, et al. Blastoid mantle cell lymphoma occurring in a patient in complete remission of chronic myelogenous leukemia. *Lab Hematol.* 2007;13(1):30-33.

47. Rodler E, Welborn J, Hatcher S, et al. Blastic mantle cell lymphoma developing concurrently in a patient with chronic myelogenous leukemia and a review of the literature. *Am J Hematol.* 2004; 75(4):231-238.

48. Zhang J, Lu A, Li L, Yue J, Lu Y. p16 Modulates VEGF expression via its interaction with HIF-1alpha in breast cancer cells. *Cancer Invest.* 2010;28(6): 588-597.

49. Ousset M, Bouquet F, Fallone F, et al. Loss of ATM positively regulates the expression of hypoxia inducible factor 1 (HIF-1) through oxidative stress: Role in the physiopathology of the disease. *Cell Cycle.* 2010;9(14): 2814-2822.

50. Grossfeld GD, Ginsberg DA, Stein JP, et al. Thrombospondin-1 expression in bladder cancer: association with p53 alterations, tumor angiogenesis, and tumor progression. *J Natl Cancer Inst.* 1997;89(3):219-227.

Relapses in Patients With Giant Cell Arteritis

Prevalence, Characteristics, and Associated Clinical Findings in a Longitudinally Followed Cohort of 106 Patients

Marco A. Alba, MD, Ana García-Martínez, MD, Sergio Prieto-González, MD, Itziar Tavera-Bahillo, MD, Marc Corbera-Bellalta, PhD, Ester Planas-Rigol, PhD, Georgina Espígol-Frigolé, MD, Montserrat Butjosa, MD, José Hernández-Rodríguez, MD, and Maria C. Cid, MD

Abstract: Giant cell arteritis (GCA) is a relapsing disease. However, the nature, chronology, therapeutic impact, and clinical consequences of relapses have been scarcely addressed. We conducted the present study to investigate the prevalence, timing, and characteristics of relapses in patients with GCA and to analyze whether a relapsing course is associated with disease-related complications, increased glucocorticoid (GC) doses, and GC-related adverse effects. The study cohort included 106 patients, longitudinally followed by the authors for 7.8 ± 3.3 years. Relapses were defined as reappearance of disease-related symptoms requiring treatment adjustment. Relapses were classified into 4 categories: polymyalgia rheumatica (PMR), cranial symptoms (including ischemic complications), systemic disease, or symptomatic large vessel involvement. Cumulated GC dose during the first year of treatment, time required to achieve a maintenance prednisone dose <10 mg/d (T10), <5 mg/d (T5), or complete prednisone discontinuation (T0), and GC-related side effects were recorded. Sixty-eight patients (64%) experienced at least 1 relapse, and 38 (36%) experienced 2 or more. First relapse consisted of PMR in 51%, cranial symptoms in 31%, and systemic complaints in 18%. Relapses appeared predominantly, but not exclusively, within the first 2 years of treatment, and only 1 patient developed visual loss. T10, T5, and T0 were significantly longer in patients with relapses than in patients without relapse (median, 40 vs 27 wk, $p < 0.0001$; 163 vs 89.5 wk, $p = 0.004$; and 340 vs 190 wk, $p = 0.001$, respectively). Cumulated prednisone dose during the first year was significantly higher in relapsing patients (6.2 ± 1.7 g vs 5.4 ± 0.78 g, $p = 0.015$). Osteoporosis was more common in patients with relapses compared to those without (65% vs 32%, $p = 0.001$). In conclusion, the results of the present study provide evidence that a relapsing course is associated with higher and prolonged GC requirements and a higher frequency of osteoporosis in GCA.

(*Medicine* 2014;93: 194–201)

Abbreviations: CRP = C-reactive protein, ESR = erythrocyte sedimentation rate, GC = glucocorticoids, GCA = giant cell arteritis, Hb = hemoglobin, IQR = interquartile range, PDN = prednisone, PMR = polymyalgia rheumatica, SD = standard deviation, SIR = systemic inflammatory response, TNF = tumor necrosis factor.

INTRODUCTION

Giant cell arteritis (GCA) is a granulomatous arteritis predominantly affecting large and medium-sized vessels.[18,27] Treatment with high-dose glucocorticoids (GC) results in prompt and remarkable improvement of symptoms and reduces the risk of ischemic complications.[2] However, reduced GC doses do not completely abolish essential pathways involved in disease persistence, and consequently, the course of GCA may be troubled by relapses.[5,8,27] Recrudescence of GCA activity is common, occurring in at least 43% of patients in population-based studies[3,26] and up to 80% in clinical trials with adjuvant therapies.[15,16,19,20,22] The remarkable variability in the reported prevalence of relapses may be related to heterogeneity in the definition of relapses and to variability in the GC-tapering schedules. Definition of relapse, flare, or recurrence considerably varies across different studies.[16,21–23,26] While in some publications definition of relapse has been based on clinical grounds,[15,16,19] in others, isolated increases in acute-phase reactants have been considered disease flares.[24]

In addition, although this has not been formally evaluated, initial doses and tapering schedules seem to influence relapse rate in GCA.[17,20] In this regard, it is noteworthy that the higher relapse rates have been observed in the context of clinical trials with adjuvant therapies where GC tapering is more aggressive than in standard of care settings, and when alternate-day GC tapering is applied.[15,16,19,20,22] Consistently, a detailed review of treatments received by patients with isolated polymyalgia rheumatica (PMR) suggests that starting with lower GC doses is associated with higher relapse rates.[13]

Relapse rate is a commonly used primary endpoint in clinical trials with patients with GCA. However, although frequency of relapses has been reported in various studies,[15,16,19,20,22,26] limited information exists regarding the

From the Vasculitis Research Unit (MAA, AG-M, SP-G, IT-B, MC-B, EP-R, GE-F, MB, JH-R, MCC), Department of Autoimmune Diseases, Hospital Clínic, University of Barcelona, Institut d'Investigacions Biomèdiques August Pi Sunyer (IDIBAPS), Barcelona, Spain.

Correspondence: Maria C. Cid, MD, Vasculitis Research Unit, Department of Systemic Autoimmune Diseases, Hospital Clínic, Villarroel 170, 08036 Barcelona, Spain (e-mail: mccid@clinic.ub.es).

Results partially presented at the Annual Scientific Meeting of the American College of Rheumatology 2012, Washington, DC (November 10–14, 2012).

Conflicts of Interest and Funding Sources: The authors declare no conflicts of interest. Supported by Ministerio de Economía y Competitividad (SAF 08/04328 y SAF 11/30073). MA Alba was supported by Consejo Nacional de Ciencia y Tecnología (CONACyT), Mexico and by the Agencia de Gestió d'Ajuts Universitaris i de Recerca (AGAUR) (Generalitat de Catalunya). G Espígol-Frigolé was supported by Instituto de Salud Carlos III. M Butjosa and S Prieto-González were supported by Premi Fi de Residència (Hospital Clínic).

ISSN: 0025-7974
DOI: 10.1097/MD.0000000000000033

clinical characteristics and predictors of relapses, and accompanying blood test abnormalities, which have been only specifically addressed in a previous study.[23] Moreover, it has not been clearly demonstrated whether a relapsing course results in increased disease or treatment-related morbidity in these patients. Therefore, we conducted the present study to investigate the prevalence, timing, predictors, and main features of relapses in a longitudinally followed cohort of patients with GCA with long-term follow-up. In addition, we analyzed whether a relapsing course was associated with disease-related ischemic complications, higher cumulated GC doses, more prolonged treatment periods, and/or higher frequency of GC-related adverse effects.

PATIENTS AND METHODS

Between 1995 and 2007, 187 individuals were diagnosed with biopsy-proven GCA at our institution (Hospital Clínic, Barcelona, Spain). Among them, patients treated by the authors who underwent a regular follow-up for at least 4 years were selected. From the initial 187 patients diagnosed, 81 were excluded for the following reasons: 31 were subsequently treated at other departments or institutions, 19 died early during follow-up, 14 were transferred to nursing homes for advanced dementia, and 17 moved to other regions or had deficient compliance with the scheduled follow-up visits.

The remaining 106 patients were uniformly evaluated, treated, and longitudinally followed by the authors for an average of 7.8 ± 3.3 years (range, 4–15 yr). Clinical and laboratory findings at disease diagnosis were recorded. A combination of clinical and blood test abnormalities was used to evaluate the intensity of the systemic inflammatory response (SIR) as previously reported.[6,7,14] These included fever $>38\,^{\circ}C$, weight loss ≥ 4 kg, hemoglobin (Hb) <11 g/L, and erythrocyte sedimentation rate (ESR) ≥ 85 mm/h. Patients with 3 or 4 of these items were considered to have a strong SIR, whereas patients with ≤ 2 were considered to have a weak SIR. Patients underwent clinical assessments in our outpatient facility every 3 months for the first 2 years after diagnosis and approximately every 4–6 months thereafter. ESR, C-reactive protein (CRP), blood cell counts, and Hb concentration were determined at each visit. The treatment protocol consisted of an initial prednisone (PDN) dose of 1 mg/kg per day (up to 60 mg/d) for 1 month. Intravenous methylprednisolone pulse therapy (1 g daily for 3 d) was initially administered to patients with recent (<48 h) visual loss. PDN was subsequently tapered at 10 mg/wk. When reaching 20 mg/d, this dose was maintained for 1–2 weeks and then reduced to 15 mg/d, which was maintained for 1 month. A further reduction to a maintenance dose of 10 mg/d was attempted. If tolerated, a reduction to 7.5 mg/d was tried after 3–6 months. Subsequent tapering was more variable. In general, a reduction to 5 mg/d was attempted approximately 3–6 months later and maintained for 1 year, after which a reduction of 1.25 mg/d was attempted every 6 months. Methotrexate at 15 mg/wk was added when patients experienced ≥ 2 relapses or had developed GC side effects. Reduction in PDN dose was performed 1 month before the scheduled follow-up visit to evaluate tolerance to the adjustment and to avoid severe relapses. If disease-related symptoms (cranial manifestations or PMR), fever, weight loss, or anemia not attributable to other reasons after the necessary work-up occurred, PDN dose was increased by 10–15 mg/d above the previous effective dose. If asymptomatic increases in acute-phase reactants were detected, PDN dose was held until the next visit. When a relapse could be defined, patients were managed as discussed above. If not, a reduction was attempted regardless of the ESR or CRP levels.

We used a consensus definition of relapse established in the context of international multicenter clinical trials.[15,16,19] Relapse or recurrence were indistinctly defined as reappearance of disease-related symptoms, usually accompanied by elevation of acute-phase reactants that required treatment adjustment. Relapses were categorized according to the clinical manifestation into 4 categories: 1) PMR, 2) cranial symptoms (headache, scalp tenderness, jaw claudication, cranial ischemic complications), 3) systemic disease (anemia, fever, and/or weight loss), or 4) symptomatic large vessel involvement (extremity claudication). Cranial ischemic manifestations included stroke, transient ischemic attacks, amaurosis fugax, GCA-related visual loss, or diplopia. Number of relapses, time (in weeks) from the initiation of treatment to first relapse, time required to reach a PDN maintenance dose <10 mg/d (T10), <5 mg/d (T5), and time required to complete GC withdrawal (T0), not followed by a relapse for at least 3 months, were recorded. Cumulated PDN doses received after the first year of treatment were calculated. For each episode of relapsing activity, the ESR, serum CRP, and Hb concentrations were determined, as well as the PDN dose received at that time. In addition, GC-related adverse effects including new or worsening hypertension, diabetes mellitus, hypercholesterolemia, osteoporosis, cataracts, and Cushing appearance were recorded. Measurement of bone mineral density with dual energy X-ray absorptiometry was performed at disease diagnosis and thereafter approximately every 2 years. Osteoporosis was diagnosed using the World Health Organization criteria–that is, bone mineral density T-score of 2.5 standard deviations (SDs) or more below the young adult mean.[4] For screening of diabetes and hyperlipidemia, patients had blood tests prior to each visit, and blood pressure was periodically assessed both at their scheduled visits and by their primary care physicians. We recorded events as adverse events when they appeared or worsened after GC treatment and required new treatment or intensification of previous therapy. The study was approved by the Ethics Committee of Hospital Clínic (Barcelona, Spain).

Statistical Analysis

Continuous variables are presented as mean±SD and/or median and interquartile range (IQR) and categorical data as percentages. Association between relapses and selected covariates was analyzed using the T-test (paired and unpaired) for quantitative variables and the chi-square test for categorical data. Time required to achieve maintenance PDN dose <10 mg/d, <5 mg/d, and time to treatment discontinuation were compared between patients with and without relapses by the Kaplan-Meier survival analysis method. Statistical significance was defined as $p < 0.05$. Calculations were performed with the statistical package PAWS statistics v 18 (SPSS Inc, Chicago, IL) and GraphPad Prism v 5.04 for Windows (GraphPad Software, La Jolla, CA).

RESULTS

We analyzed 106 patients. Mean age at diagnosis was 75 ± 7 years (range, 58–89 yr) with a male to female ratio of 1:2.6. Demographic data and main clinical features at disease onset are depicted in Table 1.

TABLE 1. Baseline Characteristics at Diagnosis (*n=106*)

General Characteristics:	
Age, mean ± SD (range), years	75 ± 7 (58–89)
Sex, No. Male/female (%)	29/77 (27/73)
Duration of Symptoms, Mean ± SD, Weeks	16 ± 21
Cranial Symptoms at Diagnosis, N (%)	
Headache	83 (78)
Jaw Claudication	47 (44)
Scalp Tenderness	49 (46)
Facial Pain[+]	50 (47)
Cranial Ischemic Complications[†]	26 (24.5)
Polymyalgia Rheumatica	54 (51)
Systemic Manifestations, N (%)	
Fever	40 (38)
Anorexia	12 (11)
Weight Loss	54 (51)
Laboratory Parameters	
ESR, mm/hour	90 ± 30.2
CRP, mg/dL	11.2 ± 17.6
Haptoglobin, g/L	3.6 ± 1.5
Hemoglobin, g/dL	11.3 ± 1.4

[+]Includes ocular pain, tongue pain, toothache, earache, odynophagia and carotidynia.

† Includes stroke, transitory ischemic attacks, amaurosis fugax, blindness and diplopia.

Chronology and Characteristics of Relapses

Sixty-eight patients (64%) relapsed during follow-up (mean, 7.8 ± 3.3 yr; range, 4–15 yr) (Figure 1). Mean time to first relapse was 79 ± 75 weeks (range, 11–339 wk) with a median of 51 (IQR, 89) weeks. Thirty-four of the 68 patients (50%) relapsed during the first year after diagnosis (Figure 2A).

PMR was the most frequent clinical manifestation observed during the first flare (Figure 2B). Of note, severe ischemic complications were not developed by any patient as part of the first relapsing episode. Most patients relapsed with the same features originally present at GCA diagnosis (n = 52, 78%). For those who developed a different clinical manifestation, PMR was the most frequent new feature (n = 9, 75%). No patients in this series relapsed with symptomatic large vessel involvement.

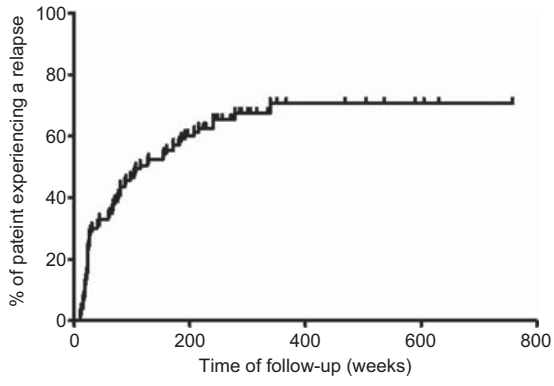

FIGURE 1. Kaplan-Meier plot of the entire series showing the probability of relapse over time.

Figure 2A shows the mean±SD and median (IQR) of PDN used by patients at the time of relapse during the first 5 years of follow-up. Mean PDN dose received by the 68 patients at the first relapse was of 5.3 ± 6.5 mg/d with a median of 2.5 (IQR, 7.5) mg/d. Fifty-two percent were receiving doses ≤2.5 mg/d (Figure 2C). PDN doses at the time of relapse tended to decrease over time (Figure 2A). Patients who relapsed during the first year received 8.3 ± 8.2 mg/d, median 7.5 mg (IQR, 15), whereas patients who relapsed during the second year were receiving 3.7 ± 2.3 mg, median 5 mg (IQR, 2.5).

Mean ESR, CRP, and Hb levels at the time of the first relapse were 61 ± 29 mm/h, 4.0 ± 3.8 mg/dL, and 12 ± 1.4 g/L, respectively. The inflammatory response at that time was comparatively lower than that observed at GCA onset (ESR 88 ± 33 vs 61 ± 29 mm/h, $p < 0.0001$; CRP 11 ± 19 vs 4.0 ± 3.8 mg/dL, $p = 0.001$; and Hb 11.3 ± 1.6 vs 12 ± 1.4 g/L, $p < 0.0001$). We observed an increase of 33 ± 14 mm/hr in ESR level, an increase of 2.9 ± 2.2 mg/dL in CRP concentration, and a decrease of 0.7 ± 0.1 g/L for Hb values between the previous laboratory tests while in remission and the ones performed at disease relapse.

There were significant differences in the PDN doses used to treat relapses according to the type of recurrence (Table 2). The lowest doses were used to treat PMR symptoms (14.5 ± 6.8 mg/d) whereas higher doses were employed to treat cranial manifestations (23.7 ± 12.9 mg/d). ESR levels and Hb concentrations were significantly more deviated from normal values in patients who relapsed with systemic manifestations (see Table 2).

Thirty-eight patients (36%) had 2 or more relapses. Distribution of relapse types was similar to that observed at the first episode (Figure 2D). One patient developed a severe ischemic complication (anterior ischemic optic neuritis) as part of her second recurrence. This patient was treated for 3.5 years and regularly followed for 5 years. She subsequently abandoned regular visits and presented with a relapse including malaise, ischemic optic neuritis, and elevation of ESR, 4 years later. The mean PDN dose at the second flare was 4.3 ± 2.7 mg/d with a median of 5 (IQR 2.5) mg. ESR (mm/h), CRP (mg/dL), and Hb (g/L) levels were 55 ± 30, 3.9 ± 6.1, and 12.1 ± 1.4 respectively.

Predictors of Relapse

To search for predictors of relapses, we compared initial clinical and laboratory findings between patients with or without recurrent disease. At disease onset, PMR and scalp tenderness were more frequently observed in relapsing patients (Table 3). Acute-phase reactants tended to be higher in patients with recurrences, but only haptoglobin reached statistical significance (3.8 ± 1.6 g/L vs 3.0 ± 1.3 g/L, $p = 0.042$). When the intensity of the SIR was evaluated combining clinical and laboratory findings, patients with multiple relapses were significantly more frequent among those with a strong SIR: 23 of 27 (85%) patients with a strong SIR relapsed 2 or more times compared with 15 of 41 (37%) of those with a weak SIR. No other predictors of recurrences could be identified.

Glucocorticoid Requirements and Side Effects According to Disease Recurrences

Treatment requirements were different in both groups of patients (Table 4). Patients with relapses required

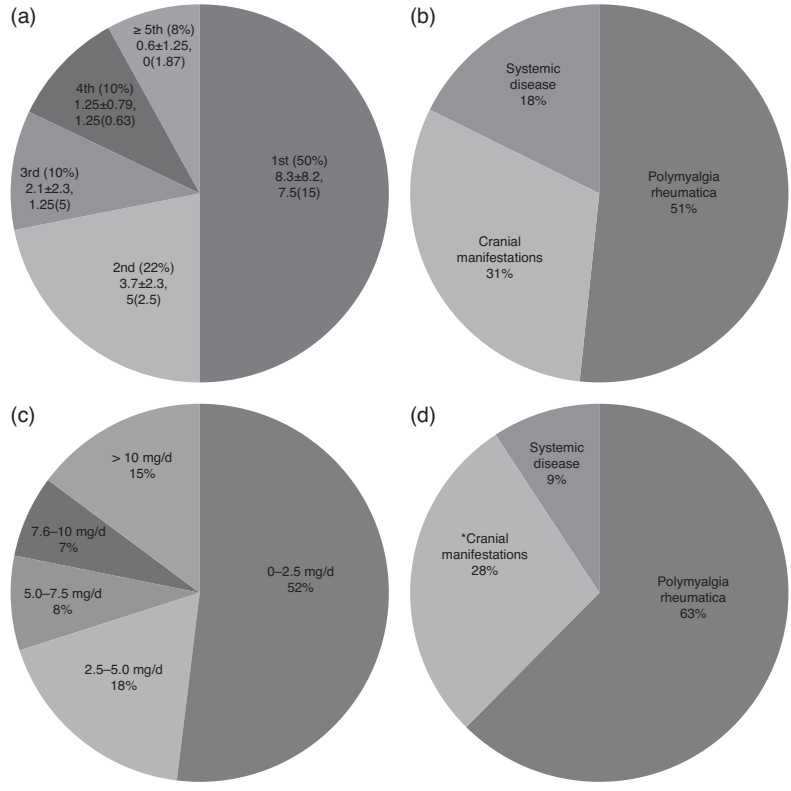

FIGURE 2. Characteristics and timing of flares in relapsing patients (n = 68). A) Percentage of patients relapsing per year of follow-up and mean±SD and median (IQR) prednisone dose (mg/d) received at the time of relapse. B) Percentage of relapsing patients with a given clinical type of relapse. C) Percentage of patients receiving the indicated dose of prednisone (mg/d) at the time of the first

significantly longer periods of time to reach a maintenance dose of PDN <10 mg/d, <5 mg/d, and to completely discontinue GC therapy (Figure 3). Cumulated PDN dose during the first year was significantly higher in relapsing patients (6.2 ± 1.7 g vs 5.4 ± 0.78 g, $p = 0.015$). Relapsing patients had an increased prevalence of osteoporosis (65% for relapsing patients vs 32% for nonrelapsing, $p = 0.001$). Other adverse effects also tended to be more frequent in patients with relapses, but differences did not reach statistical significance. As expected, methotrexate was administered more frequently in patients with relapses than in patients in sustained remission (22% vs 3%, $p = 0.009$).

DISCUSSION

Limited information about the characteristics of recurrences occurring in patients with GCA is available.[23] Here, we present detailed data about clinical and laboratory characteristics of relapses from a cohort of uniformly treated patients with GCA with long-term follow-up. The definition of relapse used in the present study was similar to that used in randomized, controlled clinical trials evaluating adjunctive therapies for GCA.[15,16,19]

In spite of the satisfactory initial response to GC treatment, 64% of patients relapsed in the present series. This percentage is somewhat higher than that reported in population-based studies,[3,26] possibly due to the more extended follow-up of our patient cohort, but some selection bias cannot be excluded. Although most relapses occurred within the first 2 years of treatment, recurrences also developed subsequently. PMR was the most frequent symptom (51%) at the time of relapse, followed by cranial manifestations (31%). In previous studies[16,22,23] headache was the leading feature (44%-60%), followed by PMR (19%-30%),[16,23] and constitutional syndrome (28%).[23] Therefore, the distribution found in the current cohort is close to that found in other studies. It is noteworthy that disease-related

TABLE 2. Laboratory Characteristics and PDN Dose at Each Relapse Type

	Polymyalgia Rheumatica	Cranial Manifestations	Systemic Disease	*p*
ESR (mm/h)	55 ± 28	59 ± 28	80 ± 26	0.038
CRP (mg/L)	3.9 ± 3.5	4.5 ± 4.2	3.6 ± 4.1	ns
Hemoglobin (g/L)	12.2 ± 1.3	12.3 ± 1.4	11.7 ± 1.2	0.017
Dose of prednisone (mg/d) used to treat relapse	14.5 ± 6.8	23.7 ± 12.9	17.9 ± 5.6	0.002
Increment in prednisone dose (mg/d)	10 ± 6.5	17 ± 12	14 ± 11	0.009

TABLE 3. Clinical Manifestations at Diagnosis in Patients With and without Relapses

Clinical characteristics	*Relapse (n=68)*	*No relapse (n=38)*	*p*
General characteristics:			
Sex, no. female/male	52/16 (76.5/23.5)	25/13 (66/34)	ns
Age, mean, yr	74 ± 6.5	76 ± 8	ns
Cranial symptoms, n (%)			
Headache	56 (82)	27 (71)	ns
Jaw claudication	34 (50)	13 (34)	ns
Scalp tenderness	40 (59)	9 (24)	0.001
Ischemic complications	17 (25)	9 (24)	ns
Stroke	2 (3)	0 (0)	ns
Transitory ischemic attack	4 (6)	0 (0)	ns
Amaurosis fugax	9 (13)	6 (16)	ns
Diplopia	9 (13)	2 (5)	ns
Permanent visual loss	6 (9)	6 (16)	ns
Polymyalgia rheumatica	40 (59)	14 (37)	0.042
Systemic manifestations, n (%)			
Fever	24 (35)	16 (42)	ns
Anorexia	7 (10)	5 (13)	ns
Weight loss	36 (53)	18 (47)	ns
Baseline laboratory parameters, mean ± SD			
ESR, mm/hour	88 ± 33	92 ± 24	ns
CRP, mg/dL	11.4 ± 18.6	10.7 ± 15.9	ns
Haptoglobin, g/L	3.8 ± 1.6	3.0 ± 1.3	0.049
Hemoglobin, g/dL	11.3 ± 1.5	11.2 ± 1.2	ns

ischemic complications seem to be extremely infrequent in the context of controlled relapses. In previous studies the occurrence of ischemic manifestations has been also found to be infrequent during follow-up (0%-6%).[1,16,23] Only 1 patient in the current series suffered anterior ischemic optic neuropathy in the context of a delayed relapse, but this patient had interrupted regular control visits at the time of disease recurrence. No patient in our series relapsed with symptomatic involvement of large vessels.

Relapses were usually accompanied by elevated levels of ESR and CRP that were, nevertheless, lower than those observed at disease onset. In accordance, PDN doses much lower than the starting doses were usually effective for treating controlled relapses. However, it must be stressed that the reported features were obtained from patients who were closely followed with reassessments performed approximately every 3 months during the first 2 years after diagnosis. We cannot exclude that severe relapses requiring higher GC doses may occur in patients controlled less tightly. These findings indicate that patients with GCA need to be indefinitely observed even after successful GC discontinuation.

As for the time at greatest risk for relapse, in 50% of patients who relapsed, recurrences occurred during the first year. Mean time to first relapse was 19.7 ± 18.7 months, similar to what has been reported by others.[21,23,26] However delayed relapses also occurred.

As shown in Figure 2, PDN dose received at the time when relapses occurred decreased over time, suggesting that

TABLE 4. Treatment Requirements and Side Effects During Follow-up

Clinical characteristic	*Relapse (n=68)*	*No relapse (n=38)*	*p*
Treatment requirements			
*Intravenous methylprednisolone pulse**	3 (4)	4 (10.5)	ns
Cumulated dose first year, mean ± SD (g)	6.2 ± 1.7	5.4 ± 0.78	0.015
Methotrexate (15 mg/week)	15 (22)	1 (3)	0.009
Glucocorticoid related adverse effects n, (%)†			
Diabetes mellitus	7 (10)	2 (5)	ns
Systemic hypertension	37 (54)	17 (45)	ns
Hypercholesterolemia	42 (62)	26 (69)	ns
Osteoporosis	44 (65)	12 (32)	0.001
Cushing appearance	8 (12)	1 (3)	ns
Cataracts	16 (23.5)	3 (8)	ns

* At disease onset.
† 100% of patients presented at least 1 side effect.

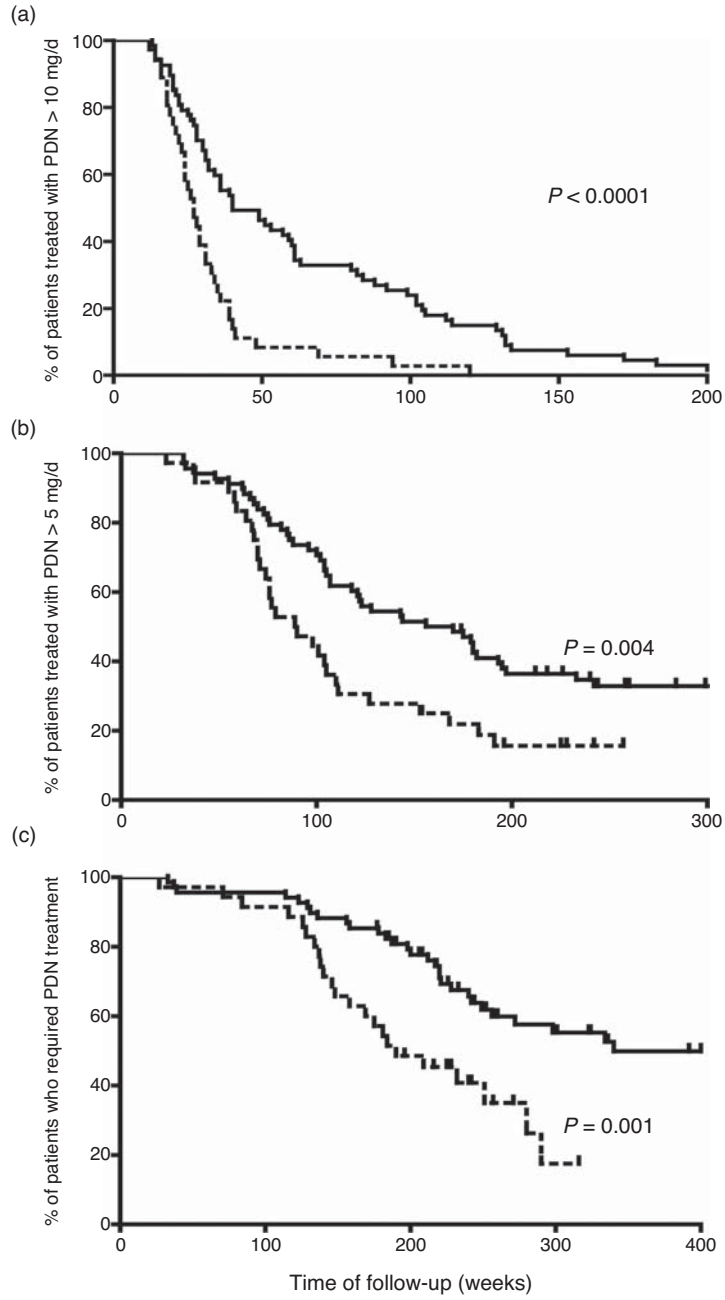

FIGURE 3. Survival curves showing the time required to reach a stable dose of prednisone <10 mg/d (A), <5 mg/d (B), and 0 mg/d (C) in patients with relapses (solid line) and with sustained remission (broken line). [Note the scale for time of follow-up is different among the 3 figure parts].

disease activity progressively decreases and, over the years, lower PDN doses are required to maintain remission. Overall, relapses occurred when patients were receiving a mean PDN dose of 5.3 ± 6.5 mg/d with median 2.5 mg/d (IQR, 7.5). This dose is lower than that reported in other series. This may be due to variability in the rate of initial PDN tapering across different studies or to other reasons. No patient in our cohort relapsed with PDN higher than 25 mg/d.

Patients with relapses required longer periods of treatment and were exposed to higher cumulated PDN doses, similar to what was found in a previous study.[23] All patients in our cohort experienced at least 1 GC-related side effect. Other studies have reported GC adverse effects in 90%-95% of GCA patients within the first 3 years of therapy.[24,26] These include new or worsening hypertension (22%-84%),[19,24,26] infections (22%-56%),[19,22,24,26] osteoporosis and bone fractures (8%-38%),[19,22–24,26] new or worsening diabetes mellitus (7%-37%),[19,22–24,26] and cataracts (4%-41%).[19,24,26] The higher frequency of side effects in our patient cohort may be related to the longer follow-up period. We observed that patients with

recurrences presented more GC-related toxicity, in particular osteoporosis despite the administration of calcium supplements, vitamin D, and bisphosphonates. These data highlight the need for more efficient and safer therapies.

In the current cohort, relapses could not be attributed to insufficient treatment because relapsing patients received more GC and for more extended periods of time. This observation indicates that some patients have a more resistant disease. From the clinical standpoint, an intense acute-phase response was associated with higher risk of relapse. Other investigators have also observed that abnormalities related to the acute-phase response are predictors of relapse.[6,9,12,14,23,25,28] Among other findings, only scalp tenderness and PMR were slightly more frequent in relapsing patients. Although this association may be spurious, a similar trend has been observed in other studies.[23] Previous studies have investigated tissue and serum biomarkers associated with persistent disease activity and relapsing course. Elevated serum concentrations of tumor necrosis factor (TNF)-α, interleukin (IL)-6, and soluble intercellular adhesion molecule (ICAM)-1 are associated with relapsing disease.[10,12,28] Increased expression of TNF-α or chemokine (C-C motif) ligand (CCL)-2 mRNA in involved arteries is associated with recurrent disease and higher GC requirements. However, TNF-α blockade was not sufficient to reduce relapses and spare corticosteroids,[16] indicating that association does not imply causality and suggesting that TNF-α effects may be compensated by other cytokines and that upstream mediators may be more relevant to perpetuate disease activity. Elevated mRNA concentrations of Th1 cytokines IL-12/23p40 and interferon (IFN)-γ have been observed after 1 year of treatment in second temporal artery biopsies of relapsing patients, suggesting reactivation of initial events able to drive subsequent inflammatory cascades.[28] In contrast, increased IL-17 expression in GCA lesions is a predictor of sustained response to GC.[11] Further research is needed to elucidate the mechanisms involved in disease persistence, to enable the design of more specific and efficient targeted therapies.

REFERENCES

1. Aiello PD, Trautmann JC, McPhee TJ, et al. Visual prognosis in giant cell arteritis. *Ophthalmology*. 1993;100:550–555.
2. Alba MA, Espigol-Frigole G, Butjosa M, et al. Treatment of large vessel vasculitis. *Curr Immunol Rev*. 2011;7:435–442.
3. Andersson R, Malmvall BE, Bengtsson BA. Long-term corticosteroid treatment in giant cell arteritis. *Acta Med Scand*. 1986;220:465–469.
4. Assessment of fracture risk and its application to screening for postmenopausal osteoporosis. *Report of a WHO Study Group. Technical Report Series*. Vol. 843. World Health Organization; 1994: 1–129.
5. Bongartz T, Matteson EL. Large-vessel involvement in giant cell arteritis. *Curr Opin Rheumatol*. 2006;18:10–17.
6. Ciccia F, Alessandro R, Rizzo A, et al. IL-33 is overexpressed in the inflamed arteries of patients with giant cell arteritis. *Ann Rheum Dis*. 2013;72:258–264.
7. Cid MC, Font C, Oristrell J, et al. Association between strong inflammatory response and low risk of developing visual loss and other cranial ischemic complications in giant cell (temporal) arteritis. *Arthritis Rheum*. 1998;41:26–32.
8. Cid MC, Garcia-Martinez A, Lozano E, et al. Five clinical conundrums in the management of giant cell arteritis. *Rheum Dis Clin North Am*. 2007;33:819–834, vii.
9. Cid MC, Hoffman MP, Hernandez-Rodriguez J, et al. *Association between increased CCL2 (MCP-1) expression in lesions and persistence of disease activity in giant-cell arteritis*. *Rheumatology (Oxford)*. 2006;45:1356–1363.
10. Coll-Vinent B, Vilardell C, Font C, et al. Circulating soluble adhesion molecules in patients with giant cell arteritis. Correlation between soluble intercellular adhesion molecule-1 (sICAM-1) concentrations and disease activity. *Ann Rheum Dis*. 1999;58:189–192.
11. Espigol-Frigole G, Corbera-Bellalta M, Planas-Rigol E, et al. Increased IL-17A expression in temporal artery lesions is a predictor of sustained response to glucocorticoid treatment in patients with giant-cell arteritis. *Ann Rheum Dis*. 2013;72:1481–1487.
12. Garcia-Martinez A, Hernandez-Rodriguez J, Espigol-Frigole G, et al. Clinical relevance of persistently elevated circulating cytokines (tumor necrosis factor alpha and interleukin-6) in the long-term followup of patients with giant cell arteritis. *Arthritis Care Res (Hoboken)*. 2010;62:835–841.
13. Hernandez-Rodriguez J, Cid MC, Lopez-Soto A, et al. Treatment of polymyalgia rheumatica: a systematic review. *Arch Intern Med*. 2009;169:1839–1850.
14. Hernandez-Rodriguez J, Garcia-Martinez A, Casademont J, et al. A strong initial systemic inflammatory response is associated with higher corticosteroid requirements and longer duration of therapy in patients with giant-cell arteritis. *Arthritis Rheum*. 2002;47:29–35.
15. Hoffman GS, Cid MC, Hellmann DB, et al. A multicenter, randomized, double-blind, placebo-controlled trial of adjuvant methotrexate treatment for giant cell arteritis. *Arthritis Rheum*. 2002;46:1309–1318.
16. Hoffman GS, Cid MC, Rendt-Zagar KE, et al. Infliximab for maintenance of glucocorticosteroid-induced remission of giant cell arteritis: a randomized trial. *Ann Intern Med*. 2007;146:621–630.
17. Hunder GG, Sheps SG, Allen GL, et al. Daily and alternate-day corticosteroid regimens in treatment of giant cell arteritis: comparison in a prospective study. *Ann Intern Med*. 1975;82:613–618.
18. Jennette JC, Falk RJ, Bacon PA, et al. Revised international Chapel Hill Consensus Conference nomenclature of vasculitides. *Arthritis Rheum*. 2013;65:1–11.
19. Jover JA, Hernandez-Garcia C, Morado IC, et al. Combined treatment of giant-cell arteritis with methotrexate and prednisone. A randomized, double-blind, placebo-controlled trial. *Ann Intern Med*. 2001;134:106–114.
20. Kyle V, Hazleman BL. Treatment of polymyalgia rheumatica and giant cell arteritis. I. Steroid regimens in the first two months. *Ann Rheum Dis*. 1989;48:658–661.
21. Kyle V, Hazleman BL. The clinical and laboratory course of polymyalgia rheumatica/giant cell arteritis after the first two months of treatment. *Ann Rheum Dis*. 1993;52:847–850.
22. Mahr AD, Jover JA, Spiera RF, et al. Adjunctive methotrexate for treatment of giant cell arteritis: an individual patient data meta-analysis. *Arthritis Rheum*. 2007;56:2789–2797.
23. Martinez-Lado L, Calvino-Diaz C, Pineiro A, et al. Relapses and recurrences in giant cell arteritis: a population-based study of patients with biopsy-proven disease from northwestern Spain. *Medicine (Baltimore)*. 2011;90:186–193.
24. Mazlumzadeh M, Hunder GG, Easley KA, et al. Treatment of giant cell arteritis using induction therapy with high-dose glucocorticoids: a double-blind, placebo-controlled, randomized prospective clinical trial. *Arthritis Rheum*. 2006;54:3310–3318.

25. Nesher G, Nesher R, Mates M, et al. Giant cell arteritis: intensity of the initial systemic inflammatory response and the course of the disease. *Clin Exp Rheumatol*. 2008;26:S30–S34.

26. Proven A, Gabriel SE, Orces C, et al. Glucocorticoid therapy in giant cell arteritis: duration and adverse outcomes. *Arthritis Rheum*. 2003;49:703–708.

27. Salvarani C, Pipitone N, Versari A, et al. Clinical features of polymyalgia rheumatica and giant cell arteritis. *Nat Rev Rheumatol*. 2012;8:509–521.

28. Visvanathan S, Rahman MU, Hoffman GS, et al. Tissue and serum markers of inflammation during the follow-up of patients with giant-cell arteritis—a prospective longitudinal study. *Rheumatology (Oxford)*. 2011;50:2061–2070.

CONCISE REPORT

Positron emission tomography assessment of large vessel inflammation in patients with newly diagnosed, biopsy-proven giant cell arteritis: a prospective, case–control study

Sergio Prieto-González,[1] Marina Depetris,[2] Ana García-Martínez,[1,3] Georgina Espígol-Frigolé,[1] Itziar Tavera-Bahillo,[1] Marc Corbera-Bellata,[1] Ester Planas-Rigol,[1] Marco A Alba,[1] José Hernández-Rodríguez,[1] Josep M Grau,[4] Franciso Lomeña,[2] Maria C Cid[1]

Handling editor Tore K Kvien

▶ Additional material is published online only. To view please visit the journal online (http://dx.doi.org/10.1136/annrheumdis-2013-204572).

For numbered affiliations see end of article.

Correspondence to
Dr Maria C Cid, Department of Autoimmune Diseases, Clinical Institute of Medicine and Dermatology, Hospital Clínic, Villarroel 170, Barcelona 08036, Spain; mccid@clinic.ub.es

FL and MCC share senior authorship.

Results presented at the European Congress of Rheumatology (EULAR) 2013, Madrid, Spain, June 2013, and at the Annual Congress of European Association of Nuclear Medicine, Lyon, France, October 2013.

Received 7 September 2013
Revised 13 February 2014
Accepted 1 March 2014
Published Online First 24 March 2014

To cite: Prieto-González S, Depetris M, García-Martínez A, *et al*. *Ann Rheum Dis* 2014;**73**:1388–1392.

ABSTRACT

Background Positron emission tomography (PET) scan is emerging as a promising imaging technique to detect large-vessel inflammation in giant cell arteritis (GCA). However, the lack of a standardised definition of arteritis based on ^{18}fluorodeoxyglucose (FDG) uptake is an important limitation to the use of PET scan for diagnostic purposes.

Objective To prospectively assess the intensity and distribution of FDG uptake at different vascular territories in patients with newly diagnosed GCA compared with controls.

Methods 32 consecutive, biopsy-proven, GCA patients treated with glucocorticoids for ≤3 days were included. The control group consisted of 20 individuals, who underwent PET/CT for cancer staging. Maximal standardised uptake value (SUVm) was calculated at four aortic segments, supraaortic branches and iliac-femoral territory. Sensitivity and specificity was calculated by receiver–operator characteristic curves (ROC) analysis.

Results Mean SUVm was significantly higher in patients than in controls in all vessels explored and correlated with acute-phase reactants and serum IL-6. Mean of the SUVm at all the vascular territories had an area under the curve (AUC) of 0.830, and a cut-off of 1.89 yielded a sensitivity of 80% and a specificity of 79% for GCA diagnosis. There were no significant differences in AUC among the vascular beds examined.

Conclusions FDG uptake by large vessels has a substantial sensitivity and specificity for GCA diagnosis.

INTRODUCTION

Temporal artery biopsy is the gold standard for the diagnosis of giant cell arteritis (GCA) due to the tropism of GCA for the epicranial arteries.[1 2] With a few exceptions,[3] histopathological demonstration of temporal artery inflammation provides the most definitive evidence of GCA. Doppler ultrasonography (DUS) of temporal arteries has emerged as a useful alternative tool in centres where biopsy is not easily available.[1]

The diagnosis of GCA may be also supported by demonstrating extracranial artery involvement by imaging. Over the past recent years, positron emission tomography/CT (PET/CT), CT angiography, magnetic resonance imaging (MRI) angiography and DUS have revealed that extracranial involvement in GCA is more frequent than previously anticipated, occurring in 30–74% of patients.[4–7]

PET detection of large-vessel involvement in patients with fever of unknown origin, unexplained constitutional symptoms or apparently isolated polymyalgia rheumatica (PMR) has emphasised its diagnostic potential.[8 9] A limitation of PET as a diagnostic tool is the lack of a standardised definition of vascular inflammation based on the intensity of ^{18}fluorodeoxyglucose (FDG) uptake. While visual assessment of intensively positive cases may be clear, there is no consensus about the minimal intensity of FDG uptake necessary to define vascular inflammation. Conversely, atherosclerosis and ageing may increase vascular FDG uptake, potentially leading to vasculitis overdiagnosis.[10]

In this study, we measured FDG uptake by different vascular territories in a cohort of newly diagnosed patients and controls and performed receiver–operator characteristic curves (ROC) analysis to determine sensitivity and specificity of FDG uptake to detect inflammation at different vascular sites. As a secondary endpoint, we analysed potential correlation between FDG uptake and inflammatory biomarkers.

MATERIALS AND METHODS

Patients

Between November 2006 and March 2011, all patients diagnosed with biopsy-proven GCA[2] at our institution were assessed for potential participation in the study. Patients who had received glucocorticoid treatment for >3 days were excluded. Clinical and laboratory data recorded are detailed in the online supplementary methods. The study was approved by the ethics committee (Hospital Clínic, Barcelona).

The control group included 20 patients with no chronic inflammatory diseases, matched for gender, age and cardiovascular risk factors (CVRF), consecutively selected among patients who underwent PET/CT during the same timeframe for early lung cancer staging.

PET/CT protocol

PET scans were performed using a hybrid PET/CT (Biograph, Siemens) with an ECAT EXACT HR+BGO PET and a helicoidal CT scanner (Somatom, Emotion). Patients fasted 4 h before injection of 370 MBq of 18F-FDG. Whole-body PET data were acquired 60 min after in three-dimensional mode and for 5 min per bed position. PET images were reconstructed both with and without CT data for attenuation correction. A region of interest (ROI) in 3-D around the vessel was placed manually in transaxial, sagittal and coronal slices. The standardised uptake value (SUV) was calculated based on the measured activity, decay-corrected injected dose and patient body weight. SUVm=maximal activity (ROI) (mBq/mL)/injected dose (mBq)/weight (g).

Four aortic segments (ascending thoracic aorta, aortic arch, descending thoracic aorta and abdominal aorta) and the main tributaries—carotid, subclavian, axillary, iliac and femoral arteries (each bilaterally)—were evaluated. The control group was subjected to the same PET/CT protocol. Assessment of PET data was carried out by two nuclear medicine specialists (FL and MD), who were blinded to clinical and pathological findings. However, unequivocal masked evaluation could not be guaranteed due to the controls' disease.

Statistical analysis

ROC were applied to each vascular territory to calculate sensitivity and specificity. Area under the curve (AUC) comparison was performed by Hanley and McNeil analysis. Cut-offs with best sensitivity and specificity were selected. Mann–Whitney U test or Student t test, when applicable, were used for quantitative data. Correlations were calculated using Pearson's or Spearman's test. Statistical significance was defined as $p<0.05$. Calculations were performed with the IBM SPSS Statistics (V.20.0, Armonk, New York, USA).

RESULTS

Clinical and laboratory findings of the GCA cohort

Seventy-one GCA patients were diagnosed during the recruitment period. Eight patients refused participation, and 31 had received glucocorticoid treatment for >3 days. The remaining 32 were included. Seventeen of them had been treated for ≤3 days at the time of imaging. Treatment consisted of oral prednisone at 1 mg/kg/day. Two patients received 250 mg intravenous methylprednisolone pulses (1 and 7 pulses, respectively) due to severe cranial ischaemic symptoms.

Online supplementary table S1 shows the clinical and laboratory data of the study group. There were no relevant differences in age, gender or CVRF between patients and controls (see online supplementary table S2).

FDG uptake cut-off for GCA diagnosis

SUVm at any vascular territory explored was significantly higher in GCA patients than in controls (table 1). ROC curves and AUCs are displayed in figure 1 and table 1, respectively. Mean of the SUVm observed at all the vascular territories had an AUC of 0.830 (0.715–0.946). A cut-off of 1.89 had a sensitivity of 80% and a specificity of 79%. Mean of the SUVm at supraaortic vessels showed the highest AUC (0.832). In this site, a cut-off of 1.70 achieved a sensitivity and specificity of 81 and 79%, respectively, for the diagnosis of GCA (95% CI 0.720 to 0.946). FDG uptake at the aorta showed lower AUC (0.738), with a sensitivity and specificity of 90 and 42, respectively, using a cut-off of 2.25, and a sensitivity of 58%, specificity of 90% with a cut-off of 2.65 (95% CI 0.598 to 0.881). However, differences in AUCs among territories did not reach statistical significance.

Vascular/liver uptake ratios were also significantly higher in patients than in controls at the right axillary and carotid arteries,

Table 1 SUVm and AUC at each vascular bed assessed

Territory	GCA patients (mean±SD)	Controls (mean±SD)	p Value	AUC (95% CI)
Ascending aorta	2.63±0.57	2.17±0.26	<0.001	0.778 (0.651 to 0.904)
Aortic arch	2.61±0.50	2.23±0.31	0.002	0.756 (0.621 to 0.891)
Descending thoracic aorta	2.78±0.65	2.39±0.33	0.007	0.739 (0.598 to 0.881)
Abdominal aorta	2.97±0.60	2.56±0.39	0.005	0.748 (0.608 to 0.888)
Right subclavian artery	2.46±0.54	2.14±0.40	0.030	0.763 (0.607 to 0.889)
Left subclavian artery	2.26±0.56	1.89±0.28	0.003	0.764 (0.610 to 0.891)
Right carotid artery	2.33±0.52	1.83±0.25	<0.001	0.812 (0.695 to 0.930)
Left carotid artery	2.32±0.51	1.97±0.30	0.004	0.733 (0.594 to 0.872)
Right axillary artery	1.21±0.31	0.88±0.17	<0.001	0.830 (0.725 to 0.940)
Left axillary artery	1.09±0.34	0.88±0.18	0.001	0.780 (0.627 to 0.886)
Right iliac artery	2.41±0.67	2.01±0.38	0.009	0.747 (0.606 to 0.888)
Left iliac artery	2.46±0.47	2.00±0.41	0.002	0.767 (0.628 to 0.905)
Right femoral artery	1.68±0.39	1.24±0.22	<0.001	0.817 (0.715 to 0.928)
Left femoral artery	1.50±0.37	1.14±0.18	<0.001	0.801 (0.679 to 0.922)
All territories*	2.15±0.37	1.79±0.17	<0.001	0.830 (0.715 to 0.946)
Aorta**	2.75±0.54	2.34±0.23	0.001	0.738 (0.612 to 0.874)
Supraaortic branches**	1.95±0.35	1.59±0.15	<0.001	0.832 (0.732 to 0.968)
Iliofemoral territory**	1.97±0.36	1.62±0.23	<0.001	0.802 (0.679 to 0.925)
Liver	2.76±0.57	2.52±0.42	0.119	0.635 (0.480 to 0.790)

Removal of the two patients who had received intravenous methylprednisolone pulses at the time of PET performance did not significantly modify the results (data not shown).
Differences in AUCs among different vascular territories did not reach statistical significance.
AUC, area under the curve; GCA, giant cell arteritis; PET, positron emission tomography.
*Values represent the mean of the SUVm observed at all the vascular beds assessed.
**Aorta, Supraaortic branches and Iliofemoral territory represents the mean of the SUVm observed at the different vessels of these areas.

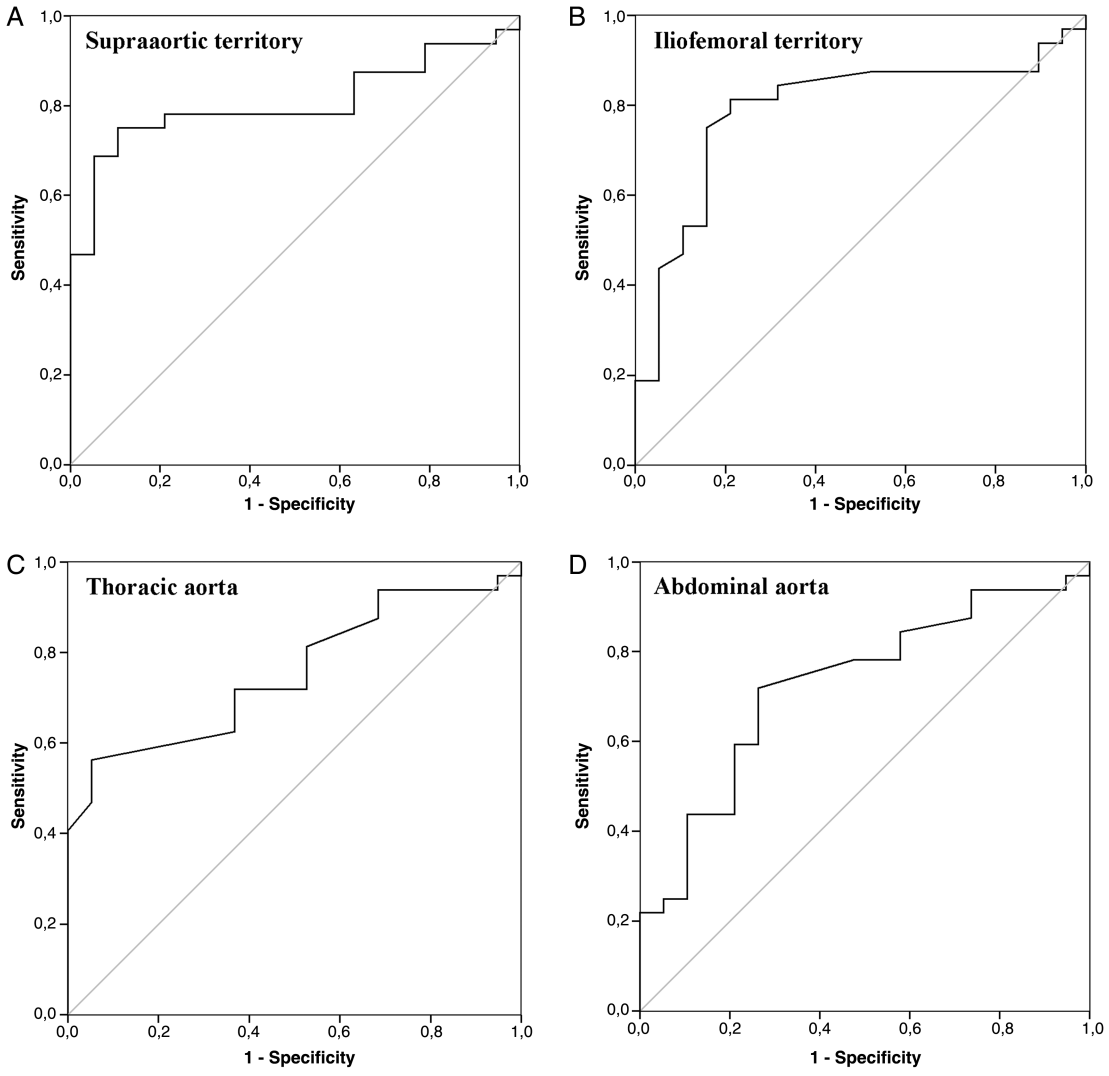

Figure 1 Receiver–operator characteristic curves of standardised uptake value at different vascular regions.

but the overall discriminatory performance was much lower (see online supplementary table S3).

Relationship between FDG uptake and clinical and laboratory findings

Patients with cranial symptoms presented significantly higher values of maximal and mean SUVm (combined average of all vascular territories) than patients lacking cranial manifestations. No relationship between the intensity of FDG uptake and other clinical findings was observed (table 2). No differences in maximal or mean SUVm were observed between treatment-naïve patients and those who had received glucocorticoids. The maximal and mean SUVm correlated with acute-phase reactants and serum IL-6 concentrations (table 2).

DISCUSSION

The present prospective study, performed in an unselected patient cohort with unequivocal GCA, shows that FDG uptake is significantly stronger in patients than in controls in all vascular territories tested, confirming the diagnostic potential of PET/CT.[4 8 9 11] PET/CT allows rapid, reproducible and broad vascular evaluation. Nevertheless, there is no standardised definition of vasculitis based on an objective FDG uptake measure, and strategies employed to establish a PET-based diagnosis of GCA has been heterogeneous. Most studies have used qualitative visual assessment or a semiquantitative score using liver uptake as a reference. Visual scoring has a remarkable investigator dependency and interobserver variability. Liver uptake is influenced by individual metabolic activity, glucocorticoid treatment and the time lapse between injection and scanning.[12]

We tried to overcome this limitation by objectively quantifying FDG uptake by different vascular beds in patients and controls and performing ROC analysis to determine the optimal cut-off for GCA diagnosis at different vascular territories. FDG uptake by supraaortic branches had the highest AUC, in accordance with a pioneer study showing that supraaortic branches were the most frequently involved when assessed by PET.[4] In this area, an FDG uptake cut-off value of 1.70 had the best sensitivity and specificity. A similar value, in the same territory but with lower performance (AUC=0.72), was reported in a retrospective study of 17 patients with GCA and 3 Takayasu arteritis patients.[13] This observation may be useful to differentiate GCA from other inflammatory aortic diseases that may produce systemic complaints and active aortic FDG uptake, including idiopathic aortitis, periaortitis, IgG4 disease and severe atherosclerosis.[10 14–17] This is crucial since a positive PET/CT may be accepted in the near future as a diagnostic criterion and is currently accepted as such in an ongoing clinical trial with tocilizumab in GCA.[18]

Table 2 Relationship between clinical and laboratory data and maximal SUV at any vascular territory (SUVm) and mean of the SUVm obtained at every vascular bed assessed (mean SUVm).

	Maximal SUVm		Mean SUVm	
		p Value		p Value
Cranial symptoms (P/A)	3.21±0.65/2.50±0.52	0.021	2.24±0.32/1.77±0.36	0.004
Systemic symptoms (P/A)	3.12±0.61/2.98±0.82	0.589	2.20±0.35/2.07±0.43	0.354
Ischaemic symptoms (P/A)	2.91±0.61/3.14±0.71	0.402	2.11±0.39/2.17±0.37	0.708
PMR (P/A)	3.11±0.62/3.06±0.71	0.886	2.27±0.35/2.12±0.38	0.321
GC treatment (Y/N)	2.97±0.44/3.20±0.81	0.385	2.14±0.36/2.17±0.40	0.858
CRP, mg/dL	r=0.551	0.001	r=0.476	0.034
ESR, mm/h	r=0.442	0.011	r=0.335	0.050
Haptoglobin, mg/dL	r=0.585	0.008	r=0.358	0.050
IL-6, pg/mL	r=0.616	0.002	r=0.544	0.007

Values are mean±SD.
Removal of the two patients who had received intravenous methylprednisolone pulses at the time of PET performance did not substantially modify the results (data not shown).
A, absence; CRP, C-reactive protein; ESR, erythrocyte sedimentation rate; F, female; GC, glucocorticoid; IL-6, interleukin 6; M, male; N, no; NS, not significant; P, presence; PET, positron emission tomography; PMR, polymyalgia rheumatica; SUV, standardized uptake value; Y, yes.

The sensitivity and specificity of PET/CT obtained in this study is close to that calculated in a recent systematic review/meta-analysis of heterogeneous, mostly retrospective studies, and those reported in a retrospective analysis evaluating the impact of PET on the management of patients with suspected large-vessel vasculitis.[19]

Interestingly, FDG uptake by the aorta showed a lower AUC, being worse in the abdominal segment where atherosclerosis is more prevalent in the general population. This fact highlights the diagnostic limitation of PET in this territory since aortic FDG uptake may be markedly influenced by ageing or atheroma plaques. Hautzel *et al* reported a higher sensitivity and specificity of thoracic aorta FDG uptake to detect large-vessel inflammation in a cohort of 18 patients with GCA.[20] A thoracic aorta/liver ratio of 1.0 had a sensitivity and specificity of 88% and 93%, respectively (AUC = 0.932). However, a substantial proportion of the patients assembled in this cohort were selected on the basis of previously known large-vessel involvement demonstrated by other techniques. In our study, direct, territory-focused comparison of SUVm between patients and controls discriminated better than vascular/liver ratios.

A retrospective study evaluating how PET/CT results influenced management of patients with suspected GCA suggested that previous glucocorticoid (GC) treatment decreased the diagnostic yield of PET/CT.[19] Sequential assessments have demonstrated, indeed, that FDG uptake decreases after 3 months of treatment.[4] The present study suggests that a short course of therapy (≤3 days) may not substantially reduce the diagnostic accuracy of PET/CT.

In conclusion, this study provides sensitive and specific, territory-focused cut-off values to detect vascular inflammation by PET/CT. A limitation of the study is that while patients were prospectively recruited, controls were retrospectively selected. Another limitation is the relatively small number of patients analysed, although our cohort is among the largest investigated. Further prospective studies using objective cut-offs are necessary to confirm their diagnostic performance in patients with suspected GCA.

Author affiliations
[1]Vasculitis Research Unit, Department of Systemic Autoimmune Diseases, Hospital Clínic, University of Barcelona, Institut d'Investigacions Biomèdiques August Pi i Sunyer (IDIBAPS), Barcelona, Spain
[2]Center for Diagnostic Imaging, Hospital Clínic, University of Barcelona, Institut d'Investigacions Biomèdiques August Pi i Sunyer (IDIBAPS), Barcelona, Spain
[3]Department of Emergency Medicine, Hospital Clínic, University of Barcelona, Institut d'Investigacions Biomèdiques August Pi i Sunyer (IDIBAPS), Barcelona, Spain
[4]Department of Internal Medicine, Hospital Clínic, University of Barcelona, Institut d'Investigacions Biomèdiques August Pi i Sunyer (IDIBAPS), Barcelona, Spain

Contributors MCC had full access to all of the data in the study and takes responsibility for the integrity of the data and the accuracy of the data analysis. Study design: SP-G, FL and MCC. Acquisition of data: SP-G, MD, AG-M, GE-F, IT-B, FL, MC-B, EP-R, MAA, JMG, JH-R and MCC. Analysis and interpretation of data: SP-G, MD, GE-F, FL, JH-R and MCC. Manuscript preparation: SP-G, FL, JH-R, JMG and MCC. Statistical analysis: SP-G, MAA, MCC.

Competing interests Supported by Ministerio de Economía y Competitividad (SAF 08/04328 and SAF11/30073). SP-G was a postresidency research award recipient from Hospital Clínic. MAA was supported by Consejo Nacional de Ciencia y Tenología (CONACyT), Mexico, and by Agencia de Gestió d'Ajuts Universitaris i de Recerca (AGAUR), Generalitat de Catalunya.

Ethics approval The study was approved by the ethics committee of our institution (Hospital Clínic, Barcelona).

Provenance and peer review Not commissioned; externally peer reviewed.

REFERENCES

1 Salvarani C, Pipitone N, Versari A, *et al*. Clinical features of polymyalgia rheumatica and giant cell arteritis. *Nat Rev Rheumatol* 2012;8:509–21.
2 Lie JT. Illustrated histopathologic classification criteria for selected vasculitis syndromes. American College of Rheumatology Subcommittee on Classification of Vasculitis. *Arthritis Rheum* 1990;33:1074–87.
3 Esteban MJ, Font C, Hernandez-Rodriguez J, *et al*. Small-vessel vasculitis surrounding a spared temporal artery: clinical and pathological findings in a series of twenty-eight patients. *Arthritis Rheum* 2001;44:1387–95.
4 Blockmans D, de Ceuninck L, Vanderschueren S, *et al*. Repetitive 18F-fluorodeoxyglucose positron emission tomography in giant cell arteritis: a prospective study of 35 patients. *Arthritis Rheum* 2006;55:131–7.
5 Prieto-Gonzalez S, Arguis P, Garcia-Martinez A, *et al*. Large vessel involvement in biopsy-proven giant cell arteritis: prospective study in 40 newly diagnosed patients using CT angiography. *Ann Rheum Dis* 2012;71:1170–6.
6 Schmidt WA, Seifert A, Gromnica-Ihle E, *et al*. Ultrasound of proximal upper extremity arteries to increase the diagnostic yield in large-vessel giant cell arteritis. *Rheumatology (Oxford)* 2008;47:96–101.
7 Aschwanden M, Kesten F, Stern M, *et al*. Vascular involvement in patients with giant cell arteritis determined by duplex sonography of 2×11 arterial regions. *Ann Rheum Dis* 2010;69:1356–9.
8 Hao R, Yuan L, Kan Y, *et al*. Diagnostic performance of 18F-FDG PET/CT in patients with fever of unknown origin: a meta-analysis. *Nucl Med Commun* 2013;34:682–8.
9 Blockmans D, De Ceuninck L, Vanderschueren S, *et al*. Repetitive 18-fluorodeoxyglucose positron emission tomography in isolated polymyalgia rheumatica: a prospective study in 35 patients. *Rheumatology (Oxford)* 2007;46:672–7.
10 Dunphy MP, Freiman A, Larson SM, *et al*. Association of vascular 18F-FDG uptake with vascular calcification. *J Nucl Med* 2005;46:1278–84.

11 Besson FL, Parienti JJ, Bienvenu B, *et al*. Diagnostic performance of (1) F-fluorodeoxyglucose positron emission tomography in giant cell arteritis: a systematic review and meta-analysis. *Eur J Nucl Med Mol Imaging* 2011;38:1764–72.
12 Iozzo P, Geisler F, Oikonen V, *et al*. Insulin stimulates liver glucose uptake in humans; an 18F-FDG uptake in humans. *J Nucl Med* 2003; 44:682–9.
13 Lehmann P, Buchtala S, Achajew N, *et al*. 18F-FDG PET as a diagnostic procedure in large vessel vasculitis-a controlled, blinded re-examination of routine PET scans. *Clin Rheumatol* 2011;30:37–42.
14 Reeps C, Essler M, Pelisek J, *et al*. Increased 18F-fluorodeoxyglucose uptake in abdominal aortic aneurysms in positron emission/computed tomography is associated with inflammation, aortic wall instability, and acute symptoms. *J Vasc Surg* 2008;48:417–23.
15 Salvarani C, Pipitone N, Versari A, *et al*. Positron emission tomography (PET): evaluation of chronic periaortitis. *Arthritis Rheum* 2005;53:298–303.
16 Vaglio A, Catanoso MG, Spaggiari L, *et al*. IL6 as an inflammatory mediator and target of therapy in chronic periaortitis. *Arthritis Rheum* 2013;65:2469–75.
17 Vaglio A, Salvarani C, Buzio C. Retroperitoneal fibrosis. *Lancet* 2006; 367:241–51.
18 Unizony SH, Dasgupta B, Fisheleva E, *et al*. Design of the tocilizumab in giant cell arteritis trial. *Int J Rheumatol* 2013;2013:912562.
19 Fuchs M, Briel M, Daikeler T, *et al*. The impact of 18F-FDG PET on the management of patients with suspected large vessel vasculitis. *Eur J Nucl Med Mol Imaging* 2012;39:344–53.
20 Hautzel H, Sander O, Heinzel A, *et al*. Assessment of large-vessel involvement in giant cell arteritis with 18F-FDG PET: introducing an ROC-analysis-based cutoff ratio. *J Nucl Med* 2008;49:1107–13.

Positron emission tomography assessment of large vessel inflammation in patients with newly diagnosed, biopsy-proven giant cell arteritis: a prospective, case–control study

Sergio Prieto-González, Marina Depetris, Ana García-Martínez, Georgina Espígol-Frigolé, Itziar Tavera-Bahillo, Marc Corbera-Bellata, Ester Planas-Rigol, Marco A Alba, José Hernández-Rodríguez, Josep M Grau, Franciso Lomeña and Maria C Cid

Ann Rheum Dis 2014 73: 1388-1392 originally published online March 24, 2014
doi: 10.1136/annrheumdis-2013-204572

EXTENDED REPORT

Changes in biomarkers after therapeutic intervention in temporal arteries cultured in Matrigel: a new model for preclinical studies in giant-cell arteritis

Marc Corbera-Bellalta,[1] Ana García-Martínez,[1,2] Ester Lozano,[1] Ester Planas-Rigol,[1] Itziar Tavera-Bahillo,[1] Marco A Alba,[1] Sergio Prieto-González,[1] Montserrat Butjosa,[1] Georgina Espígol-Frigolé,[1] José Hernández-Rodríguez,[1] Pedro L Fernández,[3] Pascale Roux-Lombard,[4] Jean-Michel Dayer,[5] Mahboob U Rahman,[6,7] Maria C Cid[1]

Handling editor Tore K Kvien

▶ Additional material is published online only. To view please visit the journal online (http://dx.doi.org/10.1136/annrheumdis-2012-202883).

For numbered affiliations see end of article.

Correspondence to
Dr Maria C Cid,
Vasculitis Research Unit, Department of Systemic Autoimmune Diseases, Hospital Clínic, University of Barcelona, Institut d'Investigacions Biomèdiques August Pi i Sunyer (IDIBAPS), Villarroel 170, 08036-Barcelona, Catalonia Spain;
mccid@clinic.ub.es

Preliminary results presented at the 71–74th Annual Scientific Meetings of the American College of Rheumatology (Boston, MA; San Francisco, CA; Philadelphia, PA; Atlanta, GA; 2007–2010)

Accepted 17 March 2013
Published Online First 27 April 2013

To cite: Corbera-Bellalta M, García-Martínez A, Lozano E, *et al*. *Ann Rheum Dis* 2014;**73**:616–623.

ABSTRACT

Background Search for therapeutic targets in giant-cell arteritis (GCA) is hampered by the scarcity of functional systems. We developed a new model consisting of temporal artery culture in tri-dimensional matrix and assessed changes in biomarkers induced by glucocorticoid treatment.

Methods Temporal artery sections from 28 patients with GCA and 22 controls were cultured in Matrigel for 5 days in the presence or the absence of dexamethasone. Tissue mRNA concentrations of pro-inflammatory mediators and vascular remodelling molecules was assessed by real-time RT-PCR. Soluble molecules were measured in the supernatant fluid by immunoassay.

Results Histopathological features were exquisitely preserved in cultured arteries. mRNA concentrations of pro-inflammatory cytokines (particularly IL-1β and IFNγ), chemokines (CCL3/MIP-1α, CCL4/MIP-1β, CCL5/RANTES) and MMP-9 as well as IL-1β and MMP-9 protein concentrations in the supernatants were significantly higher in cultured arteries from patients compared with control arteries. The culture system itself upregulated expression of cytokines and vascular remodelling factors in control arteries. This minimised differences between patients and controls but underlines the relevance of changes observed. Dexamethasone downregulated pro-inflammatory mediator (IL-1β, IL-6, TNFα, IFNγ, MMP-9, TIMP-1, CCL3 and CXCL8) mRNAs but did not modify expression of vascular remodelling factors (platelet derived growth factor, MMP-2 and collagens I and III).

Conclusions Differences in gene expression in temporal arteries from patients and controls are preserved during temporal artery culture in tri-dimensional matrix. Changes in biomarkers elicited by glucocorticoid treatment satisfactorily parallel results obtained in vivo. This may be a suitable model to explore pathogenetic pathways and to perform preclinical studies with new therapeutic agents.

INTRODUCTION

Giant-cell arteritis (GCA) is a granulomatous arteritis of the elderly, targeting the aorta and its branches with a striking tropism for the cranial arteries.[1] Although most patients with GCA experience a remarkable relief with high-dose glucocorticoids (GC), treatment has proven to be unsatisfactory. GC fail to prevent further sight deterioration in 10%–17% of patients presenting with visual impairment and are unable to avoid large vessel damage leading to aortic dilatation in about 22.5% of patients.[2 3] Moreover, more than 50% of patients relapse when GC are tapered[4 5] and GC-related adverse events occur in a more than 80% of patients with GCA.[6] There is an unmet need for more effective and specific therapies.

Search for therapeutic innovation in GCA is difficult due to the limited understanding of pathogenesis and the scarcity of functional models where the impact of therapeutic interventions can be assessed. The pathogenesis model of GCA is based on the identification of particular cell types (CD4T lymphocytes, macrophages, dendritic cells, endothelial cells),[7 8] cell activation and differentiation markers,[7–9] and inflammatory mediators in lesions.[9–13] The interpretation of immunopathology findings is often extrapolated from basic immunology principles, and the role of infiltrating cells and their products is assumed from their known biological activities and association with particular phenotypes,[10 11 13] histopathological changes or outcomes.[12–14] Proof of concept is weak for the majority of grounds on which the current pathogenetic model is sustained.

The frustrating experience with anti-tumour necrosis factor (TNF) therapy in GCA underlines the crucial need for functional systems. TNFα was considered a potential therapeutic target based on its strong upregulation in lesions[13] and correlation of tissue and serum TNFα levels with GC requirements and relapsing course.[13 15] In spite of these observations and in spite of the therapeutic efficacy of TNF blockers in other granulomatous diseases, neutralising TNFα with infliximab did not seem sufficient to abrogate inflammatory activity in GCA.[5] Blocking IL-6 receptor is currently being considered as a therapeutic option.[16] This and other interventions could benefit from preclinical functional testing.

A functional model was created by Brack *et al*[17] subcutaneously engrafting fragments of human temporal arteries into severe combined immunodeficiency (SCID) mice. This pioneer model has been useful to detect changes in cytokine expression in temporal artery tissue after pharmacological

treatment of engrafted mice[18 19] or after selective depletion of specific cell types with antibodies injected to animals,[8 17] providing proof of concept of some of the basic pathogenic principles. However, this model is complex, expensive and not widely available. Moreover, monitoring of successful engraftment is difficult and the accessibility of therapeutic agents administered to the mice cannot be controlled. Due to its complexity, the majority of published experiments have been performed with only 1–3 temporal arteries split into several mice.[8 18 19]

The Engelbreth-Holm-Swarm sarcoma-derived tri-dimensional matrix, Matrigel,[20] provides anchorage and survival signals for vascular smooth muscle cells (VSMC).[21] Based on these findings, we developed a new model to assess changes in lesions after therapeutic intervention, consisting of culture of temporal artery sections embedded in Matrigel. We found that cultured arteries remained viable for at least 2 weeks with exquisitely preserved morphology. Moreover, this system was sensitive enough to demonstrate clear differences in cytokine expression between normal and inflamed arteries as well as changes induced by therapeutic intervention.

METHODS

Patients

Temporal artery biopsies were performed to 50 consecutive patients with suspected GCA for diagnostic purposes. A 5–15 mm segment was saved for this study and the remaining fragment was processed for histopathological diagnosis. The study was approved by the Ethics Committee of the Hospital Clínic of Barcelona and patients signed informed consent.

A total of 28 biopsies disclosed histopathological features of GCA and 22 revealed no inflammatory infiltrates. Patients with a negative temporal artery biopsy were eventually diagnosed with other conditions (see online supplementary methods).

Temporal artery culture

Temporal artery fragments were placed in RPMI 1640 medium (Lonza; Verviers, Belgium) supplemented with 10% foetal bovine serum (Invitrogen, Carlsbad, California, USA), 2 mM L-glutamine (Invitrogen), amphotericin B at 2.5 µg/ml (Invitrogen) and gentamycine (Braun, Germany) at 200 µg/ml. An average of 10.79±2.91 (mean±SEM) 0.8–1 mm sections per specimen were cut in a tissue culture hood. Matrigel (Collaborative Biomedical Products, Bedford, Massachusetts, USA) was allowed to thaw on ice and 24-well tissue culture plates were coated with a 25 µl Matrigel drop per well, which was allowed to solidify at 37°C for 30 min. One temporal artery section per well was dipped in the Matrigel coating and covered with 1 ml medium. Dexamethasone (Sigma, Ayrshire, UK) at 0.5 µg/ml was added to selected wells. Each condition was tested in 3–4 replicate wells. Sections were incubated al 37°C in 5% CO_2 for 5 days. Replicates of supernatant fluids and biopsies were respectively pooled. Biopsies were frozen in TRIzol reagent (Invitrogen) and stored at −80°C. Random specimens were cultured for 2 weeks in order to assess morphology preservation after extended culture periods and fixed in 10% formalin for H&E staining and histopathological examination.

Immunostaining

Cultured temporal artery sections were de-paraffinised, washed in phosphate-buffered saline (PBS) and endogenous peroxidase was blocked with H_2O_2. Slides were incubated with mouse antihuman CD3 (clone PS1, Leica Microsystems, Wetzlar, Germany, at 1:60 dilution) or undiluted mouse antihuman CD68 (clone KP1 from Dako, Glostrup, Denmark, ready to use). Optimal dilutions were tested on human tonsils (positive control). Isotype-matched mouse immunoglobulins served as negative controls. Immunodetection was performed with a HRP-labelled polymer conjugated to a secondary antibody (EnVision, Dako) using 3-3′-diaminobenzidine as a chromogen.

Cytokine mRNA measurement by real-time quantitative RT-PCR

Three to four temporal artery sections per condition were homogenised in TRIzol reagent. RNA extraction was performed according to the chloroform-isopropanol precipitation method. Total RNA (1 µg) was reverse transcribed to cDNA using Archive kit (Applied Biosystems, Life Technologies, Carlsbad, California, USA) in a final volume of 100 µl, employing random hexamer priming. Samples were stored at −80°C until use.

Gene expression of pro-inflammatory cytokines (IL-1 β, IL-6, TNFα, interferon (IFN)γ), chemokines (chemokine ligand (CCL)2/monocyte chemoattractant protein (MCP)-1, CCL3/MIP-1α, CCL4/MIP1β, CCL5/regulated upon activation normal T cell expressed and secreted (RANTES) and CXCL8/IL-8), metalloproteases (matrix metalloproteinases (MMP)-2, MMP-9) and their inhibitors (tissue inhibitor of metalloproteinases (TIMP)-1 and TIMP-2), growth factors (platelet derived growth factor (PDGF) A and B) and vascular matrix components (collagen I, collagen III) was assessed using specific predeveloped Taqman probes from Applied Biosystems (Taqman Gene Expression Assays; see online supplementary methods). Fluorescence was detected with ABI PRISM 7900 Sequence Detection system and results were analysed with the Sequence Detection Software V.2.3 (Applied Biosystems). Comparative Ct method was used to assess the relative gene expression. All samples were normalised to the expression of the endogenous control GUSb and values were expressed as relative units.

Detection of inflammatory mediators in the supernatant fluid by immunoassay

Pro-inflammatory cytokines (IL-6, TNFα, IL-1β, IFNγ), chemokines (CCL2/MCP-1 and CCL3/MIP-1α), metalloproteases (MMP2 and MMP-9) and growth factors (PDGF AB) were detected by enzyme-linked immunoassay (Quantikine ELISA kits from R&D Systems, Minneapolis, Minnesota, USA) in the culture supernatants form all patient and control arteries.

CCL4/MIP-1β and CXCL8/IL-8 were assessed by the Multiplex Luminex system (Life Technologies, Paisley, UK) in the supernatant fluid from 10 patients and six controls.

Statistical analysis

Mann–Whitney test was applied for statistical analysis.

RESULTS

Viability of the system and preserved morphology

Arterial sections were daily monitored under an inverted microscope. In GCA arteries white blood cells were visible in the periphery of the artery and remained bright and viable as assessed by Trypan blue exclusion throughout the duration of the experiment (figure 1A). After 1 week, VSMC began to spread and extend towards the matrix, further supporting the viability of this system (figure 1B).

As shown in figure 1C and 1D histopathological examination of cultured GCA arteries disclosed that morphological details including distinct arterial layers, inflammatory infiltrates, internal elastic lamina fragments and giant-cells were perfectly preserved. Over time, the intensity of inflammatory infiltrates decreased in cultured arteries, as described in arteries engrafted into SCID mice.[17] As shown in figure 1E–H, inflammatory

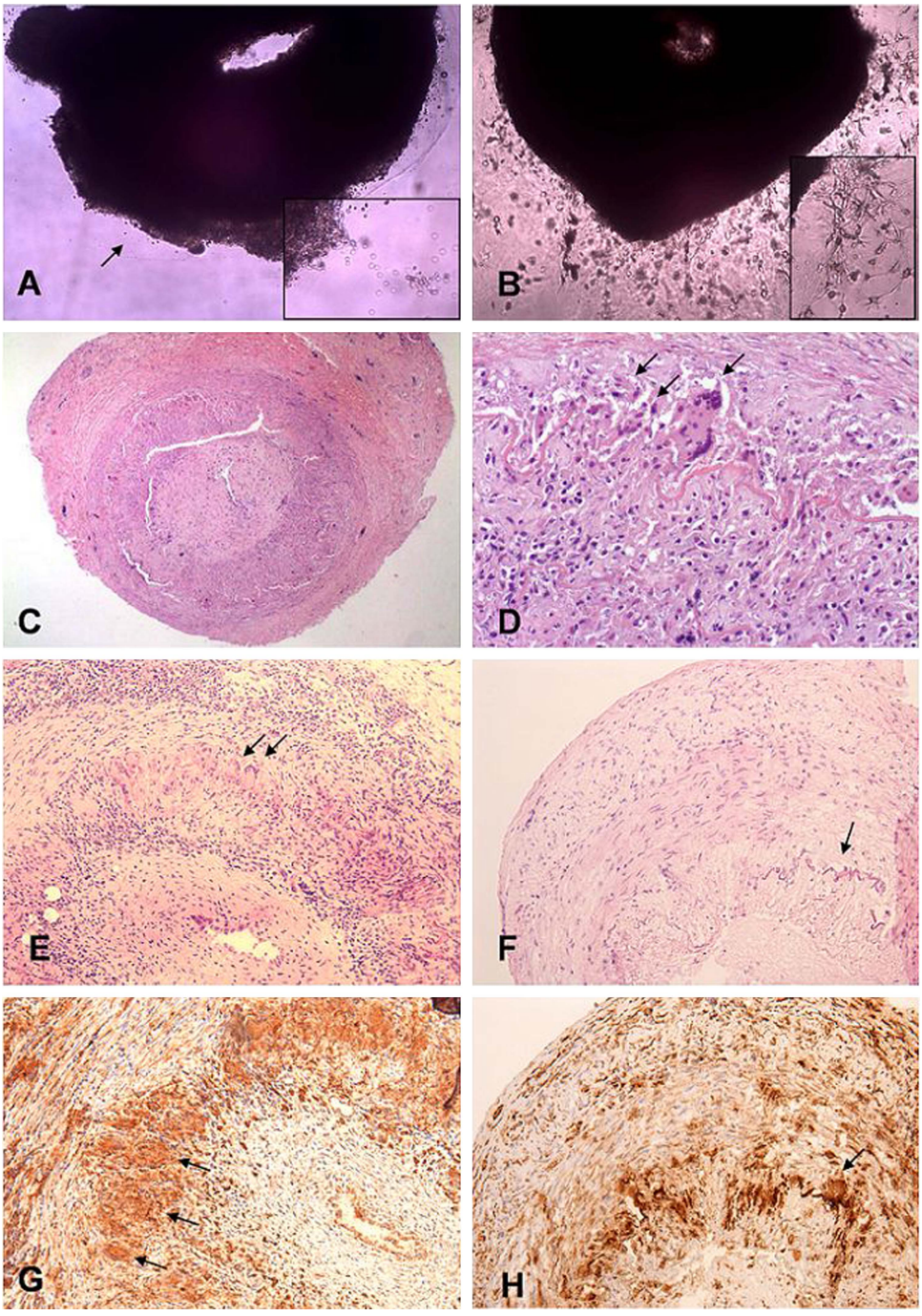

Figure 1 Histopathological findings in temporal artery sections from patients with giant-cell arteritis (GCA) cultured in Matrigel. (A) Temporal artery section from a patient with GCA cultured for 24 h and observed under an inverted, phase-contrast microscope. The arrow shows bright leukocytes cumulating in the periphery of the artery (inset shows a closer view). (B) Temporal artery section from a patient with GCA after 7-day culture. Vascular smooth muscle cells (VSMC) sprout from the artery and leukocytes migrate outwards (inset shows a closer view). Identity of these cells as VSMC has been previously demonstrated.[21] (C) H&E staining of a temporal artery section cultured for 2 weeks showing exquisite preservation of morphology. (D) Closer view of another temporal artery section cultured for 2 weeks displaying giant cells (arrows) along fragments of the internal elastic lamina. (E) H&E staining of a section of a freshly removed artery. Arrows show giant-cells. (F) Serial section of the artery disclosed in E cultured for 2 weeks showing a reduction in inflammatory infiltrates. The arrow indicates typical internal elastic lamina fragments. (G) Macrophages and numerous giant-cells (arrows) identified by anti-CD68 immunostaining in a freshly removed artery. (H) Anti-CD68 immunostaining of a serial section cultured for 2 weeks. Giant-cells (arrow) are dramatically reduced.

infiltrates, including giant-cells, decreased after 2-week culture. Examination of the cultured arteries under an inverted microscope disclosed that, over time, some inflammatory cells migrated along the outgrowing VSMC (figure 1B).

Differences in expression and release of relevant molecules between cultured GCA and control arteries

To assess the model reliability we investigated expression of pro-inflammatory cytokines, chemokines, metalloproteinases and

growth factors largely known to be expressed in GCA lesions and thought to be relevant to pathogenesis. We also explored some additional chemokines, such as CCL3/MIP-1α, CCL4/MIP-1β, CCL5/RANTES and CXCL8/IL-8, not previously investigated in GCA.

After a 5-day incubation period, remarkable differences in the spontaneous expression and release of various relevant factors were detected between GCA and control arteries, underlining the accurate sensitivity of the system to distinguish between non-inflamed and inflamed arteries (table 1). Differences in gene expression were particularly significant for IL-1β, IFNγ, chemokines CCL3/MIP-1α, CCL4/MIP-1β and CCL5/RANTES, and MMP-9. Less marked or no differences were observed for other factors known to be upregulated in GCA lesions including IL-6, TNFα and CCL2. Intense expression by cultured control arteries probably minimised differences.

Of interest, MMP-9, mainly produced by inflammatory cells, was overexpressed in patient versus control specimens whereas MMP-2, constitutively expressed by VSMC, was similar between patients and controls, paralleling again what has been observed in uncultured temporal artery biopsies.[22] As previously observed in freshly removed arteries, TIMP-1 and TIMP-2 mRNAs were decreased in inflamed arteries, leading to increased proteolytic balance.[22] Vascular remodelling factors PDGFs, CCL2, MMP-2 and collagens were strongly expressed in cultured arteries with no relevant differences between patients and controls.

Variations in the secretion of various markers were observed. TNFα and particularly IL-6 were remarkably released in the supernatant fluid (table 1). However, IFNγ and IL-1β, markedly expressed at the mRNA level, were secreted in small amounts. This parallels what happens in vivo where circulating TNFα and IL-6 are increased in sera of patients whereas IL-1β and IFNγ are not easily secreted and remain around the detection threshold in human serum. Therefore, this system allows evaluation of cytokine expression and investigation of cytokine secretion.

Similarly, while there were significant differences in chemokines CCL3/MIP1-α, CCL4/MIP-1β and CCL5/RANTES between patients and controls at the mRNA level, differences in released chemokines were less apparent.

Effect of the culture system on gene expression in cultured arteries

Since control arteries notably expressed various mediators we next investigated whether the culture system itself influenced gene expression. Frozen tissue from the original artery was available for six of the GCA patients and five controls and the expression of selected markers was compared between sections of the same specimen before and after 5-day culture in Matrigel. With the exception of IFNγ, the culture system upregulated expression of pro-inflammatory cytokines, chemokines CCL2 and CXCL8, and MMP-9 in both patients and controls. PDGFs and collagen III were markedly increased in control arteries whereas IFNγ and collagens decreased in GCA specimens (figure 2). In general, the culture system minimised differences between patients and controls.

Effect of dexamethasone on inflammatory infiltrates and on the expression and release of inflammatory and vascular remodelling markers

To assess whether this ex vivo system allowed accurate detection of changes induced by pharmacological intervention, we compared expression and release of inflammatory markers between artery sections cultured with medium alone and sections from 10 patients cultured in the presence of dexamethasone. A marked decrease in cytokine production was observed (figure 3 and table 2). Chemokines were downregulated at the mRNA level but changes in chemokine release were, again, less apparent (table 2). Vascular remodelling factors such as CCL2, MMP-2 and PDGF as well as collagens I and III were not downregulated by dexamethasone.

Dexamethasone treatment for 2 weeks induced a decrease in macrophage infiltration as assessed by CD68 mRNA expression and immunohistochemistry (figure 4). No effect on T cells was observed during the same treatment period.

Table 1 Differences in biomarker mRNA expression (*relative units*) and protein secretion (*pg/ml*) between cultured temporal artery sections from GCA patients and controls

	mRNA concentration (relative units)			Protein concentration (pg/ml)		
	GCA biopsies	Control biopsies	p Value	GCA biopsies	Control biopsies	p Value
IL-1β	35.91±8.80	14.22±2.86	**0.047**	5.61±1.33	−0.85±0.58	**0.000**
IL-6	448.54±86.88	380.04±68.37	0.543	25583±9404	7805.4±2685	0.076
TNFα	4.70±2.26	6.69±1.24	0.420	21.25±5.09	8.42±2.59	0.053
IFNγ	0.805±0.257	0.012±0.011	**0.010**	7.75±2.41	7.75±2.41	0.764
CCL-2/MCP-1	648.72±155.21	729.5±201.42	0.758	11268±1903	5850.91±4316.1	0.227
CXCL-8/IL-8	2287.9±619.9	4346.5±1092.4	0.095	81403±25050	34778.2±18253.9	0.157
CCL-3/MIP-1α	86.31±16.9	20.16±.5.10	**0.002**	25.617±2.503	26.62±4.25	0.834
CCL-4/MIP-1β	28.21±6.13	5.36±1.13	**0.003**	12.61±3.1	6.15±1.3	0.087
CCL-5/RANTES	139.83±37.34	16.42±5.58	**0.007**	21.43±5.19	17.33±6.54	0.633
MMP-2	2097.4±276.9	3450.9±1143.4	0.297	39125±11144	15250±8280	0.192
MMP-9	1283.85±408.2	304.21±90.70	**0.039**	48913±10740	7825±3512.4	**0.006**
TIMP-1	11813±3550	15126.8±5893.7	0.613	Not done	Not done	–
TIMP-2	586.68±87.77	2798.1±1135.2	0.074	Not done	Not done	–
COL I	1545.6±284.61	1065.34±196.7	0.175	Not done	Not done	–
COL III	3674.4±637.07	3979.2±991.5	0.789	Not done	Not done	–
PDGF A	71.14±24.75	163.55±40.13	0.056	Not done	Not done	–
PDGF B	40.78±7.78	43.807±7.992	0.806	Not done	Not done	–
PDGF AB	Not applicable	Not applicable	–	23.375±3.245	41.50±15.34	0.325

Values in bold are statistically significant (p<0.05). mRNA expression was detected in the entire cohort of 28 GCA patients and 22 controls. CCL3/MIP-1α, CCL4/MIP-1β and CXCL8/IL-8 protein concentrations were detected by Luminex in 10 patients and six controls. The remaining proteins were detected by ELISA in the entire cohort.
COL, Collagen; GCA, giant-cell arteritis.

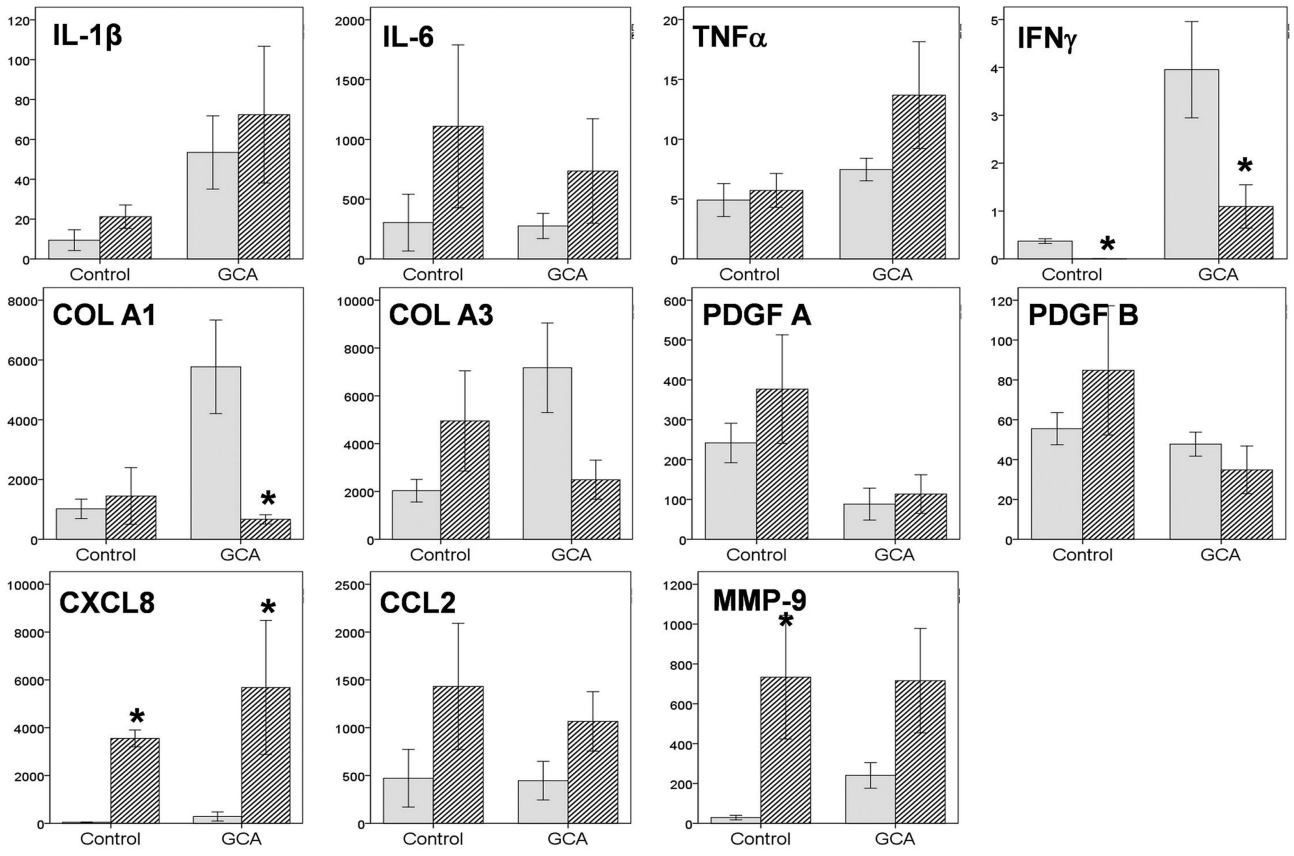

Figure 2 Effects of the culture system on biomarker expression. mRNA concentration (*relative units*) of pro-inflammatory cytokines, chemokines, vascular remodelling factors and matrix proteins in freshly removed (white bars) versus cultured, untreated, serial temporal artery sections (dashed bars) from six giant-cell arteritis patients and five controls (mean±SEM). *p<0.05 comparing fresh versus cultured arteries. Statistics are only indicative given the low number of samples studied.

DISCUSSION

Functional models are essential to explore pathogenic pathways and to test therapeutic intervention in diseases. We developed a new model of temporal artery culture in tri-dimensional matrix to perform functional studies in GCA. Short-term explant culture of involved tissue has been previously used in other conditions such as rheumatoid arthritis and has provided useful insights into involved immunopathogenic pathways.[23] A previous attempt of culturing temporal artery explants was tried by Blain *et al*.[24] However, without the use of a supporting matrix, the specimen remained viable for a short period of time. Specimens were cultured for 20 h only and the release of mediators in the supernatant fluid had to be induced with lypopolysaccharide which is an important exogenous manipulation.

The main innovation of our culture system is the embedding of the specimen in Matrigel which supports viability with active production of inflammatory mediators and their spontaneous release into the culture medium. In addition to provide an anchorage system for the wounded VSMC medial layer of the excised sections, Matrigel provides survival and proliferation signals for VSMC[21] which, in turn, may promote survival of infiltrating lymphocytes and macrophages. In this model, morphology was excellently preserved within 2-week culture.

There was a remarkable variability in the spontaneous production of inflammatory mediators, reflecting the notable differences in the density of inflammatory infiltrates and individual variation in cytokine production existing among patients with GCA. This observation underlines the need of a suitable model where testing specimens from multiple donors is feasible.

Spontaneous expression of IL-1β, IFNγ, MMP-9 and chemokines CCL3, CCL4 and CCL5 was significantly higher in explants from patients compared with controls and closely paralleled what has been described in immunopathology studies of freshly removed GCA arteries.

GC substantially reduced the production of pro-inflammatory cytokines IL-1β, IL-6 and TNFα both at the mRNA and protein level and also IFNγ mRNA. Expression of chemokines was also markedly decreased. These changes were similar to what has been observed in cross-sectional comparisons in biomarker expression between biopsies obtained from untreated patients and biopsies from patients who have already received GC,[7 22] in sequential biopsies obtained in four patients before and after 1 year of GC treatment,[14] or results obtained in temporal artery biopsies engrafted in the SCID mice.[18] GC treatment induced also a decrease in macrophage infiltration, whereas virtually no effect was observed on T cells, suggesting that T cell infiltration may be more resistant to GC therapy.

An interesting contribution of this study is that the expression of vascular remodelling factors such as CCL2/MCP-1, MMP-2, PDGFs and collagen I and III is not influenced by GC. A previous study comparing sequential biopsies obtained in four patients before and after 1 year of GC treatment showed, indeed, that vascular remodelling factors increased after long-term GC treatment.[14] This may explain why some patients

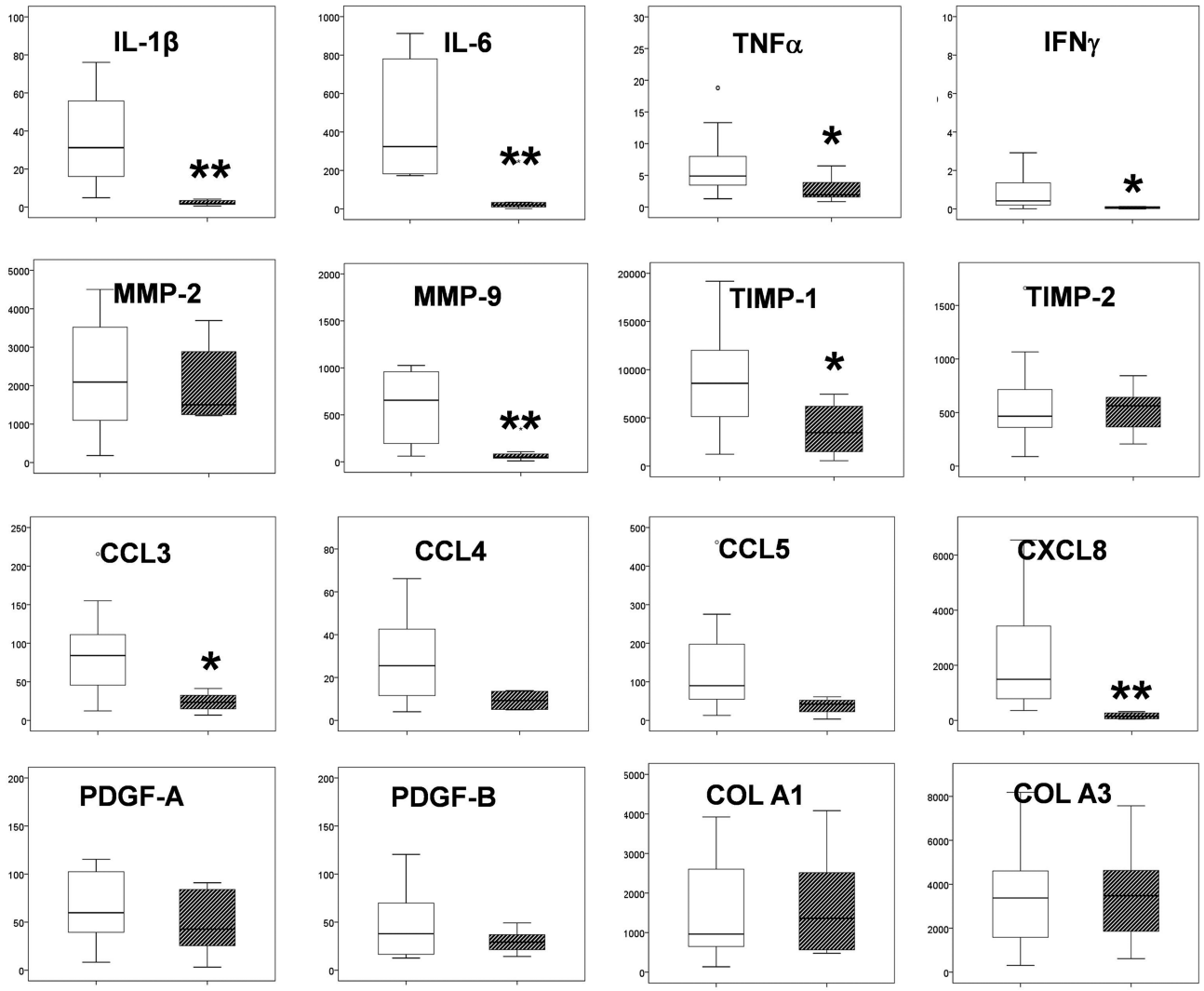

Figure 3 Changes in biomarker mRNAs induced by dexamethasone treatment. Comparison in mRNA concentration of selected biomarkers between untreated temporal artery sections from the giant-cell arteritis cohort (white box) and temporal artery sections from 10 of the patients subjected to dexamethasone at 0.5 mg/ml (grey box). *p<0.05; **p<0.005.

Table 2 Changes in biomarker protein concentration (*pg/ml*) in the supernatant fluid from untreated cultured GCA temporal artery sections and cultured GCA sections exposed to dexamethasone

	Protein concentration (pg/ml)		
	Untreated artery sections (mean ±SEM)	Dexamethasone-treated artery sections (mean±SEM)	p Value
IL-1β	6.06±1.32	2.41±0.76	**0.017**
IL-6	31059.8±10600.6	4796.5±1968.4	**0.020**
TNFα	27.043±6.398	2.22±2.104	**0.041**
IFNγ	4.901±1.8	4.792±1.66	0.961
CCL-2/ MCP-1	11759±2679.5	5130.2±598.83	0.921
CCL3/ MIP-1α	24.11±9.05	19.41±11.38	0.399
CXCL8/ IL-8	132670±41358.1	2465.5±631.76	0.056
MMP-2	39.125±11.14	27.5±7.79	0.204
MMP-9	48.91±10.74	8.64±1.89	**0.003**
PDGF AB	23.38±3.25	20±2.83	0.394

GCA, giant-cell arteritis.

continue to develop vascular occlusive events in spite of GC treatment.[2]

A limitation of this model is that Matrigel itself, by promoting survival and proliferation of smooth muscle cells, may directly influence the expression or detection of some products introducing a bias in the results. The culture system downregulated IFNγ and collagen I expression in GCA arteries and, conversely, upregulated the expression IL-6, CCL2/MCP-1, MMP-9, CXCL8/IL-8, PDGFs and collagen III in control arteries. These molecules may be part of vascular remodelling/repair programme stimulated by surgical injury and facilitated by attachment to the matrix. These observations indicate that some differences in gene expression observed between patients and controls are minimised by the culture system but, at the same time, enhance the significance of the differences observed. Furthermore, this finding underlines the need of investigating how the culture system influences the expression of any factor to be tested in this model.

Another limitation is that detection of some mediators such as chemokines in the culture medium may not accurately reflect their actual production. Chemokines act in an autocrine/paracrine manner and interact with matrix proteins to create a local

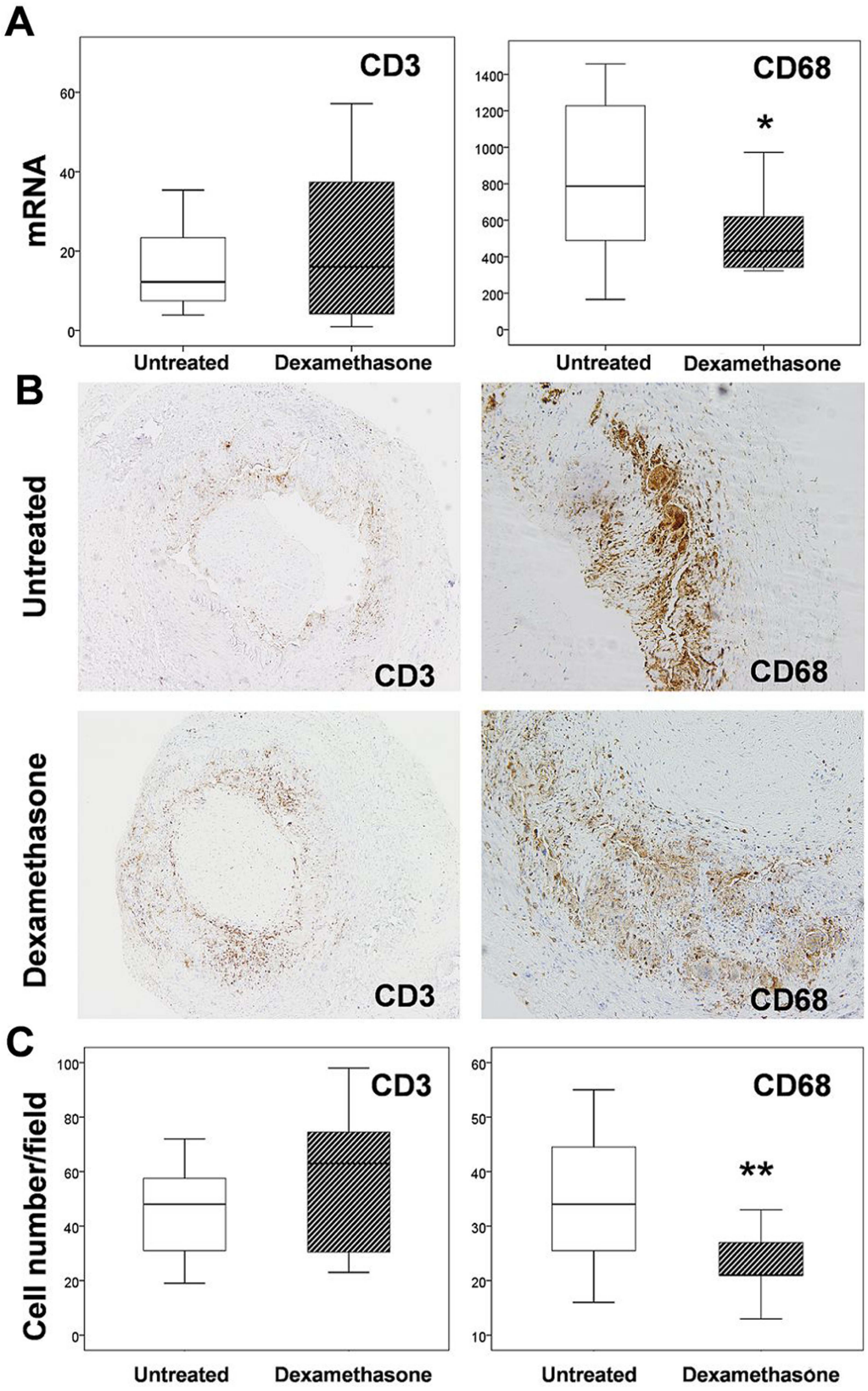

Figure 4 Effects of dexamethasone treatment on the density of infiltrating T lymphocytes and macrophages. (A) Differences in mRNA concentration of CD3 (T lymphocyte marker) and CD68 (macrophage marker) between 28 untreated giant-cell arteritis (GCA) temporal artery sections and 10 GCA sections exposed to 0.5 μg/ml dexamethasone. *p=0.059. (B) Changes in infiltrating T lymphocytes (identified by anti-CD3 immunostaining) and macrophages (identified by anti-CD68 immunostaining) upon dexamethasone treatment. (C) CD3 or CD68 cell number per field in three paired arteries cultured with or without dexamethasone. **p=0.004.

gradient. Therefore, chemokines may be retained in the artery and surrounding proteoglycan-rich matrix, according to their physiological function.[25] Dissociation between tissue and serum concentrations of relevant chemokines has been observed in several chronic inflammatory conditions.[12]

Our model overcomes some of the limitations of the temporal artery engraftment into the SCID mice. It allows daily monitoring of viability, it ensures direct accessibility of the molecules tested, it allows serial detection of proteins secreted into the culture medium and morphology is better preserved. Since retrieval of the cultured specimens is direct and simple, very thin sections can be used, allowing the assessment of replicates to assure consistency, and the testing of various conditions per specimen. This is very important given the remarkable variability in the intensity of inflammatory infiltrates and cytokine production among patients. In addition, it is cheap, easy, spares animals and does not require special equipment besides tissue culture facilities. In fact, since the initial communication of preliminary results,[26 27] this model is being used by other investigators.[28] It shares with the SCID mice model the limitation that only changes in biomarkers can be assessed and true, clinically relevant, disease outcomes cannot be investigated.

In summary, we developed an artery explant culture system based on the unique properties of Matrigel in creating a tridimensional matrix support and promoting VSMC survival. This method is sensitive enough to detect changes after intervention and may be useful to explore pathogenic pathways and to assess the impact of new therapeutic agents.

Author affiliations
[1]Vasculitis Research Unit, Department of Systemic Autoimmune Diseases, Hospital Clínic, University of Barcelona, Institut d'Investigacions Biomèdiques August Pi i Sunyer (IDIBAPS), Barcelona, Catalonia, Spain
[2]Department of Emergency Medicine, Hospital Clínic, Institut d'Investigacions Biomèdiques August Pi i Sunyer (IDIBAPS), Barcelona, Catalonia, Spain
[3]Department of Pathology, Hospital Clínic, University of Barcelona, Institut d'Investigacions Biomèdiques August Pi i Sunyer (IDIBAPS), Barcelona, Spain
[4]Immunology and Allergy Division, University Hospital of Geneva, Geneva, Switzerland
[5]Faculty of Medicine, University of Geneva, Geneva, Switzerland
[6]Department of Medicine, Rheumatology section, University of Pennsylvania Medical School, Philadelphia, Pennsylvania, USA
[7]Department of Medical Affairs, Emerging Markets Business unit, Pfizer Inc., Collegeville, Pennsylvania, USA

Acknowledgements We are thankful to Mrs Eva Fernández and Ingrid Victoria for excellent technical assistance.

Contributors MCC and MUR designed the study. J-MD contributed important input to its design. MC-B, AG-M, EL, EP-R and PR-L performed the experimental work. GE-F, SP-G, MAA, JH-R and MB contributed to clinical selection and contributed to the experimental work, PLF supervised the immunopathology studies. All authors evaluated and criticised the data and J-MD provided important contributions to their interpretation. MC-B and MCC wrote the manuscript. All authors read, made improvements and approved the final version.

Funding Supported by Ministerio de Ciencia e Innovación (SAF 08/04328), Ministerio de Economía y Competitividad (SAF 11/30073 and SAF 12/40017) and Marató TV3 (06/0710). G Espígol-Frigolé and MC Cid were supported by Instituto de Salud Carlos III. M Butjosa and I Tavera-Bahillo were supported by a Post-Residency Award from Hospital Clínic.

Competing interests MUR is a full employee by Pfizer Inc. No other competing interests.

Patient consent Obtained.

Ethics approval Ethics Committee from Hospital Clínic, Barcelona.

Provenance and peer review Not commissioned; externally peer reviewed.

REFERENCES

1 Salvarani C, Pipitone N, Versari A, *et al*. Clinical features of polymyalgia rheumatica and giant cell arteritis. *Nat Rev Rheumatol* 2012;8:509–21.
2 Cid MC, García-Martínez A, Lozano E, *et al*. Five clinical conundrums in the management of giant cell arteritis. *Rheum Dis Clin North Am* 2007;33:819–34.
3 García-Martínez A, Hernández-Rodríguez J, Arguis P, *et al*. Development of aortic aneurysm/dilatation during the follow-up of patients with giant cell arteritis: a cross-sectional screening of fifty-four prospectively followed patients. *Arthritis Rheum* 2008;59:422–30.
4 Martinez-Lado L, Calviño-Díaz C, Piñeiro A, *et al*. Relapses and recurrences in giant cell arteritis: a population-based study of patients with biopsy-proven disease from northwestern Spain. *Medicine* 2011;90:186–93.
5 Hoffman GS, Cid MC, Rendt-Zagar KE, *et al*. Infliximab for maintenance of glucocorticosteroid-induced remission of giant cell arteritis: a randomized trial. *Ann Intern Med* 2007;146:621–30.
6 Proven A, Gabriel SE, Orces C, *et al*. Glucocorticoid therapy in giant cell arteritis: duration and adverse outcomes. *Arthritis Rheum* 2003;49:703–8.
7 Cid MC, Campo E, Ercilla G, *et al*. Immunohistochemical analysis of lymphoid and macrophage cell subsets and their immunologic activation markers in temporal arteritis. Influence of corticosteroid treatment. *Arthritis Rheum* 1989;32:884–93.
8 Ma-Krupa W, Jeon MS, Spoerl S, *et al*. Activation of arterial wall dendritic cells and breakdown of self-tolerance in giant cell arteritis. *J Exp Med* 2004;199:173–83.
9 Deng J, Younge BR, Olshen RA, *et al*. Th17 and Th1 T-cell responses in giant cell arteritis. *Circulation* 2010;121:906–15.
10 Weyand CM, Tetzlaff N, Björnsson J, *et al*. Disease patterns and tissue cytokine profiles in giant cell arteritis. *Arthritis Rheum* 1997;40:19–26.
11 Hernández-Rodríguez J, Segarra M, Vilardell C, *et al*. Elevated production of interleukin-6 is associated with a lower incidence of disease-related ischemic events in patients with giant-cell arteritis: angiogenic activity of interleukin-6 as a potential protective mechanism. *Circulation* 2003;107:2428–34.
12 Cid MC, Hoffman MP, Hernández- Rodríguez J, *et al*. Association between increased CCL2 (MCP-1) expression in lesions and persistente of disease activity in giant-cell arteritis. *Rheumatology* 2006;45:1356–63.
13 Hernández-Rodríguez J, Segarra M, Vilardell C, *et al*. Tissue production of pro-inflammatory cytokines (IL-1beta, TNFalpha and IL-6) correlates with the intensity of the systemic inflammatory response and with corticosteroid requirements in giant-cell arteritis. *Rheumatology* 2004;43:294–301.
14 Visvanathan S, Rahman MU, Hoffman GS, *et al*. Tissue and serum markers of inflammation during the follow-up of patients with giant-cell arteritis—a prospective longitudinal study. *Rheumatology* 2011;50:2061–70.
15 García-Martínez A, Hernández-Rodríguez J, Espígol-Frigolé G, *et al*. Clinical relevance of persistently elevated circulating cytokines (tumor necrosis factor alpha and interleukin-6) in the long-term followup of patients with giant cell arteritis. *Arthritis Care Res* 2010;62:835–41.
16 Salvarani C, Magnani L, Catanoso M, *et al*. Tocilizumab: a novel therapy for patients with large-vessel vasculitis. *Rheumatology* 2012;51:151–6.
17 Brack A, Geisler A, Martinez-Taboada VM, *et al*. Giant cell vasculitis is a T cell-dependent disease. *Mol Med* 1997;3:530–43.
18 Brack A, Rittner HL, Younge BR, *et al*. Glucocorticoid-mediated repression of cytokine gene transcription in human arteritis-SCID chimeras. *J Clin Invest* 1997;99:2842–50.
19 Piggott K, Deng J, Warrington K, *et al*. Blocking the NOTCH pathway inhibits vascular inflammation in large-vessel vasculitis. *Circulation* 2011;123:309–18.
20 Benton G, George J, Kleinman HK, *et al*. Advancing science and technology via 3D culture on basement membrane matrix. *J Cell Physiol* 2009;221:18–25.
21 Lozano E, Segarra M, García-Martínez A, *et al*. Imatinib mesylate inhibits in vitro and ex vivo biological responses related to vascular occlusion in giant cell arteritis. *Ann Rheum Dis* 2008;67:1581–8.
22 Segarra M, García-Martínez A, Sánchez M, *et al*. Gelatinase expression and proteolytic activity in giant-cell arteritis. *Ann Rheum Dis* 2007;66:1429–35.
23 Tetlow LC, Harper N, Dunningham T, *et al*. Effects of induced mast cell activation on prostaglandin E and metalloproteinase production by rheumatoid synovial tissue in vitro. *Ann Rheum Dis* 1998;57:25–32.
24 Blain H, Abdelmouttaleb I, Belmin J, *et al*. Arterial wall production of cytokines in giant cell arteritis: results of a pilot study using human temporal artery cultures. *J Gerontol A Biol Sci Med Sci* 2002;57:M241–5.
25 Tanaka Y, Adams DH, Hubscher S, *et al*. T-cell adhesion induced by proteoglycan-immobilized cytokine MIP-1 beta. *Nature* 1993;361:79–82.
26 García-Martínez A, Lozano E, Segarra M, *et al*. Human temporal artery culture on Matrigel: a useful method for preclinical assessment of functional changes after intervention. *Arthritis Rheum* 2007;56:S497.
27 Corbera-Bellalta M, Lozano E, García-Martínez A, *et al*. Changes in inflammatory-mediators induced by glucocorticoids in cultured human temporal arteries from patients with giant-cell arteritis. *Arthritis Rheum* 2008;58:S929.
28 Molloy D, Connolly M, McCormick J, *et al*. Acute serum amyloid A and TLR2 activation induces pro-inflammatory mechanisms in a novel ex vivo temporal artery explant culture/model of giant cell arteritis. *Ann Rheum Dis* 2012;71 (Suppl 3):225.

Changes in biomarkers after therapeutic intervention in temporal arteries cultured in Matrigel: a new model for preclinical studies in giant-cell arteritis

Marc Corbera-Bellalta, Ana García-Martínez, Ester Lozano, Ester Planas-Rigol, Itziar Tavera-Bahillo, Marco A Alba, Sergio Prieto-González, Montserrat Butjosa, Georgina Espígol-Frigolé, José Hernández-Rodríguez, Pedro L Fernández, Pascale Roux-Lombard, Jean-Michel Dayer, Mahboob U Rahman and Maria C Cid

Ann Rheum Dis 2014 73: 616-623 originally published online April 27, 2013
doi: 10.1136/annrheumdis-2012-202883

EXTENDED REPORT

Increased IL-17A expression in temporal artery lesions is a predictor of sustained response to glucocorticoid treatment in patients with giant-cell arteritis

Georgina Espígol-Frigolé,[1] Marc Corbera-Bellalta,[1] Ester Planas-Rigol,[1] Ester Lozano,[1] Marta Segarra,[1] Ana García-Martínez,[2] Sergio Prieto-González,[1] José Hernández-Rodríguez,[1] Josep M Grau,[3] Mahboob U Rahman,[4,5] Maria C Cid[1]

Handling editor Tore K Kvien

▶ Additional data are published online only. To view these files please visit the journal online (http://dx.doi.org/10.1136/annrheumdis-2012-201836).

[1]Vasculitis Research Unit, Department of Autoimmune Diseases, Hospital Clínic, University of Barcelona, Institut d'Investigacions Biomèdiques August Pi iSunyer (IDIBAPS), Barcelona, Spain
[2]Vasculitis Research Unit, Department of Emergency Medicine, Hospital Clínic, University of Barcelona, Institut d'Investigacions Biomèdiques August Pi iSunyer (IDIBAPS), Barcelona, Spain
[3]Department of Internal Medicine, Hospital Clínic, University of Barcelona, Institut d'Investigacions Biomèdiques August Pi iSunyer (IDIBAPS), Barcelona, Spain
[4]University of Pennsylvania Medical School, Collegeville, Pennsylvania, USA
[5]Department of Medical Affairs, Inflammation, Pfizer Inc., Collegeville, Pennsylvania, USA

Correspondence to
Dr Maria C Cid, MD, Vasculitis Research Unit, Department of Systemic Autoimmune Diseases, Hospital Clínic, University of Barcelona, Institut d'Investigacions Biomediques August Pi Sunyer (IDIBAPS), Villarroel 170, Barcelona 08036, Spain; mccid@clinic.ub.es

Accepted 14 August 2012
Published Online First 19 September 2012

ABSTRACT

Background Interleukin 17A (IL-17A) exerts pivotal proinflammatory functions in chronic inflammatory and autoimmune diseases.

Objective To investigate IL-17A expression in temporal artery lesions from patients with giant-cell arteritis (GCA), and its relationship with disease outcome.

Methods Fifty-seven patients with biopsy-proven GCA were prospectively evaluated, treated and followed for 4.5 years (52–464 weeks). Relapses, time (weeks) required to achieve a maintenance prednisone dose <10 mg/day, and time (weeks) to complete prednisone withdrawal were prospectively recorded. IL-17A mRNA was measured by real-time quantitative RT-PCR in temporal arteries from all patients and 19 controls. IL-17 protein expression was assessed by immunohistochemistry/immunofluorescence.

Results IL-17A expression was significantly increased in temporal artery samples from GCA patients compared with controls (6.22±8.61 vs 2.50±3.9 relative units, p=0.016). Surprisingly, patients with strong IL-17A expression tended to experience less relapses, and required significantly shorter treatment periods (median 25 vs 44 weeks to achieve <10 mg prednisone/day, p=0.0079). There was no correlation between IL-17A and RORc or RORα expression suggesting that these transcription factors may not exclusively reflect Th17 differentiation, and that cells other than Th17 cells might contribute to IL-17 expression in active patients. Accordingly, $FoxP3^+IL\text{-}17A^+$ cells were identified in lesions by confocal microscopy and were dramatically reduced in specimens from treated patients.

Conclusions IL-17A expression is increased in GCA lesions, and is a predictor of response to glucocorticoid treatment. The contribution of FoxP3+ cells to IL-17A production in untreated patients suggests that induced-Tregs may facilitate disease remission when proinflammatory cytokine production is downregulated by glucocorticosteroids.

INTRODUCTION

Giant-cell arteritis (GCA) is a large and medium-sized vessel vasculitis considered to be a Th1-mediated disease on the basis of its granulomatous appearance and the strong expression of IFNγ and IFNγ-induced products in lesions.[1–5]

Patients with GCA experience a dramatic improvement with high-dose glucocorticoids (GC). However, response is not sustained, and about 40%–50% of patients relapse when GC are tapered.[6 7] Persistent activity results in prolonged GC treatment, and more than 80% of patients experience GC-related complications.[8] Mechanisms involved in disease persistence are unknown. Increased expression of TNFα and CCL2 in vascular lesions and elevated serum concentrations TNFα and IL-6 are associated with relapsing disease and prolonged GC-requirements.[5 9 10] However, blocking TNFα with infliximab did not result in reduced relapse rate or cumulated GC doses when compared with placebo in a randomised clinical trial, indicating that blocking TNFα is not sufficient to abrogate disease activity.[11] In the context of this trial, comparison of gene expression in second temporal artery biopsies performed in four patients after 1 year of treatment disclosed that IFNγ and IL12/23p40, but not IL12p35, were upregulated in relapsing patients.[3] Discrepancy between expression of the two IL-12 subunits, p35 and p40, suggested that upregulated IL-12/23p40 might be part of IL-23. This led to the search for IL-23 and its related cytokine IL-17 in GCA lesions.[3 12 13]

IL-17A production characterises a distinct T cell phenotype, Th17, with pivotal proinflammatory functions in several autoimmune and chronic inflammatory disorders previously thought to be Th1-mediated.[14 15] Several cytokines participate in Th17 differentiation in humans, including IL-1β, IL-6 and TGFβ. IL-21 also contributes, particularly in the absence or paucity of IL-6, and IL-23 participates in the expansion/maintenance of the Th17 phenotype.[15] All these cytokines are abundantly expressed in GCA lesions.[3 9 16 17]

The aim of this study was to expand these initial observations by investigating the expression of IL-17A in temporal artery biopsies from a sizable series of patients with GCA to investigate the relationship between IL-17A expression and clinically relevant findings, such as the intensity of the systemic inflammatory response, relapses and response to therapy.

PATIENTS AND METHODS

Patients

The study group consisted of 57 patients with biopsy-proven GCA diagnosed between 1997 and 2006 at our institution (Hospital Clinic, Barcelona)

(see online supplementary data S1 and figure S1 for selection criteria). All patients were prospectively evaluated and treated by the authors (GEF, JHR, SPG and MCC) with a predefined homogeneous glucocorticoid-tapering schedule.[6 10] Clinical data recorded at the time of diagnosis included disease symptoms, number of relapses, time to achieve a prednisone dose <10 mg/day, and time to complete prednisone discontinuation with no relapse within the following 6 months. The following baseline blood tests were recorded: erythrocyte sedimentation rate (ESR), haemoglobin, C-reactive protein (CRP) and haptoglobin concentrations, and platelet counts. Relapse was defined as reappearance of cranial symptoms, polymyalgia rheumatica, or systemic symptoms that could not be attributed to other conditions.[3 11] Isolated fluctuations on ESR or CRP were not considered relapses. Symptoms of relapse had to resolve by an increase of 10 mg above the previous effective dose.

Clinical data of the patients are displayed in online supplementary table S1. In 38 patients, the temporal artery was removed before starting treatment, and the remaining 19 had been treated with prednisone (60 mg/day) for a median of 7 days (range 2–12). In four patients, a contralateral temporal artery biopsy was performed after 1 year of treatment.[3]

Uninvolved temporal arteries from 19 patients (13 women and 6 men) with a median of 77 years (range 64–91) in whom GCA was considered but not confirmed, served as controls. All of them were subsequently diagnosed with other diseases (see online supplementary methods).

The study was approved by the Ethics Committee of Hospital Clínic (Barcelona), and patients signed an informed consent.

RNA Isolation and cDNA synthesis

Temporal artery biopsies were embedded in optimal cutting temperature (OCT, Sakura, The Netherlands), snap-frozen in liquid nitrogen and stored at −80°C until used. Sections consecutive to those that provided the histopathologic diagnosis were processed for RNA isolation using TRIzol Reagent (Invitrogen, Carlsbad, California, USA).

Total RNA (1 μg) was reverse-transcribed to cDNA using the Archive kit (Applied Biosystems, Foster City, California, USA), employing random hexamer priming.

Real-time quantitative PCR

cDNA was measured by quantitative real-time PCR using specific Pre-Developed TaqMan gene expression assays (see online supplementary methods) from Applied Biosystems as previously described.[9 16] All samples were normalised to the expression of the housekeeping gene, GUSb. The comparative CT method was used to assess relative gene expression.

Immunohistochemistry

To determine the topography of IL-17 expression, serial 4–6 μm sections were obtained from frozen temporal arteries of two of the patients and two controls. Sections were air-dried, fixed with cold acetone and permeabilised with 0.1% saponin. Endogenous peroxidase was blocked with H_2O_2, and the slides were incubated with the primary polyclonal antibody goat anti-human IL-17A (R&D Systems, Minneapolis, Minnesota, USA). Optimal dilutions were tested on frozen sections of human tonsils (positive control). Immunoglobulins obtained from the same species served as negative controls. Immunodetection was performed with a HRP-labeled polymer conjugated to a secondary antibody (EnVision Visualisation method, Dako, Glostrup, Denmark) using 3,3′-diaminobenzidine as a chromogen.

Enzyme-linked immunosorbent assay (ELISA) detection of IL-17A in tissue

Temporal artery protein extracts could be obtained from seven of the patients (five responders and two relapsers) from the phenolic phase during RNA extraction. IL-17A concentration was measured by immunoassay using Quantikine Human IL-17A from R&D Systems, according to the manufacturer's protocol.

Immunofluorescence staining and confocal microscopy

For qualitative assessment of cytokine distribution at the cellular level, immunofluorescence staining was performed in three additional temporal artery biopsies obtained from an active patient and from two patients who had received treatment with prednisone at 60 mg/day for 8 days at the time of the artery excision. A fragment of these biopsies was fixed in 4% paraformaldehyde with increasing concentrations of sucrose, frozen with OCT and stored at −80°C. Cryostat 10 μm sections were fixed with 4% paraformaldehyde, permeabilised with Triton 0.1% and immunostained with the primary and secondary antibodies detailed in online supplementary methods. Nuclei were stained with Hoechst dye (Molecular Probes, Life Technologies Ltd, Paisley, UK) at 1 : 1000. Slides were mounted in Mowiol 4-88 Reagent (Merck4Biosciences, Nottingham, UK) and examined using a laser scanning confocal Leica TCS *SP5* microscope (Leica Microsystems, Heildelberg, Germany). Images were processed with Leica Confocal software and Image J software (Wayne Rasband, Bethesda, Massachusetts, USA). The number of IL-17 positive and IL-17/FoxP3 double positive cells per field was counted in 10 fields per specimen at 200×magnification.

STATISTICAL ANALYSIS

Mann–Whitney test, Spearman's rho correlation coefficient, and Kaplan–Meier survival curves analysed with log-rank test were used for statistical analysis. With the exception of comparison between untreated (38) and treated (19) patients, statistical analysis was restricted to the cohort of 38 treatment-naïve patients.

RESULTS

IL-17A is upregulated in GCA lesions

IL-17A mRNA was significantly more abundant in temporal arteries from untreated patients than in control arteries (6.22±8.61 vs 2.50±3.90 relative units; p=0.016) (figure 1A). By contrast, plasma IL-17A was not detectable, or was slightly above the detection threshold in the majority of patients and controls (figure 1B).

As shown in figure 2, immunostaining revealed intense IL-17A protein expression by inflammatory cells in GCA lesions. Giant-cells immunostained negative for IL-17A. Interestingly, although control arteries had some constitutive IL-17A mRNA expression, control arteries immunostained negative for IL-17A.

Lack of correlation between IL-17A expression and systemic inflammatory findings

Given the known proinflammatory functions of IL-17A, we explored whether IL-17A mRNA expression correlated with the intensity of the systemic inflammatory response. No differences in IL-17A mRNA expression were observed between patients with strong versus weak systemic inflammatory response at diagnosis (see online supplementary table S2). No significant correlation was found between IL-17A mRNA expression and acute-phase reactants including ESR (r=0.0886, p=0.60), haemoglobin (r=−0.03563, p=0.82) or CRP concentrations (r=0.1495, p=0.45).

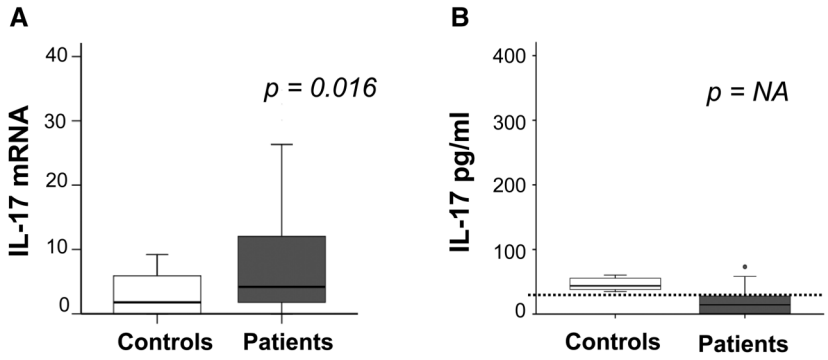

Figure 1 IL-17A concentrations in temporal artery biopsies and serum from patients with giant-cell arteritis (GCA). (A) IL-17A mRNA expression (relative units) in temporal arteries from 38 treatment-naïve patients with GCA and 19 controls. (B) IL-17A concentrations in sera from 33 GCA treatment-naïve patients and seven controls. Dotted line indicates detection threshold. NA, not applicable.

Correlation between IL-17A and other proinflammatory cytokines in GCA lesions

We next tested the potential correlation between IL-17A expression in treatment-naïve samples and the expression of cytokines known to participate in Th17 differentiation (IL-6, TGFβ) or in the maintenance and expansion of the Th17 phenotype (IL23p19).[15] IL-17A mRNA concentrations in untreated GCA arteries significantly correlated with IL-6 (r=0.363, p=0.025) and with IL23p19 mRNA (r=0.397, p=0.008). These findings suggest coordinated regulation in accordance with the role for

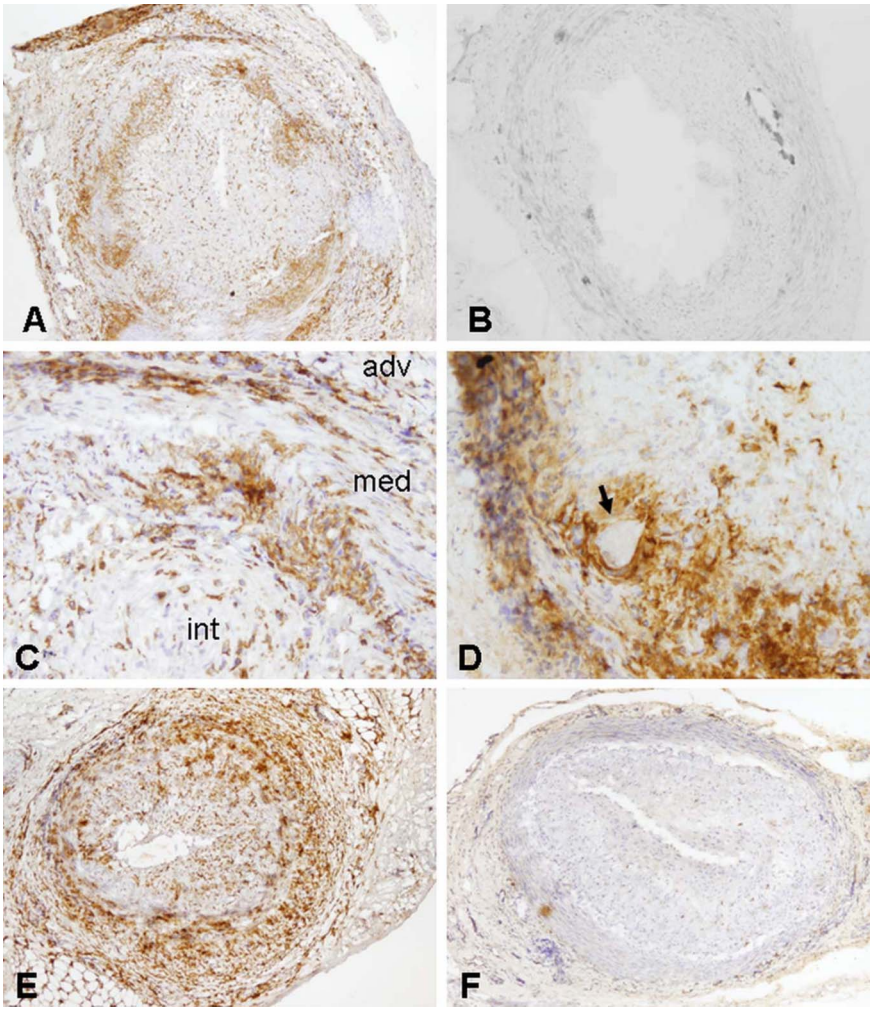

Figure 2 Immunohistochemical detection of IL-17A expression in temporal artery lesions. (A) IL-17 expression in a giant-cell arteritis (GCA)-involved temporal artery section. (B) Lack of IL-17A immunostaining in a temporal artery from a control individual. (C) Closeup view of a GCA-involved artery where distinct IL-17A+cells can be observed in all arterial layers: adventitia (adv), media (med) and intima (int). (D) Giant cells (arrow) do not express IL-17A. (E) IL-17A expression in the temporal artery from a treatment-naive patient compared with IL-17A expression in the contralateral biopsy obtained after being treated with prednisone for 1 year (F).

IL-6 and IL-23 in inducing and maintaining the Th17 phenotype, respectively. No correlation was found between IL-17A and TGFβ (r=−0.037, p=0.848).

IL-17A concentration is decreased in temporal arteries from treated GCA patients

IL-17A mRNA concentrations in temporal artery biopsies from the 19 treated patients were significantly lower than those found in the 38 treatment-naïve patients (1.74±2.48 relative units vs 6.22±8.61; p=0.017) (figure 3A). In four patients who underwent a second temporal artery biopsy after being treated for 1 year, immunohistochemical detection of IL-17 protein, which was intense at the time of diagnosis (figure 2E), was limited to scattered remaining inflammatory cells in the second specimen (figure 2F).

IL-17A expression and long-term response to glucocorticoid treatment

Surprisingly, IL-17A mRNA concentrations in lesions tended to be higher in patients who achieved sustained remission or experienced just one disease flare compared with those who experienced multiple relapses (7.46±9.73 vs 3.19±3.70 relative units; p=0.058) (figure 3B). The same trend was observed in IL-17A protein concentration which tended to be higher in non-relapsing patients (19.30±29.96 vs 0.68±0.63 pg/ml) (figure 3C). Accordingly, IL-17A mRNA levels tended to be higher in patients able to completely discontinue prednisone at 3 years (5.17±8.11 vs 0.29±0.46, p=0.06) (figure 3D).

Similarly, untreated patients with high IL-17A mRNA content (above 75% percentile) in their arteries achieved a maintenance prednisone dose <10 mg/day significantly sooner than patients with lower IL-17A mRNA values (median 25 vs 44 weeks, p=0.0079) (figure 4A). Likewise, patients with elevated IL-17A mRNA concentrations were able to completely withdraw prednisone earlier than patients with lower IL-17 mRNA levels (p=0.028) (figure 4B).

Plasticity between regulatory T lymphocytes (Tregs) and Th17 lineages may contribute to the association between increased IL-17A expression and response to therapy

We next investigated the expression of transcription factors RORα and RORc, master regulators of Th17 lineage. RORα and RORc were expressed at similar levels in GCA and control arteries; their expression tended to correlate (r=0.33, p=0.053), and were not influenced by treatment (figure 5). No correlation was found between IL-17A and RORα (r=−0.20, p=0.36) or RORc expression (r=−0.11, p=0.596). Taken together, these findings suggest that RORα and RORc may be expressed by cells other than Th17 lymphocytes, and that Th17 cells may not be the only producers of IL-17A in GCA. By contrast,

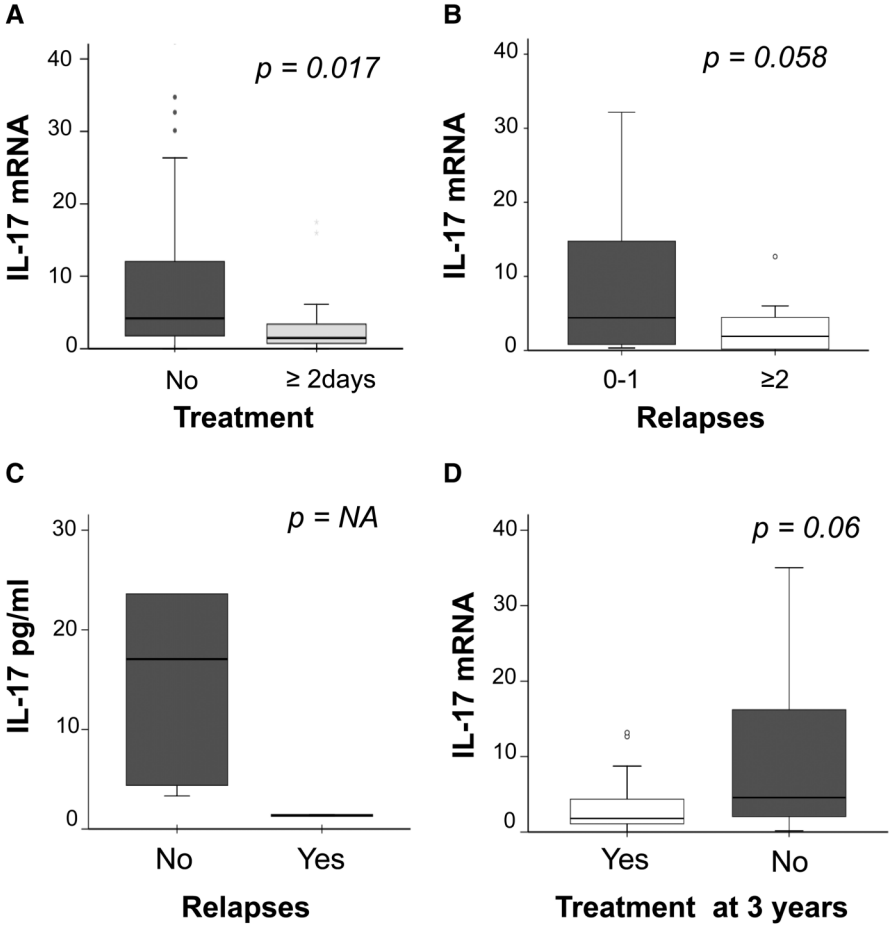

Figure 3 Relationship between IL-17A and response to therapy. (A) IL-17A mRNA expression (relative units) in temporal arteries from 38 treatment-naïve and 19 prednisone treated giant-cell arteritis (GCA) patients. (B) IL-17A mRNA content in temporal arteries from 38 treatment-naïve GCA patients according to relapses. (C) IL-17 protein content in temporal arteries from seven GCA patients according to relapses (patient numbers are too small for reliable statistics). (D) IL-17A mRNA concentration in initial temporal artery biopsies from patients still requiring prednisone compared with that obtained from patients in sustained treatment-free remission, 3 years after diagnosis. NA: not applicable

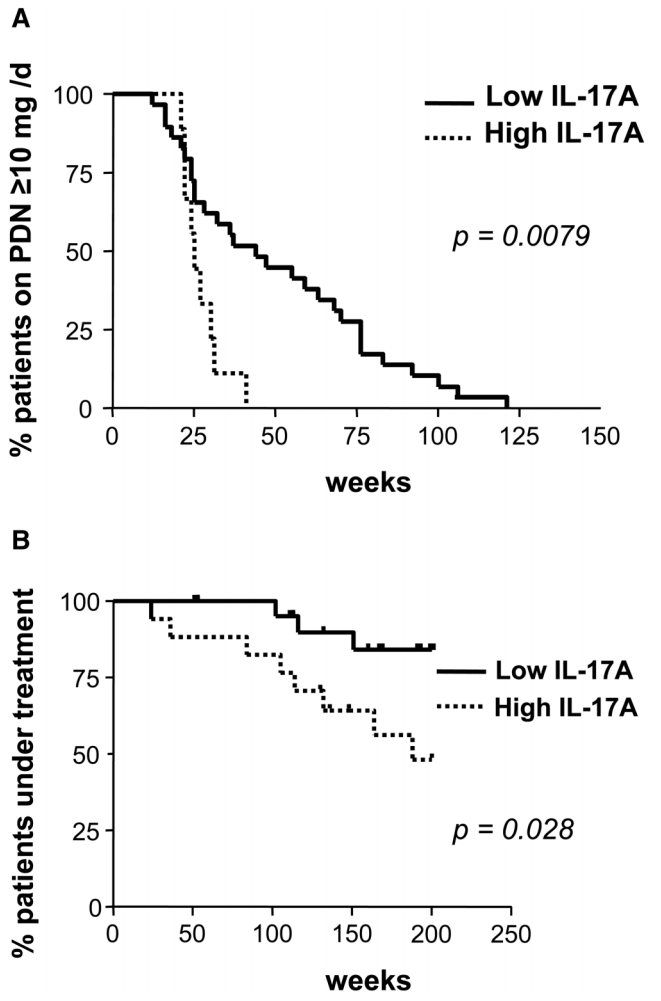

Figure 4 Association between IL-17A expression in giant-cell arteritis (GCA) lesions and treatment requirements. (A) Percentage of patients requiring >10 mg prednisone/day to maintain remission, according to the intensity of IL-17A expression in vascular lesions. High IL-17A refers to mRNA concentration within the 75th percentile, and low IL-17A below the 75th percentile. (B) Percentage of patients requiring prednisone treatment over time, according to the intensity of IL-17A expression in lesions as in A.

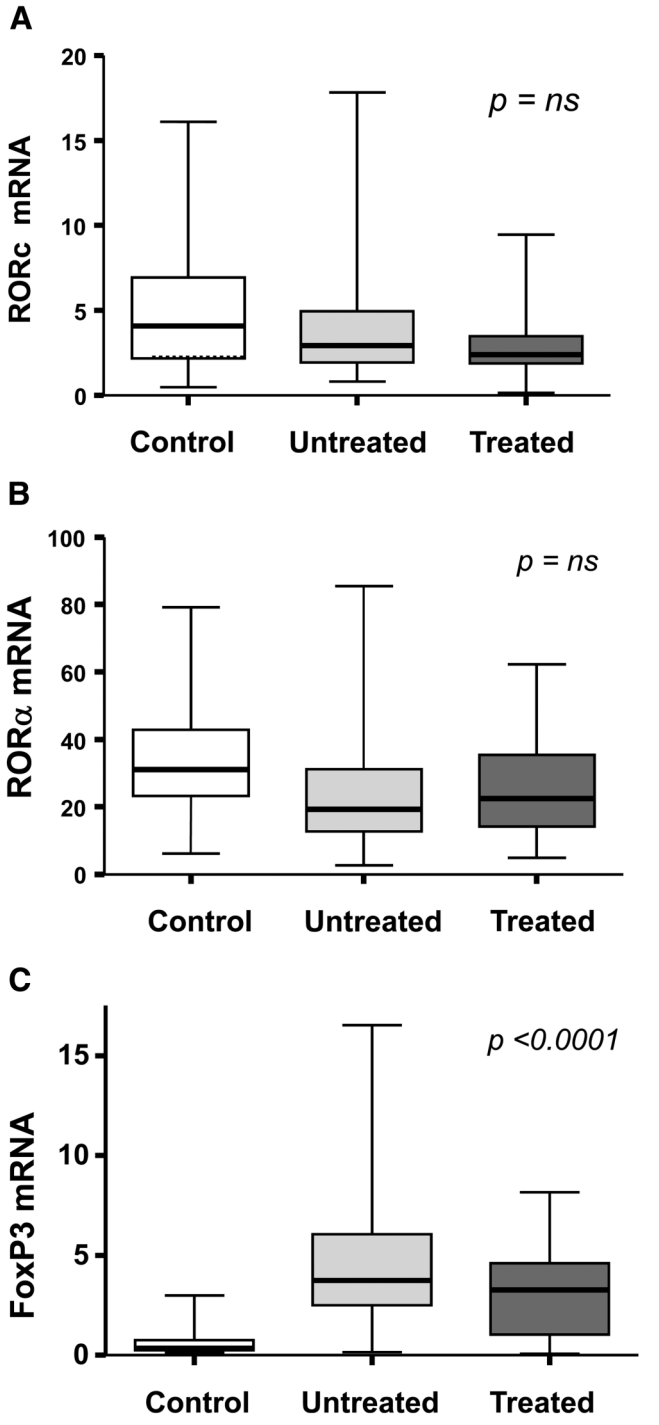

Figure 5 Expression of master regulators of Th17 (RORc and RORα) and Treg differentiation (FoxP3) in temporal artery lesions. (A) Expression of RORc (relative units) in 19 control arteries, 38 treatment-naïve patients and 19 prednisone-treated patients. Expression of RORα (B) and FoxP3 (C) in the same patient subsets.

FoxP3 was significantly upregulated in GCA lesions and significantly decreased with treatment (figure 5).

It has been recently shown that induced regulatory Tregs may transiently lose their suppressive capacity and produce IL-17A in an inflammatory microenvironment.[18–21] Confocal microscopy of temporal artery sections showed that a subset of Tregs (identified as FoxP3-positive cells) contributed, indeed, to IL-17A production in active GCA lesions, and that these cells may be reduced in specimens from treated patients (figure 6). Initial IL-17A expression may then reflect the functional activity of Th17 cells and also the contribution of IL-17A-producing FoxP3 cells with their potential to recover suppressive activity when inflammatory stimuli decrease in the microenvironment.

DISCUSSION

We found that IL-17A expression is prominent in GCA lesions. Consistently, IL-17A expression correlated with expression of IL-6, a cytokine involved in Th17 differentiation, and particularly, with expression of the IL-23 subunit IL-23p19, a cytokine involved in the maintenance and expansion of the Th17 phenotype.[15 21] The lack of correlation with TGFβ, also required for Th17 differentiation, as well as the significant correlation with IL-23, may be related to the fact that temporal artery biopsies are rarely performed during early events and are usually obtained when the inflammatory process is fully developed. At the stages when temporal arteries are obtained, TGFβ may play additional roles in vascular remodelling.[3 22] Our findings, obtained in a sizable series of patients with prospectively recorded

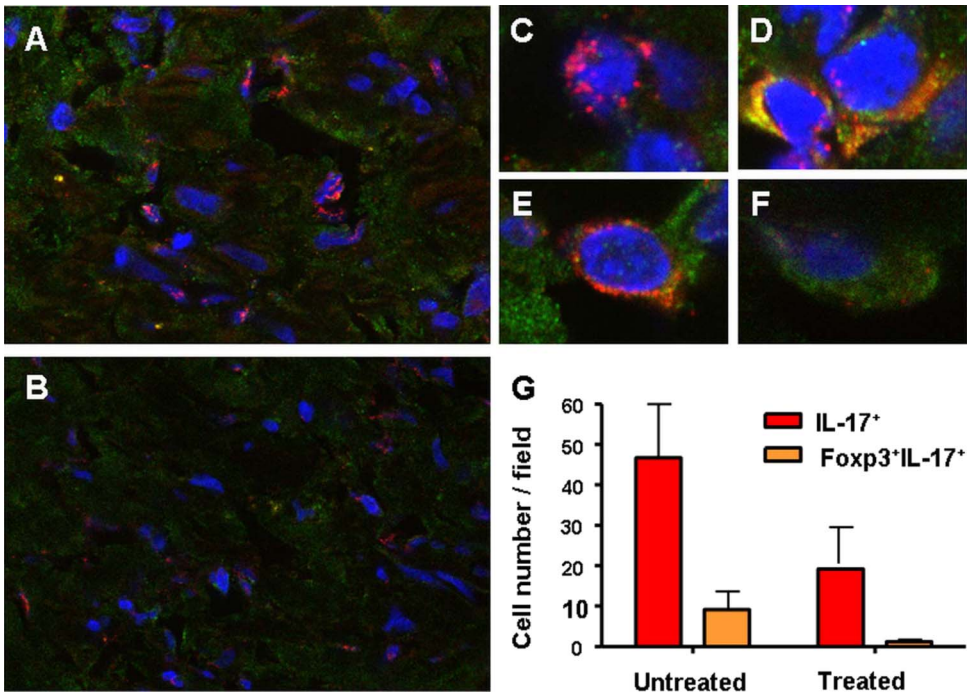

Figure 6 Expression of IL-17A and Foxp3 cells in temporal artery lesions from patients with giant-cell arteritis. (A) IL-17A expression (red colour) in a patient with active giant-cell arteritis (GCA). (B) IL-17A expression in a patient treated with 60 mg prednisone/day for 1 week. (C) Higher magnification of an inflammatory cell expressing only IL-17A (red, merged). (D) A magnified inflammatory cell intensively expressing both IL-17A and FoxP3 (orange, merged). (E) A magnified inflammatory cell from a treated patient with lower coexpression (orange, merged). (F) A magnified cell from a treated patient expressing primarily Foxp3 (green, merged). (G) IL-17A$^+$ and IL-17A$^+$FoxP3$^+$ double positive cells (mean±SD) in 10 different fields (200×) per specimen containing similar number of nuclei in lesions from an active patient versus two treated patients. $p<0.05$ (due to the small number of cases, statistics are only indicative).

clinical and follow-up data confirm preliminary observations performed in small series of patients, and support the participation of Th17 mechanisms in the pathogenesis of GCA.[3 12 13]

IL-17A, typically, but not exclusively, produced by Th17 cells, plays a central role in the development of tissue inflammation in a variety of experimental models and human diseases.[15 21] IL-17A exerts strong proinflammatory functions on a variety of cells, including endothelial cells, by inducing expression of classical proinflammatory cytokines IL-1β, IL-6 and TNFα, endothelial adhesion molecules, chemokines and metalloproteinases.[14 15 23] All these molecules are strongly expressed in GCA, and are thought to participate in proinflammatory amplification cascades.[2 9 16 23–25] The remarkable expression of IL-17A found in GCA supports a prominent role in vascular inflammation. Supporting this concept, deletion of IRF-4-binding protein leading to sustained activation of IRF-4, a transcription factor involved in Th17 differentiation, results in large-vessel vasculitis in mice.[26]

While IL-17A was remarkably upregulated in lesions, it was barely detectable in serum. Consistent with this finding, we could not find a relationship between IL-17A expression and systemic symptoms or acute-phase proteins, suggesting that IL-17A functions are predominantly exerted locally at the vascular lesions. IL-17A strongly amplifies the expression of other proinflammatory cytokines (IL-6, TNFα) which, in turn, are effectively released into the bloodstream and do correlate with the intensity of the systemic inflammatory response in GCA.[6 10]

As others and we have previously shown in small series,[3 12 13] IL-17A mRNA and IL-17A-expressing cells were dramatically reduced in specimens obtained from treated patients. This finding supports the prominent proinflammatory role of IL-17A in GCA, and suggests that downregulation of IL-17A may at least partially account for the dramatic effect of high-dose glucocorticoids in ameliorating disease-related symptoms, and in substantially decreasing vascular inflammation after long-term treatment.[3]

The most intriguing finding of this study was the association between strong initial expression of IL-17A and response to therapy. Patients with strong IL-17A expression tended to experience less relapses and were able to reduce and completely discontinue prednisone earlier than patients with weaker IL-17A expression. This may indicate that patients who develop a predominantly Th17 response are more sensitive to glucocorticoid treatment.

Recent studies have shown that, on one hand, Th17 cells are not the only producers of IL-17A[15 27] and that, on the other hand, there is remarkable plasticity among T cell lineages depending on the conditions of the microenvironment.[18–20] Particularly interesting is the fact that induced Tregs, which role was initially identified as immunosuppressive, are able to produce IL-17A when exposed to an inflammatory milieu.

We show that both RORα and RORc, markers and master regulators of Th17 are equally expressed in GCA and control arteries. Constitutive expression of RORα and RORc by non-inflamed arteries may indicate an important, previously unknown role of these factors in vascular biology. By contrast, FoxP3 was upregulated in GCA and decreased with treatment, consistent with our early findings demonstrating expression of CD25+ lymphocytes in lesions and their reduction upon treatment.[4] The lack of correlation between RORα/RORc and IL-17A expression also suggests that other cells, in addition to Th17 cells, may contribute to IL-17A production in GCA. FoxP3-positive cells contributed,

indeed, to IL-17A production. These preliminary findings suggest that induced Tregs may functionally evolve over time, and may have a role in limiting disease activity in GCA. Expanding Tregs by administration of low-dose IL-2 has been recently shown to ameliorate cryoglobulinemic-related vascular inflammation in humans.[28] Moreover, it has recently become apparent that not all Th17 cells are equally pathogenic, and that abundance of TGFβ expression may switch Th17cells to the alternative non-pathogenic phenotype.[29] We have recently shown that prednisone treatment increases TGFβ expression,[3] which may also limit the pathogenicity of Th17 cells.

In conclusion, strong IL-17A expression in involved arteries is a biomarker and predictor of response to therapy. Our preliminary data suggests that different cell lineages may contribute to IL-17A expression in GCA. However, the observational nature of this and other existing studies addressing IL-17A expression in GCA does not allow to draw strong mechanistic conclusions about the specific role of IL-17A and Th17 cells in GCA. Our findings suggest complex interplay among T cell lineages in delineating disease fate and response to therapy that deserves further investigation.

Acknowledgements We thank Mrs Montse Sánchez and Mrs Ester Tobías for excellent technical support with immunohistochemistry and Dr María Calvo for her invaluable advice with confocal microscopy.

Contributors GEF, MCC: designed the study and wrote the paper; GEF, MCB, EPR, EL, MS: performed experimental work; JHR, SPG, AGM, JMG, MCC: collected and analysed clinical data; MUR: designed the study, analysed data, provided important inputs to the writing of the manuscript and approved the final version. All the authors repeatedly discussed the results of the paper, made suggestions for improvement and contributed to generate further data. All the authors read and reviewed the drafts and approved the final version of the manuscript.

Funding Supported by Ministerio de Economía y Competitividad (SAF 08/04328 and SAF 11/30073).

Competing interests None.

Patient consent Obtained.

Ethics approval Internal Review Board, Hospital Clínic.

Provenance and peer review Not commissioned; externally peer reviewed.

REFERENCES

1. **Salvarani C,** Cantini F, Hunder GG. Polymyalgia rheumatica and giant-cell arteritis. *Lancet* 2008;**372**:234–45.
2. **Weyand CM,** Hicok KC, Hunder GG, *et al*. Tissue cytokine patterns in patients with polymyalgia rheumatica and giant cell arteritis. *Ann Intern Med* 1994;**121**:484–91.
3. **Visvanathan S,** Rahman MU, Hoffman GS, *et al*. Tissue and serum markers of inflammation during the follow-up of patients with giant-cell arteritis—a prospective longitudinal study. *Rheumatology (Oxford)* 2011;**50**:2061–70.
4. **Cid MC,** Campo E, Ercilla G, *et al*. Immunohistochemical analysis of lymphoid and macrophage cell subsets and their immunologic activation markers in temporal arteritis. Influence of corticosteroid treatment. *Arthritis Rheum* 1989;**32**:884–93.
5. **Cid MC,** Hoffman MP, Hernández-Rodríguez J, *et al*. Association between increased CCL2 (MCP-1) expression in lesions and persistence of disease activity in giant-cell arteritis. *Rheumatology* 2006;**45**:1356–63.
6. **Hernández-Rodriguez J,** García-Martinez A, Casademont J, *et al*. A strong initial systemic inflammatory response is associated with higher corticosteroid requirements and longer duration of therapy in patients with giant-cell arteritis. *Arthritis Rheum* 2002;**47**:29–35.
7. **Martinez-Lado L,** Calviño-Díaz C, Piñeiro A, *et al*. Relapses and recurrences in giant cell arteritis: a population-based study of patients with biopsy-proven disease from northwestern Spain. *Medicine (Baltimore)* 2011;**90**:186–9312.
8. **Proven A,** Gabriel S, Orces C, *et al*. Glucocorticoid therapy in giant-cell arteritis: duration and adverse outcomes. *Arthritis Rheum* 2003;**49**:703–8.
9. **Hernández-Rodríguez J,** Segarra M, Vilardell C, *et al*. Tissue production of pro-inflammatory cytokines (IL-1β, TNF-α and IL-6) correlates with the intensity of the systemic inflammatory response and with corticosteroid requirements in giant-cell arteritis. *Rheumatology* 2004;**43**:294–301.
10. **García-Martínez A,** Hernández-Rodríguez J, Espígol-Frigolé G, *et al*. Clinical relevance of persistently elevated circulating cytokines (tumor necrosis factor alpha and interleukin-6) in the long-term followup of patients with giant cell arteritis. *Arthritis Care Res* 2010;**62**:835–41.
11. **Hoffman GS,** Cid MC, Rendt-Zagar KE, *et al*. Infliximab for maintenance of glucocorticosteroid-induced remission of giant-cell arteritis. *Ann Intern Med* 2007;**146**:621–30.
12. **Espígol-Frigolé G,** Lozano E, García-Martínez A, *et al*. IL-17 expression in temporal artery lesions from patients with giant-cell arteritis (GCA). *Arthritis Rheum* 2008;**58** (Suppl):S929.
13. **Deng J,** Younge BR, Olshen RA, *et al*. Th17 and Th1 T-cell responses in giant cell arteritis. *Circulation* 2010;**121**:906–15.
14. **Miossec P,** Korn T, Kuchroo VK. Interleukin-17 and type 17 helper T cells. *N Engl J Med.* 2009;**361**:888–98.
15. **Korn T,** Bettelli E, Oukka M, *et al*. IL-17 and Th17 cells. *Ann Rev Imunol* 2009;**27**:485–517.
16. **Hernández-Rodríguez J,** Segarra M, Vilardell C, *et al*. Elevated production of interleukin-6 is associated with a lower incidence of disease-related ischemic events in patients with giant-cell arteritis: angiogenic activity of interleukin-6 as a potential protective mechanism. *Circulation* 2003;**107**:2428–34.
17. **Terrier B,** Geri G, Chaara W, *et al*. IL-21 modulates Th1 and Th17 responses in giant cell arteritis. *Arthritis Rheum* 2012;**64**:2001–11.
18. **Abdulahad WH,** Boots AM, Kallenberg CG. FoxP3+ CD4+ T cells in systemic autoimmune diseases: the delicate balance between true regulatory T cells and effector Th-17 cells. *Rheumatology* 2011;**50**:646–56.
19. **Bluestone JA,** Mackay CR, O'Shea JJ, *et al*. The functional plasticity of T cell subsets. *Nat Rev Immunol.* 2009;**9**:811–16.
20. **O'Shea JJ,** Paul WE. Mechanisms underlying lineage commitment and plasticity of helper CD4+ T cells. *Science* 2010;**327**:1098–102.
21. **Gaffen SL.** Recent advances in the IL-17 cytokine family. *Curr Opin Immunol.* 2011;**23**:613–19.
22. **Lozano E,** Segarra M, García-Martínez A, *et al*. Imatinib mesylate inhibits in vitro and ex vivo biological responses related to vascular occlusion in giant cell arteritis. *Ann Rheum Dis* 2008;**67**:1581–8.
23. **Hot A,** Lenief V, Miossec P. Combination of IL-17 and TNFα induces a pro-inflammatory, pro-coagulant and pro-thrombotic phenotype in human endothelial cells. *Ann Rheum Dis* 2012;**71**:768–76.
24. **Cid MC,** Cebrián M, Font C, *et al*. Cell adhesion molecules in the development of inflammatory infiltrates in giant cell arteritis: inflammation-induced angiogenesis as the preferential site of leukocyte-endothelial cell interactions. *Arthritis Rheum.* 2000;**43**:184–94.
25. **Segarra M,** García-Martínez A, Sánchez M, *et al*. Gelatinase expression and proteolytic activity in giant-cell arteritis. *Ann Rheum Dis* 2007;**66**:1429–35.
26. **Chen Q,** Yang W, Gupta S, *et al*. IRF-4-binding protein inhibits interleukin-17 and interleukin-21 production by controlling the activity of IRF-4 transcription factor. *Immunity* 2008;**29**:899–911.
27. **Noordenbos T,** Yeremenko N, Gofita I, *et al*. Interleukin-17-positive mast cells contribute to synovial inflammation in spondylarthritis. *Arthritis Rheum* 2012;**64**:99–109.
28. **Saadoun D,** Rosenzwajg M, Joly F, *et al*. Regulatory T-cell responses to low-dose interleukin-2 in HCV-induced vasculitis. *N Engl J Med* 2011;**365**:2067–77.
29. **McGeachy M,** Bak-Jensen KS, Chen Y, *et al*. TGFβ and IL-6 drive the production of IL-17 and Il-10 by T cells and restrain Th17 cell-mediated pathology. *Nature Immunology* 2007;**8**:1390–97.